Groundwater-Surface Water Interactions in a Eutrophic Lake – Impacts of Lacustrine Groundwater Discharge on Water and Nutrient Budgets

Dissertation

zur Erlangung des akademischen Grades
doctor rerum naturalium
(Dr. rer. nat.)
im Fach Geographie

eingereicht an der
Mathematisch-Naturwissenschaftlichen Fakultät
der Humboldt-Universität zu Berlin

von
Diplom-Landschaftsökologin Karin Meinikmann

Präsidentin der Humboldt-Universität zu Berlin
Prof. Dr.-Ing. Dr. Sabine Kunst

Dekan der Mathematisch-Naturwissenschaftlichen Fakultät
Prof. Dr. Elmar Kulke

Gutachter:
1. Prof. Dr. Tobias Krüger, Humboldt-Universität zu Berlin, Geographisches Institut
2. Prof. Dr. Stefan Peiffer, Universität Bayreuth, Hydrologie
3. Prof. Dr. Henning Jensen, University of Southern Denmark, Dep. of Biology

Tag der Einreichung: 20. Dezember 2016

Tag der mündlichen Prüfung: 26. Juni 2017

Acknowledgements

I would like to thank my supervisors Dr. Jörg Lewandowski and Prof. Dr. Gunnar Nützmann who always supported and encouraged me and never lost their faith throughout the years. It is a pleasure and a privilege for me to be a member of their working group.

Sincere thanks also go to Michael Hupfer who was an important contact in all questions regarding Lake Arendsee. Thanks a lot for several years of intense and fruitful discussions and collaborations.

Franziska Pöschke as my friend and office mate was one of the most important persons in the last years for me. Not only her expertise and active contribution to my work but also her warm and dear character helped me through the ups and downs of this time. I would like to thank her for her help, her patience and friendship and for all the wonderful experiences we had together.

Thanks a lot to Christine Sturm, Jörg Fritz Friedrich, and Grit Siegert who supported me on countless occasions in the field, the lab, and as friends. Without them this work would not have been possible.

Many thanks also to the whole team of the Department "Chemical Analytics and Biogeochemistry" at the IGB who contributed valuably to this work by analyzing hundreds of water samples. Also their mental support (especially by Elke Zwirnmann and Christiane Herzog) was very much appreciated.

A large number of interns and bachelor and students supported my field work especially at Lake Arendsee. Thanks a lot to all of them, especially to Roman, Stephi, and Andrea Sacher. Especially Andrea spent a long time with our working group and contributed substantially to the present work by maintaining, sampling, and analyzing the surface inflows of Lake Arendsee. Her high spirits and humor were a driving force for me and the whole working group.

Kirsten Pohlmann as the coordinator of the doctoral programme was a valuable contact regarding many scientific and administrative questions. I would like to thank her for her engagement not only in my work but in the IGB doctoral training and support in general.

I am very happy to have made a lot of friends at the IGB during the last years. These acquaintances are of great importance for me. Special thanks go to Sebi, Steffi, Silke, Ani, Bine, Simone, Björn, Maja, and Cris who, among a whole lot of others, accompanied me as friends and colleges. The value of their friendship cannot be put in words.

With great empathy my dear family followed the progress of my work. My biggest thanks to them for always being there for and never stopping believing in me.

Summary

The present work is a collection of studies on lacustrine groundwater discharge (LGD) and groundwater-borne phosphorus (P) loads. For a number of reasons, groundwater exfiltration (i.e., LGD) is often not considered in water and nutrient budgets of lakes. This is also and especially true for P which was often regarded to be immobile in groundwater until recently. Two chapters review the scientific literature regarding the impacts of groundwater on hydrology and nutrient budgets of lakes, respectively. Both of them present mechanisms and processes of LGD as well as techniques and methods to measure LGD and related nutrient transports. Moreover, numbers of LGD volumes and loads reported in literature are presented. A major issue is the spatial scale on which the approaches can be applied. Point measurements deliver predominantly quantitative results (LGD fluxes) while approaches on larger scales provide qualitative information (identification of exfiltration zones and LGD patterns) but often lack absolute values.

The core of the present work is represented by two case studies dealing with the quantification of P loads from LGD to Lake Arendsee in Northern Germany. A combination of the results of groundwater recharge determination at the catchment scale and temperature depth measurements of the lake sediments is applied to overcome the problem of quantitative large scale LGD determination without losing local spatial information. P concentrations in both, groundwater and LGD, are investigated by detailed spatial water sampling from groundwater observation wells, domestic wells, and temporary piezometers directly at the lake shore. The results reveal that P is actually present in concentrations far above natural background concentrations in the urban groundwater. Resulting LGD-derived P loads account for more than 50% of the overall external P loads to Lake Arendsee and by that contribute significantly to lake eutrophication. Sources for increased P concentrations could not be identified eventually.

Three further studies are devoted to the development and improvement of approaches to determine LGD. They show results of attempts to upscale point measurements of LGD, and the application of thermal infrared radiation to identify hotspots of LGD. Stable isotopes are used to confirm the separation of groundwater in- and exfiltration zones which were defined based on hydraulic head contour lines.

Critical reviews of the above mentioned studies reveal the need for further research in order to standardize and improve methods for LGD and mass load determination. It is found that the appropriate method for LGD determination depends on the spatial scale of interest. The identification of P introduced by LGD as a main driver of lake eutrophication is an important finding which should encourage scientists, policy makers, and lake managers to consider groundwater as a relevant P source for lakes.

Zusammenfassung

Die vorliegende Arbeit besteht aus mehreren Studien zur Quantifizierung des Grundwasserstroms in Seen (Exfiltration; engl.: lacustrine groundwater discharge, LGD) und damit verbundener Nährstoffeinträge. Die Bedeutung des Grundwassers für Wasser- und Nährstoffhaushalte von Seen wird häufig unterschätzt. Dies gilt insbesondere für Phosphor (P), der lange Zeit als im Grundwasser immobil galt. Das ist einer der Gründe, warum das Grundwasser vor allem im Zusammenhang mit der Gewässereutrophierung häufig ignoriert wurde. In zwei einleitenden Kapiteln dieser Arbeit werden eine Vielzahl weiterer Gründe für die Vernachlässigung der Grundwasserexfiltration in Seen und der daran gekoppelten Nährstoffeinträge identifiziert. Diese Literaturstudien fassen den aktuellen Kenntnisstand zum Einfluss des Grundwassers auf die Hydrologie von Seen und ihre Nährstoffhaushalte zusammen. Dabei werden Mechanismen und Prozesse ebenso wie entsprechende Messtechniken vorgestellt. Außerdem werden in der internationalen Fachliteratur publizierte Daten gemessener Exfiltrationsraten und -volumina präsentiert. Die Wahl der Messmethode zur Erfassung des Grundwasserzustroms ist zum großen Teil vom räumlichen Maßstab des Untersuchungsgebietes abhängig. Zwar steht eine Vielzahl von Methoden zur Verfügung; deren Anwendbarkeit ist aber häufig auf eine bestimmte räumliche Skala beschränkt. Punktmessungen liefern überwiegend quantitative Ergebnisse (z. B. Fluxraten), während Ansätzen, die es erlauben, größere Skalen abzudecken, lediglich qualitative Informationen liefern (z. B. die räumliche Eingrenzung von Bereichen mit Grundwasserzustrom und Muster des Grundwasserfluxes).

Den Kern der vorliegenden Arbeit bilden zwei empirische Studien, die sich mit der Quantifizierung der grundwasserbürtigen Phosphor-Fracht in den Arendsee im Nordosten Deutschlands befassen. Das Gesamtvolumen des Grundwasserzustroms wird basierend auf der Grundwasserneubildung im Einzugsgebiet des Sees ermittelt. Lokale Muster der Grundwasserexfiltration werden anhand von Temperaturtiefenprofilen des Seesediments bestimmt. Eine Kombination der Ergebnisse ermöglicht es, die quantitativen Daten mit lokalen Informationen zu unterstützen. Anhand von Grundwassermessstellen, privaten Hausbrunnen, sowie am Ufer installierten Piezometern werden die Phosphor-Konzentrationen im Grundwasser im Einzugsgebiet und in unmittelbarer Ufernähe untersucht. Das Grundwasser im besiedelten Bereich weist Phosphor-Konzentrationen weit oberhalb der natürlichen Hintergrund-Konzentrationen auf. Als Konsequenz daraus haben die grundwasserbürtigen Phosphor-Frachten einen Anteil von mehr als 50% an der gesamten externen P-Last des Arendsees. Das Grundwasser ist damit eine maßgebliche Ursache für die Eutrophierung des Gewässers. Quellen für die hohen P-Konzentrationen im Grundwasser können nicht abschließend identifiziert und lokalisiert werden.

Drei weitere Studien widmen sich der Entwicklung und Optimierung von Ansätzen zur qualitativen und quantitativen Bestimmung der Grundwasserexfiltration in Seen. Vorgestellt werden die Ergebnisse von Versuchen, Punktmessungen von Fluxraten hochzuskalieren, sowie die Anwendung von thermaler Infrarot-Strahlung zur räumlichen Abgrenzung von Hotspots des Grundwasserzustroms. Außerdem wird gezeigt, dass stabile Isotope des ufernahen Grundwassers zur Identifikation von In- und Exfiltrationszonen genutzt werden können. Die kritische Auseinandersetzung mit den Ergebnissen der oben genannten Studien zeigt die Notwendigkeit weiterer Forschung zur Verbesserung und Standardisierung der Methoden zur Bestimmung von LGD und damit verbundenen Stofftransporten auf. Der Fall des Arendsees sollte alle, Wissenschaftler und Praktiker, dazu motivieren, das Grundwasser als relevante Eutrophierungsquelle in Betracht zu ziehen.

Contents

Figures

Tables

1 Introduction

1.1 Eutrophication and lacustrine groundwater discharge

The ecological state of lakes is to a large extent linked to processes in the atmospheric, terrestrial, and aquatic compartments of their catchment. This is especially true for their trophic state which is closely linked to the input of allochthonous nutrients such as nitrogen (N) and phosphorus (P). The trophic state of lakes is ubiquitously impaired by the enrichment of nutrients resulting from human activities, a process referred to as "cultural eutrophication" (Smith 2003; Smith and Schindler 2009). The oversupply of P is especially considered the most relevant factor driving lake eutrophication (Schindler 2012). The present doctoral study was embedded in a series of projects developing mitigation measures against eutrophication of Lake Arendsee, a deep stratified lake in Northern Germany. This freshwater lake, as many others in Europe and all over the world, is affected by excessive P availability from an unknown source.

The problem of freshwater eutrophication is not new. The issue came up already decades ago, a little delayed but straightforward following the rapid "career" of industrialization, especially in Western Europe. The consequences of increasing N and P loads to aquatic ecosystems were as severe as they were obvious (Smith and Schindler 2009):

- Increased biomass of phytoplankton and macrophyte vegetation
- Increased biomass of consumer species
- Shifts to bloom-forming algal species that might be toxic or inedible (e.g., cyanobacteria)
- Increased biomass of benthic and epiphytic algae
- Changes in species composition of macrophyte vegetation
- Increased incidence of fish kills
- Reduction in species diversity
- Reductions in harvestable fish biomass
- Decreases in water transparency
- Taste, odor, and drinking water treatment problems
- Oxygen depletion
- Decreases in perceived aesthetic value

For several decades, a worldwide and intense scientific effort was made to understand the multi-dependent processes driving the observed changes and develop management strategies for ecosystem and human health protection. However, after about 40 years of research eutrophication is still defined to be one of the major threats to water quality worldwide (Orderud and Vogt 2013; Schindler 2012; Sharpley and Wang 2014; Smith and Schindler 2009). In 2002, Brönmark and Hansson (2002) predicted a reduced impact of eutrophication on lakes and ponds by 2025. From this, they concluded that research interests on eutrophication will decrease. However, selecting "eutrophication" and "lake" as keywords in ISI Web of Science™ shows that publication numbers have not yet decreased since 2000 (Fig. 1.1). In fact, annual publications peaked in 2012 while having similar numbers in the following years. It might take another decade to evaluate if eutrophication is of less relevance for research. However, increasing temperatures due to climate change and increasing global population might continue to promote eutrophication and by that keep up this issue as a topic of continuous research efforts.

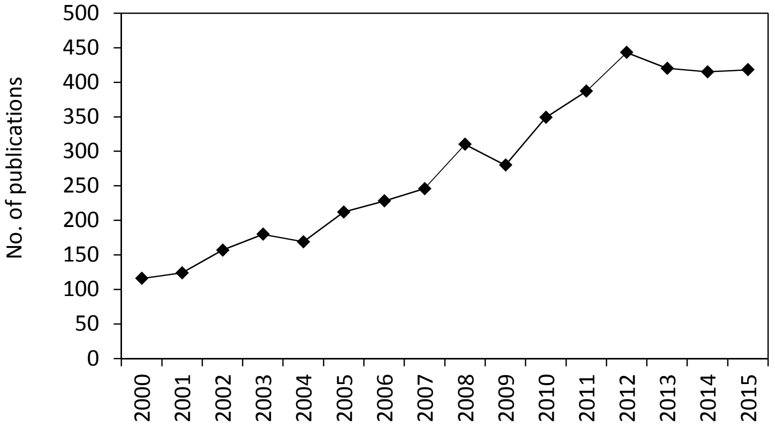

Figure 1.1 Annual number of English publications (reviews and articles filtered for the key words "eutrophication" and "lake" listed in ISI Web of Science™ as of 11/09/2016).

Actions against cultural eutrophication should primarily aim at reducing the import of nutrients to the lake (Carpenter et al. 1998). Additionally, in-lake measures might be useful to reduce the symptoms of eutrophication or to decrease adaption times during or even before load reductions (Hupfer et al. 2016). Since point sources of nutrients have been eliminated to a large extent by now (at least in the developed countries) ongoing lake eutrophication is mostly attributed to diffuse sources of N and P nowadays (Orderud and Vogt 2013; Sharpley and Wang 2014). Besides atmospheric inputs the basic diffuse transport paths for nutrients include both, surface and subsurface transport paths (Carpenter et al. 1998). Diffuse surface transport of nutrients is induced by overland flow or wind and water erosion. Subsurface flow is driven by complex mechanisms in both, the unsaturated and the saturated zone. Vadose water travelling toward the water table ends up either as near-surface flow resulting in a relatively fast lateral transport toward receiving waters or as groundwater flow which is usually slower but also has a lateral flow component. Although often neglected, groundwater travelling through the aquifers is an important input path for nutrients to lakes. Many lakes (and rivers) are hydrologically connected to the aquifer; i.e., water is constantly exchanged between the two systems (Winter 1999).

Nitrate as the most common inorganic N-species is of high solubility and thus transported relatively fast in the subsurface, and especially the groundwater. In contrast, P is of generally low solubility and shows high sorption and precipitation potentials to particulate or dissolved organic matter and other, mostly inorganic, binding molecules in soils and sediments (Correll 1998). This resulted in the paradigm that P is to a large extent immobile in the subsurface, and transported only by wind and water driven soil movements at the surface, while groundwater concentrations are low (Khan and Mohammad 2014; Roy and Bickerton 2014; Wetzel 2001). Due to a lack of significant slope overland flow is of minor importance in lowland areas. In these settings surface waters are predominantly fed by subsurface flow which has, due to the above-mentioned reasons, long been neglected in terms of P transport (Heathwaite et al. 2006; Kilroy and Coxon 2005). However, especially in lowland areas intense agriculture has resulted in an accumulation of P in soils, imposing the risk of elevated P losses with subsurface flow (Heathwaite et al. 2006; Withers and Haygarth 2007). Studies on subsurface transport of P in agricultural settings often focus on (tile) drainage (Heathwaite et al. 2006; Sharpley et al. 2007; Tiemeyer et al. 2009). The gradient imposed by such facilities enforces soluble and even particulate P to be transported with near-surface flow through the macropore systems of sediment matrices (Heathwaite et al. 2006; Simard et al. 2000). By that nutrients and contaminants travel relatively fast through the pore matrix into drainage facilities and from there into rivers and lakes.

Apart from this, a further subsurface transport of P into the groundwater is hardly considered in the international literature.

Holman et al. (2008) were probably the first ones presenting results of increased groundwater P concentrations at a large scale (UK and Ireland). They also attributed this to the ubiquitous loss of P from agricultural soils. On the local scale there is evidence that P can be present in concentrations two orders of magnitudes above 0.1 mg l^{-1} in the groundwater (Roy and Bickerton 2014 and studies therein). This value is referred to as a threshold for the classification of hypereutrophic lakes (Dodds et al. 2009; Wetzel 2001). According to Ansari et al. (2011) the "acceptable level of total inorganic phosphorus" in lake water is between 0.03 and 0.04 mg l^{-1}. Increased groundwater P concentrations on the local scale often occur as a consequence of urban wastewater contaminations (e.g., Driescher and Gelbrecht 1993; Harman et al. 1996; Ptacek 1998; McCobb et al. 2003; Robertson 2003; Wolf et al. 2012). Not all of them have a focus on ecological impacts of groundwater P to surface waters. Although there are studies showing that groundwater discharge to surface waters has high P concentrations and by that has a high potential to fuel eutrophication (McCobb et al. 2003; Palmer-Felgate et al. 2010; Roy and Malenica 2013; Roy et al. 2009; Vanek 1993) a quantitative analysis of these findings is hardly done. One reason for that is that groundwater-borne P loads to lakes and their impacts are difficult to quantify.

In the case of Lake Arendsee a detailed P budget was expected to give insights into the causes of ongoing eutrophication. In order to identify all input paths water and nutrient budgets of a lake have to be quantified. Their reliability depends on the accuracy of the determination of single input (and output) paths. Lake Arendsee is situated in a lowland area where surface inflows such as rivers and ditches are usually considered to be the main P sources for lakes. Measurements of discharge rates and P concentrations in surface inflows are relatively easy in surface inflows. Nowadays, measurement and sampling techniques allow a high temporal resolution of both components which increases the accuracy of P load determination from surface inflows significantly (Cassidy and Jordan 2011; Jordan et al. 2005).

Additionally to surface inflows, other nutrient input paths are often not or only roughly considered in lowland settings. This is especially true for groundwater although many lakes are tightly connected to contiguous aquifers (Winter 1999). Groundwater flows into (exfiltration) and/or out of (infiltration) lakes and by that transports water constituents from one compartment to the other (Winter et al. 1998). However, even if groundwater is the main contributor to a lake water balance groundwater-borne nutrient loads can be low when concentrations are low. This relation reverses when concentrations increase. Loads then grow by the factor of this increase. By this, even small volumes of groundwater exfiltration may result in significant mass fluxes (LaBaugh et al. 1995; Lee 1996; Schuster et al. 2003; Shaw et al. 1990). Nevertheless, especially regarding P inputs groundwater is often not considered or even willfully neglected. Reasons for this are discussed in detail in Chapter 2.

The present work is dealing with the process of groundwater exfiltration to lakes which is also called lacustrine groundwater discharge (LGD). The core is represented by two studies aiming at the quantification of LGD-derived P loads to Lake Arendsee (Chapter 3). Those studies are accompanied by several hydrological side-studies focusing on the determination of LGD patterns (Chapter 4). For a general overview, the following sub-chapters 1.2 and 1.3 provide a short introduction into groundwater-lake interactions, including general mechanisms and approaches to quantify LGD-derived nutrient loads. Detailed insights to the topic are given in Chapter 2.

1.2 General concepts and patterns of LGD

The exchange between groundwater and lake happens across the lake bed and is mainly driven by factors such as

a) hydraulic gradient between groundwater and lake surface,
b) hydraulic conductivity of the saturated sediments (k_{sat}),
c) degree of anisotropy , and
d) climatic settings (Winter 1999).

The hydraulic gradient drives direction and intensity of groundwater-lake interactions. Groundwater exfiltrates into a lake when the water table is higher than the lake level (Fig. 1.2a). Vice versa, lake water infiltrates into the contiguous aquifer when the water table is below the lake level (Fig. 1.2b). The hydraulic conductivity k_{sat} controls actual flow velocities and by that exchange rates between groundwater and lakes. In unconsolidated sediments porosity and permeability are major parameters determining k_{sat}. Furthermore, the ratio of k_{sat} in horizontal to vertical directions (anisotropy) plays an important role regarding flow velocities.

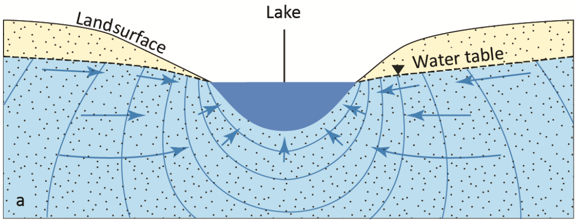

Figure 1.2 Groundwater flow (blue arrows) under exfiltrating (a) and infiltrating (b) conditions (modified from Winter et al. 1998).

Though focused to near-shore areas, groundwater-lake exchange is usually a diffuse process occurring distributed over relatively large areas of the lake bed (Rosenberry and LaBaugh 2008). This is one of the major reasons for the difficulties in measuring exchange rates since many techniques allow only point measurements which require upscaling to the area where exchange processes are assumed to occur. After all, in homogeneous and isotropic sediments main LGD is expected to take place close to the shoreline with an exponential decrease of exchange rates with increasing distance to the shore (McBride and Pfannkuch 1975; Pfannkuch and Winter 1984). This results from upward bending of groundwater flow lines towards the breaking point of the water table and the lake surface (Winter 1999, Fig. 1.3a).

.

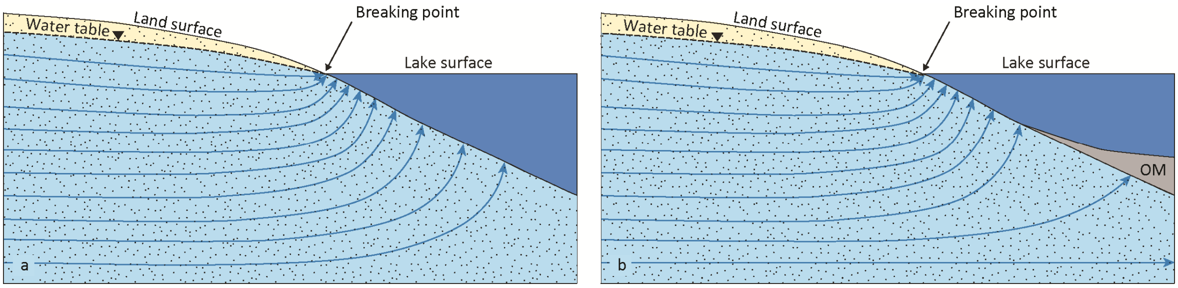

Figure 1.3 Focusing of groundwater flow (blue arrows) under exfiltrating conditions without (a) and with (b) an organic matter layer (OM) (modified from Winter et al. 1998).

Additionally, the deposition of fine organic material of low hydraulic conductivity on the lake bottom in deeper zones is assumed to cause clogging which inhibits groundwater exfiltration in the deeper parts of lakes (Krabbenhoft et al. 1990, Fig. 1.3).

Shoreline-focused LGD is advantageous regarding investigation efforts since measurements can be conducted from the shore or at least in shallow water depths. However, groundwater may also reach the lake in further distance from the shore, for example when coarse sediments surrounded by low permeable sediments serve as a preferential flow path into the lake (Krabbenhoft and Anderson 1986, Fig. 1.4). Furthermore, the focus of LGD to near-shore areas is decreased with increasing anisotropy (Genereux and Bandopadhyay 2001; Pfannkuch and Winter 1984)

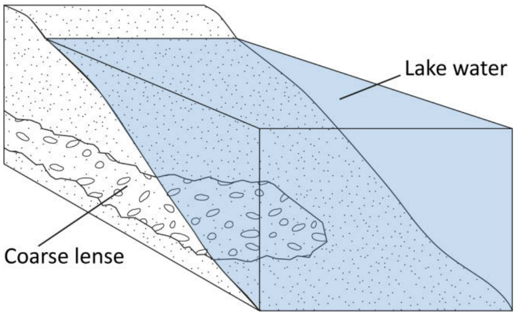

Figure 1.4. Schematic drawing of a coarse lens intersecting the lake bed and serving as a preferential flow path for lacustrine groundwater discharge (modified from Krabbenhoft and Anderson 1986).

The above-mentioned aspects only roughly describe the complex physical processes impacting on groundwater-lake interactions. In-depth view on the large variety of processes and factors impacting on groundwater-surface water interactions is given in Winter (1999) and in Chapter 2.1.

1.3 Approaches for quantification of LGD and LGD-derived nutrients

Point measurement techniques for LGD

Mass loads are typically obtained from multiplying LGD volume by parameter concentration. The determination of both terms is challenging. The diffuse inflow of LGD over large areas is hardly directly measurable. Point measurement techniques allow the determination of local LGD fluxes. The most traditional approach is the application of Darcy´s law:

$$\frac{Q}{A} = v_f = \frac{\Delta h}{L} \cdot k_{sat} \qquad \text{(Eq. 1.1)}$$

with

Q = groundwater or LGD flux, e.g., m^3 day^{-1}
A = area being crossed by groundwater or LGD flux, e.g., m^2
v_f = Darcy velocity (groundwater or LGD flow velocity), e.g., m day^{-1}
Δh = height difference between groundwater and lake water, e.g., m
l = distance/length between groundwater level measurement point and lake, e.g., m
k_{sat} = hydraulic conductivity, e.g., m day^{-1}

The sign of the hydraulic gradient $\frac{\Delta h}{L}$ between the lake level and the groundwater table indicates in- or exfiltrating conditions; the absolute value indicates the intensity (Fig. 1.2). The hydraulic conductivity (k_{sat}) of the sediment allows calculating flow velocities which can be transformed to fluxes for an area A in which an exchange between groundwater and lake takes place. Hydraulic gradients occur in two dimensions: The horizontal hydraulic gradient is the gradient between lake level and aquifer while the vertical hydraulic gradient is the gradient between lake and pore water in the sediment. Both can be relatively easily determined from water level measurements. In contrast to that, the determination of a representative k_{sat} is more difficult due to the large heterogeneity of sediment and aquifer properties on small and medium scales. Approaches and methods as well as further details about the application of hydraulic gradients and Darcy´s law can be found in Annex I (in German).

Other techniques for point measurements of LGD take advantage of the seasonal temperature differences between groundwater and surface water. The intensity of advective transport of groundwater into a lake is represented in vertical temperature distributions in the sediment. Profiles of lake sediment temperatures can be applied for an analytical solution of the heat-transport-equation, which is solved by adjusting the Darcy velocity in order to fit a modelled to the measured profile (Schmidt et al. 2006). This approach is described in more detail in Chapters 2.1 and 3.1. Furthermore, time series of sediment temperature profiles can be used to calculate LGD fluxes (Hatch et al. 2006). They depict diurnal temperature signals due to atmospheric temperature differences. The degree of dampening of such signals with increasing sediment depth is a function of the advective heat transport (Fig. 1.5). This applies also for phase shifts of temperature amplitudes in different sediment depths. Software tools such as VFLUX process time series of sediment temperatures to obtain LGD fluxes (Gordon et al. 2012; Irvine et al. 2015).

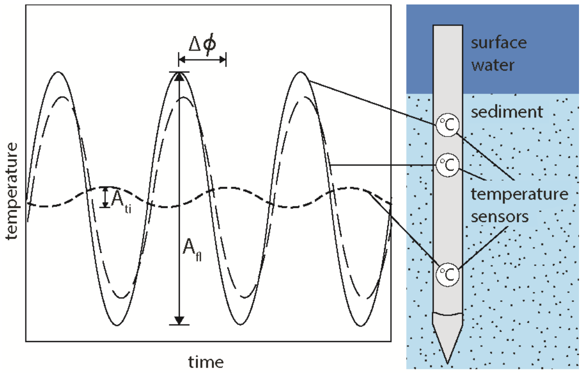

Figure 1.5 Shifting and dampening of temperature amplitudes in the sediment (modified from Hatch et al. 2006).

Seepage meters allow collecting the exfiltrating water and by that represent the only method to directly measure LGD rates. They consist of cylindrical vessels which are closed at the top and open at the bottom end. With the open end they are deployed in the lake sediment. Water exfiltrating within the enclosed area is collected by an attached plastic bag. Volume determination is done by detaching and weighing the bag. The method has been widely used and improved during the last decades (Rosenberry and LaBaugh 2008). Connecting several seepage meters to one bag integrates small scale heterogeneities of seepage rates (Fig. 1.6). A detailed description of this method can be found in Annex I (in German).

Groundwater recharge calculations for the subsurface catchment are another method to determine the overall LGD quantity. In the long run the amount of groundwater recharged in a lake catchment equals the amount of groundwater discharged to the lake. This integrating approach, in contrast to point measurements, does not deliver any spatial information about LGD distribution.

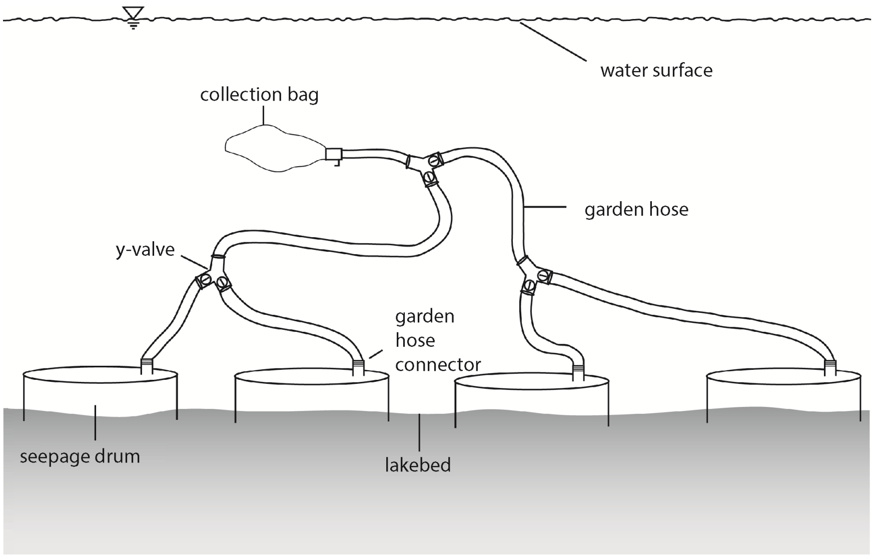

Figure 1.6 Scheme of several seepage meters connected to a single collection bag to integrate local heterogeneity of LGD rates (modified from Rosenberry 2005).

LGD pattern identification

On the local scale spatial heterogeneity of LGD can be identified by point measurements while large scale approaches deliver valuable quantitative information about overall LGD without providing distinct spatial information. However, some techniques such as fiber-optic temperature sensing also allow identifying spatial patterns of LGD on larger scales. They can be applied to localize sites of intense LGD prior to detailed investigations. Quantitative investigations of groundwater-surface water interactions are more effective when they can be directly guided to study sites where main or representative LGD occurs. Again, temperature differences between groundwater and surface water are widely used for such pattern identification. In this context, fiber-optic distributed temperature sensing (FO-DTS) has become very popular within the last years. The setup basically consists of a fiber-optic cable which is deployed on the lake bottom or into the lake sediment as a linear temperature sensor. Laser pulses sent into the cable result in different backscatter signals (Raman and Brillouin Scattering). Both types of scatterings partly depend on the temperature of the fiber (Anti-Stokes component). By that, temperatures along the fiber represent temperatures of the sediments the fiber is deployed on/in (Selker et al. 2006). Local deviations from the general temperature signal indicate the inflow of warmer or colder groundwater. By that hot spots of LGD can be identified over large ranges since cables can be 10 km long or longer. With a spatial resolution up to only a few decimeters even small scale variations of LGD can be depicted. By this the approach has the potential to identify local spatial LGD patterns for large areas (Day-Lewis et al. 2006; Fleckenstein et al. 2010; Selker et al. 2006). When applying this method it should be considered that predominantly diffuse and areal LGD fluxes may not develop distinguished temperature signals. Furthermore, no quantitative information can be gained from applying FO-DTS alone. Nevertheless, the above-mentioned endeavors certainly focus on FO-DTS as a means of upscaling point measurements to large scales (see Chapter 4.2).

Measuring nutrient concentrations in LGD

Spatial heterogeneity is often the limiting factor for representative values of parameter concentrations in groundwater and LGD. Nutrient and pollutant concentrations may be modified by a variety of processes (e.g., sorption or degradation) during their transport towards a lake. Especially the passage of the reactive interface in the lake sediment which might underlie a strong redox-gradient is expected to influence the eventual concentrations of LGD (e.g., Dean et al. 2003; Frape and Patterson 1981; LaBaugh et al. 1997; Schuster et al. 2003). For example, concentrations of some redox-sensitive species might decrease due to precipitation where redox potentials become more positive within the interface. This might imply to measure concentrations as closely as possible to the interface. However, it should be considered that lake-internal processes may also influence pore water concentrations at the interface. Organic matter from the water column deposited at the lake bottom may induce increased microbiological activity at the reactive interface resulting in an additional release of nutrients or in-/decreasing sorption rates due to changes in the redox conditions. Concentrations of pore water close to or directly at the interface may thus not represent original LGD concentrations (Chapter 3.2). The optimal approach to determine LGD concentrations depends on the underlying research question and is a matter of case-individual decisions.

Multiple techniques are available for these purposes, as there are for example multi-level samplers (Rivett et al. 2008), seepage meters (Rosenberry and LaBaugh 2008), or dialysis samplers (Schuster et al. 2003; Vroblesky et al. 2002). The installation of (temporal) piezometers and different types of suction probes enables an active sampling of pore water or near-shore, near-surface groundwater when applying a vacuum. In contrast to this, dialysis samplers do not require any pressure to sample water. They consist of a rectangular acrylic plate into which small chambers with a volume of several cm^3 are embedded. These are filled with distilled water. The plate is covered by a semi-permeable membrane allowing the parameters of interest to pass. The samplers are placed in the sediment and after an equilibrium-time of about two weeks the concentrations of the surrounding pore water have established in the chambers by diffusion. The plates are removed and the water in the chambers can be analyzed. Dialysis samplers provide vertical concentration profiles with high spatial resolution covering the processes potentially induced by the reactive interface. In contrast to them, piezometers and other suction-based devices usually sample pore water from only a single depth. This shortcoming can be overcome by installing multiple devices in different depths (Rivett et al. 2008). Furthermore, seepage meters have been introduced above as a method to quantify LGD by directly sampling the exfiltrating water. The collected water can be analyzed for nutrients and other parameters. However, insufficient flushing of the seepage meter by exfiltrating water prior to sampling or reducing conditions in the vessel due to the absence of exchange with the surrounding overlying water might result in false values for pore water concentrations.

While piezometers can be applied to both, terrestrial (i.e., near-shore or aquifer) and lake sediments seepage meters and passive samplers are installed off-shore only. Both approaches (near-shore and off-shore) have advantages and disadvantages. Near-shore groundwater sampling is usually easier (no waves, low water table depths). However, on-shore investigations do not necessarily capture the actual constitution of the groundwater eventually exfiltrating into the lake water. The above-mentioned redox-dependent processes at the lake-sediment interface may alter the LGD quality just shortly before entering the lake by either retention or further release of nutrients. Hence, exclusively relying on near-shore groundwater quality might carry the risk of over- or underestimating the potential contribution of LGD to a lake mass balance. On the other hand, results from off-shore methods to sample LGD might also reflect lake-internal processes such as organic matter deposited from the water column and mineralized in the lake sediment. A quantitative separation of external and internal nutrient loads from lake sediments becomes very difficult when no further investigations (e.g., sediment trap analysis) or measures (areal covering of lake bed to exclude sediment deposition from the lake water) are conducted. Eventually, the decision for one or the other approach and method to investigate LGD quality should be made individually depending on the research question and the state of knowledge about the system.

The above-mentioned methods to determine LGD and parameter concentrations of LGD are representative for a number of other (partly similar) approaches. All common methods in the field of groundwater-surface water interactions are introduced in Annex I (in German). This work provides advantages and shortcomings as well as practical advices for the application of each of the introduced methods. Additionally, methods to determine LGD patterns and fluxes are also described in Chapter 2.1, while Chapter 2.2 contains further information on how to gain representative parameter concentrations in LGD.

1.4 Major study site Lake Arendsee

Lake Arendsee is a deep dimictic lake in the Federal State of Saxony-Anhalt in Northern Germany. It originates from several collapses of a subsurface salt dome. Its morphometry is characterized by an abrupt decrease of lake depth in few decameters distance to the shore. The medium depth of the lake is 29 m, the maximum depth is 49 m. Together with a relatively large volume of 147 Mm^3 the water residence time results in 50 to 60 years.

From investigations of fossil and living meiobenthic communities in sediment cores, Scharf (1998) inferred that the trophic state of the lake changed dramatically from mesotrophic to eutrophic between 1960 and 1972. The average lake volume TP-concentration between 2005 and 2014 was 184 ± 7 µg l^{-1} (n = 10, Hupfer et al. 2016, see also Fig. 1.7), exceeding the limit to hypertrophy. Repeated harmful cyanobacteria blooms (*Planktothrix rubescens*, DC. Ex Gomont; *Anabaena flos-aquae*, Bory de St.-Vincent; *Aphanizomenon flos-aquae*, L.; Hupfer et al. 2016) repeatedly forced local authorities to temporally prohibit recreational activities in the lake.

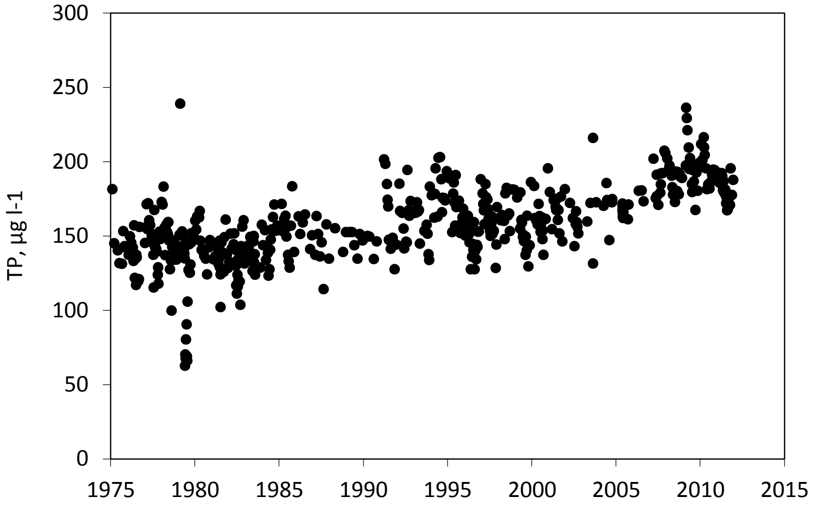

Figure 1.7 Time series of concentrations of total phosphorus (TP) in the pelagic water of Lake Arendsee.

Direct discharge of municipal, domestic, and industrial wastewaters, the intensification of agriculture in the watershed as well as fishery in the lake have been held responsible for eutrophication of Lake Arendsee. Additionally, waterfowl resting in large numbers on the lake during migration periods were discussed to contribute to the poor trophic conditions. Wastewater-derived P loads ceased largely in the 1970s when a wastewater treatment plant was built outside of the lake catchment. Nevertheless, the trophic state of the lake did not improve indicating that the major nutrient source has not been identified and eliminated yet. An effective and sustainable restoration of Lake Arendsee seems to be only possible by a combination of P elimination in the pelagic water (internal measure) with a significant reduction of external P loads (external measure, Hupfer et al. 2016).

To evaluate the impact of a single P source precise water and P budgets are required. LGD is assumed to be a major term in the water balance of the lake. Additionally, four surface inlets draining agricultural areas in the lake catchment contribute to both, water and nutrient budgets of the lake. The present work was embedded in intense investigations of the P budget of Lake Arendsee. These investigations aimed at an eventual identification of the so far unknown driver of eutrophication of Lake Arendsee.

1.5 Objectives and hypothesis of the Ph.D. study

Based on the background described in Chapter 1.4 intense investigations were initiated at Lake Arendsee which focused on the setup of precise and detailed water and nutrient budgets. As a part of this effort the two main studies presented in Chapter 3 aim at the determination of groundwater-borne P loads entering Lake Arendsee. Pre-investigations indicate that none of the common input paths (e.g., agricultural drainage discharges) explains the high P concentrations in the lake. So far, LGD has not been taken into account as a relevant P source to Lake Arendsee. However, based on studies indicating that P might be transported with the groundwater in larger concentrations than previously thought (Holman et al. 2008; Roy and Bickerton 2014) it is hypothesized that groundwater-borne P loads are mainly driving eutrophication of Lake Arendsee. The resultant research activities address the following questions:

- Where does LGD occur?
- How much LGD enters the lake?
- How much P reaches the lake via LGD?
- Do LGD-derived P loads have a significant influence on the trophic state of Lake Arendsee?
- If yes, is it due to natural conditions or are anthropogenic contaminations causing increased pelagic P concentrations?
- In the case of a contamination: Are there site-specific conditions/factors regarding LGD favoring or dampening the effect of the contamination?
- Which methods/approaches tackle the above-mentioned questions best?

Considering the difficulties reported in above chapters the importance of choosing appropriate methods in order to answer these questions becomes evident. An intense literature review about the state of knowledge on LGD and related measuring techniques resulted in a review paper which served as a basis for the studies at Lake Arendsee (Chapter 2.1). As a follow up-review, Chapter 2.2 addresses general aspects as well as examples of nutrient and contaminant transport to lakes via LGD. Based on these reviews and the background described in Chapter 1.4, the following overarching hypotheses were developed for the case study of Lake Arendsee:

1) P concentrations in LGD are increased above natural background concentrations. As a result LGD is a major input path for P and by that significantly contributes to eutrophication of Lake Arendsee.

The hypothesis is based on the assumption that an intense and long-lasting P source caused a severe groundwater contamination in the catchment of Lake Arendsee. This is the core topic of Chapter 3.

2) P concentrations are significantly increased in the catchment of Lake Arendsee and spatially highly resolved groundwater sampling allows localizing the contamination site.

Identifying location and source of the groundwater contamination might allow applying sustainable measures to mitigate eutrophication of the lake. A maximum of spatial information on groundwater quality in the catchment helps tracking a contamination to its origin. Chapter 3.2 describes how this hypothesis is handled.

3) Spatial heterogeneity of both, LGD volume and P concentrations in the near-shore groundwater, influence the magnitude of groundwater-borne P loads.

A lot of factors influence if and to what extent groundwater contaminations reach freshwaters. E.g., varying hydrogeological conditions impose spatial heterogeneity of local LGD rates and contribute to the propagation of contaminant plumes. A segmented approach captures the spatial heterogeneity of LGD-derived P loads: P loads are determined individually for single shore sections and summed up. The topic of spatial heterogeneity is discussed in Chapter 3.1 for LGD volumes, and in Chapter 3.2 for P concentrations.

1.6 Outline

Chapter 2 - State of knowledge on groundwater-lake interactions

This chapter includes a two-part review titled “Groundwater – the disregarded component in lake water and nutrient budgets.” The first part (“Effects of groundwater on hydrology”) illuminates why LGD has often been neglected in lake water budgets although it is often a relevant proportion in lake hydrology. Characteristics of LGD flow and factors driving and controlling it are described alongside a comprehensive comparison of LGD fluxes reported in the international literature. Furthermore, methods and techniques for qualitative (pattern identification) and quantitative measurements of LGD are introduced.

The second part (“Effects of groundwater on nutrients”) deals with biogeochemical processes related to LGD and resulting impacts on lake nutrient budgets. The pathways of groundwater exfiltration from the catchment to the open water are described and compared to river and marine systems. Reasons for the importance of LGD in lake nutrient budgets are identified such as the fact that small LGD volumes can carry high nutrient loads if concentrations are high. In this context, a special focus is on P as a major factor driving lake eutrophication. Since P has long been considered immobile in groundwater (Chapter 1.1) LGD has not been taken into account as a cause of eutrophication. However, recent studies reporting increased P concentrations in groundwater indicate a major importance of LGD-derived P loads. Furthermore, the complex biogeochemical reactions potentially taking place at the reactive interface between groundwater and lake complicate the determination of actual P concentrations in LGD. Besides P also the fate of N in LGD is discussed in detail. An overview on P and N loads from groundwater to lakes is presented based on data published in the international literature. Also in this part of the review, methods and techniques to measure LGD nutrient concentrations are introduced.

Chapter 3 - The case study of Lake Arendsee

In order to quantify LGD-derived P loads information on LGD volumes and P concentrations is needed. In sub-chapter 3.1 (“Lacustrine groundwater discharge: Combined determination of volumes and spatial patterns”) the total annual LGD volume for Lake Arendsee is determined by calculating groundwater recharge in the subsurface catchment. As a prerequisite for this the subsurface catchment is delimited based on groundwater head contour lines. To account for spatial patterns of LGD fluxes along the lake shore local LGD fluxes are derived from temperature profiles of the lake sediment. The sediment temperatures reflect the intensity of the LGD flux and can be applied to solve the heat conduction-advection equation for the vertical Darcy flow in a 1-D approach. The results of the two approaches are combined to calculate quantitative values of LGD fluxes for single shore sections. Based on these data and on some limited information on near-shore groundwater quality LGD-derived P loads are calculated.

In the second sub-chapter ("Phosphorus in groundwater discharge – a potential source for lake eutrophication") the information on near-shore groundwater is extended by sampling near-surface groundwater from temporal piezometers in a high spatial resolution along the shore. P concentrations are increased up to 4 mg l^{-1} in a shoreline section of about 2 km length. These data are combined with the shore sections defined by LGD flux measurements in Chapter 3.1 in order to refine the accuracy of LGD-derived P load calculations. The influence of LGD is evaluated by comparing groundwater P loads to other external P loads such as surface inflows, and atmospheric deposition. It turns out that LGD contributes more than 50% to the overall external P load of Lake Arendsee and by that fuels eutrophication of the lake. Despite intense investigations of the groundwater quality in the lake´s catchment the sources for the contamination of the groundwater with P could not be identified.

Chapter 4 - Development and improvement of approaches to determine lacustrine groundwater discharge

When working on LGD it quickly becomes obvious that many of the available approaches and techniques are not yet fully developed. Continuous development and improvement of techniques are required to increase the reliability of results of LGD-related research. In Chapter 4 three side-projects are introduced which address different aspects of method development.

Chapter 4.1 ("Empirical quantification of lacustrine groundwater discharge – different methods and their limitations") leads back to Lake Arendsee. Two sub-studies represent the ups and downs of every day LGD research by comparing the results of a) different methods and b) different measurement dates. The transition between in- and exfiltration zones along the shore is located where the boundary of the subsurface catchment meets the lake. The shape of the subsurface catchment has been assessed from groundwater head contour lines (Chapter 3.1). In order to validate the location of the transition of exfiltration to infiltration zones near-shore groundwater is sampled to determine the stable isotope composition. Stable isotopes in groundwater originating from precipitation differ substantially from those in surface water that experienced evaporation. Stable isotopes of groundwater samples originating from infiltrated surface water are thus expected to show compositions similar to surface water while in exfiltration zones the signal of precipitation dominates. The results confirm the transition from in- to exfiltration zones determined based on contour lines. While in this example a completely different approach leads to a very good agreement with previous results, results of a repeated application of the same method do not correspond as expected: Repeated temperature measurements of the lake sediment which are used to calculate local LGD fluxes (Chapter 3.1) show different results at some locations. Reasons for this might result from small-scale spatial and/or seasonal impacts on LGD.

Chapter 4.2 ("Upscaling lacustrine groundwater discharge rates by fiber-optic distributed temperature sensing") develops and tests an approach of upscaling point measurements. FO-DTS is used to upscale LGD rates with a transfer function based on point measurements of different methods (vertical hydraulic gradients or temperature depth profiles). Both FO-DTS-based upscaling approaches are able to reproduce the distinct small-scale heterogeneities in LGD patterns and quantities that are observed in an extensive reference survey using LGD estimates based on sediment temperature profiles. An exponential function describing the decrease of LGD fluxes with increasing distance to the shore performs less well.

In Chapter 4.3 ("Localization of lacustrine groundwater discharge (LGD) by airborne measurement of thermal infrared radiation"), a novel approach for the localization of LGD by thermal infrared

(TIR) is presented. Aviation-derived TIR pictures reveal a plume of warmer surface water along the southern shore of Lake Arendsee. This area corresponds to results in Chapter 3.1 where LGD flux measurements have indicated main groundwater discharge along the southern shoreline.

Chapters 5 to 7

Chapter 5 discusses the results of the two core studies at Lake Arendsee (Chapter 3). Outcomes of the studies presented in Chapter 4 are discussed in **Chapter 6**. **Chapter 7** generates conclusions from results and discussions of this work.

Please note that as a result of the cumulative nature of this thesis, references are provided at the end of every chapter.

1.7 References

Ansari, A.A., Gill, S.S., Khan, F.A., 2011. Eutrophication: Threat to Aquatic Ecosystems. In: *Eutrophication: causes, consequences and control*, Ansari, A.A., Gill, S.S., Lanza, G.R., Rast, W. (Eds.). Springer, Netherlands, 143-170.

Brönmark, C., Hansson, L.A., 2002. Environmental issues in lakes and ponds: current state and perspectives. *Environmental Conservation*, 29(3): 290-307.

Carpenter, S.R., Caraco, N.F., Correll, D.L., Howarth, R.W., Sharpley, A.N., Smith, V.H., 1998. Nonpoint pollution of surface waters with phosphorus and nitrogen. *Ecological Applications*, 8(3): 559-568.

Cassidy, R., Jordan, P., 2011. Limitations of instantaneous water quality sampling in surface-water catchments: Comparison with near-continuous phosphorus time-series data. *Journal of Hydrology*, 405(1–2): 182-193.

Correll, D.L., 1998. The role of phosphorus in the eutrophication of receiving waters: A review. *Journal of Environmental Quality*, 27(2): 261-266.

Day-Lewis, F.D., White, E.A., Johnson, C.D., Jr., J.W.L., Belaval, M., 2006. Continuous resistivity profiling to delineate submarine groundwater discharge—examples and limitations. *The Leading Edge*, 25(6): 724-728.

Dean, W.E., Neff, B.P., Rosenberry, D.O., Winter, T.C., Parkhurst, R., 2003. The Significance of Ground Water to the Accumulation of Iron and Manganese in the Sediments of Two Hydrologically Distinct Lakes in North-Central Minnesota: A Geological Perspective. *Ground Water*, 41(7): 951-963.

Dodds, W.K., Bouska, W.W., Eitzmann, J.L., Pilger, T.J., Pitts, K.L., Riley, A.J., Schloesser, J.T., Thornbrugh, D.J., 2009. Eutrophication of US Freshwaters: Analysis of Potential Economic Damages. *Environmental Science & Technology*, 43(1): 12-19.

Driescher, E., Gelbrecht, J., 1993. Assessing the Diffuse Phosphorus Input from Subsurface to Surface Waters in the Catchment-Area of the Lower River Spree (Germany). *Water Science and Technology*, 28(3-5): 337-347.

Fleckenstein, J.H., Krause, S., Hannah, D.M., Boano, F., 2010. Groundwater-surface water interactions: New methods and models to improve understanding of processes and dynamics. *Advances in Water Resources*, 33(11): 1291-1295.

Frape, S.K., Patterson, R.J., 1981. Chemistry of Interstitial Water and Bottom Sediments as Indicators of Seepage Patterns in Perch Lake, Chalk-River, Ontario. *Limnology and Oceanography*, 26(3): 500-517.

Genereux, D., Bandopadhyay, I., 2001. Numerical investigation of lake bed seepage patterns: effects of porous medium and lake properties. *Journal of Hydrology*, 241(3–4): 286-303.

Gordon, R.P., Lautz, L.K., Briggs, M.A., McKenzie, J.M., 2012. Automated calculation of vertical pore-water flux from field temperature time series using the VFLUX method and computer program. *Journal of Hydrology*, 420–421: 142-158.

Harman, J., Robertson, W.D., Cherry, J.A., Zanini, L., 1996. Impacts on a sand aquifer from an old septic system: Nitrate and phosphate. *Ground Water*, 34(6): 1105-1114.

Hatch, C.E., Fisher, A.T., Revenaugh, J.S., Constantz, J., Ruehl, C., 2006. Quantifying surface water-groundwater interactions using time series analysis of streambed thermal records: Method development. *Water Resources Research*, 42(10).

Heathwaite, A.L., Burke, S.P., Bolton, L., 2006. Field drains as a route of rapid nutrient export from agricultural land receiving biosolids. *Science of The Total Environment*, 365(1–3): 33-46.

Holman, I.P., Whelan, M.J., Howden, N.J.K., Bellamy, P.H., Willby, N.J., Rivas-Casado, M., McConvey, P., 2008. Phosphorus in groundwater-an overlooked contributor to eutrophication? *Hydrological Processes*, 22(26): 5121-5127.

Hupfer, M., Reitzel, K., Kleeberg, A., Lewandowski, J., 2016. Long-term efficiency of lake restoration by chemical phosphorus precipitation: Scenario analysis with a phosphorus balance model. *Water Research*, 97: 153-161.

Irvine, D.J., Lautz, L.K., Briggs, M.A., Gordon, R.P., McKenzie, J.M., 2015. Experimental evaluation of the applicability of phase, amplitude, and combined methods to determine water flux and thermal diffusivity from temperature time series using VFLUX 2. *Journal of Hydrology*, 531, Part 3: 728-737.

Jordan, P., Arnscheidt, J., McGrogan, H., McCormick, S., 2005. High-resolution phosphorus transfers at the catchment scale: the hidden importance of non-storm transfers. *Hydrology and Earth System Sciences*, 9(6): 685-691.

Khan, M.N., Mohammad, F., 2014. Eutrophication: Challenges and Solutions. In: *Eutrophication: Causes, consequences and control*, Ansari, A.A., Gill, S.S. (Eds.). Springer, Netherlands, 1-14.

Kilroy, G., Coxon, C., 2005. Temporal variability of phosphorus fractions in Irish karst springs. *Environmental Geology*, 47(3): 421-430.

Krabbenhoft, D.P., Anderson, M.P., 1986. Use of a numerical groundwater-flow model for hypothesis-testing. *Ground Water*, 24(1): 49-55.

Krabbenhoft, D.P., Anderson, M.P., Bowser, C.J., 1990. Estimating groundwater exchange with lakes: 2. Calibration of a three-dimensional, solute transport model to a stable isotope plume. *Water Resources Research*, 26(10): 2455-2462.

LaBaugh, J.W., Rosenberry, D.O., Winter, T.C., 1995. Groundwater contribution to the water and chemical budgets of Williams Lake, Minnesota, 1980-1991. *Canadian Journal of Fisheries and Aquatic Sciences*, 52(4): 754-767.

LaBaugh, J.W., Winter, T.C., Rosenberry, D.O., Schuster, P.F., Reddy, M.M., Aiken, G.R., 1997. Hydrological and chemical estimates of the water balance of a closed-basin lake in north central Minnesota. *Water Resources Research*, 33(12): 2799-2812.

Lee, T.M., 1996. Hydrogeologic controls on the groundwater interactions with an acidic lake in karst terrain, Lake Barco, Florida. *Water Resources Research*, 32(4): 831-844.

McBride, M.S., Pfannkuch, H.O., 1975. Distribution of seepage within lakebeds. *Journal of Research of the U.S. Geological Survey*, 3(5): 505-512.

McCobb, T.D., LeBlanc, D.R., Walter, D.A., Hess, K.M., Kent, D.B., Smith, R.L., 2003. Phosphorus in a ground-water contaminant plume discharging to Ashumet Pond, Cape Cod, Massachusetts, 1999. *U.S. Geological Survey Water Resources Investigations Report* 02-4306: 70 p.

Orderud, G.I., Vogt, R.D., 2013. Trans-disciplinarity required in understanding, predicting and dealing with water eutrophication. *International Journal of Sustainable Development and World Ecology*, 20(5): 404-415.

Palmer-Felgate, E.J., Mortimer, R.J.G., Krom, M.D., Jarvie, H.P., 2010. Impact of Point-Source Pollution on Phosphorus and Nitrogen Cycling in Stream-Bed Sediments. *Environmental Science & Technology*, 44(3): 908-914.

Pfannkuch, H.O., Winter, T.C., 1984. Effect of anisotropy and groundwater system geometry on seepage through lakebeds: 1. Analog and dimensional analysis. *Journal of Hydrology*, 75(1–4): 213-237.

Ptacek, C.J., 1998. Geochemistry of a septic-system plume in a coastal barrier bar, Point Pelee, Ontario, Canada. *Journal of Contaminant Hydrology*, 33(3-4): 293-312.

Rivett, M.O., Ellis, R., Greswell, R.B., Ward, R.S., Roche, R.S., Cleverly, M.G., Walker, C., Conran, D., Fitzgerald, P.J., Willcox, T., Dowle, J., 2008. Cost-effective mini drive-point piezometers and multilevel samplers for monitoring the hyporheic zone. *Quarterly Journal of Engineering Geology and Hydrogeology*, 41: 49-60.

Robertson, W.D., 2003. Enhanced attenuation of septic system phosphate in noncalcareous sediments. *Ground Water*, 41(1): 48-56.

Rosenberry, D.O., LaBaugh, J.W., 2008. Field Techniques for Estimating Water Fluxes Between Surface Water and Ground Water. *U.S. Geological Survey Techniques and Methods* 4-D2: 128 p.

Roy, J.W., Bickerton, G., 2014. Elevated Dissolved Phosphorus in Riparian Groundwater along Gaining Urban Streams. *Environmental Science & Technology*, 48(3): 1492-1498.

Roy, J.W., Malenica, A., 2013. Nutrients and toxic contaminants in shallow groundwater along Lake Simcoe urban shorelines. *Inland Waters*, 3(2): 125-138.

Roy, J.W., Robillard, J.M., Watson, S.B., Hayashi, M., 2009. Non-intrusive characterization methods for wastewater-affected groundwater plumes discharging to an alpine lake. *Environmental Monitoring and Assessment*, 149(1-4): 201-211.

Scharf, B.W., 1998. Eutrophication history of lake Arendsee (Germany). *Palaeogeography Palaeoclimatology Palaeoecology*, 140(1-4): 85-96.

Schindler, D.W., 2012. The dilemma of controlling cultural eutrophication of lakes. *Proceedings of the Royal Society B: Biological Sciences*, 279(1746): 4322-4333.

Schmidt, C., Bayer-Raich, M., Schirmer, M., 2006. Characterization of spatial heterogeneity of groundwater-stream water interactions using multiple depth streambed temperature measurements at the reach scale. *Hydrology and Earth System Sciences*, 10(6): 849-859.

Schuster, P.F., Reddy, M.M., LaBaugh, J.W., Parkhurst, R.S., Rosenberry, D.O., Winter, T.C., Antweiler, R.C., Dean, W.E., 2003. Characterization of lake water and ground water movement in the littoral zone of Williams Lake, a closed-basin lake in north central Minnesota. *Hydrological Processes*, 17(4): 823-838.

Selker, J.S., Thevenaz, L., Huwald, H., Mallet, A., Luxemburg, W., de Giesen, N.v., Stejskal, M., Zeman, J., Westhoff, M., Parlange, M.B., 2006. Distributed fiber-optic temperature sensing for hydrologic systems. *Water Resources Research*, 42(12): W12202.

Sharpley, A., Wang, X., 2014. Managing agricultural phosphorus for water quality: Lessons from the USA and China. *Journal of Environmental Sciences*, 26(9): 1770-1782.

Sharpley, A.N., Krogstad, T., Kleinman, P.J.A., Haggard, B., Shigaki, F., Saporito, L.S., 2007. Managing natural processes in drainage ditches for nonpoint source phosphorus control. *Journal of Soil and Water Conservation*, 62(4): 197-206.

Shaw, R.D., Shaw, J.F.H., Fricker, H., Prepas, E.E., 1990. An integrated approach to quantify groundwater transport of phosphorus to Narrow Lake, Alberta. *Limnology and Oceanography*, 35(4): 870-886.

Simard, R.R., Beauchemin, S., Haygarth, P.M., 2000. Potential for preferential pathways of phosphorus transport. *Journal of Environmental Quality*, 29(1): 97-105.

Smith, V.H., 2003. Eutrophication of freshwater and coastal marine ecosystems a global problem. *Environmental Science and Pollution Research*, 10(2): 126-139.

Smith, V.H., Schindler, D.W., 2009. Eutrophication science: where do we go from here? *Trends in Ecology & Evolution*, 24(4): 201-207.

Tiemeyer, B., Kahle, P., Lennartz, B., 2009. Phosphorus losses from an artificially drained rural lowland catchment in North-Eastern Germany. *Agricultural Water Management*, 96(4): 677-690.

Vanek, V., 1993. Transport of groundwater-borne phosphorus to Lake Bysjon, South Sweden. *Hydrobiologia*, 251(1-3): 211-216.

Vroblesky, D.A., D. Petkewich, M.D., Ted R. Campbell, T.R., 2002. Field Tests of Diffusion Samplers for Inorganic Constituents in Wells and at a Ground-Water-Discharge Zone. *U.S. Geological Survey Water-Resources Investigations Report* 02-4031: 31 p.

Wetzel, R.G., 2001. *Limnology: Lake and River Ecosystems.* Academic Press, San Diego, 1006 p.

Winter, T.C., 1999. Relation of streams, lakes, and wetlands to groundwater flow systems. *Hydrogeology Journal*, 7(1): 28-45.

Winter, T.C., Harvey, J.W., Franke, O.L., Alley, W.M., 1998. Ground Water and Surface Water - A Single Resource. *U.S. Geological Survey Circular* 1139: 79 p.

Withers, P.J.A., Haygarth, P.M., 2007. Agriculture, phosphorus and eutrophication: a European perspective. *Soil Use and Management*, 23: 1-4.

Wolf, L., Zwiener, C., Zemann, M., 2012. Tracking artificial sweeteners and pharmaceuticals introduced into urban groundwater by leaking sewer networks. *Science of The Total Environment*, 430: 8-19.

2 State of knowledge on groundwater-lake interactions

2.1 Groundwater – the disregarded component in lake water and nutrient budgets. Part 1: Effects of groundwater on hydrology

Donald O. Rosenberry[1] Jörg Lewandowski[2,3], Karin Meinikmann[2,3] and Gunnar Nützmann[2,3]

[1] US Geological Survey, Denver Federal Center, USA

[2] Department of Ecohydrology, Leibniz-Institute of Freshwater Ecology and Inland Fisheries, Berlin, Germany

[3] Department of Geography, Humboldt-Universität zu Berlin, Berlin, Germany

This is the peer reviewed version of the following article:
Rosenberry, D.O., Lewandowski, J., Meinikmann, K., Nützmann, G., 2015. Groundwater - the disregarded component in lake water and nutrient budgets. Part 1: Effects of groundwater on hydrology. *Hydrological Processes*, 29(13): 2895-2921.

Abstract

Lake eutrophication is a large and growing problem in many parts of the world, commonly due to anthropogenic sources of nutrients. Improved quantification of nutrient inputs is required to address this problem, including better determination of exchanges between groundwater and lakes. This first of a two-part review provides a brief history of the evolution of the study of groundwater exchange with lakes, followed by a listing of the most commonly used methods for quantifying this exchange. Rates of exchange between lakes and groundwater compiled from the literature are statistically summarized for both exfiltration (flow from groundwater to a lake) and infiltration (flow from a lake to groundwater), including per cent contribution of groundwater to lake-water budgets. Reported rates of exchange between groundwater and lakes span more than five orders of magnitude. Median exfiltration is 0.74 cm day^{-1}, and median infiltration is 0.60 cm day^{-1}. Exfiltration ranges from near 0% to 94% of input terms in lake-water budgets, and infiltration ranges from near 0% to 91% of loss terms. Median values for exfiltration and infiltration as percentages of input and loss terms of lake-water budgets are 25% and 35%, respectively. Quantification of the groundwater term is somewhat method dependent, indicating that calculating the groundwater component with multiple methods can provide a better understanding of the accuracy of estimates. The importance of exfiltration to a lake budget ranges widely for lakes less than about 100 ha in area but generally decreases with increasing lake area, particularly for lakes that exceed 100 ha in area. No such relation is evident for lakes where infiltration occurs, perhaps because of the smaller sample size.

2.1.1 Introduction

Eutrophication is one of the most important threats to lakes situated in temperate climatic zones (Brönmark and Hansson 2002; Wetzel 2001). Excess nutrients usually are to blame. Effective management for nutrient reduction in lakes requires that all water and nutrient source and loss terms be identified and quantified. An accurate water balance is a prerequisite for determining relative magnitudes of nutrient inputs. Surface inflows and outflows via streams, rivers and ditches usually can be quantified with relatively small errors. Nearby or on-site weather data often are available for obtaining precipitation and calculating evaporation. Overland flow is almost always assumed to be irrelevant, and it often is.

Quantifications of flow between groundwater and surface water are nearly always much more difficult. In some settings, groundwater contributions are small relative to other water-budget terms and can justifiably be ignored, but exchange with groundwater can be a large component of a lake-water or nutrient budget. Perhaps in part because of the difficulty of determining groundwater exchanges, groundwater has been assumed to be irrelevant for many lake-water-budget and nutrient budget studies (Rosenberry and Winter 2009). There are several reasons that this onerous term has often been neglected:

1. Groundwater exchange is far less visible (invisible except in the case of springs) compared with all other terms of a lake-water budget.
2. Rates of exchange between groundwater and lake water can be exceptionally small. However, the area over which this exchange occurs often is a large percentage of the lake-surface area, making even very small rates of exchange relevant to a lake-water budget.
3. The distribution of exchange between groundwater and a lake is heterogeneous both spatially and temporally. This can make quantification difficult and often requires multiple approaches.
4. The groundwater–lake interface can be difficult to access, particularly in deep lakes or lakes set in rocky terrain or lakes fringed with extensive wetland areas.

5. In lakes where groundwater exfiltration (defined here as flow from groundwater to a lake) and infiltration (flow from a lake to groundwater) both occur, net flow between groundwater and the lake could be small, whereas both exfiltration and infiltration are large (e.g., Kenoyer and Anderson 1989; LaBaugh et al. 1997; Sutula et al. 2001).
6. Although several new techniques have been developed in the past few decades for quantifying exchange between groundwater and surface water (reviews by Fleckenstein et al. 2010; Kalbus et al. 2006; Rosenberry and LaBaugh 2008), numerous challenges remain. In some lake settings, no suitable method exists for adequately quantifying groundwater exchange, leading to the hope, and assumption by default, that groundwater exchange is small because it cannot reasonably be quantified (e.g., Song et al. 2014).
7. Historical compartmentalization of scientific disciplines is slow to overcome. Hydrogeologists, surface water hydrologists and ecologists have long approached the interface between groundwater and surface water from different perspectives. Although groundwater and surface water are now more commonly considered as a single resource (Winter et al. 1998), lack of integration of scientific disciplines can impede progress in understanding flows and processes at the groundwater–surface water interface (Fleckenstein et al. 2010; Hayashi and Rosenberry 2002).

In spite of these assumptions, groundwater dominates some lake-water budgets. For example, groundwater represented 94% of inflows to a 14-ha lake in northern Minnesota (Stets et al. 2010) and 90% of all inputs to a 9-ha lake in Montana (Gurrieri and Furniss 2004). Groundwater infiltration also can be a large percentage of a lake-water budget, particularly for lakes that lack a surface-water outlet. Groundwater infiltration made up 91% of all loss terms at a 480-ha lake in Minnesota (Rosenberry et al. 2000) and 84% of loss terms for a lake in Florida (Grubbs 1995). Even for the very large (201 700 ha) Lake Nam Ko in the Tibetan Plateau, groundwater infiltration comprised 56–70% of loss terms (Zhou et al. 2013). Groundwater infiltration at Lake Nam Ko may have been larger yet because no data were available for groundwater exfiltration, which was assumed to be zero. Groundwater can be a large water-budget component even if there is a surface-water inlet or outlet. At a 16-ha lake in Denmark where annual streamflow to the lake was 7.5 times larger than annual precipitation, groundwater exfiltration was larger yet, comprising 66% of all inputs to the lake (Kidmose et al. 2013). At a 15-ha lake in New Hampshire where three streams enter the lake, more water left the lake via groundwater infiltration than via surface-water outflow or evaporation; groundwater infiltration averaged 51% of the loss terms in the lake water budget (Rosenberry and Winter 2009).

The importance of groundwater to a lake nutrient budget depends on both the volume of groundwater exchange and the concentration of nutrients associated with that exchange. In some settings where groundwater exfiltration is small from a water-budget perspective, it can be the largest input term from a nutrient-budget perspective (Jarosiewicz and Witek 2014; LaBaugh et al. 2000; Lewandowski et al. 2015).

This first of a two-part review presents a brief history of the study and quantification of groundwater exchange. A listing of methods for measuring this exchange is then presented, followed by a discussion of continuing challenges due primarily to heterogeneity of groundwater–lake exchange in both space and time. Rates of groundwater exchange reported from a broad survey of the literature are listed and summarized to provide an idea of rates of groundwater–lake exchange that are common or extreme. Because lakes occupy low places in the landscape, they often are thought to only receive flow from groundwater. However, a large percentage of lakes both receive water from groundwater and also lose water to groundwater. Descriptions of direction of flow can be confusing and depend on one's perspective. In both parts of this two-part paper, we describe flow from a groundwater perspective. Flow from groundwater to a lake (also known as lacustrine groundwater discharge) is termed exfiltration; flow from a lake to groundwater is termed infiltration. Percentage contributions of groundwater to lake-water budgets are also listed and summarized to demonstrate the importance of the groundwater component to lake-water budgets.

The companion paper by Lewandowski et al. (2015) presents similar information, but from a nutrient-budget perspective. Numerous reasons exist for conducting detailed water and chemical budgets, such as concerns over mercury in lakes and fish, acid deposition or too much or too little water in a lake. However, it is likely that concerns over excess nutrients exceed all others, hence the emphasis on nutrients in the companion paper. Lewandowski et al. emphasize exfiltration and the associated nutrient loading to lakes.

2.1.2 Quantifying groundwater exchange with lakes

Groundwater and surface water historically have been viewed and managed as separate entities. Although submerged springs have been recognized as a linkage between groundwater and surface water for thousands of years, less obvious linkages between the two resources either were unknown or assumed to be of little consequence. Only since the mid-1800s have the processes and conditions that control exchange between groundwater and surface water been discovered and investigated more thoroughly. During the past four decades, increased interest has been directed to flows of water and solutes across the sediment–water interface of lakes, which has led to an increased understanding of the physical, chemical and biological linkages at this interface (Jones and Mulholland 2000; Mann and Wetzel 2000; Wetzel 1999; Winter 1996).

There are at least three primary reasons for the growing interest in and importance of the connection between groundwater and surface water.

1. The global use of both groundwater and surface water continues to increase. In most parts of the world, the inexpensive, easily attainable water resources already have been exploited (Alley et al. 1999; Sophocleous 2002). We now are faced with utilizing water resources that have higher economic, social and environmental costs. Continuing increases in the extraction of both groundwater and surface water are inducing greater flows across the interface between groundwater and surface water.

2. Contamination of groundwater and surface water increasingly threatens the supply of water for human use and consumption. Three quarters of excessively contaminated groundwater sites (‘Superfund sites’) in the USA are within 0.8km (0.5 mi) of a surface-water body (Tomassoni 2000). Municipal water-supply wells increasingly are designed to induce flow from nearby river water (Hiscock and Grischek 2002; Lindgren and Landon 2000; Ray et al. 2003; Sheets et al. 2002) and from lake water (Miettinen et al. 1997; Wiese and Nützmann 2009) to meet water supply demands. Movement of contaminants from the adjacent river or lake to these water-supply wells is a growing concern.

3. Exchange of groundwater and surface water at and near the sediment–water interface occurs at an important ecotone where aquatic plant, invertebrate and vertebrate (fish and amphibians) communities have evolved to depend upon exchanges between surface water and their terrestrial surroundings (Gardner 1999; Gurnell et al. 2000; Hayashi and Rosenberry 2002). Many rare and endangered plants thrive in and near springs where groundwater discharges rapidly to surface water (Goslee et al. 1997; Hall et al. 2001; Rosenberry et al. 2000). However, exploitation of groundwater resources has greatly reduced the discharge of groundwater to some of these ecologically sensitive areas and has altered the communities that have evolved at this ecotone (Alley et al. 1999; Brunke and Gonser 1997; Sophocleous 2002).

Scientists have made substantial progress in quantifying flows and understanding processes that control the flow of fluid and solutes across the sediment–water interface. Advances in computer modelling, water-quality analytical techniques and our understanding of hydrological, hydrogeological, biogeochemical and ecological processes have served as foundations for this growth, but perhaps more importantly, a growing interest in interdisciplinary collaboration has been responsible for much of this recent progress. Although significant progress has been driven by needs related to water supply and contaminant hydrology, perhaps the greatest impetus for advancements has come from the ecological disciplines.

A relatively new field, ecohydrology, has evolved to focus on the biological communities and ecological processes that exist at this ecotone (Gurnell et al. 2000; Hayashi and Rosenberry 2002; Nuttle 2002; Wassen and Grootjans 1996). Baird and Wilby (1999), in the preface of their book on ecohydrology, demonstrate the interdisciplinary nature of this field by stating that only by collaboration between allied disciplines can substantial environmental problems and important research questions be addressed. Jones and Mulholland (2000) reach similar conclusions in their summary of the collaborative findings of ecological studies conducted in stream settings. The impressive collection of recent research focused at the sediment–water interface provides water-resource managers with many new ideas and methods with which to better manage these linked resources from ecological and human-health perspectives.

Interest in managing surface water and groundwater as a linked resource spawned a US Geological Survey publication titled Ground Water and Surface Water: A Single Resource (Winter et al. 1998), which generated considerable additional interest in the topic. This publication, oriented for the lay reader and the water resource manager as well as the research scientist, has greatly increased public awareness of the importance of quantifying the degree of interaction between groundwater and surface water in many hydrologic settings. However, although the interest in and understanding of this important linkage has grown remarkably during recent years, the development of new tools with which to quantify these exchanges has grown more slowly. Accurate, reliable and scale-independent methods have yet to be developed for many physical settings where quantification of flow between groundwater and surface water is needed.

2.1.3 Methods for quantifying flow between groundwater and surface water – a brief overview of the past 100 years

Many of the advances in understanding of processes and quantification of flows at the sediment–water interface are the result of new methodologies. As new methods are developed, processes are viewed from different perspectives, and a new understanding is generated. The list of methods available for quantification of flow between groundwater and surface water is still surprisingly small, however, given the historical and growing interest in the topic. Most of the methods rely on indirect measurement of water flow across the sediment–water interface, and the most frequently used methods provide information scaled to entire watersheds or entire surface-water bodies. The most commonly used methods can be categorized as follows (Kalbus et al. 2006; Rosenberry and LaBaugh 2008):

- watershed-scale studies
- lake-water budgets
- combined lake-water and chemical budgets
- wells and flow-net analysis
- groundwater flow modelling
- tracer studies
- thermal methods

- biological indicators
- seepage meters

The aforementioned methods are arranged approximately according to spatial scale, although considerable scale overlap occurs among several of the methods. The evolution of these methods also generally follows a progression in scale, with the largest-area methods being developed earliest, followed by local-scale approaches as studies have evolved to focus on questions and problems that are more site specific. A brief description and history of the evolution of each of these methods follow. Some of the methods were developed for use in other types of settings, but all are wholly suitable for lake applications.

Watershed-scale studies

This method is basically a water-budget approach, but from the perspective of the watershed (also called catchment) that supplies water to a lake. By using the topographically determined watershed divide as the boundary of the area of interest, inputs from precipitation are assumed to be distributed to a lake via stream and groundwater input minus evapotranspiration over the watershed area. Groundwater exfiltration is calculated as the residual of all other hydrological components. Most early efforts distributed groundwater exfiltration along a stream reach above a gauging station, but the method works equally well distributing the result along all or part of a lake shoreline.

Perhaps the earliest efforts that determined the interaction between groundwater and surface water at this scale were watershed studies that came into vogue during the 1920s through the 1960s. The first likely was the Wagon Wheel Gap study near Creede, Colorado, USA, begun by the US Forest Service in 1910 (Bates and Henry 1928). This watershed-hydrology approach grew in popularity for several decades; studies were conducted by the US Forest Service, US Soil Conservation Service and US Agricultural Research Service. Watershed-scale research also grew in scope and scale to include studies of biology, biogeochemistry and general ecology of entire basins and sub-basins. Programmes initiated by the US Geological Survey (e.g., Baedecker and Friedman 2000; Mast and Clow 2000), US National Park Service (Herrmann 1997) and the US National Science Foundation (Greenland et al. 2003) emphasized inter-site comparisons to address the concern of uniqueness of data and applicability of results to other watersheds.

A significant attraction of watershed-scale studies is the relative ease of defining the study on the basis of watershed boundaries, and the ability to scale the study on the basis of where streamflow is measured. One of the earliest streamflow-based approaches, commonly called the Rorabaugh (1964) method, segments the streamflow hydrograph to determine groundwater discharge to the stream. This method has since been modified and automated by applying computer programs to streamflow time-series data (Rutledge 1998; Rutledge 2000).

Numerous distributed-area 'rainfall–runoff' models have been developed that areally divide watersheds and sub-watersheds and calculate hydrologic parameters for each area; some models include the groundwater component of each area (e.g., Beven et al. 1984; Federer and Lash 1978; Leavesley et al. 1983; Leavesley et al. 2002). The current trend is to couple distributed area watershed-scale models with groundwater flow models to better determine the temporal and spatial variability of the interaction between groundwater and surface water (Beven and Feyen 2002; Leavesley and Hay 1998; Markstrom et al. 2008).

A combined water and chloride budget was used on a watershed scale to determine the volume of groundwater that discharged from the watershed to Lake Stechlin (Nützmann et al. 2003). This method was similar to those that make use of conservative chemical constituents described in the section on combined lake-water and chemical budgets.

Lake-water budgets

Quantifying all of the easier-to-measure components of a lake-water budget, and solving for the groundwater component as a residual, is a relatively simple concept that has been commonly used only since about the 1970s. The earliest examples of a lake-water budget being conducted to determine the groundwater components include a study of Lake Stechlin and other nearby lakes in eastern Germany to determine the suitability of the lake for cooling a proposed nuclear power plant (Heitmann and Schubert 1965; Schumann 1973) and a study of Lake Sallie in northern Minnesota to determine the role of groundwater in delivering excess nutrients to the lake (Mann and McBride 1972). Prior to the early 1970s, most lake-water budgets were conducted for the purpose of determining evaporation (e.g., Ficke 1972; Harbeck et al. 1958), perhaps because lakes were generally considered to be minimally influenced or even separated from groundwater (Broughton 1941).

The water-budget equation can be written as

$$\frac{\Delta V}{\Delta t} + R = P + S_i + G_i - ET - S_o - G_o \qquad \text{Eq. 2.1}$$

where $\Delta V/\Delta t$ is the change in volume of water in the lake per time, P is precipitation, S is surface-water flow, ET is evaporation plus transpiration from emergent vegetation in the lake, G is groundwater flow and R is the residual, or unaccounted water, in the water budget. Subscripts i and o refer to water flowing into and out of the lake, respectively. Missing in the equation are overland flow and flow through unsaturated sediments, the latter also known as interflow. If we make the common assumption that these terms are negligible (or are included in R), then groundwater exfiltration minus groundwater infiltration can be grouped with R to write

$$G_i - G_o - R = \frac{\Delta V}{\Delta t} + ET + S_o - P - S_i \qquad \text{Eq. 2.2}$$

Net groundwater is indicated on the left-hand side of Equation 2.2; neither groundwater exfiltration nor infiltration can be determined with this equation. However, both groundwater terms can be determined if water and chemical budgets are solved together, as described in the next section.

This equation is particularly well suited for settings where two of the three terms on the left-hand side of Equation 2.2 can be assumed to be small. For water budgets of reservoirs, where surface-water inputs and losses are the largest terms and can be measured relatively accurately, solving for groundwater as the residual can often be performed with relatively small errors. If surface flows become very large or are difficult to measure, errors associated with the surface-water terms can be so large that the resulting groundwater component is of little value (e.g., LaBaugh and Winter 1984). Settings with surface-water input but no surface-water outlet (e.g., Rosenberry et al. 2000; Zhou et al. 2013) or where there is a surface-water outlet but no inlets (e.g., Stets et al. 2010) make it more likely that a determination of the net groundwater component can be reasonably accurate.

Accurate determination of ET can be difficult and requires a substantial amount of instrumentation and data. Depending on the anticipated magnitude of ET relative to other components of a lake-water budget, several methods are available, the accuracies of which generally are commensurate with the cost of implementation (Rosenberry et al. 2007).

Combined lake-water and chemical budgets

Conservative chemicals in a watershed are those that are not altered by chemical reaction with the porous media through which they flow or by chemical or biological processes that occur in surface waters. Conservative chemicals can be used to determine the volume of groundwater that flows into or out of a surface water body, provided that all other fluxes are known. This method has been used for decades in many stream, lake and wetland studies but, perhaps because of advances in analytical methods, has grown rapidly in use since the 1980s (e.g., Brunke and Gonser 1997; Bukaveckas et al. 1998; Katz et al. 1997; LaBaugh et al. 1995; LaBaugh et al. 1997; Stauffer 1985; Wentz et al. 1995). The accuracy of the method depends greatly on the accuracy of the flow and chemical-concentration measurements. LaBaugh (1985) and Choi and Harvey (2000) provide thorough examples of proper use of error analysis to quantify the uncertainty associated with flux results obtained using this method.

The concept and procedure for determining a chemical budget are similar to a water-budget equation; the chemical concentration is multiplied by the mass (or volume) of each water-budget component to determine the chemical mass:

$$\frac{\Delta(C_L V)}{\Delta t} + R = C_P P + C_{Si} S_i + C_{Gi} G_i - C_{ET} ET - C_{So} S_o - C_{Go} G_o \qquad \text{Eq. 2.3}$$

where *C* is the concentration of the chemical constituent in each of the water-budget components as indicated by the subscript that follows *C* and the other terms are the same as for Equation 2.1 except for *R*, which now indicates concentration times water volume. The equation can be simplified for shallow, well-mixed lakes where the concentrations for So and G_o equal the lake-water concentration, C_L, and for all lakes, assuming no chemical mass is lost in the evaporation process:

$$\frac{\Delta(C_L V)}{\Delta t} + R = C_P P + C_{Si} S_i + C_{Gi} G_i - C_L (S_o + G_o) \qquad \text{Eq. 2.4}$$

Equation 2.1 can be rearranged to isolate G_o and then substituted for G_o in Equation 2.4 (again, without the *ET* term, assuming no chemical mass is lost in the *ET* process) to solve for G_i:

$$G_i + \varepsilon = \frac{C_L \frac{\Delta V}{\Delta t} + (C_L - C_P)P + (C_L - C_{Si})S_i}{C_{Gi} - C_L} \qquad \text{Eq. 2.5}$$

where ε is the combined errors of measurements of water mass and chemical concentration. *R* is lumped with ε in Equation 2.5 for convenience. G_i determined with Equation 2.5 can now be inserted in Equation 2.1 or 2.2 to solve for G_o.

This method is particularly well suited for settings where the concentration of the chemical constituent of interest is spatially consistent within the groundwater that discharges to the lake. If this is not the case, the groundwater flow field that discharges to the lake can be segmented into areas where the chemical concentration is relatively consistent, and $C_{Gi}G_i$ can be determined for each area where C_{Gi} is relatively uniform. This method is not well suited for settings where C_{Gi} is nearly the same as *Cl* because as the denominator in Equation 2.5 approaches zero, measurement errors cause the result to become unstable.

Combining water and chemical budgets to determine G_i and G_o separately requires the use of a conservative constituent dissolved in the water. Chloride is commonly used in this application, although it is not always conservative (e.g., LaBaugh et al. 1997). Isotopes of oxygen and hydrogen have been used for the last several decades to determine various source and loss terms of surface-water bodies, including groundwater exfiltration and infiltration (Dinçer 1968; Katz et al. 1997; Kendall et al. 1995; Krabbenhoft et al. 1990; LaBaugh et al. 1997; Sacks et al. 1998). These isotopes are inherently conservative because they are part of the water as opposed to solutes dissolved in the water. The method works well when the degree of isotopic fractionation of the water is different for different sources of water (Kendall et al. 1995). The simple mixing models described earlier then can be used to identify sources of water, with one caveat. The isotopic signature of the evaporating water needs to be determined, and the term $C_{ET}ET$ needs to be subtracted on the right-hand side of Equation 2.4.

Additional variables, such as air temperature at the water–atmosphere interface, relative humidity and the isotopic content of local atmospheric water vapour, need to be determined (e.g., Krabbenhoft et al. 1990), making $C_{ET}ET$ particularly difficult to determine accurately. This method was rarely used until the mid-1980s when new analytical tools, such as the mass spectrometer, became less expensive and more readily available. Data richness in some locations has grown to the point that decadal-scale studies of seasonal and inter-annual variability in groundwater–surface water exchange are now possible using this isotope-mass-budget approach (Sacks et al. 2014).

Wells and flow-net analysis

The flow-net analysis, sometimes called the 'Darcy approach', is probably the most frequently used field-based method for quantifying flow between groundwater and surface water. This method requires determination of horizontal hydraulic gradient and hydraulic conductivity in the portion of the aquifer near the lake, so calculations can be made on the basis of Darcy's law. The method uses a combination of near-shore water-table wells along with a device to measure surface-water stage to determine water-table gradients between the wells and the shoreline of the surface-water body. Hydraulic conductivity commonly is determined from single-well slug tests (e.g., Bouwer and Rice 1976) conducted in the same wells used to obtain hydraulic gradients. A multiple-well aquifer test would provide a better indication of hydraulic conductivity, but the greater cost usually precludes this option. Other options include grain-size analysis of sediments removed during well installation (e.g., Shepherd 1989) or a lab analysis of an intact sediment core collected during well installation. One of two approaches is commonly used to determine spatial distribution of hydraulic properties. One approach segments the shoreline of the surface-water body according to the number and location of nearby wells, and flows to or from the lake are determined for the lake segment attributed to each monitoring well on the basis of data collected from that well. Another approach uses hydraulic-head and surface-water-stage data to generate equipotential lines and flow paths. Flows to and from the surface-water body are then calculated using flow-net analysis (Cedergren 1997; Fetter 1994; Rosenberry et al. 2008). Flow-net analysis has existed for many decades, but prior to the mid-1990s, use of the method required subjective hand-drawn lines to generate equipotential lines and groundwater flow paths (e.g., Kenoyer and Anderson 1989; Schafran and Driscoll 1993). Commercially or freely available computer programs (e.g., Hsieh 2001) have made the method much more popular during recent years.

This method typically is used for all or a portion of a watershed or a lake or wetland basin. It is relatively expensive for use with large lakes or where the depth to groundwater makes well installations costly. Detail and accuracy of the method are directly proportional to the density of the well network (Rosenberry and Hayashi 2013). The literature contains numerous examples of the method being used successfully to quantify exchange of water (and also solutes) between groundwater and surface water (e.g., Belanger and Kirkner 1994; Lee and Swancar 1997; Pfannkuch and Winter 1984). One benefit of this method over many others is the ability to determine flow direction and magnitude for specific shoreline segments or portions or embayments of irregularly shaped lakes. An even finer-scale approach has been to use small diameter portable wells that are driven into the shallow lakebed to determine the vertical hydraulic-head gradient (Winter et al. 1988). This local-scale approach can be far less expensive and less labour-intensive than typical well installations.

Groundwater flow modelling

Prior to the mid-1970s, most people concerned with modelling flow between groundwater and surface water used analytical models or electric analogue models, both of which were limited to relatively simple flow geometry and boundary conditions. Early finite-difference and finite-element numerical models were a substantial improvement in modelling groundwater fluid flow, but they also were relatively restrictive regarding the physical settings that could be modelled. One of the limitations was the requirement that the elevation of the water table and surface-water body be specified and fixed. Although this restriction did not substantially affect most watershed-scale studies, it severely limited simulations of local-scale, near-shore processes adjacent to surface water bodies. Richard Cooley developed a two-dimensional, variably saturated, transient finite-element model that allowed the water table to fluctuate in response to temporally variable recharge conditions (Cooley 1983), and Thomas Winter used this model to simulate groundwater flow adjacent to lakes in response to snowmelt (Winter 1976; Winter 1978; Winter 1981; Winter 1983). Winter's (1976, 1978) results indicated that flow conditions adjacent to lakes were highly variable and that a hydraulic-head dam could form in the aquifer, reverse the direction of flow between groundwater and the lake and hydraulically isolate the lake from other nearby lakes. Winter's (1983) subsequent modelling further developed this new concept and initiated a rapid increase in research on processes that control flow between groundwater and surface water.

Groundwater-flow models are now commonly used to assess the interaction between groundwater and surface water, in part because the popular US Geological Survey MODFLOW finite-difference code (Harbaugh et al. 2000; McDonald and Harbaugh 1984) is modular in implementation and relatively easy to use. The newest (circa 2014) version of this model (http://water.usgs.gov/ogw/modflow/) includes modules for simulating flows to or from a river, detailed stream–groundwater interaction, flows to and from reservoirs, and two modules exist for simulating flows to and from lakes. For some settings, other simpler modelling approaches (e.g., analytical element, Strack 1999, and high conductivity) can produce similar results (Hunt et al. 2003). Detailed simulations of the spatial distribution of groundwater discharge to a lake were recently made for a lake in Kenya using the high-conductivity modelling method and setting hydraulic conductivity of the lake domain at three orders of magnitude larger than the surrounding porous media (Yihdego and Becht 2013). Anderson et al. (2002) indicated a four-orders-of-magnitude contrast between lake and aquifer hydraulic conductivity would be better but less efficient than using the MODFLOW lake package. Temporal variability also has been emphasized in many modelling studies. Some studies have investigated the importance of temporal variability in groundwater divides (Holzbecher 2001), which commonly diverge substantially from surface-water divides (Winter et al. 2003). Other studies investigated the effects of climate change on the groundwater contribution to lake water budgets (Hunt et al. 2013) and on near-shore processes that control exchanges between groundwater and a lake underlain by karst, the latter incorporating simulated changes in lake-surface area that accompany simulated changes in lake stage (Virdi et al. 2013). Nearshore temporal variability in hydraulic gradients also was shown to enhance dispersion of solutes when groundwater flow between an upgradient and nearby downgradient lake was modelled (Kim et al. 2000).

Many studies that are primarily field oriented also include a groundwater flow model, often in an attempt to further verify the results of the study. However, problems arise when insufficient field data exist to properly calibrate the models (Hill 1992; Konikow and Bredehoeft 1992; Munter and Anderson 1981; Tiedeman and Gorelick 1993). Alternately, overly complex models can be developed with the intent of matching field data as opposed to increasing understanding of hydrogeological processes (Voss 2011a; Voss 2011b). Rapidly increasing computer power allows newer calibration methods that were unheard of only a few years ago (e.g., Hunt and Zheng 2012).

Tracer studies

The addition of chemicals to streams and rivers, and subsequent sampling of water downgradient of the source to determine the mean flow velocity, has been used for many years in the surface-water community. However, only since the 1980s, and the concern with discovery and movement of groundwater-contamination plumes, has the use of tracers become widespread among groundwater scientists. Tracers have been used in several ways to track the movement of groundwater, including single-point (slug-type) tracer injection and constant-discharge tracer injection. Naturally occurring tracers also can be used if the chemical signature of groundwater is sufficiently different from lake water. Perhaps the first well-documented use of tracers to determine the discharge of groundwater to a lake was at Perch Lake, Ontario. Salt was injected in an upgradient line of wells, and a dense grid of monitoring wells installed adjacent to and in the lake was sampled to determine the route and velocity of the salt mass as it moved towards and discharged to the lake (Lee et al. 1980). Other studies have used fluorescent dye (Smart and Smith 1976), as well as other conservative chemical constituents, to track movement of groundwater to surface water (Bertin and Bourg 1994; Harvey et al. 1996; Hayashi et al. 1998; Thies et al. 2002). Studies have even made use of contaminant plumes to determine rates of discharge of groundwater to surface water (Ferrey et al. 2001).

Tracers also can be injected into a lake to determine movement of surface water to groundwater (a ‘whole-lake’ injection test). If a tracer is selected that has exceptionally low natural, or background, concentrations in all of the other water-budget terms (lithium or bromide commonly meets this criterion), then Equation 2.3 reduces to

$$\frac{\Delta(C_L V)}{\Delta t} + R = C_L(S_o + G_o) \quad \text{Eq. 2.6}$$

Lithium bromide solution, for example, was injected into several small lakes in Michigan in order to quantify water movement from the lakes to groundwater (Cole and Pace 1998).

Despite their wide applicability, tracer studies are not as commonly used to study the interaction between groundwater and surface water as some of the other available methods. This likely is due, in part, to the relative cost, in both equipment and time, for application and monitoring of tracer movement or to restrictions that prohibit addition of chemicals to a lake. Another problem with use of tracers at the sediment–water interface is detection of the tracer once it enters or leaves the surface-water body. Tracer dilution in the surface water often results in tracer concentrations that are below detection limits.

Thermal methods

Temperature is one of the simplest and most accurately measured properties of water. Temperature anomalies long have been used to locate near-shore springs in surface water bodies (Lee 1985). Commonly, temperature has been used qualitatively as an indicator of groundwater discharge (Baskin 1998; Bundschuh 1993), especially in karstic terrain where spring discharge is focused and rapid. Remote sensing temperature-measurement methods have proven useful for identifying areas of rapid groundwater discharge to shallow surface water (Baskin 1998; Gosselin et al. 2000; Kang et al. 2005; Lee and Tracey 1984; Lewandowski et al. 2013), including hand-held thermal-infrared units (Cardenas et al. 2012). Spatial variability in temperature also has been used to locate areas of rapid groundwater discharge in deeper portions of lakes and rivers (Lee 1985; Stark et al. 1994). This is accomplished by towing a tethered temperature (and sometimes also specific-conductance, Lee 1985) probe and recording temperature anomalies. Relatively new technology, commonly referred to as distributed temperature sensing, is now routinely used to map temperatures at the sediment-water interface of lakebeds with 0.25- to about 1-m spatial resolution and about 0.05–0.1 °C temperature resolution along distances of up to several kilometres, providing the ability to identify areas where groundwater exfiltration is likely focused (e.g., Blume et al. 2013; Day-Lewis et al. 2006; Fleckenstein et al. 2010; Sebok et al. 2013; Selker et al. 2006).

Previously mentioned temperature-measurement methods have primarily been qualitative. Recent analytical methods have provided convenient means for temperature to be used quantitatively to determine rates of groundwater discharge. Several authors (Anibas et al. 2009; Conant 2004; Schmidt et al. 2006) assumed steady-state conditions when they measured thermal depth profiles and applied a one-dimensional analytical solution of the heat conduction–advection equation to the measured profiles. Others have made use of seasonal differences between shallow groundwater and surface water temperature (Bartolino and Niswonger 1999; Lapham 1989) or diurnal changes in temperature difference (Briggs et al. 2012; Constantz et al. 1994; Gordon et al. 2012; Silliman and Booth 1993; Stonestrom and Constantz 2003). Because measurement of temperature is so simple and inexpensive, it is one of the fastest-growing methods for determining the interaction between groundwater and surface water on a small scale (e.g., Briggs et al. 2012; Briggs et al. 2013; Gordon et al. 2012; Hatch et al. 2010; Lautz and Ribaudo 2012). Several recent local-scale studies have used thermal methods in lake settings (Blume et al. 2013; Kidmose et al. 2011; Sebok et al. 2013). However, geologic heterogeneity often makes the results from temperature methods difficult to extrapolate to scales at which watershed managers typically are interested (Conant 2000; Fryar et al. 2000; Rau et al. 2012).

Analogous to thermal profiles discussed earlier, vertical profiles of conservative, natural chemicals also can be used to calculate rates of exchange between groundwater and surface water. Several authors have used conservative constituents, such as chloride, bromide, tritium and the water isotopes deuterium and oxygen^{-18}, to determine fluxes at the sediment–water interface of lakes (Cornett et al. 1989; Mortimer et al. 1999; Schuster et al. 2003).

Biological indicators

The biological response to flow at the sediment–water interface can be used as an indicator of direction of flow and relative magnitude of groundwater exfiltration or infiltration. Hydrologists have used plants to locate areas of groundwater discharge for many years, as evidenced by O. E. Meinzer's classic report titled *Plants as Indicators of Ground Water* (Meinzer 1927). Numerous more recent examples from the growing field of ecohydrology use distributions of specific types of plants and animals to indicate areas of groundwater–surface water interaction (Danielopol 1984; Danielopol et al. 1997; Goslee et al. 1997; Lillie and Barko 1990; Lodge et al. 1989; Loeb and Hackley 1988; Malard et al. 1996; Rosenberry et al. 2000; Sebestyen and Schneider 2004; Wetzel 1999). The density of submerged macrophytes also can be related to groundwater exfiltration, particularly if nutrients are being supplied by groundwater (Frandsen et al. 2012; Lodge et al. 1989). These methods provide a qualitative indication of the direction and magnitude of flow between groundwater and surface water and are good reconnaissance tools to aid in locating areas in need of more detailed investigations. Typically, they involve identifying species or groups of species of plants or animals that are known to thrive in places where groundwater discharges to surface water, but some of the species also indicate areas where surface water flows into groundwater. Although identification of specific plant and animal species is necessary for use of these methods, some of the species are so simple to identify that biological or ecological training is not required (Rosenberry et al. 2000).

A considerable impetus for the increased interest in quantifying flows between groundwater and surface water is related to fish. Fisheries biologists for years have suspected that many species of fish position spawning redds on the basis of water flow across the sediment–water interface in streams, commonly termed hyporheic exchange (e.g, Malcolm et al. 2004; Pollard 1955; Shepherd et al. 1986; Vaux 1968). Some fish species construct spawning redds in locations of focused groundwater discharge (e.g., Warren et al. 2005), and others seemingly do not. More recent research is advancing the understanding of this linkage with regard to fish in lake settings (Ridgway and Blanchfield 1998; Warren et al. 2005).

Seepage meters

The seepage meter is a device placed over the sediment of a surface-water body, in this case a lake, that records the net flow of water to or from the lake through the bed area covered by the meter. The device funnels all flow through the isolated portion of the lakebed either to or from a collection bag, depending on whether water is flowing to or from the lake. The change in volume of water contained in the bag during the bag-attachment period gives a time-integrated and space-integrated indication of seepage. Of all the methods listed in this review, the seepage meter alone provides a direct measurement of water flow across the sediment–water interface. All other methods rely on measurement of related parameters that indirectly determine flow across the sediment–water interface. The seepage meter provides a local-scale measurement, integrating flow over a lakebed area typically between 0.03 and 1.7m^2, with 0.25m^2 being the area covered by the most commonly used type of seepage meter (Lee 1977).

Early versions of the seepage meter developed during the 1940s and 1950s were designed to measure seepage losses in irrigation canals (Israelson and Reeve 1944; Rasmussen and Lauritzen 1953; Robinson and Rohwer 1952; Warnick 1951). Many of these devices were expensive and unwieldy and were little used beyond the application to canals. David Lee (1977) developed an inexpensive and simple meter that has evolved little in the decades since its inception. Lee's meter consists of the cut-off end of a 208-l (55-gal) storage drum, to which a plastic bag that is partially filled with a known volume of water is attached. The bag is attached to the chamber for a measured amount of time, after which the bag is removed and the volume of water contained in the bag is re-measured. The change in volume per bag-attachment time is the volumetric rate of flow through the portion of the bed covered by the chamber, which then can be divided by the approximately 0.25-m^2 area covered by the chamber to obtain a flux velocity (distance/time). Values commonly are expressed as cubic metre per square metre per second or centimetre per day. This value typically is multiplied by a coefficient that compensates for inefficiencies in flow within the meter as well as restrictions to flow through the connector between the bag and the chamber and any resistance to movement of the bag. Correction factors reported in the literature have ranged from 1.05 to 1.74 (Rosenberry and Menheer 2006). This basic design is used in most seepage-meter studies, although several modifications exist for use in a variety of specific stream and lake settings, including shallow, near-shore waters (Lee and Cherry 1978), deep lakes (Boyle 1994) and large lakes with large waves (Cherkauer and McBride 1988). Placing the bag inside a shelter minimizes velocity-head effects associated with waves and currents in lakes (Rosenberry 2008; Sebestyen and Schneider 2001). Increasing the area covered by the seepage meter better integrates local-scale seepage heterogeneity (Rosenberry 2005), whereas seepage meters that cover a smaller bed area are far easier to install. Additional information regarding methods of use and sources of error is presented by Rosenberry et al. (2008).

Several automated seepage meters have been developed that replace the seepage bag with a flow meter. Taniguchi and Fukuo (1993) introduced the first automated seepage meter when they used heat-pulse sensors, originally designed to measure sap flow in trees, to measure lakebed seepage. They were able to extend the range over which they could measure seepage by using pairs of thermistor thermometers that were various distances away from a heat source. They also logged results from this system with a digital data logger. Taniguchi and others have used this device to investigate temporal variability in seepage responses to seiches in lakes and ocean tides (Taniguchi et al. 2002; Taniguchi and Fukuo 1996). Although information regarding this device has been readily available for nearly two decades, only a few similar devices have been built (Krupa et al. 1998), likely because considerable engineering and electronics expertise is required. Ultrasonic flow sensors have been used to measure seepage with good results (Fritz et al. 2009; Menheer 2004; Paulsen et al. 2001). An electromagnetic flow meter designed for use in boreholes has been used to measure seepage in several freshwater and marine settings (Rosenberry and Morin 2004; Swarzenski et al. 2007). This device is capable of measuring seepage on the order of seconds to minutes, which allows investigation of short-term temporal variability in response to rainfall, evapotranspiration, lake seiches and other processes (Rosenberry et al. 2013).

2.1.4 Distribution of exchange between groundwater and lakes in space and time

Seepage, whether exfiltration or infiltration, is focused near the shoreline of lakes and decreases exponentially with distance from shore (McBride and Pfannkuch 1975; Pfannkuch and Winter 1984), but only if the geology beneath and adjacent to the lake is homogeneous. Lakebeds rarely are homogeneous for a wide variety of reasons, including (1) wave-induced erosion of sediments focused at the shoreline, which can remove fines and leave behind the coarser-grained fraction; (2) deposition of sediments focused at the shoreline brought in via overland flow associated with intense rainfall events; (3) changes in lake stage that result in lateral movement of the shoreline, as well as the associated near-shore processes listed in 1 and 2; (4) erosion and deposition of sediment caused by seiche-induced, wind-induced and wave-induced currents; (5) accumulation of biomass and/or woody debris from the adjacent upland; (6) manipulation of near-shore sediments by physical (e.g., ice shove, Rosenberry et al. 2010) or biological processes such as plant roots, benthic invertebrates, freshwater mussels, crayfish, fish and ducks; (7) geologic heterogeneity; and (8) anthropogenic manipulations (e.g., shoreline alteration and/or stabilization). Anisotropy, the ratio of horizontal to vertical hydraulic conductivity, also is common in lacustrine sediments. The greater the anisotropy, the less that seepage is focused near the shoreline (Genereux and Bandopadhyay 2001; Pfannkuch and Winter 1984). Numerous studies have indicated atypical distribution of seepage with distance from shore in lake settings (e.g, Cherkauer and Nader 1989; Kidmose et al. 2013; Schneider et al. 2005; Woessner and Sullivan 1984), including increase in seepage with distance from shore. In all of these cases, geologic controls were stronger than the local or regional physiographic setting that otherwise would control seepage distribution (Winter 1999).

In addition to spatial heterogeneity, temporal variability also confounds determination and interpretation of exchange between groundwater and lakes. Seepage rates are affected by numerous hydrologic processes that commonly are focused at or near the shoreline, such as troughs of depression in the adjacent groundwater system resulting from evapotranspiration (Rosenberry and Winter 1997). Near-shore hydraulic gradients and seepage change when rainfall infiltrates through an unsaturated zone that thins to zero with proximity to the lake. Enhanced groundwater recharge near the shoreline can also create water-table mounds that reverse seepage direction in near-shore margins. Anthropogenic effects, such as withdrawal of groundwater for private or municipal water supply or addition of water associated with septic leachate, can locally affect exchange between lakes and the adjacent groundwater. Some large-volume water-supply wells are intentionally placed near a lake to induce flow from the lake to the well; this process is commonly termed bank filtration(Miettinen et al. 1997; Wiese and Nützmann 2009). Fine-grained sediments that accumulate in lakes are re-suspended by waves and currents focused in the near-shore margins; the net effect of this frequent process is that fines are preferentially deposited in the deeper portions of the lake. Suspension of fines by waves and currents increases sediment permeability and enhances the focusing of seepage in the near-shore margins. For all these reasons, lakebeds are notoriously heterogeneous, which creates one of the greatest challenges in determining representative seepage rates for lakeshore segments, embayments or entire lakes.

2.1.5 Seepage values commonly measured in lakes

Rates of exchange between groundwater and lakes were obtained from the published literature to statistically summarize seepage in lake settings. Data presented in Table 2.1 are indicative almost entirely of variability among lakes. In a few instances, multiple values are presented for the same lake, either because different methods were used to indicate seepage or because multiple studies were conducted by different groups of authors. These multiple values for a single lake additionally provide an indication of either methodological biases or temporal variability.

Seepage, when determined as part of a lake-water budget, commonly is reported in units of volume per time. However, for the purpose of comparing seepage among lakes that vary over many orders of magnitude in surface area or to compare seepage that has been determined with a variety of methods, each of which has a different measurement scale, it is useful to normalize seepage values by dividing the volumetric seepage value by the surface area of the lake, or the area over which the measurement represents, to determine a seepage rate. Here (Table 2.1), we present seepage in units of volume per area per time, or distance per time, in centimeter per day (equivalent to 10 l m^{-2} day^{-1}).

On the basis of studies conducted in 102 lakes where exfiltration was measured (Fig. 2.1 and Table 2.1), the median value for exfiltration is 0.74 cm day^{-1} (Table 2.2).

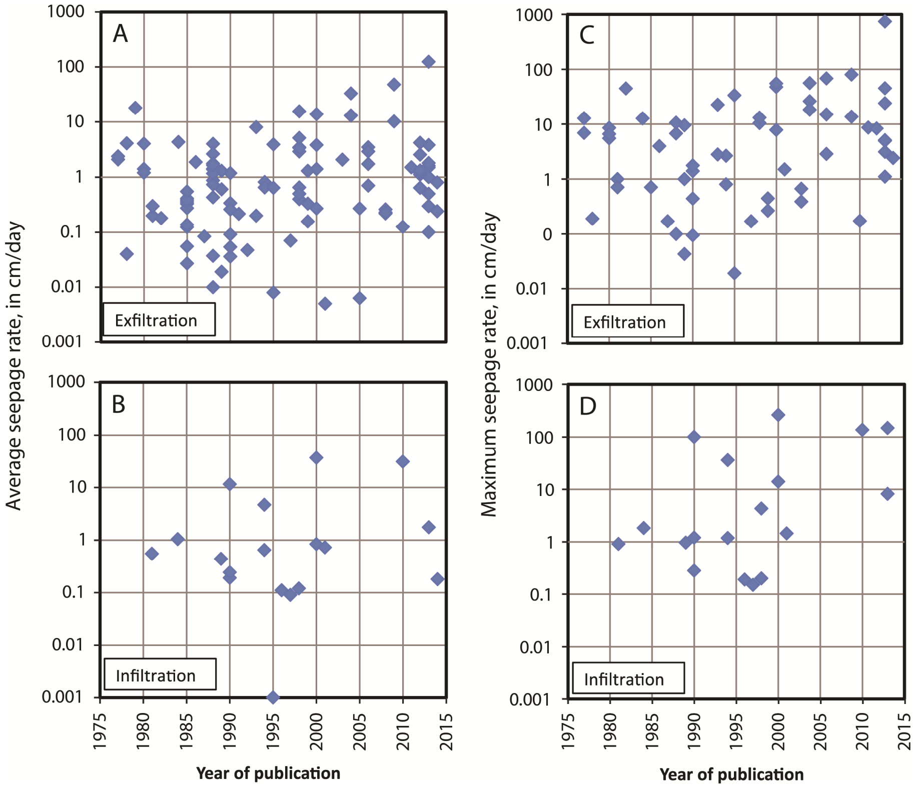

Figure 2.1 Published rates of groundwater exfiltration (A, C) and infiltration (B, D). References are listed in Table 2.3. Panels A and B are based on average values reported in the literature for specific study lakes. Panels C and D list maximum values from each studied lake.

Far fewer studies have been conducted in lakes where infiltration occurs. The median value for 18 lakes where infiltration was measured is 0.60 cm day^{-1}, nearly the same as at exfiltration locations. These values represent average seepage rates reported for a wide range of lakes situated around the world, with 70% of the studied lakes being in the USA. Although data in Table 2.1 are extensive, they are by no means an exhaustive representation of the seepage literature. Median values would better represent seepage than average values because seepage datasets commonly are skewed. However, data from the ‘Average value’ column in Table 2.1 were used to summarize data because median values were only rarely reported in the literature. The same comparison of seepage rates can be made on the basis of maximum rather than average values from the literature. The median of 59 maximum exfiltration values reported in the literature is 5.10 cm day^{-1}. The median of 18 maximum infiltration seepage rates is 1.64 cm day^{-1} (Table 2.2). In the case of maximum values, the largest reported exfiltration seepage rate is 745 cm day^{-1}; the largest reported infiltration rate is 263 cm day^{-1}. Interestingly, extreme values for maximum seepage are larger for infiltration than for exfiltration. Four of the 18 values of reported maximum infiltration are larger than 100 cm day^{-1}, whereas only one of the 59 maximum values for exfiltration is larger than 100 cm day^{-1} (Figure 2.1C, D). The largest exfiltration value based on our literature review is 745 cm day^{-1} at Lake Væng in central Jutland, Denmark (Kidmose et al. 2013). The largest value for infiltration is 263 cm day^{-1} at Lake Belle Taine, in northern Minnesota (Rosenberry 2000). Bed sediment at both lakes is medium-to-coarse-grained sand.

Table 2.1 Summaries of rates of groundwater exfiltration and infiltration reported in the literature.

Reference	Location	Average	Median	Minimum	Maximum	Measurement method
Rates of groundwater exfiltration:						
Mitchell et al. (1988)	11 lakes in Massachusetts, USA				10.6	Seepage meter
Ala-aho et al. (2013)	L. Ahveroinen, Finland	1.49	0.78	0	4.92	Seepage meter
Boyle (1994)	Alexander Lake, Ontario, Canada	0.65		0.5	0.8	Seepage meter
McCobb et al. (2009)	Ashumet Pond, Massachusetts, USA	47.7		25	80.4	Seepage meter
Rosenberry and Morin (2004)	Ashumet Pond, Massachusetts, USA	33		11	56	Seepage meter
Rosenberry et al. (2013)	Ashumet Pond, Massachusetts, USA				55	Seepage meter
Herczeg et al. (2003)	Blue Lake, Australia	1.07				Isotopes
Dimova et al. (2013)	Butler Lake, Florida, USA	0.3				Radon
Dimova et al. (2013)	Clear Lake, Florida, USA	0.3				Radon
Simpkins (2006)	Clear Lake, Iowa, USA	2.9		0	14.9	Model
Pina-Ochoa and Alvarez-Cobelas (2009)	Colgada Lake, Spain	10.2		6.8	13.6	Flow meters
Stauffer (1985)	Columbia Lake, Wisconsin, USA	0.329				Chemistry
Schafran and Driscoll (1993)	Dart´s Lake, Pennsylvania, USA	1.8		0.35	5.1	Seepage meter
Stauffer (1985)	Deep Lake, Wisconsin, USA	0.274				Chemistry
Lillie and Barko (1990)	Devils Lake, Wisconsin, USA	0.34	0.24	0.02	1.76	Seepage meter
Ridgway and Blanchfield (1998)	Dickson Lake, Ontario, Canada	15.5				Seepage meter
Mitchell et al. (1988)	Dimmock Pond, Massachusetts, UA	1.74				Seepage meter
Belanger et al. (1985)	East Lake Tohopekaliga, Florida, USA	0.411	0.488	0.016	0.708	Seepage meter
Cole and Pace (1998)	East Long Lake, Michigan, USA	0.4				Chemistry
Stauffer (1985)	Emrick Lake, Wisconsin, USA	0.123				Chemistry
Stauffer (1985)	Fish Lake, Wisconsin, USA	0.027				Chemistry
Mitchell et al. (1988)	Five Mile Pond, Massachusetts, USA	1.42				Seepage meter
Weilhartner et al. (2012)	Gravel Pit Lake 1, Austria	1.11				Budget
Weilhartner et al. (2012)	Gravel Pit Lake 2, Austria	1.19				Budget
Weilhartner et al. (2012)	Gravel Pit Lake 3, Austria	2.54				Budget
Weilhartner et al. (2012)	Gravel Pit Lake 4, Austria	1.32				Budget
Weilhartner et al. (2012)	Gravel Pit Lake 5, Austria	4.17				Budget
Anderson et al. (2014)	Great Salt Lake, Utah, USA	0.8		0.1	2.4	Seepage meter
Rosenberry et al. (2013)	Great Salt Lake, Utah, USA				24	Seepage meter
Dimova et al. (2013)	Haines Lake, Florida, USA	1		0.3	1.1	Radon
Harvey et al. (2000)	Hamilton Harbor, Lake Ontario, Canada	3.8				Budget
Harvey et al. (2000)	Hamilton Harbor, Lake Ontario, Canada	0.27				Darcy
Dimova et al. (2013)	Josephine Lake, Florida, USA	1.6		1	3.1	Radon
Mitchell et al. (1988)	Knopp´s Pond, Massachusetts, USA	2.62				Seepage meter
Cherkauer and McBride (1988)	Lake Michigan, Michigan, USA	0.01				Seepage meter

Table 2.1 Continued.

Reference	Location	Average	Median	Minimum	Maximum	Measurement method
Lee (1977)	Lake Sallie, Minnesota, USA	2.37	1.90	0.03	6.91	Seepage meter
Loeb and Goldman (1979)	Lake Tahoe, California, USA	18				Darcy
Loeb and Hackley (1988)	Lake Tahoe, California, USA	0.04	0.01	0.004	0.1	Seepage meter
Connor and Belanger (1981)	Lake Washington, Florida, USA	0.2		-0.3	1	Seepage meter
Bruckner et al. (1989)	Lake Anna, Virginia, USA	0.019	0.016	0.002	0.043	Seepage meter
Fellows and Brezonik (1980)	Lake Apopka, Florida, USA	1.4		0.1	8.5	Seepage meter
Taniguchi and Fukuo (1993)	Lake Biwa, Japan	8		0	22.5	Seepage meter
Vanek (1991)	Lake Bysjön, Sweden	0.216				Recharge
Lesack (1995)	Lake Calado, Brazil	3.9		0.12	33.5	Seepage meter
Cullmann et al. (2006)	Lake Camaleao, Brazil	0.7				Budget
Cullmann et al. (2006)	Lake Camaleao, Brazil	1.73	1.42	1.22	2.86	Chemistry
Cullmann et al. (2006)	Lake Camaleao, Brazil	3.48			67.8	Seepage meter
Fellows and Brezonik (1980)	Lake Conway, Florida, USA	1.2		0.3	5.5	Seepage meter
Kidmose et al. (2011)	Lake Hampen, Denmark	1.5		0	8.6	Seepage meter
Oliveira Ommen et al. (2012)	Lake Hampen, Denmark	0.64			8.3	
Mortimer et al. (1999)	Lake Kinneret, Israel	0.33	0.323	0.226	0.444	Chemistry
Mortimer et al. (1999)	Lake Kinneret, Israel	0.16	0.157	0.049	0.266	Seepage meter
Mitchell et al. (1988)	Lake Lorraine, Massachusetts, USA	1.75				Seepage meter
Lee and Swancar (1997)	Lake Lucerne, Florida, USA	0.07		0.003	0.17	Darcy
Woessner and Sullivan (1984)	Lake Maed, Nevada, USA	4.30	3.06	0.2	12.63	Seepage meter
Sonzogni and Lee (1974)	Lake Mendota, Wisconsin, USA	0.19				Budget
Brock et al. (1982)	Lake Mendota, Wisconsin, USA	0.18		0.6	44.5	Seepage meter
Downing and Peterka (1978)	Lake Metigoshe, North Dakota, USA	0.04			0.19	Seepage meter
Schneider et al. (2005)	Lake Oneida, New York, USA	0.2		0	2.8	Seepage meter
Kang et al. (2005)	Lake Persimmon, Florida, USA	0.0063				Chemistry
Misztal et al. (1992)	Lake Piaseczno, Poland	0.047				Darcy
McBride (1987)	Lake St. Clair, Michigan, USA	0.08		0.03	0.17	Seepage meter
Lee et al. (2014)	Lake Starr, Florida, USA	0.24				Model
Kidmose et al. (2013)	Lake Væng, Denmark	124.1	19.0	0.3	745	Seepage meter
Kidmose et al. (2013)	Lake Væng, Denmark	3.8				Budget
Mitchell et al. (1988)	Little Sandy Bottom Pond, Massachusetts, USA	0.87				Seepage meter
Menheer (2004)	Long Lake, Minnesota, USA	13		1.8	26	Seepage meter
Attanayake and Waller (1988)	Long Lake, Nova Scotia, Canada	4.0		1.3	6.7	Seepage meter
Mitchell et al. (1988)	Loon Pond, Massachusetts, USA	1.38				Seepage meter
Mitchell et al. (1988)	Lost Lake, Massachusetts, USA	1.16				Seepage meter
Cherkauer and Zager (1989)	Lower Nashotah Lake, Wisconsin, USA	0.6		0.02	1	Seepage meter
Sebestyen and Schneider (2001)	Lower Sylvan Pond, New York, USA	0.005		0	1.5	Seepage meter
Stauffer (1985)	Marl Lake, Wisconsin, USA	0.356				Chemistry
Hofmann et al. (2008)	Mining Lake Plessa 117, Germany	0.22				Budget
Hofmann et al. (2008)	Mining Lake Plessa 117, Germany	0.26				Isotopes
Hofmann et al. (2008)	Mining Lake Plessa 117, Germany	0.23				Model
Asbury (1990)	Mirror Lake, New Hampshire, USA		0.0115	0.004	0.094	Seepage meter
Toran et al. (2010)	Mirror Lake, New Hampshire, USA	0.125		0.004	0.17	Seepage meter
Belanger and Kirkner (1994)	Mountain Lake, Florida, USA	0.813	0.432	0.0336	2.64	Seepage meter
Ridgway and Blanchfield (1998)	Mykiss Lake, Ontario, Canada	2.9				Seepage meter
Shaw et al. (1990)	Narrow Lake, Alberta, Canada	0.091				Budget

Table 2.1 Continued.

Reference	Location	Average	Median	Minimum	Maximum	Measurement method
Shaw et al. (1990)	Narrow Lake, Alberta, Canada	0.054				Darcy
Shaw and Prepas (1990)	Narrow Lake, Alberta, Canada	0.26	0.22	0.14	0.44	Seepage meter
Shaw et al. (1990)	Narrow Lake, Alberta, Canada	0.036				Seepage meter
Mitchell et al. (1988)	Nashawannuck Pond, Massachusetts, USA	0.43				Seepage meter
Dimova et al. (2013)	Newnans Lake, Florida, USA	0.5				Radon
Stauffer (1985)	Parker Lake, Wisconsin, USA	0.383				Chemistry
Lee and Cherry (1978)	Perch Lake, Ontario, USA	4.1				Seepage meter
Lee et al. (1980)	Perch Lake, Ontario, USA	4.04	4.63	1.42	6.56	Seepage meter
Cole and Pace (1998)	Peter Lake, Michigan, USA	0.65				Chemistry
Stauffer (1985)	Pickerel Lake, Wisconsin, USA	0.055				Chemistry
Mitchell et al. (1988)	Richmond Pond, Massachusetts, USA	0.74				Seepage meter
John and Lock (1977)	Rotorua Lake, New Zealand	2.09	0.96	0.27	12.8	Seepage meter
Stauffer (1985)	Round Lake, Wisconsin, USA	0.548				Chemistry
Ridgway and Blanchfield (1998)	Scott Lake, Ontario, Canada	3.4		0.86	13	Seepage meter
Rosenberry et al. (2013)	Shingobee Lake, Minnesota, USA				45	Seepage meter
Rosenberry et al. (2000)	Shingobee Lake, Minnesota, USA – nonsprings	1.4		0.09	7.8	Seepage meter
Rosenberry et al. (2000)	Shingobee Lake, Minnesota, USA – springs	13.8		0.39	47.5	Seepage meter
Dimova et al. (2013)	Shipp Lake, Florida, USA	0.1				Radon
Mitchell et al. (1988)	Silver Lake, Massachusetts, USA	1.64				Seepage meter
Hagerthey and Kerfoot (1998)	Sparkling Lake, Wisconsin, USA	3.45		0.04	10.4	Seepage meter
Krabbenhoft et al. (1990)	Sparkling Lake, Wisconsin, USA	1.18	1.21	0.8	1.39	Seepage meter
Lodge et al. (1989)	Sparkling Lake, Wisconsin, USA	1.3		0.17	9.5	Seepage meter
Menheer (2004)	Square Lake, Minnesota, USA	13.1		5.9	18.3	Seepage meter
Mitchell et al. (1988)	Stetson Pond, Massachusetts, USA	1.3				Seepage meter
Ridgway and Blanchfield (1998)	Stringer Lake, Ontario, Canada	5.1				Seepage meter
Krabbenhoft and Anderson (1986)	Trout Lake, Wisconsin, USA	1.87	1.47	0.86	3.97	Seepage meter
Wentz et al. (1995)	Vandercook Lake, Wisconsin, USA	0.008	0.005	0	0.02	Darcy
Cole and Pace (1998)	West Long Lake, Michigan, USA	0.5				Chemistry
LaBaugh et al. (1995)	Williams Lake, Minnesota, USA	0.64				Darcy
Schuster et al. (2003)	Williams Lake, Minnesota, USA	0.271				Darcy
Schuster et al. (2003)	Williams Lake, Minnesota, USA			0.234	0.39	Isotopes
Erickson (1981)	Williams Lake, Minnesota, USA	0.3		0	0.71	Seepage meter
Schuster et al. (2003)	Williams Lake, Minnesota, USA			0.013	0.665	Seepage meter
Stauffer (1985)	Wolf Lake, Wisconsin, USA	0.137				Chemistry
Stauffer (1985)	Wood Lake, Wisconsin, USA	0.137				Chemistry
Rates of groundwater infiltration:						
Mitchell et al. (1988)	11 lakes in Massachusetts, USA				-4.3	Seepage meter
Ala-aho et al. (2013)	L. Ahveroinen, Finland	-1.76	-0.6	-0.09	-8.21	Seepage meter
Boyle (1994)	Alexander Lake, Ontario, Canada	-0.65		-0.02	-1.18	Seepage meter
Choi and Harvey (2000)	Everglades, Florida, USA	-0.84		-0.004	-14	Seepage meter
Rosenberry (2000)	Lake Belle Taine, Minnesota, USA	-37		-0.08	-263	Seepage meter
Isiorho and Matisoff (1990)	Lake Chad, Cameroon, Chad, Niger, and Nigeria, Africa	-0.19	-0.11	-0.002	-1.2	Seepage meter
Lee and Swancar (1997)	Lake Lucerne, Florida, USA	-0.09		-0.006	-0.15	Budget
Dorrance (1989)	Lake Mary, Arizona, USA	-0.44	-0.34	-0.15	-0.96	Seepage meter

Table 2.1 Continued.

Reference	Location	Average	Median	Minimum	Maximum	Measurement method
Woessner and Sullivan (1984)	Lake Maed, Nevada, USA	-1.05	-1.02	-0.61	-1.83	Seepage meter
Lee et al. (2014)	Lake Starr, Florida, USA	-0.18				Model
Isiorho et al. (1996)	Long Lake, Indiana, USA	-0.11		-0.002	-0.19	Seepage meter
Sebestyen and Schneider (2001)	Lower Sylvan Pond, New York, USA	-0.73		0	-1.45	Seepage meter
Asbury (1990)	Mirror Lake, New Hampshire, USA	-11.52		-0.008	-100.12	Seepage meter
Rosenberry et al. (2010)	Mirror Lake, New Hampshire, USA	-31.2		-1.9	-137	Seepage meter
Rosenberry et al. (2013)	Mirror Lake, New Hampshire, USA				-148	Seepage meter
Belanger and Kirkner (1994)	Mountain Lake, Florida, USA	-4.69	-1.008	-0.067	-36	Seepage meter
Krabbenhoft and Webster (1995)	Nevins Lake, Michigan, USA	-0.001				Chemistry
Hagerthey and Kerfoot (1998)	Sparkling Lake, Wisconsin, USA	-0.12		-0.02	-0.2	Seepage meter
Krabbenhoft et al. (1990)	Sparkling Lake, Wisconsin, USA	-0.24	-0.24	-0.2	-0.28	Seepage meter
Erickson (1981)	Williams Lake, Minnesota, USA	-0.55		0	-0.91	Seepage meter

Values are in cm per day.

Early measurements of seepage indicated substantially smaller seepage rates. Not until 1990 were rates as large as 100 cm day^{-1} reported (Figure 1D), and maximum measured seepage rates generally increase with time after 1990, particularly for lakes where exfiltration was measured (Fig. 2.1). This trend may be in part due to improving measurement methods. For example, the efficiency of seepage meters has improved substantially since the mid-1970s (Rosenberry and Menheer 2006). Some scientists also have focused more on the larger seepage rates found in near-shore margins or in unusual geologic settings. Seepage rates one to two orders of magnitude larger than those presented here have been reported for fluvial settings, and also in lakes where infiltration occurs and the sediment has been disturbed or altered (Rosenberry et al. 2010).

Table 2.2 Seepage rates for upward seepage (exfiltration) and downward seepage (infiltration at 108 lakes across the world.

	Exfiltration average	Exfiltration maximum	Infiltration average	Infiltration maximum
Count	109	59	18	18
Minimum	0.0005	0.019	0.001	0.15
25th percentile	0.23	0.76	0.18	0.92
Median	0.74	5.10	0.6	1.64
75th percentile	2.09	13.30	1.58	30.5
Maximum	124.1	745.0	37.0	263.0

2.1.6 Significance of the groundwater component in lake-water budgets

The significance of the groundwater component of a lake-water budget varies greatly and often is larger than expected. On the basis of 110 determinations of the groundwater component of a lake-water budget, including 73 for groundwater exfiltration and 37 for groundwater infiltration, groundwater as a percentage of the water budget ranged from 0.01 to 94.4 with a median value of 31.0%. Groundwater exfiltration determined at 65 lakes (some lakes had multiple determinations) ranged from 0.01% to 94.4% of the lake-water-budget input terms, with a median value of 25.0%. Groundwater infiltration determined at 44 lakes ranged from 0.1% to 91.0% of the lake-water-budget loss terms, with a median value of 34.5% (Table 2.3). As with Table 2.1, this gleaning of lakes for which water budgets have been determined is comprehensive but by no means exhaustive. Given the broad range of lake sizes represented in the table, it is likely that adding data from other studies would not substantially affect the statistical summaries of the results. However, there may be some overall bias in this dataset because some of these studies were conducted in lakes where quantification of exchange with groundwater was a goal of the study, likely because the groundwater component of the lake budget was substantial. In other studies, the groundwater component was so small as to be 'negligible' (e.g, Schindler et al. 1976) and was, therefore, not included in this analysis because no value for a groundwater component was given.

Because exchange between groundwater and lake water commonly is focused near the shoreline, it is logical to expect that groundwater would be a larger component of the water budget for small lakes where the ratio of perimeter to surface area is larger. One would be hard pressed to make this case for lakes smaller than about 100 ha. Percentages of the groundwater component of a lake-water budget range from nearly 0% to nearly 95% of inputs to lakes (Fig. 2.2A) and from nearly 0% to 91% of losses from lakes (Fig. 2.2B). For lakes larger than about 100 ha, groundwater as a percentage of a lake-water budget rarely exceeds 40%. A log-normal fit of the exfiltration data shown in Figure 2.2A indicates a poor relation between per cent groundwater component of a lake-input budget and lake surface area, explaining only 25% of the variance. If the data are binned and surface area is averaged for each order of magnitude range in surface area, a log-normal regression shows a good relation and explains 85% of the variance (Fig. 2.3). However, no such relation is evident, no matter the data manipulation, for lakes where groundwater infiltration occurs (Fig. 2.2B). One particularly interesting lake is Lake Nam Co on the Tibetan plateau with a lake-surface area greater than 100 000 ha. In spite of the large surface area for evaporating water, groundwater makes up over 60% of the water-budget loss terms (Zhou et al. 2013).

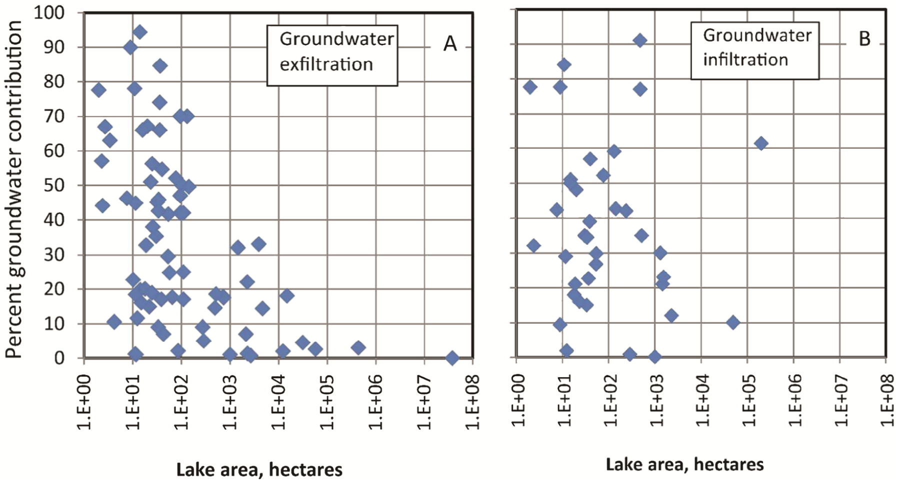

Figure 2.2 Groundwater exfiltration (A) and infiltration (B) as a percentage of a lake-water budget versus lake-surface area.

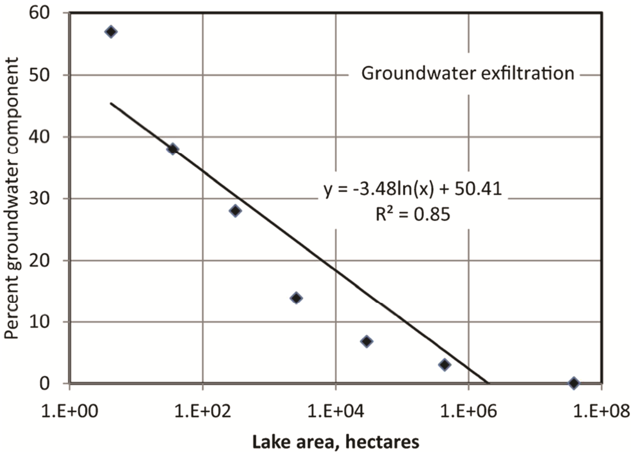

Figure 2.3 Average groundwater exfiltration as a percentage of the lake-water budget when data are grouped into orders of magnitude of lake-surface area.

Table 2.3 Groundwater exfiltration and infiltration as percentage (%) of a lake-water budget.

Reference	Location	Lake area (ha)	%	Measurement method
Exfiltration				
Brown and Cherkauer (1991)	Beaver Lake, Wisconsin, USA	132	70	Budget
Ozyavas et al. (2010)	Caspian Sea	38350000	0.01	Budget
Simpkins (2006)	Clear Lake, Iowa, USA	1468	32	Model
Gurrieri and Furniss (2004)	Cliff Lake, Montana, USA	9	90	Budget
Pina-Ochoa and Alvarez-Cobelas (2009)	Colgada Lake, Spain	103	50	Flow meter
Stets et al. (2010)	Crystal Lake, Minnesota, USA	77	52	Isotopes
Field and Duerk (1988)	Delavan Lake, Wisconsin, USA	725	17.8	Budget
Mitchell et al. (1988)	Dimmock Pond, Massachusetts, UA	42.2	10.5	Seepage meter
Belanger et al. (1985)	East Lake Tohopekaliga, Florida, USA	4680	14.3	Seepage meter
Cole and Pace (1998)	East Long Lake, Michigan, USA	2.3	57	Chemistry
Mitchell et al. (1988)	Five Mile Pond, Massachusetts, USA	14.3	19.7	Seepage meter
Sacks et al. (1998)	Grassy Lake, Florida, USA	30.4	35	Isotopes
Arnow (1985)	Great Salt Lake, Utah, USA	440000	3	Budget
Harvey et al. (2000)	Hamilton Harbor, Ontario, Canada	2150	7	Darcy
Bayer et al. (2008)	Hayes Lake, New Zealand	276	9	Seepage meter
Stets et al. (2010)	Island Lake, Minnesota, USA	32	45	Isotopes
Mitchell et al. (1988)	Knopp´s Pond, Massachusetts, USA	25.1	56.2	Seepage meter
Sacks et al. (1998)	Lake Annie, Florida, USA	36.8	85	Isotopes
Fellows and Brezonik (1980)	Lake Apopka, Florida, USA	12400	2	Seepage meter
Colman (1998)	Lake Baikal, Russia	31722	4.5	Budget
Lee (1996)	Lake Barco, Florida, USA	11.7	1	Model
Yihdego and Webb (2012)	Lake Buninjon, Australia	290	5	Budget
Yihdego and Webb (2012)	Lake Burrumbeet, Australia	2300	1.3	Budget
Wentz and Rose (1991)	Lake Clara, Wisconsin, USA	33.6	9	Darcy
Fellows and Brezonik (1980)	Lake Conway, Florida, USA	739	17.5	Seepage meter
Grubbs (1995)	Lake Five-O, Florida, USA	10.9	78	Model
Sacks et al. (1998)	Lake George, Florida, USA	23.6	51	Isotopes
Sacks et al. (1998)	Lake Hollingsworth, Florida, USA	142.4	50	Isotopes
Sacks et al. (1998)	Lake Isis, Florida, USA	20	67	Isotopes
Yihdego and Webb (2012)	Lake Linlithgow, Australia	1010	1	Budget

Table 2.3 Continued.

Reference	Location	Lake area (ha)	%	Measurement method
Mitchell et al. (1988)	Lake Lorraine, Massachusetts, USA	11.5	18.4	Seepage meter
Lee and Swancar (1997)	Lake Lucerne, Florida, USA	18	20	Darcy
Brock et al. (1982)	Lake Mendota, Wisconsin, USA	3940	33	Seepage meter
Grannemann et al. (2000)	Lake Michigan, Michigan, USA	58000	2.6	Budget
Hood et al. (2006)	Lake O´Hara, British Columbia, Canada	26	38	Budget
Sacks et al. (1998)	Lake Olivia, Florida, USA	34.4	46	Isotopes
McBride et al. (2011)	Lake Panasoffkee, Florida, USA	2280	22	Budget
Mann and McBride (1972)	Lake Sallie, Minnesota, USA	492	14.5	Darcy
Dalton et al. (2004)	Lake Seminole, Georgia, USA	15040	18	Model
Lee et al. (2014)	Lake Starr, Florida, USA	54	42	Budget
Sacks et al. (1998)	Lake Starr, Florida, USA	53.6	29	Isotopes
Kidmose et al. (2013)	Lake Vaeng	16	66	Budget
Connor and Belanger (1981)	Lake Washington, Florida, USA	2700	0.7	Seepage meter
Mitchell et al. (1988)	Little Sandy Bottom Pond, Massachusetts, USA	21.9	14.9	Seepage meter
Mitchell et al. (1988)	Loon Pond, Massachusetts, USA	10.2	22.65	Seepage meter
Mitchell et al. (1988)	Lost Lake, Massachusetts, USA	57.5	24.8	Seepage meter
Motz et al. (2001)	Lowry Lake, Florida, USA	519	19	Darcy
Jarosiewicz and Witek (2014)	Maly Borek Lake, Poland	7.6	42.6	Darcy
Stets et al. (2010)	Mary Lake, Minnesota, USA	14	94	Isotopes
Hofmann and Lessmann (2006)	Mining Lake Plessa 117, Germany	95	70	Isotopes
Hofmann et al. (2008)	Mining Lake Plessa 117, Germany	95	42	Model
Hofmann et al. (2008)	Mining Lake Plessa 117, Germany	95	47	Isotopes
Rosenberry and Winter (2009)	Mirror Lake, New Hampshire, USA	15	16	Darcy
Shaw et al. (1990)	Narrow Lake, Alberta, Canada	110	17	Seepage meter
Shaw et al. (1990)	Narrow Lake, Alberta, Canada	110	25	Darcy
Shaw et al. (1990)	Narrow Lake, Alberta, Canada	110	42	Budget
Mitchell et al. (1988)	Nashawannuck Pond, Massachusetts, USA	11.3	1.2	Seepage meter
Cole and Pace (1998)	Peter Lake, Michigan, USA	2.7	67	Chemistry
Mitchell et al. (1988)	Richmond Pond, Massachusetts, USA	86.6	2.1	Seepage meter
Gurrieri and Furniss (2004)	Rock Lake, Montana, USA	18.9	33	Budget
Sacks et al. (1998)	Round Lake, Florida, USA	12.4	12	Isotopes
Sacks et al. (1998)	Saddle Blanket Lake, Florida, USA	2.4	44	Isotopes
Stets et al. (2010)	Shingobee Lake, Minnesota, USA	65	18	Isotopes
Mitchell et al. (1988)	Silver Lake, Massachusetts, USA	11.5	44.8	Seepage meter
Stets et al. (2010)	Steel Lake, Minnesota, USA	25	19	Isotopes
Mitchell et al. (1988)	Stetson Pond, Massachusetts, USA	33.8	42.6	Seepage meter
Sacks et al. (1998)	Swim Lake, Florida, USA	2	78	Isotopes
Wentz and Rose (1991)	Vandercook Lake, Wisconsin, USA	38.8	17	Darcy
Wentz et al. (1995)	Vandercook Lake, Wisconsin, USA	43	7	Darcy
Cole and Pace (1998)	West Long Lake, Michigan, USA	3.4	63	Chemistry
LaBaugh et al. (1995)	Williams Lake, Minnesota, USA	36	66	Darcy
LaBaugh et al. (1997)	Williams Lake, Minnesota, USA	36	74	Darcy
Stets et al. (2010)	Williams Lake, Minnesota, USA	40	55	Isotopes
Infiltration				
Deevey (1988)	10 lakes in central Florida, USA	1317	30	Budget
Brown and Cherkauer (1991)	Beaver Lake, Wisconsin, USA	132	59	Budget

Table 2.3 Continued.

Reference	Location	Lake area (ha)	%	Measurement method
Simpkins (2006)	Clear Lake, Iowa, USA	1468	21	Model
Gurrieri and Furniss (2004)	Cliff Lake, Montana, USA	9	78	Budget
Stets et al. (2010)	Crystal Lake, Minnesota, USA	77	52	Isotopes
Choi and Harvey (2000)	Everglades Nutrient Removal Project, Florida, USA	1544	23	Seepage meter
Sacks et al. (1998)	Grassy Lake, Florida, USA	30.4	35	Budget
Sacks et al. (1998)	Lake Annie, Florida, USA	36.8	23	Budget
Lee (1996)	Lake Barco, Florida, USA	11.7	29	Model
Rosenberry (2000)	Lake Belle Taine, Minnesota, USA	480	91	Seepage meter
Yihdego and Webb (2012)	Lake Buninjon, Australia	290	0.8	Budget
Yihdego and Webb (2012)	Lake Burrumbeet, Australia	2300	12	Budget
Wentz and Rose (1991)	Lake Clara, Wisconsin, USA	33.6	15	Darcy
Grubbs (1995)	Lake Five-O, Florida, USA	10.9	84	Model
Sacks et al. (1998)	Lake George, Florida, USA	23.6	16	Budget
Sacks et al. (1998)	Lake Hollingsworth, Florida, USA	142.4	43	Budget
Sacks et al. (1998)	Lake Isis, Florida, USA	20	48	Budget
Yihdego and Webb (2012)	Lake Linlithgow, Australia	1010	0.1	Budget
Lee and Swancar (1997)	Lake Lucerne, Florida, USA	18	18	Budget
Dorrance (1989)	Lake Mary, Arizona, USA	240	42	Seepage meter
Zhou et al. (2013)	Lake Nam Co, Tibet	201700	6	Budget
Sacks et al. (1998)	Lake Olivia, Florida, USA	34.4	35	Budget
Lee et al. (2014)	Lake Starr, Florida, USA	54	30	Budget
Sacks et al. (1998)	Lake Starr, Florida, USA	53.6	27	Budget
Vallet-Coulomb et al. (2001)	Lake Ziway, Ethiopia	50000	10	Budget
Motz (1998)	Lowry Lake, Florida, USA	519	35	Budget
Jarosiewicz and Witek (2014)	Maly Borek Lake, Poland	7.6	42.3	Darcy
Healy et al. (2007)	Mirror Lake, New Hampshire, USA	15	51	Darcy
Rosenberry and Winter (2009)	Mirror Lake, New Hampshire, USA	15	50	Darcy
Belanger and Kirkner (1994)	Mountain Lake, Florida, USA	483	77	Seepage meter
Gurrieri and Furniss (2004)	Rock Lake, Montana, USA	18.9	21	Budget
Sacks et al. (1998)	Round Lake, Florida, USA	12.4	2	Budget
Sacks et al. (1998)	Saddle Blanket Lake, Florida, USA	2.4	32	Budget
Hines and Brezonik (2007)	Spring Lake, Minnesota, USA	8.9	9	Budget
Sacks et al. (1998)	Swim Lake, Flolrida, USA	2	78	Budget
Wentz and Rose (1991)	Vandercook Lake, Wisconsin, USA	38.8	39	Darcy
Stets et al. (2010)	Williams Lake, Minnesota, USA	40	57	Isotopes

2.1.7 Influence of measurement method on determination of groundwater exfiltration and infiltration

The interpreted exchange between groundwater and surface water depends substantially on the method of quantification. Calculating a groundwater component as the residual of a water budget or using a conservative water or chemical tracer or combining water and chemical budgets provides a value that is integrated across the entire lake, or in some cases an entire bay or other lake component that may be reasonably isolated from the rest of the lake. Segmenting a lakeshore according to locations of monitoring wells (Darcy approach), from which hydraulic gradients and estimates of hydraulic conductivity are obtained, including incorporating that information into a groundwater-flow model, provides groundwater exfiltration and infiltration data for specific portions of lakes that then need to be summed to represent the whole lake. Although conceptually sound, this method comes with the large uncertainty in the scale-appropriate value for hydraulic conductivity (e.g., Rovey and Cherkauer 1995). Calculating a groundwater component on the basis of seepage-meter measurements is only representative of the portion of the lakebed covered by the seepage cylinders; results from multiple meters must then be extrapolated across the rest of the lakebed area.

Table 2.4 Groundwater component of lake-water budget based on measurement method.

	Water budget	Chemistry budget	Darcy method	Seepage meter
All data				
n	37	23	27	23
Average	28.8	51.8	33.1	27.6
Median	22.6	52.0	29.0	19.7
Maximum	89.9	94.4	84.0	91.0
Minimum	0.01	11.5	1.0	0.7
Exfiltration only				
n	15	21	18	19
Average	26.4	51.5	29.6	21.1
Median	17.8	50.9	19.3	17.5
Maximum	89.9	94.4	78.0	56.2
Minimum	0.01	11.5	1.0	0.7
Infiltration only				
n	22	2	9	4
Average	30.5	54.5	40.1	58.3
Median	28.4	54.5	39.0	59.5
Maximum	77.6	56.9	84.0	91.0
Minimum	0.1	52.2	15.0	23.0

Values in percentage of the sum of all input or loss terms of the lake-water budget. Chemistry budget includes entries listed as 'Isotopes' in Table 2.3. Darcy method includes entries listed as 'Model' in Table 2.3. Seepage meter includes entries listed as 'Flow meter' in Table 2.3.

In spite of these issues of scale, parsing 110 quantifications of the groundwater component of a lake budget (data from Table 2.3) on the basis of the measurement method results in surprisingly little difference in the method-averaged groundwater component for the lake-water budgets available for this analysis (Table 2.4). When exfiltration and infiltration are lumped together, median values based on water budget, chemical budget, Darcy or seepage-meter measurements range from about 20% to 52%. The scale of measurement appears to have little to do with the range in percentages. The median groundwater percentages resulting from the two methods that integrate the whole lake, the lake-water and lake-chemistry budget methods, are 23% and 52%, respectively. Similar ranges occur for both exfiltration-only and infiltration-only analyses (Table 2.4). The median groundwater percentage based on the most locally determined measurements, seepage meters, is 20% if both exfiltration and infiltration lakes are considered, 18% for exfiltration-only lakes and 60% for infiltration-only lakes.

Although generally smaller, the seepage-meter percentages are not appreciably smaller given the range of percentages indicated by the methods that integrate a larger portion of the lake area.

Some studies have quantified groundwater exfiltration and/or infiltration using several methods. Results often are substantially different among methods. LaBaugh et al. (1997) determined exfiltration and infiltration using Darcy calculations, and also with combined water and chemical budgets using several chemical constituents, including water isotopes. The Darcy-based estimate of groundwater exfiltration was close to 400m^3/year. The best estimate using oxygen isotopes of water was 525, although that value ranged from 320 to 650, depending on the range in estimates of the isotopic value of evaporating water. Values for groundwater exfiltration using major ions ranged from 60 based on chloride to 300 based on sodium. An estimate using dissolved organic carbon was over 1000. Precipitation, at 140m^3/year, was the only other input term. Therefore, the Darcy-based best estimate for groundwater exfiltration was 74% of the water-budget input terms. Estimates from combined water and chemical mass budgets ranged from 30% to 88% (LaBaugh et al. 1997). Meinikmann et al. (2013) compared groundwater exfiltration rates to a lake using temperature-depth profiles with watershed-scale equipotential lines drawn from field data. As might be expected, spatial variability of exfiltration rates was greater on the basis of temperature; however, the temperature-based results also indicated that the largest rates of groundwater exfiltration were not always located where hydraulic gradients were largest. Discrepancies likely arose from limited opportunities for measurement of hydraulic head in groundwater, especially near the shoreline.

Others have combined Darcy-based flow determinations with water-budget calculations to reduce the uncertainty associated with estimates of hydraulic conductivity. Lee and Swancar (1997), in a very detailed study of a lake in Florida, used a flow-net analysis based on an extensive network of monitoring wells to calculate flows of groundwater to and from the lake. They determined that groundwater exfiltration occurred around the entire perimeter of the lake and groundwater infiltration occurred in the middle, deepest portion of the lake. Darcy-based estimates were determined to be too small when compared with an analysis of water-budget terms over a period of several months. By comparing net groundwater flow based on the residual of monthly water budgets with net groundwater flow from their Darcy-based flow-net calculations, they were able to determine that actual groundwater exfiltration was about 1.2 times larger than their flow-net estimates. Others also have adjusted Darcy-based calculations of groundwater flows to match more closely values from combined water and chemical budgets (e.g., Sacks et al. 1998). Combining results from multiple methods often reduces the uncertainty of estimates of groundwater exfiltration or infiltration (e.g, Hines and Brezonik 2007; Hofmann et al. 2008; Kidmose et al. 2011; Yihdego and Webb 2012). Perhaps the greatest potential for advancement in understanding and quantification of flow across the groundwater–lakebed interface will come from combining measurement methods in clever new ways.

2.1.8 Summary

Measured rates of groundwater exfiltration and groundwater infiltration vary by five orders of magnitude in lacustrine settings, on the basis of 127 values gleaned from the literature. Of these values, 85% were groundwater exfiltration, and 15% were groundwater infiltration. The median rate of exfiltration (0.74 cm day^{-1}) was nearly the same as the median rate of infiltration (0.60 cm day^{-1}). Maximum measured exfiltration (745 cm day^{-1}) was almost three times larger than the maximum infiltration rate of 263 cm day^{-1}. However, four values for maximum infiltration were larger than 100 cm day^{-1}, whereas the second largest value for maximum exfiltration was 80 cm day^{-1}.

The groundwater component of 110 measured lake- water budgets ranged from near 0% to just under 95%, with a median value of 31%. Although surprisingly large, this value may be somewhat biased; several of the cited studies were conducted for the specific purpose of determining what was suspected to be a substantial groundwater contribution to a lake-water budget. The percentage of the groundwater component generally decreased as lake area increased, but only in the case of groundwater exfiltration and only for lakes greater than about 100 ha in area. No percentage-versus-lake area relation was evident for groundwater infiltration on the basis of 37 lake-water budget calculations. Determination of per cent groundwater contribution to a lake budget depends substantially on the method used to quantify the groundwater term. Use of multiple methods to estimate the groundwater component is suggested to reduce this uncertainty.

2.1.9 References

Ala-aho, P., Rossi, P.M., Kløve, B., 2013. Interaction of esker groundwater with headwater lakes and streams. *Journal of Hydrology*, 500(0): 144-156.

Alley, W.M., Reilly, T.E., Franke, O.L., 1999. Sustainability of ground-water resources. *U.S. Geological Survey Circular* 1186: 79 p.

Anderson, M.P., Hunt, R.J., Krohelski, J.T., Chung, K., 2002. Using High Hydraulic Conductivity Nodes to Simulate Seepage Lakes. *Ground Water*, 40(2): 117-122.

Anderson, R.B., Naftz, D.L., Day-Lewis, F.D., Henderson, R.D., Rosenberry, D.O., Stolp, B.J., Jewell, P., 2014. Quantity and quality of groundwater discharge in a hypersaline lake environment. *Journal of Hydrology*, 512: 177-194.

Anibas, C., Fleckenstein, J.H., Volze, N., Buis, K., Verhoeven, R., Meire, P., Batelaan, O., 2009. Transient or steady-state? Using vertical temperature profiles to quantify groundwater-surface water exchange. *Hydrological Processes*, 23(15): 2165-2177.

Arnow, T., 1985. Water-level and water-quality changes in Great Salt Lake, Utah 1843–1985. In: *Orogenic Patterns and Stratigraphy of Northcentral Utah and Southeastern Idaho*, Kerns, G.J., Kerns, J.R.L. (Eds.). Utah Geological Association, Salt Lake City, 227–236.

Asbury, C., 1990. The role of groundwater seepage in sediment chemistry and nutrient budgets in Mirror Lake, New Hampshire. Ph.D. Thesis, Cornell University, p.

Attanayake, M.P., Waller, D.H., 1988. Use of seepage meters in a groundwater – lake interaction study in a fractured rock basin — a case study. *Canadian Journal of Civil Engineering*, 15(6): 984-989.

Baedecker, M.J., Friedman, L.C., 2000. Water, Energy, and Biogeochemical Budgets: A Watershed Research Program. *Fact Sheet*, FS 165-99: 4.

Baird, A.J., Wilby, R.L., 1999. *Eco-hydrology: Plants and Water in Terrestrial and Aquatic Environments Routledge Physical Environment Series*. Routledge, London, 402 p.

Bartolino, J.R., Niswonger, R.G., 1999. Numerical simulation of vertical ground-water flux of the Rio Grande from ground-water temperature profiles, central New Mexico. *U.S. Geological Survey Water-Resources Investigations Report* 99-4212: 40 p.

Baskin, R.L., 1998. Locating Shoreline and Submarine Springs in Two Utah Lakes using Thermal Imagery. In: *Modern and Ancient Lake Systems: New Problems and Perspectives*, Pitman, J.K., Carroll, A.R. (Eds.). Utah Geological Association, Salt Lake City, Utah, 51-57.

Bates, C.G., Henry, A.J., 1928. Forests and streamflow at Wagon Wheel Gap, Colorado. *Monthly Weather Review*, 30: 1-79.

Bayer, T.K., Schallenberg, M., Martin, C.E., 2008. Investigation of nutrient limitation status and nutrient pathways in Lake Hayes, Otago, New Zealand: A case study for integrated lake assessment. *New Zealand Journal of Marine and Freshwater Research*, 42(3): 285-295.

Belanger, T.V., Kirkner, R.A., 1994. Groundwater/Surface Water Interaction in a Florida Augmentation Lake. *Lake and Reservoir Management*, 8: 165–174.

Belanger, T.V., Mikutel, D.F., Churchill, P.A., 1985. Groundwater seepage nutrient loading in a Florida lake. *Water Research*, 19(6): 773-781.

Bertin, C., Bourg, A.C.M., 1994. Radon-222 and Chloride as Natural Tracers of the Infiltration of River Water into an Alluvial Aquifer in Which There Is Significant River/Groundwater Mixing. *Environmental Science & Technology*, 28(5): 794-798.

Beven, K., Feyen, J., 2002. The future of distributed modelling - Special issue. *Hydrological Processes*, 16(2): 169-172.

Beven, K.J., Kirkby, M.J., Schofield, N., Tagg, A.F., 1984. Testing a physically-based flood forecasting model (TOPMODEL) for three U.K. catchments. *Journal of Hydrology*, 69(1): 119-143.

Blume, T., Krause, S., Meinikmann, K., Lewandowski, J., 2013. Upscaling lacustrine groundwater discharge rates by fiber-optic distributed temperature sensing. *Water Resources Research*, 49(12): 7929-7944.

Bouwer, H., Rice, R.C., 1976. A slug test for determining hydraulic conductivity of unconfined aquifers with completely or partially penetrating wells. *Water Resources Research*, 12(3): 423-428.

Boyle, D.R., 1994. Design of a seepage meter for measuring groundwater fluxes in the non-littoral zones of lakes - evaluation in a boreal forest lake. *Limnology and Oceanography*, 39(3): 670-681.

Briggs, M.A., Lautz, L.K., McKenzie, J.M., Gordon, R.P., Hare, D.K., 2012. Using high-resolution distributed temperature sensing to quantify spatial and temporal variability in vertical hyporheic flux. *Water Resources Research*, 48(2): W02527.

Briggs, M.A., Voytek, E.B., Day-Lewis, F.D., Rosenberry, D.O., Lane, J.W., 2013. Understanding Water Column and Streambed Thermal Refugia for Endangered Mussels in the Delaware River. *Environmental Science & Technology*, 47(20): 11423-11431.

Brock, T.D., Lee, D.R., Janes, D., Winek, D., 1982. Groundwater seepage as a nutrient source to a drainage lake - Lake Mendota, Wisconsin. *Water Research*, 16(7): 1255-1263.

Brönmark, C., Hansson, L.A., 2002. Environmental issues in lakes and ponds: current state and perspectives. *Environmental Conservation*, 29(3): 290-307.

Broughton, W., 1941. The geology, ground water, and lake basin seal of the region south of the Muskellunge Moraine, Vilas County, Wisconsin. *Transactions of the Wisconsin Academy of Sciences, Arts and Letter*, 33: 5–20.

Brown, B.E., Cherkauer, D.S., 1991. Phosphate and carbonate mass balances and their relationships to groundwater inputs at Beaver Lake, Waukesha County, Wisconsin. *University of Wisconsin Water Resources Center Technical Completion Report*, G1458-04: 43.

Bruckner, A.E., Hornberger, G.M., Mills, A.L., 1989. Field measurement and associated controlling factors for groundwater seepage in a piedmont impoundment. *Hydrological Processes*, 3(3): 223-235.

Brunke, M., Gonser, T.O.M., 1997. The ecological significance of exchange processes between rivers and groundwater. *Freshwater Biology*, 37(1): 1-33.

Bukaveckas, P.A., Likens, G.E., Winter, T.C., Buso, D.C., 1998. A Comparison of Methods for Deriving Solute Flux Rates Using Long-Term Data from Streams in the Mirror Lake Watershed. In: *Biogeochemical Investigations at Watershed, Landscape, and Regional Scales: Refereed papers from BIOGEOMON, The Third International Symposium on Ecosystem Behavior; Co-Sponsored by Villanova University and the Czech Geological Survey; held at Villanova University, Villanova Pennsylvania, USA, June 21–25, 1997*, Wieder, R.K., Novák, M., Černý, J. (Eds.). Springer Netherlands, Dordrecht, 277-293.

Bundschuh, J., 1993. Modeling annual variations of spring and groundwater temperatures associated with shallow aquifer systems. *Journal of Hydrology*, 142(1): 427-444.

Cardenas, M.B., Lagmay, A.M.F., Andrews, B.J., Rodolfo, R.S., Cabria, H.B., Zamora, P.B., Lapus, M.R., 2012. Terrestrial smokers: Thermal springs due to hydrothermal convection of groundwater connected to surface water. *Geophysical Research Letters*, 39.

Cedergren, H.R., 1997. *Seepage, Drainage, and Flow Nets. Wiley Professional Paper Back Series*. Wiley and Sons, New York, 496 p.

Cherkauer, D.A., McBride, J.M., 1988. A Remotely Operated Seepage Meter for Use in Large Lakes and Rivers. *Ground Water*, 26(2): 165-171.

Cherkauer, D.S., Nader, D.C., 1989. Distribution of groundwater seepage to large surface-water bodies: The effect of hydraulic heterogeneities. *Journal of Hydrology*, 109(1–2): 151-165.

Cherkauer, D.S., Zager, J.P., 1989. Groundwater interaction with a kettle-hole lake: Relation of observations to digital simulations. *Journal of Hydrology*, 109(1): 167-184.

Choi, J., Harvey, J.W., 2000. Quantifying time-varying ground-water discharge and recharge in wetlands of the northern Florida Everglades. *Wetlands*, 20(3): 500-511.

Cole, J.J., Pace, M.L., 1998. Hydrologic Variability of Small, Northern Michigan Lakes Measured by the Addition of Tracers. *Ecosystems*, 1(3): 310-320.

Colman, S.M., 1998. Water-level changes in Lake Baikal, Siberia: tectonism versus climate. *Geology*, 26(6): 531-534.

Conant, J.B., 2000. Ground-water plume behavior near the ground-water/surface water interface of a river. *Proceedings of the Ground-water/Surface-water Interactions Workshop*: 23–30.

Conant, J.B., 2004. Delineating and quantifying ground water discharge zones using streambed temperatures. *Ground Water*, 42(2): 243-257.

Connor, J.N., Belanger, T.V., 1981. Ground water seepage in Lake Washington and the Upper St. Johns River Basin, Florida. *Journal of the American Water Resources Association*, 17(5): 799-805.

Constantz, J., Thomas, C.L., Zellweger, G., 1994. Influence of diurnal variations in stream temperature on streamflow loss and groundwater recharge. *Water Resources Research*, 30(12): 3253-3264.

Cooley, R.L., 1983. Some new procedures for numerical solution of variably saturated flow problems. *Water Resources Research*, 19(5): 1271-1285.

Cornett, R.J., Risto, B.A., Lee, D.R., 1989. Measuring groundwater transport through lake sediments by advection and diffusion. *Water Resources Research*, 25(8): 1815-1823.

Cullmann, J., Junk, W.J., Weber, G., Schmitz, G.H., 2006. The impact of seepage influx on cation content of a Central Amazonian floodplain lake. *Journal of Hydrology*, 328(1–2): 297-305.

Dalton, M.S., Aulenbach, B.T., Torak, L.J., 2004. Ground-water and surface-water flow and estimated water budget for Lake Seminole, southwestern Georgia and northwestern Florida. *U.S. Geological Survey Scientific Investigations Report* 2004-5073: 49 p.

Danielopol, D.L., 1984. Ecological investigations on the alluvial sediments of the Danube in the Vienna area – a phreatobiological project. *Verhandlungen. Internationale Vereinigung fur theoretische und angewandte Limnologie*, 22: 1755–1761.

Danielopol, D.L., Rouch, R., Pospisil, P., Torreiter, P., Moeszlacher, F., 1997. Ecotonal animal assemblages; their interest for groundwater studies. In: *Groundwater/Surface Water Ecotones: Biological and Hydrological Interactions and Management Options*, Gibert, J., Mathieu, J., Fournier, F. (Eds.). International Hydrology Series. Cambridge University Press, Cambridge, 11–20.

Day-Lewis, F.D., White, E.A., Johnson, C.D., Jr., J.W.L., Belaval, M., 2006. Continuous resistivity profiling to delineate submarine groundwater discharge—examples and limitations. *The Leading Edge*, 25(6): 724-728.

Deevey, E.S., 1988. Estimation of downward leakage from Florida lakes. *Limnology and Oceanography*, 33(6): 1308-1320.

Dimova, N.T., Burnett, W.C., Chanton, J.P., Corbett, J.E., 2013. Application of radon-222 to investigate groundwater discharge into small shallow lakes. *Journal of Hydrology*, 486: 112-122.

Dinçer, T., 1968. The Use of Oxygen 18 and Deuterium Concentrations in the Water Balance of Lakes. *Water Resources Research*, 4(6): 1289-1306.

Dorrance, D.W., 1989. Streaming potential and seepage meter studies at Upper Lake Mary near Flagstaff, Arizona, University of Arizona, 182 p.

Downing, J.A., Peterka, J.J., 1978. Relationship of rainfall and lake groundwater seepage. *Limnology and Oceanography*, 23(4): 821-825.

Erickson, D.R., 1981. A study of littoral groundwater seepage at Williams Lake, Minnesota using seepage meters and wells. MS Thesis, University of Minnesota, 153 p.

Federer, C.A., Lash, D., 1978. BROOK: A hydrologic simulation model for eastern forests. *Research report / Water Resource Research Center, University of New Hampshire*, 19: 84.

Fellows, C.R., Brezonik, P.L., 1980. Seepage inflow into Florida lakes. *Journal of the American Water Resources Association*, 16(4): 635-641.

Ferrey, M.L., Lundy, J.R., Estuesta, P., 2001. The Effect of Groundwater Aeration on PCE Natural Attenuation Patterns. *Bioremediation Journal*, 5(3): 211-224.

Fetter, J.C.W., 1994. *Applied Hydrogeology*. Prentice Hall, Englewood Cliffs, 691 p.

Ficke, J.F., 1972. Comparison of evaporation computation methods, Pretty Lake, Lagrange County, northeastern Indiana. *U.S. Geological Survey Professional Paper* 686-A: 48 p.

Field, S.J., Duerk, M.D., 1988. Hydrology and water quality of Delavan Lake in southeastern Wisconsin. *U.S. Geological Survery Water-Resources Investigations Report* 87-4168: 61 p.

Fleckenstein, J.H., Krause, S., Hannah, D.M., Boano, F., 2010. Groundwater-surface water interactions: New methods and models to improve understanding of processes and dynamics. *Advances in Water Resources*, 33(11): 1291-1295.

Frandsen, M., Nilsson, B., Engesgaard, P., Pedersen, O.L.E., 2012. Groundwater seepage stimulates the growth of aquatic macrophytes. *Freshwater Biology*, 57(5): 907-921.

Fritz, B.G., Mendoza, D.P., Gilmore, T.J., 2009. Development of an electronic seepage chamber for extended use in a river. *Ground Water, 47(1):136-140*: Medium: X.

Fryar, A.E., Wallin, E.J., Brown, D.L., 2000. Spatial and temporal variability in seepage between a contaminated aquifer and tributaries to the Ohio River. *Ground Water Monitoring and Remediation*, 20(3): 129-146.

Gardner, K.M., 1999. Importance of Surface Water/groundwater Interactions - Issue Paper. *U.S. Environmental Protection Agency*, 23 p.

Genereux, D., Bandopadhyay, I., 2001. Numerical investigation of lake bed seepage patterns: effects of porous medium and lake properties. *Journal of Hydrology*, 241(3–4): 286-303.

Gordon, R.P., Lautz, L.K., Briggs, M.A., McKenzie, J.M., 2012. Automated calculation of vertical pore-water flux from field temperature time series using the VFLUX method and computer program. *Journal of Hydrology*, 420–421: 142-158.

Goslee, S.C., Brooks, R.P., Cole, C.A., 1997. Plants as indicators of wetland water source. *Plant Ecology*, 131(2): 199-206.

Gosselin, D.C., Rundquist, D.C., McFeeters, S.K., 2000. Remote monitoring of selected ground-water dominated lakes in the Nebraska Sand Hills. *Journal of the American Water Resources Association*, 36(5): 1039-1051.

Grannemann, N.G., Hunt, R.J., Nicholas, J.R., Reilly, T.E., Winter, T.C., 2000. The importance of ground water in the Great Lakes Region. *Water-Resources Investigations Report*, 00–4008: 19.

Greenland, D., Goodin, D.G., Smith, R.C., 2003. *Climate Variability and Ecosystem Response at Long-term Ecological Research Sites. Long-term Ecological Research Network Series.* Oxford University Press, 480 p.

Grubbs, J.W., 1995. Evaluation of ground-water flow and hydrologic budget for Lake Five-O, a seepage lake in northwestern Florida. *U.S. Geological Survey Water-Resources Investigations Report* 94-4145: 41 p.

Gurnell, A.M., Hupp, C.R., Gregory, S.V., 2000. Linking hydrology and ecology. *Hydrological Processes*, 14: 2813-2815.

Gurrieri, J.T., Furniss, G., 2004. Estimation of groundwater exchange in alpine lakes using non-steady mass-balance methods. *Journal of Hydrology*, 297(1-4): 187-208.

Hagerthey, S.E., Kerfoot, W.C., 1998. Groundwater flow influences the biomass and nutrient ratios of epibenthic algae in a north temperate seepage lake. *Limnology and Oceanography*, 43(6): 1227-1242.

Hall, B.R., Raynal, D.J., Leopold, D.J., 2001. Environmental influences on plant species composition in ground-water seeps in the Catskill Mountains of New York. *Wetlands*, 21(1): 125-134.

Harbaugh, A.W., Banta, E.R., Hill, M.C., McDonald, M.G., 2000. MODFLOW-2000, The U.S. Geological Survey Modular Ground-Water Model - User Guide to Modularization Concepts and the Ground-Water Flow Process. *U.S. Geological Survey Open-File Report* 00-0092: 121 p.

Harbeck, G.E.J., Kohler, M.A., Koberg, G.E., 1958. Water-loss investigations: Lake Mead studies. *U.S. Geological Survey Professional Paper* 298: 100 p.

Harvey, F.E., Rudolph, D.L., Frape, S.K., 2000. Estimating ground water flux into large lakes: Application in the Hamilton Harbor, western Lake Ontario. *Ground Water*, 38(4): 550-565.

Harvey, J.W., Wagner, B.J., Bencala, K.E., 1996. Evaluating the Reliability of the Stream Tracer Approach to Characterize Stream-Subsurface Water Exchange. *Water Resources Research*, 32(8): 2441-2451.

Hatch, C.E., Fisher, A.T., Ruehl, C.R., Stemler, G., 2010. Spatial and temporal variations in streambed hydraulic conductivity quantified with time-series thermal methods. *Journal of Hydrology*, 389(3–4): 276-288.

Hayashi, M., Rosenberry, D.O., 2002. Effects of ground water exchange on the hydrology and ecology of surface water. *Ground Water*, 40(3): 309-316.

Hayashi, M., van der Kamp, G., Rudolph, D.L., 1998. Water and solute transfer between a prairie wetland and adjacent uplands, 1. Water balance. *Journal of Hydrology*, 207(1-2): 42-55.

Healy, R.W., Winter, T.C., LaBaugh, J.W., Franke, O.L., 2007. Water Budgets: Foundations for Effective Water-Resources and Environmental Management. *U.S. Geological Survey Circular* 1308: 98 p.

Heitmann, M., Schubert, H., 1965. Lake Stechlin – a hydrometeorological research area. *Publ. IASH: Budapest*, 66: 429–440.

Herczeg, A.L., Leaney, F.W., Dighton, J.C., Lamontagne, S., Schiff, S.L., Telfer, A.L., English, M.C., 2003. A modern isotope record of changes in water and carbon budgets in a groundwater-fed lake: Blue Lake, South Australia. *Limnology and Oceanography*, 48(6): 2093-2105.

Herrmann, R., 1997. Long-term watershed research and monitoring to understand ecostystem change in parks and equivalent reserves. *Journal of the American Water Resources Association*, 33(4): 747-753.

Hill, M.C., 1992. A computer program (MODFLOWP) for estimating parameters of a transient, three-dimensional ground-water flow model using nonlinear regression. *Open-File Report.*

Hines, N.A., Brezonik, P.L., 2007. Mercury inputs and outputs at a small lake in northern Minnesota. *Biogeochemistry*, 84(3): 265-284.

Hiscock, K.M., Grischek, T., 2002. Attenuation of groundwater pollution by bank filtration. *Journal of Hydrology*, 266(3–4): 139-144.

Hofmann, H., Knöller, K., Lessmann, D., 2008. Mining lakes as groundwater-dominated hydrological systems: assessment of the water balance of Mining Lake Plessa 117 (Lusatia, Germany) using stable isotopes. *Hydrological Processes*, 22(23): 4620-4627.

Hofmann, H., Lessmann, D., 2006. Hydrogeochemistry of groundwater seepage into an acidic mining lake. *Proceedings of the International Association of Theoretical and Applied Limnology*, 29: 1452–1456.

Holzbecher, E., 2001. The dynamics of subsurface water divides—watersheds of Lake Stechlin and neighbouring lakes. *Hydrological Processes*, 15(12): 2297-2304.

Hood, J.L., Roy, J.W., Hayashi, M., 2006. Importance of groundwater in the water balance of an alpine headwater lake. *Geophysical Research Letters*, 33(13): L13405.

Hsieh, P.A., 2001. TopoDrive and ParticleFlow--Two Computer Models for Simulation and Visualization of Ground-Water Flow and Transport of Fluid Particles in Two Dimensions. *Open-File Report*.

Hunt, R.J., Haitjema, H.M., Krohelski, J.T., Feinstein, D.T., 2003. Simulating ground water-lake interactions: Approaches and insights. *Ground Water*, 41(2): 227-237.

Hunt, R.J., Walker, J.F., Selbig, W.R., Westenbroek, S.M., Regan, R.S., 2013. Simulation of climate-change effects on streamflow, lake water budgets, and stream temperature using GSFLOW and SNTEMP, Trout Lake Watershed, Wisconsin. *Scientific Investigations Report*: 128 p.

Hunt, R.J., Zheng, C., 2012. The current state of modeling. *Ground Water*, 50(3): 330-333.

Isiorho, S.A., Beeching, F.M., Stewart, P.M., Whitman, R.L., 1996. Seepage measurements from Long Lake, Indiana Dunes National Lakeshore. *Environmental Geology*, 28(2): 99-105.

Isiorho, S.A., Matisoff, G., 1990. Groundwater recharge from Lake Chad. *Limnology and Oceanography*, 35(4): 931-938.

Israelson, O.W., Reeve, R.C., 1944. Canal Lining Experiments in the Delta Area, Utah. *Utah Agricultural Experimental Station Bulletin*, 313: 15–35.

Jarosiewicz, A., Witek, Z., 2014. Where do nutrients in an inlet-less lake come from? The water and nutrient balance of a small mesotrophic lake. *Hydrobiologia*, 724(1): 157-173.

John, P.H., Lock, M.A., 1977. The spacial distribution of groundwater discharge into the littoral zone of a New Zealand lake. *Journal of Hydrology*, 33(3): 391-395.

Jones, J.B., Mulholland, P.J., 2000. *Streams and Ground Waters*. Academic Press, San Diego, 425 p.

Kalbus, E., Reinstorf, F., Schirmer, M., 2006. Measuring methods for groundwater - surface water interactions: a review. *Hydrology and Earth System Sciences*, 10(6): 873-887.

Kang, W.J., Kolasa, K.V., Rials, M.W., 2005. Groundwater inflow and associated transport of phosphorus to a hypereutrophic lake. *Environmental Geology*, 47(4): 565-575.

Katz, B.G., Coplen, T.B., Bullen, T.D., Davis, J.H., 1997. Use of Chemical and Isotopic Tracers to Characterize the Interactions Between Ground Water and Surface Water in Mantled Karst. *Ground Water*, 35(6): 1014-1028.

Kendall, C., Sklash, M.G., Bullen, T.D., 1995. Isotope tracers of water and solute sources in catchments. In: *Solute Modelling in Catchment Systems*, Trudgill, S.T. (Ed.). John Wiley & Sons, Chichester, UK, 261–303.

Kenoyer, G.J., Anderson, M.P., 1989. Groundwater's dynamic role in regulating acidity and chemistry in a precipitation-dominated lake. *Journal of Hydrology*, 109(3): 287-306.

Kidmose, J., Engesgaard, P., Nilsson, B., Laier, T., Looms, M.C., 2011. Spatial Distribution of Seepage at a Flow-Through Lake: Lake Hampen, Western Denmark. *Vadose Zone Journal*, 10(1): 110-124.

Kidmose, J., Nilsson, B., Engesgaard, P., Frandsen, M., Karan, S., Landkildehus, F., Sondergaard, M., Jeppesen, E., 2013. Focused groundwater discharge of phosphorus to a eutrophic seepage lake (Lake Væng, Denmark): implications for lake ecological state and restoration. *Hydrogeology Journal*, 21(8): 1787-1802.

Kim, K., Anderson, M.P., Bowser, C.J., 2000. Enhanced dispersion in groundwater caused by temporal changes in recharge rate and lake levels. *Advances in Water Resources*, 23(6): 625-635.

Konikow, L.F., Bredehoeft, J.D., 1992. Ground-water models cannot be validated. *Advances in Water Resources*, 15(1): 75-83.

Krabbenhoft, D.P., Anderson, M.P., 1986. Use of a numerical groundwater-flow model for hypothesis-testing. *Ground Water*, 24(1): 49-55.

Krabbenhoft, D.P., Bowser, C.J., Anderson, M.P., Valley, J.W., 1990. Estimating groundwater exchange with lakes. 1. The stable isotope mass balance method. *Water Resources Research*, 26(10): 2445-2453.

Krabbenhoft, D.P., Webster, K.E., 1995. Transient hydrogeological controls on the chemistry of a seepage lake. *Water Resources Research*, 31(9): 2295-2305.

Krupa, S.L., Belanger, T.V., Heck, H.H., Brock, J.T., Jones, B.J., 1998. Krupaseep—The Next Generation Seepage Meter. *Journal of Coastal Research*: 210-213.

LaBaugh, J.W., 1985. Uncertainty in Phosphorus Retention, Williams Fork Reservoir, Colorado. *Water Resources Research*, 21(11): 1684-1692.

LaBaugh, J.W., Rosenberry, D.O., Winter, T.C., 1995. Groundwater contribution to the water and chemical budgets of Williams Lake, Minnesota, 1980-1991. *Canadian Journal of Fisheries and Aquatic Sciences*, 52(4): 754-767.

LaBaugh, J.W., Winter, T.C., 1984. The impact of uncertainties in hydrologic measurement on phosphorus budgets and empirical models for two Colorado reservoirs. *Limnology and Oceanography*, 29(2): 322-339.

LaBaugh, J.W., Winter, T.C., Rosenberry, D.O., 2000. Comparison of the variability in fluxes of ground water and solutes in lakes and wetlands in central North America. *Proceedings - International Association of Theoretical and Applied Limnology*, 27: 420-426.

LaBaugh, J.W., Winter, T.C., Rosenberry, D.O., Schuster, P.F., Reddy, M.M., Aiken, G.R., 1997. Hydrological and chemical estimates of the water balance of a closed-basin lake in north central Minnesota. *Water Resources Research*, 33(12): 2799-2812.

Lapham, W.W., 1989. Use of temperature profiles beneath streams to determine rates of vertical ground-water flow and vertical hydraulic conductivity. *U.S. Geological Survey Water-Supply Paper* 2337: 35 p.

Lautz, L.K., Ribaudo, R.E., 2012. Scaling up point-in-space heat tracing of seepage flux using bed temperatures as a quantitative proxy. *Hydrogeology Journal*, 20(7): 1223-1238.

Leavesley, G.H., Hay, L., 1998. The use of coupled atmospheric and hydrological models for water-resources management in headwater basins. *Proceedings of the Hydrology, Water Resources and Ecology in Headwaters*: 259–265.

Leavesley, G.H., Lichty, R.W., Troutman, B.M., Saindon, L.G., 1983. Precipitation-runoff modeling system; user's manual. *U.S. Geological Survey Water-Resources Investigations Report* 83-4238: 207 p.

Leavesley, G.H., Markstrom, S.L., Restrepo, P.J., Viger, R.J., 2002. A modular approach to addressing model design, scale, and parameter estimation issues in distributed hydrological modelling. *Hydrological Processes*, 16(2): 173-187.

Lee, D.R., 1977. A device for measuring seepage flux in lakes and estuaries. *Limnology and Oceanography*, 22(1): 140-147.

Lee, D.R., 1985. Method for locating sediment anomalies in lakebeds that can be caused by groundwater flow. *Journal of Hydrology*, 79(1): 187-193.

Lee, D.R., Cherry, J.A., 1978. A field exercise on groundwater flow using seepage meters and mini-piezometers. *Journal of Geological Education*, 27: 6–20.

Lee, D.R., Cherry, J.A., Pickens, J.F., 1980. Groundwater transport of a salt tracer through a sandy lakebed1. *Limnology and Oceanography*, 25(1): 45-61.

Lee, D.R., Tracey, J.P., 1984. Identification of groundwater discharge locations using thermal infrared imagery. *Proceedings of the Ninth Canadian Symposium on Remote Sensing, Saint Johns, Newfoundland*: 301–308.

Lee, T.M., 1996. Hydrogeologic controls on the groundwater interactions with an acidic lake in karst terrain, Lake Barco, Florida. *Water Resources Research*, 32(4): 831-844.

Lee, T.M., Sacks, L.A., Swancar, A., 2014. Exploring the long-term balance between net precipitation and net groundwater exchange in Florida seepage lakes. *Journal of Hydrology*, 519, Part D: 3054-3068.

Lee, T.M., Swancar, A., 1997. Influence of evaporation, ground water, and uncertainty in the hydrologic budget of Lake Lucerne, a seepage lake in Polk County, Florida. *U.S. Geological Survey Water Supply Paper* 2439: 61 p.

Lesack, L.F.W., 1995. Seepage exchange in an Amazon floodplain lake. *Limnology and Oceanography*, 40(3): 598-609.

Lewandowski, J., Meinikmann, K., Nützmann, G., Rosenberry, D.O., 2015. Groundwater – the disregarded component in lake water and nutrient budgets. Part 2: effects of groundwater on nutrients. *Hydrological Processes*, 29(13): 2922-2955.

Lewandowski, J., Meinikmann, K., Ruhtz, T., Pöschke, F., Kirillin, G., 2013. Localization of lacustrine groundwater discharge (LGD) by airborne measurement of thermal infrared radiation. *Remote Sensing of Environment*, 138: 119-125.

Lillie, R.A., Barko, J.W., 1990. Influence of sediment and groundwater on the distribution and biomass of *Myriophyllum spicatum* L. in Devils Lake, Wisconsin. *Journal of Freshwater Ecology*, 5(4): 417-426.

Lindgren, R.J., Landon, M.K., 2000. Effects of ground-water withdrawals on the Rock River and associated valley aquifer, eastern Rock County, Minnesota. *Water-Resources Investigations Report.*

Lodge, D.M., Krabbenhoft, D.P., Striegl, R.G., 1989. A positive relationship between groundwater velocity and submersed macrophyte biomass in Sparkling Lake Wisconsin. *Limnology and Oceanography*, 34(1): 235-239.

Loeb, S.L., Goldman, C.R., 1979. Water and nutrient transport via groundwater from Ward Valley into Lake Tahoe. *Limnology and Oceanography*, 24(6): 1146-1154.

Loeb, S.L., Hackley, S.H., 1988. The distribution of submerged macrophytes in Lake Tahoe, California and Nevada, and the possible influence of groundwater seepage. *Verhandlungen. Internationale Vereinigung fur theoretische und angewandte Limnologie*, 23: 927–1933.

Malard, F., Plenet, S., Gibert, J., 1996. The Use of Invertebrates in Ground Water Monitoring: A Rising Research Field. *Ground Water Monitoring & Remediation*, 16(2): 103-113.

Malcolm, I.A., Soulsby, C., Youngson, A.F., Hannah, D.M., McLaren, I.S., Thorne, A., 2004. Hydrological influences on hyporheic water quality: implications for salmon egg survival. *Hydrological Processes*, 18(9): 1543-1560.

Mann, C.J., Wetzel, R.G., 2000. Hydrology of an impounded lotic wetland—subsurface hydrology. *Wetlands*, 20(1): 33-47.

Mann, W.B., McBride, M.S., 1972. The hydrologic balance of Lake Sallie, Becker County, Minnesota. *U.S. Geological Survey Professional Paper*, 800-D: 189–191.

Markstrom, S.L., Niswonger, R.G., Regan, R.S., Prudic, D.E., Barlow, P.M., 2008. GSFLOW - Coupled Ground-Water and Surface-Water Flow Model Based on the Integration of the Precipitation-Runoff Modeling System (PRMS) and the Modular Ground-Water Flow Model (MODFLOW-2005). *Techniques and Methods.*

Mast, M.A., Clow, D.W., 2000. Environmental characteristics and water quality of hydrologic benchmark network stations in the western United States, 1963-95. *Circular.*

McBride, J.M., 1987. Measurement of ground water flow to the Detroit River, Michigan and Ontario. M.S. Thesis, University of Wisconsin - Milwaukee, Wisconsin, 107 p.

McBride, M.S., Pfannkuch, H.O., 1975. Distribution of seepage within lakebeds. *Journal of Research of the U.S. Geological Survey*, 3(5): 505-512.

McBride, W.S., Bellino, J.C., Swancar, A., 2011. Hydrology, water budget, and water chemistry of Lake Panasoffkee, west-central Florida. *U.S. Geological Survey Scientific Investigations Report* 2010-5237: 96 p.

McCobb, T.D., LeBlanc, D.R., Massey, A.J., 2009. Monitoring the removal of phosphate from ground water discharging through a pond-bottom permeable reactive barrier. *Ground Water Monitoring and Remediation*, 29(2): 43-55.

McDonald, M.G., Harbaugh, A.H., 1984. A modular three-dimensional finitedifference ground-water flow model. *U.S. Geological Survey Open-File Report* 83-0875: 528 p.

Meinikmann, K., Lewandowski, J., Nutzmann, G., 2013. Lacustrine groundwater discharge: Combined determination of volumes and spatial patterns. *Journal of Hydrology*, 502(0): 202-211.

Meinzer, O.E., 1927. Plants as indicators of ground water. *U.S. Geological Survey Water-Supply Paper* 577: 95 p.

Menheer, M.A., 2004. Development of a benthic-flux chamber for measurement of ground-water seepage and water sampling for mercury analysis at the sediment-water interface. *Scientific Investigations Report*: 20 p.

Miettinen, I.T., Vartiainen, T., Martikainen, P.J., 1997. Changes in water microbial quality during bank filtration of lake water. *Canadian Journal of Microbiology*, 43(12): 1126-1132.

Misztal, M., Smal, H., Gorniak, A., 1992. Ground-water inflow of nutrients to a lake from differently utilized catchments. *Water Research*, 26(9): 1237-1242.

Mitchell, D.F., Wagner, K.J., Asbury, C., 1988. Direct measurement of groundwater flow and quality as a lake management tool. *Lake and Reservoir Management*, 4: 169–178.

Mortimer, R.J.G., Krom, M.D., Boyle, D.R., Nishri, A., 1999. Use of a high-resolution pore-water gel profiler to measure groundwater fluxes at an underwater saline seepage site in Lake Kinneret, Israel. *Limnology and Oceanography*, 44(7): 1802-1809.

Motz, L.H., 1998. Vertical leakage and vertically averaged vertical conductance for Karst Lakes in Florida. *Water Resources Research*, 34(2): 159-167.

Motz, L.H., Sousa, G.D., Annable, M.D., 2001. Water budget and vertical conductance for Lowry (Sand Hill) Lake in north-central Florida, USA. *Journal of Hydrology*, 250(1–4): 134-148.

Munter, J.A., Anderson, M.P., 1981. The Use of Ground-Water Flow Models for Estimating Lake Seepage Rates. *Ground Water*, 19(6): 608-616.

Nuttle, W.K., 2002. Eco-hydrology's past and future in focus. *Eos, Transactions American Geophysical Union*, 83(19): 205-212.

Nützmann, G., Holzbecher, E., Pekdeger, A., 2003. Evaluation of the water balance of Lake Stechlin with the help of chloride data. *Advances in Limnology*, 58: 11-23.

Oliveira Ommen, D.A., Kidmose, J., Karan, S., Flindt, M.R., Engesgaard, P., Nilsson, B., Andersen, F.O., 2012. Importance of groundwater and macrophytes for the nutrient balance at oligotrophic Lake Hampen, Denmark. *Ecohydrology*, 5(3): 286-296.

Ozyavas, A., Khan, S.D., Casey, J.F., 2010. A possible connection of Caspian Sea level fluctuations with meteorological factors and seismicity. *Earth and Planetary Science Letters*, 299(1-2): 150-158.

Paulsen, R.J., Smith, C.F., O'Rourke, D., Wong, T.F., 2001. Development and evaluation of an ultrasonic ground water seepage meter. *Ground Water*, 39(6): 904-911.

Pfannkuch, H.O., Winter, T.C., 1984. Effect of anisotropy and groundwater system geometry on seepage through lakebeds: 1. Analog and dimensional analysis. *Journal of Hydrology*, 75(1–4): 213-237.

Pina-Ochoa, E., Alvarez-Cobelas, M., 2009. Seasonal nitrogen dynamics in a seepage lake receiving high nitrogen loads. *Marine and Freshwater Research*, 60(5): 335-445.

Pollard, R.A., 1955. Measuring Seepage through Salmon Spawning Gravel. *Journal of the Fisheries Research Board of Canada*, 12(5): 706-741.

Rasmussen, W., Lauritzen, C.W., 1953. Measuring seepage from irrigation canals. *Agricultural Engineering*, 34: 26–330.

Rau, G.C., Andersen, M.S., Acworth, R.I., 2012. Experimental investigation of the thermal time-series method for surface water-groundwater interactions. *Water Resources Research*, 48(3): n/a-n/a.

Ray, C., Melin, G., Linsky, R.B., 2003. Riverbank Filtration: Improving Source-water Quality. In: *Water Science and Technology Library*, Singh, V.P. (Ed.). Springer Netherlands, 366.

Ridgway, M.S., Blanchfield, P.J., 1998. Brook trout spawning areas in lakes. *Ecology of Freshwater Fish*, 7(3): 140-145.

Robinson, A.R., Rohwer, C., 1952. Study of seepage losses from irrigation channels. *U.S. Department of Agriculture, Soil Conservation Service Progress Report*: 42 p.

Rorabaugh, M.I., 1964. Estimating changes in bank storage and groundwater contribution to streamflow. *International Association of Scientific Hydrology Publication*, 63: 432–441.

Rosenberry, D.O., 2000. Unsaturated-zone wedge beneath a large, natural lake. *Water Resources Research*, 36(12): 3401-3409.

Rosenberry, D.O., 2005. Integrating seepage heterogeneity with the use of ganged seepage meters. *Limnology and Oceanography-Methods*, 3: 131-142.

Rosenberry, D.O., 2008. A seepage meter designed for use in flowing water. *Journal of Hydrology*, 359(1–2): 118-130.

Rosenberry, D.O., Hayashi, M., 2013. Assessing and Measuring Wetland Hydrology. In: *Wetland Techniques: Volume 1: Foundations*, Anderson, J.T., Davis, C.A. (Eds.). Springer Netherlands, Dordrecht, 87-225.

Rosenberry, D.O., La Baugh, J.W., Hunt, R.J., 2008. Use of monitoring wells, portable piezometers, and seepage meters to quantify flow between surface water and ground water. In: *Field Techniques for Estimating Water Fluxes between Surface Water and Ground Water*, Rosenberry, D.O., La Baugh, J.W. (Eds.). U.S. Geological Survey Techniques and Methods 4-D2, Reston, Virginia, 39–70.

Rosenberry, D.O., LaBaugh, J.W., 2008. Field Techniques for Estimating Water Fluxes Between Surface Water and Ground Water. *U.S. Geological Survey Techniques and Methods* 4-D2: 128 p.

Rosenberry, D.O., Menheer, M.A., 2006. A system for calibrating seepage meters used to measure flow between ground water and surface water. *Scientific Investigations Report*: 27 p.

Rosenberry, D.O., Morin, R.H., 2004. Use of an electromagnetic seepage meter to investigate temporal variability in lake seepage. *Ground Water*, 42(1): 68-77.

Rosenberry, D.O., Sheibley, R.W., Cox, S.E., Simonds, F.W., Naftz, D.L., 2013. Temporal variability of exchange between groundwater and surface water based on high-frequency direct measurements of seepage at the sediment-water interface. *Water Resources Research*, 49(5): 2975-2986.

Rosenberry, D.O., Striegl, R.G., Hudson, D.C., 2000. Plants as indicators of focused ground water discharge to a northern Minnesota lake. *Ground Water*, 38(2): 296-303.

Rosenberry, D.O., Toran, L., Nyquist, J.E., 2010. The effect of surficial disturbance on exchange between groundwater and surface water in near-shore margins. *Water Resources Research*, 46(W06518).

Rosenberry, D.O., Winter, T.C., 1997. Dynamics of water-table fluctuations in an upland between two prairie-pothole wetlands in North Dakota. *Journal of Hydrology*, 191(1): 266-289.

Rosenberry, D.O., Winter, T.C., 2009. Hydrologic processes and the water budget: Chapter 2. *Mirror Lake: Interactions among air, land, and water*: 23-68.

Rosenberry, D.O., Winter, T.C., Buso, D.C., Likens, G.E., 2007. Comparison of 15 evaporation methods applied to a small mountain lake in the northeastern USA. *Journal of Hydrology*, 340(3–4): 149-166.

Rovey, C.W., Cherkauer, D.S., 1995. Scale dependency of hydraulic conductivity measurements. *Ground Water*, 33(5): 769-780.

Rutledge, A.T., 1998. Computer programs for describing the recession of ground-water discharge and for estimating mean ground-water recharge and discharge from streamflow records-update. *U.S. Geological Survey Water-Resources Investigations Report* 98-4148: 44 p.

Rutledge, A.T., 2000. Considerations for use of the RORA program to estimate ground-water recharge from streamflow records. *U.S. Geological Survey Open-File Report* 00-156: 44 p.

Sacks, L.A., Lee, T.M., Swancar, A., 2014. The suitability of a simplified isotope-balance approach to quantify transient groundwater-lake interactions over a decade with climatic extremes. *Journal of Hydrology*, 519: 3042-3053.

Sacks, L.A., Swancar, A., Lee, T.M., 1998. Estimating ground-water exchange with lakes using water-budget and chemical mass-balance approaches for ten lakes in ridge areas of Polk and Highlands counties, Florida. *U.S. Geological Survey Water-Resources Investigations Report* 98-4133: 52 p.

Schafran, G.C., Driscoll, C.T., 1993. Flow path-composition relationships for groundwater entering an acidic lake. *Water Resources Research*, 29(1): 145-154.

Schindler, D.W., Newbury, R.W., Beaty, K.G., Campbell, P., 1976. Natural Water and Chemical Budgets for a Small Precambrian Lake Basin in Central Canada. *Journal of the Fisheries Research Board of Canada*, 33(11): 2526-2543.

Schmidt, C., Bayer-Raich, M., Schirmer, M., 2006. Characterization of spatial heterogeneity of groundwater-stream water interactions using multiple depth streambed temperature measurements at the reach scale. *Hydrology and Earth System Sciences*, 10(6): 849-859.

Schneider, R.L., Negley, T.L., Wafer, C., 2005. Factors influencing groundwater seepage in a large, mesotrophic lake in New York. *Journal of Hydrology*, 310(1-4): 1-16.

Schumann, D., 1973. Annual variation of seepage of lakes in the moraine area of the German Democratic Republic. *Hydrology of Lakes IAHS Publication*, 109: 101–108.

Schuster, P.F., Reddy, M.M., LaBaugh, J.W., Parkhurst, R.S., Rosenberry, D.O., Winter, T.C., Antweiler, R.C., Dean, W.E., 2003. Characterization of lake water and ground water movement in the littoral zone of Williams Lake, a closed-basin lake in north central Minnesota. *Hydrological Processes*, 17(4): 823-838.

Sebestyen, S.D., Schneider, R.L., 2001. Dynamic temporal patterns of nearshore seepage flux in a headwater Adirondack lake. *Journal of Hydrology*, 247(3-4): 137-150.

Sebestyen, S.D., Schneider, R.L., 2004. Seepage patterns, pore water, and aquatic plants: hydrological and biogeochemical relationships in lakes. *Biogeochemistry*, 68(3): 383-409.

Sebok, E., Duque, C., Kazmierczak, J., Engesgaard, P., Nilsson, B., Karan, S., Frandsen, M., 2013. High-resolution distributed temperature sensing to detect seasonal groundwater discharge into Lake Væng, Denmark. *Water Resources Research*, 49(9): 5355-5368.

Selker, J.S., Thevenaz, L., Huwald, H., Mallet, A., Luxemburg, W., de Giesen, N.v., Stejskal, M., Zeman, J., Westhoff, M., Parlange, M.B., 2006. Distributed fiber-optic temperature sensing for hydrologic systems. *Water Resources Research*, 42(12): W12202.

Shaw, R.D., Prepas, E.E., 1990. Groundwater-lake interactions: I. Accuracy of seepage meter estimates of lake seepage. *Journal of Hydrology*, 119(1): 105-120.

Shaw, R.D., Shaw, J.F.H., Fricker, H., Prepas, E.E., 1990. An integrated approach to quantify groundwater transport of phosphorus to Narrow Lake, Alberta. *Limnology and Oceanography*, 35(4): 870-886.

Sheets, R.A., Darner, R.A., Whitteberry, B.L., 2002. Lag times of bank filtration at a well field, Cincinnati, Ohio, USA. *Journal of Hydrology*, 266(3–4): 162-174.

Shepherd, B.G., Hartman, G.F., Wilson, W.J., 1986. Relationships Between Stream and Intragravel Temperatures in Coastal Drainages, and Some Implications for Fisheries Workers. *Canadian Journal of Fisheries and Aquatic Sciences*, 43(9): 1818-1822.

Shepherd, R.G., 1989. Correlations of Permeability and Grain Size. *Ground Water*, 27(5): 633-638.

Silliman, S.E., Booth, D.F., 1993. Analysis of time-series measurements of sediment temperature for identification of gaining vs. losing portions of Juday Creek, Indiana. *Journal of Hydrology*, 146: 131-148.

Simpkins, W.W., 2006. A multiscale investigation of ground water flow at Clear Lake, Iowa. *Ground Water*, 44(1): 35-46.

Smart, P.L., Smith, D.I., 1976. Water tracing in tropical regions, the use of fluorometric techniques in Jamaica. *Journal of Hydrology*, 30(1): 179-195.

Song, C., Huang, B., Ke, L., Richards, K.S., 2014. Seasonal and abrupt changes in the water level of closed lakes on the Tibetan Plateau and implications for climate impacts. *Journal of Hydrology*, 514: 131-144.

Sonzogni, W.C., Lee, G.F., 1974. Nutrient sources for Lake Mendota - 1972. *Transactions of the Wisconsin Academy Sciences Arts and Letters*, 62: 133-164.

Sophocleous, M., 2002. Interactions between groundwater and surface water: the state of the science (vol 10, pg 52, 2002). *Hydrogeology Journal*, 10(2): 348-348.

Stark, J.R., Armstrong, D.S., Zwilling, D.R., 1994. Stream-aquifer interactions in the Straight River area, Becker and Hubbard counties, Minnesota. *U.S. Geological Survey Water-Resources Investigations Report* 94-4009: 83 p.

Stauffer, R.E., 1985. Use of solute tracers released by weathering to estimate groundwater inflow to seepage lakes. *Environmental Science & Technology*, 19(5): 405-411.

Stets, E.G., Winter, T.C., Rosenberry, D.O., Striegl, R.G., 2010. Quantification of surface water and groundwater flows to open- and closed-basin lakes in a headwaters watershed using a descriptive oxygen stable isotope model. *Water Resources Research*, 46: W03515.

Stonestrom, D.A., Constantz, J., 2003. Heat as a tool for studying the movement of ground water near streams. *U.S. Geological Survey Circular* 1260: 96 p.

Strack, O.D.L., 1999. Principles of the analytic element method. *Journal of Hydrology*, 226(3–4): 128-138.

Sutula, M., Day, J.W., Cable, J., Rudnick, D., 2001. Hydrological and nutrient budgets of freshwater and estuarine wetlands of Taylor Slough in Southern Everglades, Florida (U.S.A.). *Biogeochemistry*, 56(3): 287-310.

Swarzenski, P.W., Simonds, F.W., Paulson, A.J., Kruse, S., Reich, C., 2007. Geochemical and geophysical examination of submarine groundwater discharge and associated nutrient loading estimates into Lynch Cove, Hood Canal, WA. *Environmental Science and Technology*, 41(20): 7022-7029.

Taniguchi, M., Burnett, W.C., Cable, J.E., Turner, J.V., 2002. Investigation of submarine groundwater discharge. *Hydrological Processes*, 16(11): 2115-2129.

Taniguchi, M., Fukuo, Y., 1993. Continuous Measurements of Ground-Water Seepage Using an Automatic Seepage Meter. *Ground Water*, 31(4): 675-679.

Taniguchi, M., Fukuo, Y., 1996. An Effect of Seiche on Groundwater Seepage Rate into Lake Biwa, Japan. *Water Resources Research*, 32(2): 333-338.

Thies, H., Nickus, U., Arnold, C., Psenner, R., 2002. A hydrological tracer experiment with LiCl in a high mountain lake. *Hydrological Processes*, 16(12): 2329-2337.

Tiedeman, C., Gorelick, S.M., 1993. Analysis of uncertainty in optimal groundwater contaminant capture design. *Water Resources Research*, 29(7): 2139-2153.

Tomassoni, G., 2000. A federal statutory/regulatory/policy perspective on remedial decision-making with respect to ground-water/surface-water interaction, Proceedings of the Ground-Water/Surface-Water Interactions Workshop. United States Environmental Protection Agency, Denver, Colorado, p. 13-14.

Toran, L., Johnson, M., Nyquist, J., Rosenberry, D., 2010. Delineating a road-salt plume in lakebed sediments using electrical resistivity, piezometers, and seepage meters at Mirror Lake, New Hampshire, U.S.A. *GEOPHYSICS*, 75(4): WA75-WA83.

Vallet-Coulomb, C., Legesse, D., Gasse, F., Travi, Y., Chernet, T., 2001. Lake evaporation estimates in tropical Africa (Lake Ziway, Ethiopia). *Journal of Hydrology*, 245(1–4): 1-18.

Vanek, V., 1991. Riparian zone as a source of phosphorus for a groundwater-dominated lake. *Water Research*, 25(4): 409-418.

Vaux, W.G., 1968. Intragravel flow and interchange of water in a streambed. *Fishery Bulletin*, 66: 479–489.

Virdi, M.L., Lee, T.M., Swancar, A., Niswonger, R.G., 2013. Simulating the Effect of Climate Extremes on Groundwater Flow Through a Lakebed. *Ground Water*, 51(2): 203-218.

Voss, C.I., 2011a. Editor's message: Groundwater modeling fantasies—part 2, down to earth. *Hydrogeology Journal*, 19(8): 1455-1458.

Voss, C.I., 2011b. Editor's message: Groundwater modeling fantasies —part 1, adrift in the details. *Hydrogeology Journal*, 19(7): 1281-1284.

Warnick, C.C., 1951. Methods of measuring seepage loss in irrigation canals. *University of Idaho Engineering Experiment Station Bulletin*, 8: 42.

Warren, D.R., Sebestyen, S.D., Josephson, D.C., Lepak, J.M., Kraft, C.E., 2005. Acidic groundwater discharge and in situ egg survival in redds of lake-spawning brook trout. *Transactions of the American Fisheries Society*, 134: 1193–1201.

Wassen, M.J., Grootjans, A.P., 1996. Ecohydrology: An Interdisciplinary Approach for Wetland Management and Restoration. *Vegetatio*, 126(1): 1-4.

Weilhartner, A., Muellegger, C., Kainz, M., Mathieu, F., Hofmann, T., Battin, T.J., 2012. Gravel pit lake ecosystems reduce nitrate and phosphate concentrations in the outflowing groundwater. *Science of The Total Environment*, 420: 222-228.

Wentz, D.A., Rose, W.J., 1991. Hydrology of Lakes Clara and Vandercook in north-central Wisconsin. *U.S. Geological Survey Water-Resources Investigations Report* 89-4204: 28 p.

Wentz, D.A., Rose, W.J., Webster, K.E., 1995. Long-Term Hydrologic and Biogeoehemieal Responses of a Soft Water Seepage Lake in North Central Wisconsin. *Water Resources Research*, 31(1): 199-212.

Wetzel, R.G., 1999. Plants and water in and adjacent to lakes. In: *Eco-hydrology: Plants and Water in Terrestrial and Aquatic Environments*, Baird, A.J., Wilby, R.L. (Eds.). Routledge, London, New York, 269–299.

Wetzel, R.G., 2001. *Limnology: Lake and River Ecosystems*. Academic Press, San Diego, 1006 p.

Wiese, B., Nützmann, G., 2009. Transient Leakance and Infiltration Characteristics during Lake Bank Filtration. *Ground Water*, 47(1): 57-68.

Winter, T.C., 1976. Numerical simulation analysis of the interaction of lakes and ground water. *U.S. Geological Survey Professional Paper* 1001: 45 p.

Winter, T.C., 1978. Numerical simulation of steady state three-dimensional groundwater flow near lakes. *Water Resources Research*, 14(2): 245-254.

Winter, T.C., 1981. Effects of water-table configuration on seepage through lakebeds. *Limnology and Oceanography*, 26(5): 925-934.

Winter, T.C., 1983. The interaction of lakes with variably saturated porous media. *Water Resources Research*, 19(5): 1203-1218.

Winter, T.C., 1996. Hydrological and biogeochemical research in the Shingobee River Headwaters Area, north-central Minnesota. *U.S. Geological Survey Water Resources Investigations Report* 96-4215: 210 p.

Winter, T.C., 1999. Relation of streams, lakes, and wetlands to groundwater flow systems. *Hydrogeology Journal*, 7(1): 28-45.

Winter, T.C., Harvey, J.W., Franke, O.L., Alley, W.M., 1998. Ground Water and Surface Water - A Single Resource. *U.S. Geological Survey Circular* 1139: 79 p.

Winter, T.C., LaBaugh, J.W., Rosenberry, P.O., 1988. The design and use of a hydraulic potentiomanometer for direct measurement of differences in hydraulic head between groundwater and surface water. *Limnology and Oceanography*, 33(5): 1209-1214.

Winter, T.C., Rosenberry, D.O., LaBaugh, J.W., 2003. Where Does the Ground Water in Small Watersheds Come From? *Ground Water*, 41(7): 989-1000.

Woessner, W.W., Sullivan, K.E., 1984. Results of Seepage Meter and Mini-Piezometer Study, Lake Mead, Nevada. *Ground Water*, 22(5): 561-568.

Yihdego, Y., Becht, R., 2013. Simulation of lake–aquifer interaction at Lake Naivasha, Kenya using a three-dimensional flow model with the high conductivity technique and a DEM with bathymetry. *Journal of Hydrology*, 503: 111-122.

Yihdego, Y., Webb, J., 2012. Modelling of seasonal and long-term trends in lake salinity in southwestern Victoria, Australia. *Journal of Environmental Management*, 112: 149-159.

Zhou, S., Kang, S., Chen, F., Joswiak, D.R., 2013. Water balance observations reveal significant subsurface water seepage from Lake Nam Co, south-central Tibetan Plateau. *Journal of Hydrology*, 491: 89-99.

2.2 Groundwater – the disregarded component in lake water and nutrient budgets. Part 2: Effects of groundwater on nutrients

Jörg Lewandowski[1,2] Karin Meinikmann[1,2] Gunnar Nützmann[1,2] and Donald O. Rosenberry[3]

[1] Department of Ecohydrology, Leibniz-Institute of Freshwater Ecology and Inland Fisheries, Berlin, Germany

[2] Geography Department, Humboldt-Universität zu Berlin, Berlin, Germany

[3] US Geological Survey, Denver Federal Center, USA

This is the peer reviewed version of the following article:
Lewandowski, J., Meinikmann, K., Nützmann, G., Rosenberry, D.O., 2015. Groundwater – the disregarded component in lake water and nutrient budgets. Part 2: Effects of groundwater on nutrients. *Hydrological Processes*, 29(13): 2922-2955.

Abstract

Lacustrine groundwater discharge (LGD) transports nutrients from a catchment to a lake, which may fuel eutrophication, one of the major threats to our fresh waters. Unfortunately, LGD has often been disregarded in lake nutrient studies. Most measurement techniques are based on separate determinations of volume and nutrient concentration of LGD: Loads are calculated by multiplying seepage volumes by concentrations of exfiltrating water. Typically low phosphorus (P) concentrations of pristine groundwater often are increased due to anthropogenic sources such as fertilizer, manure or sewage. Mineralization of naturally present organic matter might also increase groundwater P. Reducing redox conditions favour P transport through the aquifer to the reactive aquifer-lake interface. In some cases, large decreases of P concentrations may occur at the interface, for example, due to increased oxygen availability, while in other cases, there is nearly no decrease in P. The high reactivity of the interface complicates quantification of groundwater-borne P loads to the lake, making difficult clear differentiation of internal and external P loads to surface water. Anthropogenic sources of nitrogen (N) in groundwater are similar to those of phosphate. However, the environmental fate of N differs fundamentally from P because N occurs in several different redox states, each with different mobility. While nitrate behaves essentially conservatively in most oxic aquifers, ammonium's mobility is similar to that of phosphate. Nitrate may be transformed to gaseous N_2 in reducing conditions and permanently removed from the system. Biogeochemical turnover of N is common at the reactive aquifer-lake interface. Nutrient loads from LGD were compiled from the literature. Groundwater-borne P loads vary from 0.74 to 2900 mg PO_4-P m^{-2} $year^{-1}$; for N, these loads vary from 0.001 to 640 g m^{-2} $year^{-1}$. Even small amounts of seepage can carry large nutrient loads due to often high nutrient concentrations in groundwater. Large spatial heterogeneity, uncertain areal extent of the interface and difficult accessibility make every determination of LGD a challenge. However, determinations of LGD are essential to effective lake management.

2.2.1 Introduction

Motivation. Eutrophication is one of the most important threats to lakes in temperate climatic zones (e.g., Conley et al. 2009; Kira 1993; Sigua et al. 2010). Usually, phosphorus (P) is considered the limiting nutrient in most freshwater ecosystems in these regions (e.g., Griffioen 1994; Lamontagne 2002; Ptacek 1998; Schelske 2009; Schindler and Hecky 2009). In contrast, most marine and some freshwater systems are nitrogen (N) limited (Conley et al. 2009; Howarth 1988; Kilinc and Moss 2002; Lewis and Wurtsbaugh 2008; Slomp and Van Cappellen 2004; Sterner 2008). It is necessary to determine the relative importance of various N and P sources and pathways within the catchment to evaluate their role in in-lake processes, to conduct effective management measures and to model future scenarios. Water budgets are a prerequisite for such nutrient budgets. Surface inflows from streams, rivers, ditches and precipitation can be quantified quite accurately. Evaporation can be calculated roughly based on local weather data. Quantifications of groundwater infiltration (here, flow from the lake to groundwater) and exfiltration (flow from groundwater to the lake) are more difficult. Often, they are neglected or determined as the residual in a water budget equation (Charette and Buesseler 2004; Crowe and Schwartz 1981; Kang et al. 2005; Kidmose 2010; Shaw et al. 1990; Winter 1978).

Hydrological considerations. In the first part of this review (Rosenberry et al. 2015), several methods for quantification of seepage fluxes (water volume per time) are presented; here, we transfer and extend those methods towards quantification of nutrient exfiltration. While the accurate quantification of the exfiltrating groundwater volume (per time) is already an enormous challenge (e.g., Burnett et al. 2006), the quantification of nutrient loads is even more challenging because of the spatial and temporal variations in groundwater composition in addition to the heterogeneous nature of groundwater fluxes.

Although spatial heterogeneity in chemical concentrations is more common, temporal variations also occur, particularly in karstic areas where groundwater flow velocities are high (Kilroy and Coxon 2005; Norrström and Jacks 1996) and source areas can differ depending on rainfall rate (Holzbecher 2001; Norrström and Jacks 1996). Thus, to determine nutrient loads, fluctuating concentrations have to be combined with the corresponding temporally and spatially varying water fluxes. In the first part of this review, it was shown that lacustrine groundwater discharge (LGD) exhibits a wide range, from 0.05 to 1240 l m^{-2} day^{-1}. Similarly, Taniguchi et al. (2002) showed in a compilation of worldwide submarine groundwater discharge (SGD) measurements a range from 0.08 to 1300 l m^{-2} day^{-1}.

River-aquifer interface. Although some authors realized quite early the importance of seepage for lakes (e.g., Meyboom 1967; Schumann 1973; Williams 1968), relationships between a lake and the adjacent groundwater are still the least known factors of lake hydrology and ecology (Healy et al. 2007; LaBaugh et al. 2009; Rosenberry and Winter 2009; Vanek 1987). Because of this knowledge gap, we also transfer knowledge collected for other interfaces to the aquifer-lake interface; for example, knowledge collected for the river-aquifer interface, commonly known as the hyporheic zone (e.g., Brunke and Gonser 1997; Grannemann and Sharp 1979; Grimm and Fisher 1984; Vaux 1968).

The hyporheic zone is an active ecotone that influences whole system metabolism and nutrient retention (Grimm and Fisher 1984; Triska et al. 1989; Valett et al. 1997). Retention varies under different hydrologic conditions (Valett et al. 1997). There are fundamental differences between the groundwater-surface water interface in lakes versus streams (Fig. 2.4). In streams (Fig. 2.4B), surface water can infiltrate the hyporheic zone (downwelling), travel for some time/path through that zone, and then return to the stream again (upwelling). Groundwater is mixed with the water that originated from the stream along the flow path, giving the water that discharges back into the stream channel characteristics of both surface and groundwater. Concepts, such as the 'nutrient spiraling concept' (Newbold et al. 1981; Valett et al. 1997), are based on that exchange. At the aquifer-lake interface (Fig. 2.4A), such processes are greatly diminished because, unlike in rivers and streams, virtually no hydraulic gradient exists across the lake surface or within the lake's water column. There might be brief reversals of the hydraulic gradient. For example, Krabbenhoft and Webster (1995) and report for Nevins Lake and Williams Lake, respectively, that there is infiltration during most periods of the year but exfiltration of previously infiltrated water during spring snowmelt or following substantial rain events. Also, there might be infiltration/exfiltration reversals due to waves or seiches (Rosenberry et al. 2013) as well as reversals in flow direction across the sediment-water interface at sediment structures or obstacles on the lakebed. Diffusion might also cause transport in the opposite direction. However, usually, these processes are of minor importance. A further difference between lake and stream interfaces is that, in floodplains, flooding events can result in a spreading of riverbed sediment including organic material onto the soil surface, whereas there is no similar process in most lakes. Nevertheless, basic biogeochemical processes at the aquifer-river interface are comparable with the aquifer-lake interface.

Submarine groundwater discharge (SGD). Groundwater exfiltration into marine systems, referred to as SGD in the international literature, is defined as 'any and all flow of water on continental margins from the seabed to the coastal ocean, regardless of the fluid composition or driving force' (Burnett et al. 2003). Tides create a subsurface flow cell of saltwater at and below the high water mark, and there is a freshwater flow tube entering the ocean below this cell and above the saltwater wedge. A further difference between SGD and LGD is that some deep seawater is recirculated upwards in coastal zones (up to 90% of the total SGD volume) and thus comprised under the marine exfiltration term (Fig. 2.4C). Topography-driven flow of fresh water 'drags' saline water from the underlying saline groundwater body (Slomp and Van Cappellen 2004). This intrusion of seawater might cause changes of the water composition due to ion exchange reactions with the aquifer matrix and dissolution of carbonate minerals. For example, Price et al. (2006) observed an increase in total phosphorus (TP) concentrations compared with fresh groundwater and intruded seawater. Nevertheless, we assume that basic biogeochemical processes are similar at both interfaces. In analogy to the term SGD, we introduce the abbreviation LGD for lacustrine groundwater discharge. The total flux of SGD to the Atlantic Ocean is huge, similar in volume to the amount of riverine discharge into the ocean (Burnett et al. 2006; Moore 1996; Moore et al. 2006; Moore and Church 1996; Moore et al. 2008). However, because nutrient concentrations in groundwater are often higher than in stream water, SGD is probably even more important in oceanic chemical budgets than surface water discharge to the oceans. This is especially true for N, which is typically the limiting nutrient in marine systems.

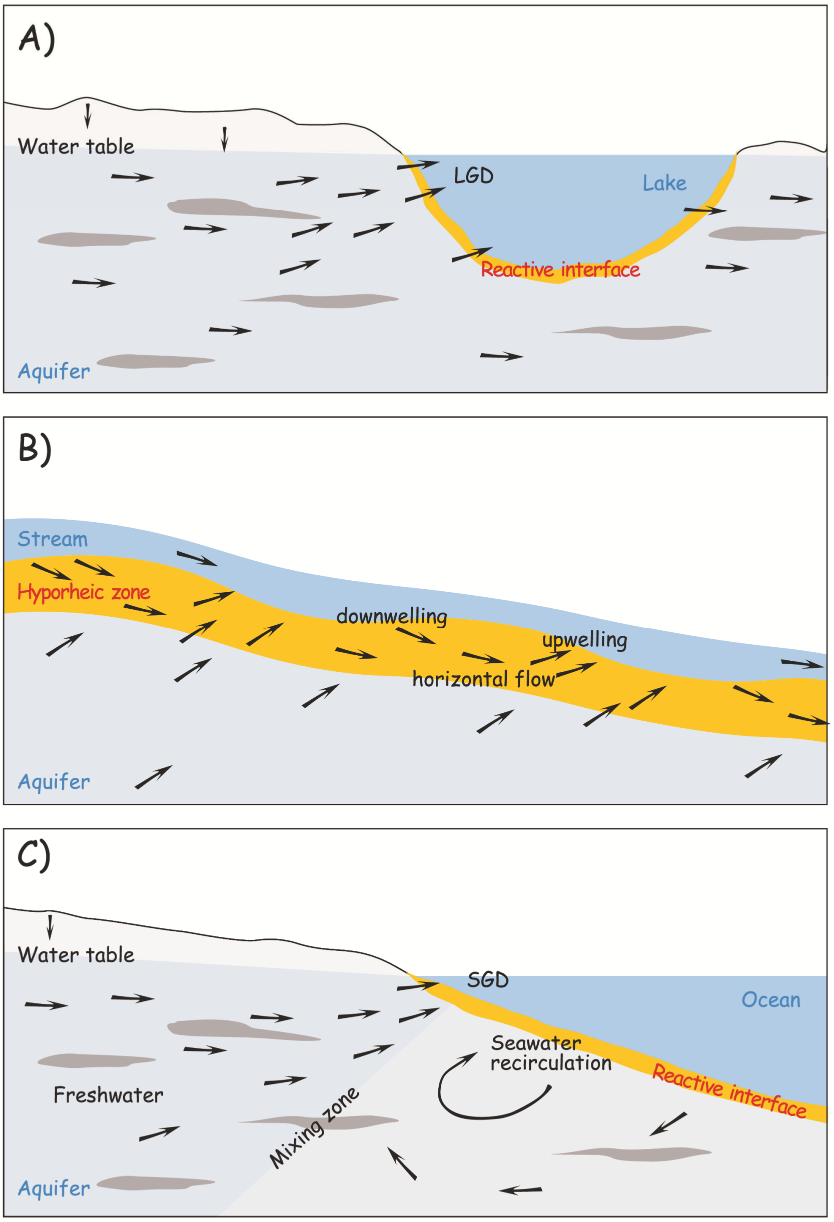

Figure 2.4 Conceptual model (longitudinal sections) of major hydrodynamic transport processes (black arrows) across aquifer-surface water interfaces for (a) lacustrine groundwater discharge (LGD), (b) the aquifer-river interface (hyporheic zone), and (c) submarine groundwater discharge (SGD).

Due to this significance, the literature on SGD has grown rapidly since the beginning of the new millennium (Moore 2010). Some scientists of the marine community argue that nutrient transport across the aquifer-lake interface is well-known while nutrient transport associated with SGD is an emerging topic. We agree that LGD was noticed much earlier than SGD, because, after all, there were some early studies investigating and quantifying LGD (Belanger and Mikutel 1985; Sonzogni and Lee 1974; Winter 1978). Nevertheless, LGD has been overlooked or at least disregarded in most eutrophication studies and funding focusing on LGD has been quite limited. In contrast, the marine community advanced the topic of SGD at the beginning of the century and the number of SGD studies exploded in the last decade.

Controls on nutrient fluxes by LGD. The nutrient input by LGD is controlled by (1) the length of the flow path and the groundwater flow velocity, both of which have important impacts on the residence time and, thus, on the opportunity for chemical processes between groundwater and the aquifer matrix; that is, the contact time (Buso et al. 2009; Winter 1978). Thus, the position of a lake within the regional hydrologic flow system is important (Hagerthey and Kerfoot 2005; Kratz et al. 1997; Webster et al. 1996). (2) Additionally, groundwater flow rates determine the magnitude of land-derived nutrient transport (Bowen et al. 2007). In analogy to the controlling factors of SGD identified by Slomp and Van Cappellen (2004), the nutrient input by LGD is additionally controlled by (3) supply rates and forms of N and P from natural and anthropogenic sources; (4) the redox conditions in the subsurface, which strongly affect transformation processes and mobility of N and P (Slomp and Van Cappellen 2004); and (5) further attenuation along the flow path depending on aquifer lithology (Bowen et al. 2007).

Goals of this review. Lacustrine groundwater discharge is still often disregarded in lake nutrient budgets, although several authors indicated this shortcoming decades ago (e.g, Loeb and Goldman 1979; Stauffer 1985) and identified LGD as a significant nutrient source (e.g., Enell 1982). Our overall aim in this paper is to advance the notion that LGD can be a substantial component in lake water and nutrient budgets and should be routinely considered in future lake studies. Due to the increasing effort that has been taken to reduce point sources, the relative importance of diffuse sources such as LGD is increasingly important in lake-budget studies. Because of space limitation, we focus in the present review exclusively on nutrients, although LGD of other biogeochemical compounds might also be of ecological concern, but without doubt LGD of nutrients is the most widespread and important impact. Our goal is to review existing studies on LGD, to describe the reasons why LGD has been disregarded so long, to draw together scientific knowledge from adjacent disciplines relevant for processes in the transition zone between aquifer and lake, to give an overview of existing and emerging measurement techniques, and to emphasize the relevance of the topic by citing numbers reported in the literature. We will closely look at the pathways of nutrients from different sources in the catchment through the aquifer, across the reactive interface and into the lake (Fig. 2.5).

2.2.2 Why has LGD been disregarded so long?

Transfers of nutrients (especially P) via groundwater discharge have traditionally received little attention and were largely neglected (Cherkauer et al. 1992; Kilroy and Coxon 2005; Vanek 1987). However, results from a growing number of studies (e.g., Kang et al. 2005; Roy and Malenica 2013; Shaw and Prepas 1990) have indicated that groundwater can influence the chemical composition of some precipitation-dominated lakes and can be a significant source of nutrients (Enell 1982), even in some large lakes (e.g., Lake Tahoe, Loeb and Goldman 1979).

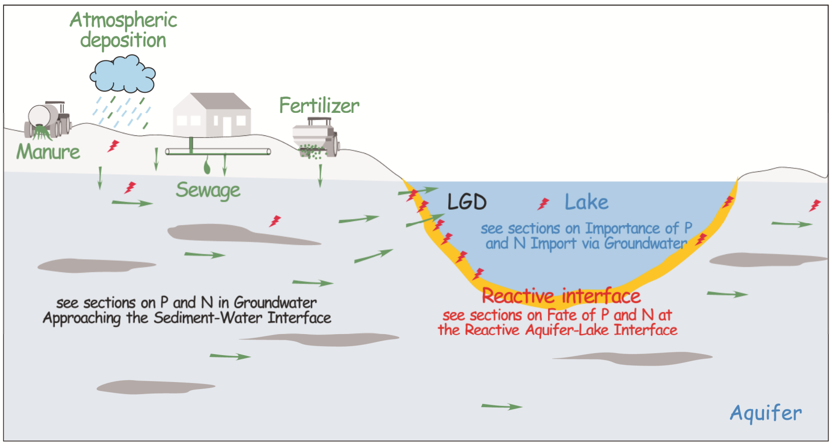

Figure 2.5 Schematic diagram of nutrient pathways (green arrows) from the sources in the catchment into the aquifer and from there across the reactive aquifer-lake interface into the receiving water body. Transport of nutrients is usually retarded compared with water transport shown in Figure 2.4. Red symbols indicate biogeochemical turnover of nutrients. Gray areas indicate lower-permeability deposits within a heterogeneous aquifer.

(1–7) Hydrologic considerations. Some reasons for neglecting the groundwater discharge to lakes have already been given in the first part of this review (Rosenberry et al. 2015) such as (1) the invisibility of the groundwater import; (2) the size of the aquifer-lake interface; (3) the spatial heterogeneity of seepage volumes (per time); (4) difficulties in accessing and quantifying fluxes through deeper parts of the interface; (5) the commonly small size of the net groundwater component (difference of groundwater exfiltration minus groundwater infiltration) even if gross groundwater exfiltration and infiltration are large; (6) methodological and/or measurement difficulties; and (7) the compartmentalisation of scientific disciplines.

(8) Small seepage – large concentrations. When concerning nutrient loads, some additional reasons for neglecting the groundwater discharge can be identified, such as small seepage but high concentrations. Groundwater, because of its generally higher concentrations of most water compounds, plays a relatively larger role in lake chemical budgets than it does in lake water budgets (Buso et al. 2009; Cherkauer et al. 1992; LaBaugh et al. 2000; Shaw and Prepas 1990; Vanek 1987). Even small water fluxes might result in substantial mass fluxes to lakes and might have significant impacts on chemical budgets of lakes. For example, Lee (1996) estimated that groundwater seepage contributed only 9–14% to the water budget of Lake Barco but approximately 50% to the budget of the acid neutralizing capacity. For Williams Lake, Minnesota, groundwater inputs represented only half of the annual water input but most of the chemical inputs (LaBaugh et al. 1995; Schuster et al. 2003). Groundwater contributed less than one third to the water budget of Narrow Lake, Alberta, but was the major single source of P to epilimnetic lakewater (Shaw and Prepas 1990). Even for estuaries with their large surface inflows, seepage might be relevant because nutrient concentrations in groundwater is, in general considerably, higher than concentrations in receiving estuaries (Bowen et al. 2007). Small amounts of LGD can have large impacts on nutrient budgets due to high concentrations of exfiltrating groundwater.

(9) Reactive interface. Biogeochemical reactions along the flow path through the aquifer often alter the groundwater composition, especially as groundwater approaches the sediment-water interface (Beck et al. 2007; Carlyle and Hill 2001; Dean et al. 2003; Frape and Patterson 1981; Kroeger and Charette 2008; LaBaugh et al. 1997; Moore 2010; Moore et al. 2006; Schuster et al. 2003). Temperature,

pressure, and chemical concentration can change substantially as water flows across the interface. Loading estimates based on conservative behaviour during exfiltration can be erroneous (Beck et al. 2007; Griffioen 2006; Kroeger and Charette 2008). Several studies have shown that groundwater samples taken from piezometers some meters upgradient from the shore can have compositions significantly different from the water discharging across the interface (Beck et al. 2007; Brock et al. 1982; Fellows and Brezonik 1980; John and Lock 1977; Krabbenhoft 1988; Krabbenhoft and Webster 1995; Kroeger and Charette 2008; McIntire et al. 1988; Weinstein et al. 2011). A major difference between the aquifer matrix and the sediment close to the interface is that the sediment close to the interface is often of lacustrine origin (e.g., Frape and Patterson 1981). The high level of organic matter may favour mineralization that alters the redox milieu and releases nutrients. Reducing conditions cause dissolution of redox-sensitive species and, as a consequence, sorbed phosphate is released. Furthermore, the higher content of organic matter close to the interface can encourage biological activity and promote sorption and desorption reactions (Frape and Patterson 1981).

Another reason for increased biogeochemical reactivity in groundwater approaching the groundwater-lake interface is topography. From investigations in floodplains, it is known that the thin unsaturated zone above the aquifer can cause high metabolic activity in floodplain aquifers (Lewandowski and Nützmann 2010). Plant cover on the land surface might deliver much fresh, easily degradable organic matter. The decay of this material consumes oxygen, and the shallow water table reduces the subsequent delivery of oxygen because oxygen diffusion is several magnitudes slower in the water-filled pores than in air-filled pores (Wilhelm et al. 1994).

Additional reasons for increased biogeochemical reactivity at the groundwater-lake interface involve transport processes from the lake into the sediment. For example, diffusion might result in downward transport of compounds due to concentration gradients or temporal fluctuation of water levels can cause an alternation of exfiltration and infiltration. Bioturbation and bioirrigation transport both pore-water and particulate material into deeper sediment layers. Furthermore, tube dwelling organisms restructure the sediment and affect nutrient pore-water chemistry (e.g., Aller 1978; Lewandowski et al. 2007; Stief and de Beer 2006). Flux rates have been found to be higher in areas of greater benthic invertebrate densities (Zimmermann et al. 1985). Macrophytes can also interact with exfiltrating groundwater and affect the composition of the seepage (Frandsen et al. 2012). Because most LGD usually occurs in near-shore areas, plant-seepage interactions are especially important in the shallow, near-shore margins of lakes. Several authors described the reactions in the rhizosphere without being aware of the delivery of water compounds by LGD (Christensen and Sorensen 1986; Holmer et al. 1998; e.g., Ottosen et al. 1999). Christensen et al. (1997) showed that *Littorella uniflora* was able to precipitate and retain a large percentage of iron in the LGD because of oxygen release from the roots (Oliveira Ommen et al. 2012). This led to efficient binding of phosphate to iron in the sediment, which in addition to the plant uptake of phosphate, may be very important for immobilizing P in the sediment (e.g., Christensen et al. 1997; Hupfer and Dollan 2003; Oliveira Ommen et al. 2012).

(10) Spatial and temporal heterogeneity in concentrations. The heterogeneity of seepage fluxes and volumes was already mentioned under 3. In addition, the concentrations of nutrients and other water compounds in groundwater entering lakes vary considerably in space and sometimes in time as well (Brock et al. 1982; Frape and Patterson 1981; Hagerthey and Kerfoot 1998; Schafran and Driscoll 1990; Schafran and Driscoll 1993; Schot and Pieber 2012; Shaw and Prepas 1990; Vanek 1991; Zimmermann et al. 1985). Krabbenhoft (1988) reports spatial variations of soluble reactive phosphorus (SRP) and NH_4^+ concentrations of LGD in Sparkling Lake at 14 littoral LGD sites (1–65 µg PO_4-P l^{-1}, 120–2540 µg NH_4 -N l^{-1}). Variations occur over relatively short distances within the same stratigraphic horizon at the same depth (Frape and Patterson 1981). However, among different lithologic types, there is even more variability of groundwater composition (McIntire et al. 1988; Valett

et al. 1997). Schafran and Driscoll (1990) indicate that variations in sediment organic matter could potentially be responsible for variations in sediment microbial activity and substantially different biogeochemical processes. Heterogeneities of groundwater composition can also be caused by varying hydraulic conductivities. Water in zones of low hydraulic conductivity is susceptible to reducing conditions that favour a release of P. The extent to which this P release will influence SRP fluxes depends on its proximity to hydrologically active zones with permeable sediments that function as conduits to the surface water body (Carlyle and Hill 2001). Several authors report that there is little temporal variability in P loading. For example, Hagerthey and Kerfoot (1998) report that P varied spatially but was temporally static. Similarly, Kilroy and Coxon (2005) wrote that groundwater quality is often considered more stable than that of surface water primarily due to greater residence times. Karstic areas may exhibit much greater temporal variability of exfiltrating groundwater; short-lived pollutant pulses may occur (Kilroy and Coxon 2005).

(11) Delayed impact. Even if a nutrient source has been eliminated long ago, there might be lingering adverse impacts on receiving water bodies. The water residence time of aquifers can be very long (decades to millennia) and thus, there is a mismatch between groundwater contamination and the observed nutrient delivery to surface waters by seepage (Lamontagne 2002; McCoy and Corbett 2009). Conversely, once a problem has been identified and management measures to reduce the sources are conducted, a long time may be required before the quality of seepage improves (Lamontagne 2002).

(12) Long-held belief of immobile P. Little attention has been paid to P transfers via groundwater because of the long-held belief that phosphate readily sorbs in the unsaturated zone (soil), in the saturated zone (aquifer) or precipitates with other groundwater constituents (Holman et al. 2010; Holman et al. 2008). Recently, a new understanding of the migration of P in groundwater is developing and analyses of long-term data sets have demonstrated that P does migrate in groundwater, raising concerns that P-containing groundwater may accelerate eutrophication of receiving water bodies (e.g., McCobb et al. 2003; Stollenwerk 1996; Walter et al. 1995).

(13) Extensive data sets needed. Due to the extensive data set required for construction of nutrient budgets that include groundwater, only relatively few such studies are reported in literature (Buso et al. 2009; Juckem and Robertson 2013; Oliveira Ommen et al. 2012; Robertson et al. 2009; Sutula et al. 2001).

2.2.3 Nutrient budgets of lakes

The quantification of water budgets based on measurements and modelling is discussed in detail in part 1 of this review (Rosenberry et al. 2015). Groundwater has been identified as one of several potentially important terms in the water budgets of lakes. Nutrient budgets are even more complex; spatial and temporal fluctuations of chemical concentrations have to be combined with the temporal and spatial fluctuations of the water fluxes for each of the different input paths of the budget. For example, TP concentrations in streams that flow into lakes are known to increase during periods of high flow so that loads increase disproportionally with increasing discharge (increase of water flux and TP concentration, e.g., Jordan et al. 2005). It is useful to establish flexible sampling strategies with increased sampling frequency during high flow periods (Sonzogni and Lee 1974) to quantify this process. However, only a part of the nutrient import to a lake is coupled to the water budget. For nutrient budgets, some additional input paths have to be taken into account, for example, dry deposition, waterfowl, swimmers and anglers. Temporal and spatial fluctuations of those budget terms have to be considered as well.

Although the quantification of each single term is quite ambitious, the overall concept of a mass budget is simple (Healy et al. 2007). The change in mass storage equals mass inflow minus mass outflow, plus or minus reactions (Lin et al. 1987). These reactions include biological, chemical and physical source and sink reactions of the compound in the lake water, losses to the atmosphere via processes such as gaseous exchange and losses at the sediment-water interface due to sedimentation of particulate matter and diffusion of dissolved substances. In addition, there is also some release from lake sediments due to diffusion, bioturbation, advective transport and resuspension. Few authors, such as Wentz et al. (1995)et al. (1995), LaBaugh et al. (1995), LaBaugh et al. (1997), Robertson et al. (2003), Oliveira Ommen et al. (2012) and Juckem and Robertson (2013), have presented chemical budgets that explicitly include groundwater inflow and outflow.

2.2.4 Measurement techniques and modelling

In the first part of this review (Rosenberry et al. 2015), several measurement techniques and modelling approaches for the quantification of water fluxes have been presented. Some of those methods are also appropriate for investigating chemical constituents in the exfiltrating groundwater. Applicable techniques will be discussed briefly here; see Rosenberry et al. (2015) for further details. Additional criteria to consider when choosing a sampling method are accessibility, costs, robustness, unattractiveness for vandalism and aesthetical aspects (McCobb et al. 2009). All approaches listed in the succeeding text require multiplying the estimates of the water fluxes by the nutrient concentrations in the seepage water (e.g., Kroeger and Charette 2008; Meinikmann et al. 2013; Robertson et al. 2003; Winter 1978; Zimmermann et al. 1985). Under the assumption that transport through the aquifer-lake interface is conservative, P fluxes are often determined as the product of seepage flux times groundwater concentration (Kroeger and Charette 2008). However, the sediment-water interface is a chemically reactive interface, and thus such calculation can be problematic. Consequently, it is more desirable to measure the concentration of the exfiltrating water directly at the interface. Because most LGD occurs in nearshore areas (McBride and Pfannkuch 1975), it is sufficient to sample predominantly in littoral regions of lakes, which are more easily accessible than deeper areas of the lake (Rosenberry et al. 2015; Schafran and Driscoll 1993).

One approach that does not require the multiplication of water fluxes and nutrient concentrations is determination of the net groundwater nutrient component as residual in the lake's nutrient budget (e.g., Lerman and Brunskill 1971; Schaffner and Oglesby 1978; Sutula et al. 2001; Vanek 1987). However, as discussed in Rosenberry et al. (2015), we doubt that such an approach is useful for lake water budgets, and we have even more doubts regarding nutrient budgets because the errors of all budget terms are even larger in nutrient budgets than in water budgets.

Groundwater observation wells. Groundwater observation wells, occasionally including private wells near lake shorelines, can be sampled to estimate nutrient concentrations of LGD (e.g., Belanger et al. 1985; McCobb et al. 2003; Vanek 1993). An advantage of such an approach is that already existing wells can be used in the investigations. Often, these wells have been built as a part of a hydrogeological observation network, and sometimes long-term data sets are available. Furthermore, groundwater sampling is a well-established technique, required devices are easily available, sampling strategies are standardized and consulting companies are familiar with such tasks. A disadvantage, however, is the potential for the water chemistry at the sampled well to not be representative of the water chemistry that enters the lake. Because of the high reactivity of the sediment-water interface (section on Why has LGD been Disregarded so Long?), especially within decimeters of the interface, groundwater chemistry can change greatly just prior to discharging to a lake. A further disadvantage might be the suboptimal location or depth of the wells, unsuitable well materials that interfere with the chemical composition of the groundwater (e.g., iron in metal well casing might react with phosphate in the groundwater), and heterogeneities in the catchment (e.g., Schot and Pieber 2012; section 2) that result in the need for a large number of wells.

Suction samplers in lake bottom sediments. Several different devices can be used to collect water samples from approximately 0.1 to 2m beneath the sediment water interface by applying suction(McCobb et al. 2009). Although they all rely on the same basic principle of applying less than 1 atm of vacuum, there are several different designs for accessing these shallow sediments and for applying such a vacuum. Whereas some techniques require drilling a hole in the sediments prior to insertion of the sampler, other devices are pushed or hammered directly into the sediment. Some designs have the well screen protected inside a pipe casing during installation. The casing is pulled out of the sediment after installation and prior to sample collection, for example, drive point samplers (Lewandowski et al. 2011b; McCobb et al. 2003; Rivett et al. 2008b). Other simple sampling designs consist of plastic or metal pipes with a screen (also called filter) made of slits or perforations (with or without a gauze cover) at its lower end, also called piezometers. Some of these designs have a diameter large enough to allow a tube or pump to be lowered inside the well for sample collection. Several authors also have used multilevel samplers, multilevel wells or multilevel piezometers that consist of a bundle of tubes ending at different sediment depths (Brock et al. 1982; Hauxwell et al. 2001; Lee et al. 1980; Lewandowski et al. 2011b; McCobb et al. 2009; McCobb et al. 2003; Rivett et al. 2008b). A gauze or nylon mesh fabric is typically wrapped around the lower end of each tube to serve as a well screen. Tubes commonly are color-coded to distinguish the different well depths. A simpler suction sampler used by Brock et al. (1982) is a 10ml pipette modified by melting holes near the tapered end of the pipette with a hot metal rod and wrapping the perforated end with nylon mesh fabric. Oliveira Ommen et al. (2012) introduced ‘pore-water sippers’, which are basically small metal tubes (inner diameter 1 to 2.5 mm) sealed at one end and perforated with several holes (0.5 to 1 mm diameter) along the first few centimetres of the sippers. Silicone tubing attached to the metal tube is used to connect the sipper to a plastic syringe. Muendo et al. (2005) used ‘rhizon samplers’ (Eijkelkamp Agrisearch Equipment, Gelderland, Netherlands), which are basically made of a thin polymer tube with 1mm inner diameter and 0.1µm pores. The rhizon samplers are connected to 10ml vacuum tubes that fill within a few hours.

After installation of suction sampling devices, an equilibration time of a few days is recommended to allow any disturbance of the sediment biogeochemistry to dissipate with re-equilibration of the system. All suction samplers require sufficient hydraulic conductivity of the surrounding sediment to transmit water through the screen at a reasonable rate. If hydraulic conductivity is low (because of fine-grained silty sediments), either no sampling is possible or sampling times may take too long. An advantage of these sampling techniques relying on suction is that they are relatively fast and inexpensive. Problems might arise from short-circuiting of flow downward along the sampler or from changes of the chemical pore-water composition during sampling. For example, oxygen diffusion through the tube walls or oxygen contact at the outlet of the sampling device might alter the composition of reduced pore-water samples. Furthermore, the applied suction might cause degassing. Fortunately, the small sample volumes limit mixing of the targeted water with water from above or below the well screen, and thus will increase the representativeness of the sample.

Dialysis samplers. Dialysis samplers (Hesslein 1976), also called diffusion samplers or peepers, are a common method to collect pore-water in marine and lacustrine sediments. Dialsysis samplers consist of a plastic plate with several chambers, which are initially filled with distilled deoxygenated water before a dialysis membrane, for example, a polysulfone membrane, is attached to hold the water in place. Once the sampler is installed in the sediment, the water in the chambers equilibrates with the pore-water outside the sampler. After an exposition time of approximately 2 weeks, the sampler is retrieved, and the water in the chambers is preserved for analytics. Several studies used dialysis samplers to characterize solute fluxes at the sediment-water interface in lake areas where groundwater exfiltration was likely (Schuster et al. 2003; Vroblesky et al. 2002). Because common dialysis samplers have to be pulled out of the sediment for analysis, a repetition at exactly the same location is impossible. However, there are some designs that allow a repetitive analysis at the same location. McCobb et al. (2009) developed a sampler with an outer casing that can remain in the sediment while the sampler itself is replaced. Jacobs (2002) developed a sampler with tubes attached to each chamber so that the water in the chambers can be collected for analysis and substituted by distilled water without recovering the sampler.

An advantage of dialysis samplers is that they allow high spatial resolutions; 1-cm vertical sampling resolution is common. An additional advantage of passive sampling is that mixing of water from different zones is avoided (McCobb et al. 2009). Oxygenation of the samples during sampling is only a minor problem compared with suction samplers. In contrast with suction samplers, dialysis samplers also can be used in sediments with low hydraulic conductivity. A design of dialysis samplers also exists that provides a 2D horizontal and vertical resolution of 0.9cm (Lewandowski et al. 2002). A disadvantage of all aforementioned dialysis samplers is the quite long equilibration time of 1 to 2 weeks.

Instead of water-filled chambers, a thin layer of gel on a plastic plate covered by a dialysis membrane is used in gel samplers. They allow a much shorter equilibration time. Due to the thin gel layer, equilibration can be completed within less than a day (Krom et al. 1994; Mortimer et al. 1998; Pagès et al. 2011; Robertson 2008). After recovery of the samplers, the gel is divided into sections and re-equilibration with a solvent is used to re-dissolve the pore-water constituents. Mortimer et al. (1999) used gel samplers to quantify exfiltrating groundwater. A novel technique deploying gel samplers developed by Robertson (2008) and Pagès et al. (2011) allows a fast and easy analysis of pore-water P, Fe(II) and sulphide concentrations at the sediment-water interface with 1mm spatial resolution simply by using photometrical reactions and a conventional digital office scanner. Unquestionably, this method has much potential for the investigation of LGD.

Coring. Coring in conjunction with pore-water extraction by squeezing or centrifugation is another technique to collect pore-water (Cornett et al. 1989; Frape and Patterson 1981; Harvey et al. 2000; Patterson et al. 1978). A disadvantage of these methods is that oxygenation and degassing might alter the pore-water composition during handling of the samples and separation of pore-water and sediment matrix.

Seepage meters. Exfiltrating groundwater can be collected using seepage meters (Rosenberry et al. 2015). During insertion of the seepage meter, a volume of overlying water is enclosed inside the seepage meter. Thus, flushing with several seepage meter volumes by exfiltrating water should be carried out prior to sampling. The bags attached to the seepage meters to determine seepage volume can also be used to collect water quality samples. The bags are usually partially prefilled with water to reduce the resistance caused by an empty bag. For determinations of the water composition of the exfiltrating water, it is then necessary to consider the composition of that initial water (distilled water, lake water or previously collected water of the seepage meter). Seepage meters can experience several complications. Some authors (Belanger and Mikutel 1985; Belanger et al. 1985; Downing and Peterka 1978; Zimmermann et al. 1985) have described that the enclosure of lake sediment by seepage meters can cause anoxic conditions that might produce anomalously high P concentrations and increased release rates of ammonium nitrogen. Although this seems reasonable, none of the aforementioned authors present reliable evidence for this being a problem. The observed changes in chemistry of water collected from seepage meters compared with groundwater collected from shallow piezometers or pore-water samplers might also be caused by biogeochemical reactivity of the interface (compare sections on "*Why has LGD been disregarded so long?*", "*Importance of Phosphorus Import via Groundwater*" and "*Importance of Nitrogen Import via Groundwater*"). Another artifact of the deployment of seepage meters is the interruption of sedimentation on the portion of the bed covered by the seepage meter, which might reduce delivery of easily degradable organic matter and thus alter biogeochemical processes.

Modelling. Although groundwater-flow models are commonly used to assess hydrological interactions between groundwater and surface water (Rosenberry et al. 2015), nutrient transport from aquifers to surface waters has less frequently been modelled. There are only some studies that use reactive transport modelling to investigate the fate of nutrients on the flow path from an aquifer, through the (reactive) transition zone and into a surface water body. These few studies can be grouped according to the three interfaces shown in Figure 2.4: LGD (Kidmose et al. 2010; Parkhurst et al. 2003), hyporheic zone (Bardini et al. 2012; Bardini et al. 2013; Gu et al. 2012; Zarnetske et al. 2012) and SGD (Ibánhez et al. 2011; Spiteri et al. 2008a; Spiteri et al. 2007; Spiteri et al. 2008b). In addition to the few studies that have focused on reactive transport modelling of groundwater discharge, there are a few studies (Greskowiak et al. 2006; Horner et al. 2007) that have investigated the opposite flow direction, that is, infiltration of surface water into the aquifer, a special type of groundwater recharge. The main motivation for the latter studies is concern about the quality of bank filtrate used for drinking water abstraction.

Different processes driving the transport across the groundwater-surface water interface have to be considered depending on the interface setting. In the case of LGD, Parkhurst et al. (2003) and Kidmose et al. (2010) used a standard groundwater flow model based on hydraulic gradients and hydraulic conductivities combined with a chemical reaction network. For a hyporheic setting, Bardini et al. (2012); Bardini et al. (2013) employed a numerical model to simulate the turbulent water flow and the pressure distribution over submerged dunes, and then they evaluated the flow field and the biogeochemical reactions in the hyporheic sediments. In the case of SGD, Spiteri et al. (2008a); Spiteri et al. (2007); Spiteri et al. (2008b) used a model that couples density-dependent flow to a reaction network. The most common code for modelling the reaction network is PHREEQC (Parkhurst and Appelo 1999).

Horner et al. (2007) list a number of reactive transport models, which are available to simulate processes at aquifer-surface water interfaces: RT3D (Clement 1997), COTREM (Adler et al. 2000; Landenberger et al. 1997), STEADYSED (Van Cappellen and Wang 1995), HYDROGEOCHEM (Yeh et al. 1998), TBC (Schäfer et al. 1998), MIN3P (Mayer and Frind 2003), PHAST (Parkhurst et al. 2003) and PHT3D (Prommer 2002). COTREM and STEADYSED are mainly used for marine environments. RT3D and TBC preferentially solve kinetic reaction problems without, or only partially, addressing geochemical equilibrium processes (Horner et al. 2007). The computer codes MIN3P, HYDROGEOCHEM, PHAST and PHT3D couple kinetically controlled processes (biodegradation, non-aqueous phase liquid dissolution) to the relevant background geochemical reactive processes, such as aqueous complexation, mineral precipitation and dissolution, thus providing modelling of real hydrochemical situations.

2.2.5 Phosphorus in seepage

We start this section with a short description of basic chemical characteristics of phosphate mobility in soils and aquifers. Then, we follow the transport of P (Fig. 2.5) from the catchment through the aquifer to the reactive aquifer-lake interface, and finally into the receiving water body. We describe both background P concentrations and major anthropogenic sources because this information is important to understand why P input from LGD is a major concern for many freshwater systems.

Furthermore, there is still a need to promote the environmental hazards of high phosphate concentrations in aquifers because mobility and concentrations of phosphate in aquifers were underestimated until recently. Now, there may be a shift in thinking reflected in headlines such as: 'Phosphate doesn't migrate in groundwater? Better think again' (USGS 2012) and 'Phosphorus in groundwater – an overlooked contributor to eutrophication?' (Holman et al. 2008).

Basic chemical characteristics of phosphate mobility

Primary and secondary reactions of P immobilisation. Reactive phosphate in the aquifer is mostly present as dissolved inorganic phosphate (Slomp and Van Cappellen 2004) while little is known about concentrations of dissolved organic phosphate in groundwater (Kalbitz et al. 2000). Fast surface sorption of the dominant forms of phosphate, which are HPO_4^{2-} and $H_2PO_4^-$, occur by anion exchange (Isenbeck-Schroeter et al. 1993; Ptacek 1998; Robertson 2008)

- onto positively charged mineral surfaces such as Al-containing, Mn(IV)-containing and Fe(III)-containing oxides and (oxy)hydroxides, and calcite (e.g., Ptacek 1998; Spiteri et al. 2007; Wilhelm et al. 1994; Zanini et al. 1998);
- onto clay surfaces by complexing with calcium, aluminum and iron (Loeb and Goldman 1979; Ptacek 1998);
- onto solid organic carbon (Harman et al. 1996).

Most studies describe an additional loss of phosphate and a tendency for increasing irreversibility of phosphate sorption with time (Detenbeck and Brezonik 1991; Munns and Fox 1976). Robertson (2008) states that there is an additional loss and irreversibility caused by secondary reactions, such as (1) molecular diffusion of P into micropores or through mineral coatings onto internal sorption sites (Torrent et al. 1992); (2) slow crystallisation of sorbed P into insoluble metal phosphate minerals (Stumm and Morgan 1996); and/or (3) slow direct precipitation of secondary Ca/Fe/Al/Mn-phosphate minerals with extremely low solubility, such as hydroxyapatite ($Ca_5(PO_4)_3(OH)$), vivianite ($Fe_3(PO_4)_2 \cdot 8H_2O$), strengite ($Fe(PO_4) \cdot 2H_2O$), variscite ($Al(PO_4) \cdot 2H_2O$) (e.g., Isenbeck-Schroeter et al. 1993; Ptacek 1998; Stumm and Morgan 1996; Zanini et al. 1998). Geochemical equilibrium calculations are useful for identifying which minerals might precipitate when concentrations become close to or exceed their saturation indices (Ptacek 1998). However, even if saturation indices are exceeded, the formation of the minerals might be kinetically hindered (Ptacek 1998; Stumm and Morgan 1996). It is likely that a variety of minerals are present in most lakebed sediments, including amorphous mixtures for which limited solubility data are available (Zurawsky et al. 2004). The distinction between fast reversible sorption and secondary processes is important because reversible sorption does not permanently remove P from solution, here as secondary processes have impacts on the total amount of P in the system even if the processes are very slow (Robertson 2008).

Sorption and precipitation. The reason for usually low P concentrations in groundwater is that most soils have a high P sorption capacity under oxic conditions (>100mg kg^{-1} PO_4-P according to Vanek (1993), 15–30mg kg^{-1} according to Harman et al. (1996)) and extremely high P loads are necessary to exhaust it (Vanek 1993). It has been shown that under prolonged high nutrient loading, phosphate can be mobile (Robertson 1995; Robertson et al. 1998; Slomp and Van Cappellen 2004). Furthermore, some authors report a competition between Si and P for sorption sites because both adsorb specifically to the surface of iron and aluminum oxides through ligand exchange (Brinkman 1993; Tallberg and Koski-Vahala 2001; Tallberg et al. 2008; Tuominen et al. 1998). Thus, the presence of Si can induce a release of sorbed P. In addition to P sorption onto mineral surfaces, mineral precipitation with dissolved Ca, Al or Fe might cause P attenuation, for example, hydroxyapatite ($Ca_5(PO_4)_3(OH)$), varisite ($AlPO_4 \cdot 2H_2O$), strengite ($FePO_4 \cdot 2H_2O$) (Dean et al. 2003; Garcia-Solsona et al. 2010; Harman et al. 1996; Robertson 1995; Robertson et al. 1998; Simmons and Lyons 1994; Slomp and Van Cappellen 2004; Zanini et al. 1998).

P transport in the vadose and in the saturated zone; impact of oxic and anoxic conditions. P is typically immobilized in the vadose zone, that is, in the upper soil layers before reaching the aquifer (Robertson et al. 1998). However, the P sorption capacity is low in soils poor in clay minerals, calcium and metals. Thus, leaching and loss of calcium during soil genesis will result in decreased P sorption capacities (Vanek 1993). P sorption in the saturated zone is impacted by additional processes. Reducing conditions in saturated sediments will lower the P sorption capacity due to the dissolution of iron(oxy) hydroxides and the release of iron-bound and other redox-sensitive bound P species (Carlyle and Hill 2001; Patrick et al. 1973). Under sub-oxic conditions, the transport of phosphate with groundwater flow is enhanced compared with oxic conditions (McCobb et al. 2003). Under anaerobic conditions, however, phosphate removal is often less efficient than under oxic conditions (Carlyle and Hill 2001) and occurs mainly through precipitation of mineral phases such as hydroxyapatite ($Ca_5(PO_4)_3(OH)$ or vivianite ($FePO_4 \cdot 2\,H_2O$) (Slomp and Van Cappellen 2004). Processes are generally more complicated when different redox environments are involved. At redox boundaries, the iron oxides that bind phosphate quickly precipitate upon oxygenation (Griffioen 1994; Griffioen 2006).

P retardation and de-mixing of contaminant plumes. P migration is usually retarded compared with water and conservative water compounds by a factor of 5 to 100 because of sorption (Appelo and Postma 1999; Harman et al. 1996; Lamontagne 2002; Robertson 2008; Robertson et al. 1998; Stumm and Morgan 1996). Thus, P plumes usually move much slower than groundwater flow (McCobb et al. 2003; Ptacek 1998). The adsorption of P creates a reservoir of P in the aquifer sediments (McCobb et al. 2003; Stollenwerk 1996). P might desorb as water with lower P concentrations flushes through the previously contaminated aquifer (Stollenwerk 1996; Walter et al. 1995). McCobb et al. (2003) state that the flux of P may continue for decades after eliminating the source because of the large amount of P sorbed onto the aquifer sediments. Furthermore, variations of pH and ionic strength might alter P sorption capacity (McCobb et al. 2003; Ptacek 1998). In most systems, sorption of phosphate decreases as pH increases, and surface charge becomes more negative (Detenbeck and Brezonik 1991).

Ptacek (1998), McCobb et al. (2003) and Roy et al. (2009) determined that transport and exfiltration pattern of different sewage constituents are clearly asynchronous. Whereas chloride and boron are conservative tracers passing through the aquifer without retention, other constituents such as P are retarded. Thus, a contaminant plume containing both chloride and phosphate is de-mixed (separated) while travelling through the aquifer. Consequently, P might reach a site some distance from the source much later than a sewage indicator, such as boron. After repairing a leaking sewage source, the sewage indicator boron will soon be gone due to its mobility, whereas phosphate contamination is much more enduring. Under oxic conditions nitrate might also exhibit a nearly conservative behaviour, and thus travel much faster than P. The mobility of other redox-sensitive constituents, such as iron and manganese, also depends on the redox conditions in the aquifer. As a consequence, there is an increasing separation of the different sewage contaminants with travel time and travel distance.

Phosphate in groundwater approaching the sediment-water interface

Background P. Phosphate concentrations in groundwater are usually quite low (<50 µg PO_4-P l^{-1}), especially background P concentrations in areas without anthropogenic impact (Table 2.5). For Germany, natural groundwater concentrations throughout the country were determined in a research project for the German Working Group of the Federal States on Water Problems. The investigations were conducted separately for different hydrogeological typologies using data from 26 000 sampling locations. Based on statistical analysis, natural and anthropogenically influenced groundwater components were separated. The 90% percentiles of the natural components are given in Table 2.5 as maximum natural groundwater P concentration (Kunkel et al. 2004; Wendland et al. 2005).

Holman et al. (2008) and Holman et al. (2010) assessed phosphate concentrations in the groundwater of the Republic of Ireland, Northern Ireland, Scotland, England and Wales. They concluded that groundwater phosphate concentrations were more important contributors to surface water P concentrations than previously thought, especially during base-flow conditions that are quite common during spring and summer. Furthermore, they concluded that ecosystems were of highest vulnerability to P input in the period of maximum primary productivity in late spring and summer (Holman et al. 2010; Holman et al. 2008). The largest problem for a reliable estimation of background P concentrations in Holman et al. (2008) and Holman et al. (2010) was the analytical detection limit for P. The reason for that is that the primary driver for monitoring P in groundwater is the drinking water quality standard (EU drinking water standard 2200µg PO_4-P l^{-1}) and not an ecologically relevant threshold (Holman et al. 2010). There is no widely accepted in-lake target P concentration because the threshold depends on the potential trophic state of the lake. Thresholds of 50µg TP l^{-1} or lower have been common. The acceptable areal annual P load and the target P concentration depend on the potential trophic state of the system and morphometric characteristics of the lake (Correll 1998; Schauser et al. 2003; Vollenweider 1976). It might be desirable that groundwater P concentrations are below the target set for the receiving water body. However, even groundwater P concentrations lower than the target P concentration of the lake water might be a problem in some cases such as lakes in geographic regions with high evaporation rates resulting in an accumulation of P concentration in the water body. Furthermore, in stratified lakes P accumulations in the hypolimnion during stratification periods are common resulting in infiltrating epilimnetic water having lower than average P concentrations and resulting in increasing average P concentrations.

Although background P concentrations are usually low (<50 µg PO_4-P l^{-1}, Table 2.5), this is not always the case. Schaffner and Oglesby (1978) noted that losses of P from the landscape to receiving waters are a function of bedrock geology. A source of groundwater P is the weathering of mineral phases (Slomp and Van Cappellen 2004). For example, Reynolds (1979) suggested that extremely high phosphate concentrations of some lakes in England are caused by catchments rich in apatite. Inputs of P from the catchment need to be large enough to offset the annual net loss of P to sedimentation to maintain the actual trophic level of a system. Natural P inputs to groundwater are also caused by downward leaching of P from soil organic matter, *in situ*-release from organic matter in the aquifer and release from Fe-oxides under anoxia (Carlyle and Hill 2001; Slomp and Van Cappellen 2004). According to Griffioen (1994); Griffioen (2006), natural sources of high groundwater P concentrations include the degradation of organic matter in wetlands, moors and bogs. Similarly, Ptacek (1998) reports elevated groundwater P concentrations of 100 to 900 µg PO_4-P l^{-1} in the lower reduced zone of the investigated aquifer that is similar to the concentrations reported in Table 2.5 for reducing groundwater in low-lying areas of North German Plains. However, Ptacek (1998) could not completely rule out the possibility that the high groundwater P concentrations are caused by anthropogenic impacts. Carlyle and Hill (2001) report that, beside external inputs of P from adjacent landscapes, internal P sources account for the presence of SRP in groundwater and SRP transport to streams. They identified abandoned channel-fill and bar deposits as P pools in the aquifer. The stored P can be remobilized due to mineralization of organic matter and due to dissolution of iron(oxy)-hydroxides at low redox potentials. This is analogously true for lake shores, which are often bordered by silting up areas with their high organic matter and P content.

Agriculture. Traditionally, water and wind erosion are regarded as main routes of P transport from terrestrial to aquatic systems, and thus factors such as vegetation cover, cultivation, tillage and precipitation control P mobility (Hillbricht-Ilkowska and Sharpley 1995) and external P loads to surface waters. When applied judiciously, manure and fertilizer should usually result in only small amounts of dissolved P draining into the aquifer because soil adsorption properties and high biological uptake rates prevent excessive mobility of P. However, according to Spiteri et al. (2007), groundwater P concentrations have increased worldwide as a result of the agricultural application of manure and synthetic fertilizers. Most authors agree that the main anthropogenic sources of P to groundwater are fertilizer applications, manure and wastewater (Hwang et al. 2010; Kroeger et al. 2007; Slomp and Van Cappellen 2004). Thus, land uses such as grasslands, arable soils or urban settlements impact groundwater P concentrations (Cherkauer et al. 1992; Griffioen 2006; Holman et al. 2010; Holman et al. 2008; Roy and Malenica 2013). For decades, P was applied in excess of crop requirements leading to a well-documented P accumulation in many soils and a consequently increased risk of P transport to groundwater (Heckrath et al. 1995). Withers et al. (2001) report that as part of agriculture in the UK, productive grasslands and arable soils have resulted in an average P surplus of 1000 kg ha^{-1} over the last 65 years. Further potential causes of agricultural groundwater contamination are animal slurry lagoons (dairy, beef and pig farms) and manure heaps (Gooddy 2002; Harper 1992; Holman et al. 2010; Holman et al. 2008; Withers et al. 1998). The largest surpluses occur in regions with intensive hog and poultry units where the resulting amounts of manure exceed the carrying capacity of soils (Withers et al. 2001).

Urban settlements, industry and sewage. Urban aquifers receive P via multiple pathways. P originates from infiltration of precipitation in unsealed urban areas and infiltration of road and roof runoff through storm water infiltration facilities. Hazardous sites (e.g., caused by chemical industry, foods industry, wastewater treatment facilities and fertilizer storage) are other possible causes of high groundwater P concentrations. A variety of sewage infiltration techniques were used in previous centuries and are still common in several countries to dispose (more or less) treated sewage. For example, decentralized sewage pits were quite common in Germany until the second half of the 20th century. With the development of the sewage canalization in the 19th and 20th centuries in Germany, centralized sewage treatment facilities were established. At some locations, for example in Berlin (Horner et al. 2009) or on Massachusetts Military Reservation (McCobb et al. 2003), large sewage infiltration beds were used. In the US, conventional septic systems are still a source of ongoing groundwater degradation because approximately one-third of the nation's sewage is disposed of by systems consisting of septic tanks and drain fields (Harman et al. 1996; Wakida and Lerner 2005; Wilhelm et al. 1994; Zanini et al. 1998). Such systems are also common in Canada and Western Australia (Harman et al. 1996; Wakida and Lerner 2005; Wilhelm et al. 1994; Wilhelm et al. 1996). Similarly, in Ireland, one-third of the population uses on-site treatment systems (Holman et al. 2008). In properly operating systems, the water percolating downwards is almost completely oxidized in the unsaturated zone, which it passes through before reaching the aquifer so that most organic compounds are oxidized. Nevertheless, septic systems are a potential source of P to groundwater and receiving waters (Lapointe et al. 1990), especially if they are located near lakeshores. For example, in some jurisdictions (e.g., province of Ontario, Robertson 2008; Robertson et al. 1998; Zanini et al. 1998; Zurawsky et al. 2004), the minimum setback distance for septic systems from lakes shorelines is only 15 to 20m. According to Zurawsky et al. (2004), mass loading studies have suggested that septic systems can represent the largest source of P loading to some lakes (e.g., up to 55% in Ontario lakes). Harman et al. (1996) also conclude that septic systems can result in significant amounts of phosphate entering nearby surface water bodies. Swarzenski et al. (2007) and Simonds et al. (2008) found that

Table 2.5 Examples for typical groundwater phosphate-concentrations for pristine and anthropogenically impacted aquifers.

Aquifer typology	PO_4-P (µg l^{-1})	Type of value	Reference
Loose rock, Germany			
Sand and gravel of the North German Plain	33	Maximal natural groundwater concentration (90% percentile of the natural groundwater component)	Kunkel et al. (2004); Wendland et al. (2005) [a]
Sampling depth 0-10 m	26		
Sampling depth 10-25 m	16		
Sampling depth 25-50 m			
Fluvial sand and gravel of the Upper Rhine Valley	59		
Fluvial gravel deposits and glacial moraine deposits in Alpine piedmont	39		
Tertiary sediments	20		
Carbonate rock, Germany			
Jurassic limestones	46		
Triassic limestones	46		
Carbonate rock (marl) interbedded with clay and sand layers	68		
Silicate rock, Germany			
Sandstones and sandstone interbedded with clay stone (different eras)	3		
Paleozoic sedimentary rock	23		
Magmatic and metamorphic rock	16		
Reducing groundwater in low-lying areas of North German Plains	500	Typical values	Kunkel et al. (2004)
Semi-natural land cover		Mean groundwater P concentration	Holman et al. (2010)
Republic of Ireland	23		
Scotland	20		
England and Wales	48		
Woodland			
Republic of Ireland	28		
Scotland	16		
England and Wales	58		
Natural background level, Republic of Ireland	20	90% percentile concentration within confined portions Irish aquifers	
Various sites, Ontario, Canada:		Background	Harman et al. (1996); Wilhelm et al. (1996); Zanini et al. (1998)
Fine to medium-grained calcareous sand, Cambridge, Canada	< 10		
Fine to coarse sand, Muskoka	< 10		
Fine to medium sand, Langton	30		
Groundwater, U.S.		Median	Nolan and Stoner (2000)
Shallow groundwater, agricultural land use	10		
Shallow groundwater, urban land use	20		
Deeper groundwater, major aquifers	10		
Nearshore surface water, Florida Keys		Arithmetic mean	Lapointe et al. (1990)
Groundwater close to septic systems	527		
Groundwater impacted by septic systems	303		
Background groundwater	3.4		
Sewage plumes	4900	Maximum	Robertson et al. (1998)
Anthropogenically impacted groundwater, Swaziland	100-490	Range of 15 wells	Fadiran et al. (2008)

[a] The method to estimate maximum natural groundwater concentrations in described in Wendland et al. (2005). Unfortunately, the values for phosphate are only published in German in Kunkel et al. (2004).

leaky or improperly functioning septic systems are the major source of excess nutrients in LGD entering Puget Sound, and thus its water quality deterioration. Mallin and McIver (2012) state that most septic systems in a popular tourist area in North Carolina are failing because high groundwater tables reduce the pathway of wastewater through the unsaturated zone, and thus preclude the proper functioning of septic systems.

Leaky sewers are another potential source of groundwater contamination (Bishop et al. 1998; Rutsch et al. 2008; Schirmer et al. 2013; Wakida and Lerner 2005) and high P emissions (Wolf et al. 2004). Typical sewage P concentrations range between 9 and 15mg PO_4-P l^{-1} (Bishop et al. 1998; Holman et al. 2008). The exfiltration of sewage from defective sewer systems into the aquifer in the city of Hanover is about 17 m^3 day^{-1} km^{-1} while it is 1.2m^3 day^{-1} km^{-1} in the city of Rastatt (Eiswirth et al. 2004). For Germany, it is estimated that several 100 million m^3 $year^{-1}$ of sewage, that is, approximately 10% of the total sewage load, drain through leaking sewers into soils and aquifers (Eiswirth and Hötzl 1999). The flux from the sewer pipe into the unsaturated and saturated zones is 16 kg P ha^{-1} yr^{-1} for Rastatt and 11 kg P ha^{-1} yr^{-1} for Hanover. A similar problem to leaking sewers is main water pipes. Their losses of 20% are considered routine in the UK (Holman et al. 2010; Holman et al. 2008; Wakida and Lerner 2005). About 95% of the public water supplies in the UK are regularly dosed with 0.5 to 1.5 mg PO_4-P l^{-1} to reduce plumbosolvency (Hayes et al. 2008; Holman et al. 2010; Holman et al. 2008), and thus also drinking water losses result in contamination of the aquifer.

Fate of phosphate at the reactive aquifer-lake interface

Is the interface a P source or sink? It is controversial whether phosphate concentrations increase or decrease as exfiltrating water passes through the reactive groundwater-lake interface (Fig. 2.5; section on Why has LGD been Disregarded so Long?). Hofmann and Lessmann (2006) report a decrease of phosphate concentrations in water exfiltrating to a mining lake compared with adjacent groundwater. Griffioen (1994) also describes P fixation at the oxic/anoxic interface. Holman et al. (2010) note that elevated groundwater P concentrations do not necessarily result in an increased P load via LGD because a number of attenuating reactions may occur along the flow path. Vanek (1991) states that riparian zones of lakes are usually phosphate sinks. However, he also describes that after accumulating P for many years, changes of environmental conditions might result in a subsequent release of P to the lake. Vanek's data show that significant amounts of P were liberated in the riparian zone and increased the transport of P to Lake Bysjön due to increased decomposition of organic matter and a gradual decrease in calcium in aquifer sediments. Patrick et al. (1973) describe a release of P from flooded soils and Gilliom and Patmont (1983) also report a transport of P towards a lake from areas with periodically perched water tables. For Lake Mendota, Brock et al. (1982) observed that P concentrations were increased about one order of magnitude in exfiltrating water compared with groundwater collected from nearby piezometers. Similar P concentrations in groundwater and exfiltrating seepage indicate that P in the exfiltrating water is groundwater-borne P (Brock et al. 1982; Kang et al. 2005).

Exfiltration pattern. As already discussed in the first part of this review (Rosenberry et al. 2015), groundwater flow-lines bend upwards as groundwater discharges to lakes. Thus, a vertical depth differentiation of groundwater composition that might be present where water flows primarily horizontally through an adjacent aquifer is depicted more or less horizontally on the lake bottom. For example, McCobb et al. (2003) show that in groundwater approaching, Ashumet Pond highest P concentrations of up to 3 mg PO_4-P l^{-1} occur approximately 10m below the groundwater table. This high concentration groundwater exfiltrates about 5m offshore where the water depth is approximately 0.5 m. Lateral shifts in the plume's discharge area occur as a result of varying pond stage (McCobb et al. 2009). Most exfiltration usually occurs close to the shore, so that P transported by groundwater usually enters the epilimnion where it can be directly utilized by lake biota (Enell 1982; McCobb et al. 2003; Shaw and Prepas 1990; Vanek 1991). Increasing groundwater exfiltration might have negative impacts on surface water quality. Downing and Peterka (1978) investigated at Lake Metigoshe the relationship between LGD and P input by LGD. They found a nearly linear relationship between fluctuating LGD and P input by LGD because there were little changes in P concentrations of the exfiltrating water. For management considerations, Kang et al. (2005) suggest that the organic-rich sediments may not be considered as a significant source of P, but rather as an effective cover that impedes the delivery of groundwater P to the lake.

Origin of interface P. P released from the reactive interface as approaching groundwater crosses the sediment-water interface to enter the lake may previously have been immobilized and accumulated at the same interface during different environmental conditions. When changes of environmental conditions occur, previously accumulated P can be released (Carlyle and Hill 2001; Vanek 1991). For example, a combination of processes consuming oxygen with a high water table lead, at least temporarily, to anoxic conditions. Reducing conditions result in the mobilization of redox-sensitive bound P and its transport into the lake (Vanek 1991). It is also possible that the released P is originally of lacustrine origin, that is, that P was previously deposited as particulate P by sedimentation or as dissolved P by sorption and covered by additional sediment over long time scales. For example, Brock et al. (1982) assume that P in seepage to Lake Mendota is of lacustrine origin. This release of P reduces the exhaustible previously stored P pool but the pool might be sufficient to supply P for decades or even centuries.

Differentiation of internal and external P. Care is required to differentiate between internal P cycling and external P sources. P dissolved in the lake water is taken up very efficiently by biological processes and fixed in the lake biomass. Additional P might be sorbed by particulate material suspended in the lake water or imported as particulate P from the catchment. Sedimentation causes a downward transport of dead organic matter and inorganic particles to the lake sediment. Part of the P is released back to the water column during settling and the rest reaches the sediment (Hupfer and Lewandowski 2005). There, mineralization of organic matter and other early diagenetic processes can cause a release of some of the previously settled P into the pore-water while another part is permanently buried in the sediment (Hupfer and Lewandowski 2008). Thus, pore-water P concentrations are usually much higher than P in the overlying water. Diffusion causes a transport of pore-water P into the overlying lake water. Some authors also indicate that bioirrigation is a substantial driver for the release of pore-water P (Andersson et al. 1988) to the water column, whereas others have found decreased P release due to an increased oxidized sediment volume caused by bioirrigation (Lewandowski et al. 2007).

In some lakes, exfiltrating groundwater is an important transport process for pore-water P into the water body (Sonzogni and Lee 1974). However, there is usually a mismatch between zones of high groundwater exfiltration and zones with high pore-water P concentrations. Highest pore-water P occurs usually in the deepest areas of lakes where thick layers of fine sediments have accumulated during millennia. The low hydraulic conductivity of that sediment essentially seals the lake bottom and inhibits exfiltration. In contrast, exfiltration is usually focused at near-shore areas where the sediment is commonly sandy and pore-water P commonly is small. Nevertheless, groundwater exfiltration into lakes can be considered as a mechanism fueling the internal P cycle by increasing P recycling from the lake sediments to the overlying water (Shaw and Prepas 1990). Cornett et al. (1989) introduced a one-dimensional advection-diffusion model to differentiate between advection and diffusion in sediments with low groundwater flow velocities. Advective transport of pore-water P released by diagenetic processes has an important impact on the shape of the pore-water profiles in the sediment and the fluxes. However, that P is the result of internal recycling and should not be mistaken for or be considered part of groundwater-borne P. The release of P from the sediment is usually smaller than the amount of P deposited with previously settled sediment. In lakes that are in a steady state with respect to P, the sediment is a net sink for P on an annual basis. After substantial changes occur in the lake or its catchment, especially after load reduction, the sediment might function, for a limited time or as long as decades, as a net P source (Hupfer and Lewandowski 2008).

The border between groundwater-borne P and internal P is somewhat arbitrary because groundwater concentrations change when groundwater approaches the interface. Diagenetic processes, mineralization of organic matter (e.g., Simmons and Lyons, 1994) and reducing conditions result in a release of phosphate and ammonium. Although these processes lead to an increase in nutrient concentrations, a thin oxic surface layer might concurrently cause a decrease. It is unclear whether P immobilized in that aerobic surface layer is permanently eliminated or its delivery to the lake only delayed (Hupfer and Lewandowski 2008; Roy and Malenica 2013). Furthermore, there might be uptake of nutrients by macrophytes. That uptake might occur over several decimeter sediment depth by roots. Is that P entering the lake or not? Oliveira Ommen et al. (2012) assumed a cut-off depth in the sediment of 25 cm. P released from sediment that settled some years ago unquestionably is internal P and P detected in piezometers some meters upstream of the shoreline unquestionably is groundwater-borne P. But what about P in sediment within 50 or 100cm of the sediment-water interface? Even if that P is of lacustrine origin and mobilized by diagenetic processes, its transport into the overlying water is extremely slow or even zero without the aid of groundwater exfiltration. We suggest that a depth of 50 to 100cm is below the root zone of most macrophytes and below the depth usually reached by bio-irrigation and bioturbation in lakes. Due to the 'large' distance between that sediment depth and the overlying water, diffusion is not an effective transport mechanism. The chemical gradient is too small, and usually there are higher pore-water P concentrations close to the sediment water interface due to mineralization of freshly settled organic matter. Thus, there could even be a diffusive P flux in the opposite direction. Based on the aforementioned considerations, we suggest that the border between groundwater-borne P and internal P should be set at about 50 to 100 cm sediment depth. Of course, the best way to differentiate P is to sample along the flow path (methods of flow path identification are described in Lewandowski et al. 2011a) to observe the concentration changes of groundwater with distance from the sediment-water interface. This would lead to an understanding of P mobilization processes as well as the advective and diffusive transport processes. However, due to the difficulties in differentiating between internal and external P, in some cases, the resulting estimates of P loads from LGD may actually include P released from sediments as indicated by Corbett et al. (1999) for SGD into Florida Bay.

Biogeochemical turnover processes in the aquifer-lake transition zone. Several factors make the transition zone between aquifer and lake a highly reactive interface: delivery of easily degradable organic matter of lacustrine and riparian origin; slow oxygen diffusion in saturated sediment causes reducing conditions; and bioturbation, wave-induced pumping, bioturbation and diffusion transport oxygen from the lake water into the subsurface (for details, see section on Why has LGD been Disregarded so Long?). At the redox interface – no matter whether it is above or below the sediment-water interface – iron(oxy) hydroxides and manganese oxides that quickly bind P precipitate upon oxygenation at neutral pH while at slightly alkaline pH, nearly no P is fixed by the solid (Griffioen 1994). Mixing of groundwater with different composition due to converging streamlines in near-shore areas might also cause a precipitation of iron at the interface, creating an 'iron curtain' that effectively sequesters phosphate (Spiteri et al. 2008a). In some lakes, such as Ashumet Pond, the black color of the sand and rocks along the shore is the visual evidence of the discharge of (sewage-contaminated) reduced groundwater. The black color is caused by coatings formed by precipitation of manganese oxide (McCobb et al. 2003). Phosphate may also be bound in Ca precipitates following $_{CO2}$ degassing and pH increase at the interface. However, that reaction is extremely slow (Griffioen 2006). P might also be bound to organic matter before it reaches the surface water (Griffioen 1994).

In some cases, phosphate is sorbed by sediments due to a high sorption capacity of the sediment or high concentration in the water. As a management measure, the sorption capacity of the interface might be artificially increased to capture P in the sediment. McCobb et al. (2009) describe the installation of a permeable reactive barrier in the near-shore lake bottom where a P plume discharges to the lake. The barrier is composed of 3% zero-valent-iron mixed with native sediments from the lakebed to 0.6-m sediment depth. Steep decreases of P concentrations occurred in the groundwater flowing upward through the barrier (McCobb et al. 2009). Detenbeck and Brezonik (1991) studied P sorption by sediments from a soft-water seepage lake and conducted batch experiments with sediment from Little Rock Lake. They tried to fit different kinetic and equilibrium models to the results. Equilibria and kinetic data for P sorption did not fit well to simple models that assume homogenous binding sites. A maximum sorption capacity was not exhibited by the sediments, but sorption continued to increase slowly as solution P increased. The rapid initial sorption (primary reactions, see section on Basic Chemical Characteristics of Phosphate Mobility) followed by a reduced rate of sorption (secondary reactions, see section on Basic Chemical Characteristics of Phosphate Mobility) was also observed for Little Rock Lake sediments (Detenbeck and Brezonik 1991). However, sorption of P is an equilibria reaction, which means that desorption might also occur, especially if geochemical conditions change. The extent to which P concentration in groundwater is maintained during transfers to the receiving surface water is generally uncertain (Holman et al. 2008). Any reversals in flow direction, whether they occur for days or years, only complicate these processes (e.g., Schuster et al. 2003).

Importance of phosphorus import via groundwater

In marine science, it is now well accepted that on a global scale, SGD nutrient loads are of the same order of magnitude as riverine inputs and on a regional scale can even exceed riverine inputs (e.g., Kroeger et al. 2007; Slomp and Van Cappellen 2004; Taniguchi et al. 2002). It can be assumed that the overall role of groundwater-borne nutrients in freshwater systems is even more important than in marine systems because the proportion of interface area to the volume of the water body is much larger in freshwaters.

Overview of data reported in literature. Tables 2.6 and 2.7 present N and P loads by LGD reported in the literature. Table 2.6 presents basic site descriptions, such as the location, the geology, the trophic state, main N and P sources and some morphometric data. Figure 2.6 displays the locations of the sites.
Table 2.7 reports volumetric seepage rates and N and P loads. Loads from the literature are reported in a variety of units, such as (1) mass per area per unit time; (2) mass per length of shoreline per unit time; (3) mass per unit time; or (4) mass per volume per unit time. A conversion is possible if the length of the shoreline, the lake area and its mean depth are known. We compiled the reported loads if morphometric data were reported into g m^{-2} $year^{-1}$ to make data sets comparable. However, care is required when interpreting the data because some loads pertain to the whole lake or the area of a specific bay (which may include areas with little to no LGD) and other reported loads pertain to limited nearshore areas, where loads are usually higher. Several authors associated loads to a specific length of shoreline (g m^{-1} $year^{-1}$ or l m^{-1} day^{-1}) but did not report shoreline length; in those instances, data cannot be converted to mass per area per time (Table 2.7). We also report the concentrations of the exfiltrating water, which is usually the basis for calculating the nutrient loads (seepage volume flux times concentration). Ranges of loads are also visualized in Figure 2.7.

Table 2.6 Description of sites for which nutrient loads by lacustrine groundwater discharge were determined.

		Catchment and lake characteristics					
No.	Lake and Location	Geology and hydraulic conductivity	Trophic state	Main groundwater N and P sources	Lake area (ha)	Mean depth (m)	Reference
1	Williams Lake, Minnesota	Thick, calcareous glacial drift	n. d.	Little anthropogenic impact (low population density)	36	9.8 (max. depth)	LaBaugh et al. (1995)
2	Colgada Lake, Spain	Karst aquifer	Mesotrophic	Fertilizer	103	8	Pina-Ochoa and Alvarez-Cobelas (2009)
3	Lake Bysjön, Sweden	Sand	Hypereutrophic	Agriculture and sewage	12	3.6	Vanek (1991); Vanek (1993)
4	Sparkling Lake, Wisconsin	Unconsolidated glacial outwash sediment	Oligomeso-trophic	n. d.	81	11	Hagerthey and Kerfoot (1998); Krabbenhoft (1988); Krabbenhoft et al. (1990)
5	Lake Hampen, Denmark	Glacial deposits (mainly sand and gravel)	Oligotrophic	Mainly natural (forest), some agriculture	76	4.3	Oliveira Ommen et al. (2012)
6	Lake Tahoe, only Ward Valley watershed, California	Alluvium (glacial outwash sediment)	n. d.	n. d.	n. d.	n. d.	Loeb and Goldman (1979)
7	Narrow Lake, Alberta	Moraine material	Mesotrophic	Natural (forest)	110	14.4	Shaw et al. (1990)
8	East Lake Tohopekaliga, Florida	Lake bottom is sand covered in some areas with varying thickness of fine organic matter	Mesotrophic	Agriculture	4680	5.2	Belanger and Mikutel (1985); Belanger et al. (1985)
9	Lake Metigoshe, North Dakota	Primary stony-sandy clay, clay, or clayey silt (low permeability)	n. d.	n. d.	n. d.	n. d.	Downing and Peterka (1978)
10	Lake Piaseczno, Poland	Periglacial sands	Mesotrophic	Different land use (forest, bog, agriculture), not very intensive, largest nutrient source is agriculture	84	11.3	Misztal et al. (1992)
11A	Lake Conway, Florida (East Pool)	Fine sand (low permeability)	Mesotrophic	Anthropogenic impact	739	5.3	Fellows and Brezonik (1980); Fellows and Brezonik (1981)
11B	(West Pool)	Sand (medium permeability)		Fertilizer (citrus grove)			
11C	(South Pool)	Fine sand (low permeability)		Low anthropogenic impact			
12A	Lake Apopka, Florida (site Magnolia Park)	Mucky peat (very low permeability)	Hypereutrophic	Low anthropogenic impact	12 400	1.7	Fellows and Brezonik (1980); Fellows and Brezonik (1981)
12B	(site Winter Garden)	Fine sand (low permeability)		Anthropogenic impact			
12C	(site Monteverde)	Sand (high permeability)		Anthropogenic impact (citrus grove)			
13	Blue Lake, South Australia	Karstic limestone aquifer	Oligotrophic (since P limited system)	Disposal of agricultural waste directly into the aquifer	60.3	58	Herczeg et al. (2003)
14	Vandercook Lake, Wisconsin	Glacial deposits (sand and gravel outwash sediments)	n. d.	Forest with few sediments	43	7.2 (max. depth)	Wentz et al. (1995)
15A	Dart´s Lake, New York (reducing sites)	Crystaline granitic gneiss	n. d.	Natural (forest)	58	n. d.	Schafran and Driscoll (1993)
15B	(oxic sites)						

Table 2.6 Continued

		Catchment and lake characteristics					
No.	Lake and Location	Geology and hydraulic conductivity	Trophic state	Main groundwater N and P sources	Lake area (ha)	Mean depth (m)	Reference
16	Lake Mendota, Wisconsin	n. d.	Eutrophic	Agriculture and urban areas	3940	14.4	Brock et al. (1982); Keeney et al. (1971); Sonzogni and Lee (1974)
17	Lake Persimmon, Florida	Unconsolidated clay and silt	Hypereutrophic	n. d.	15	4 (max. depth)	Kang et al. (2005)
18	Devil´s Lake, Wisconsin	n. d.	n. d.	n. d.	151	9.3	Lillie and Barko (1990)
19	Ashumet Pond, Massachusetts	Medium to coarse glacio-fluvial sand and gravel	Mesotrophic	Sewage infiltration beds (secondary treated sewage)	88	7.1	Bussey and Walter (1996); McCobb et al. (2003); Walter and LeBlanc (1997)
20	Hayes Lake, New Zealand	n. d.	n. d.	Pastoral farming and residential	276	10	Bayer et al. (2008)
21A	Garvel pit lake 1, Austria	Carbonate rich Quaternary fluvial deposits (mainly sand and gravel)	n. d.	Agriculture	3.8	n. d.	Muellegger et al. (2013); Weilhartner et al. (2012)
21B	Garvel pit lake 2, Austria				16.4		
21C	Garvel pit lake 3, Austria				5.9		
21D	Garvel pit lake 4, Austria				6.0		
21E	Garvel pit lake 5, Austria				8.6		
22	Mirror Lake, New Hampshire	Glacial deposits (mainly sand and gravel)	Oligotrophic	Forest with few settlements	15	5.75	Buso et al. (2009); Likens (2009); Rosenberry and Winter (2009)
23	Lake Kasumigaura, Japan	Alluvium (sand and gravel; clay below the center of the lake)	Eutrophic	Agriculture	22 0000	4	Nakayama and Watanabe (2008)
24	Lake Arendsee, Germany	Glacial deposits (mainly sand with some interbedded low conductivity layers)	Eutrophic	Urban sources	510	30	Meinikmann et al. (2013)
25	Muskellunge Lake, Wisconsin	n. d.	Eutrophic	Low anthropogenic impact	110	2.8	Robertson et al. (2003)
26	Whitefish Lake, Wisconsin	Sandy, glacial outwash sediments	Oligotrophic	Low anthropogenic impact (forest)	337	8.8	Robertson and Rose (2011); Robertson et al. (2009)
27	Shell Lake, Wisconsin	Glacial deposits of sands and gravel with interbedded layers of silts and clay	Eutrophic	Sewage	1034	7.1	Juckem and Robertson (2013)

n. d. not determined; no data

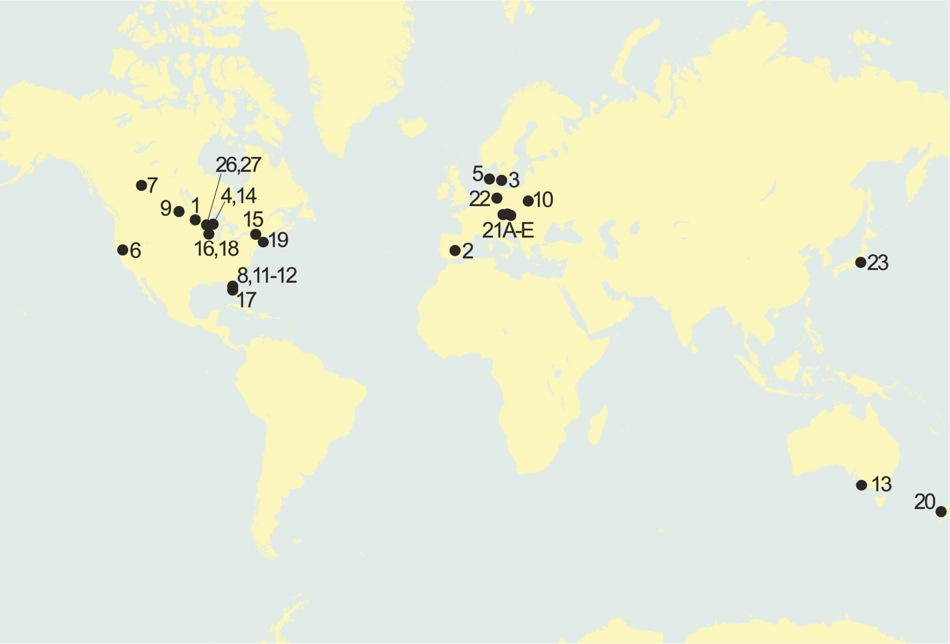

Figure 2.6 Geographic location of studies of lacustrine groundwater discharge reported in Tables 2.6 and 2.7. The numbers in the figure are identical with the numbers in those tables.

In the same way, volumetric seepage rates are reported in l m^{-2} day^{-1} and either refer to the whole lake or a specific bay or other limited area. In some studies (and in part 1 of this review), seepage rates are reported in the form of a velocity in m year^{-1}. If this is the Darcy flux (volume per area per time), it can be directly transformed into l m^{-1} day^{-1}. However, if the velocity was presented as a linear interstitial velocity, a conversion could be made only if porosity was reported. We also cite the percent of LGD in the water or nutrient budget as an indication of the relevance of LGD. Nutrient loads by LGD reported in Table 2.7 vary over orders of magnitude. The wide range reflects the importance of hydrogeologic controls on LGD as well as potential anthropogenic impacts (Swarzenski et al. 2006).

Table 2.7 Seepage rates and nutrient loads by lacustrine groundwater discharge for sites described in Table 2.6.

	Method		Seepage rate			P load by LGD		N load by LGD		
No.	for seepage volume	for seepage conc.	(l m^{-2} day^{-1}) [a]	(% of water balance)	(mg m^{-2} year^{-1}) [a]	(conc. of exfiltrating water, µg P l^{-1})	(% of total P load)	(g m^{-2} year^{-1}) [a]	(conc. of exfiltrating water, µg N l^{-1})	(% of total N load)
1	Darcy´s law for 8 shoreline segments (measurement of hydraulic conductivity and hydraulic gradient)	Near-shore gw observation wells	3.2 (whole lake)	66 (simplified balance consisting of gw and precip.)	5.7 (whole lake)	5	52 (total load simplified as load by gw and precip.)	0.43 (whole lake)	370 (TN)	61 (total load simplified as load by gw and precip.)
2	Hand-held flowmeter for surface springs and ADCP for subaquatic springs (diffuse LGD negligible)	Water samples of surface and subaquatic springs (collected by SCUBA divers)	68-136* (whole lake)	>50 (simplified balance consisting of gw and surface inflows)	n. d.	n. d.	n. d.	260-1000* (whole lake)	10000-17000 (NO_3-N)	58
3	Method not mentioned but probably determined as gw recharge in the catchment	gw observation wells, near-shore drive-point sampler and shoreline seepages	2.4 (whole lake)	n. d.	1700-2900* (whole lake)	2570	n. d.	n. d.	n. d.	n. d.
4	(1) gw flow meter; (2) Isotopic mass balance; (3) Seepage meter	Pore-water concentrations collected by a suction technique	0.54 (whole lake, method 1) 0.78 (whole lake, method 2) 0.70 (whole lake, method 3)	n. d.	1141 (mean for two sites with high LGD)	1-65 (SRP)	>50	0.59 (mean for two sites with high LGD)	120-2540 (NH_4-N)	37

Table 2.7 Continued.

	Method		Seepage rate		P load by LGD			N load by LGD		
No.	for seepage volume	for seepage conc.	(l m^{-2} day^{-1}) [a]	(% of water balance)	(mg m-^{2} year^{-1}) [a]	(conc. of exfiltrating water, µg P l^{-1})	(% of total P load)	(g m-^{2} year^{-1}) [a]	(conc. of exfiltrating water, µg N l^{-1})	(% of total N load)
5	(1) Segmented Darcy approach, (2) Seepage meter	Pore-water concentration in 25 cm depth	5.9 (whole lake, both methods)	70	52 (whole lake)	4.3-52	85	3 (whole lake)	120-7500 (DIN)	67
6	Darcy´s law (wells along a transect parallel to the lake shore)	gw observation wells	5800 l m^{-1} day^{-1} (1.9 km long section of shore-line; conservative estimate) 8900 l m^{-1} day^{-1} (1.9 km long section of shoreline; arithmetic mean)	n. d.	158 000 mg m^{-1} yr^{-1} (1.9 km long section of shore-line; conservative estimate) 237 000 m^{-1} yr^{-1} (1.9 km long section of shore-line; arithmetic mean)	73	44	347 g m^{-1} yr^{-1} (1.9 km long section of shoreline; conservative estimate) 1370 g m^{-1} yr^{-1} (1.9 km long section of shore-line; arithmetic mean)	162 (NO_3-N, conservative estimate) 421 (NO_3-N, arithmetic mean)	49 (NO_3-N)
7	(1) Residual in the water balance (2) Darcy´s law (wells around the lake) (3) Darcy´s law (mini-piezometers) (4) Seepage meters	(A) Pore-water concentration (B) gw observation wells	0.91 (whole lake, method 1) 0.54 (whole lake, method 2) 0.08 (point estimate, method 3 - evaluated by authors as unreliable) 0.36 (point estimate, method 4) 0.61 (arithmetic mean without method 3)	28 (arithmetic mean of methods 1, 2, and 4)	58 (methods 1 and A, whole lake) 35 (methods 2 and A, whole lake) 23 (methods 2 and A, point estimate) 39 (arithmetic mean, whole lake)	175 (method A) 21 (method B – evaluated by authors as unreliable)	53 (arithmetic mean; total load includes atmospheric deposition, surface runoff, and molecular diffusion from sediment)	n. d.	n. d.	n. d.
8	Seepage meters	(1) Seepage meters 2) Near-shore landside piezometer	4.3 (whole lake)	14	297 (method 1, whole lake) 47 (method 2, whole lake)	253 (method 1) 50 (method 2)	38 (method 1) 9 (method 2)	4.7 (method 1, whole lake) 1.6 (method 2, whole lake)	<20/74 (method 1/2, NO_3-N) 3490/733 (method 1/2, NH_4-N) 4145/1570 (method 1/2 TKN)	39 (method 1) 18 (method 2)
9	Seepage meters	(1) Seepage meters (2) One lakeside groundwater observation well	0.43 (near-shore area. max 12 m from shoreline)	2	7.9 (method 1, near-shore area) 9.4 (method 2, near-shore area)	51 (method 1) 60 (method 2)	n. d.	0.53 (method 1, near-shore area) 0.08 (method 2, near-shore area)	3395 (method 1, NH_4-N) 480 (method 2, NH_4-N)	n. d.
10	Unclear method description: residual in the water balance or Darcy´s law (gw observation well)	Near-shore landside gw observation wells	0.47 (whole lake)	n. d.	35	257	n. d.	0.92	1305 (NO_3-N) 1063 (NH_4-N) 4724 (TN)	n. d.
11A	Transects of seepage meters perpendicular to the shoreline	Transects of seepage meters perpendicular to the shoreline	0.83 (whole lake) 140 l m^{-1} day^{-1} (shoreline of section)	17.5	n. d.	n. d.	n. d.	105 g m^{-1} year^{-1} (shoreline of section)	9.3 (NO_3-N) 1320 (NH_4-N) 1100 (TON) 2060 (TN)	n. d.
11B			203/217 l m^{-1} day^{-1} (shoreline of section) Regular seepage rate/seepage rate shortly after fertilizer application					133 g m^{-1} year^{-1} (shoreline of section)	17.4/3170 (NO_3-N) 1210/2260 (NH_4-N) 800/460 (TON) 1800/5890 (TN) Regular conc./ conc. shortly after fertilizer application	
11C			304 l m^{-1} day^{-1} (shoreline of section)					272 g m^{-1} year^{-1} (shoreline of section)	5.5 (NO_3-N) 1390 (NH_4-N) 1050 (TON) 2450 (TN)	
12A	Transects of seepage meters perpendicular to the shoreline	Transects of seepage meters perpendicular to the shoreline	0.09 (whole lake) 64 l m^{-1} day^{-1} (shoreline of section)	2	n. d.	n. d.	n. d.	483 g m^{-1} year^{-1} (shoreline of section)	4.9 (NO_3-N) 6070 (NH_4-N) 14510 (TON) 20560 (TN)	n. d.
12B			21 l m^{-1} day^{-1} (shoreline of section)					482 g m^{-1} year^{-1} (shoreline of section)	14.3 (NO_3-N) 13450 (NH_4-N) 49330 (TON) 62800 (TN)	
12C			524 l m^{-1} day^{-1} (shoreline of section)					462 g m^{-1} year^{-1} (shoreline of section)	4.0 (NO_3-N) 900 (NH_4-N) 1510 (TON) 2410 (TN)	

Table 2.7 Continued.

	Method		Seepage rate		P load by LGD			N load by LGD		
No.	for seepage volume	for seepage conc.	(l m^{-2} day^{-1}) [a]	(% of water balance)	(mg m^{-2} year^{-1}) [a]	(conc. of exfiltrating water, µg P l^{-1})	(% of total P load)	(g m^{-2} year^{-1}) [a]	(conc. of exfiltrating water, µg N l^{-1})	(% of total N load)
13	Sedimentary isotopic records used for mass balance of $\delta^{18}O$ and $\delta^{13}C$ in carbonates	gw observation wells	20.7 (whole lake)	n. d.	n. d.	n. d.	n. d.	80 (whole lake)	10500 (NO_3-N)	n. d.
14	Darcy´s law (piezometers around the lake)	Piezometers finished just below the water table	0.17/0.03/0.00 (whole lake) Annual hydrologic changes depending on weather conditions and gw recharge in the catchment: 1981-83/1984-86/1987-88	0-9 (interannual changes depending on weather conditions and groundwater recharge in the catchment)	n. d.	n. d.	n. d.	0.006/0.001/0.000 (whole lake) Annual hydrologic changes depending on weather conditions and gw recharge in the catchment: 1981-83/1984-86/1987-88	53 (NO_3-N) 35 (NH_4-N)	n. d.
15A	Seepage meters	Mini-Piezometer in lake bed close to the shore	2.1 (near shore seepage rates)	<5	n. d.	n. d.	n. d.	0.31 (near-shore TN-fluxes)	5,6 (NO_3-N) 750 (NH_4-N)	n. d.
15B			26 (near shore seepage rates)	<5	n. d.	n. d.	n. d.	7.4 (near-shore TN-fluxes)	476 (NO_3-N) 0 (NH_4-N)	n. d.
16	(1) Rough estimate of water balance of the catchment (2) Seepage meters	(A) Few groundwater concentrations (B) Dialysis samplers in 3 cm sediment depth (C) Gentle suction devices in 4 cm depth (D) Groundwater observation wells	1.9 (whole lake, method 1) 1.8 (whole lake, method 2)	30 (method 2)	11.5 (whole lake, method 1 and A) 113 (whole lake, method 2 and mean of methods C and D) 20 (whole lake, method D)	10 (method A) 172 (arithmetic mean of methods B and C) 33 (method B) 270 (method C) 30 (method D)	0.5 (methods 1 and A) 12 (methods 2 and arithmetic mean of methods B and C)	2.0 (whole lake, method 1 and A) 0.28 (whole lake, method 2 and arithmetic mean of methods B and C) 1.1 (whole lake, method 2 and D)	2500 (NO_3-N, method A) 256/508/156/1605 (NO_3-N, method A) 161/97158/33 (NH_4-N) (arithmetic mean of methods B and C/method B/ method C/ method D)	13.5 (methods 1 and A) 1.9 (method 2 and arithmetic mean of B and C)
17	(1) Mass balance approach (fluctuations of Cl$^-$ in lake water) (2) Cl$^-$ depth profile (3) Seepage meters	(A) gw observation wells (B) Pore-water conc. of deepest layer (72 cm) after centrifugation of sectioned sediment core (C) Seepage meters	0.06 (whole lake, method 1) 0.15 (whole lake, method 2)	n. d.	8.0 (whole lake, media method A and arithmetic mean of method 1 and 2) 7.4 (whole lake, method B and arithmetic mean of methods 1 and 2) 3.4-7.3* (whole lake, methods 3 and C)	242 (method A, arithmetic mean) 202 (method A, median) 191 (method B)	n. d.	0.004 (method A and arithmetic mean of methods 1 and 2)	106 (method A, arithmetic mean) (NH_4-N)	n. d.
18	Seepage meters	Seepage meters	3.4 (near-shore area)	n. d.	96 (near-shore area)	77.5 (near-shore area)	n. d.	1.0 (near-shore area)	818 (near-shore area) (TN)	n. d.
19	Steady state groundwater flow model	(A) gw in the catchment (plume data set 1995) (B) gw in the catchment (plume data set 1999) (C) Pore-water conc. approx.. 60 cm lake depth	3512 l m^{-1} day^{-1} (shoreline of 300 m long modelled section Fishermans Cove)	Fishermans Cove comprises 8% of total groundwater inflow	360 (whole lake, method A) 202 (whole lake, method 2) 141 (whole lake, method C) 1000000 mg m^{-1} yr^{-1} (shoreline section of Fishermans Cove, method A)	808 (method A, arithmetic mean for Fishermans Cove)	84-98 (whole lake) (19-70% by sewage plume discharging in Fishermans Cove; different estimates)	n. d.	12000 (NO_3-N) 7000 (NH_4-N) (method C, maximum)	
20	Digital propeller flow meter for spring at the lake shore	Water sampling of spring	n. d.	9 (spring)	n. d.	5 (spring) 7 (groundwater)	4 (spring)	n. d.	791/897 (NO_3-N + NO_2-N) 13/18 (NH_4-N) (spring/gw)	26 (spring, NO_3-N + NO_2-N) 21 (spring, TN)
21A	Water budget	gw observation well	11.1 (whole lake)	n. d.	n. d.	n. d.	n. d.	143 (whole lake)	n. d.	n. d.
21B			11.9 (whole lake)	n. d.	n. d.	n. d.	n. d.	82 (whole lake)	n. d.	n. d.
21C			25.4 (whole lake)	n. d.	n. d.	n. d.	n. d.	456 (whole lake)	n. d.	n. d.
21D			13.2 (whole lake)	n. d.	n. d.	n. d.	n. d.	112 (whole lake)	n. d.	n. d.
21E			41.7 (whole lake)	n. d.	n. d.	n. d.	n. d.	453 (whole lake)	n. d.	n. d.
22	Darcy, stable isotopes and groundwater model	gw observation wells	2.1 (whole lake)	16	0.74 (whole lake)	9.3	1.0	0.013 (whole lake)	1.4 (NH_4-N) 15.4 (NO_3-N)	15.5 (NH_4-N) 2.3 (NO_3-N)
23	Darcy, stable isotopes and nice-lake model	gw observation wells and nice-lake model	1.6 (whole lake)	9 (simplified balance consisting of gw and surface inflows)	n. d.	n. d.	n. d.	5.7 (whole lake)	7000 (TN)	23 (simplified balance consisting of gw and surface inflows)

Table 2.7 Continued.

	Method		Seepage rate			P load by LGD			N load by LGD	
No.	for seepage volume	for seepage conc.	(l m^{-2} day^{-1}) [a]	(% of water balance)	(mg m-^{2} year^{-1}) [a]	(conc. of exfiltrating water, µg P l^{-1})	(% of total P load)	(g m-^{2} year^{-1}) [a]	(conc. of exfiltrating water, µg N l^{-1})	(% of total N load)
24	Mean annual gw recharge in the catchment; temperature depth profiles for spatial distribution of the calculated discharge	Near-shore gw observation wells	0.68 (whole lake)	n. d.	83 (whole lake)	80 – 1210	n. d.	n. d.	n. d.	n. d.
25	Residual in the water balance	Near-shore shall-ow piezometers	4.2 (whole lake)	49	104 (whole lake)	13-130	58	n. d.	n. d.	n. d.
26	Steady state gw flow model	Near-shore shallow piezometers	1.3 (whole lake)	52.4	8.3 (whole lake)	5-80	27	n. d.	n. d.	n. d.
27	gw flow model	Near-shore gw observation wells	0.1 (whole lake)	4.8	16 (whole lake)	445	21	n. d.	n. d.	n. d.
		Arithmetic mean	7.83	(*n* = 55)	174	(*n* = 30)		76.7	(*n* = 26)	
		Median	1.86		34.7			1.31		
		10% to 90% Quantile	0.094...23.6		5.19…303			0.0049…298		

[a] area for which the reported load was determined.

n. d., not determined; no data; gw, groundwater; precip., precipitation; TKN, total kjeldahl nitrogen; SRP, soluble reactive phosphorus.

Values in grey were calculated based on the data given in the references reported in Table 2.6. Values reported in black are directly reported in the references or only the units of the data had to be transformed.

* For the calculation of the mean, median, and quantiles we used arithmetic means instead of ranges.

Indirect impacts. In addition to the direct impact on the P budget due to delivery of P via LGD, there can also be indirect effects due to other chemical constituents in the discharging groundwater that alter the P biogeochemistry of the lake water. For example, the import of calcium-rich groundwater might cause calcite precipitation; examples are Blue Lake of Mount Gambier, South Australia (Lamontagne 2002), and Lake Stechlin, Germany (Holzbecher and Nützmann 2000). Calcite precipitation depends on the availability of carbonate, and highest rates of calcite precipitation are found in moderately eutrophic lakes (Holzbecher and Nützmann 2000). P co-precipitation is a very efficient removal mechanism for in-lake P.

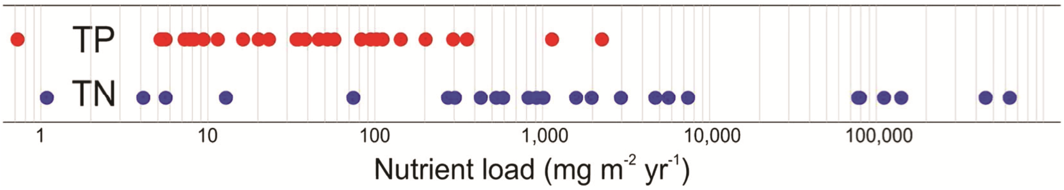

Figure 2.7 Ranges of groundwater-borne nutrient (phosphorus and nitrogen) loads to lakes (lacustrine groundwater discharge) reported in literature (data of case studies presented in Tables 2.6 and 2.7; in instances where ranges are reported in Table 2.7, we used the arithmetic mean of that range in the present figure).

2.2.6 Nitrogen in seepage

Basic chemical characteristics of nitrogen mobility

Nitrate and Denitrification. Nitrate is nearly ubiquitous in oxic groundwater, it is frequently the dominant form of N, and it is highly mobile and travels through oxic aquifers with minimal physical retention (Bowen et al. 2007; Cherkauer et al. 1992; Keeney 1986; Korom 1992; Slomp and Van Cappellen 2004; Spiteri et al. 2007; Weiskel and Howes 1992; Wilhelm et al. 1994). Denitrification, the anaerobic microbial respiratory pathway in which nitrate is converted to N_2, is the predominant removal process for groundwater N. Denitrification requires anoxia and an electron donor, which can be organic carbon, sulphide or Fe^{2+} (Slomp and Van Cappellen 2004; Starr and Gillham 1993; Tesoriero et al. 2000). The highest rates of denitrification are restricted to the upper layers of groundwater where DOC concentrations are largest (Bowen et al. 2007; Crandall 2000; Pabich et al. 2001).

Ammonium. The mobility of ammonium in anoxic aquifers is much lower than the corresponding mobility of nitrate in oxic aquifers because sorption to clays and other cation exchangers causes ammonium retention (Bowen et al. 2007; Ceazan et al. 1989; Kroeger et al. 2007). Ammonium might also be bound by humic substances. In oxic aquifers, ammonium is converted to nitrate by nitrification. However, anaerobic ammonium oxidation (sometimes abbreviated as Anammox) provides a microbially mediated ammonium removal process under anoxic conditions (Burgin and Hamilton 2007; Kroeger and Charette 2008). Ammonium is regenerated in the aquifer by the decomposition of sedimentary and dissolved organic N (Bowen et al. 2007; Hagerthey and Kerfoot 1998). A further source of ammonium is dissimilatory nitrate reduction to ammonium (Burgin and Hamilton 2007).

Dissolved organic nitrogen. Large concentrations of dissolved organic nitrogen (DON), a reduced N form, might also occur in groundwater. For example, (Kroeger et al. 2006) reported that about 60% of total dissolved nitrogen was in the form of DON in the near-shore groundwater of 10 Cape Cod watersheds. Qualls and Richardson (2003) concluded that over 90% of the N transported downstream in the Everglades is in the form of DON. However, still little is known about DON (Bowen et al. 2007; Kalbitz et al. 2000; Kroeger et al. 2007; McDowell 2003; Slomp and Van Cappellen 2004). The limited studies carried out for soils suggest that N fertilization may increase DON concentration in soils, particularly in soils with low sorption capacities (McDowell 2003; Slomp and Van Cappellen 2004). Although DON is generally attributed to natural sources, Kroeger et al. (2007) assume that DON in groundwater in an urban setting is from wastewater or other anthropogenic sources because it occurs in high concentrations in close proximity to landfills and wastewater disposal sites.

Comparison of N and P mobility. There are some fundamental differences between N and P that result in completely different properties and fate of both in soils and aquifers. Whereas P occurs mainly in the redox state P(+V) and is only indirectly impacted by the redox potential due to redox reactions of its binding partners, N occurs in the environment usually in several different redox states, especially as N(-III) in ammonium, N(+III) in nitrite, N (+V) in nitrate and N(0) in gaseous N_2. Gaseous N_2 is usually lost from the system, although some microorganisms are able to fix gaseous N_2. There is no comparable reaction for P that results in a loss of P across the sediment-air or water-air interface. While soils and oxidized aquifers reveal high P retention capacities, nitrate behaves essentially conservatively in oxic aquifers. Mobility of both ammonium and phosphate is limited in aquatic systems.

The contrasting behaviour of nitrate and phosphate in oxic groundwater systems typically results in a strong increase of the dissolved N:P ratio along a groundwater flow path compared to the Redfield ratio of 16 : 1, particularly in contaminated systems (compare also de-mixing described in the section on Basic Chemical Characteristics of Phosphate Mobility) (Kroeger et al. 2007; Moore 2010; Slomp and Van Cappellen 2004). A high N:P ratio may significantly impact the ecology of marine coastal waters by driving N-limited systems to P-limitation (Slomp and Van Cappellen 2004; Valiela et al. 1990), and thus stimulating harmful algal blooms (Lee et al. 2010). In contrast, Kroeger et al. (2007) report that strictly reducing conditions result in N:P ratios below the Redfield ratio because reductive dissolution of iron (oxy)hydroxides will result in a release of P. In other words: effective nitrate removal by denitrification in riparian zones may produce redox conditions, which increase the release of SRP (Carlyle and Hill 2001; Lewandowski and Nützmann 2010).

Nitrogen in groundwater approaching the sediment-water interface

Typical nitrate concentrations in groundwater are reported in Table 2.8. Even within one site, there can be three orders of magnitude difference in concentrations at spatial scales of meters (Bowen et al. 2007). Ammonium concentrations show a similar variability among sites and can also be high, but in general, there is less ammonium-N in groundwater than nitrate-N (Bowen et al. 2007).

Background N. Nitrate and ammonium are usually scarce in pristine aquatic and terrestrial systems (Table 2.8; Reddy et al. 1999; Vanek 1991). Natural N inputs are caused by downward leaching of N from soil organic matter and *in situ*-release from organic matter in the aquifer. Compared with anthropogenically-impacted N concentrations, natural N concentrations of groundwater are smaller (Table 2.8; Slomp and Van Cappellen 2004).

Anthropogenic N sources. Similar to P, the main anthropogenic sources of N in groundwater are comercial fertilizers, manure, sewage (Appelo and Postma 1999; Cherkauer et al. 1992; Crandall 2000; Johannes and Hearn 1985; Keeney 1986; Lamontagne 2002; Misztal et al. 1992; Slomp and Van Cappellen 2004; Tiessen 1995; Wakida and Lerner 2005) and atmospheric deposition (Slomp and Van Cappellen 2004; Tiessen 1995; Wakida and Lerner 2005). Wakida and Lerner (2005) mention that contaminated land (e.g., abandoned landfills and industrial sites) is also an important non-agricultural source of groundwater nitrate. Groundwater N from anthropogenic sources is usually supplied in the form of nitrate, which can easily leach from the vadose zone, whereas ammonium is nitrified in the unsaturated oxic zone (Jordan et al. 1997; Slomp and Van Cappellen 2004; Wilhelm et al. 1994). Ammonium and nitrate also are decreased in the vadose zone due to plant and other biotic uptake (e.g., Reay et al. 1992). The only places with substantial amounts of ammonium in groundwater are where ammonium-rich wastewater is directly released into the saturated, anoxic zone (Ceazan et al. 1989; Slomp and Van Cappellen 2004), where significant decomposition of organic matter occurs under anoxic conditions, for example, in landfill leachate plumes (Brun and Engesgaard 2002; Christensen et al. 2001; Slomp and Van Cappellen 2004) or in aquifers naturally rich in organic matter. Land use types cause characteristic isotopic signatures of groundwater (Bowen et al. 2007). Thus, differences in the ratio of 15N to 14N can be used to discriminate among the different N sources, such as wastewater, atmospheric deposition and fertilizer application (Bowen et al. 2007; Kreitler et al. 1978). Nowadays, human activities fix more atmospheric N into the global N cycle than the remainder of earth's ecosystems combined (Ibánhez et al. 2011; Vitousek et al. 1997). Erisman et al. (2008) report that the invention of ammonia synthesis based on the Haber-Bosch process altered the planet seriously and was the basis for a growing world population in the 20th century. Due to low N-use efficiency of agriculture, unused N from fertilizer application causes multiple adverse environmental impacts such as unintentional fertilization of terrestrial and aquatic ecosystems (eutrophication), reduced biodiversity, polluted air, greenhouse gas emissions and increased human health risks (Erisman et al. 2008).

Fate in the watershed. Anthropogenic addition of bioavailable N to the biosphere is increasingly causing additional bioavailable N to enter groundwater and surface waters (Burgin and Hamilton 2007; Galloway et al. 2004; Johnes and Butterfield 2002; Mulholland et al. 2008). Hence, natural systems have become artificially enriched in N (Ibánhez et al. 2011; Puckett et al. 2011), and nitrate contamination is a common worldwide problem (Johannes and Hearn 1985; Lamontagne 2002; Wakida and Lerner 2005). In general, a considerable portion of the N that enters a watershed is immobilized or eliminated (Bowen et al. 2007). Denitrification of nitrate and retention of ammonium and DON by adsorption take place in aquifers (Bowen et al. 2007) with denitrification being the largest of these terms (Bowen et al. 2007). Factors decreasing nitrate in the aquifer include poorly drained soils, greater depth to groundwater table, artificial drainage systems, intervening layers of unfractured bedrock, a low rate of groundwater recharge, lithologic sources of DOC and sulphides and anaerobic conditions in the aquifer (Crandall 2000; Nolan and Stoner 2000; Tesoriero and Puckett 2011). A lack of labile organic matter in the aquifer is responsible for often high concentrations of oxidized nitrogen arriving in seepage areas (Ibánhez et al. 2011; Kroeger et al. 2007; Rivett et al. 2008a; Slomp and Van Cappellen 2004). Denitrification of nitrate in the groundwater below properly operating septic systems is generally much less than assumed in previous decades because newer septic systems are designed to eliminate organic carbon from the downward percolating effluent already in the oxidized unsaturated zone. Furthermore, in most aquifers there is not much carbon from other sources available for denitrification (Wilhelm et al. 1994). Already several years ago, European legislation, such as the (EU Water Framework Directive (2000) and the EU Nitrate Directive (1991), acknowledged the existence of excessive levels of nitrate in groundwater and implemented strategies to reduce nitrate. Nevertheless, groundwater nitrate is still high due to an insufficient set of standards, long response times and further intensification of agriculture. Worldwide regulations could recognize and counteract substantial additions of nitrate to groundwater from conventional septic systems (Wilhelm et al. 1994) and common agricultural practises.

Fate of nitrogen at the interface

Biogeochemical turnover processes in the aquifer-lake interface. A significant portion of nitrate being transported from the subsurface catchment towards the lake might be lost as water crosses the sediment-water interface and enters the lake (Bowen et al. 2007; Dahm et al. 1998; Ibánhez et al. 2011; Oliveira Ommen et al. 2012; Sonzogni and Lee 1974; Spiteri et al. 2008a; Valiela et al. 1990). The uppermost layers of lake sediments often contain much freshly settled easily degradable organic matter, which creates a reduced redox potential and potentially intense denitrification at the sediment-water interface (Ibánhez et al. 2011; Keeney et al. 1971). Pore-water depth profiles taken in shallow lake sediments reveal a decrease of nitrate and nitrite concentrations within the last decimetres to centimetres as groundwater approaches the sediment-water interface (Capone and Slater 1990; Keeney et al. 1971). Chen and Keeney (1974) also showed in laboratory experiments that nitrate-rich groundwater passing through certain lake sediments loses nitrate. As a consequence of these processes, nitrate in LGD is often lower than in nearby groundwater observation wells. Therefore, Brock et al. (1982) pointed out that well chemistry does not provide a good indication of the composition of groundwater entering lakes. At some lakes, denitrification occurs before reaching the vicinity of a lake because many lakes are surrounded by areas with wet soils, fens, bogs or silting-up. All of these generally wet areas, as well as near-surface aquifers, in combination with a high content of easily degradable organic matter provide circumstances favouring denitrification (Bowen et al. 2007; Pinay and Decamps 1988).

However, if there is no decline in oxygen at the groundwater-lake interface, nitrate may be transported freely into the lake (Reay et al. 1992). Such conditions occur in sandy, near-shore groundwater discharge areas where little or no organic matter is present, especially under winter conditions (Schafran and Driscoll 1990; Vanek 1987). The associated high flux of oxygen with the exfiltrating groundwater exceeds the sediment microbial demand, and thus the pore-water remains oxic (Schafran and Driscoll 1990). High flow velocities result in little denitrification due to short contact time (Capone and Slater 1990). Consequently, denitrification is also less important in karstic areas (Garcia-Solsona et al. 2010). Aquifer heterogeneities might also support nitrate exfiltration. Although highest potential denitrification rates occur in peat deposits, their low hydraulic conductivity diverts groundwater flow around peat lenses through surrounding sand and gravel deposits where faster flow and shorter contact time results in less potential for denitrification (Devito et al. 2000).

Table 2.8 Examples for typical groundwater nitrite, nitrate, and ammonium concentrations for pristine and anthropogenically impacted aquifers.

Aquifer typology	NO_2-N (mg l^{-1})	NO_3-N (mg l^{-1})	NH_4-N (mg l^{-1})	Type of value	Reference
Loose rock, Germany				Maximal natural groundwater concentration (90% percentile of the natural groundwater component)	Kunkel et al. (2004); Wendland et al. (2005) [a]
Sand and gravel of the North German Plain					
Sampling depth 0-10 m	0.018	0.20	0.08		
Sampling depth 10-25 m	0.012	0.11	0.27		
Sampling depth 25-50 m	0.012	0.14	0.34		
Fluvial sand and gravel of the Upper Lower Valley	n. d.	2.94	0.18		
Fluvial sand and gravel of the Upper Rhine Valley	n. d.	0.27	0.03		
Fluvial gravel deposits and glacial moraine deposits in Alpine piedmont	n. d.	5.65	0.01		
Tertiary sediments	0.003	0.12	0.03		
Carbonate rock, Germany					
Jurassic limestones	0.003	4.07	0.01		
Triassic limestones	0.006	9.04	0.01		
Alpine limestones	n. d.	1.63	0.01		
Paleozoic limestones	n. d.	4.29	0.02		
Carbonate rock (marl) interbedded with clay and sand layers	0.003	3.16	0.01		
Silicate rock, Germany					
Sandstones and sandstone interbedded with clay stone (different eras)	0.003	1.92	0.01		
Earlier Triassic (sandstone)	0.003	5.87	0.01		
Paleozoic sedimentary rock	0.003	2.71	0.02		
Volcanic rock	0.000	2.94	0.02		
Magmatic and metamorphic rock	0.003	3.84	0.01		
Various sites, Ontario, Canada:				Background	Harman et al. (1996); Wilhelm et al. (1996)
Fine to medium-grained calcareous sand, Cambridge, Canada		28.1	<0.05		
Fine to coarse sand, Muskoka		3.9	0.18		
Fine to medium sand, Langton		4.2	<0.05		
Groundwater, U.S.				Median	Nolan and Stoner (2000)
Shallow groundwater, agricultural land use	<0.01	3.4	0.02		
Shallow groundwater, urban land use	<0.01	1.6	0.03		
Deeper groundwater, major aquifers	<0.01	0.48	0.02		
Groundwater in coastal aquifers [b]				Range	Bowman (1977); (1979); Gaines et al. (1983); Gilliam et al. (1974); Meade and Vaccaro (1971)
Orleans, MA		0-9.8			
North Carolina, Forest		0.01-1.01	0.02-1.73		
North Carolina, Agriculture		0.02-31.5	0.01-5.1		
Falmouth, MA	0.001-0.08	0.01-9.7	0.002-0.9		
Cape Cod, MA		0-6.3	0-0.9		
Long Island, NY		0.11-8.5			
Florida				Arithmetic mean	Lapointe et al. (1990)
Groundwater impacted by septic systems		4.1	6.1		
Background		0.007	0.023		
Unconfined aquifer in the south-east of South Australia (impacted by agriculture, urbanization and waste disposal)		0-100 8		Range Median	Lamontagne (2002)
Septic system plume, Ontario, Canada		10-80	1-15	Range	Ptacek (1998)

n. d., not determined or no data.

a The method to estimate maximum natural groundwater concentrations is described in Wendland et al. (2005). Some of the values for nitrogen species presented here are only published in German in Kunkel et al. (2004).

b Values cited here were collected by Valiela et al. (1990) and Bowen et al. (2007).

Differentiation of internal and external N. Because of the difficulties in differentiating between internal and external N, in some cases, estimates of external N inputs by LGD may actually include internally originated N mobilization from lake sediments. For example, as noted earlier, organic matter degradation in lake sediments releases ammonium and that ammonium is transported with exfiltrating groundwater into the water body (Brock et al. 1982; Corbett et al. 1999; Fellows and Brezonik 1981).

Exfiltration pattern. Lee (1977) found that groundwater with high nitrate concentrations seeped into a lake primarily within the first few meters of the shore. Similarly, Reay et al. (1992) report that nitrate was the predominant nitrogen species discharging in nearshore areas of a marine bay. However, discharge that was primarily nitrate gradually became discharge that was primarily ammonium with distance offshore. Also, in the study of Fellows and Brezonik (1981), groundwater deeper in the flow system had lower nitrate concentrations and appeared to enter the lake farther from shore. The vertical distribution of N concentrations in horizontally flowing groundwater that discharges to a lake is rotated 90° and distributed across the lake bottom with distance from shore. In an example presented by McCobb et al. (2003) mentioned earlier, areas of elevated ammonium concentrations in a vertical groundwater chemical profile are surrounded by areas of elevated nitrate. This same pattern of chemicals and concentrations is distributed across the lakebed with increasing distance from the shoreline.

Importance of nitrogen import via groundwater

As described in the section on the Importance of Phosphorus Import via Groundwater, Table 2.7 lists N and P loads entering lakes by LGD, and Figure 2.5 displays their ranges. It is clear that groundwater is an important N source for some lakes. Even under best management practise goals of reducing N in groundwater, N loads by LGD might be high. Excess fertilizer application can result in a high transport to adjacent lakes. For example, the application of a 2.7 times greater than usual fertilizer amount to a citrus grove resulted in a rapid increase of groundwater-borne N in nearby Lake Conway; 9.5% of the nitrate applied on the citrus grove ended up in the lake (Fellows and Brezonik 1981). A rapid response of in-lake nitrate concentrations was also observed in a study by Lamontagne (2002) at Blue Lake, South Australia,

where lake water was withdrawn for drinking water production. Due to the high hydraulic conductivity of the unconfined aquifer, changes of the pumping management schemes influenced seepage rates, water residence time and in-lake nitrate concentrations. Although increased groundwater inputs increase nutrient loading (Herczeg et al. 2003; Lamontagne 2002), this may not be a linear correlation and differences in biogeochemical characteristics of nutrients have to be considered.

2.2.7 Outlook

Lacustrine groundwater discharge can be important to lakes, both as it affects their overall water budget and their water quality by carrying large nutrient loads and may have detrimental ecological and human health impacts. LGD is often a more important component in lake nutrient budgets than reflected by the majority of literature. Nutrient budgets are even more complex than hydrological budgets (reported in Rosenberry et al. 2015), because there is much heterogeneity both in seepage rates and nutrient composition of LGD; the uncertainties of both are multiplied. To cope with that uncertainty, we suggest a combination of different techniques, although this increases efforts and costs of investigations. For example, we suggest using distributed temperature sensing or airborne thermal infrared to identify major water exfiltration zones (Lewandowski et al. 2013) and then focusing more detailed measurements in those locations. A quantification of LGD on a whole lake basis is possible using natural geochemical tracers such as stable isotopes or radon and on local scales based on temperature gradients and head differences at the groundwater-lake interface (comparison of methods-based results in Rosenberry et al. 2015). Nutrient concentrations can then be determined with seepage meters and diffusion samplers at the same locations in addition to groundwater sampling in the catchment and along the shoreline. Modelling is a useful tool for upscaling and integrating point measurements.

Our review reveals the importance to decrease nutrient concentrations in anthropogenically affected groundwater, especially for aquifers located in the catchment of seepage lakes. In this context, the different mobility of N and P should be considered as well as redox conditions favouring denitrification and thus permanent removal of N from the groundwater. One of the basic problems is that redox conditions favouring nitrate removal increase phosphate mobility and thus phosphate input by LGD. Leaching of nutrients from agricultural sources into the aquifer could be reduced, sewage disposal facilities (infiltration beds) could be gradually replaced by more modern wastewater cleaning technologies and leaky sewers could be repaired or rebuilt.

Our review focuses on the exfiltration of groundwater into lakes though the opposite process, the infiltration of lake water into aquifers, is often also of ecological significance. Enell (1982) was one of the first authors to view groundwater-exfiltration lakes as a nutrient trap, especially for P (here, Lake Bysjön in Sweden). Several other authors report a high retention of nutrients and other compounds in groundwater-dependent lakes, because concentrations in exfiltrating groundwater are often much higher than concentrations in surface water infiltrating to the aquifer (e.g., LaBaugh et al. 1995; Muellegger et al. 2013). For example, Oliveira Ommen et al. (2012) report a retention of 92% regarding N and 96% regarding P for an oligotrophic lake in Denmark. Weilhartner et al. (2012) also found that gravel-pit lakes significantly decrease nutrient (nitrate and phosphate) concentrations as groundwater passes through the lake ecosystems because dissolved P is taken up very efficiently by the biomass and the formed particulate P remains in the lake (sedimentation/filtration of particulate matter). Furthermore, in stratified lakes P is transported as particulate P from the epilimnion to the hypoliminion (e.g., Hupfer and Lewandowski 2008), whereas both infiltration and exfiltration occur mainly in the epilimnion (Rosenberry et al. 2015), and thus concentrations are decreased before infiltration occurs.

Summarizing, the relevance of discharge of nutrients via groundwater has generally been underestimated with regard to freshwater ecological quality and represents a future concern for environmental policy in Europe and beyond (Holman et al. 2008). Given the adverse impacts of high nutrient concentrations in ecosystems, there is an urgent need for detailed research to quantify different groundwater nutrient sources and the likelihood of transport, transformation and storage along flow paths (Holman et al. 2010; Moore et al. 2006). Effects of land use changes and climatic changes on the long-term hydrological budget of groundwater-fed lakes, and their effects on biogeochemical cycles, are also poorly understood (Herczeg et al. 2003). The close coupling of hydrologic and biogeochemical processes in the catchment and at the aquifer-lake interface requires close collaboration of scientists from different disciplines (Cirmo and McDonnell 1997).

2.2.8 References

EU Nitrate Directive, 1991. Council Directive 91/676/EEC of 12 December 1991 concerning the protection of waters against pollution caused by nitrates from agricultural sources.

EU Water Framework Directive, 2000. Directive 2000/60/EC of the European Parliament and of the Council of 23 October 2000 establishing a framework for Community action in the field of water policy.

Adler, M., Hensen, C., Kasten, S., Schulz, H.D., 2000. Computer simulation of deep sulfate reduction in sediments of the Amazon Fan. *International Journal of Earth Sciences*, 88(4): 641-654.

Aller, R.C., 1978. Experimental studies of changes produced by deposit feeders on pore water, sediment, and overlying water chemistry. *American Journal of Science*, 278(9): 1185-1234.

Andersson, G., Graneli, W., Stenson, J., 1988. The influence of animals on phosphorus cycling in lake ecosystems. *Hydrobiologia*, 170: 267-284.

Appelo, C.A.J., Postma, D., 1999. *Geochemistry, groundwater and pollution*. Balkema, Rotterdam, 536 p.

Bardini, L., Boano, F., Cardenas, M.B., Revelli, R., Ridolfi, L., 2012. Nutrient cycling in bedform induced hyporheic zones. *Geochimica et Cosmochimica Acta*, 84: 47-61.

Bardini, L., Boano, F., Cardenas, M.B., Sawyer, A.H., Revelli, R., Ridolfi, L., 2013. Small-scale permeability heterogeneity has negligible effects on nutrient cycling in streambeds. *Geophysical Research Letters*, 40(6): 1118-1122.

Bayer, T.K., Schallenberg, M., Martin, C.E., 2008. Investigation of nutrient limitation status and nutrient pathways in Lake Hayes, Otago, New Zealand: A case study for integrated lake assessment. *New Zealand Journal of Marine and Freshwater Research*, 42(3): 285-295.

Beck, A.J., Tsukamoto, Y., Tovar-Sanchez, A., Huerta-Diaz, M., Bokuniewicz, H.J., Sanudo-Wilhelmy, S.A., 2007. Importance of geochemical transformations in determining submarine groundwater discharge-derived trace metal and nutrient fluxes. *Applied Geochemistry*, 22(2): 477-490.

Belanger, T.V., Mikutel, D.F., 1985. On the use of seepage meters to estimate groundwater nutrient loading to lakes. *Water Resources Bulletin*, 21(2): 265-273.

Belanger, T.V., Mikutel, D.F., Churchill, P.A., 1985. Groundwater seepage nutrient loading in a Florida lake. *Water Research*, 19(6): 773-781.

Bishop, P.K., Misstear, B.D., White, M., Harding, N.J., 1998. Impacts of sewers on groundwater quality. *Journal of the Chartered Institution of Water and Environmental Management*, 12(3): 216-223.

Bowen, J.L., Kroeger, K.D., Tomasky, G., Pabich, W.J., Cole, M.L., Carmichael, R.H., Valiela, I., 2007. A review of land-sea coupling by groundwater discharge of nitrogen to New England estuaries: Mechanisms and effects. *Applied Geochemistry*, 22(1): 175-191.

Bowman, M.J., 1977. Nutrient distributions and transport in Long Island Sound. *Estuarine and Coastal Marine Science*, 5(4): 531-548.

Brinkman, A.G., 1993. A double-layer model for ion adsorption onto metal oxides, applied to experimental data and to natural sediments of Lake Veluwe, The Netherlands. *Hydrobiologia*, 253(1): 31-45.

Brock, T.D., Lee, D.R., Janes, D., Winek, D., 1982. Groundwater seepage as a nutrient source to a drainage lake - Lake Mendota, Wisconsin. *Water Research*, 16(7): 1255-1263.

Brun, A., Engesgaard, P., 2002. Modelling of transport and biogeochemical processes in pollution plumes: literature review and model development. *Journal of Hydrology*, 256(3–4): 211-227.

Brunke, M., Gonser, T.O.M., 1997. The ecological significance of exchange processes between rivers and groundwater. *Freshwater Biology*, 37(1): 1-33.

Burgin, A.J., Hamilton, S.K., 2007. Have we overemphasized the role of denitrification in aquatic ecosystems? A review of nitrate removal pathways. *Frontiers in Ecology and the Environment*, 5(2): 89-96.

Burnett, W.C., Aggarwal, P.K., Aureli, A., Bokuniewicz, H., Cable, J.E., Charette, M.A., Kontar, E., Krupa, S., Kulkarni, K.M., Loveless, A., Moore, W.S., Oberdorfer, J.A., Oliveira, J., Ozyurt, N., Povinec, P., Privitera, A.M.G., Rajar, R., Ramessur, R.T., Scholten, J., Stieglitz, T., Taniguchi, M., Turner, J.V., 2006. Quantifying submarine groundwater discharge in the coastal zone via multiple methods. *Science of The Total Environment*, 367(2–3): 498-543.

Burnett, W.C., Bokuniewicz, H., Huettel, M., Moore, W.S., Taniguchi, M., 2003. Groundwater and pore water inputs to the coastal zone. *Biogeochemistry*, 66(1-2): 3-33.

Buso, D.C., Likens, G.E., LaBaugh, J.W., Bade, D., 2009. Nutrient dynamics. In: *Mirror Lake: Interactions among air, land, and water*, Winter, T.C., Likens, G.E. (Eds.). University of California Press, Berkeley, 69–203.

Bussey, K.W., Walter, D.A., 1996. Spatial and temporal distribution of specific conductance, boron, and phosphorus in a sewage-contaminated aquifer near Ashumet Pond, Cape Cod, Massachusetts. *USGS Open-File Report* 96-472: 48 p.

Capone, D.G., Slater, J.M., 1990. Interannual patterns of water table height and groundwater derived nitrate in nearshore sediments. *Biogeochemistry*, 10(3): 277-288.

Carlyle, G.C., Hill, A.R., 2001. Groundwater phosphate dynamics in a river riparian zone: effects of hydrologic flowpaths, lithology and redox chemistry. *Journal of Hydrology*, 247(3-4): 151-168.

Ceazan, M.L., Thurman, E.M., Smith, R.L., 1989. Retardation of ammonium and potassium transport through a contaminated sand and gravel aquifer: the role of cation exchange. *Environmental Science & Technology*, 23(11): 1402-1408.

Charette, M.A., Buesseler, K.O., 2004. Submarine groundwater discharge of nutrients and copper to an urban subestuary of Chesapeake bay (Elizabeth River). *Limnology and Oceanography*, 49(2): 376-385.

Chen, R.L., Keeney, D.R., 1974. The fate of nitrate in lake sediment colums. *JAWRA Journal of the American Water Resources Association*, 10(6): 1162-1172.

Cherkauer, D.S., McKereghan, P.F., Schalch, L.H., 1992. Delivery of Chloride and Nitrate by Ground Water to the Great Lakes: Case Study for the Door Peninsula, Wisconsin. *Ground Water*, 30(6): 885-894.

Christensen, K.K., Andersen, F.Ø., Jensen, H.S., 1997. Comparison of iron, manganese, and phosphorus retention in freshwater littoral sediment with growth of Littorella uniflora and benthic microalgae. *Biogeochemistry*, 38(2): 149-171.

Christensen, P.B., Sorensen, J., 1986. Temporal variation of denitrification activity in plant-covered, littoral sediment from Lake Hampen, Denmark. *Applied and Environmental Microbiology*, 51(6): 1174-1179.

Christensen, T.H., Kjeldsen, P., Bjerg, P.L., Jensen, D.L., Christensen, J.B., Baun, A., Albrechtsen, H.-J., Heron, G., 2001. Biogeochemistry of landfill leachate plumes. *Applied Geochemistry*, 16(7–8): 659-718.

Cirmo, C.P., McDonnell, J.J., 1997. Linking the hydrologic and biogeochemical controls of nitrogen transport in near-stream zones of temperate-forested catchments: a review. *Journal of Hydrology*, 199(1): 88-120.

Clement, T.P., 1997. A modular computer code for simulating reactive multispecies transport in 3-dimensional groundwater aquifers. *Technical Report, Pacific Northwest National Laboratory*: 59 p.

Conley, D.J., Paerl, H.W., Howarth, R.W., Boesch, D.F., Seitzinger, S.P., Havens, K.E., Lancelot, C., Likens, G.E., 2009. Controlling Eutrophication: Nitrogen and Phosphorus. *Science*, 323(5917): 1014-1015.

Corbett, D.R., Chanton, J., Burnett, W., Dillon, K., Rutkowski, C., Fourqurean, J.W., 1999. Patterns of groundwater discharge into Florida Bay. *Limnology and Oceanography*, 44(4): 1045-1055.

Cornett, R.J., Risto, B.A., Lee, D.R., 1989. Measuring groundwater transport through lake sediments by advection and diffusion. *Water Resources Research*, 25(8): 1815-1823.

Correll, D.L., 1998. The role of phosphorus in the eutrophication of receiving waters: A review. *Journal of Environmental Quality*, 27(2): 261-266.

Crandall, C.A., 2000. Distribution, movement, and fate of nitrate in the surficial aquifer beneath citrus groves, Indian River, Martin, and St Lucie Counties, Florida. *Water-Resources Investigations Report.*

Crowe, A.S., Schwartz, F.W., 1981. Simulation of lake-watershed systems. 1. Description and sensitivity analysis of the model. *Journal of Hydrology*, 52(1-2): 71-105.

Dahm, C.N., Grimm, N.B., Marmonier, P., Valett, H.M., 1998. Nutrient dynamics at the interface between surface waters and groundwaters. *Freshwater Biology*, 40(3): 427–451.

Dean, W.E., Neff, B.P., Rosenberry, D.O., Winter, T.C., Parkhurst, R., 2003. The Significance of Ground Water to the Accumulation of Iron and Manganese in the Sediments of Two Hydrologically Distinct Lakes in North-Central Minnesota: A Geological Perspective. *Ground Water*, 41(7): 951-963.

Detenbeck, N.E., Brezonik, P.L., 1991. Phosphorus sorption by sediments from a soft-water seepage lake. 1. An evaluation of kinetic and equilibrium models. *Environmental Science & Technology*, 25(3): 395-403.

Devito, K.J., Fitzgerald, D., Hill, A.R., Aravena, R., 2000. Nitrate Dynamics in Relation to Lithology and Hydrologic Flow Path in a River Riparian Zone. *Journal of Environmental Quality*, 29(4): 1075-1084.

Downing, J.A., Peterka, J.J., 1978. Relationship of rainfall and lake groundwater seepage. *Limnology and Oceanography*, 23(4): 821-825.

Eiswirth, M., Hötzl, H., 1999. Gefährdungspotential von Abwasserversickerungen auf urbane Grundwasserleiter. *Wasser-Abwasser-Praxis*, 5: 10–15.

Eiswirth, M., Wolf, L., Hötzl, H., 2004. Balancing the contaminant input into urban water resources. *Environmental Geology*, 46(2): 246-256.

Enell, M., 1982. The phosphorus economy of a hypertrophic seepage lake in Scania, south Sweden groundwater influence. *Hydrobiologia*, 86(1): 153-158.

Erisman, J.W., Sutton, M.A., Galloway, J., Klimont, Z., Winiwarter, W., 2008. How a century of ammonia synthesis changed the world. *Nature Geosci*, 1(10): 636-639.

Fadiran, A.O., Diamini, S.C., Mavuso, A., 2008. A comparative study of the phosphate levels in some surface and ground water bodies of Swaziland. *Bulletin of the Chemical Society of Ethiopia*, 22(2): 197–206.

Fellows, C.R., Brezonik, P.L., 1980. Seepage inflow into Florida lakes. *Journal of the American Water Resources Association*, 16(4): 635-641.

Fellows, C.R., Brezonik, P.L., 1981. Fertilizer Flux into Two Florida Lakes via Seepage1. *Journal of Environmental Quality*, 10(2): 174-177.

Frandsen, M., Nilsson, B., Engesgaard, P., Pedersen, O.L.E., 2012. Groundwater seepage stimulates the growth of aquatic macrophytes. *Freshwater Biology*, 57(5): 907-921.

Frape, S.K., Patterson, R.J., 1981. Chemistry of Interstitial Water and Bottom Sediments as Indicators of Seepage Patterns in Perch Lake, Chalk-River, Ontario. *Limnology and Oceanography*, 26(3): 500-517.

Frimpter, M.H., Gay, F.B., 1979. Chemical quality of groundwater on Cape Cod, Massachusetts. *U.S. Geological Survey Water Resources Investigations Report* 79-65: 11 p.

Gaines, A.G., Giblin, A.E., lodzinska-Kijowski, Z., 1983. Freshwater discharge and nitrate input into Town Cove. In: *The Coastal Impact of Groundwater Discharge: An Assessment of Anthropogenic Nitrogen Loading in Town Cove, Orleans. Final Report*, Teal, J.M. (Ed.). Woods Hole Oceanographic Institution, Woods Hole, Massachusetts, 13-37.

Galloway, J.N., Dentener, F.J., Capone, D.G., Boyer, E.W., Howarth, R.W., Seitzinger, S.P., Asner, G.P., Cleveland, C.C., Green, P.A., Holland, E.A., Karl, D.M., Michaels, A.F., Porter, J.H., Townsend, A.R., Vöosmarty, C.J., 2004. Nitrogen Cycles: Past, Present, and Future. *Biogeochemistry*, 70(2): 153-226.

Garcia-Solsona, E., Garcia-Orellana, J., Masqué, P., Garcés, E., Radakovitch, O., Mayer, A., Estradé, S., Basterretxea, G., 2010. An assessment of karstic submarine groundwater and associated nutrient discharge to a Mediterranean coastal area (Balearic Islands, Spain) using radium isotopes. *Biogeochemistry*, 97(2): 211-229.

Gilliam, J.W., Daniels, R.B., Lutz, J.F., 1974. Nitrogen Content of Shallow Ground Water in the North Carolina Coastal Plain1. *Journal of Environmental Quality*, 3(2): 147-151.

Gilliom, R.J., Patmont, C.R., 1983. Lake phosphorus loading from septic systems by seasonally perched groundwater. *Journal Water Pollution Control Federation*, 55(10): 1297-1305.

Gooddy, D.C., 2002. Movement of leachate from beneath turkey litter sited over chalk in southern England. *Journal of Environmental Science and Health, Part B*, 37(1): 81-91.

Grannemann, N.G., Sharp, J.M., 1979. Alluvial hydrogeology of the lower Missouri River valley. *Journal of Hydrology*, 40(1): 85-99.

Greskowiak, J., Prommer, H., Massmann, G., Nützmann, G., 2006. Modeling seasonal redox dynamics and the corresponding fate of the pharmaceutical residue phenazone during artificial recharge of groundwater. *Environmental Science & Technology*, 40(21): 6615-6621.

Griffioen, J., 1994. Uptake of Phosphate by Iron Hydroxides during Seepage in Relation to Development of Groundwater Composition in Coastal Areas. *Environmental Science & Technology*, 28(4): 675-681.

Griffioen, J., 2006. Extent of immobilisation of phosphate during aeration of nutrient-rich, anoxic groundwater. *Journal of Hydrology*, 320(3-4): 359-369.

Grimm, N.B., Fisher, S.G., 1984. Exchange between interstitial and surface water: Implications for stream metabolism and nutrient cycling. *Hydrobiologia*, 111(3): 219-228.

Gu, C., Anderson, W., Maggi, F., 2012. Riparian biogeochemical hot moments induced by stream fluctuations. *Water Resources Research*, 48(9): n/a-n/a.

Hagerthey, S.E., Kerfoot, W.C., 1998. Groundwater flow influences the biomass and nutrient ratios of epibenthic algae in a north temperate seepage lake. *Limnology and Oceanography*, 43(6): 1227-1242.

Hagerthey, S.E., Kerfoot, W.C., 2005. Spatial variation in groundwater-related resource supply influences freshwater benthic algal assemblage composition. *Journal of the North American Benthological Society*, 24(4): 807-819.

Harman, J., Robertson, W.D., Cherry, J.A., Zanini, L., 1996. Impacts on a sand aquifer from an old septic system: Nitrate and phosphate. *Ground Water*, 34(6): 1105-1114.

Harper, D.M., 1992. Preface. In: *Eutrophication of Freshwaters : Principles, Problems and Restoration*, Harper, D.M. (Ed.). Chapman and Hall, London, i–viii.

Harvey, F.E., Rudolph, D.L., Frape, S.K., 2000. Estimating ground water flux into large lakes: Application in the Hamilton Harbor, western Lake Ontario. *Ground Water*, 38(4): 550-565.

Hauxwell, A.M., Neill, C., Valiela, I., Kroeger, K.D., 2001. Small-scale heterogeneity of nitrogen concentrations in groundwater at the seepage face of Edgartown Great Pond. *Biological Bulletin*, 201(2): 290-292.

Hayes, C.R., Incledion, S., Balch, M., 2008. Experience in Wales (UK) of the optimisation of orthophosphate dosing for controlling lead in drinking water. *Journal of Water and Health*, 6(2): 177–185.

Healy, R.W., Winter, T.C., LaBaugh, J.W., Franke, O.L., 2007. Water Budgets: Foundations for Effective Water-Resources and Environmental Management. *U.S. Geological Survey Circular* 1308: 98 p.

Heckrath, G., Brookes, P.C., Poulton, P.R., Goulding, K.W.T., 1995. Phosphorus leaching from soils containing different phosphorus concentrations in the Broadbalk experiment. *Journal of Environmental Quality*, 24(5): 904-910.

Herczeg, A.L., Leaney, F.W., Dighton, J.C., Lamontagne, S., Schiff, S.L., Telfer, A.L., English, M.C., 2003. A modern isotope record of changes in water and carbon budgets in a groundwater-fed lake: Blue Lake, South Australia. *Limnology and Oceanography*, 48(6): 2093-2105.

Hesslein, R.H., 1976. An in situ sampler for close interval pore water studies. *Limnology and Oceanography*, 21(6): 912-914.

Hillbricht-Ilkowska, A., Sharpley, A., 1995. Phosphorus transfers and landscape structure: riparian sites and diversified land use patterns. In: *Phosphorus in the Global Environment*, Tiessen, H. (Ed.). Wiley, New York, 201–227.

Hofmann, H., Lessmann, D., 2006. Hydrogeochemistry of groundwater seepage into an acidic mining lake. *Proceedings of the International Association of Theoretical and Applied Limnology*, 29: 1452–1456.

Holman, I.P., Howden, N.J.K., Bellamy, P., Willby, N., Whelan, M.J., Rivas-Casado, M., 2010. An assessment of the risk to surface water ecosystems of groundwater P in the UK and Ireland. *Science of The Total Environment*, 408(8): 1847-1857.

Holman, I.P., Whelan, M.J., Howden, N.J.K., Bellamy, P.H., Willby, N.J., Rivas-Casado, M., McConvey, P., 2008. Phosphorus in groundwater-an overlooked contributor to eutrophication? *Hydrological Processes*, 22(26): 5121-5127.

Holmer, M., Jensen, H.S., Christensen, K.K., Wigand, C., Andersen, F.Ø., 1998. Sulfate reduction in lake sediments inhabited by the isoetid macrophytes Littorella uniflora and Isoetes lacustris. *Aquatic Botany*, 60(4): 307-324.

Holzbecher, E., 2001. The dynamics of subsurface water divides—watersheds of Lake Stechlin and neighbouring lakes. *Hydrological Processes*, 15(12): 2297-2304.

Holzbecher, E., Nützmann, G., 2000. Influence of the subsurface watershed on eutrophication — Lake Stechlin case study. *Ecological Engineering*, 16(1): 31-38.

Horner, C., Engelmann, F., Nützmann, G., 2009. Model based verification and prognosis of acidification and sulphate releasing processes downstream of a former sewage field in Berlin (Germany). *Journal of Contaminant Hydrology*, 106(1–2): 83-98.

Horner, C., Holzbecher, E., Nützmann, G., 2007. A coupled transport and reaction model for long column experiments simulating bank filtration. *Hydrological Processes*, 21(8): 1015-1025.

Howarth, R.W., 1988. Nutrient limitation of net primary production in marine ecosystems. *Annual Review of Ecology and Systematics*, 19: 89-110.

Hupfer, M., Dollan, A., 2003. Immobilisation of phosphorus by iron-coated roots of submerged macrophytes. *Hydrobiologia*, 506(1): 635-640.

Hupfer, M., Lewandowski, J., 2005. Retention and early diagenetic transformation of phosphorus in Lake Arendsee (Germany) - consequences for management strategies. *Archiv fuer Hydrobiologie*, 164(2): 143-167.

Hupfer, M., Lewandowski, J., 2008. Oxygen Controls the Phosphorus Release from Lake Sediments – a Long-Lasting Paradigm in Limnology. *International Review of Hydrobiology*, 93(4-5): 415-432.

Hwang, D.-W., Kim, G., Lee, W.-C., Oh, H.-T., 2010. The role of submarine groundwater discharge (SGD) in nutrient budgets of Gamak Bay, a shellfish farming bay, in Korea. *Journal of Sea Research*, 64(3): 224-230.

Ibánhez, J.S.P., Leote, C., Rocha, C., 2011. Porewater nitrate profiles in sandy sediments hosting submarine groundwater discharge described by an advection–dispersion-reaction model. *Biogeochemistry*, 103(1): 159-180.

Isenbeck-Schroeter, M., Doring, U., Moller, A., Schroter, J., Matthess, G., 1993. Experimental approach and simulation of the retention processes limiting orthophosphate transport in groundwater. *Journal of Contaminant Hydrology*, 14(2): 143-161.

Jacobs, P.H., 2002. A new rechargeable dialysis pore water sampler for monitoring sub-aqueous in-situ sediment caps. *Water Research*, 36(12): 3121-3129.

Johannes, R.E., Hearn, C.J., 1985. The effect of submarine groundwater discharge on nutrient and salinity regimes in a coastal lagoon off Perth, Western Australia. *Estuarine, Coastal and Shelf Science*, 21(6): 789-800.

John, P.H., Lock, M.A., 1977. The spacial distribution of groundwater discharge into the littoral zone of a New Zealand lake. *Journal of Hydrology*, 33(3): 391-395.

Johnes, P.J., Butterfield, D., 2002. Landscape, regional and global estimates of nitrogen flux from land to sea: Errors and uncertainties. *Biogeochemistry*, 57(1): 429-476.

Jordan, P., Arnscheidt, J., McGrogan, H., McCormick, S., 2005. High-resolution phosphorus transfers at the catchment scale: the hidden importance of non-storm transfers. *Hydrology and Earth System Sciences*, 9(6): 685-691.

Jordan, T.E., Correll, D.L., Weller, D.E., 1997. Relating nutrient discharges from watersheds to land use and streamflow variability. *Water Resources Research*, 33(11): 2579-2590.

Juckem, P.F., Robertson, D.M., 2013. Hydrology and water quality of Shell Lake, Washburn County, Wisconsin, with special emphasis on the effects of diversion and changes in water level on the water quality of a shallow terminal lake. *Scientific Investigations Report*.

Kalbitz, K., Solinger, S., Park, J.-H., Michalzik, B., Matzner, E., 2000. Controls on the dynamics of dissolved organic matter in soils: a review. *Soil Science*, 165(4): 277-304.

Kang, W.J., Kolasa, K.V., Rials, M.W., 2005. Groundwater inflow and associated transport of phosphorus to a hypereutrophic lake. *Environmental Geology*, 47(4): 565-575.

Keeney, D., 1986. Sources of nitrate to groundwater. *Crc Critical Reviews in Environmental Control*, 16(3): 257-304.

Keeney, D.R., Chen, R.L., Graetz, D.A., 1971. Importance of Denitrification and Nitrate Reduction in Sediments to the Nitrogen Budgets of Lakes. *Nature*, 233(5314): 66-67.

Kidmose, J., 2010. Groundwater - surface water interaction: From catchment to interfaces at lakes and streams, University of Copenhagen, Copenhagen, 181 p.

Kidmose, J., Dahl, M., Engesgaard, P., Nilsson, B., Christensen, B.S.B., Andersen, S., Hoffmann, C.C., 2010. Experimental and numerical study of the relation between flow paths and fate of a pesticide in a riparian wetland. *Journal of Hydrology*, 386(1-4): 67-79.

Kilinc, S., Moss, B., 2002. Whitemere, a lake that defies some conventions about nutrients. *Freshwater Biology*, 47(2): 207-218.

Kilroy, G., Coxon, C., 2005. Temporal variability of phosphorus fractions in Irish karst springs. *Environmental Geology*, 47(3): 421-430.

Kira, T., 1993. Major environmental problems in world lakes. *Memorie dell' Istituto Italiano di Idrobiologia*, 52: 1-7.

Korom, S.F., 1992. Natural denitrification in the saturated zone: A review. *Water Resources Research*, 28(6): 1657-1668.

Krabbenhoft, D.P., 1988. Hydrologic and geochemical investigations of aquifer-lake interactions at Sparkling Lake, Wisconsin, University Wisconsin-Madison, 205 p.

Krabbenhoft, D.P., Anderson, M.P., Bowser, C.J., 1990. Estimating groundwater exchange with lakes: 2. Calibration of a three-dimensional, solute transport model to a stable isotope plume. *Water Resources Research*, 26(10): 2455-2462.

Krabbenhoft, D.P., Webster, K.E., 1995. Transient hydrogeological controls on the chemistry of a seepage lake. *Water Resources Research*, 31(9): 2295-2305.

Kratz, T.K., Webster, K.E., Bowser, C.J., Magnuson, J.J., Benson, B.J., 1997. The influence of landscape position on lakes in northern Wisconsin. *Freshwater Biology*, 37(1): 209-217.

Kreitler, C.W., Ragone, S.E., Katz, B.G., 1978. N15/N14 Ratios of Ground-Water Nitrate, Long Island, New Yorka. *Ground Water*, 16(6): 404-409.

Kroeger, K.D., Charette, M.A., 2008. Nitrogen biogeochemistry of submarine groundwater discharge. *Limnology and Oceanography*, 53(3): 1025-1039.

Kroeger, K.D., Cole, M.L., Valiela, I., 2006. Groundwater-transported dissolved organic nitrogen exports from coastal watersheds. *Limnology and Oceanography*, 51(5): 2248-2261.

Kroeger, K.D., Swarzenski, P.W., Greenwood, W.J., Reich, C., 2007. Submarine groundwater discharge to Tampa Bay: Nutrient fluxes and biogeochemistry of the coastal aquifer. *Marine Chemistry*, 104(1-2): 85-97.

Krom, M.D., Davison, P., Zhang, H., Davison, W., 1994. High-resolution pore-water sampling with a gel sampler. *Limnology and Oceanography*, 39(8): 1967-1972.

Kunkel, R., Wendland, F., Voigt, H.-J., Hannappel, S., 2004. Die natürliche, ubiquitär überprägte Grundwasserbeschaffenheit in Deutschland. In: GmbH, F.J. (Ed.), Schriften des Forschungszentrums Jülich, Reihe Umwelt. Forschungszentrum Jülich.

LaBaugh, J.W., Buso, D.C., Likens, G.E., 2009. Evaluation of Methods and Uncertainties in the Chemical Budgets: Chapter 5.

LaBaugh, J.W., Rosenberry, D.O., Winter, T.C., 1995. Groundwater contribution to the water and chemical budgets of Williams Lake, Minnesota, 1980-1991. *Canadian Journal of Fisheries and Aquatic Sciences*, 52(4): 754-767.

LaBaugh, J.W., Winter, T.C., Rosenberry, D.O., 2000. Comparison of the variability in fluxes of ground water and solutes in lakes and wetlands in central North America. *Proceedings - International Association of Theoretical and Applied Limnology*, 27: 420-426.

LaBaugh, J.W., Winter, T.C., Rosenberry, D.O., Schuster, P.F., Reddy, M.M., Aiken, G.R., 1997. Hydrological and chemical estimates of the water balance of a closed-basin lake in north central Minnesota. *Water Resources Research*, 33(12): 2799-2812.

Lamontagne, S., 2002. Groundwater delivery rate of nitrate and predicted change in nitrate concentration in Blue Lake, South Australia. *Marine and Freshwater Research*, 53(7): 1129-1142.

Landenberger, H., Hensen, C., Zabel, M., Schulz, H.D., 1997. Softwareentwicklung zur computerunterstützten Simulation frühdiagenetischer Prozesse in marinen Sedimenten. *Zeitschrift der Deutschen Gesellschaft für Geowissenschaften*, 148((3-4)): 447–455.

Lapointe, B.E., O'Connell, J.D., Garrett, G.S., 1990. Nutrient couplings between on-site sewage disposal systems, groundwaters, and nearshore surface waters of the Florida Keys. *Biogeochemistry*, 10(3): 289-307.

Lee, D.R., 1977. A device for measuring seepage flux in lakes and estuaries. *Limnology and Oceanography*, 22(1): 140-147.

Lee, D.R., Cherry, J.A., Pickens, J.F., 1980. Groundwater transport of a salt tracer through a sandy lakebed1. *Limnology and Oceanography*, 25(1): 45-61.

Lee, T.M., 1996. Hydrogeologic controls on the groundwater interactions with an acidic lake in karst terrain, Lake Barco, Florida. *Water Resources Research*, 32(4): 831-844.

Lee, Y.-W., Kim, G., Lim, W.-A., Hwang, D.-W., 2010. A relationship between submarine groundwater borne nutrients traced by Ra isotopes and the intensity of dinoflagellate red-tides occurring in the southern sea of Korea. *Limnology and Oceanography*, 55(1): 1-10.

Lerman, A., Brunskill, G.J., 1971. Migration of major constituents from lake sediments into lake water and its bearing on lake water composition. *Limnology and Oceanography*, 16(6): 880-890.

Lewandowski, J., Angermann, L., Nutzmann, G., Fleckenstein, J.H., 2011a. A heat pulse technique for the determination of small-scale flow directions and flow velocities in the streambed of sand-bed streams. *Hydrological Processes*, 25(20): 3244-3255.

Lewandowski, J., Laskov, C., Hupfer, M., 2007. The relationship between Chironomus plumosus burrows and the spatial distribution of pore-water phosphate, iron and ammonium in lake sediments. *Freshwater Biology*, 52(2): 331-343.

Lewandowski, J., Meinikmann, K., Ruhtz, T., Pöschke, F., Kirillin, G., 2013. Localization of lacustrine groundwater discharge (LGD) by airborne measurement of thermal infrared radiation. *Remote Sensing of Environment*, 138: 119-125.

Lewandowski, J., Nützmann, G., 2010. Nutrient retention and release in a floodplain's aquifer and in the hyporheic zone of a lowland river. *Ecological Engineering*, 36(9): 1156-1166.

Lewandowski, J., Putschew, A., Schwesig, D., Neumann, C., Radke, M., 2011b. Fate of organic micropollutants in the hyporheic zone of a eutrophic lowland stream: Results of a preliminary field study. *Science of The Total Environment*, 409(10): 1824-1835.

Lewandowski, J., Ruter, K., Hupfer, M., 2002. Two-dimensional small-scale variability of pore water phosphate in freshwater lakes: Results from a novel dialysis sampler. *Environmental Science & Technology*, 36(9): 2039-2047.

Lewis, W.M., Wurtsbaugh, W.A., 2008. Control of Lacustrine Phytoplankton by Nutrients: Erosion of the Phosphorus Paradigm. *International Review of Hydrobiology*, 93(4-5): 446-465.

Likens, G.E., 2009. A limnological introduction to Mirror Lake. In: *Mirror Lake: Interactions among air, land, and water*, Winter, T.C., Likens, G.E. (Eds.). University of California Press, Berkely, 1-22.

Lillie, R.A., Barko, J.W., 1990. Influence of sediment and groundwater on the distribution and biomass of *Myriophyllum spicatum* L. in Devils Lake, Wisconsin. *Journal of Freshwater Ecology*, 5(4): 417-426.

Lin, J.C., Schnoor, J.L., Glass, G.E., 1987. Ion budgets in a seepage lake. *Advances in Chemistry Series*(216): 209-227.

Loeb, S.L., Goldman, C.R., 1979. Water and nutrient transport via groundwater from Ward Valley into Lake Tahoe. *Limnology and Oceanography*, 24(6): 1146-1154.

Mallin, M.A., McIver, M.R., 2012. Pollutant impacts to Cape Hatteras National Seashore from urban runoff and septic leachate. *Marine Pollution Bulletin*, 64(7): 1356-1366.

Mayer, K.U., Frind, E.O., 2003. Reactive transport modeling for variably saturated groundwater systems - the state of the art. In: *GeoProc 2002 Geochemical Processes in Soil and Groundwater*, Schulz, H.D., Hadeler, A. (Eds.). Wiley - VCH, Weinheim, Germany, 468–480.

McBride, M.S., Pfannkuch, H.O., 1975. Distribution of seepage within lakebeds. *Journal of Research of the U.S. Geological Survey*, 3(5): 505-512.

McCobb, T.D., LeBlanc, D.R., Massey, A.J., 2009. Monitoring the removal of phosphate from ground water discharging through a pond-bottom permeable reactive barrier. *Ground Water Monitoring and Remediation*, 29(2): 43-55.

McCobb, T.D., LeBlanc, D.R., Walter, D.A., Hess, K.M., Kent, D.B., Smith, R.L., 2003. Phosphorus in a ground-water contaminant plume discharging to Ashumet Pond, Cape Cod, Massachusetts, 1999. *U.S. Geological Survey Water Resources Investigations Report* 02-4306: 70 p.

McCoy, C.A., Corbett, D.R., 2009. Review of submarine groundwater discharge (SGD) in coastal zones of the Southeast and Gulf Coast regions of the United States with management implications. *Journal of Environmental Management*, 90(1): 644-651.

McDowell, W.H., 2003. Dissolved organic matter in soils—future directions and unanswered questions. *Geoderma*, 113(3–4): 179-186.

McIntire, P.E., Mills, A.L., Hornberger, G.M., 1988. Interactions between groundwater seepage and sediment porewater sulfate concentration profiles in Lake Anna, Virginia. *Hydrological Processes*, 2(3): 207-217.

Meade, R.H., Vaccaro, R.F., 1971. Sewage disposal in Falmouth, MA. III. Predicted effects of inland disposal and sea outfall on groundwater. *Boston Society of Civil Engineers Journal*, 58: 278–297.

Meinikmann, K., Lewandowski, J., Nutzmann, G., 2013. Lacustrine groundwater discharge: Combined determination of volumes and spatial patterns. *Journal of Hydrology*, 502(0): 202-211.

Meyboom, P., 1967. Mass-transfer studies to determine the groundwater regime of permanent lakes in hummocky moraine of Western Canada. *Journal of Hydrology*, 5(0): 117-142.

Misztal, M., Smal, H., Gorniak, A., 1992. Ground-water inflow of nutrients to a lake from differently utilized catchments. *Water Research*, 26(9): 1237-1242.

Moore, W.S., 1996. Large groundwater inputs to coastal waters revealed by Ra-226 enrichments. *Nature*, 380(6575): 612-614.

Moore, W.S., 2010. The Effect of Submarine Groundwater Discharge on the Ocean. *Annual Review of Marine Science*, 2: 59-88.

Moore, W.S., Blanton, J.O., Joye, S.B., 2006. Estimates of flushing times, submarine groundwater discharge, and nutrient fluxes to Okatee Estuary, South Carolina. *Journal of Geophysical Research-Oceans*, 111(C9).

Moore, W.S., Church, T.M., 1996. Submarine groundwater discharge - Reply. *Nature*, 382(6587): 122-122.

Moore, W.S., Sarmiento, J.L., Key, R.M., 2008. Submarine groundwater discharge revealed by 228Ra distribution in the upper Atlantic Ocean. *Nature Geosci*, 1(5): 309-311.

Mortimer, R.J.G., Krom, M.D., Boyle, D.R., Nishri, A., 1999. Use of a high-resolution pore-water gel profiler to measure groundwater fluxes at an underwater saline seepage site in Lake Kinneret, Israel. *Limnology and Oceanography*, 44(7): 1802-1809.

Mortimer, R.J.G., Krom, M.D., Hall, P.O.J., Hulth, S., Ståhl, H., 1998. Use of gel probes for the determination of high resolution solute distributions in marine and estuarine pore waters. *Marine Chemistry*, 63(1–2): 119-129.

Muellegger, C., Weilhartner, A., Battin, T.J., Hofmann, T., 2013. Positive and negative impacts of five Austrian gravel pit lakes on groundwater quality. *Science of The Total Environment*, 443: 14-23.

Muendo, P.N., Stoorvogel, J.J., Gamal, N.E., Verdegem, M.C.J., 2005. Rhizons improved estimation of nutrient losses because of seepage in aquaculture ponds. *Aquaculture Research*, 36(13): 1333-1336.

Mulholland, P.J., Helton, A.M., Poole, G.C., Hall, R.O., Hamilton, S.K., Peterson, B.J., Tank, J.L., Ashkenas, L.R., Cooper, L.W., Dahm, C.N., Dodds, W.K., Findlay, S.E.G., Gregory, S.V., Grimm, N.B., Johnson, S.L., McDowell, W.H., Meyer, J.L., Valett, H.M., Webster, J.R., Arango, C.P., Beaulieu, J.J., Bernot, M.J., Burgin, A.J., Crenshaw, C.L., Johnson, L.T., Niederlehner, B.R., O/'Brien, J.M., Potter, J.D., Sheibley, R.W., Sobota, D.J., Thomas, S.M., 2008. Stream denitrification across biomes and its response to anthropogenic nitrate loading. *Nature*, 452(7184): 202-205.

Munns, D.N., Fox, R.L., 1976. Slow reaction which continues after phosphate adsorption - kinetics and equilibrium in some tropical soils. *Soil Science Society of America Journal*, 40(1): 46-51.

Nakayama, T., Watanabe, M., 2008. Missing role of groundwater in water and nutrient cycles in the shallow eutrophic Lake Kasumigaura, Japan. *Hydrological Processes*, 22(8): 1150-1172.

Newbold, J.D., Elwood, J.W., Oneill, R.V., Vanwinkle, W., 1981. MEASURING NUTRIENT SPIRALLING IN STREAMS. *Canadian Journal of Fisheries and Aquatic Sciences*, 38(7): 860-863.

Nolan, B.T., Stoner, J.D., 2000. Nutrients in Groundwaters of the Conterminous United States, 1992−1995. *Environmental Science & Technology*, 34(7): 1156-1165.

Norrström, A.C., Jacks, G., 1996. Water Pathways and Chemistry at the Groundwater/Surface Water Interface to Lake Skjervatjern, Norway. *Water Resources Research*, 32(7): 2221-2229.

Oliveira Ommen, D.A., Kidmose, J., Karan, S., Flindt, M.R., Engesgaard, P., Nilsson, B., Andersen, F.O., 2012. Importance of groundwater and macrophytes for the nutrient balance at oligotrophic Lake Hampen, Denmark. *Ecohydrology*, 5(3): 286-296.

Ottosen, L.D.M., Risgaard-Petersen, N., Nielsen, L.P., 1999. Direct and indirect measurements of nitrification and denitrification in the rhizosphere of aquatic macrophytes. *Aquatic Microbial Ecology*, 19(1): 81-91.

Pabich, W.J., Valiela, I., Hemond, H.F., 2001. Relationship between DOC concentration and vadose zone thickness and depth below water table in groundwater of Cape Cod, U.S.A. *Biogeochemistry*, 55(3): 247-268.

Pagès, A., Teasdale, P.R., Robertson, D., Bennett, W.W., Schäfer, J., Welsh, D.T., 2011. Representative measurement of two-dimensional reactive phosphate distributions and co-distributed iron(II) and sulfide in seagrass sediment porewaters. *Chemosphere*, 85(8): 1256-1261.

Parkhurst, D.L., Appelo, C.A.J., 1999. User's guide to PHREEQC (Version 2) : a computer program for speciation, batch-reaction, one-dimensional transport, and inverse geochemical calculations. *Water-Resources Investigations Report.*

Parkhurst, D.L., Stollenwerk, K.G., Colman, J.A., 2003. Reactive-transport simulation of phosphorus in the sewage plume at the Massachusetts Military Reservation, Cape Cod, Massachusetts. *Water-Resources Investigations Report.*

Patrick, W.H., Gotoh, S., Williams, B.G., 1973. Strengite dissolution in flooded soils and sediments. *Science*, 179(4073): 564-565.

Patterson, R.J., Frape, S.K., Dykes, L.S., McLeod, R.A., 1978. A coring and squeezing technique for the detailed study of subsurface water chemistry. *Canadian Journal of Earth Sciences*, 15(1): 162-169.

Pina-Ochoa, E., Alvarez-Cobelas, M., 2009. Seasonal nitrogen dynamics in a seepage lake receiving high nitrogen loads. *Marine and Freshwater Research*, 60(5): 335-445.

Pinay, G., Decamps, H., 1988. The role of riparian woods in regulating nitrogen fluxes between the alluvial aquifer and surface water: A conceptual model. *Regulated Rivers: Research & Management*, 2(4): 507-516.

Price, R.M., Swart, P.K., Fourqurean, J.W., 2006. Coastal groundwater discharge – an additional source of phosphorus for the oligotrophic wetlands of the Everglades. *Hydrobiologia*, 569(1): 23-36.

Prommer, H., 2002. A reactive multicomponent transport model for saturated porous media.

Ptacek, C.J., 1998. Geochemistry of a septic-system plume in a coastal barrier bar, Point Pelee, Ontario, Canada. *Journal of Contaminant Hydrology*, 33(3-4): 293-312.

Puckett, L.J., Tesoriero, A.J., Dubrovsky, N.M., 2011. Nitrogen Contamination of Surficial Aquifers—A Growing Legacy. *Environmental Science & Technology*, 45(3): 839-844.

Qualls, R.G., Richardson, C.J., 2003. Factors controlling concentration, export, and decomposition of dissolved organic nutrients in the Everglades of Florida. *Biogeochemistry*, 62(2): 197-229.

Reay, W.G., Gallagher, D.L., Simmons, G.M., 1992. Groundwater discharge and its impact on surface water quality in a Chesepeake bay. *JAWRA Journal of the American Water Resources Association*, 28(6): 1121-1134.

Reddy, K.R., Kadlec, R.H., Flaig, E., Gale, P.M., 1999. Phosphorus retention in streams and wetlands: A review. *Critical Reviews in Environmental Science and Technology*, 29(1): 83-146.

Reynolds, C.S., 1979. The limnology of the eutrophic meres of the Shropshire-Cheshire plain: a review. *Field Studies*, 5(93): 173.

Rivett, M.O., Buss, S.R., Morgan, P., Smith, J.W.N., Bemment, C.D., 2008a. Nitrate attenuation in groundwater: A review of biogeochemical controlling processes. *Water Research*, 42(16): 4215-4232.

Rivett, M.O., Ellis, R., Greswell, R.B., Ward, R.S., Roche, R.S., Cleverly, M.G., Walker, C., Conran, D., Fitzgerald, P.J., Willcox, T., Dowle, J., 2008b. Cost-effective mini drive-point piezometers and multilevel samplers for monitoring the hyporheic zone. *Quarterly Journal of Engineering Geology and Hydrogeology*, 41: 49-60.

Robertson, D.M., Rose, W.J., 2011. Response in the trophic state of stratified lakes to changes in hydrology and water level: potential effects of climate change. *Journal of Water and Climate Change*, 2(1): 1-18.

Robertson, D.M., Rose, W.J., Juckem, P.F., 2009. Water Quality and Hydrology of Whitefish (Bardon) Lake, Douglas County, Wisconsin, With Special Emphasis on Responses of an Oligotrophic Seepage Lake to Changes in Phosphorus Loading and Water Level. *Scientific Investigations Report.*

Robertson, D.M., Rose, W.J., Saad, D.A., 2003. Water quality and the effects of changes in phosphorus loading to Muskellunge Lake, Vilas County, Wisconsin. *Water-Resources Investigations Report*: 26 p.

Robertson, W.D., 1995. Development of steady-state phosphate concentrations in septic system plumes. *Journal of Contaminant Hydrology*, 19(4): 289-305.

Robertson, W.D., 2008. Irreversible phosphorus sorption in septic system plumes? *Ground Water*, 46(1): 51-60.

Robertson, W.D., Schiff, S.L., Ptacek, C.J., 1998. Review of phosphate mobility and persistence in 10 septic system plumes. *Ground Water*, 36(6): 1000-1010.

Rosenberry, D.O., Lewandowski, J., Meinikmann, K., Nützmann, G., 2015. Groundwater - the disregarded component in lake water and nutrient budgets. Part 1: effects of groundwater on hydrology. *Hydrological Processes*, 29(13): 2895-2921.

Rosenberry, D.O., Sheibley, R.W., Cox, S.E., Simonds, F.W., Naftz, D.L., 2013. Temporal variability of exchange between groundwater and surface water based on high-frequency direct measurements of seepage at the sediment-water interface. *Water Resources Research*, 49(5): 2975-2986.

Rosenberry, D.O., Winter, T.C., 2009. Hydrologic processes and the water budget: Chapter 2. *Mirror Lake: Interactions among air, land, and water*: 23-68.

Roy, J.W., Malenica, A., 2013. Nutrients and toxic contaminants in shallow groundwater along Lake Simcoe urban shorelines. *Inland Waters*, 3(2): 125-138.

Roy, J.W., Robillard, J.M., Watson, S.B., Hayashi, M., 2009. Non-intrusive characterization methods for wastewater-affected groundwater plumes discharging to an alpine lake. *Environmental Monitoring and Assessment*, 149(1-4): 201-211.

Rutsch, M., Rieckermann, J., Cullmann, J., Ellis, J.B., Vollertsen, J., Krebs, P., 2008. Towards a better understanding of sewer exfiltration. *Water Research*, 42(10-11): 2385-2394.

Schäfer, D., Schäfer, W., Kinzelbach, W., 1998. Simulation of reactive processes related to biodegradation in aquifers - 2. Model application to a column study on organic carbon degradation. *Journal of Contaminant Hydrology*, 31(1-2): 187-209.

Schaffner, W.R., Oglesby, R.T., 1978. Phosphorus loadings to lakes and some of their responses. Part 1. A new calculation of phosphorus loading and its application to 13 New York lake 1. *Limnology and Oceanography*, 23(1): 120-134.

Schafran, G.C., Driscoll, C.T., 1990. Porewater acid/base chemistry in near-shore regions of an acidic lake. *Biogeochemistry*, 11(2): 131-150.

Schafran, G.C., Driscoll, C.T., 1993. Flow path-composition relationships for groundwater entering an acidic lake. *Water Resources Research*, 29(1): 145-154.

Schauser, I., Lewandowski, J., Hupfer, M., 2003. Decision support for the selection of an appropriate in-lake measure to influence the phosphorus retention in sediments. *Water Research*, 37(4): 801-812.

Schelske, C.L., 2009. Eutrophication: Focus on Phosphorus. *Science*, 324(5928): 722-722.

Schindler, D.W., Hecky, R.E., 2009. Eutrophication: More Nitrogen Data Needed. *Science*, 324(5928): 721-722.

Schirmer, M., Leschik, S., Musolff, A., 2013. Current research in urban hydrogeology - A review. *Advances in Water Resources*, 51: 280-291.

Schot, P.P., Pieber, S.M., 2012. Spatial and temporal variations in shallow wetland groundwater quality. *Journal of Hydrology*, 422–423: 43-52.

Schumann, D., 1973. Annual variation of seepage of lakes in the moraine area of the German Democratic Republic. *Hydrology of Lakes IAHS Publication*, 109: 101–108.

Schuster, P.F., Reddy, M.M., LaBaugh, J.W., Parkhurst, R.S., Rosenberry, D.O., Winter, T.C., Antweiler, R.C., Dean, W.E., 2003. Characterization of lake water and ground water movement in the littoral zone of Williams Lake, a closed-basin lake in north central Minnesota. *Hydrological Processes*, 17(4): 823-838.

Shaw, R.D., Prepas, E.E., 1990. Groundwater-lake interactions: II. Nearshore seepage patterns and the contribution of ground water to lakes in central Alberta. *Journal of Hydrology*, 119(1): 121-136.

Shaw, R.D., Shaw, J.F.H., Fricker, H., Prepas, E.E., 1990. An integrated approach to quantify groundwater transport of phosphorus to Narrow Lake, Alberta. *Limnology and Oceanography*, 35(4): 870-886.

Sigua, G.C., Hubbard, R.K., Coleman, S.W., 2010. Quantifying phosphorus levels in soils, plants, surface water, and shallow groundwater associated with bahiagrass-based pastures. *Environmental Science and Pollution Research*, 17(1): 210-219.

Simmons, J.A.K., Lyons, W.B., 1994. The ground water flux of nitrogen and phosphorus to Bermuda´s coastal waters. *JAWRA Journal of the American Water Resources Association*, 30(6): 983-991.

Simonds, F.W., Swarzenski, P.W., Rosenberry, D.O., Reich, C.D., Paulson, A.J., 2008. Estimates of Nutrient Loading by Ground-Water Discharge into the Lynch Cove Area of Hood Canal, Washington. *Scientific Investigations Report.*

Slomp, C.P., Van Cappellen, P., 2004. Nutrient inputs to the coastal ocean through submarine groundwater discharge: controls and potential impact. *Journal of Hydrology*, 295(1–4): 64-86.

Sonzogni, W.C., Lee, G.F., 1974. Nutrient sources for Lake Mendota - 1972. *Transactions of the Wisconsin Academy Sciences Arts and Letters*, 62: 133-164.

Spiteri, C., Slomp, C.P., Charette, M.A., Tuncay, K., Meile, C., 2008a. Flow and nutrient dynamics in a subterranean estuary (Waquoit Bay, MA, USA): Field data and reactive transport modeling. *Geochimica et Cosmochimica Acta*, 72(14): 3398-3412.

Spiteri, C., Slomp, C.P., Regnier, P., Meile, C., Van Cappellen, P., 2007. Modelling the geochemical fate and transport of wastewater-derived phosphorus in contrasting groundwater systems. *Journal of Contaminant Hydrology*, 92(1-2): 87-108.

Spiteri, C., Slomp, C.P., Tuncay, K., Meile, C., 2008b. Modeling biogeochemical processes in subterranean estuaries: Effect of flow dynamics and redox conditions on submarine groundwater discharge of nutrients. *Water Resources Research*, 44(2): n/a-n/a.

Starr, R.C., Gillham, R.W., 1993. Denitrification and Organic Carbon Availability in Two Aquifers. *Ground Water*, 31(6): 934-947.

Stauffer, R.E., 1985. Use of solute tracers released by weathering to estimate groundwater inflow to seepage lakes. *Environmental Science & Technology*, 19(5): 405-411.

Sterner, R.W., 2008. On the Phosphorus Limitation Paradigm for Lakes. *International Review of Hydrobiology*, 93(4-5): 433-445.

Stief, P., de Beer, D., 2006. Probing the microenvironment of freshwater sediment macrofauna: Implications of deposit-feeding and bioirrigation for nitrogen cycling. *Limnology and Oceanography*, 51(6): 2538-2548.

Stollenwerk, K.G., 1996. Simulation of phosphate transport in sewage-contaminated groundwater, Cape Cod, Massachusetts. *Applied Geochemistry*, 11(1): 317-324.

Stumm, W., Morgan, J.J., 1996. *Aquatic Chemistry*. Wiley, New York.

Sutula, M., Day, J.W., Cable, J., Rudnick, D., 2001. Hydrological and nutrient budgets of freshwater and estuarine wetlands of Taylor Slough in Southern Everglades, Florida (U.S.A.). *Biogeochemistry*, 56(3): 287-310.

Swarzenski, P.W., Orem, W.H., McPherson, B.F., Baskaran, M., Wan, Y., 2006. Biogeochemical transport in the Loxahatchee River estuary, Florida: The role of submarine groundwater discharge. *Marine Chemistry*, 101(3–4): 248-265.

Swarzenski, P.W., Simonds, F.W., Paulson, A.J., Kruse, S., Reich, C., 2007. Geochemical and geophysical examination of submarine groundwater discharge and associated nutrient loading estimates into Lynch Cove, Hood Canal, WA. *Environmental Science and Technology*, 41(20): 7022-7029.

Tallberg, P., Koski-Vahala, J., 2001. Silicate-induced phosphate release from surface sediment in eutrophic lakes. *Archiv Fur Hydrobiologie*, 151(2): 221-245.

Tallberg, P., Treguer, P., Beucher, C., Corvaisier, R., 2008. Potentially mobile pools of phosphorus and silicon in sediment from the Bay of Brest: Interactions and implications for phosphorus dynamics. *Estuarine Coastal and Shelf Science*, 76(1): 85-94.

Taniguchi, M., Burnett, W.C., Cable, J.E., Turner, J.V., 2002. Investigation of submarine groundwater discharge. *Hydrological Processes*, 16(11): 2115-2129.

Tesoriero, A.J., Liebscher, H., Cox, S.E., 2000. Mechanism and rate of denitrification in an agricultural watershed: Electron and mass balance along groundwater flow paths. *Water Resources Research*, 36(6): 1545-1559.

Tesoriero, A.J., Puckett, L.J., 2011. O-2 reduction and denitrification rates in shallow aquifers. *Water Resources Research*, 47.

Tiessen, H., 1995. *Phosphorus in the Global Environment: Transfers, Cycles and Management.* . Scope 54. Wiley, New York, 462 p.

Torrent, J., Schwertmann, U., Barron, V., 1992. Fast and slow phosphate sorption by goethite-rich natural materials. *Clays and Clay Minerals*, 40(1): 14-21.

Triska, F.J., Kennedy, V.C., Avanzino, R.J., Zellweger, G.W., Bencala, K.E., 1989. Retention and transport of nutrients in a third-order stream in northwestern California; hyporheic processes. *Ecology*, 70(6): 1893-1905.

Tuominen, L., Hartikainen, H., Kairesalo, T., Tallberg, P., 1998. Increased bioavailability of sediment phosphorus due to silicate enrichment. *Water Research*, 32(7): 2001-2008.

USGS, 2012. Toxic Substances Hydrology Program. U.S. Geological Survey.

Valett, H.M., Dahm, C.N., Campana, M.E., Morrice, J.A., Baker, M.A., Fellows, C.S., 1997. Hydrologic Influences on Groundwater-Surface Water Ecotones: Heterogeneity in Nutrient Composition and Retention. *Journal of the North American Benthological Society*, 16(1): 239-247.

Valiela, I., Costa, J., Foreman, K., Teal, J.M., Howes, B., Aubrey, D., 1990. Transport of groundwater-borne nutrients from watersheds and their effects on coastal waters. *Biogeochemistry*, 10(3): 177-197.

Van Cappellen, P., Wang, Y., 1995. STEADYSED1, a steady-state reaction-transport model for C, N, S, O, Fe and Mn in surface sediments, Version 1.0 User´s manual.

Vanek, V., 1987. The interactions between lake and groundwater and their ecological significance. *Stygologia*, 3: 1-23.

Vanek, V., 1991. Riparian zone as a source of phosphorus for a groundwater-dominated lake. *Water Research*, 25(4): 409-418.

Vanek, V., 1993. Transport of groundwater-borne phosphorus to Lake Bysjon, South Sweden. *Hydrobiologia*, 251(1-3): 211-216.

Vaux, W.G., 1968. Intragravel flow and interchange of water in a streambed. *Fishery Bulletin*, 66: 479–489.

Vitousek, P.M., Mooney, H.A., Lubchenco, J., Melillo, J.M., 1997. Human Domination of Earth's Ecosystems. *Science*, 277(5325): 494-499.

Vollenweider, R.A., 1976. Advances in defining critical loading levels for phosphorus in lake eutrophication. *Memorie dell'Istituto Italiano di Idrobiologia*, 33: 53–84.

Vroblesky, D.A., D. Petkewich, M.D., Ted R. Campbell, T.R., 2002. Field Tests of Diffusion Samplers for Inorganic Constituents in Wells and at a Ground-Water-Discharge Zone. *U.S. Geological Survey Water-Resources Investigations Report* 02-4031: 31 p.

Wakida, F.T., Lerner, D.N., 2005. Non-agricultural sources of groundwater nitrate: a review and case study. *Water Research*, 39(1): 3-16.

Walter, D.A., LeBlanc, D.R., 1997. Geochemical and hydrologic considerations in remediating phosphorus-contaminated ground water in a sewage plume near Ashumet Pond, Cape Cod, Massachusetts. *Open-File Report.*

Walter, D.A., Rea, B.A., Stollenwerk, K.G., Savoie, J.G., 1995. Geochemical and hydrologic controls on phosphorus transport in a sewage-contaminated sand and gravel aquifer near Ashumet Pond, Cape Cod, Massachusetts. *Open-File Report.*

Webster, K.E., Kratz, T.K., Bowser, C.J., Magnuson, J.J., Rose, W.J., 1996. The influence of landscape position on lake chemical responses to drought in northern Wisconsin. *Limnology and Oceanography*, 41(5): 977-984.

Weilhartner, A., Muellegger, C., Kainz, M., Mathieu, F., Hofmann, T., Battin, T.J., 2012. Gravel pit lake ecosystems reduce nitrate and phosphate concentrations in the outflowing groundwater. *Science of The Total Environment*, 420: 222-228.

Weinstein, Y., Yechieli, Y., Shalem, Y., Burnett, W.C., Swarzenski, P.W., Herut, B., 2011. What Is the Role of Fresh Groundwater and Recirculated Seawater in Conveying Nutrients to the Coastal Ocean? *Environmental Science & Technology*, 45(12): 5195-5200.

Weiskel, P.K., Howes, B.L., 1992. Differential transport of sewage-derived nitrogen and phosphorus through a coastal watershed. *Environmental Science & Technology*, 26(2): 352-360.

Wendland, F., Hannappel, S., Kunkel, R., Schenk, R., Voigt, H.J., Wolter, R., 2005. A procedure to define natural groundwater conditions of groundwater bodies in Germany. *Water Science and Technology*, 51(3-4): 249-257.

Wentz, D.A., Rose, W.J., Webster, K.E., 1995. Long-Term Hydrologic and Biogeoehemieal Responses of a Soft Water Seepage Lake in North Central Wisconsin. *Water Resources Research*, 31(1): 199-212.

Wilhelm, S.R., Schiff, S.L., Cherry, J.A., 1994. Biogeochemical evolution of domestic waste-water in septic systems. 1. Conceptual model. *Ground Water*, 32(6): 905-916.

Wilhelm, S.R., Schiff, S.L., Robertson, W.D., 1996. Biogeochemical Evolution of Domestic Waste Water in Septic Systems: 2. Application of Conceptual Model in Sandy Aquifers. *Ground Water*, 34(5): 853-864.

Williams, R.E., 1968. Flow of ground water adjacent to small closed basins in glacial till. *Water Resources Research*, 4(4): 777-784.

Winter, T.C., 1978. Numerical simulation of steady state three-dimensional groundwater flow near lakes. *Water Resources Research*, 14(2): 245-254.

Withers, P.J.A., Edwards, A.C., Foy, R.H., 2001. Phosphorus cycling in UK agriculture and implications for phosphorus loss from soil. *Soil Use and Management*, 17(3): 139-149.

Withers, P.J.A., McDonald, H.G., Smith, K.A., Chumbley, C.G., 1998. Behaviour and impact of cow slurry beneath a storage lagoon: 1. Groundwater contamination 1975-1982. *Water Air and Soil Pollution*, 107(1-4): 35-49.

Wolf, L., Held, I., Eiswirth, M., Hotzl, H., 2004. Impact of leaky sewers on groundwater quality. *Acta Hydrochimica Et Hydrobiologica*, 32(4-5): 361-373.

Yeh, G.T., Salvage, K.M., Gwo, J.P., Zachara, J.M., Szecsody, J.E., 1998. HydroBioGeoChem: A coupled model of hydrologic transport and mixed biogeochemical kinetic/equilibrium reactions in saturatedunsaturated media. *Report ORNL/TM-13668*.

Zanini, L., Robertson, W.D., Ptacek, C.J., Schiff, S.L., Mayer, T., 1998. Phosphorus characterization in sediments impacted by septic effluent at four sites in central Canada. *Journal of Contaminant Hydrology*, 33(3-4): 405-429.

Zarnetske, J.P., Haggerty, R., Wondzell, S.M., Bokil, V.A., González-Pinzón, R., 2012. Coupled transport and reaction kinetics control the nitrate source-sink function of hyporheic zones. *Water Resources Research*, 48(11): n/a-n/a.

Zimmermann, C.F., Montgomery, J.R., Carlson, P.R., 1985. Variability of dissolved reactive phosphate flux rates in nearshore estuarine sediments: Effects of groundwater flow. *Estuaries*, 8(2): 228-236.

Zurawsky, M.A., Robertson, W.D., Ptacek, C.J., Schiff, S.L., 2004. Geochemical stability of phosphorus solids below septic system infiltration beds. *Journal of Contaminant Hydrology*, 73(1–4): 129-143.

3 The case study of Lake Arendsee

3.1 Lacustrine groundwater discharge: Combined determination of volumes and spatial patterns

Karin Meinikmann[1,2], Jörg Lewandowski[1,2], and Gunnar Nützmann[1,2],

[1] Department of Ecohydrology, Leibniz-Institute of Freshwater Ecology and Inland Fisheries, Berlin, Germany

[2] Geography Department, Humboldt-Universität zu Berlin, Berlin, Germany

This is the peer reviewed version of the following article:

Meinikmann, K., Lewandowski, J., Nützmann, G., 2013. Lacustrine groundwater discharge: Combined determination of volumes and spatial patterns. *Journal of Hydrology*, 502(0): 202-211. DOI: 10.1016/j.jhydrol.2013.08.021.

Abstract

The quantification of lacustrine groundwater discharge (LGD) in water and nutrient balances of lakes is challenging and thus often neglected. However, by carrying large nutrient loads, groundwater might play a key role in a lake´s nutrient budget even if its contribution to the water balance is small. In the present study, we quantify the total annual LGD of a lake in northeastern Germany by the calculation of annual groundwater recharge in the subsurface catchment. Furthermore, spatial variability of LGD is expected to have significant influence on the nutrient balance due to heterogeneous nutrient concentrations. To assess its spatial variability, LGD is calculated for single sites based on vertical temperature profiles of the lake bed along the shoreline. The combination of the total LGD and the spatial LGD patterns allows calculating LGD volumes for single shoreline sub-sections. These calculations reveal that a large portion of the total LGD enters the lake within a relatively limited section of the shoreline. Scenarios including different phosphorus concentrations demonstrate the importance of both, quantity and patterns of LGD, when groundwater-borne phosphorus loads are calculated. At high, heterogeneous groundwater nutrient concentrations, it is crucial for lake nutrient budgets to reliably determine LGD patterns and volume.

3.1.1 Introduction

Research on groundwater–surface water interactions focused mainly on streams and rivers in the past decades (Kalbus et al. 2006; Stonestrom and Constantz 2003). Although there have been some early studies on lake interactions with groundwater (e.g., Meyboom, 1967, and a review by Winter, 1999) lake ecosystems were far less intensely investigated. This may be attributable to the fact that lakes had already been recognized as integrated systems in limnology for a long time while hydrologists and stream ecologists had predominantly been focusing on stream-specific topics (Moss 2012). A revision of this one-dimensional view on river ecosystems might have led to the intense focus on the interactions of streams and groundwater, rather than of lakes and groundwater.

Furthermore, a general underestimation of the influence of groundwater on the omnipresent phenomenon of lake eutrophication might have led to a strong focus on in-lake processes and above-ground nutrient inputs. In this context, point sources of nutrients were identified as major threats for surface waters. In Europe, great effort was undertaken to reduce these point sources during the last decades. However, a “good chemical and ecological status” as being demanded by the European Water Framework Directive is still not established in many European freshwaters. After a significant reduction of point sources it becomes more and more obvious that the diffuse transport of nutrients into lakes limits their ecological regeneration to a larger extent than previously expected. Gelbrecht et al. (2005) attributed this to an ongoing nutrient leaching from agricultural areas on the one hand, and to the degradation of natural retention areas on the other hand. Widely discussed is also the contamination of groundwater by domestic wastewater exfiltration from faulty sewers and septic systems (Bremer and Harter 2012; Katz et al. 2011; Ptacek 1998; Robertson 2008). Apart from the causes of groundwater contamination, the quantification of resulting nutrient loads to lakes is difficult and still lacking practical approaches. As a consequence, the groundwater path is often disregarded which might lead to a severe underestimation of its impact on the trophic state of a lake.

In the case of Lake Arendsee in northeastern Germany the groundwater path was also disregarded as a source of eutrophication. During the last four decades an increase of total phosphorus (TP) concentrations in the lake water from 0.15 to currently 0.19 mg l^{-1} has been observed. As a result, severe blooms of cyanobacteria occurred periodically, which have stimulated discussion and request of lake restoration measures. While investigating different phosphorus (P) sources, we detected high (>1 mg l^{-1}) concentrations of soluble reactive phosphorus (SRP) in some parts of the near-shore groundwater. Accordingly, we hypothesized that groundwater-borne nutrients, especially P, have a significant impact on the nutrient budget of the lake.

To reliably quantify the groundwater component in the P budget of the lake, an approach is required that considers both spatial variations of P concentrations and spatial heterogeneities in lacustrine groundwater discharge (LGD). These heterogeneities are introduced by small- to medium-scale variability of the aquifer characteristics, which in most cases are neither homogeneous nor isotropic (Rosenberry and LaBaugh 2008). To address both, LGD quantity and quality, the approach needs to incorporate total LGD volumes as well as spatial LGD patterns. Thus, we combine a method of point measurements to detect LGD patterns with an integrating approach for total groundwater recharge quantification. In particular, we hypothesize that LGD into Lake Arendsee underlies a variety of small- to medium-scale geologic and anthropogenic impacts resulting in a large variability of LGD patterns along the shoreline. We furthermore hypothesize that hydraulic head contour lines (as a prerequisite for further investigations) do not depict this heterogeneity adequately due to an insufficient number of groundwater observation wells. Moreover, a large hydraulic gradient might indicate intense groundwater exfiltration, but can also be a consequence of low hydraulic conductivity (k_{sat}). Additionally, even an aquifer with a high k_{sat} can result in little exfiltration in case that its thickness is small.

In recent years, using heat as a natural tracer has become more and more popular in research addressing small- to medium-scale interactions between groundwater and streams (Anderson 2005; Constantz 2008; Stonestrom and Constantz 2003). We thus assume a great benefit by applying such a method also to groundwater-lake interfaces. Vertical temperature profiles in the sediment of surface waters are a function of advective and conductive heat exchange across the groundwater–surface water interface. Significant differences between temperatures of groundwater and surface water typically occur during summer and winter seasons. Therefore, the curvatures of temperature gradients in the sediment close to the interface represent the direction and intensity of vertical groundwater exchange. As described by Schmidt et al. (2006), a quantification of LGD rates from temperature profiles is possible using the heat transport equation to calculate the exchange rates. In the present study, temperature gradients of the lake sediment were used to determine spatial LGD patterns and intensity, rather than for calculation of absolute LGD.

Point measurements of LGD based on temperature depth profiles are combined with an integrating approach of groundwater recharge calculation for the whole catchment in order to derive LGD volumes for shoreline sub-sections. Based on a couple of near-shore groundwater wells P loads of three scenarios are calculated to evaluate the necessity of segmented approaches. With this study we demonstrate the importance of heterogeneities in LGD for the accuracy of groundwater-borne nutrient loads in lakes.

3.1.2 Methods

Study site

Lake Arendsee in north–northeastern Germany (Federal State of Saxony-Anhalt) is a deep stratified lake with a maximum depth of 50 m and a mean depth of about 30 m. A bathymetric map is provided in Hupfer and Lewandowski (2005). The lake covers an area of 5.1 km^2. Originally it was solely groundwater-fed and had no surface in- or outflows. Nowadays, there are four drainage ditches artificial outlet exists, where a weir regulates the outflow. The surface catchment (29.5 km^2 of size) is dominated by agricultural and forest land use, while the homonymous city of Arendsee is situated directly at the southern and south-western shoreline (Fig. 3.1A). Inclination is low in the surface catchment and thus, no significant surface runoff occurs.

For the subsurface catchment, previous (unpublished) studies agreed on a mainly northern groundwater flow direction resulting in LGD at the southern shoreline. However, size, shape, and hydraulic characteristics of the subsurface catchment were unknown. The setup of ten new groundwater observation wells at four sites along the southern shoreline (Fig. 3.1A) at the beginning of the present study revealed a variety of Pleistocene substrates. Values for k_{sat} ranged from 0.33 x 10^{-4} to 5.69 x 10^{-4} m s^{-1} in different depths from 3 to 34 m below surface, with maximum values at Sites 2 and 3 (Fig. 3.1A and B). Furthermore, the borehole profiles revealed that several near-surface aquifers exist that are hydrologically connected by geologic windows. The upper one, consisting of Saalian substrates, is separated from the aquifer below by Saalian or Holsteinian aquitards. South and south-east of the lake the lower aquifer originates mainly from Pleistocene sediments of the Saalian and Elstarian glacials. In western direction the deeper parts of the aquifer become dominated by Miocene substrates. However, the aquitard is not everywhere present, and thus, in some areas the sediments form a single aquifer. In some parts, the uppermost sediments consist of Pleistocene boulder clay formations with low k_{sat}, which also might have an influence on LGD intensities at the shoreline (Fig. 3.1B). Groundwater SRP concentrations at these four sites vary broadly between 0.08 and 1.21 mg SRP l^{-1} with maximum concentrations at Site 3 in Figure 3.1A and B.

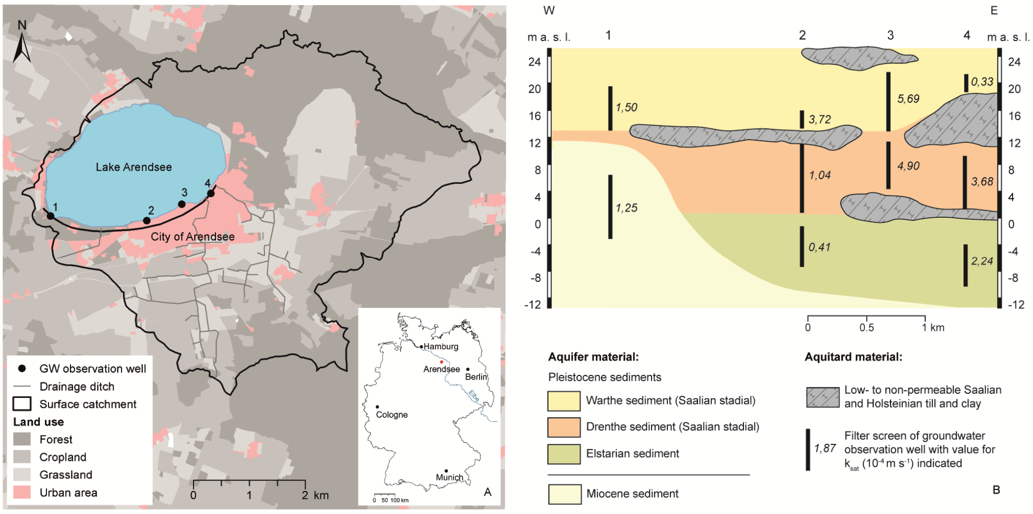

Figure 3.1 Land use in the surface catchment and position of near-shore groundwater (GW) observation wells (A) and scheme of the geologic conditions along the southern shoreline of Lake Arendsee (B). The black line along the southern shoreline in A represents the cross-section in B. Mean concentrations of soluble reactive phosphorus (SRP, mg l^{-1}) observed in the different GW observation wells at each site are 0.09 (Site 1), 0.16 (Site 2), 1.21 (Site 3), and 0.08 (Site 4). Data are available from monthly or trimonthly measurements from April 2010 to December 2012, and means are weighted by the thicknesses of geologic layers in which the wells are located.

Delineation of subsurface catchment

The size of the subsurface catchment is a necessary prerequisite to calculate groundwater recharge. We collected and evaluated available geological data to select appropriate groundwater observation wells and used 33 wells for the delineation of the subsurface catchment. Measurements were conducted at two consecutive days in July 2012. There was no rainfall during the campaign and a few days before. Thus, the measured groundwater heads can be assumed to be in a steady state.

Based on groundwater head data and the lake water level, hydraulic head contour lines were interpolated. All data were referred to sea level with the help of a tachymeter (Leica TSP 1200+). Measured groundwater head data were interpolated to contour lines by kriging using Surfer 8.0

(Golden Software©). Catchment boundaries were defined as the divide between groundwater flowing into the lake and groundwater flowing in other directions.

Mean annual groundwater recharge

According to the definition of a lake's catchment the mean total annual volume of LGD is equivalent to the mean total annual groundwater recharge in the whole catchment. Groundwater recharge can be quantified by a range of different approaches and methods have to be chosen carefully and on an individual basis (Scanlon et al. 2002). Due to the medium scale of the subsurface catchment, a method was chosen that calculates mean annual actual evapotranspiration $\overline{ET_a}$ (l m^{-2} yr^{-1}) as a factor controlling mean annual groundwater recharge. The approach by Glugla et al. (2003) is a refined method to calculate $\overline{ET_a}$ based on the differential equation by Bagrov (1953):

$$\frac{d\overline{ET_a}}{\overline{P_{korr}}} = 1 - \left(\frac{\overline{ET_a}}{\overline{ET_{max}}}\right)^n \qquad \text{Eq. 3.1}$$

where $\overline{P_{korr}}$ (l m^{-2} yr^{-1}) is the corrected mean annual precipitation, $\overline{ET_{max}}$ (mm yr^{-1}) is the mean maximum annual evapotranspiration, and n is the parameter of effectiveness. $\overline{ET_{max}}$ is the result of a land use-dependent modification of the mean annual potential evapotranspiration $\overline{ET_{pot}}$ (l m^{-2} yr^{-1}) by a factor *f*. This modification is one of several aspects that had been advanced compared to the original method in order to represent land use and soil parameters that influence site-specific $\overline{ET_{pot}}$. The method in general aims to determine $\overline{ET_a}$ from its ratio to $\overline{ET_{max}}$. For a known *n* this ratio can be derived from the graphical depiction of the Bagrov-Relation for any site of interest in Germany (Fig. 3.2). *n* represents site conditions for the utilization of water and energy supply.

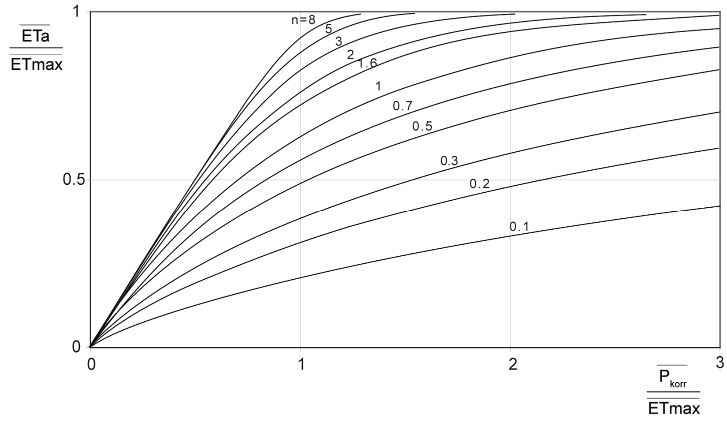

Figure 3.2 Graphical scheme of the Bagrov-Relation (Eq. 3.1) including corrected mean annual precipitation ($\overline{P_{korr}}$)and mean maximum annual evapotranspiration ($\overline{ET_{max}}$) as well as the parameter of effectiveness *n* (modified from Glugla et al., 2003).

As a further advance of the method (Glugla et al. 2003), site-specific values for both, *n* and *f*, can be determined by algorithms which base upon the evaluation of extensive lysimeter and climatic measurements in whole Germany and upon land use types. Six different land use types are covered by this method, namely sealed areas, areas without vegetation, grassland, cropland, deciduous forests and coniferous forests. Further data on specific field capacity and other specifications (e.g., population ages of forest stands and height of grassland vegetation) are required. Due to the availability of relevant soil data (especially specific field capacity) from a database of the Federal State of Saxony-Anhalt, the calculations were conducted at a higher spatial resolution than suggested by Glugla et al. (2003). Combinations of these data with land use data using ArcGIS 10.1 software (ESRI©) resulted in sub-areas for which groundwater recharge calculations were done individually. Due to a lack of this high resolution soil data for urban areas we used the soil survey map of the German Federal Institute for Geosciences and Natural Resources (BÜK 1998), which presents soil types at a lower resolution as originally suggested by Glugla et al. (2003). The predominant soil types defined three further sub-areas located in the area of the City of Arendsee. In these cases, values for specific field capacity as a prerequisite for the following calculations were chosen according to the recommendation of Glugla et al. (2003). Calculations were conducted for only 70% of the urban area, assuming a general portion of 30% being sealed and thus not contributing to groundwater recharge. Urban sub-areas were furthermore treated as grasslands, since it can be assumed that most of the unsealed area is covered with vegetation (e.g., lawns in public parks or private gardens).

Values for n were employed to derive the ratio of $\overline{ET_a}$ to $\overline{ET_{max}}$ for the sub-areas arising from intersections of soil and land use data (Fig. 3.2). Resulting $\overline{ET_a}$ is subtracted from $\overline{P_{korr}}$ to derive the total discharge $\overline{R}$ (l m^{-2} yr^{-1}):

$$\overline{R} = \overline{P_{korr}} - \overline{ET_a} \qquad \text{Eq. 3.2}$$

Since inclination is not relevant in the catchment of the lake, surface and lateral runoff were set to zero and groundwater recharge equals R. However, for cropland grasslands, drainage water extractions had to be considered. In general, such data are rarely existent but in the present case study they were available as drainage intensities. Four drainage intensity classes were assigned to single sub-areas of the catchment (0–30, 30–60, 60–90, and 90–100% drainage intensity). They were combined with the aforementioned data using ArcGIS 10.1 (ESRI©) to finally generate groundwater recharge rates and volumes for each sub-area. To distinguish the results of these drainage calculations from actual drainage measurements (see Section 2.4) we call them “calculated drainage”.

Measured drainage water extraction in the subsurface catchment

A validation of groundwater recharge calculation was performed using a dataset of a one-year-period of high resolution measurements of discharge in the aforementioned drainage ditches. The measurement equipment was mainly established for the quantification of P loads from agricultural drainage discharging into Lake Arendsee. Three of four drainage ditches contribute to discharge generated in the subsurface catchment of Lake Arendsee (Fig. 3.1A). The fourth ditch is situated outside of the subsurface catchment of the lake and is thus not relevant in the present context. Measurements were conducted close to the outlets into the lake. In one case, discharge was measured in 10 min-intervals by an ultrasonic flow measurement device. The other two ditches were equipped with V-weirs and pressure sensors to record water levels discharge and thus discharge in 30 min-intervals. The measurement period was from beginning of August 2010 until the end of July 2011.

Identification of LGD patterns using vertical lake bed temperature profiles

Lake bed temperature profiles at Lake Arendsee were measured approximately every 200 m along the southern part of the lake shoreline, where according to the delineation of the catchment LGD was expected to take place. LGD is known to primarily occur close the shore (Kishel and Gerla 2002) and to decrease at least for homogeneous sediments with increasing distance to the shoreline (McBride and Pfannkuch 1975). Based on this we focused our studies on the shoreline of the lake. Four vertical temperature profiles were obtained at each of 26 observation sites, arranged in transects of increasing distance to the shoreline (0.5 m, 1 m, 2 m, and 4 m, respectively). We used a stainless steel multilevel temperature probe including 16 equidistant thermistors of the type NTC 10 K (TDK EPCOS; Munich, Germany). Precision of the thermistors is ±0.2 C. They had a distance of 7 cm to each other and the probe was installed with the upper two of the sensors placed in the pelagic water of the lake. Profiles were generally measured down to 0.91 m (n = 13). In some cases the sediments did not allow such a deep penetration of the probe, but the measurement depth was never less than 0.84 m (n = 12).

Measurements were conducted in an eight-day-period at the end of July 2012. In the eastern parts of the shoreline a section of 900 m was not covered by sediment temperature investigations because a broad belt of shoreline vegetation inhibited access and appropriate measurements. The analytical solution of the heat-transport equation results in the vertical Darcy velocity q_z (m s^{-1}) (Bredehoeft and Papadopulos 1965):

$$\frac{T(z)-T_0}{T_L-T_0} = \frac{exp\left(\frac{q_z \, \rho_f c_f}{K_{fs}} z\right)-1}{exp\left(\frac{q_z \, \rho_f c_f}{K_{fs}} L\right)-1} \qquad \text{Eq. 3.3}$$

where L is the vertical extent of the domain where temperature changes due to LGD (m), $T(z)$ is the lake bed temperature (°C) at sediment depth z (m), $\varrho_f c_f$ is the volumetric heat capacity of the fluid (J m 3 K 1), K_{fs} is thermal conductivity of the saturated sediment (J s^{-1} m^{-1} K^{-1}), T_0 is the temperature for z = 0 (i.e., surface water temperature, C), and T_L is the temperature for z = L (i.e., groundwater temperature, °C). The vertical Darcy velocity q_z is derived by minimizing the root mean squared error (RMSE) between the n measured temperatures of a profile and the related simulated temperatures (Schmidt et al., 2006):

$$RMSE = \sqrt{\frac{1}{n}\sum_{j=1}^{n}\left[T_j - \left(\frac{exp\left(\frac{q_z \, \rho_f c_f}{K_{fs}} z_j\right)-1}{exp\left(\frac{q_z \, \rho_f c_f}{K_{fs}} L\right)-1}(T_L - T_0) + T_0\right)\right]^2} \qquad \text{Eq. 3.4}$$

Boundary conditions were set to lake water temperatures for T_0 and to groundwater temperature for T_L. Groundwater at the four near-shore sites (Fig. 3.1) showed depth-dependent temperature differences, ranging from 10.5 °C to 12.7 C. Thus, in a first approach T_L was set to 11 °C, representing the mean temperature measured in the ten wells. But for this case simulated temperature profiles did not show good fits to the measured profiles. It seemed that a value of 11 °C for T_L was too low. Thus, T_L was set to 13 C, which seemed to be plausible since near-surface groundwater showed similar temperatures (12.7 °C in 2–4 m below surface, at site 4, Fig. 3.1A) and most LGD was expected to originate from near-surface groundwater and might thus be heated up to >11 °C during the summer season. The value for $\varrho_f c_f$ is 4.19 x 10^{-6} J m^{-3} K^{-1} for water. According to (Stonestrom and Constantz 2003) K_{fs} was set to 2 J s^{-1} m^{-1} K^{-1} for the predominantly sandy sediments of Lake Arendsee. Since the temperature probe was inserted only about 1 m into the sediment it never covered the whole thickness L of the transition zone. A range of different values for the transition zone L was tested to identify the best fit of measured and simulated sediment temperatures. This revealed that at low values for the transition zone L LGD increases with increasing L while the RMSE of measured versus simulated temperatures decreased. This observation was independent of the temperature T_L at the lower boundary (Fig. 3.3). T_L was set to 13 °C which resulted in best fits in most cases (Fig. 3.3E). Due to the fact that the RMSE did not change at L > 5, L was set to 5 m (Fig. 3.3C and D). Resulting values for q_z were converted from discharge velocity (m s^{-1}) into daily LGD volume (l m^{-2} d^{-1}).

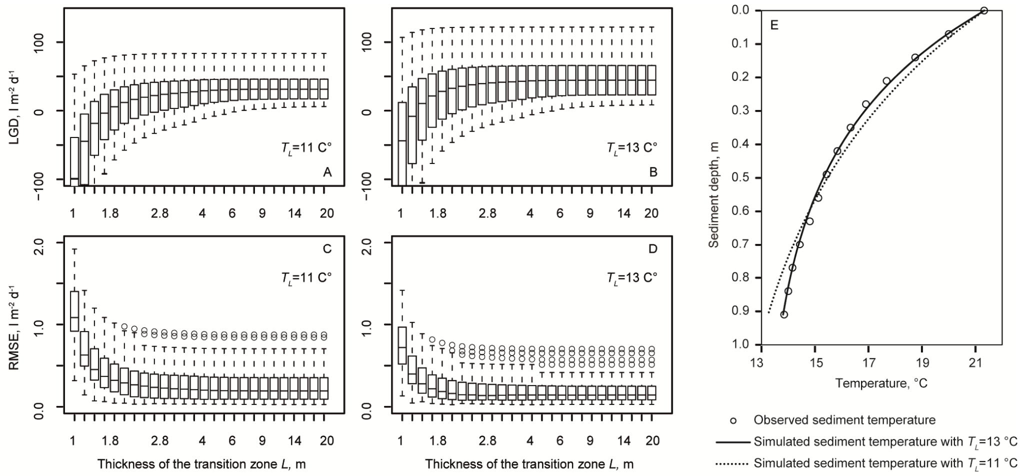

Figure 3.3 Visualization of different parameters used in the heat transport equation (Eq. 3.3). Boxplots of calculated lacustrine groundwater discharge (LGD) rates for T_L = 11 °C (A) and T_L = 13 °C (B) and root mean squared errors (RMSE) of measured versus simulated sediment temperatures for different values of the thickness of the transition zone L (m) for T_L = 11 °C (C) and T_L = 13 °C (D). Note the irregular scaling of the x-axis in Fig. 3.3A–D. Figure 3.3E shows an example for the results of temperature simulations for T_L = 13 °C (continuous line) and T_L = 11 °C (dotted line), based on measured temperatures (empty dots) and l = 5 m. Simulations led to better fits and higher LGD for T_L = 13 °C (RMSE: 0.09, LGD: 106 l m^{-2} d^{-1}) compared to T_L = 11 °C (RMSE: 0.37, LGD: 69 l m^{-2} d^{-1}).

Combination of hydraulic methods

Finally, we combined the results of the total annual volume of LGD and the LGD pattern to specify the amount of LGD for single shoreline sub-sections. Please note that from lake bed temperature derived LGD volumes only the maximum value of a transect was applied for further calculations. According to the numbers of lake bed temperature transects the shoreline was divided into 26 sub-sections by cutting the shoreline at each midpoint between two neighboring transects. The total annual volume of LGD based on groundwater recharge was split into 26 portions ($Q_{rech,i}$ in l yr^{-1}, in Eq. 3.5) which considered the individual length l_i of each shoreline sub-section. The ultimate amount of LGD discharging along a shoreline sub-section i (Q_i in l yr^{-1}) was calculated by the following equation:

$$Q_i = Q_{rech,i} \cdot \frac{q_{z,i}}{\overline{q_z}} \qquad \text{Eq. 3.5}$$

where $q_{z,i}$ is the maximum LGD rate (l m^{-2} d^{-1}) derived from each four lake bed temperature profiles in shoreline section i (q_z in Eqs. 3.1c and 3.1d) and $\overline{q_z}$ is weighted arithmetic mean (l m^{-2} d^{-1}) of all maximum lake bed temperature derived LGD rates ($q_{z,i}$) weighted by the individual length of the shoreline section l_i:

$$\overline{q_z} = \frac{\sum_{i=1}^{26} q_{z,i} \cdot l_i}{\sum_{i=1}^{26} l_i} \qquad \text{Eq. 3.6}$$

Phosphorus loads

To evaluate the necessity to determine LGD patterns with high spatial resolution we calculated three scenarios for groundwater- borne P loads to Lake Arendsee. Analysis of TP and SRP concentrations revealed that both are almost identical in this catchment. Thus, all scenarios are based on groundwater SRP concentrations measured at the four near-shore sites along the southern shoreline (Fig. 3.1A). At each site, either two or three groundwater observation wells are set up in different aquifer depths

(Fig. 3.1B). Results of monthly or trimonthly measurements of SRP from April 2010 to December 2012 were available for each well. The four SRP concentrations used in the present study are means of these measurements, weighted by the thicknesses of geologic layers in which the wells are situated. Given that in many other case studies only a single groundwater observation well is available (if at all), Scenario 1 consists of four variants (1a to 1d), each based on the SRP concentration of one of the four sites for all 26 shoreline sub-sections. They correspond in their order to the order of the groundwater observation wells in Figure 3.1A, with SRP concentrations of 0.09 mg l^{-1} (1a), 0.16 mg l^{-1} (1b), 1.21 mg l^{-1} (1c), and 0.08 mg l^{-1} (1d). P loads of each variant were calculated by multiplying the annual LGD volumes of each of the 26 shoreline sub-sections (Q_i in Eq. 3.5) by the corresponding SRP concentrations and summing up all 26 P loads. In Scenario 2, SRP concentrations all four sites were included simultaneously. Annual LGD volumes of the 26 sub-sections were multiplied by the mean SRP concentration of the closest measurement site. Scenario 3 considered the large heterogeneity of the near-shore groundwater concentrations at the four sites. The actual variation of the SRP concentrations in the near-shore wells might be log-normal distributed. Thus, for this scenario we assumed that SRP concentrations in the LGD of the 26 segments are as well log-normal distributed and that the concentrations found in the four groundwater observation wells characterize the arithmetic mean and the standard deviation of the log-normal distribution sufficiently well. With Microsoft Excel, we calculated 250 data sets, each consisting of 26 random SRP concentrations, which were log-normal distributed with the same arithmetic mean. We furthermore restricted the standard deviation to a 37% smaller value compared to the original standard deviation in order to avoid excessively high SRP concentrations. Each of the 26 SRP concentrations was assigned to one of the 26 shoreline sub-sections and multiplied by the corresponding annual LGD volume. Summing up all 26 values resulted in the total annual groundwater-borne P load of that data set. Thus, we finally ended up with 250 different groundwater-borne P loads in Scenario 3.

3.1.3 Results

Delineation of subsurface catchment

Hydraulic head data of 33 groundwater observation wells in the surrounding of Lake Arendsee facilitated the delineation of its subsurface catchment. The size and shape of the catchment were derived from the resulting hydraulic head contour lines. The catchment covered an area of 15.2 km with a main expansion south- southeasterly of the lake (Fig. 3.4A). Dominating land use types were cropland and forest (35% each). The city of Arendsee, located directly at the southern shoreline, contributed with 14% and grassland with 18% to the area of the subsurface catchment (Table 3.1).

Hydraulic head contour lines indicated a northern groundwater flow direction, with a steep hydraulic gradient in the western part of the catchment in the vicinity of Lake Arendsee that flattened in eastern direction (Fig. 3.4A).

Table 3.1 Mean annual groundwater recharge rates (l m^{-2} yr^{-1}) of different land use types in the subsurface catchment of Lake Arendsee, calculated according to Glugla et al. (2003).

	Area (km^2)	Groundwater recharge rate (l m^{-2} yr^{-1})
Forest	5.3	45
Cropland	5.3	130
Grassland	2.4	102
Urban area	2.2	189

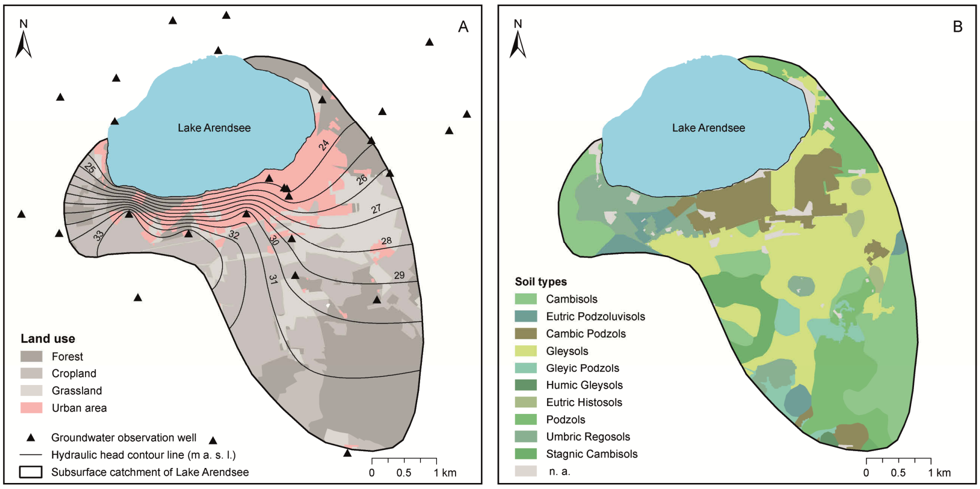

Figure 3.4 Dominating land use types and hydraulic head contour lines (in m above sea level, narrow black lines) in the subsurface catchment of Lake Arendsee (bold black line), derived from hydraulic head measurements of observation wells (black triangles) in July 2012 (A). Soil types in the catchment of Lake Arendsee (B).

Annual groundwater recharge and calculated drainage

Combinations of soil types and land uses in the subsurface catchment (Fig. 3.4A and B) resulted in 51 sub-areas for which groundwater recharge was individually calculated. Four land use types were included, as there are coniferous forest, cropland, grassland, and urban areas. Groundwater recharge rates were lowest in forested areas and highest in the urban area (Table 3.1). Croplands and grasslands differed in annual groundwater recharge rates (130 and 102 l m^{-2} yr^{-1}, respectively), while the calculation of drainage from drainage intensity classes resulted in similar values for absolute volumes (0.37 and 0.39 Mm^3 yr^{-1}, respectively, Fig. 3.5). Taking the land use in the catchment into account, croplands contributed most to the LGD volume of Lake Arendsee (0.69 Mm^3 yr^{-1}) followed by urban areas, mainly represented by the city of Arendsee (0.41 Mm^3 yr^{-1}), grasslands and forests (0.25 and 0.24 Mm^3 yr^{-1}, respectively) (Fig. 3.5). Accordingly, 1.27 Mm^3 entered Arendsee as total groundwater discharge per year (after having subtracted 0.32 Mm^3 for drinking water supply), while calculated drainage water extractions summed up to for 0.76 Mm^3 yr^{-1}.

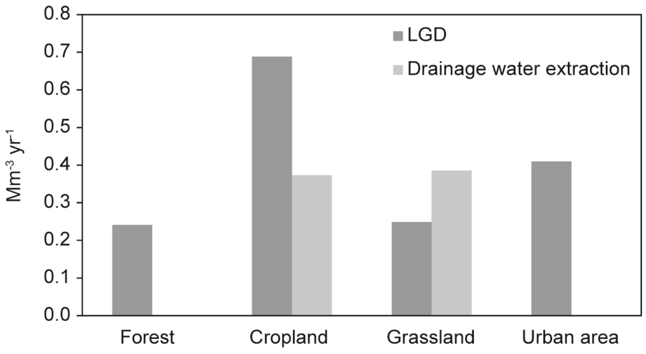

Figure 3.5 Volumes of drainage water extracted from agricultural areas and land use dependent mean annual contribution to lacustrine groundwater discharge (LGD) (Mm^3 yr^{-1}) derived from groundwater recharge calculations for the subsurface catchment according to Glugla et al. (2003).

Measured drainage from agriculture

The one-year-period of drainage water measurements at the inflows of the drainage ditches to Lake Arendsee resulted in an overall drainage volume of 1.54 Mm^3. This exceeds the calculated mean annual drainage water extraction (0.76 Mm^3), and can be attributed to an above-average amount of precipitation during the year of that study. While mean annual precipitation sums up to 593 $l\ m^{-2}$ (1976–2007), this value was 746 $l\ m^{-2}$ in the measurement period from August 2010 until the end of July 2011. Measured drainage at the inflows to the lake accounted for 13.7% of precipitation, while a value of 8.4% of $\overline{P_{korr}}$ was calculated to discharge as drainage water from agricultural areas.

Spatial patterns of LGD

In many cases, the four measurements along one transect revealed a decrease of LGD with increasing distance to the shoreline. This decline occurred independently of flux intensities although sites with generally high LGD rates still showed high rates at large distances to the shoreline (Fig. 3.6) while sites with less intense LGD often did not reveal any LGD at these distances any more. We found maximum LGD rates in the central reach of the southern shoreline while in eastern and western directions, LGD was generally lower (Fig. 7). Also within the central part of the southern shoreline variation of LGD rates occurred: The maximum LGD rate was 122 $l\ m^{-2}\ d^{-1}$, while adjacent LGD rates in this section varied between 60 and 108 $l\ m^{-2}\ d^{-1}$. In western direction LGD rates decreased with one exception in a little bay at the south-western shoreline where LGD was much higher than at neighboring sites. A slight increase of LGD is also found along the eastern shoreline, although the subsurface catchment had a small extension in that area.

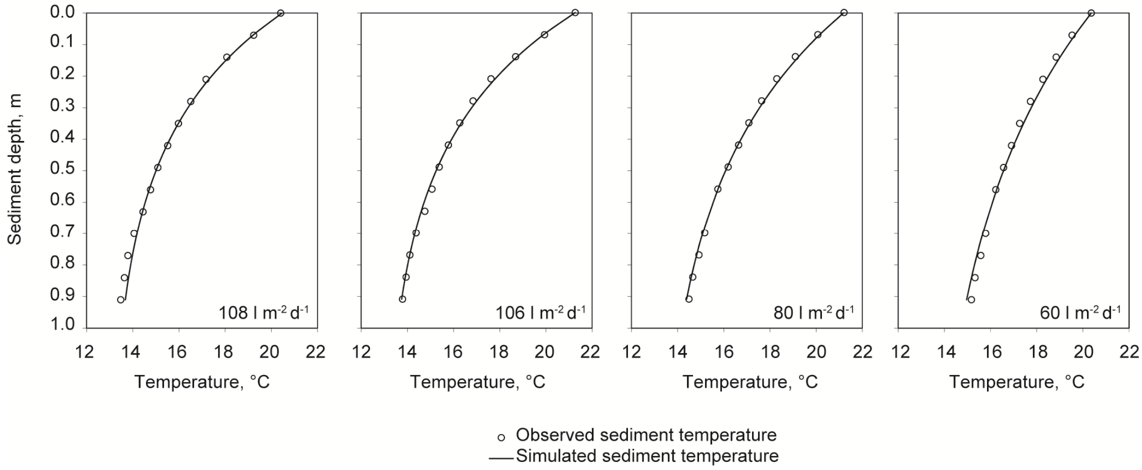

Figure 3.6 Profiles of lake bed temperatures and resulting LGD rates in different distances to shoreline (0.5, 1.0, 2.0, and 4.0 m from left to right).

Shoreline sub-section LGD amounts

The 26 shoreline sub-sections had a mean length of 196 m, with a maximum of 245 m and a minimum of 113 m. This results from different distances between single transects of lake bed temperature profiles due to restricted accessibility of the shoreline in some cases. Main LGD occurred within a section of 2.19 km at the southern shoreline, where an amount 0.69 $Mm^3\ yr^{-1}$ of LGD is calculated. This equaled an amount of 54% of the total LGD entering the lake along 36% of the shoreline bordering on the subsurface catchment and 24% of the total shoreline. Results normalized to 200 m shoreline sub-sections ranged between 0.004 and 0.093 $Mm^3\ yr^{-1}$.

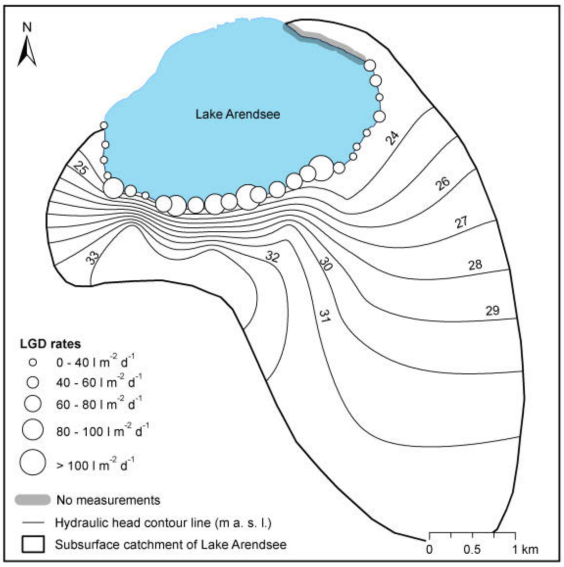

Figure 3.7 Maximum LGD rates (l m^{-2} d^{-1}) derived from transects of four sediment temperature depth profiles at each observation site in Lake Arendsee. A 900 m-reach along the north-eastern shoreline (shaded in grey) was not accessible and thus excluded from sediment temperature measurements. Narrow black lines represent hydraulic head contour lines (in m above sea level) in the subsurface catchment (bold black line).

Groundwater-borne phosphorus loads

Based on the results for annual LGD in sub-sections of the shoreline, groundwater-borne P loads were calculated for three different scenarios. P loads in the scenario-variants 1a, b and d (based on the same single groundwater SRP concentration for all shoreline sub-sections), range between 81 and 170 kg P yr^{-1}. For variant 1c the calculated P load is about ten times higher (1307 kg P yr^{-1}, Table 3.2).

Table 3.2 Means and coefficients of variance (CV) for the three different scenarios used for P load calculations. Results for sub-sectional P loads are normalized to a P load entering the lake along one meter of shoreline per year (kg m^{-1} yr^{-1}). Concentrations used for Scenarios 1a to 1d are mean SRP concentrations of one of the four near-shore groundwater (GW) observation sites that are also used as SRP concentrations in Scenario 2 but are allocated to different sub-sections in that scenario. Scenario 3 uses random distributions of SRP concentrations based on the arithmetic mean and standard deviation of the four measured SRP concentrations.

	Scenario 1a (0.09 mg l^{-1})	Scenario 1b (0.16 mg l^{-1})	Scenario 1c (1.21 mg l^{-1})	Scenario 1d (0.08 mg l^{-1})	Scenario 2	Scenario 3
Corresponding GW observation site in Fig. 3.1	1	2	3	4	1-4	-
n (different P concentrations of LGD)	1	1	1	1	4	26 · 250
n (different P loads of shoreline sub-sections)	26	26	26	26	26	26 · 250
Mean P load of shoreline sub-sections (kg P m^{-1} yr^{-1})	0.02	0.033	0.255	0.016	0.081	0.079
CV	0.581	0.581	0.581	0.581	1.650	1.222
Total P load (kg P yr^{-1})	102	170	1307	81	425	212–891

Scenario 2, in which the SRP concentrations of the four observation sites along the shoreline are considered, results in an annual P load of 425 kg P yr^{-1}. Scenario 3 was calculated for 250 variants resulting in total annual P loads of 212–891 kg P yr^{-1}. Mean P loads of shoreline segments (normalized to P load discharging along one meter of shoreline per year, kg m^{-1} yr^{-1}), and mean total P load (not shown) are similar to those of Scenario 2 since the data set was created based on this similarity. The maximum out of 26 · 250 SRP concentrations was 3.71 mg l^{-1}. This seems to be quite high but measurements of near-shore groundwater close to the surface (unpublished data) revealed SRP concentrations of >4 mg l^{-1}. Thus, a value of 3.71 mg l^{-1} is adequate to represent maximum groundwater SRP concentrations. Coefficients of variance were the same for all variants in Scenario 1 since LGD was the only variation between sub-sections while concentrations were the same in all of them. In contrast, coefficients of variance were clearly increased in Scenarios 2 and 3 to a value of >1. The impact of LGD on P loads is demonstrated by the comparison of P concentrations and resulting P loads in Scenario 3 (Fig. 3.8). It becomes obvious that P loads can be low although the corresponding P concentration is high and vice versa. For example, the two maximum SRP concentrations generated in Scenario 3 (3.69 and 3.71 mg l^{-1}) resulted in strongly differing sub-section P loads (1.07 and 0.078 kg m^{-1} yr^{-1}, respectively) because of different LGD rates.

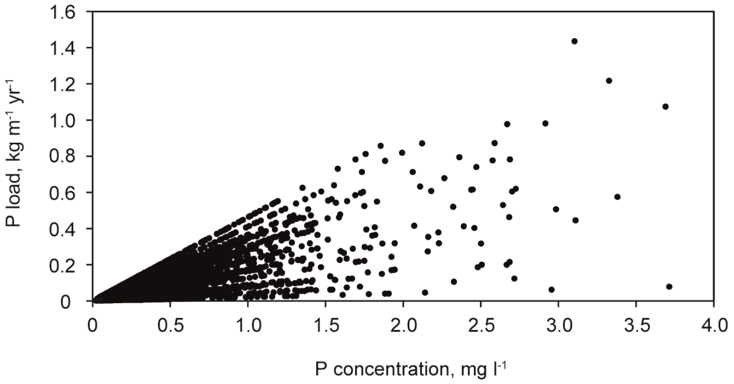

Figure 3.8 Random P concentrations (mg SRP l^{-1}) for shoreline sub-sections and resulting sub-sectional groundwater P loads calculated for Scenario 3. For comparability P loads are normalized to P entering the lake along one meter of shoreline during a one-year-period (kg P m^{-1} yr^{-1}).

3.1.4 Discussion

Groundwater recharge

By calculating groundwater recharge according to Glugla et al. (2003) based on the available data on land use and soil parameters, the estimated groundwater recharge rates are reliable with a high spatial resolution. Although the method is based on data for Germany, comparable approaches should be available for any region of interest, at least in humid climates. However, problems may arise in many regions due to a lack of data concerning artificial reduction of groundwater recharge. For example, as mentioned in the result section, an amount of 0.32 Mm^3 of groundwater is annually extracted from the aquifer for drinking water supply. Another ubiquitous reduction of groundwater recharge is the drainage of agricultural areas for melioration. In the present study, 35% of the total discharge ($\bar{R}$ in Eq. 3.2) from croplands was calculated to be drainage water (section 2.3), while this value even exceeds 60% below grasslands (Fig. 3.5). Mathematically, these drainage efforts lead to a reduction of the actual groundwater recharge by 32% compared to original (natural) conditions. This highlights the enormous impact of drainage for water balances of mainly agricultural catchments. Nevertheless, quantitative information on drainage of agricultural plains might be hardly available and of limited reliability. Depending on the context, this might restrict the validity of groundwater recharge calculations. In the present case, fortunately, data on drainage intensities were available and additionally confirmed by actually measured drainage volumes. Measured results were even higher than calculated, which underlines the importance of drainage extractions for actual groundwater recharge in agricultural areas. However, the drainage portions of 13.7% (measured) and 8.4% (calculated) of ($\overline{P_{korr}}$) confirm the general results of the groundwater recharge calculations, since the reference period experienced an amount of precipitation that was 25% larger than the mean annual precipitation. This probably led to a corresponding increase of drainage.

Although the urban area covers a relatively small portion of the subsurface catchment (Table 3.1) it contributes the second largest portion to the total LGD volume (Fig. 3.5). Considered as grassland without drainage water extraction, groundwater recharge exceeds rates calculated for agricultural grasslands by far although 30% of the urban area is sealed and thus inactive regarding groundwater recharge.

LGD patterns and P loads

A total of 33 groundwater observation wells is a fairly good basis for an overview of the hydraulic characteristics of a subsurface catchment of this size. With these data, it is possible to determine the spatial extent of the subsurface catchment with a high degree of accuracy. Furthermore, the hydraulic head contour lines that are interpolated from the groundwater head data reveal general groundwater flow directions that confirmed the assumption of main LGD in the southern part of the shoreline (Fig. 3.7). However, they do not represent actual small scale heterogeneity of LGD at the shoreline at all. Changes in geologic composition of the aquifer material close to the lake are expected to cause substantial heterogeneity in LGD. For example, coarse material embedded in less permeable sediments may cause preferential flow paths, resulting in significantly higher, but spatially isolated LGD rates (Krabbenhoft and Anderson 1986). This might be the reason for the above mentioned single site in the south-western part of the shoreline showing a relatively high LGD rate. Another reason for increased LGD at that site might be its location in an embayment. LGD in bays is commonly larger since flow paths originating from different directions are focused in these locations (Cherkauer and McKereghan 1991). Measured LGD rates at the eastern shore (public sand beach) are surprisingly high and in no agreement with the size of the catchment or the surface topography. We assume that the high rates are caused by lake water recirculation. Sea water recirculation is well known for submarine groundwater discharge (SGD; Taniguchi et al. 2002). Due to the intense wave activity at the eastern shore lake water might recirculate at this shore. However, to the best of our knowledge such a process has never been reported for lacustrine settings.

Anthropogenic alteration of the shoreline might additionally affect the LGD patterns. For example, shoreline stabilization might inhibit LGD. Vegetation growth along the shoreline might cause a decrease of LGD since vegetation usually results in an accumulation of fine sediments, thus a lower hydraulic conductivity and emersed vegetation might even result in a transpiration of subsurface water prior to its discharge into the lake.

Compared to what was expected based on hydraulic head contour lines, sediment temperature profiles revealed that the shoreline section of main LGD is shifted eastwards by several hundreds of meters. Furthermore, using heat as a tracer showed an intense variety of LGD rates on the medium-scale. This variety occurred even within the limited section in the south of the lake where LGD was largest (60–122 $\mathrm{l\ m^{-2}\ d^{-1}}$). It should be noted that studies on small-scale heterogeneity of groundwater–surface water interaction revealed a spatial variability that is beyond the scale of the present study (e.g., Kishel and Gerla, 2002). But these small-scale heterogeneities are likely superimposed by the medium-scale local groundwater flow regime. A higher measurement resolution of lake bed temperatures would have certainly resulted in a finer pattern of LGD rates in the present study. However, it is doubtful whether that increase of accuracy is worth the substantial effort of further field measurements. By upscaling the results to shoreline sub-sections with a length of approximately 200 m we generally improved the qualitative and quantitative description of LGD volumes and groundwater-borne P loads to a large extent compared to integrating approaches. For the determination of P loads the knowledge of both, spatial patterns of LGD and SRP concentrations is essential. This is illustrated by the three different scenarios of P load determination (Table 3.2). In Scenario 1, P loads of all 26 shoreline sections are based on the SRP concentration of a single groundwater observation site. Consequently, P loads vary in the same range as sub-sectional LGD volumes do and the section of intense P loads is consistent with major LGD all along the southern shoreline (Fig. 3.7). In these cases, the spatial pattern of LGD controls the P input to the lake. With heterogeneous SRP concentrations in the discharging groundwater a stronger variation in sub-sectional P loads occurs. In the case of Scenario 2, the actually measured SRP concentrations at four different sites imply a main P load in a relatively short section at the south-southeastern shoreline around Site 3 in Figure 3.1. Both, LGD and the SRP concentration are high in that area. In other sub-sections P loads are low although LGD is relatively high. This heterogeneity of P loads induced by SRP concentration is also represented by a much higher coefficient of variation (Table 3.2). However, P loads in Scenario 3 range from 212 to 891 kg yr^{-1} which demonstrates the influence of spatial LGD patterns on groundwater-borne nutrient loads, especially in combination with heterogeneous nutrient concentrations.

If high variability of nutrient concentrations occur or are expected, spatial patterns of LGD should be carefully considered: Scenario 2 results in an overall P load of 425 kg yr^{-1}. Without considering the results of lake bed temperature measurements as a weighting factor for spatial LGD patterns, the calculation of the P load yielded only 327 kg yr^{-1}. This deviation of approximately 25% might still be acceptable compared to uncertainties of other input paths in the P balance of the lake. However, the relatively good agreement of the calculation with and without weighting factor is based on the fact that that the zones of major LGD volumes and highest groundwater SRP concentrations coincidence in the present case study. As illustrated by Scenario 3 total P loads can broadly vary because of this dependency of P loads on both LGD volumes and SRP concentrations (Table 3.2).

Furthermore, not only actual values for nutrient loads but also the localization of their sources might be of interest. LGD patterns help to find hot spots or sections of intense nutrient exfiltration along the shoreline. Tracking back groundwater flow directions from there might help to identify contaminated sites. Another reason for taking LGD patterns into account is the planning of effective *in situ*-restoration measures.

However, uncertainties in LGD pattern identification might arise from improper estimation of boundary conditions in the procedure of solving the heat transport equation (Equations 3.3 and 3.4). As described above, groundwater temperatures might vary in time, as well as in horizontal and lateral space. The approach is designed for assumed 1-D vertical fluxes only, although actual groundwater flow lines would describe a mixture of both, vertical and lateral fluxes (Rosenberry and LaBaugh 2008). In the present case relatively high temperatures for the lower boundary condition L indicate a rather lateral inflow of near-surface (and thus warmer) groundwater. This issue is especially discussed by (Ferguson and Bense 2011). Further uncertainty might be introduced by the term of thermal conductivity (K_{fs}). This value is commonly estimated from literature, since its empirical determination is elaborate, especially under heterogeneous sediment conditions. In general, values for K_{fs} in saturated sediments vary only little (between 1.4 J s^{-1} m^{-1} K^{-1} for clayey and 2.2 J s^{-1} m^{-1} K^{-1} for sandy sediments, as shown in Stonestrom and Constantz, 2003). Nevertheless, this might be an important factor if absolute LGD rates are required, since resulting exfiltration rates change by the degree of changes in K_{fs}. If, as in this study, resulting LGD rates are not processed as absolute results, but used as a measure for exfiltration intensity, this issue is reduced. Many critiques for using heat as a tracer for groundwater–surface water interactions deal with different aspects of diverse boundary conditions (Ferguson and Bense 2011; Kalbus et al. 2006; Schmidt et al. 2007).

3.1.5 Conclusion

Calculating groundwater recharge in the catchment to determine the groundwater component in the water balance of a lake is no new approach. However, special care is required when the water balance serves as a prerequisite of the nutrient budget. As shown in the present study, it might be insufficient to multiply the total annual LGD volume with the mean groundwater nutrient concentration to determine the absolute nutrient load. Spatial heterogeneities of groundwater quality and LGD need to be considered carefully for reliable quantifications of groundwater-borne nutrient loads. Unfortunately, an adequate number of groundwater observation wells or other possibilities to capture heterogeneities in nutrient concentrations are often not available. Thus, the nutrient concentrations finally applied to the setup of the budget underlie some uncertainty. If the total LGD volume is imprecise, a factor of uncertainty is imposed on the nutrient budget. If additionally fine-scaled spatial patterns of LGD are unconsidered, further uncertainty is introduced. Accordingly, the groundwater impact on the lake´s ecosystem might be severely over- or underestimated. As a consequence, this might even lead to a failure of restoration efforts, if measures are based on insufficient nutrient budgets. The presented approach of combining total groundwater recharge volumes and LGD patterns drastically reduces the uncertainty of the groundwater component in the nutrient balance of Lake Arendsee. Uncertainties of temperature based LGD rates are minimized by reducing their role to a weighting factor (instead of using absolute values) for groundwater recharge calculations. Different scenarios proved the great importance of spatial LGD patterns for groundwater-borne nutrient loads.

3.1.6 References

Anderson, M.P., 2005. Heat as a Ground Water Tracer. *Ground Water*, 43(6): 951-968.

Bagrov, N.A., 1953. O srednem mnogoletnem ísparenii s poverchnosti suši (On the mean long-term evaporation rates from the continental surface, in Russian). *Meteorologia i Gidrologia*, 10: 10-20.

Bredehoeft, J.D., Papadopulos, I.S., 1965. Rates of vertical groundwater movement estimated from the Earth's thermal profile. *Water Resources Research*, 1(2): 325-328.

Bremer, J.E., Harter, T., 2012. Domestic wells have high probability of pumping septic tank leachate. *Hydrology and Earth System Sciences*, 16(8): 2453-2467.

BÜK, 1998. Soil Map of the Federal Republic of Germany 1:1,000,000 (Bodenübersichtskarte 1000). In: Resources, F.I.f.G.a.N. (Ed.), Berlin.

Cherkauer, D.S., McKereghan, P.F., 1991. Groundwater discharge to lakes - focusing in embayments. *Ground Water*, 29(1): 72-80.

Constantz, J., 2008. Heat as a tracer to determine streambed water exchanges. *Water Resources Research*, 44.

Ferguson, G., Bense, V., 2011. Uncertainty in 1D Heat-Flow Analysis to Estimate Groundwater Discharge to a Stream. *Ground Water*, 49(3): 336-347.

Gelbrecht, J., Lengsfeld, H., Pöthig, R., Opitz, D., 2005. Temporal and spatial variation of phosphorus input, retention and loss in a small catchment of NE Germany. *Journal of Hydrology*, 304(1–4): 151-165.

Glugla, G., Jankiewicz, P., Rachimow, C., Lojek, K., Richter, K., Fürtig, G., Krahe, P., 2003. Wasserhaushaltsverfahren zur Berechnung vieljähriger Mittelwerte der tatsächlichen Verdunstung und des Gesamtabflusses (Hydrological balance model to determine regional annual evapotranspiration losses and runoff rates under different climatic conditions, in German). *BfG-Report* 1342: 118 p.

Hupfer, M., Lewandowski, J., 2005. Retention and early diagenetic transformation of phosphorus in Lake Arendsee (Germany) - consequences for management strategies. *Archiv fuer Hydrobiologie*, 164(2): 143-167.

Kalbus, E., Reinstorf, F., Schirmer, M., 2006. Measuring methods for groundwater - surface water interactions: a review. *Hydrology and Earth System Sciences*, 10(6): 873-887.

Katz, B.G., Eberts, S.M., Kauffman, L.J., 2011. Using Cl/Br ratios and other indicators to assess potential impacts on groundwater quality from septic systems: A review and examples from principal aquifers in the United States. *Journal of Hydrology*, 397(3-4): 151-166.

Kishel, H.F., Gerla, P.J., 2002. Characteristics of preferential flow and groundwater discharge to Shingobee Lake, Minnesota, USA. *Hydrological Processes*, 16(10): 1921-1934.

Krabbenhoft, D.P., Anderson, M.P., 1986. Use of a numerical groundwater-flow model for hypothesis-testing. *Ground Water*, 24(1): 49-55.

McBride, M.S., Pfannkuch, H.O., 1975. Distribution of seepage within lakebeds. *Journal of Research of the Us Geological Survey*, 3(5): 505-512.

Meyboom, P., 1967. Mass-transfer studies to determine the groundwater regime of permanent lakes in hummocky moraine of Western Canada. *Journal of Hydrology*, 5(0): 117-142.

Moss, B., 2012. Cogs in the endless machine: Lakes, climate change and nutrient cycles: A review. *Science of The Total Environment*, 434(0): 130-142.

Ptacek, C.J., 1998. Geochemistry of a septic-system plume in a coastal barrier bar, Point Pelee, Ontario, Canada. *Journal of Contaminant Hydrology*, 33(3-4): 293-312.

Robertson, W.D., 2008. Irreversible phosphorus sorption in septic system plumes? *Ground Water*, 46(1): 51-60.

Rosenberry, D.O., LaBaugh, J.W., 2008. *Field Techniques for Estimating Water Fluxes Between Surface Water and Ground Water*.

Scanlon, B.R., Healy, R.W., Cook, P.G., 2002. Choosing appropriate techniques for quantifying groundwater recharge. *Hydrogeology Journal*, 10(1): 18-39.

Schmidt, C., Bayer-Raich, M., Schirmer, M., 2006. Characterization of spatial heterogeneity of groundwater-stream water interactions using multiple depth streambed temperature measurements at the reach scale. *Hydrology and Earth System Sciences*, 10(6): 849-859.

Schmidt, C., Conant Jr, B., Bayer-Raich, M., Schirmer, M., 2007. Evaluation and field-scale application of an analytical method to quantify groundwater discharge using mapped streambed temperatures. *Journal of Hydrology*, 347(3–4): 292-307.

Stonestrom, D.A., Constantz, J., 2003. Heat as a tool for studying the movement of ground water near streams. *Circular* 1260: 105 p.

Taniguchi, M., Burnett, W.C., Cable, J.E., Turner, J.V., 2002. Investigation of submarine groundwater discharge. *Hydrological Processes*, 16(11): 2115-2129.

Winter, T.C., 1999. Relation of streams, lakes, and wetlands to groundwater flow systems. *Hydrogeology Journal*, 7(1): 28-45.

3.2 Phosphorus in lacustrine groundwater discharge – a potential source for lake eutrophication

Karin Meinikmann[1,2], Michael Hupfer[3], Jörg Lewandowski[1,2]

[1] Department of Ecohydrology, Leibniz-Institute of Freshwater Ecology and Inland Fisheries, Berlin, Germany

[2] Geography Department, Humboldt-Universität zu Berlin, Berlin, Germany

[3] Department of Chemical Analytics and Biogeochemistry, Leibniz-Institute of Freshwater Ecology and Inland Fisheries, Berlin, Germany

This is the peer reviewed version of the following article:
Meinikmann, K., Hupfer, M., Lewandowski, J., 2015. Phosphorus in groundwater discharge – A potential source for lake eutrophication. *Journal of Hydrology*, 524(0): 214-226. DOI: 10.1016/j.jhydrol.2015.02.031.

Abstract

Lake eutrophication has long been mainly associated with phosphorus (P) inputs from overland flow. The present study gives evidence that also groundwater can carry significant loads of dissolved P. We quantified P loads from groundwater to Lake Arendsee using near-shore measurements of P concentrations at a high spatial resolution and volume fluxes of lacustrine groundwater discharge (LGD) derived from a previous study. Results show that LGD accounts for more than 50% of the overall external P load, thus fuelling the eutrophication of the lake. Several different approaches of groundwater sampling (groundwater observation wells, temporary piezometers, and domestic wells) reveal a broad spatial heterogeneity of P concentrations in the subsurface catchment of the lake. The highest P concentrations (above 4 mg l^{-1}) were found below a settled area along the southern lake shore. Contrary to expectations, other parameters (dissolved iron, ammonium, etc.) were not correlated with P, indicating that natural processes are superimposed by heavy contaminations. Both the intensity of the contamination and its proximity to the lake inhibit nutrient retention within vadose zone and aquifer and allow significant P loads to be discharged into the lake. Although the groundwater quality was investigated intensely, the results eventually give no clear evidence of the location and sources of the pollution. As a consequence, measures to decrease LGD-derived P loads cannot target the contamination at its source in the catchment. They need to be implemented in the riparian area to eliminate groundwater P directly before it enters the lake.

3.2.1 Introduction

Phosphorus (P) overloads are still a major threat to lake ecosystems worldwide. As a limiting nutrient P often controls the trophic state of temperate freshwater systems (Heathwaite et al. 2005; Sondergaard and Jeppesen 2007). After the significant reduction of P from point sources to improve freshwater quality it became more and more obvious that diffuse transport of P also has a critical ecological relevance. Nowadays, many studies claim agriculture is the main source of diffuse P in freshwater systems (Heathwaite et al. 2005; Orderud and Vogt 2013; Withers and Haygarth 2007), especially since sewage discharges from point sources have been eliminated to a large extent (Orderud and Vogt 2013). Depending on site conditions (i.e., inclination, sediment retention capacity, etc.) diffuse P transport occurs as particulate or dissolved P in overland flow, channelized surface runoff, drainage, or groundwater. In groundwater natural dissolved P concentrations are usually low, since potentially mobile P (i.e., in general orthophosphate) is adsorbed in the soil and sediment matrix either in the vadose or the saturated zone. As a consequence groundwater was evaluated to be of “low source strength” by Edwards and Withers (2007). However, it needs to be accepted that dissolved P concentrations can increase largely above natural background conditions in groundwater. Interestingly, studies have again found wastewater to cause heavy groundwater P contaminations (McCobb et al. 2003; Ptacek 1998; Robertson 2008; Roy et al. 2009), although this was considered to be eliminated as a nutrient source with the reduction of point sources. However, especially among practitioners it still is a common paradigm that P is completely immobile in groundwater. This might also be supported by a generally low data basis on this issue. Since P is non-hazardous for human health it is often not regularly monitored, neither in drinking water nor in groundwater. This is one of the reasons why lacustrine groundwater discharge (LGD) is often dismissed as a major source of external P inputs to lakes. In recent years the awareness of groundwater P is growing and it is becoming more and more accepted that groundwater can indeed have P concentrations exceeding thresholds of ecological relevance (e.g., Burkart et al. 2004; Holman et al. 2010; Kidmose et al. 2013).

Studies on groundwater P often deal with the determination of P concentrations on the catchment scale in order to determine natural background concentrations and to separate them from contamination-derived concentrations. Based on these findings thresholds are raised and discussed for groundwater discharging into surface waters (Burkart et al. 2004; Lewandowski et al. 2015). So far only a few studies tried to actually quantify groundwater-borne P loads to lakes and rivers and to evaluate the impact on their trophic state (Ala-aho et al. 2013; Jarosiewicz and Witek 2014; McCobb et al. 2003; Ouyang 2012; Shaw et al. 1990). However, the quantification of LGD-derived P loads is difficult. Usually LGD volume fluxes and nutrient concentrations are determined separately and are subsequently multiplied. Both, hydrological (i.e., LGD volume fluxes) and geochemical (i.e., nutrient concentrations) factors may be affected by spatial and temporal heterogeneities, which impede the empirical determination of representative values. Simplification and upscaling of point measurements are often necessary to approximate nutrient loads. In many studies the groundwater path is simply considered as the residual in budget calculations (Rosenberry et al. 2015) or even is completely neglected.

With the present study we aim to provoke an intensified discussion on the potentially harmful contribution of groundwater to lake nutrient budgets and to demonstrate that groundwater P can fuel eutrophication of lakes. The study site is Lake Arendsee in Northern Germany where the mean total phosphorus (TP) concentrations in the lake water showed a gradual increase in the past decades to more than 150 μg l^{-1}. First investigations indicated a large spatial variability of near-shore groundwater P concentrations, with concentrations of soluble reactive P (SRP) higher than 1000 μg l^{-1} at one site. These results enforced the effort to better understand and quantify LGD and its contribution to the nutrient budget of Lake Arendsee. As a first step towards the determination of groundwater-borne P loads detailed investigations on LGD volume fluxes and patterns were conducted (Lewandowski et al. 2013; Meinikmann et al. 2013). To incorporate spatial heterogeneity of LGD, the shoreline was subdivided into sections of about 200 m length, for which individual volume fluxes of LGD were calculated. Based on these results P loads were calculated by applying P concentrations of four near-shore groundwater observation wells (sites 1–4 in Fig. 3.9). This resulted in a groundwater-derived P load of 425 kg yr^{-1}. However, it was hypothesized that detailed spatial information on groundwater P concentrations increases the accuracy of P load calculations. The present study focuses on groundwater P concentrations as the second factor of groundwater-borne P loads (volume fluxes x concentration) to Lake Arendsee. We hereby aim to (1) localize crucial areas for P input by detailed measurements of P concentrations in near-shore groundwater, (2) calculate LGD-derived P loads and evaluate them within the context of overall P inputs to the lake, as well as (3) localize the origin of the P contamination in the catchment of the lake.

3.2.2 Methods

Study site

Lake Arendsee in Northern Germany is 5.14 km^2 in size. As already described in previous studies (e.g., Hupfer and Lewandowski 2005; Meinikmann et al. 2013) it is a deep stratified lake (max. depth 49 m, mean depth 29 m) which was originally solely groundwater-fed. Currently, four ditches draining adjacent agricultural fields discharge into the lake and an artificial runoff channel transports water out of the lake (Fig. 3.9). Since the middle of the last century the lake is eutrophied. The annual mean TP concentration from 2009 to 2013 ranged between 179 and 199 μg l^{-1} resulting in mass developments of phytoplankton dominated by cyanobacteria. Due to its morphometric characteristics the lake has a large volume (147 Mm^3) resulting in a water residence time of 50–60 years. Accordingly the lake reacts with significant delay to changes of external nutrient loads.

In March 2010 two to three groundwater observation wells with screens in different depths were installed at four different sites along the southern shoreline, where most of the LGD was expected to occur (Fig. 3.9). Groundwater sampling revealed a contamination with SRP, especially at site 3, where the shallower well had a mean SRP concentration of 1210 μg l^{-1} (Meinikmann et al. 2013). The subsurface catchment mainly expands south of the lake. Surface inclination is generally low in the catchment. However, a steep slope of up to 6 m can be found at the north-western shoreline. Groundwater exfiltration occurs along the western, southern, and (north-) eastern shoreline, while lake water infiltration into the aquifer primarily takes place at the northern and northwestern shoreline (Fig. 3.9). Hydraulic head contour lines indicate generally northern groundwater flow directions, with main LGD occurring along the southern shoreline. LGD rates derived from point measurements of sediment temperatures confirmed these findings, but revealed significant heterogeneity at the medium scale of the shoreline segments (Fig. 3.9, Meinikmann et al. 2013). Aquifer sediments are dominated by Saalian and Elstarian substrates above Miocene sands (Fig. 3.10). Spatial information on hydraulic conductivity is scarce. It is assumed that within the geologic layers of relatively high values (3–6 10^{-4} m s^{-1}) lenses of significantly lower ones are frequent (Fig. 3.10), introducing some spatial heterogeneity in groundwater flow velocity and exfiltration on the medium scale (Fig. 3.9). The predominant land use type in the subsurface catchment is agriculture (pasture and croplands, 18% and 35%, respectively), followed by forestry (35%). Settled areas are focused on the city of Arendsee which is situated all along the southern, southeastern, and -western shoreline, and accounts for 14% of the subsurface catchment.

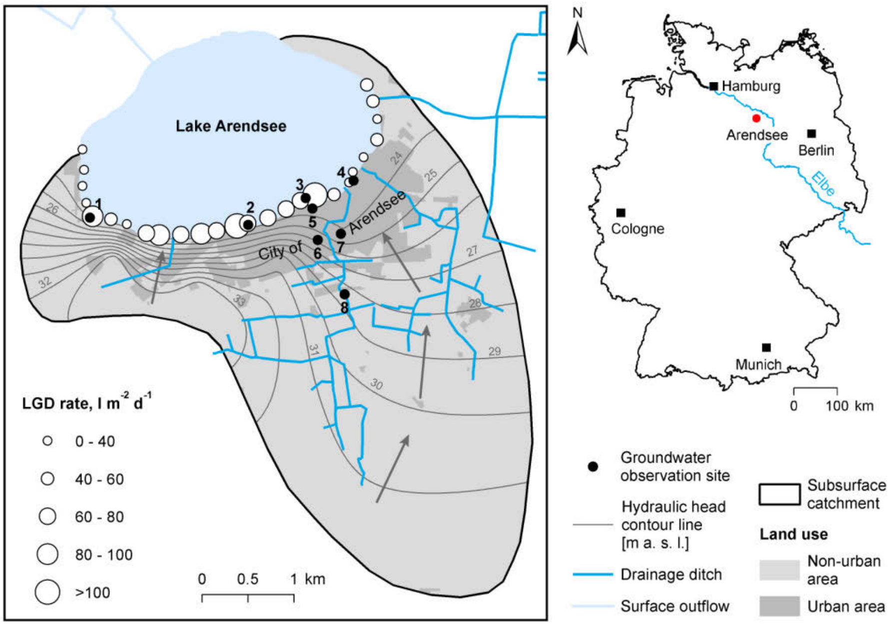

Figure 3.9 Subsurface catchment of Lake Arendsee including hydraulic head contour lines (m above sea level) and resulting groundwater flow directions (grey arrows). Black dots depict locations equipped with one, two, or three groundwater observation wells, respectively (see also Table 3.3). White circles represent rates of lacustrine groundwater discharge (LGD) determined from temperature measurements in the lake sediment (Meinikmann et al. 2013).

Near-shore groundwater quality

Groundwater observation wells. Due to the first results of high SRP concentrations at near-shore site 3 (Fig. 3.8), a monitoring program was setup to investigate temporal variations in groundwater chemistry at those shoreline sites. In order to track back the potential SRP plume, which enters the lake in the vicinity of site 3, seven additional wells were established at four different locations south of site 3 in November 2011. They represented the general groundwater flow direction, and covered the settled area of the city (sites 5–7) as well as the agricultural background (site 8, Fig. 3.9). While at site 7 one well was installed, at sites 5, 6, and 8 two wells had been built in different aquifer depths, respectively (Table 3.3). Groundwater observation wells at sites 1–4 (Fig. 3.9) were sampled monthly from April

2010 to April 2011 and bimonthly until October 2012. Monthly investigations at site 3 were continued. In 2012 SRP concentrations at sites 5–8 were measured monthly while afterwards the sampling frequency was reduced (see also Table 3.3). In the following sections, wells will be referred to as shallow, deep, or middle due to their position in the aquifer when compared to other wells at a specific site.

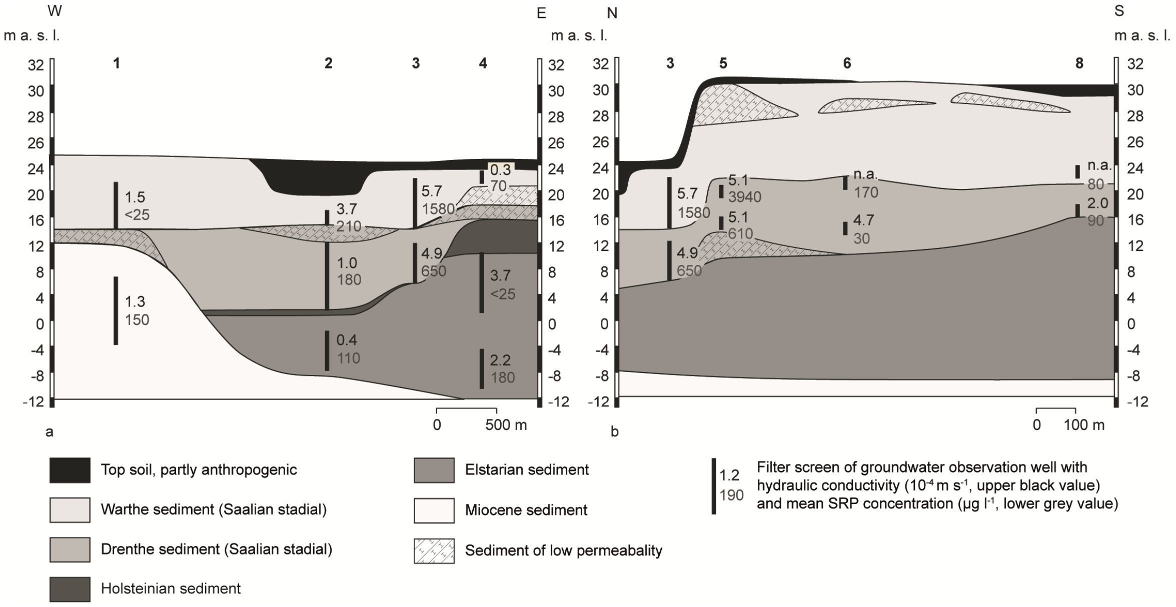

Figure 3.10 Geological cross-sections along the southern shore including groundwater observation sites 1–4 (a) and perpendicular to the southern shore including groundwater observation sites 3, 5, 6, and 8 in Figure 3.9. Mean SRP concentrations (grey values) result from regular investigations as documented in Table 3.3.

Temporary piezometers. To increase spatial information on SPR concentrations between the four near-shore groundwater observation sites, hand-drilled temporary piezometers were installed along a section of the shoreline where exfiltration occurred. With a drilling-set of Eijkelkamp Agrisearch Equipment boreholes (with a maximum depth of 2.5 m below ground surface) were drilled in close proximity to the shoreline. Then a 1-in.-diameter bottom-screened (20 cm filter length) polyethylene-pipe was put into the borehole. With a peristaltic pump groundwater was extracted until the water turbidity allowed its filtration with 0.45 lm syringe filters. This was usually the case after 10–30 min. The spatial distance between the boreholes was generally about 300 m, but spacing was decreased at sites with extraordinary high SRP concentrations. In some sections of the shoreline, manual drilling and/or groundwater pumping was not possible, either due to sediment characteristics (fine grained sediments with very low hydraulic conductivity) or inaccessibility of the shoreline (private property). In total, groundwater was sampled from 44 temporary boreholes.

LGD-derived P loads

The sub-section LGD volume fluxes presented in Meinikmann et al. (2013) were multiplied with the SRP concentrations derived from temporary piezometers to achieve SRP loads for single shoreline segments. In cases where more than one SRP concentration was available a weighted mean concentration based on the represented length of the shoreline section was calculated. Eventually, sub-sectional SRP loads were summed up to an overall LGD- derived SRP load.

Table 3.3 Characteristics of groundwater observation wells at sites 1-8 in Figure 3.9.

Site	ID	Max. depth of filter screen [m below surface]	Filter screen length [m]	Location of filter screen [m above sea level]	Investigation period	Number of measurements
1	1a	10.8	7	21.4 – 14.4	04/2010 – 12/2013	22
	1b	27.8	9.9	7.4 – -2.5		
2	2a	9.3	2	17.2 – 15.2	04/2010 – 12/2013	22
	2b	21.9	9.6	11.8 – 2.2		
	2c	31.1	6	-1.2 – -7.2		
3	3a	10	8	22.1 – 14.1	04/2010 – 12/2013	33
	3b	17.6	5.4	11.8 – 6.4		
4	4a	3.9	1.8	22.5 – 20.7	04/2010 – 12/2013	22
	4b	22.9	8.9	10.5 – 1.6		
	4c	34	5.8	-3.8 – - 9.6		
5	5a	12.2	2	20.6 – 18 .6	12/2011-12/2013	15
	5b	17.2	2	15.7 – 13.7		
6	6a	10.2	2	22.3 – 20.3	12/2011-12/2013	15
	6b	17.2	2	15.2 – 13.2		
7	7	15.8	2	15.5 – 13.5	12/2011-12/2013	15
8	8a	8.1	2	23.9 – 21.9	12/2011-12/2013	15
	8b	13.9	2	18.1 – 16.1		

Groundwater P concentrations in the catchment

To achieve an overview on groundwater quality in the catchment, as many groundwater samples as possible were included in the monitoring program. This was done to localize the source of groundwater pollution.

Groundwater observation wells

Overall, at 15 additional sites groundwater observation wells were available. At most of these sites only one well existed. However, at two sites two wells were available with screens in different aquifer depths. This resulted in a total of 17 groundwater observation wells. Most of these wells were sampled seven to nine times between September 2010 and December 2013. Due to access constraints some of them were only monitored four times or less.

Domestic wells

To further improve the overview on groundwater P concentrations in the catchment, the citizens of the catchment were asked to bring water from their private wells for chemical analyses. After a successful campaign in September 2011, this was repeated a second time in August 2012. At a central public location in the city of Arendsee citizens could get 250 ml-PE-bottles and a leaflet with instructions for the sampling procedure as well as questions regarding location and depth of the well. Participants were asked to discard at least 20 l of water before collecting the sample to avoid sampling of standing pipe water. Furthermore, participants were instructed to not leave a head space to prevent oxidation and precipitation. Afterwards, they were asked to store samples in refrigerators and return samples within 24 h.

Other sources of external P loads

To evaluate the relative importance of groundwater P for the trophic state of Lake Arendsee additional paths of P import were quantified:

Atmospheric deposition. To quantify P import by atmospheric deposition, which comprises wet and dry deposition, bulk samplers were installed. Between 2009 and 2012 sampling stations were located around the lake (up to six stations), at a landing stage at the lake shore (one station) and on the lake itself (up to four stations). Installation and sampling of the samplers were done following the recommendations of the German Working Group of the Federal States on Water (LAWA 1998). Sampling details are reported in (Lewandowski et al. 2011). Samples were collected monthly.

Water fowl. During the winter half-year different geese species and some other water fowl stay overnight on Lake Arendsee. Their numbers were counted 80 times from 1994 to 2010. Average numbers were multiplied by five months (duration of stay) and literature values for the P concentration of their excrements (Lewandowski et al. 2011).

Drainage from agricultural areas. Large parts of the agricultural subsurface catchment are drained by a ditch system, resulting in four drainage ditches discharging into the lake. For a one-year-period (August 2010 to July 2011), daily measurements of discharge and P concentrations were conducted to quantify P loads from agricultural drainage. As already described in Meinikmann et al. (2013) two of the ditches were equipped with V-weirs and pressure sensors recording water levels in 30 min-intervals. Discharge in a third ditch was determined with an ultrasonic flow measurement device. Three of the ditches drain parts of the subsurface catchment which is mainly characterized by agricultural land use. The fourth ditch drains a pasture which is situated to the west of the lake outside the subsurface catchment. Discharge here was also measured with a pressure sensor recording water levels in a 30 min-interval, which were translated into discharge via a water stage-discharge relation. SRP was measured from each single daily sample while total phosphorus (TP) was measured from samples that were mixed due to similar discharge rates and SRP values of several consecutive days. Daily (SR)P loads were calculated by multiplying the concentrations with 24 h-summed up discharge volumes for each drainage ditch.

Storm water discharge into the lake. Wastewater is mostly collected and treated in a centralized wastewater treatment plant outside of the lake's catchment. However, during heavy rainfalls storm water overflow is discharged into the lake. Discharge was measured with an ultrasonic flow measurement device and, in case of an overflow event, samples were taken for SRP and TP analysis. Additionally rainwater discharge is considered, although only 1.7 ha of paved area is directly discharging into the lake (data provided from public authorities).

Overland flow. There is no significant inclination in the catchment of Lake Arendsee. Thus overland flow was expected to be low. However, P load from overland flow was modelled based on the ABAG approach, which represents an adaption to the USLE (universal soil loss equation, Wischmeier and Smith 1965) to German conditions (Gebel et al. 2010).

Bathers. According to a study by Schulz (1981) bathers introduce 94 mg P per person and day into a lake. Based on this value and current numbers of bathing tourists at the lake P inputs were calculated.

Evaluation of external P loads estimations by mass balance

External P loads (P_{load}) equal the sum of P retention in the lake sediment (P_{sed}), P export from the lake by surface and groundwater outflow (P_{exp}), and changes in P inventory of the lake water (ΔP_{lake}):

$$P_{load} = P_{sed} + P_{exp} + \Delta P_{lake} \qquad \text{Eq. 3.7}$$

This equation was used to validate external P load determinations described above. Hupfer and Lewandowski (2005) calculated P_{sed} from dated sediment cores taken at different water depths and referred it to the lake area deeper than 30 m (3.0 km^2).

P_{exp} was estimated based on mean epilimnic P concentrations from 1993 until 2013. However, since no hydrological data were available for surface and groundwater outflow from the lake (Q_{out}) this term was calculated from the lake's water balance:

$$Q_{out} = Q_{in} - E_{lake} \qquad \text{Eq. 3.8}$$

Water inflow to the lake (Q_{in}) is the sum of all hydrological input paths. Water loss from the lake surface by evaporation (E_{lake}) was determined as a long-term value for the period from 1990 until 2009. Q_{out} and P_{exp} are cumulated values for water and P losses from the lake, respectively, allowing no distinction between groundwater and surface water outflow. ΔP_{lake} was derived from the mean linear trend of lake water P content from 1993 until 2013.

Chemical analysis

SRP samples were filtered using a 0.45 µm syringe filter (cellulose acetate). P concentrations were determined with the ammonium molybdate spectrometric method with a limit of quantification (LOQ) of 25 µg l^{-1}. Domestic well samples were additionally digested and analyzed for total phosphorus (TP, ISO 6878:2004).

Although the present study focuses on P, some additional parameters were determined in all groundwater samples. Analysis included the two most relevant N-fractions (ammonium and nitrate), dissolved iron, boron, and redox potential. The latter could not be determined for domestic wells since the redox potential has to be measured on-site during sampling in flow-through cells.

Nitrate-N concentrations were determined by ion-chromatography (ISO 10304-^{1}:2007.), while ammonium-N was measured photometrically (ISO 11732:2005). Boron and dissolved iron concentrations were determined via inductively coupled plasma optical emission spectrometry (ICP-OES). Redox potentials of well samples were measured on-site in a flow-through cell with a potentiometry probe (Multi3430, WTW).

3.2.3 Results

Near-shore groundwater quality

Groundwater observation wells. Mean SRP concentrations at the eight monitoring sites (Fig. 3.9) vary by orders of magnitudes (Fig. 3.11). Most remarkable are the results of sites 3 and (upgradient to it) site 5 where the shallow wells have mean SRP concentrations of 1600 and 3900 µg l^{-1}, respectively. The deeper wells at these sites show concentrations of 650 and 610 µg SRP l^{-1}, respectively. At near-shore sites 2 and 6 SRP concentrations also decrease with increasing aquifer depths. At both sites the shallowest wells still have SRP concentrations with a potential relevance for lake eutrophication (210 and 170 µg l^{-1} at 2a and 6a, respectively). The pattern of decreasing SRP concentrations with depth is not valid at all monitoring sites. At sites 1, 4, and 8 SRP concentrations are slightly higher in the deeper wells than in the shallower ones. Thus, there is no consistency in P concentrations with regard to aquifer depth.

With one exception, time series of SRP concentrations in the ten groundwater observation wells at sites 1 to 8 (Fig. 3.9) from April 2010 to December 2013 demonstrate that no significant changes take place (Fig. 3.12). Variations over time may be driven by seasonal factors (e.g., weather conditions) or analytical errors but do not seem to be caused by general changes in groundwater chemistry. However, at well 5a which has the highest SRP concentrations, a decrease occurred. In January 2012 a maximum concentration of 3630 µg SRP l^{-1} was recorded in December 2013. In contrast, the deeper well at site

5b revealed an ongoing increase of SRP concentrations from 510 µg l^{-1} at the beginning of the monitoring period to 770 µg l^{-1} in December 2013.

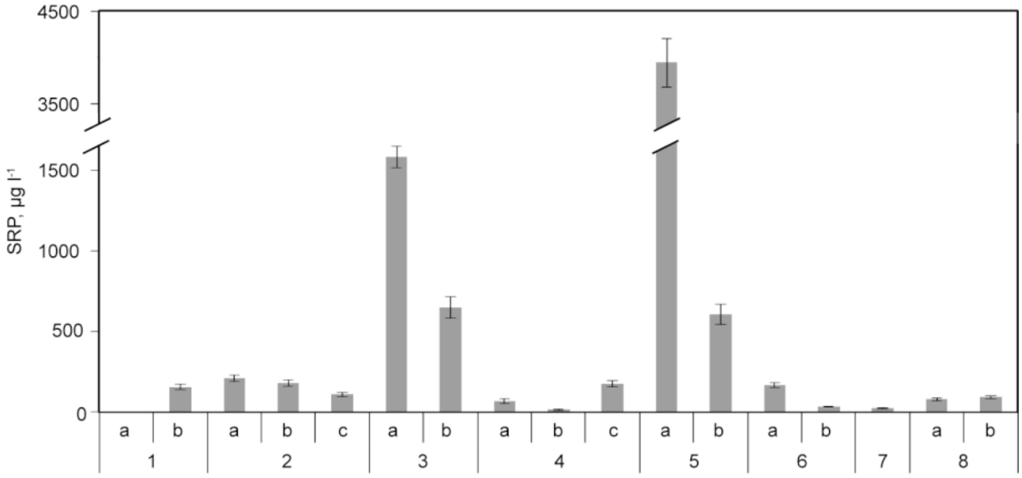

Figure 3.11 Mean concentrations and standard deviations (error bars) of soluble reactive phosphorus (SRP in µg l^{-1}) in groundwater observation wells at sites 1–8 (sites 1, 2, and 4: *n* = 22, site 3: *n* = 33 in a period from April 2010 to December 2013; sites 5–8: *n* = 15 from December 2011 to December 2013). Letters (a, b, and/or c) represent shallow, middle, and/or deep well according to Table 3.3.

Temporary piezometers. Samples from temporary near-shore piezometers in the upper part of the aquifer reveal a large heterogeneity of SRP concentrations (Fig. 3.13a). Concentrations range from less than 25 to above 4000 µg SRP l^{-1} in overall 44 piezometer samples. The results show that SRP concentrations of more than 100 µg l^{-1} almost exclusively occur in a 1.9 km long section along the southern and southeastern shoreline, including sites 2 and 3, where increased concentrations are also found in the deeper observation wells (Fig. 3.11). The section, where LGD is heavily contaminated with P, is restricted to urban areas of the city of Arendsee. Concentrations up to 4060 µg SRP l^{-1} are found in this reach. There are only two sites outside the area where near-shore groundwater has concentrations of more than 100 µg SRP l^{-1}. They are located at the western shoreline, where a settlement of vacation cottages is situated (Fig. 3.13a).

LGD-derived P loads. The largest portion of LGD-derived P loads enters the lake along a 1.4 km long reach where not only SRP concentrations are high, but also LGD rates are largest (Meinikmann et al. 2013, Fig. 3.9). Standardized SRP loads in the shoreline sections range from less than 1 to 1060 g SRP discharging to the lake along one meter of shoreline per year (g SRP m^{-1} yr^{-1}, Fig. 3.13b), with a median of 12 g m^{-1} yr^{-1}. Segmented SRP loads sum up to an overall groundwater-borne load of 830 kg SRP yr^{-1}. Of this, 94% enters the lake along 23% of the shoreline where exfiltration occurs.

Groundwater P concentrations in the catchment

Mapping of SRP concentrations at sites 1–8 indicates a plume which encompasses groundwater observation sites 2, 3, and 5 (Fig. 3.14a). Site 6 with a mean of 170 µg l^{-1} might also be part of this plume, while sites 7 and 8 are not considered to be impacted by a contamination (<100 µg SRP l^{-1}). However, in the settled area of the city of Arendsee, another well with a concentration of 1900 µg SRP l^{-1} occurs north of site 7 (Fig. 3.14b). In the remaining, mostly rural parts of the catchment, SRP concentrations are relatively low. There are only two groundwater observation wells in the south and at the eastern border of the subsurface catchment with SRP concentrations of more than 100 mg l^{-1} (140 and 190 µg l^{-1}, respectively). However, these concentrations are relatively low compared to some found in the urban area (Fig. 3.14b).

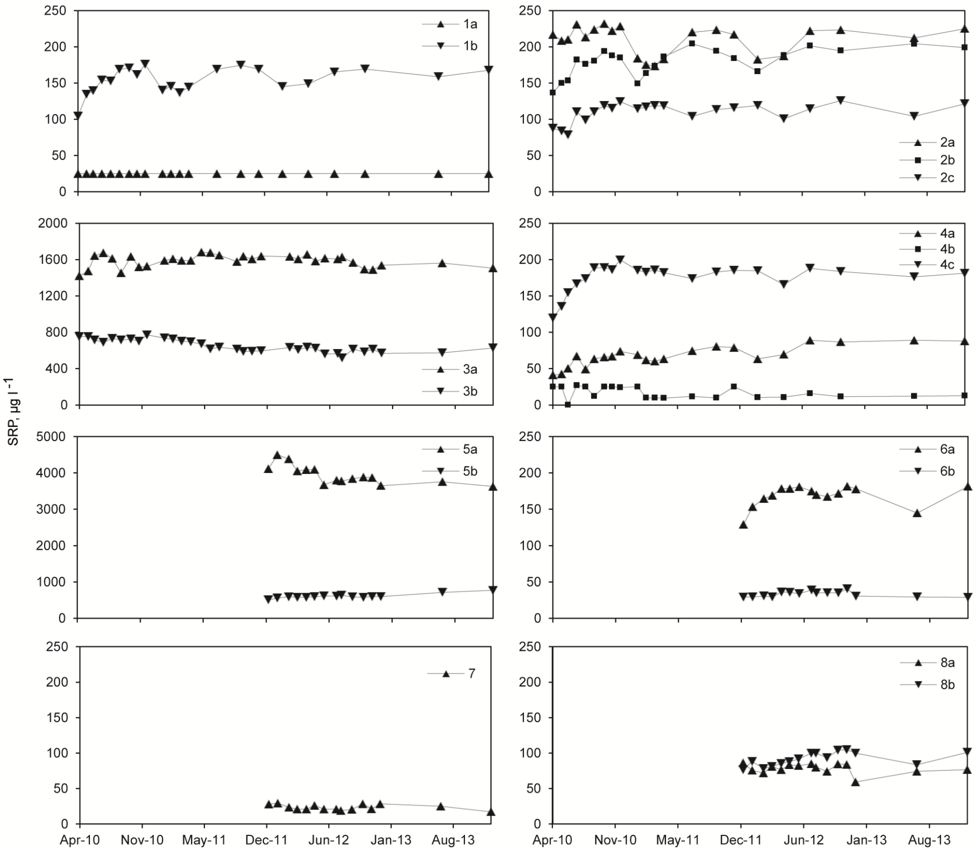

Figure 3.12 Time series of concentrations of soluble reactive phosphorus (SRP) in groundwater observation wells at sites 1–8. Letters (a, b, and/or c) indicate shallow, middle, and/or deepest well at a specific site (see Table 3.3). Note the differing scales at sites 3 and 5.

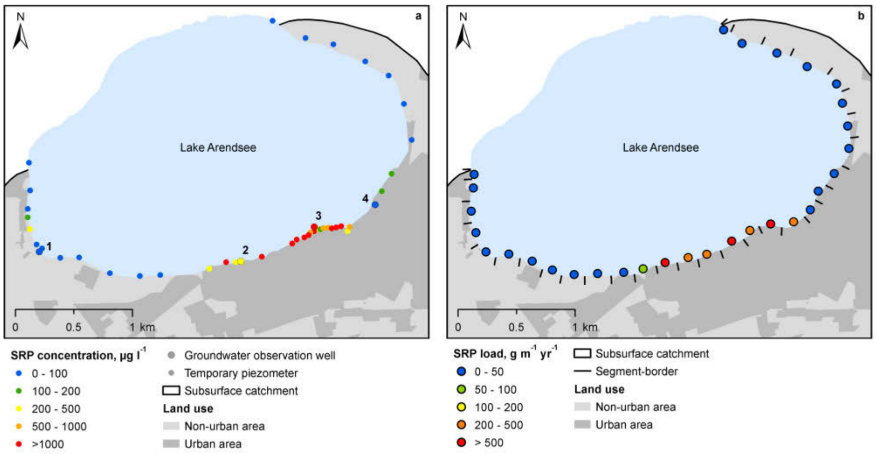

Figure 3.13 (a) Near-shore groundwater concentrations of soluble reactive phosphorus (SRP) in groundwater observation wells (big outlined circles) and temporary piezometers (small circles), and (b) resulting standardized SRP loads (g SRP entering the lake along one meter of shoreline per year) for shoreline segments (based on hydrological data by Meinikmann et al. (2013).

The call for groundwater samples from domestic wells was successful and resulted in 56 additional samples. Most of them are from the city of Arendsee. Only a few came from other small villages in the subsurface catchment (6c). At first glance, P concentrations confirm the existence of a P plume in the area south and southeasterly of the impacted sites 3 and 5. Concentrations of more than 500 µg P l^{-1} are found south of site 7, which was previously not considered to be located in the potential P plume. Furthermore, the area around site 6 as well as south and west of site 7 is dominated by P concentrations between 100 and 200 µg l^{-1}. Although these concentrations are relatively low the agglomeration of slightly increased P concentrations may also indicate a contamination of this area. Compared to the eastern part of the city, information on groundwater quality west of the transect is scarce. Geological conditions are assumed to be dominated by sediments of low hydraulic conductivity. The installation of groundwater wells, at least for private water abstraction, is presumably not worthwhile in that area. As a consequence, no samples are available from the central part of the city of Arendsee. Alternatively, many samples were brought from the southwestern part of the city of Arendsee (Fig. 3.14d). Except one, they all show P concentrations of less than 100 µg l^{-1}.

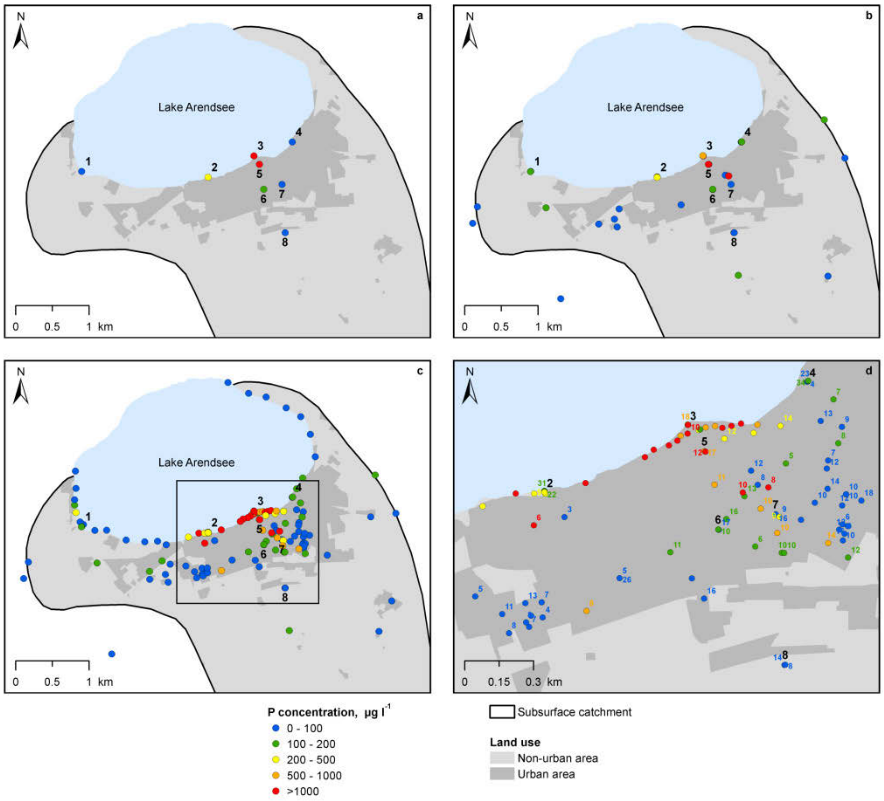

Figure 3.14 Spatial variation of phosphorus (P) concentrations in the catchment of Lake Arendsee and stepwise increase of investigation extent and its spatial resolution. (a) Most shallow groundwater observation wells at sites 1–8; (b) in addition groundwater observation wells in and close to the subsurface catchment of the lake; and (c) in addition domestic wells and temporary piezometers. (d) Enlargement of the rectangle in (c) which depicts the urban area of the city of Arendsee. It includes well depths (m below ground surface, coloured according to the corresponding P concentration) to additionally visualize results from different wells at the same place and/or sampling depths.

Although the results indicate a P plume reaching the lake from southeast of site 3, the focus here should also be on medium to small scale results. There is considerable heterogeneity in groundwater P concentrations in this area. Two wells north of site 7 reveal a discrepancy of P concentrations within a small distance. One of them had a concentration of 1900 µg l^{-1}, while the other well (although located

50 m away) had 40 µg P l^{-1}. Both wells had similar depths of about 8 m below ground surface. Furthermore, two domestic wells in even closer proximity to site 7 were found to have the same depth (9 m) but significantly different P concentrations (400 and 35 µg l^{-1}, respectively) (Fig. 3.14d). According to the owners these two wells are located less than 20 m apart from each other. Also around near-shore site 2 P concentrations are heterogenic. Within a distance of 130 m two samples collected in six and three meters depth below ground, respectively, have concentrations of 3200 and less than 25 µg P l^{-1}. Near-shore well 2a in close proximity to them has a mean P concentration of about 220 µg l^{-1} but is with 9 m below ground deeper than the other ones (Table 3.3).

Although no general dependency on aquifer depth can be identified, concentrations of more than 1000 µg P l^{-1} are restricted to wells with depths ranging from 6 to 12 m below top ground surface (Fig. 3.14d). At those of the heavily contaminated sites which are equipped with a shallow and a deep well, a decrease of P concentrations with increasing well depths is determined (e.g., sites 3 and 5, Fig. 3.11).

To summarize, the investigation reveals an area south of near- shore site 3 which seems to be impacted by a P plume. However, its origin is not traceable. Furthermore, upgradient of near-shore observation site 2 another plume exists. Within the contaminated areas there are sites in close proximity to heavily impacted wells which do not show any increase in P concentrations.

Correlations of phosphorus with other groundwater parameters

With the exception of boron, P concentrations show hardly any correlation with other groundwater parameters. The majority of coefficients of determination (R^2) are less than 0.02 (Fig. 3.15). Boron shows a slightly positive correlation with P (R^2 = 0.16, Fig. 3.15e). In some samples with P concentrations of less than 250 µg l^{-1}, both, ammonium-N and dissolved iron increase with increasing P concentrations, indicating a dependency on the redox potential. However, at higher P concentrations this positive relation is not valid anymore (Fig. 3.15a and b). Redox potential data themselves do not show any correlation with P concentrations (Fig. 3.15d). Increased P concentrations occur at both, high and low redox potentials. It is noteworthy that out of the five highest P concentrations four occur at positive redox potentials of more than 50 mV. Nitrate-N concentrations also do not correlate with P concentrations. High and low nitrate concentrations occur together with high P concentrations, while ammonium and dissolved iron have concentrations predominantly below the LOQ at high P concentrations.

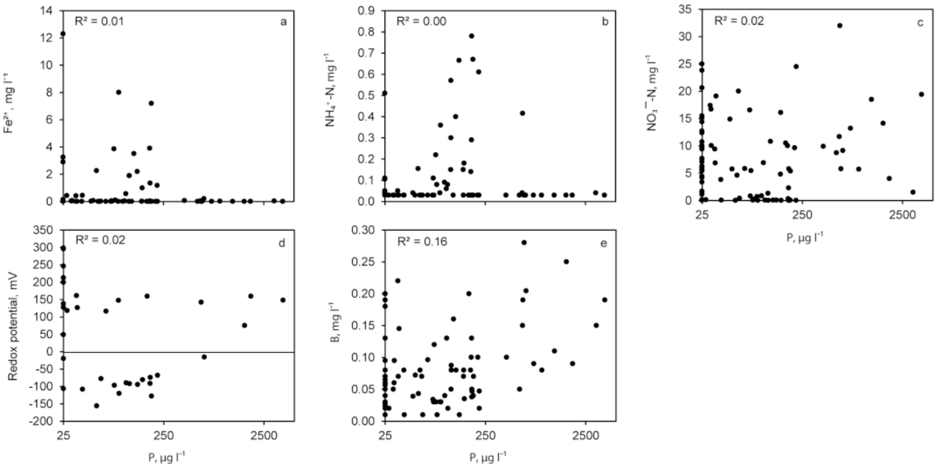

Figure 3.15 Concentrations of phosphorus (P) vs. concentrations of Fe^{2+} (a), NH$_4^+$-N (b), NO$_3^-$-N (c), B (e) and redox potential (d). a, b, c and e include median concentrations of time series of groundwater observation wells as well as results from domestic wells which were sampled once. Data depicted in (d) contain only results from groundwater observation wells, since no redox potential measurements were possible for domestic well samples. Note log-transformation of x-axis.

External phosphorus inputs into Lake Arendsee

Overall, P inputs from external sources sum up to 1560 kg yr^{-1} (Table 3.3). Due to the results presented above, LGD accounts for 53% of this value which is equivalent to 161 mg m^{-2} yr^{-1} (referred to the whole lake area). This is followed by atmospheric deposition (19%), water fowl (13%), and drainage from agriculture (12%). Rainwater and storm water overflow discharge, overland flow, as well as bathers did not contribute significantly to the overall external P load (Table 3.4). To evaluate these results, additional calculations were performed with a background concentration of 50 µg P l^{-1} in LGD (generally discussed as maximum background P concentrations in areas without anthropogenic impact; Lewandowski et al. 2015). In this scenario LGD accounts for only 9% of the overall external P load to Lake Arendsee (Table 3.4).

Table 3.4 External phosphorus (P) loads to Lake Arendsee.

P input path	Actual P input [a]			Background P input [b]		
	kg yr^{-1}	%	mg m^{-2} yr^{-1}	kg yr^{-1}	%	mg m^{-2} yr^{-1}
Groundwater	830	53	161	70	9	14
Atmospheric deposition	300	19	58	300	38	58
Waterfowl	200	13	39	200	25	39
Drainage ditches	180	12	35	180	23	35
Bathers	20	1	4	20	3	4
Surface runoff	10	1	2	10	1	2
Storm water overflow	10	1	2	10	1	2
Rainwater discharge	10	1	2	10	1	2
Sum of P inputs	1560	100	304	800	100	156

[a] Groundwater P load based on measured data presented in this study.

[b] Groundwater P loads based on a theoretical maximum background concentration of 50 µg P l^{-1}.

Phosphorus mass balance

Q_{in} (Eq. 3.8) sums up the total runoff in the catchment (as presented Meinikmann et al. 2013), precipitation on the lake surface, discharge of a ditch draining pastures west of the subsurface catchment (see Fig. 3.9), and groundwater abstraction for drinking water supply (Table 3.5). Subtracting water losses due to evaporation of lake water (E_{lake}) yields the amount of water leaving the lake with groundwater outflow and surface runoff (Q_{out} in Eq. 3.8 and Table 3.5). The long-term epilimnetic P concentration is 134 µg l^{-1}, resulting in a P_{exp} of 355 kg P yr^{-1}. 1400 kg P yr^{-1} are retained in the lake sediment (P_{sed} in Eq. 3.7). Between 1993 and 2013 ΔP_{lake} increased on average by 215 kg yr^{-1}. P_{exp}, P_{sed}, and ΔP_{lake} sum up to 1970 kg yr^{-1} (Eq. 3.7) compared to an external P load (P_{load}) of 1560 kg yr^{-1} determined by summing up all input paths (Table 3.4).

Table 3.5 Water balance of Lake Arendsee with water inflow to the lake (Q_{in}), evaporation of lake water (E_{lake}), and resulting outflow of the lake (Q_{out}) based on Equation 3.8 (in Mm^3 yr^{-1}).

Q_{in}	6.03
Precipitation on lake surface	3.00
Total runoff in subsurface catchment	2.35
Discharge from drainage ditch outside of subsurface catchment	1.00
Groundwater abstraction for drinking water supply	- 0.32
E_{lake}	- 3.38
Q_{out}	2.65

3.2.4 Discussion

The role of LGD at Lake Arendsee

Groundwater P concentrations found in the catchment of Lake Arendsee partly exceed ecological thresholds discussed in literature by far (Burkart et al. 2004; Holman et al. 2010; Lewandowski et al. 2015). Moreover, main LGD takes place where the groundwater is most contaminated. As a result, LGD-derived P loads from the segmented approach account for 53% of all quantified external P inputs to Lake Arendsee, compared to only 9% based on natural background concentrations of P. Temporary piezometer investigations increased the spatial resolution of SRP concentrations along the shore significantly. Accordingly, the application of the results to LGD rates also increased the accuracy of P load determinations and led to a groundwater-borne P load of 830 kg yr^{-1}. A first approach by Meinikmann et al. (2013) based on only four near- shore groundwater concentrations yielded a P load of 425 kg yr^{-1}. The underestimation of about 50% can be attributed to the large heterogeneity in near-shore SRP concentrations which was not captured by the four near-shore observation sites alone.

However, both approaches showed that LGD contributes the largest proportion of external P loads to the lake. This confirms that groundwater P drives the ongoing eutrophication of Lake Arendsee. The area P loading via LGD is 161 mg m^{-2} yr^{-1}. Values reported for other lakes range from 6 to about 2900 mg P m^{-2} yr^{-1} via LGD (e.g., Belanger et al. 1985; Brock et al. 1982; Kang et al. 2005; LaBaugh et al. 1995; Lewandowski et al. 2015; McCobb et al. 2003; Misztal et al. 1992; Oliveira Ommen et al. 2012; Shaw et al. 1990; Vanek 1991). Other studies also found LGD as a major contributor to lake P bud gets. For example, Oliveira Ommen et al. (2012) showed for oligotrophic Lake Hampen in Denmark that groundwater accounts for 85% of external P loads, with groundwater P concentrations ranging from 4 to 52 µg l^{-1}. However, while LGD in Lake Hampen had a much higher proportion of the P budget than at Lake Arendsee, its eutrophication potential is significantly lower due to generally lower groundwater P concentrations. Nevertheless, the authors still attributed the potential for lake eutrophication to LGD derived P loads. There are probably many other lakes where LGD significantly enhances eutrophication.

Common neglect of LGD in lake nutrient budgets has several reasons. Groundwater is an invisible input path, and the quantification of its contribution to lake nutrient budgets is challenging (Lewandowski et al. 2015). Temporal and especially spatial heterogeneities in LGD and nutrient concentrations have to be carefully considered, to minimize uncertainties in the nutrient budget. This has recently been confirmed for groundwater-borne N inputs to a lake by Kidmose et al. (2015). But in contrast to N, P has long been assumed to be immobile in the aquifer and thus generally low groundwater P concentrations are expected (Lewandowski et al. 2015). This paradigm has changed within the last years and as an indicator for contrary findings the USGS (2014) issued the following statement on its webpage: "*Phosphorus Doesn't Migrate in Ground Water? Better Think Again!*". The results of the present study show that groundwater P concentrations can increase far beyond natural values and by that alter the trophic condition of surface waters. Lake Arendsee might represent a "worst case" where extremely high P concentrations coincide with the area of main LGD volume fluxes. Our findings should encourage scientists and practitioners dealing with surface water eutrophication to also take groundwater into account as a significant source of external P. Furthermore, it needs to be considered that in close proximity to surface waters water tables are usually low. Consequently, near-shore groundwater is especially prone to contaminations: The thickness of the vadose zone and by that its adsorption and retention capacities decrease with decreasing distance to the shoreline. Moreover, the closer a contamination source is to surface water the less time and flow path length is available for restoration and retention of pollutants during the passage of the saturated zone.

Temporal variability of phosphorus concentrations

Low temporal dynamics of P concentrations at near-shore site 3 indicate a contamination source that has been active for a long time with more or less constant intensity. Since no improvement of groundwater quality could be determined during almost four years of monitoring it cannot be excluded that the contamination source is still active. Moreover, increasing SRP concentrations at well 5b indicate, that at least for deeper parts of the aquifer, the maximum extent of the plume might not have reached the lake yet. The generally low temporal variability at the near-shore sites supports the approach to use a one-time-sampling of groundwater from temporary piezometers for representative P load calculations. These results also support the utilization of one-time-measurements of P concentrations from private domestic wells.

Spatial variability of phosphorus concentrations in the catchment

Groundwater observation and domestic wells reveal a large degree of spatial heterogeneity in the urban area. Several locations with low P concentrations were found in closest proximity to severely contaminated sites. In some cases these heterogeneities can be explained by different depths of well screens, since plumes have a limited horizontal as well as vertical extent. A vertical concentration gradient within the plume might be responsible for differing measured P concentrations at neighboring sites when the lengths of the screens differ. An example are strongly differing SRP concentrations at sites 3 and 5, which are located only 150 m apart from each other. Flow directions indicate that groundwater first passes site 5 before it reaches the lake at site 3 (Figs. 3.8 and 3.9). Mean SRP concentrations of about 3900 $\mu g\ l^{-1}$ at well 5a compared to 1600 $\mu g\ l^{-1}$ at well 3a (Fig. 3.11) might imply that the maximum extent of the contamination has not reached the lake yet, but actually well 5a covers only 2 m of the upper vertical extent of the aquifer while well 3a covers 8 m of the aquifer (Table 3.3 and Fig. 3.10b). Samples from well 5a are likely taken from the more contaminated upper part of the aquifer, while samples from well 3a are diluted with less contaminated deeper groundwater. Thus, drilling depths and screen lengths should be considered when evaluating spatial groundwater quality data.

A vertical gradient might also be responsible for relatively low P concentrations at well 7 (arithmetic means 25 $\mu g\ l^{-1}$), although surrounding wells indicate a P plume in that area. Since here groundwater is sampled from 9 m below the water table, the maximum P concentration within the vertical aquifer extent might not be captured. In addition, spatially varying aquifer substrates can cause heterogeneous P concentrations due to differences in hydraulic conductivities. A sediment layer with a larger hydraulic conductivity compared to surrounding sediments can function as a preferential flow path for groundwater and its constituents. Also, the commonly higher retention capacity of sediments with low hydraulic conductivity might reduce groundwater P concentrations more efficiently than sediments of large hydraulic conductivity. Nevertheless, since retention capacities are exhaustible this effect will be suspended at one point.

Although the number of available monitoring sites is quite high in the present study, it still is not possible to identify a contamination site. The spatial variety of P concentrations indicates that the pollution is caused not only by one but by several contamination sources.

However, the detailed picture of groundwater quality below the city of Arendsee could only be accurately assessed due to the inclusion of domestic wells into the investigation. They provide a fast, simple and cheap supplement of traditional investigations based on groundwater observation wells.

Correlations with other parameters

Ammonium-N, dissolved iron, and P are usually known to occur under anaerobic conditions (i.e., at negative redox potentials). In contrast, at higher redox potentials nitrogen exists as nitrate-N, while P mobility is decreased due to adsorption to iron(oxy)hydroxides. In the present study, none of these assumptions seems to be valid; P concentrations do not correlate with other parameters (Fig. 3.15). Moreover, in several cases there are even contrasting findings. High P concentrations go along with high redox potentials, and with low ammonium and dissolved iron concentrations. In several cases high P concentrations occur in combination with high nitrate concentrations. We suspect that the following processes are responsible for this:

Organic matter enters the unsaturated zone from an unknown source and is mineralized. Nutrients mobilized by mineralization underlie different mechanisms and processes: Nitrogen is percolated with the groundwater down the unsaturated zone as nitrate-N, as long as the redox potential is positive. In contrast, under oxic conditions, P derived from the degradation of organic matter is predominantly immobilized in the vadose zone by sorption onto different mineral surfaces (e.g., Fe(III)-containing oxides or hydroxides) and therefore, does not reach the groundwater. However, with ongoing pollution these retention capacities of the unsaturated zone become exhausted and freshly delivered P starts to constantly travel towards the saturated zone, even though the redox potential is clearly positive. At some sites with negative redox potentials, the usual pattern of co-existence between redox-dependent species are still visible, i.e., increased P concentrations correlate with increased ammonium and dissolved iron concentrations. However, this seems to be only valid for groundwater with P concentrations less than 250 $\mu g\ l^{-1}$ (Fig. 3.15). Heavier contaminations (P concentrations > 250 $\mu g\ l^{-1}$) are restricted to oxic conditions, indicating already exhausted retention capacities at those sites.

Additionally, spatial separation of plume constituents during the passage of the aquifer might cause discrepancies between P concentrations and other contamination indicators at a single site. It is known that P travel times are at least one magnitude lower than actual groundwater flow velocity while boron or nitrate show nearly no retardation in the aquifer.

Overall we assume that the present distribution of nutrients and other compounds in the aquifer of the subsurface catchment results from a complex overlay of different processes. Furthermore, we interpret these findings as resulting from the immense impact of a severe pollution.

Origins of the groundwater P contamination

Agricultural or urban origin? The intense investigation of the groundwater quality in the subsurface catchment of Lake Arendsee leads to the conclusion that the sources of the P contamination are located somewhere in the urban area of the city of Arendsee. In particular, results from near-shore temporal piezometers did not reveal increased SRP concentrations in non- settled areas. There is no evidence that agriculture is a significant source of P enrichment of the aquifer in the catchment of Lake Arendsee. In fact, according to an independent modelling approach based on land use types (Gebel et al. 2010) diffuse P loads from agriculture accounts for only 13% of the overall P loads calculated in this study. Even less (3% of overall P load) are delivered by forested areas.

Higher P concentrations in urban groundwater compared to agricultural or other land use types have been reported in several other studies before (Holman et al. 2008; Qian et al. 2011), demonstrating a potential vulnerability of urban aquifers to P contamination.

Potential sources. According to paleoecological investigations a change from a mesotrophic to a eutrophic state happened in Lake Arendsee in the middle of the 20th century (Scharf 1998). This was mainly attributed to the discharge of untreated communal and industrial wastewater into the lake. Furthermore, the drainage of an adjacent lake to reclaim arable land and the overall intensification of agriculture in the catchment probably also contributed to increased nutrient loads.

Since the end of the 1970s a sewage system transports wastewater to a treatment plant outside of the catchment. It was assumed that this measure would eliminate the largest portion of external P. However, the trophic state of the lake did not recover, which at the time was explained by the very long water residence time of Lake Arendsee. Nevertheless, TP concentrations still increased during the subsequent decades. Results from the present study now reveal that it is mainly P contaminated groundwater from settled areas at the southern shore that contributes to the ongoing lake eutrophication.

Contamination of groundwater below urban areas is often caused by leakages from wastewater systems (Bishop et al. 1998; Rutsch et al. 2008; Schirmer et al. 2013; Wakida and Lerner 2005). This includes on-site septic tank-systems, or sewer channels, with the latter including the municipal sewage system, as well as house connection sewers. Sewage P concentrations range between 9 and 15 mg PO_4-P l^{-1} (Bishop et al. 1998; Holman et al. 2008). However, a part of the wastewater P can be assumed to be retained in the vadose zone matrix during percolation (Gilliom and Patmont 1983; Zanini et al. 1998). The amount of nutrients and pollutants from leaky sewers that actually reaches the groundwater depends on filtering and retention capacities of the vadose zone. Under oxic conditions P is usually adsorbed as phosphate onto positively charged mineral surfaces, e.g., Al-, Mn(IV)- and Fe(III)-containing oxides and (oxy)hydroxides, and calcite (Ptacek 1998; Spiteri et al. 2007; Wilhelm et al. 1994; Zanini et al. 1998) or onto solid organic carbon (Harman et al. 1996). Thus, P concentrations do not necessarily increase instantly after a contamination. However, as mentioned above, a long-lasting continuous supply of P exhausts the aforementioned retention capacities. In such a case pollution-derived P is transported through the vadose zone and finally reaches the groundwater. Depending on the thickness of the vadose zone, its retention capacities, and due to slow groundwater flow velocities it might take decades before the groundwater pollution is recognized (McCobb et al. 2003).

Leakages from wastewater facilities within the city of Arendsee would easily explain the observed heterogeneity of the groundwater P concentrations. Especially house connection sewers and on- site septic tanks are known to be malfunctioning (e.g., Katz et al. 2011). Some studies even warn of pumping septic tank leachate from domestic wells since it might cause serious health threats (Bremer and Harter 2012; Katz et al. 2011).

Other potential sources for P in groundwater are abandoned contaminated sites such as agricultural fertilizer storage units, and/or industrial sites. The excessive application of fertilizers in private gardens may also cause groundwater contaminations (Vanek 1993; Zhao et al. 2011).

In the case of Lake Arendsee the large heterogeneity of P concentrations prevented the identification of contamination sites and origins. Reasons for this heterogeneity might be the following:

- Small- to medium-scale differences in aquifer material cause preferential flow paths and a heterogenic dispersion of a potential plume.
- The contamination is/was happening at several sites simultaneously (e.g., leaking of wastewater at several malfunctioning sites) causing plumes of varying intensity.
- Incompatible parameters of observation sites (e.g., well depths and screen lengths) or lacking information on them prevented a reliable interpretation of the results.

Evaluation of external phosphorus load estimations

The sum of separately determined external P loads (Table 3.4) agrees well with the sum of P retention in the lake sediment, P export from the lake, and changes in lake P inventory (Eq. 3.7). The good agreement confirms that all relevant P input paths have been considered in the investigations. Discrepancies might result from small errors in individual terms. Uncertainties in LGD arise from the determination of the subsurface catchment, from groundwater recharge calculations, as well as P concentrations in LGD (e.g., due to inappropriate resolution of near-shore measurements along the lake and with depth). One year-measurements of P loads from agriculture via drainage ditches might differ from a long-term mean. Storm water overflows might have been underestimated due to a small and thus non-representative number of discharge events during the experimental period (data not shown). Additionally, P retention in the lake sediment underlies some uncertainty. The relatively good agreement of total P loads (Table 3.4) with the sum of P_{sed}, P_{exp}, and ΔP_{lake} (Eq. 3.7) provides significant evidence for the importance of LGD-derived P loads to the lake.

Implications

Because of the long water residence time an immediate reduction of the P concentration in Lake Arendsee is only possible by internal P inactivation (Schauser et al. 2003). Due to the high external P loads P concentrations in the lake will gradually exceed critical threshold values necessary for controlling primary production within only one decade after a chemical inactivation. Therefore, a restoration is only sustainable when the internal measure is accompanied by a decrease of external P loads. Since the results do not indicate if and when a decrease in groundwater P loads can be expected, further measures should be considered to reduce P loads from LGD. Calculations of section-wise groundwater P loads allow the delineation of a reach at the shore where most groundwater P is entering the lake (Fig. 3.13b). Thus, it seems promising to establish groundwater remediation measures along this reach. One possibility is the installation of a permeable reactive barrier close to the shoreline to directly remove diffuse P from shallow groundwater before it enters the lake. For this P sorbing materials (e.g., metal cations) are blended with filter sediment material (e.g., zero-valent-iron) and implemented into the soil/aquifer matrix or, like described for Ashumet Pond in Cape Cod, as a permeable reactive layer directly into the lake bottom (McCobb et al. 2009). Also, the abstraction of contaminated near-shore groundwater to an off-site treatment facility may be a feasible option to remove P from the system. After treatment the water could either be reinserted into the aquifer or directly discharged into the lake. The deviation of the untreated groundwater to a treatment plant outside of the lake's catchment could also be taken into account. However, the resulting shift in the lake water balance should be carefully considered in that case.

3.2.5 Summary and Conclusion

1. Completing the segmented approach introduced by Meinikmann et al. (2013) with near-shore groundwater P concentrations from temporary piezometers enabled us to quantify LGD-derived P loads and to evaluate their impact on the lake's trophic state.

2. Groundwater can be a main cause of lake eutrophication, especially when a contamination leads to high nutrient concentrations in those parts of the shoreline where main lacustrine groundwater discharge (LGD) takes place.

3. Despite a large number of observation sites it was not possible to clearly locate a contamination site and to identify the source for the severe groundwater pollution.

4. It is conceivable that groundwater P pollution is more common than previously thought. Special care should be taken when human settlements are located in close proximity to those reaches of a lake shore where significant groundwater exfiltration takes place. Adsorption and retention potentials of both, vadose and saturated zones usually decrease with decreasing distance to the lake.

5. Heavy contaminations may alter natural patterns of co-existence of groundwater constituents. At Lake Arendsee groundwater P concentrations are highest at high positive redox potentials, indicating a severe contamination to superimpose the usual redox dependency of P mobility in groundwater.

6. Sustainable restoration of Lake Arendsee will only be achieved by a reduction of the P inventory in the lake on the one hand and external P loads on the other hand. Since groundwater is by far

the largest contributor to the overall P load, measures for P elimination from near-shore groundwater should be evaluated for their applicability.

3.2.6 References

Ala-aho, P., Rossi, P.M., Kløve, B., 2013. Interaction of esker groundwater with headwater lakes and streams. *Journal of Hydrology*, 500(0): 144-156.

Belanger, T.V., Mikutel, D.F., Churchill, P.A., 1985. Groundwater seepage nutrient loading in a Florida lake. *Water Research*, 19(6): 773-781.

Bishop, P.K., Misstear, B.D., White, M., Harding, N.J., 1998. Impacts of sewers on groundwater quality. *Journal of the Chartered Institution of Water and Environmental Management*, 12(3): 216-223.

Bremer, J.E., Harter, T., 2012. Domestic wells have high probability of pumping septic tank leachate. *Hydrology and Earth System Sciences*, 16(8): 2453-2467.

Brock, T.D., Lee, D.R., Janes, D., Winek, D., 1982. Groundwater seepage as a nutrient source to a drainage lake - Lake Mendota, Wisconsin. *Water Research*, 16(7): 1255-1263.

Burkart, M.R., Simpkins, W.W., Morrow, A.J., Gannon, J.M., 2004. Occurrence of total dissolved phosphorus in unconsolidated aquifers and aquitards in Iowa. *Journal of the American Water Resources Association*, 40(3): 827-834.

Edwards, A.C., Withers, P.J.A., 2007. Linking phosphorus sources to impacts in different types of water body. *Soil Use and Management*, 23: 133-143.

Gebel, M., Halbfaß, S., Bürger, S., Uhlig, M., Pöschke, F., 2010. Quellen- und pfadbezogene Modellierung diffuser Phosphoreinträge in den Arendsee (Source- and input path-related modelling of diffuse phosphorus to Lake Arendsee). Project report on behalf of the State Agency for Flood Protection and Water Management Saxony-Anhalt, in German. 36 p.

Gilliom, R.J., Patmont, C.R., 1983. Lake phosphorus loading from septic systems by seasonally perched groundwater. *Journal Water Pollution Control Federation*, 55(10): 1297-1305.

Harman, J., Robertson, W.D., Cherry, J.A., Zanini, L., 1996. Impacts on a sand aquifer from an old septic system: Nitrate and phosphate. *Ground Water*, 34(6): 1105-1114.

Heathwaite, A.L., Dils, R.M., Liu, S., Carvalho, L., Brazier, R.E., Pope, L., Hughes, M., Phillips, G., May, L., 2005. A tiered risk-based approach for predicting diffuse and point source phosphorus losses in agricultural areas. *Science of The Total Environment*, 344(1–3): 225-239.

Holman, I.P., Howden, N.J.K., Bellamy, P., Willby, N., Whelan, M.J., Rivas-Casado, M., 2010. An assessment of the risk to surface water ecosystems of groundwater P in the UK and Ireland. *Science of The Total Environment*, 408(8): 1847-1857.

Holman, I.P., Whelan, M.J., Howden, N.J.K., Bellamy, P.H., Willby, N.J., Rivas-Casado, M., McConvey, P., 2008. Phosphorus in groundwater-an overlooked contributor to eutrophication? *Hydrological Processes*, 22(26): 5121-5127.

Hupfer, M., Lewandowski, J., 2005. Retention and early diagenetic transformation of phosphorus in Lake Arendsee (Germany) - consequences for management strategies. *Archiv fuer Hydrobiologie*, 164(2): 143-167.

ISO, 6878:2004. Water quality – Determination of phosphorus – Ammonium molybdate spectrometric method. International Organization for Standardization, p. 21.

ISO, 10304-1:2007. Water quality - Determination of dissolved anions by liquid chromatography of ions - Part 1: Determination of bromide, chloride, fluoride, nitrate, nitrite, phosphate and sulfate. International Organization for Standardization, p. 15.

ISO, 11732:2005. Water quality - Determination of ammonium nitrogen - Method by flow analysis (CFA and FIA) and spectrometric detection. International Organization for Standardization, p. 18.

Jarosiewicz, A., Witek, Z., 2014. Where do nutrients in an inlet-less lake come from? The water and nutrient balance of a small mesotrophic lake. *Hydrobiologia*, 724(1): 157-173.

Kang, W.J., Kolasa, K.V., Rials, M.W., 2005. Groundwater inflow and associated transport of phosphorus to a hypereutrophic lake. *Environmental Geology*, 47(4): 565-575.

Katz, B.G., Eberts, S.M., Kauffman, L.J., 2011. Using Cl/Br ratios and other indicators to assess potential impacts on groundwater quality from septic systems: A review and examples from principal aquifers in the United States. *Journal of Hydrology*, 397(3-4): 151-166.

Kidmose, J., Engesgaard, P., Ommen, D.A.O., Nilsson, B., Flindt, M.R., Andersen, F.Ø., 2015. The Role of Groundwater for Lake-Water Quality and Quantification of N Seepage. *Groundwater*, 53(5): 709-721.

Kidmose, J., Nilsson, B., Engesgaard, P., Frandsen, M., Karan, S., Landkildehus, F., Sondergaard, M., Jeppesen, E., 2013. Focused groundwater discharge of phosphorus to a eutrophic seepage lake (Lake Væng, Denmark): implications for lake ecological state and restoration. *Hydrogeology Journal*, 21(8): 1787-1802.

LaBaugh, J.W., Rosenberry, D.O., Winter, T.C., 1995. Groundwater contribution to the water and chemical budgets of Williams Lake, Minnesota, 1980-1991. *Canadian Journal of Fisheries and Aquatic Sciences*, 52(4): 754-767.

LAWA, 1998. Atmosphärische Deposition. Richtlinie für die Beobachtung und Auswertung der Niederschlagsbeschaffenheit (Atmospheric deposition: Directive for observation and evaluation of precipitation quality, in German). Bund/Länder-Arbeitsgemeinschaft Wasser (German Working Group of the Federal States on Water) (ed.), p. 65.

Lewandowski, J., Hupfer, M., Meinikmann, K., 2011. Vorplanung zur Sanierung und Restaurierung des Arendsees, Teilprojekt III (Planning of restoration measuresfor Lake Arendsee, part III). Project report on behalf of the State Agency for Flood Proection and Water Mangement Saxony-Anhalt, in German. 101 p.

Lewandowski, J., Meinikmann, K., Nützmann, G., Rosenberry, D.O., 2015. Groundwater – the disregarded component in lake water and nutrient budgets. Part 2: effects of groundwater on nutrients. *Hydrological Processes*, 29(13): 2922-2955.

Lewandowski, J., Meinikmann, K., Ruhtz, T., Pöschke, F., Kirillin, G., 2013. Localization of lacustrine groundwater discharge (LGD) by airborne measurement of thermal infrared radiation. *Remote Sensing of Environment*, 138: 119-125.

McCobb, T.D., LeBlanc, D.R., Massey, A.J., 2009. Monitoring the removal of phosphate from ground water discharging through a pond-bottom permeable reactive barrier. *Ground Water Monitoring and Remediation*, 29(2): 43-55.

McCobb, T.D., LeBlanc, D.R., Walter, D.A., Hess, K.M., Kent, D.B., Smith, R.L., 2003. Phosphorus in a ground-water contaminant plume discharging to Ashumet Pond, Cape Cod, Massachusetts, 1999. *U.S. Geological Survey Water Resources Investigations Report* 02-4306: 70 p.

Meinikmann, K., Lewandowski, J., Nutzmann, G., 2013. Lacustrine groundwater discharge: Combined determination of volumes and spatial patterns. *Journal of Hydrology*, 502(0): 202-211.

Misztal, M., Smal, H., Gorniak, A., 1992. Ground-water inflow of nutrients to a lake from differently utilized catchments. *Water Research*, 26(9): 1237-1242.

Oliveira Ommen, D.A., Kidmose, J., Karan, S., Flindt, M.R., Engesgaard, P., Nilsson, B., Andersen, F.O., 2012. Importance of groundwater and macrophytes for the nutrient balance at oligotrophic Lake Hampen, Denmark. *Ecohydrology*, 5(3): 286-296.

Orderud, G.I., Vogt, R.D., 2013. Trans-disciplinarity required in understanding, predicting and dealing with water eutrophication. *International Journal of Sustainable Development and World Ecology*, 20(5): 404-415.

Ouyang, Y., 2012. Estimation of shallow groundwater discharge and nutrient load into a river. *Ecological Engineering*, 38(1): 101-104.

Ptacek, C.J., 1998. Geochemistry of a septic-system plume in a coastal barrier bar, Point Pelee, Ontario, Canada. *Journal of Contaminant Hydrology*, 33(3-4): 293-312.

Qian, J.Z., Wang, L.L., Zhan, H.B., Chen, Z., 2011. Urban land-use effects on groundwater phosphate distribution in a shallow aquifer, Nanfei River basin, China. *Hydrogeology Journal*, 19(7): 1431-1442.

Robertson, W.D., 2008. Irreversible phosphorus sorption in septic system plumes? *Ground Water*, 46(1): 51-60.

Rosenberry, D.O., Lewandowski, J., Meinikmann, K., Nützmann, G., 2015. Groundwater - the disregarded component in lake water and nutrient budgets. Part 1: effects of groundwater on hydrology. *Hydrological Processes*, 29(13): 2895-2921.

Roy, J.W., Robillard, J.M., Watson, S.B., Hayashi, M., 2009. Non-intrusive characterization methods for wastewater-affected groundwater plumes discharging to an alpine lake. *Environmental Monitoring and Assessment*, 149(1-4): 201-211.

Rutsch, M., Rieckermann, J., Cullmann, J., Ellis, J.B., Vollertsen, J., Krebs, P., 2008. Towards a better understanding of sewer exfiltration. *Water Research*, 42(10-11): 2385-2394.

Scharf, B.W., 1998. Eutrophication history of lake Arendsee (Germany). *Palaeogeography Palaeoclimatology Palaeoecology*, 140(1-4): 85-96.

Schauser, I., Lewandowski, J., Hupfer, M., 2003. Decision support for the selection of an appropriate in-lake measure to influence the phosphorus retention in sediments. *Water Research*, 37(4): 801-812.

Schirmer, M., Leschik, S., Musolff, A., 2013. Current research in urban hydrogeology - A review. *Advances in Water Resources*, 51: 280-291.

Schulz, L., 1981. Nährstoffeintrag in seen durch Badegäste (Nutrient inputs to lakes by bathers, in German). *Zentralbl Bakteriol Mikrobiol Hyg B.*, 73(6): 528-548.

Shaw, R.D., Shaw, J.F.H., Fricker, H., Prepas, E.E., 1990. An integrated approach to quantify groundwater transport of phosphorus to Narrow Lake, Alberta. *Limnology and Oceanography*, 35(4): 870-886.

Sondergaard, M., Jeppesen, E., 2007. Anthropogenic impacts on lake and stream ecosystems, and approaches to restoration. *Journal of Applied Ecology*, 44(6): 1089-1094.

Spiteri, C., Slomp, C.P., Regnier, P., Meile, C., Van Cappellen, P., 2007. Modelling the geochemical fate and transport of wastewater-derived phosphorus in contrasting groundwater systems. *Journal of Contaminant Hydrology*, 92(1-2): 87-108.

USGS, 2014. Phosphorus Doesn't Migrate in Ground Water? Better Think Again! US Geological Survey.

Vanek, V., 1991. Riparian zone as a source of phosphorus for a groundwater-dominated lake. *Water Research*, 25(4): 409-418.

Vanek, V., 1993. Transport of groundwater-borne phosphorus to Lake Bysjon, South Sweden. *Hydrobiologia*, 251(1-3): 211-216.

Wakida, F.T., Lerner, D.N., 2005. Non-agricultural sources of groundwater nitrate: a review and case study. *Water Research*, 39(1): 3-16.

Wilhelm, S.R., Schiff, S.L., Cherry, J.A., 1994. Biogeochemical evolution of domestic waste-water in septic systems. 1. Conceptual model. *Ground Water*, 32(6): 905-916.

Wischmeier, W.H., Smith, D.D., 1965. Predicting rainfall-erosion losses from cropland east of the Rocky-Mountains. *Agriculture Handbook* 282: 49 p.

Withers, P.J.A., Haygarth, P.M., 2007. Agriculture, phosphorus and eutrophication: a European perspective. *Soil Use and Management*, 23: 1-4.

Zanini, L., Robertson, W.D., Ptacek, C.J., Schiff, S.L., Mayer, T., 1998. Phosphorus characterization in sediments impacted by septic effluent at four sites in central Canada. *Journal of Contaminant Hydrology*, 33(3-4): 405-429.

Zhao, S., Zhang, P.F., Crusius, J., Kroeger, K.D., Bratton, J.F., 2011. Use of pharmaceuticals and pesticides to constrain nutrient sources in coastal groundwater of northwestern Long Island, New York, USA. *Journal of Environmental Monitoring*, 13(5): 1337-1343.

4 Development and improvement of approaches to determine lacustrine groundwater discharge

4.1 Empirical quantification of lacustrine groundwater discharge – different methods and their limitations

Karin Meinikmann,[1,2] Gunnar Nützmann,[1,2] and Jörg Lewandowski[1,2]

[1] Department of Ecohydrology, Leibniz-Institute of Freshwater Ecology and Inland Fisheries, Berlin, Germany

[2] Geography Department, Humboldt-Universität zu Berlin, Berlin, Germany

Citation:

Meinikmann, K., Nützmann, G., Lewandowski, J., 2015. Empirical quantification of lacustrine groundwater discharge – different methods and their limitations. *Proceedings of IAHS-IAPSO-IASPEI Assembly*, 365: 85-90. DOI: 10.5194/piahs-365-85-2015.

Abstract

Groundwater discharge into lakes (lacustrine groundwater discharge, LGD) can be an important driver of lake eutrophication. Its quantification is difficult for several reasons, and thus often neglected in water and nutrient budgets of lakes. In the present case several methods were applied to determine the expansion of the subsurface catchment, to reveal areas of main LGD and to identify the variability of LGD intensity. Size and shape of the subsurface catchment served as a prerequisite in order to calculate long-term groundwater recharge and thus the overall amount of LGD. Isotopic composition of near-shore groundwater was investigated to validate the quality of catchment delineation in near-shore areas. Heat as a natural tracer for groundwater–surface water interactions was used to find spatial variations of LGD intensity. Via an analytical solution of the heat transport equation, LGD rates were calculated from temperature profiles of the lake bed. The method has some uncertainties, as can be found from the results of two measurement campaigns in different years. The present study reveals that a combination of several different methods is required for a reliable identification and quantification of LGD and groundwater-borne nutrient loads.

4.1.1 Introduction

Lacustrine groundwater discharge (LGD) is probably the term most difficult to determine in lake water balances. Due to its invisibility, its spatial and temporal variability, and other reasons (Lewandowski et al. 2015) LGD is mostly neglected and/or handled as a residual in the water balance. However, with high nutrient concentrations LGD might play a key role in lake nutrient budgets and should thus be considered carefully when external nutrient loads of lakes are calculated. For groundwater-borne nutrient loads the amount of groundwater entering a lake in a certain time period is a necessary prerequisite. It might be additionally important to consider spatial heterogeneity of LGD along the shoreline section where groundwater primarily enters the lake. Since nutrient concentrations can also vary along relatively small distances, LGD can drive the actual influence of high nutrient concentrations on the trophic state of a lake: nutrient loads can be low despite high concentrations, when LGD is small in the corresponding reach, while a combination of high concentrations and intense LGD leads to large nutrient loads (Meinikmann et al. 2013).

4.1.2 Methods

Study site

The study site is Lake Arendsee in northeastern Germany (Fig. 4.1) where intensive research on LGD was done to quantify the impact of groundwater on the water and nutrient budget of the lake. It has a size of 5.1 km^2, a maximum depth of 50 m, and a mean depth of about 30 m. Geologic composition of the aquifer material is highly diverse, with values for hydraulic conductivity (k_{sat}) ranging from 0.33×10^{-4} to 5.69×10^{-4}, indicating an equivalent spatial heterogeneity in LGD.

Validation of in- and exfiltration along the shoreline

The size and shape of the subsurface catchment of Lake Arendsee were determined by interpolation (kriging) of groundwater head measurements in the surrounding of Lake Arendsee (Meinikmann et al. 2013). Hydraulic head contour lines are a prerequisite for the determination of groundwater catchments. However, their reliability strongly depends on the amount of available head observation sites. To validate the expansion of the catchment in the close vicinity of the lake (i.e., to separate recharge (infiltration) and discharge (exfiltration) areas) knowledge about isotopic composition of near-shore groundwater can be helpful. Due to evaporation, surface waters have in general a different isotopic signature than groundwater:

Since water molecules with the lighter isotopes ^{1}H and ^{16}O evaporate faster than water molecules with the heavier isotopes ^{2}H and ^{18}O, the latter become enriched in the surface water. Resulting from this, near-shore groundwater in recharge (infiltration) areas should show an isotopic composition that is similar to that of the lake water, but different from discharging (exfiltrating) groundwater. In August 2013, near-shore groundwater was sampled from boreholes hand-drilled to 2 m below ground and at a distance of 5 to 20 m from the lake shore. Along the southern shoreline where most groundwater was expected to reach the lake, only a few samples were taken. In the eastern and western parts, as well as along the northern shoreline, sampling density was increased to 200 - 400 m distance between sampling sites. Additionally, a lake water sample was collected. Furthermore, 11 groundwater observation wells at six different sites south of the lake were also included in the isotopic investigations.

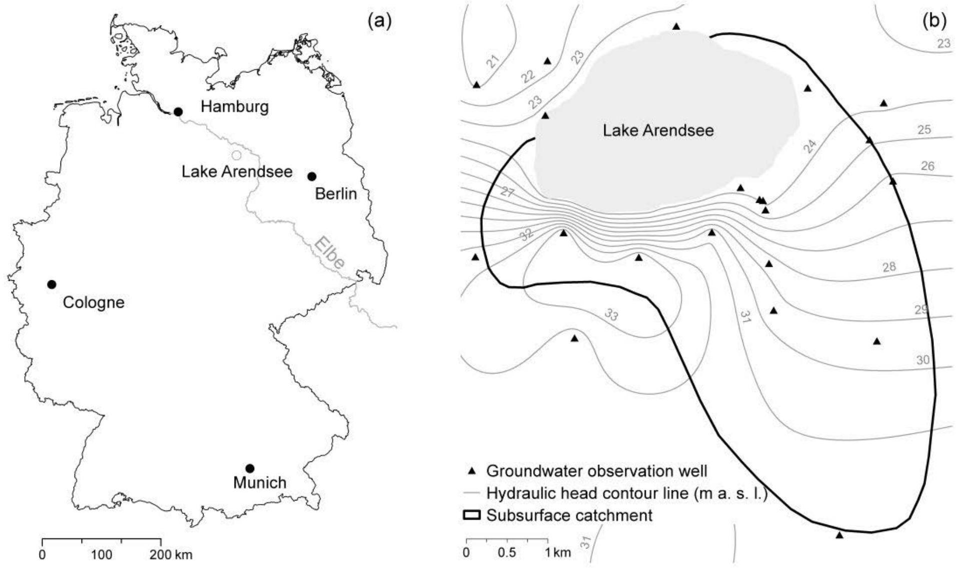

Figure 4.1 Location of Lake Arendsee within Germany (a), and hydraulic head contour lines (grey lines) interpolated from head measurements in groundwater observation wells (black triangles) as well as resulting expansion of the subsurface catchment of Lake Arendsee (black line) (b) (Meinikmann et al. 2013).

In situ-measurement of lacustrine groundwater discharge using heat as a tracer

Temperature differences between groundwater and surface water can be used as a natural tracer for groundwater–surface water interaction. By solving the heat transport equation (Eq. 4.1), profiles of lake bed temperatures can be analysed for Darcy velocities (q_z) or LGD rates, respectively.

$$\frac{T(z)-T_0}{T_L-T_0}=\frac{exp\left(\frac{q_z\,\rho_f c_f}{K_{fs}}z\right)-1}{exp\left(\frac{q_z\,\rho_f c_f}{K_{fs}}L\right)-1} \qquad \text{Eq. 4.1}$$

where L (m) is the vertical extent of the domain where temperature changes due to LGD, $T(z)$ is the lake bed temperature (°C) at sediment depth z (m), $T0$ is the temperature for $z = 0$ (i.e., surface water temperature, °C), T_L is the temperature for $z = L$ (i.e., groundwater temperature, °C), ρfcf is the volumetric heat capacity of the fluid (J m^{-3} K^{-1}), and Kfs is thermal conductivity of the saturated sediment (J s^{-1}m^{-1} K^{-1}). Schmidt et al. (2006) presented an analytical solution to derive q_z from

Equation 4.2 by minimizing the root mean squared error (RMSE) between the *n* measured temperatures of a profile and the related simulated temperatures:

$$RMSE = \sqrt{\frac{1}{n}\sum_{j=1}^{n}\left[T_j - \left(\frac{exp\left(\frac{q_z \rho_f c_f}{K_{fs}} z_j\right) - 1}{exp\left(\frac{q_z \rho_f c_f}{K_{fs}} L\right) - 1}(T_L - T_0) + T_0\right)\right]^2} \qquad \text{Eq. 4.2}$$

In September 2011 and July 2012, transects of four lake bed temperature profiles were measured in about 200 m distances along the southern, western and eastern shoreline. The western and eastern shorelines were not included in the first measurement campaign. A probe consisting of 16 temperature sensors (NTC 10K, TDK EPCOS, Munich, Germany) with a distance of 7 cm to each other, sampled sediment temperatures down to a depth of 0.98 cm. LGD is focused to near-shore areas of lakes (Kishel and Gerla 2002). Therefore, the investigations were done close to the shoreline. At each sampling site profiles were measured at 0.5, 1, 2 and 4 m distance to the shoreline. The goal of the measurements was to identify spatial patterns of LGD intensities along the shoreline. For maximal comparability the data of both measurement campaigns were analysed based on the same boundary conditions (i.e., L and T_L).

4.1.3 Results

Validation of in- and exfiltration along the shoreline

Hydraulic head contour lines indicated a main expansion of the subsurface catchment south of Lake Arendsee, with groundwater also discharging (exfiltrating) along the western and north-eastern shoreline (Fig. 4.1). Lake water recharging (infiltrating into) the aquifer was thus expected to appear along the northwestern and northern shoreline. Contour lines furthermore revealed a large hydraulic gradient at the south southeastern shoreline, indicating high LGD-rates in that area.

Measurements of the stable isotopes of oxygen and hydrogen identified two obviously differing groups of groundwater samples (Fig. 4.2a). Six near-shore samples as well as all samples from the subsurface catchment (ellipse in Fig. 4.2a) showed major differences to the lake water signature (black triangle in Fig. 4.2a). The rest of the samples showed compositions similar to the lake water, or indicated a mixture of lake water and groundwater. In Fig. 4.2b these results are depicted as the difference between lake water-δ^{18}O and groundwater-δ^{18}O. Accordingly, the symbol size in the map represents the similarity of the lake water signature to the groundwater signature. The above-mentioned six samples differing from lake water composition were exclusively taken along the southern part of the lake, while the rest of the near-shore sites are situated along the northern and northwestern shoreline. The results also indicate that the change in isotopic signature happens along a relatively short distance of 200 m at the western shoreline and 250 m at the northeastern shoreline, respectively.

In situ-measurement of lacustrine groundwater discharge

In September 2011 LGD rates derived from lake bed temperature profiles ranged between 0 and 131 l m^{-2} d^{-1} along the southern shoreline (Fig. 4.3a). Main LGD was indicated to occur along the southeastern shoreline, while along the southwestern shoreline no significant LGD was found from this method. Mean LGD of all measurements was 29 l m^{-2} d^{-1}. The measurements of July 2012 show a higher mean LGD rate of 44 l m^{-2} d^{-1}, although the maximum value was slightly lower (122 l m^{-2} d^{-1}). Highest exfiltration rates (60–122 l m^{-2} d^{-1}) were found along a 1900-m section at the southern shoreline. At the western and eastern shorelines LGD rates decreased and at some sites even turned to zero (Fig. 4.3b).

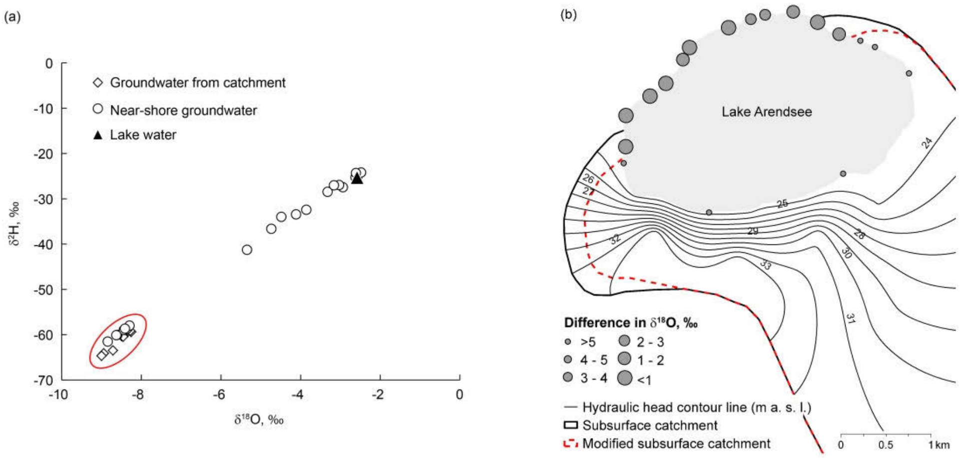

Figure 4.2 (a) Values for δ^{18}O and δ^{2}H for near-shore groundwater (circles), catchment groundwater (rectangles) and lake water (triangle). Two groups of samples are apparent, as there are those which show the isotopic composition of pure groundwater (within ellipse) and those which reveal an influence of lake water that infiltrates into the aquifer. (b) Subsurface catchment of Lake Arendsee (black line) derived from hydraulic head contour lines (grey lines) (Meinikmann et al., 2013). Results of stable isotope measurements are depicted as the difference between lake water-δ^{18}O and groundwater-δ^{18}O (in ‰). Due to the stable isotope signatures the subsurface catchment of the lake was slightly modified (dashed line).

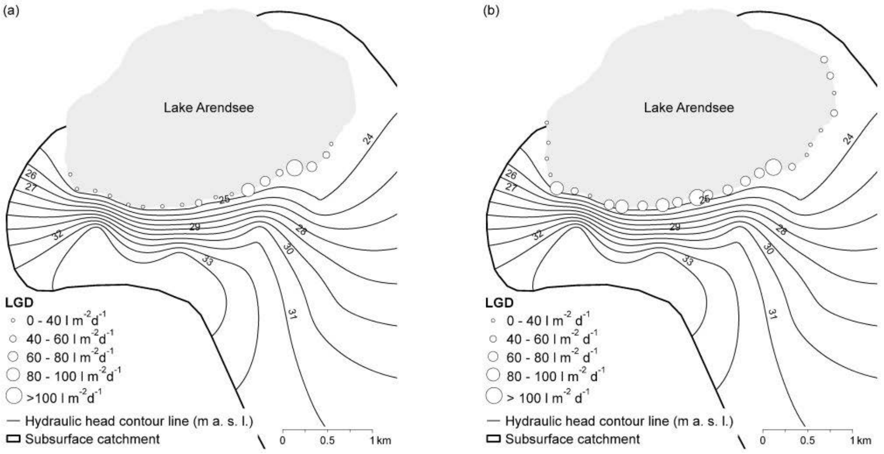

Figure 4.3. Maximum rates of lacustrine groundwater discharge (LGD, in l m^{-2} d^{-1}) derived from transects of four sediment temperature depth profiles at each observation site in September 2011 (a) and in July 2012 (b).

Some transects showed a good agreement of LGD rates between the two measurement campaigns in September 2011 and July 2012. Other transects revealed at least the same spatial pattern in both campaigns, even though the absolute values differ (triangles in Fig. 4.4a). There were also transects for which resulting LGD rates differ clearly between the different measurements (Fig. 4.4b). Many of the investigated transects showed a decreasing LGD rate with increasing distance to the shoreline, which is common for isotropic and homogenous sediments (McBride and Pfannkuch 1975).

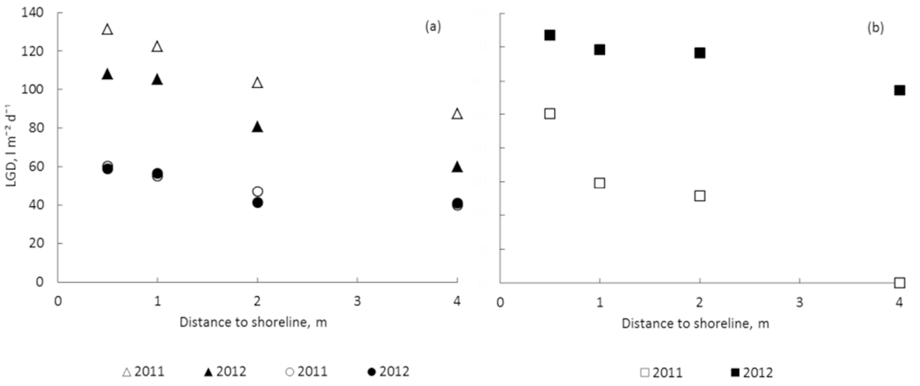

Figure 4.4 Lacustrine groundwater discharge (LGD) rates (in l m^{-2} d^{-1}) derived from temperature depth profiles of the lake bed sampled in September 2011 (empty symbols) and July 2012 (filled symbols) for three exemplary chosen transects. Circles represent a transect with a good agreement of both measurement, while triangles show a transect which shows the same spatial pattern of LGD with increasing distance to shoreline, but different absolute rates (a). Rectangles present a transect for which neither absolute LGD rates, nor spatial pattern of the two measurements coincide (b).

4.1.4 Discussion

In the case of Lake Arendsee the isotopic signatures of near-shore groundwater in general supported the delineation of the catchment based on hydraulic head contour lines. Modifying the subsurface catchment due to isotopic composition led to a slightly smaller catchment (4% of original size, see also Fig. 4.2b). A zone of mixing between groundwater and lake water due to fast temporal changes from recharging (infiltrating) to discharging (exfiltrating) conditions and *vice versa* cannot be identified from the data. Nevertheless, it is still possible that a sampling with higher spatial resolution or with a temporal resolution would reveal such zones.

Although the isotopic composition allows the determination of recharging (infiltrating) and discharging (exfiltrating) zones along the shoreline, it is not possible to deduce the quantity of LGD at the observation sites from these data. Therefore, other methods are needed. In the present study heat as a tracer was used to find out about the intensity of LGD along the shoreline. From the two measurement campaigns only the one in 2012 covered the entire LGD section. The results go well along with what was expected due to hydraulic head contour lines and reveal major LGD along the southern shoreline. Additionally, they disclose a spatial heterogeneity of LGD that could not be depicted adequately by hydraulic head contour lines alone. This heterogeneity can have a serious impact on groundwater-borne nutrient loads to the lake. With equal groundwater concentrations the main nutrient input would take place where the main LGD occurs. If spatially high nutrient concentrations occur (e.g., due to point contaminations of the aquifer) a "worst case scenario" has to be considered in which high LGD rates multiply with high concentrations to extraordinary large nutrient loads (Meinikmann et al. 2013). The temperature profiles revealed that in parts of the eastern and western shoreline, where isotopic compositions indicated discharging conditions, almost no flux of groundwater to the lake occurs. This can be attributed to decreased hydraulic gradients and the small expansion of the subsurface catchment.

LGD rates derived from lake bed temperature measurements in September 2011 indicated main groundwater exfiltration along the southeastern shoreline. Compared to the results of 2012 the section of main LGD was shifted slightly eastwards, while at the central southern shoreline no significant LGD occurred. Although the maximum LGD rate was higher than in 2012 the mean value of all calculated rates was clearly lower in 2011 (44 *vs* 29 l m^{-2} d^{-1}) and large parts of the southwestern shoreline did not contribute to LGD. Due to coverage of the entire discharge zone and better agreement to hydraulic head contour lines, the results from 2012 were determined to represent actual hydraulic conditions best. There might be several reasons for the discrepancies of the results of both measurement campaigns:

(a) Seasonality effects (maximum temperature difference between groundwater and surface water is required).
(b) Wrong estimation, measurement, or spatial upscaling of boundary conditions (e.g., T_L, L, or K_{fs} in Equations 4.1 and 4.2).
(c) Measurement and/or calibration errors.
(d) Small-scale heterogeneities in the lake bed (e.g., changes in k_{sat}).
(e) Temporal variations of hydraulic conditions along the shoreline.
(f) Abnormality in temperature profiles that are not caused by LGD (e.g., in coastal areas surface water enters the shore sediments and recirculates before being discharged again; Burnett et al. 2003).

Due to the aforementioned reasons the approach using heat as a tracer has some uncertainties concerning absolute values. Resulting LGD rates should not be used as a basis for upscaling to an overall amount of LGD. Still, they can be used as a powerful tool to gain insight into hydraulic patterns along a lake's shoreline. For example, we combined the results of temperature derived LGD rates with long-term annual groundwater recharge in the catchment of Lake Arendsee (Meinikmann et al. 2013). In the long run it can be assumed that a lake in a steady state receives the same amount of groundwater that is recharged in its catchment. Therefore, the calculation of groundwater recharge was found to be the most reliable method to derive a value for the overall amount of groundwater entering Lake Arendsee. In this context, temperature derived LGD rates were applied as a weighting factor for LGD intensity in shoreline sections. This reduced the influence of uncertainty in temperature-derived LGD rates.

4.1.5 Conclusion

Groundwater–surface water interactions are hard to quantify. Different methods, but also repetitions of the same method, lead to different results. Based on the study presented here we recommend a combination of as many methods as possible to validate the results of one method with those of another approach. The combination of point measurements and integrating approaches (taking the catchment into account) might help to reduce uncertainties. Furthermore, a high spatial resolution of measurements will increase the quality of the results, especially at heterogeneous sites. It might also be advantageous to find out about temporal variations of LGD, e.g., due to seasonal changes of groundwater heads or lake level control.

The current knowledge of eutrophication processes shows that groundwater can be the main reason for ongoing nutrient enrichment of surface waters. And although the investigations of LGD are labour-intensive, it might be of great importance to gain information on spatial quality and overall quantity of groundwater and related nutrient loads entering a lake.

4.1.6 References

Burnett, W.C., Bokuniewicz, H., Huettel, M., Moore, W.S., Taniguchi, M., 2003. Groundwater and pore water inputs to the coastal zone. *Biogeochemistry*, 66(1-2): 3-33.

Kishel, H.F., Gerla, P.J., 2002. Characteristics of preferential flow and groundwater discharge to Shingobee Lake, Minnesota, USA. *Hydrological Processes*, 16(10): 1921-1934.

Lewandowski, J., Meinikmann, K., Pöschke, F., Nützmann, G., Rosenberry, D.O., 2015. From submarine to lacustrine groundwater discharge. *Proceedings of IAHS-IAPSO-IASPEI Assembly*, 365: 72-78.

McBride, M.S., Pfannkuch, H.O., 1975. Distribution of seepage within lakebeds. *Journal of Research of the U.S. Geological Survey*, 3(5): 505-512.

Meinikmann, K., Lewandowski, J., Nutzmann, G., 2013. Lacustrine groundwater discharge: Combined determination of volumes and spatial patterns. *Journal of Hydrology*, 502(0): 202-211.

Schmidt, C., Bayer-Raich, M., Schirmer, M., 2006. Characterization of spatial heterogeneity of groundwater-stream water interactions using multiple depth streambed temperature measurements at the reach scale. *Hydrology and Earth System Sciences*, 10(6): 849-859.

4.2 Upscaling lacustrine groundwater discharge rates by fiber-optic distributed temperature sensing

Theresa Blume,[1] Stefan Krause,[2] Karin Meinikmann,[3,4] and Jörg Lewandowski[3,4]

[1] GFZ German Research Centre for Geosciences, Potsdam, Germany.

[2] School of Geography, Earth and Environmental Sciences, University of Birmingham, Birmingham, UK.

[3] Department of Ecohydrology, Leibniz-Institute of Freshwater Ecology and Inland Fisheries, Berlin, Germany.

[4] Geography Department, Humboldt-Universität zu Berlin, Berlin, Germany

This is the peer reviewed version of the following article:

Blume, T., Krause, S., Meinikmann, K., Lewandowski, J., 2013. Upscaling lacustrine groundwater discharge rates by fiber-optic distributed temperature sensing. *Water Resources Research*, 49(12): 7929-7944. DOI: 10.1002/2012WR013215.

Abstract

Despite the importance of groundwater inflow for water quantity and quality of many lakes worldwide, adequate methodologies for the determination of lacustrine groundwater discharge (LGD) rates at scales larger than the point scale and with sufficient spatial resolution are still lacking. Observations of suitably large data sets for the calculation of groundwater discharge rates by traditional methods are very time and labor intensive, often limiting the spatial extent or resolution of experimental investigations. The present study compares upscaling approaches that utilize information on LGD rates derived from a single transect of either sediment temperature profiles or vertical hydraulic gradients. Two transfer functions that integrate the single-transect information with spatially detailed temperature measurements based on fiber-optic distributed temperature sensing (FO-DTS) were developed and tested for their ability to identify 2-D patterns of LGD rates at larger scales. Results were compared with a simplified approach, based on the pragmatic assumption of exponential decline of LGD rates perpendicular to the shoreline. Both FO-DTS based upscaling approaches were able to reproduce the distinct small-scale heterogeneities in LGD patterns and quantities that were observed in an extensive reference survey using LGD estimates based on sediment temperature profiles. The transfer functions generated satisfactory representations of flow patterns, even when only low numbers (4 in this case) of reference measurements were used for their calibration, thus providing a successful proof of concept for this methodology and encouraging its further application at large scales.

4.2.1 Introduction

The water balance and chemistry of lakes with little or no surface inflow can be substantially impacted by the spatial pattern of lacustrine groundwater discharge (LGD) and corresponding fluxes of nutrient or pollutant inputs across the groundwater-surface water interface (Enell 1982; Loeb and Goldman 1979). The quantification of groundwater-borne loads requires the determination of both, water fluxes and concentrations of relevant compounds in groundwater discharge. Due to the spatial heterogeneity of exchange fluxes at the sediment-water interface, the determination of groundwater discharge and its chemical load is often a challenge. This study focuses on the identification and quantification of groundwater discharge and its spatial pattern.

Spatial patterns of seepage fluxes

Exchange fluxes between groundwater and surface water are controlled (i) by hydraulic head gradients between aquifer and lake as the driving force and (ii) by the spatial distribution of hydraulic conductivity of sediments at the aquifer-lake interface. Spatial variability in drivers (hydraulic head gradients) and controls (hydraulic conductivity) of exchange fluxes determine patterns of lacustrine groundwater discharge (LGD). Significant spatial heterogeneity of seepage fluxes has been revealed by a number of experimental studies (e.g., Cherkauer and Nader 1989; Kidmose et al. 2011; Kishel and Gerla 2002; Lautz and Ribaudo 2012). For example, Kishel and Gerla (2002) identified significant horizontal and vertical heterogeneity of flow directions and fluxes within a densely spaced grid of piezometers (every 2 m in a 10 x 10 m domain). Lautz and Ribaudo (2012) used flux rates from heat transport modeling based on time series and streambed temperatures to develop an upscaling approach for a 30 m stream reach.

For homogenous isotropic aquifers, LGD has been found to concentrate in a narrow band close to the shore (McBride and Pfannkuch 1975). As a consequence, shallow groundwater usually discharges close to the shore whereas smaller fluxes of deeper groundwater discharge more offshore (Frape and Patterson 1981; McBride and Pfannkuch 1975). Increased seepage rates at nearshore areas may also result from the spatial distribution of fine-grained, low-permeability muddy sediments in a lake. The depth of the muddy sediment is usually largest in the central parts of a lake and decreases toward the shore. Wave action can re-suspend light, freshly deposited material from shallow areas while material that settled in deeper parts of a lake is less affected. Thus, hydraulic conductivities of shoreline sediments are usually higher than of sediments from deeper lake sections (Kishel and Gerla 2002; Krabbenhoft et al. 1990a; McBride and Pfannkuch 1975). The fact that highest seepage rates usually occur in near vicinity to the shore is convenient for the experimental determination of seepage rates as measurements can be conducted in the shallowest and most accessible parts of the lake. In many lakes, this means that seepage measurements can be conducted by wading, rather than from boats or by diving (Shaw et al. 1990).

The spatial patterns of seepage rates in their relation to shore distances have been studied by direct measurements with seepage meters (Brock et al. 1982; Harvey et al. 2000; Lee 1977) and by the application of numerical models (e.g., Pfannkuch and Winter 1984; Schafran and Driscoll 1993; Shaw and Prepas 1990). However, the identification of spatial patterns and quantification of seepage fluxes across aquifer-lake interfaces is a major challenge. Quantitative approaches either treated an entire lake as a lumped system, and therefore estimations lacked detailed information on spatial patterns (Brock et al. 1982; Harvey et al. 2000; Krabbenhoft et al. 1994) or were based on point measurements, i.e., point estimates of local fluxes (Lee 1977). As point observations are representative for the specific local conditions and processes only, a large number of labor-intensive measurements is required and an extrapolation of these observations to the entire lake encompasses high uncertainty. Hence, current studies of lake water balances and nutrient budgets often lack adequate information of spatial patterns of seepage fluxes across the aquifer-lake interface, which critically limits the representativeness of results.

Quantitative methods for estimating seepage flow

Recent years have seen the development and application of a wide range of approaches for monitoring and quantifying LGD. Net exchange of groundwater has been estimated by identifying and solving the different components of the water balance equation (Belanger et al. 1985; Brock et al. 1982; Harvey et al. 2000). Furthermore, mass balances of stable isotopes (Krabbenhoft et al. 1994) or conservative chemical tracers such as chloride (Krabbenhoft and Webster 1995) have been used to quantify LGD. However, all mass balance approaches integrated spatial heterogeneities and temporal variability of the flow field and thus, did not provide spatially detailed information of exchange flow patterns (Krabbenhoft et al. 1990b).

In contrast to the aforementioned lumped approaches for entire lakes, seepage meters that are deployed at the sediment-water interface for measuring water fluxes over a specified area of the lake bed (Kalbus et al. 2006; Lee 1977) provide a possibility for direct monitoring of small-scale exchange fluxes between groundwater and surface water (Rosenberry 2005). Further indirect methods for quantifying LGD rates are based on Darcy's law and require detailed observations of pressure head gradients (e.g., in piezometers) and hydraulic conductivity of the local aquifer (Kishel and Gerla 2002; Stauffer 1985). Sediment depth profiles of temperature (Anibas et al. 2009; Meinikmann et al. 2013; Schmidt et al. 2006; Stonestrom and Constantz 2003) or conservative ions (Mortimer et al. 1999; Schuster et al. 2003) at the sediment-water interface have been successfully analyzed for indirect determination of water fluxes at the groundwater-surface water interface. However, the application of these methods is subject to certain assumptions (see sub-sections "*Depth Profiles of Sediment Temperatures to Determine LGD rates*" in the Material and Methods-section above and "*Estimation of LGD Rates*" in the Discussion-section below) and requires the existence of distinct differences in the respective characteristics of the groundwater and surface water end-members. If end-member characteristics are distinctive, fluxes can be calculated from the curvature of the observed gradient at the sediment-water interface. Dampening and phase shifts of diurnal temperature oscillations can be used if time series of temperature profiles are available (Constantz 2008; Hatch et al. 2006). Despite some problems in using temperature as a tracer arising from diurnal signal propagation during snapshot sampling or retardation effects (since temperature is not a conservative tracer) these methods have been successfully applied for the quantification of 1-D vertical fluxes at the groundwater-stream interface (Hannah et al. 2009; Hatch et al. 2006; Krause et al. 2011; Meinikmann et al. 2013).

Fiber-optic temperature sensing

Recent developments in fiber-optical sensor technologies provide a novel and robust methodology for investigating spatial patterns of exchange fluxes between groundwater and surface water by Fiber-Optic Distributed Temperature Sensing (FO-DTS) (Krause et al. 2012; Selker et al. 2006a; Selker et al. 2006b; Tyler et al. 2009). Based on the differences in groundwater and surface water temperatures, spatial patterns of groundwater discharge can be identified by tracing temperature anomalies at the sediment-water interface. Temperatures can be traced along fiber-optic cables of several kilometers length with currently 0.3–4 m spatial resolution and measurement precision of 0.05–0.1 °C for sampling intervals of 30 s (Hausner et al. 2011; Selker et al. 2006b; van de Giesen et al. 2012). In contrast to the aforementioned methodologies, FO-DTS is useful for spatially detailed measurements at larger scales, and therefore has the potential to provide temperature information for tracing LGD with high spatial resolution at scales exceeding previous detailed investigations of local flow. FO-DTS has successfully been applied for qualitative identification of complex of groundwater upwelling patterns in streams (Mwakanyamale et al. 2012; Slater et al. 2010), wetlands (Lowry et al. 2007), and coastal zones (Henderson et al. 2009). Hence, spatially detailed FO-DTS observations may provide an adequate measure to upscale detailed point observations or provide an efficient screening tool for identifying locations for detailed analyses of groundwater upwelling. The upscaling approach based on DTS data described in this study is novel as here DTS data are related to lacustrine groundwater discharge determined by both temperature profile gradients and vertical hydraulic gradients and thus allows for the quantification of flux rates. This is an important improvement of DTS application beyond simply visualizing the spatial pattern of groundwater discharge.

Objectives

The objective of the present study is to test whether FO-DTS-based upscaling of point measurements of lacustrine groundwater discharge rates is an adequate and feasible approach to represent the spatial heterogeneity of LGD rates. A transect of piezometers for determination of vertical hydraulic gradients is therefore combined with a manually measured grid of vertical temperature profiles and a FO-DTS survey of temperatures at the lake-aquifer interface. Obtaining a large data set of temperature profiles or vertical hydraulic gradients (VHG) is time consuming and tedious and hence often limits the spatial extent and resolution of experimental studies. We therefore derived and tested two upscaling methodologies based on information from a single transect of either temperature profile or VHG-derived LGD estimations. The two transfer functions combined this information with FO-DTS temperature measurements to identify detailed 2-D patterns of LGD rates at a larger scale. These DTS-based upscaling approaches were compared to a very simple 1-D-upscaling approach based on the assumption of exponential decline of LGD with distance to the shore.

4.2.2 Material and Methods

Research area: Lake Hinnensee

Lacustrine groundwater discharge (LGD) was investigated at a shore section of Lake Hinnensee, a groundwater dominated lake located in the north-eastern lowlands of Germany in the Mueritz National Park (Fig. 4.5). The landscape has been shaped by glacial and postglacial processes of the Weichsel glaciations and Lake Hinnensee was formed in a glacio-fluvial tunnel valley. The lake covers an area of 49 ha and has a maximum depth of 14 m (on average 7 m). At the southern end Lake Hinnensee is connected to Lake Fürstensee. The northern catchment boundary is constituted by a terminal moraine which coincides with the North Sea/Baltic Sea groundwater divide. However, most of the catchment is located in the outwash plain and soils are generally sandy. Elevations of the catchment range from 63 to 124 m above sea level. The majority of the catchment area is covered by forest with predominantly beech, pine and oak species. The lake is mesotrophic.

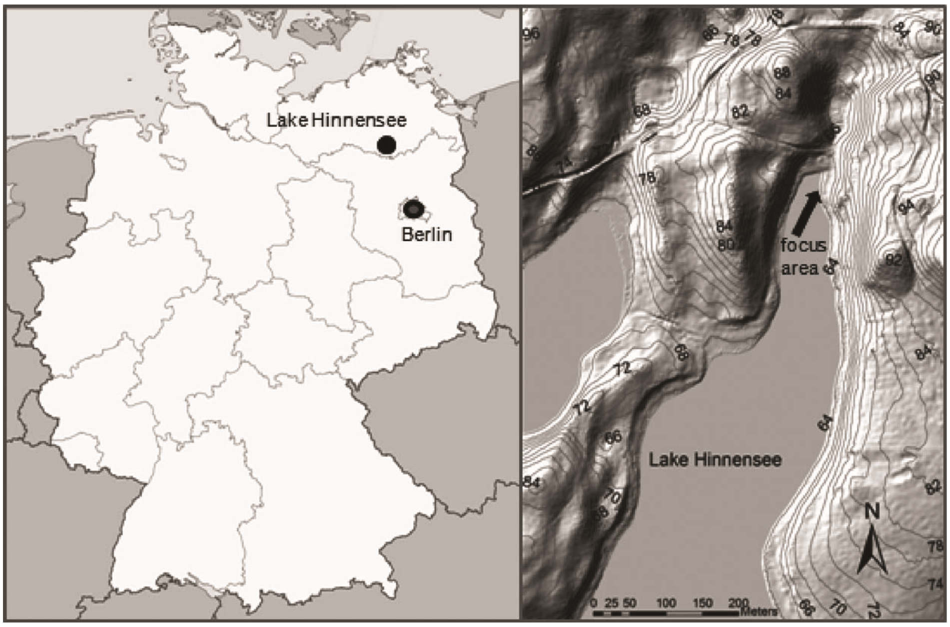

Figure 4.5 Location of Lake Hinnensee and the focus area.

The climate of the area is continental; mean annual rainfall recorded in Neustrelitz (10 km northwest of Lake Hinnensee) amounts to 610 mm (1901–2005, DWD German Weather Service) and mean annual temperature is 8.1 °C (1901–2005, DWD-German Weather Service).

The experimental investigations of this study focused on a 20 m long shore section at the northern tip of Lake Hinnensee (Figures 4.5 and 4.6). The land side of the study site is characterized by a margin of moderate slopes which become steeper with greater distance to the lake. The lake sediment of the study site is predominantly composed of fine and medium sand with some organic materials like branches, roots, and leaves. The southern end of the field site is covered by reeds. The topography of the lake bed at the field site is characterized by gentle slopes developing into steeper gradients at approximately 2–3 m distance to the shore (Fig. 4.6). The lake bed topography was surveyed along 10 transects perpendicular to the shoreline reaching 3–5 m into the lake.

Experimental design

The heterogeneity and patterns of groundwater-surface water interactions at the shore section were investigated by three different methods: (a) a transect of piezometers to determine vertical hydraulic gradients, (b) sediment temperature depth profiles measured manually with a temperature probe along a grid, and (c) temperature measurements along a fiber-optic cable (FO-DTS) deployed at the lake bed surface (Fig. 4.6).

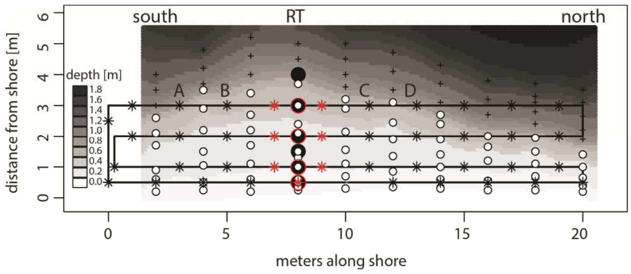

Figure 4.6 Experimental layout: Lake bathymetry along the investigated shoreline. White circles indicate locations where sediment temperature profiles and water depth were measured, black crosses show locations where only water depth was surveyed and black circles mark the locations of piezometers. The transect where the piezometers are located is called the reference transect (RT). The black line indicates the positioning of the fiber-optic cable and the stars mark the DTS sampling locations (note that DTS data is integrated over 4 m with the DTS system used here). The sediment core was taken at 1 m distance from shore at the reference transect (RT). Data points used for the final transfer functions are plotted in red while the other transects are indicated by the letters A to D.

Vertical hydraulic head gradients at piezometers and determination of LGD rates

Vertical hydraulic gradients (VHG), indicating the strength and direction of exchange fluxes between groundwater and lake, were determined from hydraulic head measurements along a transect of nearshore piezometers. Polyvinyl chloride (PVC) piezometers of 32 mm inner diameter and a 10 cm bottom screening section were installed within the lake sediments to depths of 50, 100, and 150 cm at 0.5, 1.0, 1.5, 2.0, 2.5, and 3.5 m distance to the shoreline (reference transect RT, Fig. 4.6). Hydraulic heads in the piezometers were monitored manually on 15 September 2010 and 16 September 2010 using a graduated electric contact meter (dip-meter). Based on Δh, the elevation difference of the groundwater observed inside and the lake water table outside the piezometer and Δl given by the distance between the mid-screen depth and the sediment-water interface, VHG were calculated by $\Delta h/\Delta l$. The accuracy of dip-meter-based hydraulic head observations was approximately ±2 mm head and accounts for uncertainties in the measurements introduced by small wind-induced waves around the piezometers, which can affect the outside head estimates but are assumed to be smaller than in river environments with turbulent flow (Käser et al. 2009; Krause et al. 2009), especially as wind velocities were low during the measurements (1 m s^{-1} on average). The hydraulic conductivity of the lake sediment was estimated using four different methodologies. A 108 cm long sediment core was taken at 1 m distance from the shore at the piezometer transect (see Fig. 4.6). The core was split into 11 samples of approximately 10 cm length and grain size distributions were determined in the lab. In order to obtain hydraulic conductivities, these grain size distributions were used as input for the pedotransfer function model Rosetta (United States Salinity Laboratory, release date 1999, http://www.ars.usda.gov/Services/docs.htm?docid58953) and the Hazen approximation $Ks = 0.0116 \cdot d_{10}^2$, with Ks being the hydraulic conductivity in m s^{-1} and d_{10} being the grain size diameter that bounds the lowest 10% percentile of the sample in mm. For both methods, Ks was determined for each sample individually and then was averaged over the profile using the geometric mean. These results were compared to the Ks value determined with the Hvorslev method based on pump test data from a piezometer at the field site at 1.8 m distance from shore (pump test carried out in 2012). Finally, Ks was also inferred as a result of an optimization by fitting the VHG-based exfiltration rates to the temperature profile-based exfiltration rates at the same locations.

LGD rates were calculated using the observed vertical hydraulic gradients and the estimated hydraulic conductivities:

$$LGD_{rate} = K_s \times A \times VHG \times 1000 \quad \text{Eq. 4.3}$$

with LGD_{rate} in l m^{-2} d^{-1}, K_s being the mean hydraulic conductivity in m d^{-1}, and A the unit area in m^2. Vertical hydraulic gradients (VHG) are given in m m^{-1}.

Depth profiles of sediment temperatures to determine LGD rates

Temperature depth profiles of the lake sediment were measured from 14th to 16th September (two thirds of the profiles on 15th September) with a high-precision digital thermometer (Greisinger GMH 3750) equipped with a needle thermocouple (Greisinger GES 401, needle of 45 cm length and 3 mm diameter, sensor element Pt100 in the tip of the needle, accuracy ±0.03°C). The needle was inserted several centimeters deep into the sediment and after reaching a constant temperature, sediment depth and temperature were recorded. Usually, constant temperature values were reached within less than 2 min. Afterward, the needle was pushed deeper into the sediment. That procedure was repeated until reaching the maximum penetration depth of the needle which was limited to 45 cm. At five locations, reaching the maximum depth was prevented by obstacles (stones, roots) in 35 to 45 cm depth. Usually surface water temperature and temperatures at six or seven depths were recorded for each depth profile. Depth profiles were measured along a gridded design with 10 transects from the shore into the lake (see Fig. 4.6). Transects were spaced 2 m apart. The extent of the transects into the lake depended on the local bathymetry and was limited by the requirement to reach the lake bottom for probe injection. Thus, transects varied in length between 1 and 4 m. The reference transect (RT) was measured both on 14th and 15th September. Surface water temperature during the 3 days of the measurement campaign varied from 16.1 to 17.3°C.

For calculating LGD rates based on depth profiles of sediment temperature, the procedure described by Schmidt et al. (2006) was followed. With the assumption that groundwater flow in the sediment is vertical, the governing equation for 1-D conductive and advective heat transport is

$$K_{fs}\frac{\partial^2 T(z)}{\partial z^2} - q_z \rho_f c_f \frac{\partial T(z)}{\partial z} = \rho c \frac{\partial T(z)}{\partial t} \qquad \text{Eq. 4.4}$$

where: K_{fs} (J s^{-1} m^{-1} K^{-1}) is the thermal conductivity of the saturated sediment; $T(z)$ (°C) is the streambed temperature at depth z; q_z is the vertical flux (m s^{-1}); $\varrho_f c_f$ (J m^{-3} K^{-1}) is the volumetric heat capacity of the fluid; ϱc (J m^{-3} K^{-1}) is the volumetric heat capacity of the saturated sediment; and t is the time (s).

A further prerequisite for the application of the method using temperature depth profiles is the assumption that the system is at steady state. Under this condition, the term right of the equal sign of Equation 4.4 is zero (Anibas et al. 2009). Bredehoeft and Papadopulos (1965) presented an analytical solution for this case given in Equation 4.5.

$$T(z) = \frac{exp\left(\frac{q_z \rho_f c_f}{K_{fs}} z\right) - 1}{exp\left(\frac{q_z \rho_f c_f}{K_{fs}} L\right) - 1}(T_L - T_0) + T_0 \qquad \text{Eq. 4.5}$$

where: L (m) is the depth of the lower boundary, i.e., the thickness of the zone in which vertical changes of the temperature occur due to temperature differences between groundwater and lake water; T_0 (°C) and T_L (°C) are the constant temperatures at the upper (surface water) and lower (groundwater) boundaries, respectively.

The temperature of the lower boundary T_L was estimated as 11°C based on measurements in the 1–1.5 m deep piezometers close to the shoreline. 11°C seems a plausible value for the near-surface aquifer underneath a forest. The value for the volumetric heat capacity $\varrho_f c_f$ of the water ($4.19 \cdot 10^6$ J m^{-3} K^{-1}) was obtained from literature. Values for the thermal conductivity K_{fs} of saturated sediments have a much smaller range (1.4–2.2 J s^{-1} m^{-1} °C^{-1}) than the hydraulic conductivity and are almost independent of sediment texture (Stonestrom and Constantz 2003). The thermal conductivity K_{fs} of Lake Hinnensee sediment was not measured within this study but based on values reported by Stonestrom and Constantz (2003) was estimated to be 2 J s^{-1} m^{-1} °C^{-1}.

The flux q_z was estimated by fitting the analytical solution of the heat transport equation (using the Microsoft Office Excel 2003 Solver) for each temperature depth profile so that the root mean squared error (RMSE) between measured temperatures $T_{meas}(z)$ and the ones modeled based on Equation 4.4 was minimal for the profiles consisting of *m* points:

$$RMSE = \sqrt{\frac{1}{m}\sum_{j=1}^{m}\left(T_{meas}(z_j) - T(z_j)\right)^2} \qquad \text{Eq. 4.6}$$

The calculation of the RMSE (Eq. 4.6) requires $T(z)$ to be calculated which furthermore requires information on the interface thickness L Equation 4.5. For every depth profile, 34 different values for L ranging from 0.5 to 10 m (with 0.1 m intervals between 0.5 and 2.6 m and then gradually larger spacing) were tested in order to establish the impact of a change of L on q_z and on the quality of the fit. To determine the optimal interface thickness L, we calculated for each L the arithmetic mean of the RMSEs of all 67 temperature depth profiles and determined for which L the minimum of the arithmetic mean of the RMSEs was reached.

Distributed fiber-optic temperature sensing (FO-DTS)

Fiber-optic Distributed Temperature Sensing (FO-DTS) was used to investigate temperature patterns at the sediment-water interface as this pattern can be strongly linked to patterns in LGD. FO-DTS uses the temperature-dependent backscatter properties of a laser signal that propagates through a fiber-optic cable (Selker et al. 2006a; Selker et al. 2006b; Tyler et al. 2009). The FO-DTS method applied in this project analyses the offset in the backscatter of Raman Stokes (temperature independent) and anti-Stokes (temperature dependent) signals from a 10 ns light pulse to undertake and locate temperature measurements along the fiber-optic cable (Selker et al. 2006a; Selker et al. 2006b). The applied DTS system (Sensornet Halo) is capable of measuring temperature at high precision (0.05 °C) with a sampling resolution of 2 m (Sensornet 2009) and a spatial resolution of 4 m (van de Giesen et al. 2012). For the temperature survey, a gel-coated, plastic covered two channel fiber-optic cable (Bru-Pro, Brugg/CH) was deployed at the sediment surface (ensured by carefully inspecting cable position during installation) in a setup of four parallel loops with 0.5, 1, 2, and 3 m distance to the shoreline (Fig. 4.6). Good contact to the sediment is essential as floating cables will measure lake water temperature only.

DTS measurements were carried out on 15th September. A single-ended measurement setup was deployed with alternating sampling directions that applied the laser pulse to different ends of the fiber-optic cable. Measurements were taken for 30 s intervals in each direction. As one direction showed much less noise than the other, only these traces were averaged (average over 20 traces resulting in a 20 in temporal average). In order to calculate temperature offset and losses along the cable, sections of both cable ends were calibrated in temperature controlled warm/cold baths covering length sections 8–10 times the sampling resolution. Control bath temperatures determined by the DTS measurements after calibration reproduced the temperatures measured with the handheld temperature probe with an RMSE of 0.029, 0.028, 0.050, and 0.102°C for the four calibration sections. The effect of solar radiation on cable temperature is likely to be of minor importance for this study, as the shoreline is well shaded by trees (with even more pronounced shading during the first half of the day when the cable was installed and measurements were carried out). Furthermore, the days of the study were cloudy to partially cloudy and quite cool.

Upscaling LGD rates: From single transect to shore section

The potential of upscaling single-transect measurements of LGD to the entire shore section was investigated with three different methodologies: (a) a transfer function upscaling temperature profile-based LGD rates by using DTS temperatures, (b) a transfer function upscaling VHG-based LGD rates by using DTS temperatures, and (c) a simple exponential decline function fitted to the reference transect of temperature profile-based LGD rates. All data used for the development for the three transfer functions stemmed from the reference transect (RT) where measurements of both VHG and temperature profiles were available. The interpolated surface of LGD rates based on the entire data set of temperature profiles was used for the purpose of comparison and model evaluation.

In case a and b, a simple regression was carried out to obtain the transfer function. Based on the data set from the temperature profiles, three different model types were investigated for their suitability: linear, exponential and quadratic. This was done using the entire data set, for half the data set and for five different single transects: transects A–D and the reference transect (RT) (for locations see Fig. 4.6). As only one of the DTS sample points is located directly at the reference transect (RT), the DTS measurements to the left and right of the reference transect were simply averaged to obtain paired values of DTS temperatures and LGD rates based either on VHGs or temperature profiles ($n = 4$). The exponential function of case c is based on 12 values of LGD derived from sediment temperature depth profiles and was fitted using Microsoft Excel Solver. Model/upscaling performance was evaluated using RMSE, sum of residuals and comparing the median, mean, minimum and maximum LGD rates of the predicted data set versus the LGD rates determined from the temperature profiles. Note that the LGD rates based on temperature profiles are also not a direct measurement and subject to a number of assumptions. Unless otherwise indicated data analysis was carried out with the statistical computing software R.

4.2.3 Results

Vertical hydraulic gradients

Observations of VHGs along the piezometer transect installed into the lake sediment revealed positive values throughout (Fig. 4.7), ranging from 0 to 0.047. VHGs varied strongly horizontally along the piezometer transect and slightly for different observation depths. VHGs steadily declined with increasing distance to the shore (Fig. 4.7). LGD rates were determined using the vertical hydraulic gradients for 1.5 m depth and the estimated *Ks* value as input to Equation 4.3. VHGs from this depth were chosen as they showed a similar decline with distance to shore as the LGD rates determined from temperature profiles. VHG uncertainty at this depth is much smaller compared to the shallower depth (the smaller Δh, the larger the effect of the error of ±2 mm). Hydraulic conductivities *Ks* estimated by

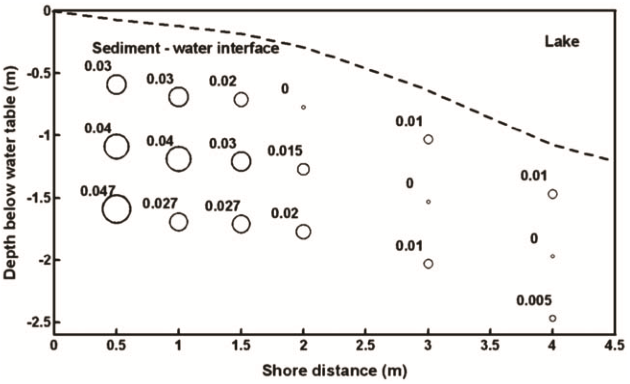

Figure 4.7 Vertical hydraulic gradients at the piezometer transect (RT).

both the pedotransfer function model Rosetta and the Hazen approximation were based on the grain size distributions of the sediment core samples summarized in Table 4.1. *Ks* values ranged from 1.4 to $1.6 \cdot 10^{-4}$ m s^{-1} with a geometric mean of $1.53 \cdot 10^{-4}$ m s^{-1} for the Rosetta model and from 0.5 to $1.8 \cdot 10^{-4}$ m s^{-1} with a geometric mean of $0.6 \cdot 10^{-4}$ m s^{-1} for the Hazen approximation. However, both the pump test analysis using the Hvorslev method as well as the optimization of *Ks* based on fitting VHG exfiltration rates to the exfiltration rates determined from temperature profiles resulted in lower *Ks* with values of $2.45 \cdot 10^{-5}$ m s^{-1} for the pump test and $3.1 \cdot 10^{-5}$ m s^{-1} for the optimization. The optimized *Ks* is quite close to *Ks* determined from the single-pump test (a more reliable method compared to the approximations based on grain sizes as it is carried out *in situ*).

Table 4.1 Mean grain size distribution including standard deviations obtained from the sediment core taken at the investigated shore section.[a]

Grain Size (µm)	%	Standard Deviation
>2000	5.6	2.2
>1000	5.3	2.2
>500	14.3	6.4
>250	38.6	11.6
>125	29.3	9.8
>63	6.3	4.5
>32	0.3	0.2
<32	0.4	0.2

[a] Values are averaged over the 11 samples taken every 10 cm along the core.

As the optimized *Ks* is furthermore based on four data points instead of a single measurement the optimized value was chosen for the determination of LGD rates. Based on this *Ks* and the VHGs, the LGD rates ranged from 27 l m^{-2} d^{-1} at 3 m, 55 l m^{-2} d^{-1} at 2 m, 73 l m^{-2} d^{-1} at 1 m, and 128 l m^{-2} d^{-1} at 0.5 m distance to the shore (Fig. 4.11c).

Temperature depth profiles

Temperature patterns. Surface water temperature varied from 16.1 to 17.3 °C during the 3 days of the measurement campaign, while groundwater temperature was constant with approximately 11 °C.

The entire data set of manual measurements in combination with the corresponding depths below the water table is shown in Figure 4.8. Transects are plotted starting from the south (to the left) of the shore section. Lowest temperatures were measured at the deepest parts of the profiles in the first meter closest to the shore. This is found to be less pronounced in both of the most southern and northern transects. No clear relationship between temperature patterns and bathymetry could be identified. However, a strong increase of temperatures with increasing distance to the shoreline (exemplary for one depth in Fig. 4.9) was found for all sediment depths.

Determination of LGD rates from temperature profiles. For each vertical temperature profile the flux q_z was calculated based on the solution to the heat transport equation (Eq. 4.5) by minimizing the root mean squared error (RMSE) between measured and simulated temperature profiles (Eq. 4.6). Simulated temperature depth profiles generally fit the measured temperature depth profiles well (RMSE: minimum 0.021 °C, arithmetic mean 0.082 °C, 90% quantil 0.132 °C, maximum 0.187 °C, $n = 67$) as can be seen for five examples in Figure 4.10. The model sensitivity to different interface thicknesses L was tested using the approach described in section 2.2.2. Based on the analysis of all 67 depth profiles, an interface thickness L of 2 m resulted in the lowest RMSE. In result, q_z appeared to be independent of L for L larger than a certain threshold (specific to each depth profile), i.e., the resulting fluxes were not influenced by L as long as L was chosen large enough to extend into the zone of spatially constant groundwater temperature. At Lake Hinnensee, LGD rates were found to be essentially independent of L at interface thicknesses L>2 m with a slight optimum at L = 2 m. This agreed with the findings of Schmidt et al. (2006), while Jensen and Engesgaard simply assumed an L of 5 m for their study (Jensen and Engesgaard 2011).

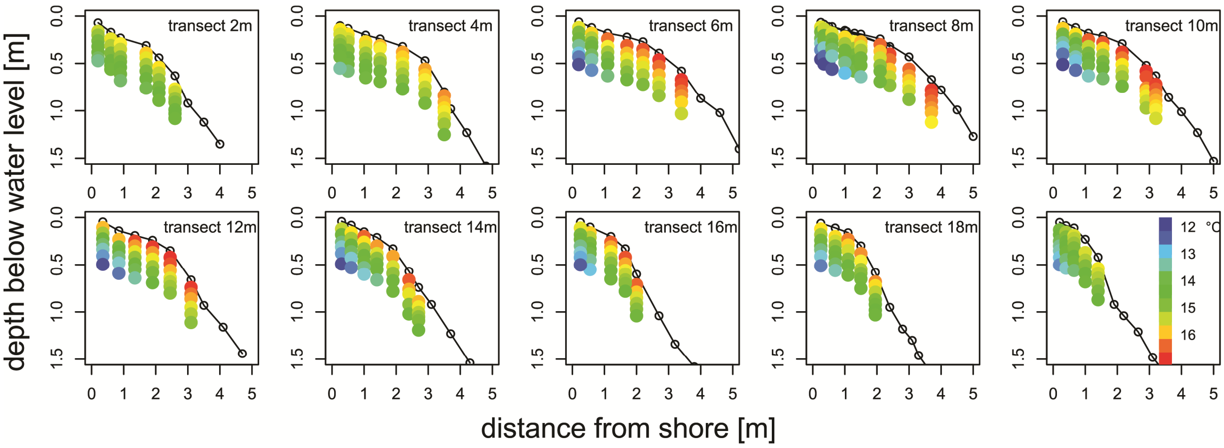

Figure 4.8 Transects of depth profiles of temperatures along the investigated shore section from south to north including the corresponding bathymetry (black line). Open circles indicate positions where the water depth was measured but no temperature depth profiles were recorded.

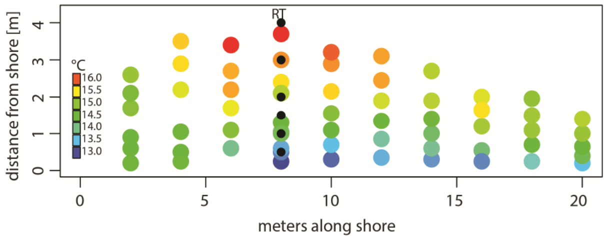

Figure 4.9 Exemplary temperature pattern along the shore section at a specific depth in the sediment, here for the depth of 26 - 32 cm. Black circles indicate the location of the piezometers and the reference transect (RT).

LGD rates determined by fitting the heat transport equation to the temperature profiles generally showed a rapid decrease with distance to shore (Fig. 4.11), similar to the LGD rates determined using VHGs (Figure 4.11c). The maximum LGD rate was found in 25 cm distance to the shore with 169 l m^{-2} d^{-1} at the reference transect (RT) (Fig. 4.11). For the neighboring transects (at 6 - 16 m), maximum LGD rates of 129 - 157 l m^{-2} d^{-1} were found at 20 - 35 cm distance to the shore (Fig. 4.11b). LGD rates at greater distances to the shore dropped to almost zero. It was found that LGD rates (q_z) decreased exponentially:

$$q_z(d_s) = a \cdot e^{-bd_s} \qquad \text{Eq. 4.7}$$

where d_s is the distance to the shore and a and b are fitting parameters.

Parameters *a* and *b* were estimated with the Microsoft Office Excel 2003 Solver based on all q_z estimates of a transect so that the root mean squared error (RMSE) between q_z estimates and $q_z(d_s)$ calculations (Eq. 4.7) was minimal. As shown in Figure 4.11b, the estimates of $q_z(d_s)$ based on ds matched the values for q_z estimated by fitting the heat transport equation quite well (RMSE: minimum 1.19 l m^{-2} d^{-1}, arithmetic mean 4.93 l m^{-2} d^{-1}, 90%-quantil 7.28 l m^{-2} d^{-1}, maximum 7.37 l m^{-2} d^{-1}, $n = 12$). Under the assumption that the exponential decrease of q_z defined by Equation 4.7 can be extrapolated further offshore we calculated that for all except the most southern transect more than 70% of LGD occurred within the first 2 m and more than 90% within the first 4 m distance from the shore. For the most southern transect of the study site, 90% of LGD occurred within 8.4 m from the shore.

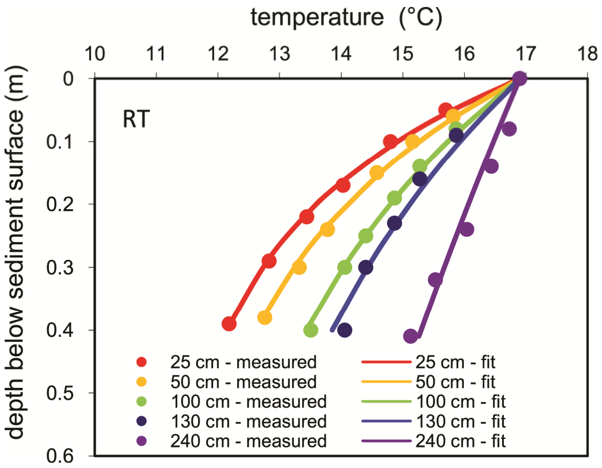

Figure 4.10 Comparison of measured and simulated depth profiles of sediment temperature based on the heat transport equation. Distance from shore increases from 25 to 240 cm. Examples shown here are from the reference transect (RT).

Fiber-Optic Distributed Temperature Sensing

Temperature patterns obtained with DTS showed a general increase of lake bed surface temperature with distance to the shore (Fig. 4.12). The lowest temperatures measured by FO-DTS were found in the midsection of the fiber-optic cable line closest to the shore. FO-DTS data covered a range of only 15.0–15.7 °C, while profile temperatures closest to the surface at 4–8 cm depth ranged from 14.9 to 17.0 °C. This discrepancy is possibly due to temperature fluctuations in the cold bath (which would be causing a general underestimation of temperatures) as well as a result of the fact that DTS measurements were carried out at noon, while most of the manual temperature measurements were carried out later in the day. However, these discrepancies are unlikely to affect our analyses (for more details see section "*Upscaling Transect Measurements of LGD*" below). The fact that the range of the DTS temperatures is smaller than that of the manual measurements is discussed below in section 4.2.4.

Upscaling transect measurements of LGD to the shore section

DTS temperatures and LGD rates determined with depth profiles of sediment temperature were well correlated with a correlation coefficient of 0.87 for the entire shore section. A transfer function relating FO-DTS temperatures to LGD rates determined with temperature depth profiles was derived based on a number of different setups from using the entire data set to using only four data pairs of FO-DTS temperatures and LGD rates at either of the transects A to D and at the reference transect (RT). As these transfer functions rely only on the patterns of DTS temperatures and their correlation with LGD

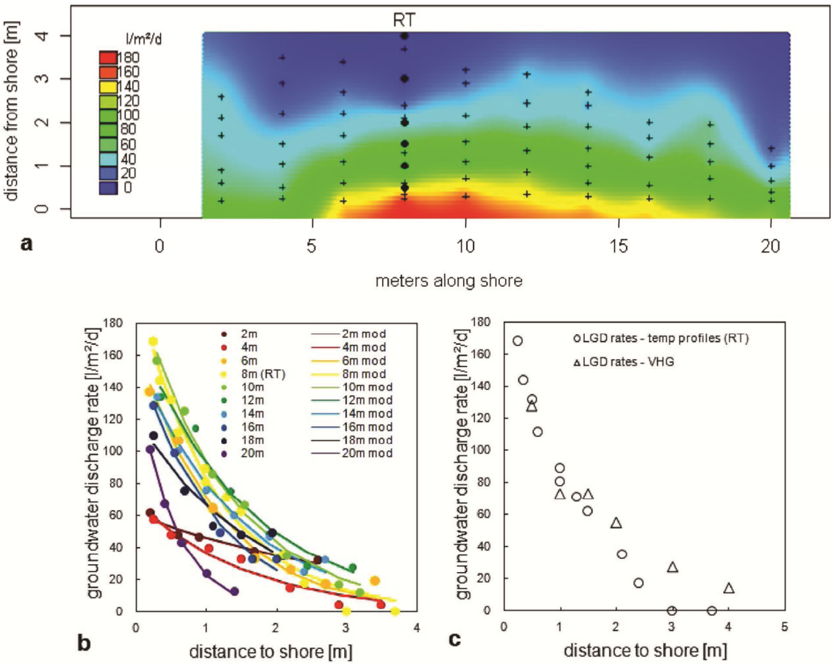

Figure 4.11 (a) Interpolated LGD rates in l m^{-2} d^{-1}; crosses mark locations of temperature depth profile measurements on which LGD rate calculations using the heat transport equation were based, black circles mark the location of piezometers. (b) LGD rates for all transects. Circles show values determined from temperature profiles with the heat transport equation, lines show LGD rates modeled with Equation 4.2e as exponential decrease with distance to shore. (c) Comparison of LGD rates for the reference transect (RT) based on temperature profiles and VHGs.

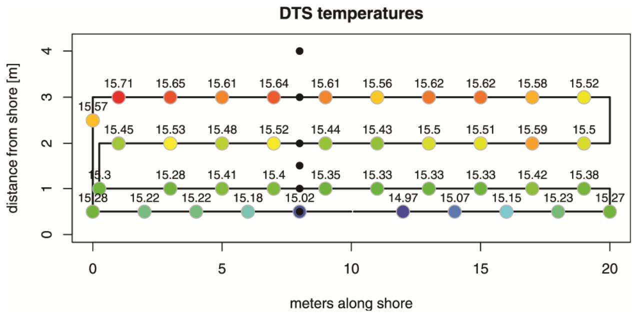

Figure 4.12 FO-DTS temperature data (2 m sampling resolution along the DTS cable).

rates a general shift in DTS temperatures due to possible underestimation will not affect model efficiency. Comparing linear models with exponential and quadratic transfer functions yielded that the exponential model produced consistently worse correlation coefficients and was therefore excluded from further analysis. In a next step, the linear and the quadratic models were evaluated in their performance and concerning the choice of calibration data set. It was found that the quadratic model did not produce better results than the simple linear model (even when using larger data sets than just one transect) (Fig. 4.13 and Table 4.2). Given its simplicity we therefore chose the linear model as a transfer function of DTS temperatures to LGD rates. We furthermore found that the choice of transect influences the performance of the model (Table 4.2). Transect A seems to be the least suited transect for this type of analysis, likely because it covers both a smaller range of DTS temperatures as well as LGD rates. Transect B and the reference transect RT performed best among the transects.

However, if we remove transect A from the comparison all linear transect models produce reasonable RMSE values. Median LGD rates can be overestimated by up to about 20% depending on choice of transect, mean and maximum LGD rates can also be slightly overestimated (generally less than 15%). The 50% model is generally just as good as the model using all data points for calibration (100% model). Both these models perform better than the models based on single transects alone. However, given their conservativeness in data needs the transect-based models perform surprisingly well and have the definite advantage of minimizing field effort. The performance measures for all models are summarized in Table 4.2. The lower left plot of Figure 4.13 shows the linear regressions of the five transect models and the lower mid plot the predicted values for the entire data set. The bad performance of transect model A becomes clear in a significant under-prediction of LGD rates.

Table 4.2 RMSE (calculated between output of the three upscaling methodologies at the DTS sampling locations and the interpolated surface of the temperature profile-based LGD rates), the sum of the residuals (as measure of bias) as well as mean, median, and range of LGD rates.

Upscaling methodology	RMSE ($l\ m^{-2}\ day^{-1}$)	Sum of residuals ($l\ m^{-2}\ day^{-1}$)	Median LGD ($l\ m^{-2}\ day^{-1}$)	Mean LGD ($l\ m^{-2}\ day^{-1}$)	Range of LGD ($l\ m^{-2}\ day^{-1}$)
From temperature profiles: Linear					
Transect A	33.3	353	31.5	33.2	11.5-65.1
Transect B	23.4	-63	48.1	54.3	-23.9-169.4
Transect C	18.7	192	55.2	59.4	6.3-137.5
Transect D	20.7	396	60.1	63.9	15.7-134.8
Ref. transect (RT)	19.4	-63	46.3	51.5	-14.0-147.8
50% of profiles	17.7	5	49.4	53.7	-0.2-132.9
100% of profiles	17.7	-1	49.4	53.5	0.7-131.3
Quadratic					
Transect A	33.17	-732	32.8	35	11.5-62.6
Transect B	24.98	-35	42.3	52	-179-183.3
Transect C	28.14	407	69.1	64.1	-48.3-135.9
Transect D	28.4	751	77.24	74.4	2.7-121.7
Ref. transect (RT)	24.9	174	59.9	57.7	-46-139.2
50% of profiles	17.77	-5.71	50.62	53.31	-7.1-128
100% of profiles	17.69	-2.33	50.06	53.47	-1.9-128.4
VHG based					
Ks (pump test)	20.1	-186	45.6	48.7	9.2-106.9
Ks (optimized)	19.2	260	57.0	60.9	11.3-133.8
Simplified					
Exponential function	27.5	396	34.3	64.7	14.0-132.2
LGD rates directly from temperature profiles	/	/	47.3	54.8	6.6-132.3

The model based on the reference transect RT was chosen for further analysis and comparison as this transect is the only location where LGD rates from both VHG and temperature profiles are available. The transfer function resulting from the linear regression was ($R^2 = 0.92$):

$$LGD\text{-}Rate_{Temp\ depth\ profile} = 3429.1 - 219.2 \cdot FO\text{-}DTS\ temp \qquad \text{Eq. 4.8}$$

A similar regression analysis was carried out between the LGD rates derived from the VHGs at the same transect (Fig. 4.11c) and resulted in the following transfer function ($R^2 = 0.998$):

$$LGD\text{-}Rate_{VHG} = 2618.3 - 166.0 \cdot FO\text{-}DTS\ temp \qquad \text{Eq. 4.9}$$

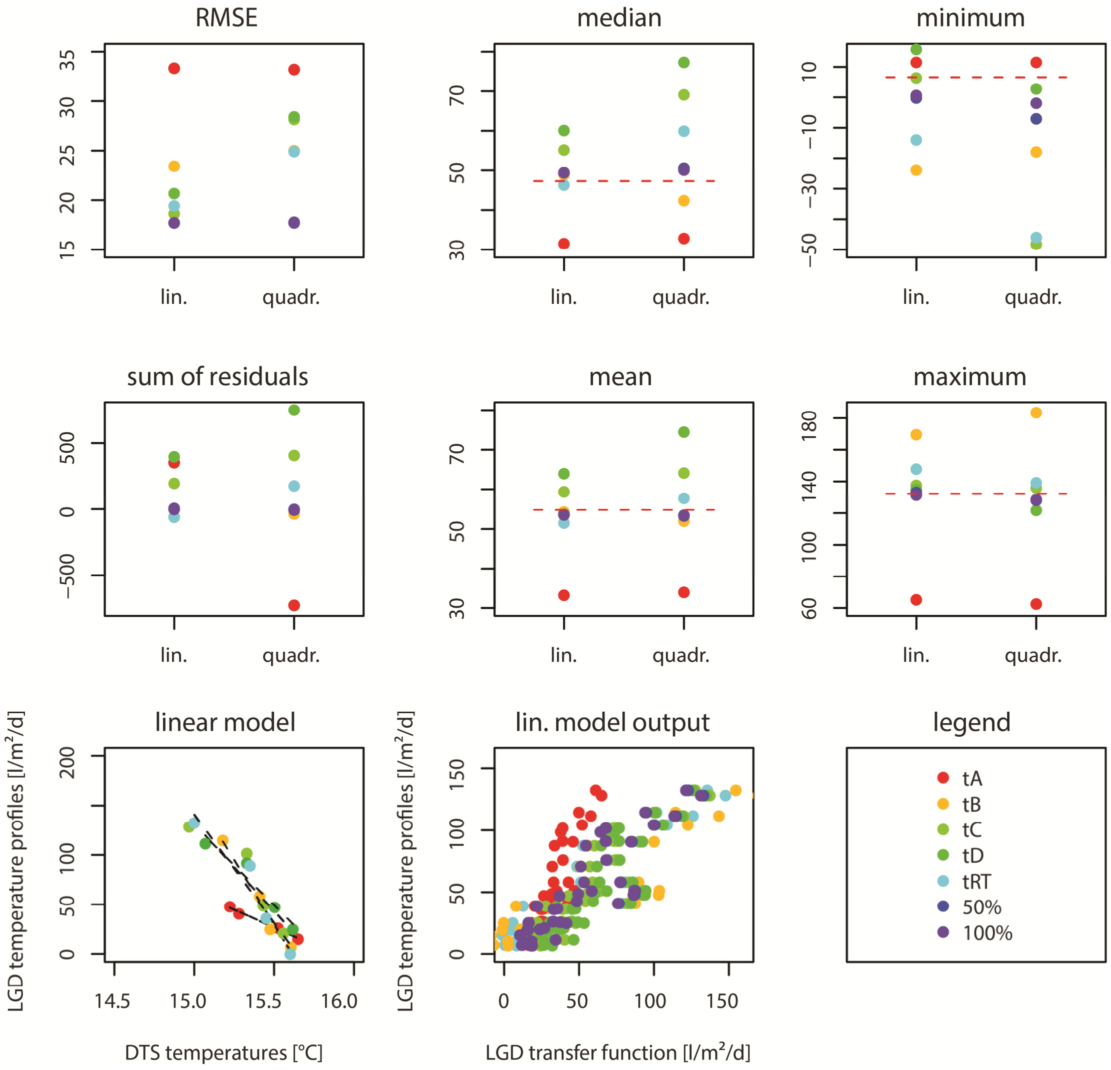

Figure 4.13 Evaluating model performance using the root mean square error (RMSE), the sum of residuals, and comparing the median, mean, minimum and maximum LGD rates of the predicted data set versus the LGD rates determined from the temperature profiles. This analysis was carried out for both linear and quadratic models based on different transects (transects A–D and the reference transect RT) as well as using every second value for calibration (50% model, *n* = 21) and the entire data set (100% model, *n* = 41). The red dashed lines show the corresponding "target values" of the temperature profile generated LGD rates. The two lower left plots show the linear regressions for the five transects models and the predicted values of LGD rates based on all linear transfer functions.

The third method employed to scale the transect measurements to the entire shore section was based on the simple exponential decline function fitted to the LGD rates determined with temperature depth profiles and does not make use of the FO-DTS measurements ($R^2 = 0.98$):

$$LGD\text{-}Rate_{exponential\ decline} = 205.2 \cdot e^{(-0.895 \cdot distance\ to\ shore)} \qquad \text{Eq. 4.10}$$

Results from all three upscaling methodologies were compared with the interpolated surface of LGD rates based on the entire grid of sediment temperature profiles (Fig. 4.14). It was found that both upscaling methodologies based on FO-DTS data were able to reproduce the patterns of LGD. However, while the exponential decline function produces acceptable results along the main gradient (away from the shoreline), the lateral variability especially in close vicinity to the shore could only be reproduced by the DTS-based methodologies (Fig. 4.14). This also becomes apparent when comparing the residuals between LGD rates from upscaling and based on temperature profiles (Fig. 4.15). A comparison of RMSE, median and mean values for all three methodologies can be found in Table 4.2. The fact that several models also produce negative values does not suggest groundwater recharge at these locations but is due to the simple statistical relationship which is not bounded by zero.

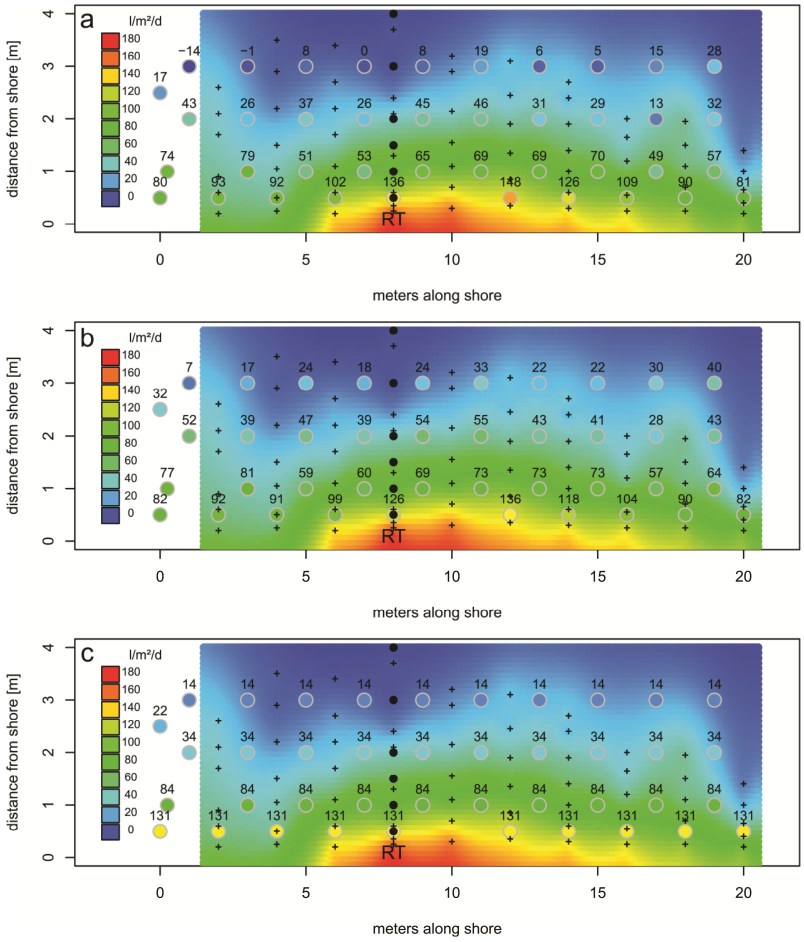

Figure 4.14 LGD rates determined with the three different upscaling methodologies. (a) Upscaling based on temperature profile transect, (b) upscaling based on VHG transect, (c) upscaling based on exponential function. The background colors depict the interpolated LGD rates from the sediment temperature profile grid. The circles and their corresponding numbers show the LGD rates determined with the upscaling methodologies at the sampling locations of the FO-DTS grid. The interpolated surface and the circle signatures are plotted using the same color scale.

4.2.4 Discussion

Estimation of LGD rates

The quantification of LGD rates based on temperature depth profiles or on VHGs is based on several assumptions:

1. It is a prerequisite that interpreted temperature differences are caused solely by the spatial variability of water fluxes and do not result from temporal variation of groundwater or surface water end-member temperatures. Since measurements were conducted in mid-September on days where diurnal variation of air temperature did not exceed 6 °C and as the investigation site is generally shaded by large beech trees, diurnal variations in surface water temperatures were assumed to be negligible and day to day variability of water temperature was only 1 °C. Two small rainfall events occurred prior to

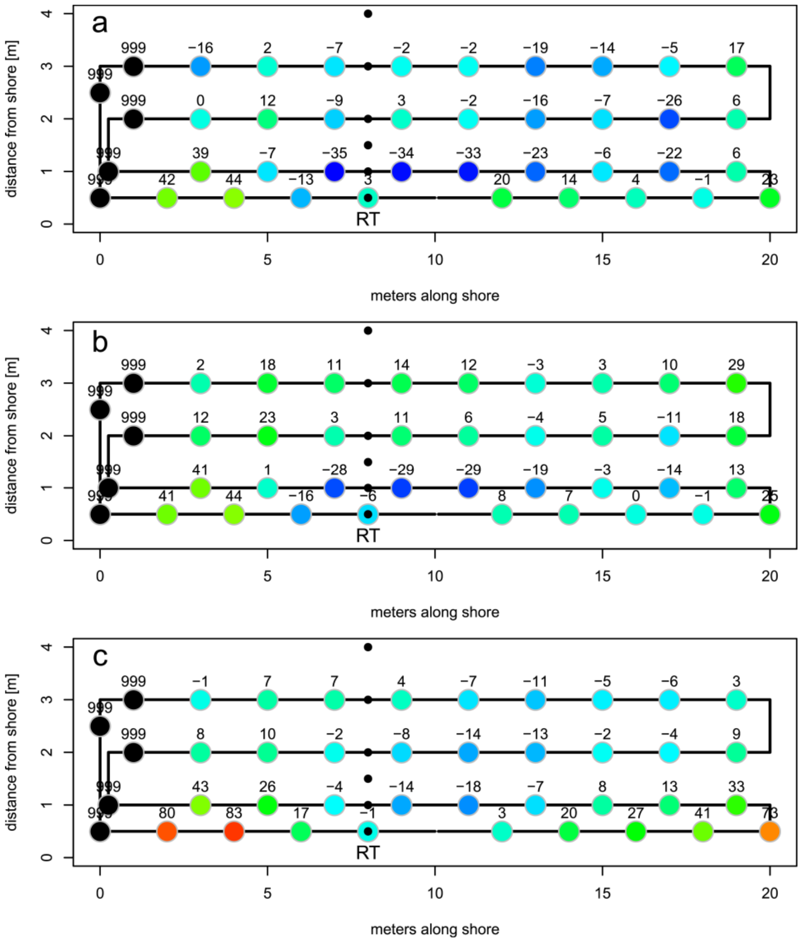

Figure 4.15 Residuals between LGD rates from the three upscaling methods and LGD rates based on temperature profiles. (a) Upscaling based on temperature profile transect, (b) upscaling based on VHG transect, (c) upscaling based on exponential function. Overestimations by the upscaling methodologies are shown as positive numbers. The color scale simply visualizes the corresponding values above the circles. 999 values correspond to no data values and indicate locations where DTS temperatures exist but no LGD data from temperature profiles is available for comparison.

the field measurements and could have introduced temporal dynamics to the head gradients at the site. As no pressure sensors were installed in the piezometers during this study, we have little information about the actual dynamics in gradients during these days. However, a piezometer installed at this location in the following year was equipped with a pressure sensor (OTT Orpheus Mini, accuracy ±2 mm). Its rainfall response in October 2012 (similar sized rainfall events) was analyzed to estimate dynamics during our field campaign. It was found that the difference between piezometer and lake level had a very stable continuous baseline. Rainfall response resulted in small deviations (2–4 mm) from this baseline during the rainfall events and values very quickly returned to prior levels. Due to the quick recovery to baseline values we assume that our measurements are not strongly influenced by the dynamics in head gradients over the period when the measurements were taken. Repetition of several temperature profile measurements on consecutive days showed little change, which is another indication of quasi stable conditions during the measurement period. The fitting parameters a and b in Equation 4.7 for the reference transect RT had similar values on both days: $a = 210.4$, $b = 0.887$ on the first day and $a = 196.3$, $b = 0.881$ on the second day. q_z values were also quite similar on both days, revealing a good reproducibility of the measurements. This implies that temporal variability of temperature and LGD rates was rather limited during the measurement campaign.

2. It is furthermore usually regarded as a necessary prerequisite that groundwater flow in the interface layer with a thickness *L* is exclusively vertical (e.g., Schmidt et al. 2006). However, in fact it is only necessary that groundwater flow into the lake is parallel to all measurement points of the sediment temperature profile. In general, groundwater flow directions follow horizontal directions within the aquifer. Tracer tests (Lee 1980) and modeling studies (McBride and Pfannkuch 1975; Pfannkuch and Winter 1984) have shown that upward curvature of flow paths occurs when groundwater approaches a lake. When applying the heat transport equation to calculate LGD rates, a flow path of length *L* has to be set which represents the flow in the transition zone in the lake sediment where groundwater temperatures approach lake temperatures (Eq. 4.7). Traditionally, *L* is regarded as the thickness of the interface. However, if the extent of the temperature depth profile (here 0.45 m) is smaller than *L* (here 2 m) it is only required that vertical flow occurs in the uppermost 45 cm where measurements are conducted while more horizontal flow paths below 45 cm have no negative impact on the quality of the estimate. In our study, an optimum value of $L = 2$ m was found, however, another possible approach would have been to use *L* tending toward infinity, thus eliminating this parameter from the equation and further simplifying it, similar to the solution by Turcotte and Schubert (1982). This solution was also used by Schmidt et al. (2007) and Ferguson and Bense (2011) and here applied to single-point measurements of temperature. Comparing the results of the two approaches did not produce significant differences for most of the data points (also found by Ferguson and Bense 2011) and differed slightly for a few locations with very low fluxes.

3. Both, the hydraulic conductivity used in the calculation of LGD from VHG and the thermal conductivity used in the heat transport equation have not been determined directly (the first one having been estimated with a three different indirect methods and also through a single-pump test and the second one having been taken from the literature). It was found that if *Ks* was determined using grain size distributions, values were significantly higher than the values determined both with the pump test as well as by optimizing LGD to the LGD rates determined from the temperature profiles. The optimization of *Ks* results in a VHG transfer function which is not entirely independent of the temperature profile data set. For purposes of comparison, the pump test-based model was also included in Table 4.2.

4. The applied approach assumed that thermal and hydraulic properties of the lake bed were homogenous. This assumption introduces some uncertainty to the interpretation of the results of this study. As *Ks* values generally show a much stronger variability compared to thermal conductivities, relying on a single *Ks* value is likely to introduce more uncertainty than using a single value of thermal conductivity. However, from the 108 cm long sediment core taken at the site of the reference transect it is known that the sediment consisted of 94% sand and it can be assumed that thermal and hydraulic properties did not vary significantly with depth. The outwash plain sands surrounding the lake are generally quite uniform and also show little anisotropy, with a ratio of 1.02 (from 47 data pairs of vertical and horizontal *Ks* determined in soil cores extracted from the saturated zone during installation of observation wells in 2012—unpublished data). However, the fact that the lake sediment core did not reach the lower end of the interface and that its representative character for the entire field site was not tested, introduces further uncertainty into the interpretation of our results. Additional core samples or a higher number of piezometers and thus locations for pump tests would make it possible to test the assumption of relative homogeneity of the sediment and are subject of an ongoing study at the field site.

5. The approaches based on temperatures are only applicable when groundwater and lake water temperatures differ significantly (i.e., in summer and winter) and will also fail at very high flow rates when the entire profile tends toward groundwater temperatures.

Concentration of seepage in nearshore areas

As previously reported by other authors in a homogeneous and isotropic aquifer, highest seepage rates occur usually close to the shore (Belanger et al. 1985; Harvey et al. 2000; Kishel and Gerla 2002; Pfannkuch and Winter 1984; Schafran and Driscoll 1993; Shaw and Prepas 1990). Similarly, our study also revealed that most seepage is focused in a very narrow band along the shore perimeter. For Lake Sallie, (McBride and Pfannkuch 1975) report a decrease of 1 order of magnitude for every 60 m. In Lake Hinnensee, the observed nearshore decrease of LGD rates was even more intense (Eq. 4.7, Fig. 4.11). Other authors also report exponential decrease of LGD rates (Kishel and Gerla 2002; Lee 1980).

Spatial patterns of FO-DTS, VHGs, and temperature depth profiles

As mentioned above, patterns of groundwater inflow into the lake were found to be highly heterogeneous along the investigated shore section with large differences in the y direction (distance to shore) and smaller differences in the x direction (along the shore).

All three methods were able to capture these patterns characterized by the strongly declining groundwater influence with increasing distance to the shore. The reduced total range of temperatures determined by FO-DTS compared to the near-surface measurements of the temperature profiles can probably be attributed to two factors: (a) the fact that FO-DTS surveys averaged temperatures over the length of 4 m along the cable, which resulted in a smoothing of temperatures and (b) as the cable was deployed at the sediment surface the surface water temperature also had a dampening effect on the temperature patterns resulting from groundwater inflow. This dampening effect of surface temperature could be avoided if the fiber-optic cable was placed in the sediment instead of at the sediment surface (Krause et al. 2012). However, special care would have to be taken to ensure a constant depth of deployment in the sediment over the entire length of the cable as temperatures are not only negatively correlated with groundwater discharge but also with sediment depth. It was found that VHGs determined at 50 cm depth (the depth closest to the measured temperature profiles) showed a weaker trend with distance to shore. This is most likely due to the large relative error and the relatively small differences in water level between lake and piezometer at this depth. As the relative error is smaller at 150 cm depth (larger differences in water level), the pattern emerges more clearly and therefore this data set was used for the transfer model. An evaluation of all three methods with respect to their potential in capturing LGD patterns on the one hand and main uncertainties on the other hand is summarized in Table 4.3

Besides the decrease of LGD with increasing distance to the shore, substantial heterogeneity of LGD rates has also been found along the shore. This spatial heterogeneity was indicated by the temperature depth profiles as well as FO-DTS. Large and small-scale stratigraphic heterogeneities and lake bed topographic structures can cause irregular LGD patterns. A decrease of LGD was observed at both ends of the study site (see Fig. 4.11a and 4.14). At the northern end it was assumed that decreased LGD rates were caused by a concave bend of the shoreline so that a part of the groundwater flow paths approaching the shoreline are diverging. At the southern end of the study site reduced LGD rates were assumed to result from the impact of a large beech tree in close vicinity to the shore with some of its roots in the nearshore sediment. We assume that the free cross-sectional area for LGD is drastically reduced due to the dense root network. Furthermore, the reed stands observed in the same area have resulted in an accumulation of fine organic matter in the sediment, likely to be sealing fractions of the pore space and thus reducing the hydraulic conductivity. The impact of increased organic matter content at these locations might also be the reason for the overestimation of LGD rates by the FO-DTS data, as surface temperatures might be reduced due to differing thermal characteristics of this material.

Table 4.3 Evaluation of the three methods for their usefulness in capturing the heterogeneity and patterns of LGD.

	Temperature profiles	VHG	DTS
Capturing spatial variability and heterogeneity	Yes	Yes, even vertically if piezometer nets are used	Yes, but signals are smoothed out due to spatial averaging
Data accuracy	High	Medium	Strongly depending on effort of calibration
Estimation of LGD possible	Using heat transport equation	Using flow equation	Only through transfer function
Causes for uncertainties in determining LGD	Estimation of thermal characteristics; diurnal temperature variations; assumption of uni-form characteristics; assumption of 1-D vertical flow	Estimation of hydraulic characteristics ; assumption of uniform characteristics ; assumption of 1-D vertical flow	Contact to sediment surface; dampening effects; calibration

Comparison of upscaling methodologies

All three methods employed for upscaling measurements taken along a single transect to the entire shore section were able to reproduce the general pattern of heterogeneity, i.e., the strong decline of LGD with distance to shore described above (Fig. 4.14). While the simple exponential decline function has the advantage of being low cost in both time and space it is intrinsically unable to reproduce the alongshore variability of LGD rates (Fig. 4.14). On the other hand, upscaling approaches based on FO-DTS data sets are able to capture the spatial variability in both dimensions (Fig. 4.14). However, the residuals for these methodologies are also quite high at both the northern and the southern end of the investigated shore section (Fig. 4.15), indicating that the dampening of DTS temperatures due to (a) averaging and (b) the dampening effect of the surface water temperature, also dampens the variability of the upscaled LGD rates. The exponential decline upscaling approach overestimates LGD rates for the shore section, as the sum of the residuals is strongly positive and mean values are higher than for the "validation" data set (the LGD rates determined from the grid of temperature profiles) (Table 4.2). When comparing the two DTS-based approaches, the combination with the VHG transect seems to produce slightly better results; with RMSE of 19.2 $l\ m^{-2}\ d^{-1}$ compared to 19.4 $l\ m^{-2}\ d^{-1}$ of the temperature profile-DTS combination (linear model RT, Table 4.2). However, for the VHG-DTS combination both median and mean values are higher than the LGD rates determined with the temperature profile-DTS combination and also compared to the rates of the validation data set (Table 4.2). RMSE values for the exponential decline-based upscaling are significantly higher with 27.5 $l\ m^{-2}\ d^{-1}$; furthermore, median values are low and mean values are high compared to all other data sets, indicating a generally different frequency distribution. LGD rates appear to be slightly underestimated by the temperature profile-DTS-based methodology as the sum of residuals has a negative value (Table 4.2), in contrast to the strongly positive values of the other two upscaling approaches. Taking all evaluation measures into account, the temperature profile-DTS combination proves to be the most promising with mean and median LGD rates close to those of the validation data set, low bias, and low RMSE. The DTS-based approach can here be used only to estimate LGD rates, water fluxes from lake to groundwater cannot be determined. As a result, zero flux will be estimated also for locations of groundwater recharge. All methodologies assume 1-D vertical flow and homogeneous sediment, concerning both its hydraulic as well as thermal characteristics. This simplification seems viable along the studied shore section but might not hold for larger scale applications. In this case, sediment variability will need to be included in the upscaling approach.

4.2.5 Conclusions

The determination of water fluxes between groundwater and surface water is a major challenge due to strong spatial variability and the need of integrating measurements at various scales. Therefore, the combination of methods tested within the present study, combining FO-DTS with methods for spot quantifications of seepage rates (in this case temperature depth profiles and vertical hydraulic gradients) proved to be a successful upscaling approach. The DTS-based upscaling approaches reliably reproduced 2-D patterns of lacustrine groundwater discharge rates using only four data points of either VHG- or sediment temperature profile determined LGD rates and the DTS temperature grid. The proof of concept and of reliability of FO-DTS applications for quantifying spatial patterns of exchange fluxes across aquifer-lake interfaces that are provided in this study encourage the extension of investigations to larger scales.

4.2.6 References

Anibas, C., Fleckenstein, J.H., Volze, N., Buis, K., Verhoeven, R., Meire, P., Batelaan, O., 2009. Transient or steady-state? Using vertical temperature profiles to quantify groundwater-surface water exchange. *Hydrological Processes*, 23(15): 2165-2177.

Belanger, T.V., Mikutel, D.F., Churchill, P.A., 1985. Groundwater seepage nutrient loading in a Florida lake. *Water Research*, 19(6): 773-781.

Bredehoeft, J.D., Papadopulos, I.S., 1965. Rates of vertical groundwater movement estimated from the Earth's thermal profile. *Water Resources Research*, 1(2): 325-328.

Brock, T.D., Lee, D.R., Janes, D., Winek, D., 1982. Groundwater seepage as a nutrient source to a drainage lake - Lake Mendota, Wisconsin. *Water Research*, 16(7): 1255-1263.

Cherkauer, D.S., Nader, D.C., 1989. Distribution of groundwater seepage to large surface-water bodies: The effect of hydraulic heterogeneities. *Journal of Hydrology*, 109(1–2): 151-165.

Constantz, J., 2008. Heat as a tracer to determine streambed water exchanges. *Water Resources Research*, 44.

Enell, M., 1982. The phosphorus economy of a hypertrophic seepage lake in Scania, south Sweden groundwater influence. *Hydrobiologia*, 86(1): 153-158.

Ferguson, G., Bense, V., 2011. Uncertainty in 1D Heat-Flow Analysis to Estimate Groundwater Discharge to a Stream. *Ground Water*, 49(3): 336-347.

Frape, S.K., Patterson, R.J., 1981. Chemistry of Interstitial Water and Bottom Sediments as Indicators of Seepage Patterns in Perch Lake, Chalk-River, Ontario. *Limnology and Oceanography*, 26(3): 500-517.

Hannah, D.M., Malcolm, I.A., Bradley, C., 2009. Seasonal hyporheic temperature dynamics over riffle bedforms. *Hydrological Processes*, 23(15): 2178-2194.

Harvey, F.E., Rudolph, D.L., Frape, S.K., 2000. Estimating ground water flux into large lakes: Application in the Hamilton Harbor, western Lake Ontario. *Ground Water*, 38(4): 550-565.

Hatch, C.E., Fisher, A.T., Revenaugh, J.S., Constantz, J., Ruehl, C., 2006. Quantifying surface water-groundwater interactions using time series analysis of streambed thermal records: Method development. *Water Resources Research*, 42(10).

Hausner, M.B., Suárez, F., Glander, K.E., van de Giesen, N., Selker, J.S., Tyler, S.W., 2011. Calibrating Single-Ended Fiber-Optic Raman Spectra Distributed Temperature Sensing Data. *Sensors (Basel, Switzerland)*, 11(11): 10859-10879.

Henderson, R.D., Day-Lewis, F.D., Harvey, C.F., 2009. Investigation of aquifer-estuary interaction using wavelet analysis of fiber-optic temperature data. *Geophysical Research Letters*, 36(6): n/a-n/a.

Jensen, J.K., Engesgaard, P., 2011. Nonuniform Groundwater Discharge across a Streambed: Heat as a Tracer. *Vadose Zone Journal*, 10(1): 98-109.

Kalbus, E., Reinstorf, F., Schirmer, M., 2006. Measuring methods for groundwater - surface water interactions: a review. *Hydrology and Earth System Sciences*, 10(6): 873-887.

Käser, D.H., Binley, A., Heathwaite, A.L., Krause, S., 2009. Spatio-temporal variations of hyporheic flow in a riffle-step-pool sequence. *Hydrological Processes*, 23(15): 2138-2149.

Kidmose, J., Engesgaard, P., Nilsson, B., Laier, T., Looms, M.C., 2011. Spatial Distribution of Seepage at a Flow-Through Lake: Lake Hampen, Western Denmark. *Vadose Zone Journal*, 10(1): 110-124.

Kishel, H.F., Gerla, P.J., 2002. Characteristics of preferential flow and groundwater discharge to Shingobee Lake, Minnesota, USA. *Hydrological Processes*, 16(10): 1921-1934.

Krabbenhoft, D.P., Anderson, M.P., Bowser, C.J., 1990a. Estimating groundwater exchange with lakes: 2. Calibration of a three-dimensional, solute transport model to a stable isotope plume. *Water Resources Research*, 26(10): 2455-2462.

Krabbenhoft, D.P., Bowser, C.J., Anderson, M.P., Valley, J.W., 1990b. Estimating groundwater exchange with lakes. 1. The stable isotope mass balance method. *Water Resources Research*, 26(10): 2445-2453.

Krabbenhoft, D.P., Bowser, C.J., Kendall, C., Gat, J.R., 1994. Use of O-18 and deuterium to assess the hydrology of groundwater-lake systems. In: *Environmental Chemistry of Lakes and Reservoirs*, Baker, L.A. (Ed.). Advances in Chemistry Series, 67-90.

Krabbenhoft, D.P., Webster, K.E., 1995. Transient hydrogeological controls on the chemistry of a seepage lake. *Water Resources Research*, 31(9): 2295-2305.

Krause, S., Blume, T., Cassidy, N.J., 2012. Investigating patterns and controls of groundwater up-welling in a lowland river by combining Fibre-optic Distributed Temperature Sensing with observations of vertical hydraulic gradients. *Hydrology and Earth System Sciences*, 16(6): 1775-1792.

Krause, S., Hannah, D.M., Blume, T., 2011. Interstitial pore-water temperature dynamics across a pool-riffle-pool sequence. *Ecohydrology*, 4(4): 549-563.

Krause, S., Heathwaite, L., Binley, A., Keenan, P., 2009. Nitrate concentration changes at the groundwater-surface water interface of a small Cumbrian river. *Hydrological Processes*, 23(15): 2195-2211.

Lautz, L.K., Ribaudo, R.E., 2012. Scaling up point-in-space heat tracing of seepage flux using bed temperatures as a quantitative proxy. *Hydrogeology Journal*, 20(7): 1223-1238.

Lee, D.R., 1977. A device for measuring seepage flux in lakes and estuaries. *Limnology and Oceanography*, 22(1): 140-147.

Lee, D.R., 1980. Groundwater - Solute Influx. *Limnology and Oceanography*, 25(1): 183-186.

Loeb, S.L., Goldman, C.R., 1979. Water and nutrient transport via groundwater from Ward Valley into Lake Tahoe. *Limnology and Oceanography*, 24(6): 1146-1154.

Lowry, C.S., Walker, J.F., Hunt, R.J., Anderson, M.P., 2007. Identifying spatial variability of groundwater discharge in a wetland stream using a distributed temperature sensor. *Water Resources Research*, 43(10).

McBride, M.S., Pfannkuch, H.O., 1975. Distribution of seepage within lakebeds. *Journal of Research of the U.S. Geological Survey*, 3(5): 505-512.

Meinikmann, K., Lewandowski, J., Nutzmann, G., 2013. Lacustrine groundwater discharge: Combined determination of volumes and spatial patterns. *Journal of Hydrology*, 502(0): 202-211.

Mortimer, R.J.G., Krom, M.D., Boyle, D.R., Nishri, A., 1999. Use of a high-resolution pore-water gel profiler to measure groundwater fluxes at an underwater saline seepage site in Lake Kinneret, Israel. *Limnology and Oceanography*, 44(7): 1802-1809.

Mwakanyamale, K., Slater, L., Day-Lewis, F.D., Elwaseif, M., Johnson, C.D., 2012. Spatially variable stage-driven groundwater-surface water interaction inferred from time-frequency analysis of distributed temperature sensing data. *Geophysical Research Letters*, 39(6).

Pfannkuch, H.O., Winter, T.C., 1984. Effect of anisotropy and groundwater system geometry on seepage through lakebeds: 1. Analog and dimensional analysis. *Journal of Hydrology*, 75(1–4): 213-237.

Rosenberry, D.O., 2005. Integrating seepage heterogeneity with the use of ganged seepage meters. *Limnology and Oceanography-Methods*, 3: 131-142.

Schafran, G.C., Driscoll, C.T., 1993. Flow path-composition relationships for groundwater entering an acidic lake. *Water Resources Research*, 29(1): 145-154.

Schmidt, C., Bayer-Raich, M., Schirmer, M., 2006. Characterization of spatial heterogeneity of groundwater-stream water interactions using multiple depth streambed temperature measurements at the reach scale. *Hydrology and Earth System Sciences*, 10(6): 849-859.

Schmidt, C., Conant Jr, B., Bayer-Raich, M., Schirmer, M., 2007. Evaluation and field-scale application of an analytical method to quantify groundwater discharge using mapped streambed temperatures. *Journal of Hydrology*, 347(3–4): 292-307.

Schuster, P.F., Reddy, M.M., LaBaugh, J.W., Parkhurst, R.S., Rosenberry, D.O., Winter, T.C., Antweiler, R.C., Dean, W.E., 2003. Characterization of lake water and ground water movement in the littoral zone of Williams Lake, a closed-basin lake in north central Minnesota. *Hydrological Processes*, 17(4): 823-838.

Selker, J., van de Giesen, N., Westhoff, M., Luxemburg, W., Parlange, M.B., 2006a. Fiber optics opens window on stream dynamics. *Geophysical Research Letters*, 33(24): n/a-n/a.

Selker, J.S., Thevenaz, L., Huwald, H., Mallet, A., Luxemburg, W., de Giesen, N.v., Stejskal, M., Zeman, J., Westhoff, M., Parlange, M.B., 2006b. Distributed fiber-optic temperature sensing for hydrologic systems. *Water Resources Research*, 42(12): W12202.

Sensornet, 2009. Sentinal DTS User Guide SEN2-UM1.0, London, UK.

Shaw, R.D., Prepas, E.E., 1990. Groundwater-lake interactions: II. Nearshore seepage patterns and the contribution of ground water to lakes in central Alberta. *Journal of Hydrology*, 119(1): 121-136.

Shaw, R.D., Shaw, J.F.H., Fricker, H., Prepas, E.E., 1990. An integrated approach to quantify groundwater transport of phosphorus to Narrow Lake, Alberta. *Limnology and Oceanography*, 35(4): 870-886.

Slater, L.D., Ntarlagiannis, D., Day-Lewis, F.D., Mwakanyamale, K., Versteeg, R.J., Ward, A., Strickland, C., Johnson, C.D., Lane, J.W., 2010. Use of electrical imaging and distributed temperature sensing methods to characterize surface water–groundwater exchange regulating uranium transport at the Hanford 300 Area, Washington. *Water Resources Research*, 46(10): n/a-n/a.

Stauffer, R.E., 1985. Use of solute tracers released by weathering to estimate groundwater inflow to seepage lakes. *Environmental Science & Technology*, 19(5): 405-411.

Stonestrom, D.A., Constantz, J., 2003. Heat as a tool for studying the movement of ground water near streams. *U.S. Geological Survey Circular* 1260: 96 p.

Turcotte, D.L., Schubert, G., 1982. *Geodynamics: Application of Continuum Physics to Geological Problems.* Wiley, New York, 464 p.

Tyler, S.W., Selker, J.S., Hausner, M.B., Hatch, C.E., Torgersen, T., Thodal, C.E., Schladow, S.G., 2009. Environmental temperature sensing using Raman spectra DTS fiber-optic methods. *Water Resources Research*, 45(4): n/a-n/a.

van de Giesen, N., Steele-Dunne, S.C., Jansen, J., Hoes, O., Hausner, M.B., Tyler, S., Selker, J., 2012. Double-Ended Calibration of Fiber-Optic Raman Spectra Distributed Temperature Sensing Data. *Sensors*, 12(5): 5471.

4.3 Localization of lacustrine groundwater discharge (LGD) by airborne measurement of thermal infrared radiation

Jörg Lewandowksi,[1,2] Karin Meinikmann,[1,2] Thomas Ruhtz,[3] Franziska Pöschke,[1,2] and Georgiy Kirillin[1]

[1] Department of Ecohydrology, Leibniz-Institute of Freshwater Ecology and Inland Fisheries, Berlin, Germany

[2] Geography Department, Humboldt-Universität zu Berlin, Berlin, Germany

[3] Free University, Institute for Space Science, Berlin, Germany

This is the peer reviewed version of the following article:
Lewandowski, J., Meinikmann, K., Ruhtz, T., Poschke, F., Kirillin, G., 2013. Localization of lacustrine groundwater discharge (LGD) by airborne measurement of thermal infrared radiation. *Remote Sensing of Environment*, 138: 119-125. DOI: 10.1016/j.rse.2013.07.005.

Abstract

Although lacustrine groundwater discharge (LGD) might be important in water and nutrient budgets, it has often been neglected due to the required effort to measure LGD and due to intense spatial heterogeneity of LGD limiting the validity of measurements. Therefore, fast, easy applicable methods for a first snapshot of the LGD pattern are required and might be the basis for choosing relevant and representative sampling sites. In the present case study, which is actually the first application of an airborne measurement of thermal infrared radiation (TIR) to identify LGD pattern for entire deep freshwater lakes, the measurement was substantiated with thermal profiles in sediments and a water-table map. We found that measurement of TIR is a powerful tool to identify LGD pattern in lake-related studies provided that there is a lack of warm surface inflows. A TIR image taken in March 2012 shows that warm groundwater entering the relatively colder lake water in some near-shore areas is visible as a plume floating on top of the lake water. Prerequisites for the application of TIR to detect LGD pattern are the positive buoyancy of the groundwater relative to lake water and weak mixing in the water column. We propose a dimensionless scale for identifying groundwater floating conditions based on weather conditions. Attributing a surface thermal anomaly to LGD depends on careful consideration of other factors that could produce similar patterns and careful consideration of lake physics.

4.3.1 Introduction

Lacustrine groundwater discharge (LGD) is an important component in water balances of some lakes (Harvey et al. 2000). Even if its contribution to the water balances is small, it might be important to nutrient balances since nutrient concentrations in groundwater are often much higher than in other components of the water balance and in the lake water itself (Vanek 1987). During the last decades much effort was spent on localization of discharge zones and quantification of LGD as well as the development of measurement and modeling tools for that purpose. Due to intense small-scale spatial heterogeneity of LGD (Kishel and Gerla 2002; Oliveira Ommen et al. 2012), the large area covered by the interface and its difficult accessibility for direct measurements all methods have limitations. In principle, there are three different types of methods for the identification of LGD: (1) Spatially explicit methods measuring LGD rates at a single point or over a small area (e.g., seepage meters Lee 1977, sediment temperature depth profiles Schmidt et al. 2006), (2) integrating methods quantifying the whole groundwater import into the lake (e. g., radon balances, Kluge et al. 2007), stable isotope approaches (Dinçer 1968; Hofmann et al. 2008; Krabbenhoft et al. 1994), annual groundwater recharge in the entire subsurface catchment, mostly determined by modeling or calculation of the water budget) and (3) methods for identification of discharge pattern without quantification of LGD (e.g., fiber-optic distributed temperature sensing (FO-DTS, Selker et al. 2006), geophysical approaches around the lake perimeter (Ong et al. 2010), airborne measurements of thermal infrared radiation (TIR) (present study)).When interested in nutrient budgets integrating methods alone are not sufficient. Nutrient budgets are calculated by multiplication of LGD rates and nutrient concentrations in discharging water. Due to the large spatial heterogeneity of nutrient concentrations in groundwater, segmented approaches are much more reliable than integrating approaches: local discharge rates should be multiplied with the corresponding nutrient concentrations instead of multiplying total discharge rates with mean nutrient concentrations (Oliveira Ommen et al. 2012). Thus, fast methods for pattern identification could be useful to localize the most relevant and representative zones for further more time-consuming investigations. With the present study we tested whether airborne TIR measurements are a suitable tool for pattern identification.

Airborne and ground-based TIR measurements have been used in several studies to detect groundwater discharge or hyporheic exchange flow in streams and rivers (Schuetz and Weiler 2011;

Torgersen et al. 2001). Fast mixing of groundwater discharge and stream water results in the visibility of discharging groundwater at the stream surface as small temperature increase or decrease compared to the river water not impacted by groundwater discharge. The volume of the stream water is relatively small so that the discharge of groundwater or hyporheic water with its temperature different than stream water results in a significant deviation of the impacted stream water compared to the not impacted stream water. The fundamental differences of lake–groundwater interactions compared to stream–groundwater interactions are the absence of hyporheic exchange flows in lakes, smaller groundwater discharge rates, less turbulent mixing of the water body and a larger volume-ratio of the water body to the discharging groundwater. Thus, analogies of groundwater discharge to streams and lakes that would be relevant for airborne TIR measurements are minor.

Airborne TIR measurements have been used in several studies to detect submarine groundwater discharge (SGD) in coastal zones (Danielescu et al. 2009; Duarte et al. 2006; Garcia-Solsona et al. 2010; Johnson et al. 2008; Peterson et al. 2009; Shaban et al. 2005) and in studies of saline lakes (Lee 1969; Whiting 1976). In saline systems, there is a large density difference between discharging fresh groundwater and saline water due to different salinities. Thus, the less dense groundwater will always float on top of the sea water and if there are some temperature differences between groundwater and sea water the groundwater can be detected with airborne TIR measurements. In freshwaters, lake water and groundwater have similar salinities and thus no salinity-induced floating of groundwater occurs. However, under certain circumstances temperature differences might cause small density differences that result in the same groundwater buoyancy as previously observed in saline systems.

To the best of our knowledge the present study is the first application of an airborne TIR measurement to identify LGD pattern for an entire deep freshwater lake. There are studies of Cook et al. (1991) who used a handheld infrared camera to detect LGD along the shore line (linescan survey) of a Scottish lake; a study of (Anderson et al. 1995) who also used a handheld infrared camera to visualize surface water temperatures and to detect cold springs along a geologic fault zone, water circulation and an influent plunging plume; and an airborne TIR study of Rundquist et al. (1985) in a shallow lake in the Nebraska Sandhills to detect groundwater discharge. The two latter studies investigated LGD in relatively shallow water bodies where mixing processes similar to the ones described above for streams might occur and cause visible surface anomalies despite the absence of floating characteristics of the groundwater discharge. In both studies groundwater relatively colder, and thus, heavier than lake water (of approximately 20 °C) was observed at the lake surface. Also, some authors (e.g., Hook et al. 2003) used satellite images to determine lake surface temperatures but data were not used to identify LGD pattern.

We hypothesize that at low lake water temperatures under relatively calm weather conditions, warmer groundwater discharge might float on top of the water body and can be detected by TIR measurements. The aim of the present study is to test the method and identify conditions favoring application of TIR to detect LGD.

4.3.2 Material and methods

The method was tested at Lake Arendsee (max. depth 49 m, mean depth 29 m, surface area 5.13 km^2) which is a highly eutrophic (total phosphorus concentration approximately 200 µg P L^{-1}) seepage lake located in north eastern Germany. The littoral zone along the shore is very narrow except an approximately 200 m broad shallow zone (<10 m water depth) at the Northern shore of the lake (Hupfer et al. 2000). The use of TIR to localize LGD is discussed and evaluated based on physical considerations, a water temperature depth profile taken with a YSI probe (Model 6600 V2/4) on 20 March 2012 at the deepest point of the lake, continuously measured water temperatures in 1.5 m depth, and weather data collected by a weather station (EcoTech Bonn, Germany) on an unmanned raft.

The TIR data were collected on 22 March 2012 from 10:59 to 11:03 local time during an airborne mission with a Cessna 207 T operated by the Free University Berlin with two transects above Lake Arendsee. The TIR camera (VarioCam HR, head 600) was installed on a stabilized platform (GSM 3000) together with an inertial navigation system (IGI Aerocontrol). The stabilized platform was controlled by the inertial system and the corresponding altitude and navigation data were collected by this system. The camera has a resolution of 640 × 480 pixels, a focal length of 30 mm and was used with a frame rate of 1 image per second synchronized and triggered by the GPS–PPS pulse of the navigation system. The very low lens distortion of the camera and the stabilized platform made it possible to mosaic the data rapidly with a common imaging program (Gimp) without major photo- and geometric correction. For this procedure only a limited number of 6 pictures were used to cover the whole lake and to compile the resulting image. A more sophisticated mosaic would include more time consuming laboratory calibrations, measurements of the camera distortion and a bore site calibration flight. That was not the scope of the study aiming at a first snapshot of the LGD pattern and would also contradict to the advantage to have a fast and easily applicable method. The flight was performed at an altitude of approximately 1500 m with a velocity of approximately 50 m s^{-1}. The resulting image was rotated by 104° and scaled from a spatial pixel resolution of approximately 1.6m× 1.2 m to 1.5m × 1.5m. For the temperature calibration the specific data of the manufacturer of the TIR camera were used. The absolute temperatures of the TIR image should be considered with care but for the present application only relative temperature differences are important.

In addition to the above-mentioned physical considerations we also used information about the study site to discuss the collected TIR images and as basis for Figure 4.16. We summarize that information here since the original sources are reports in German and similar gray literature. Results of our own below-mentioned investigations are not published yet since the time-consuming and manpower-intensive ground-based investigations are still ongoing with the TIR image of the present study being a helpful tool for selecting the best sites for further investigations. Based on 40 wells, previous studies and hydrogeological maps we determined groundwater contour lines and the delimitation of the subsurface catchment (Fig. 4.16). Groundwater in the catchment is flowing in northern directions towards the lake (perpendicular to the contour lines in Fig. 4.16) with a steep hydraulic gradient along the south-southeastern shoreline. There, relatively high LGD rates are expected while in the east and west of the lake less LGD is assumed due to a smaller extent of the subsurface catchment and lower groundwater gradients.

Aquifer sediments along the southern shoreline originate from different Pleistocene stadials which had been deposited on Miocene material. Borehole profiles indicate an increasing thickness of the Pleistocene layers from about 10 to >35 m in eastern direction along the southern shoreline. In some parts, an aquitard separates the sediments into two aquifers. However, this aquitard is not consistently present, and thus, a general hydraulic connection between the different geologic sediments can be assumed. Values for hydraulic conductivity (*ksat*) in the upper parts of the aquifer (less than 11 m below surface) show an increase in eastern direction, from $1.4 \cdot 10^{-4}$ in the south-west to $4.9 \cdot 10^{-4}$ in the south-east. Further eastwards, *ksat* decreases again.

In the north and north-west lake water infiltrates into the aquifer and in the north-east the subsurface catchment is extremely small so that nearly no LGD is expected to occur along the northern shore. Local LGD rates calculated from curvature of temperature depth profiles (Schmidt et al. 2006) in the lake sediments (dots in Fig. 4.16 along the shoreline) support in principle the aforementioned description of LGD pattern. Temperature depth profiles are based on the temperature difference between groundwater (e.g., 10 °C) and lake water (e.g., 4 °C). At high groundwater discharge rates temperatures of upwards flowing groundwater remain high while the groundwater approaches the sediment surface. Only on the last decimeters to centimeters heat conduction and diffusion result in a relatively sharp decrease of the temperatures from 10 °C to 4 °C. At lower groundwater discharge rates conductive and diffusive heat transport processes affect deeper sediment layers so that the curvature of the profiles is more flat. We also applied FO-DTS (Selker et al. 2006) to investigate LGD in deeper zones of the lake. Results suggest that no significant LGD occurs far away from the shore. Theoretical considerations, modeling exercises and the local hydrogeology also support a focusing of LGD to near-shore zones (e.g., Kishel & Gerla 2002, Pfannkuch & Winter 1984, Shaw & Prepas 1990).

4.3.3 Results

Figure 4.16 shows the TIR image of Lake Arendsee taken on 22 March 2012. For its interpretation some background information described in the Material and methods section, such as the delimitation of the subsurface catchment, water table contour lines and near shore groundwater discharge rates is additionally shown in the same figure. Surface water temperatures in areas impacted by LGD are close to 7 °C which is more than 1 °C warmer than the rest of the lake surface (Fig. 4.16) and exceeds the temperature of maximum density of freshwater (4 °C). A lake water depth profile taken on 20 March 2012 shows a difference between the top and the bottom of the water body of only 0.26 °C and 1 µS cm^{-1} with a temperature at the lake bottom of 4.12 °C and an electrical conductivity of 483 µS cm^{-1}, i.e., the lake had been completely mixed short before the measurement campaign. Groundwater temperatures in 10 groundwater observation wells close to the shore were 10.5 ± 0.3 °C (arithmetic mean ± standard error) and electrical conductivities were 643 ± 69 µS cm^{-1}. Calculated electrical conductivities based on water compounds agreed well: 727 ± 77 µS cm^{-1}. Total dissolved solids (TDS) were approximately 302 ± 36 mg l^{-1} compared to approx. 220 mg l^{-1} of the lake water. There was no

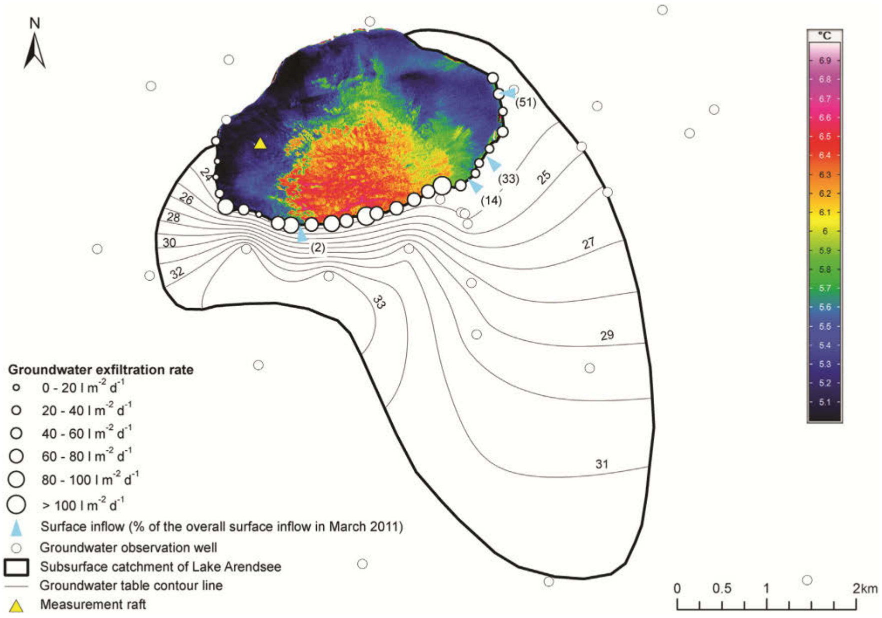

Figure 4.16 Thermal infrared image of Lake Arendsee taken on 22 March 2012. Groundwater entering the lake in near-shore zones in the south of the lake floats as thin warm layer on top of the water body and spreads out onto open waters. Water table contour lines in the catchment of Lake Arendsee and delimitation of the catchment were determined based on 32 groundwater observation wells. Size of near-shore circles indicates rates of groundwater discharge in that shore section based on sediment–temperature depth profiles (Schmidt et al., 2006) taken at the end of July and the beginning of August 2012. Blue triangles indicate location of the 4 small ditches entering the lake and the numbers in parentheses indicate the percentage of the overall surface water inflow entering the lake via that ditch in March 2011 (no measurements conducted in March 2012).

rain in the days before the flight and the measurement day was warm and cloudless which resulted in fast warming of the lake surface due to solar radiation (Fig. 4.17).

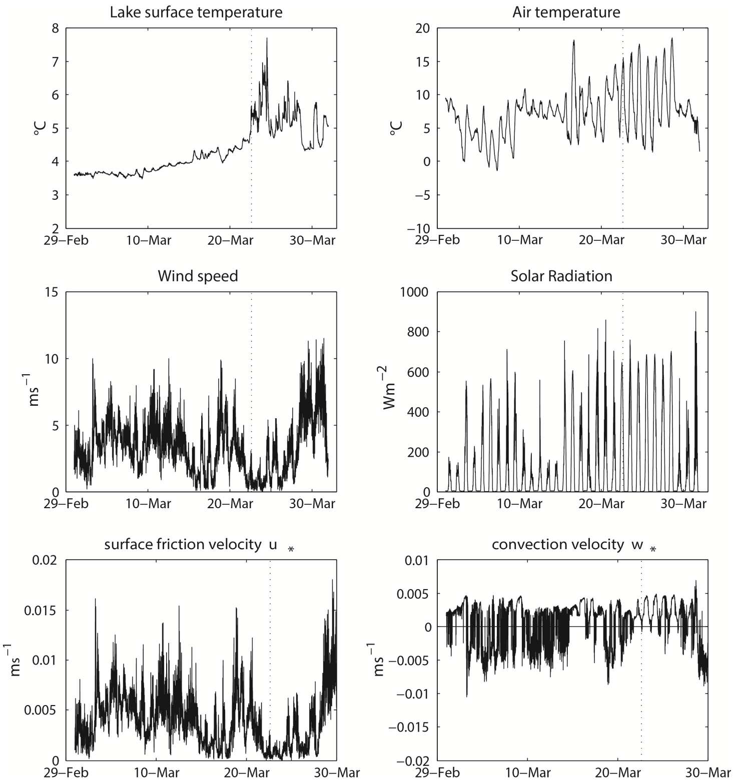

Figure 4.17 Water temperatures (T_{Water}) of Lake Arendsee in 1.5 m water depth and weather conditions over Lake Arendsee (air temperature T_{Air}, wind velocity and radiation) in March 2012. Vertical dashed lines designate the date of the TIR survey.

4.3.4 Discussion

The TIR image shows an area of warmer surface water spreading from the southern shoreline onto the lake (Fig. 4.16). Dispersion of the warm slick is driven by advection due to residual currents and by turbulent diffusion. Both mechanisms are dampened alongshore by boundary friction. Therefore, diffusion is stronger in the direction normal than parallel to the shoreline (Ozmidov 1990). The area of maximum LGD along the southern shoreline in the TIR image agrees well with our previous knowledge of zones where major LGD occurs. This is a first indication that the TIR image is a good approximation of the LGD pattern derived from ground-based methods. For the data interpretation it is not really necessary that the absolute values of the measured temperatures are correct since only the relative differences are of interest. Therefore, a labor intensive and time consuming calibration of the flight data is not required as long as data for the whole lake surface can be collected nearly instantaneously.

During the day at which the TIR image was taken and some days before, lake water temperatures measured in 1.5 m water depth were slowly approaching 5 °C. The warmer groundwater (10 °C) discharging into the lake was less dense than lake water even though TDS concentrations were slightly higher (approx. 60 mg l^{-1}) in groundwater compared to lake water. Density difference based on temperature and TDS: 236 ± 53 mg l^{-1} ($n = 10$); density difference based on temperature, TDS and changed volume due to dissolved ions: 183 ± 53 mg l^{-1} ($n = 10$, calculation according to Dietz et al. 2012) respectively 190 ± 53 mg l^{-1} ($n = 10$, calculations according to Boehrer et al. 2010). Therefore, LGD is immediately forced to the lake surface by denser lake water. During the ascent some mixing might have occurred and the contact with surrounding water resulted in some cooling of the groundwater. Nevertheless, it was still warmer than the rest of the water body and thus, floated on the top of the water body. From there the warmer less dense water gradually spread as a plume on the lake surface.

We can rule out the possibility that the observed temperature anomaly in Figure 4.16 is caused by shortwave solar radiation. If shortwave solar radiation had been the driver of the increased surface water temperatures on a cloudless day heating would be evenly distributed on a lake with the size of Lake Arendsee or it might be increased in the shallow areas at the northern shore (compare Material and methods section and Hupfer et al. (2000) for a bathymetric map of Lake Arendsee). However, Figure 4.16 shows no signal in the northern shore section of the lake. Nevertheless, it might be advantageous to conduct future flight missions pre-dawn to relieve all uncertainty associated with shortwave solar radiation.

Some authors report temperature anomalies in lakes due to surface inflows (Schott 1979). However, it can be ruled out that warm surface water entering the lakes through four drainage ditches is the major source of the observed temperature pattern since the drainage ditches enter the lake outside of the plume area or at its edges (Fig. 4.16). Also, it is impossible that upwelling of the bottom lake water by wind or seiches causes the observed lateral variations of surface water temperature since temperature differences between the upper water layers and the bottom water were only 0.26 °C. Only the immediate water surface is in some areas much warmer. Another explanation combining shortwave solar radiation and wind would be that the wind might have mixed and destroyed the warmer surface layer along the eastern, western and northern shore. However, there is no reasoning or indication for such wind pattern. Besides, the weather was quite calm before the flight (mean wind velocity in the last 14 h was 0.8 m s^{-1}). Shading can also be excluded as cause of the observed TIR temperature pattern due to the flat topography and the large size of the lake. Trees can cause some shading at the southern shore, but there water surface temperatures were highest. Also, the sky above Lake Arendsee was cloudless during the flight mission so that shading by clouds could not have any impact on the TIR image.

As described in the Material and methods section ground-based labor-intensive methods such as the measurement of the curvature of temperature depth profiles in the sediment showed a major groundwater discharge at the south-southeastern shore (Fig. 4.16). The size and shape of the catchment, hydraulic gradients (groundwater contour-lines), and k_{sat} data reported in the Material and methods section also support that the major LGD occurs in this shore section (Fig. 4.16).

The present study demonstrates a strong potential of airborne TIR imaging for investigation of groundwater inflow in lakes. However, the success of the method depends on the combination of external factors, which should favor buoyancy of groundwater and maintaining of temperature differences between groundwater and lake surface. A basic prerequisite for this is the positive buoyancy of the subsurface inflow, strong enough to reach the surface without being completely mixed with the lake water. A measure of the ratio of inflow buoyancy to the mixing forces is the densimetric Froude number *Fr*, which may be defined as

$$Fr = \frac{u_*}{\left(g \cdot \frac{\Delta\rho}{\rho_w} \cdot h_{LGD}\right)^{1/2}} = \frac{u_*}{u_g} \qquad \text{Eq. 4.11}$$

or its counterpart, the Richardson number *Ri*, used often in the studies on buoyancy flows

$$Ri = \frac{{u_g}^2}{{u_*}^2} = \frac{1}{Fr^2}. \qquad \text{Eq. 4.12}$$

Here, u_* is the characteristic scale of shear velocity, which is the measure of turbulent momentum flux (Reynolds stress), g is the acceleration due to gravity, $\Delta\varrho$ is the density difference between the groundwater and the lake water of density ϱw, h_{LGD} is a height scale relevant to the LGD, and u_g has the physical meaning of the internal gravitational wave speed based on the buoyancy $b = g \Delta\varrho\ \varrho w^{-1}$:

$$u_g = (b \cdot h_{LGD})^{1/2} \qquad \text{Eq. 4.13}$$

Fr becomes imaginary at negative buoyancy of the groundwater b < 0, whereas *Ri* is defined for both positively buoyant ($Ri > 0$) and negatively buoyant ($Ri \leq 0$) flows. Hence, a necessary (but not sufficient) condition for groundwater to reach the lake surface is the positive buoyancy of the groundwater, i.e., $\Delta\varrho i > 0$, $b > 0$, and $Ri > 0$. In addition, turbulent mixing should be weak to allow the groundwater to reach the surface without being completely mixed within the water column. Eq. 4.3c can be combined with Eq. 4.3b as

$$\frac{{u_*}^2}{b} < C_1 \cdot h_{LGD} \qquad \text{Eq. 4.14}$$

where C_1 is a dimensionless constant subject to empirical estimation. The wind friction velocity at the lake surface is a major source of the lake mixing (Wuest and Lorke 2003) and can be adopted for u_* in Equation 4.13. An appropriate choice for the LGD height scale h_{LGD} could be the vertical extension of the LGD area or the lake depth at the point of LGD. For Lake Arendsee an appropriate choice for the LGD height scale is the mean lake depth (29 m).

Another factor affecting strongly the mixing of the groundwater with the lake water is the vertical heat (or, more precisely, buoyancy) flux across the lake–atmosphere interface. If the downward heat flux is positive it depresses wind-driven turbulence and prevents mixing of the warm floating groundwater with the surrounding colder lake water. The balance between the wind mixing and the stabilizing buoyancy flux is expressed by the Monin–Obukhov length scale L_{MO} (Monin and Obukhov 1954)

$$L_{MO} \sim \frac{{u_*}^3}{B} \qquad \text{Eq. 4.15}$$

where $B = g\alpha Q$ is the buoyancy flux at the lake surface. Here, Q is the surface temperature (heat) flux and α is the coefficient of thermal expansion for the surface water. An upward heat flux destabilizes the lake water column and produces strong convective mixing, which homogenizes the water temperature. The Deardorff's (1970) convective velocity scale w_* quantifies the intensity of convective motions

$$w_* = (-h_{mix} \cdot B)^{1/3} \qquad \text{Eq. 4.16}$$

where h_{mix} is the thickness of the surface mixed layer. The two criteria 5 and 6 can be combined for both positive and negative surface buoyancy flux *B* as,

$$0 < \frac{{u_*}^3}{{w_*}^3} < C_2 \qquad \text{Eq. 4.17(a)}$$

or

$$0 = \frac{L_{MO}}{h_{mix}} < C_2 \qquad \text{Eq. 4.17(b)}$$

where C_2 is another dimensionless constant. The lower boundary is set here to 0 since convection in lakes has generally a higher potential for vertical mixing of water masses than the wind-driven turbulence at the background of the stabilizing buoyancy flux. Thus, we suggest that tracing of groundwater at the lake surface is impossible as long as the surface buoyancy flux is directed into the atmosphere and produces convective mixing in the upper lake water.

A simple interpolation formula combining Equations 4.14 and 4.17(a) provides a criterion G for groundwater floating at the lake surface

$$0 < G \ll 1 \qquad \text{Eq. 4.18}$$

where G is a dimensionless number defined as

$$G = \frac{u_*^{\,3}}{C_1 \cdot w_*^{\,3} + C_2 \cdot u_* \cdot b \cdot h_{LGD}} \qquad \text{Eq. 4.19}$$

Equation 4.18 is equivalent to Equation 4.14 at infinitesimal w_*; if, in turn b vanishes, Equation 4.18 turns into Equation 4.17. The qualitative balance between buoyancy and mixing expressed by Equation 4.19 can be used for quantification of the groundwater floating, if the constants C_1 and C_2 are defined. Their thorough estimations require more detailed field data than we possess. However, the first-guess estimations can be derived directly from our dataset. Intrinsic for scaling analysis, the constant of proportionality in a dimensionless criterion is close to 1, if the chosen scales are representative for the mean balance between the governing forces (Barenblatt 2003). Indeed, reported values of C_1 vary in the range 0.1 to 10 (Padman 1991; Stigebrandt 1985; Zilitinkevich and Mironov 1996), so that we assume $C_1 = O(1)$ in what follows. Because the LGD height scale h_{LGD} is not clearly defined, the observation data can be used for backward estimation of $C_2 h_{LGD}$. The same considerations of the approximate balance between the governing forces as above suggest that $u_*^3 w_*^{-3}$ and $u_*^2 (C_2 b h_{LGD})^{-1}$ should vary within the same orders of magnitude (compare Equations 4.14, 4.17(a) and 4.18). Substitution of u_*, w_* and b from the observational data from Lake Arendsee for March 2012 into both terms shows that the condition is equivalent to $C_2 h_{LGD} \sim 10^{-3}$. After tentative adopting of this value, the variability of G within the month allows to clearly identify the periods of potential groundwater floating events in Lake Arendsee (Fig. 4.18): in the first half of March the mixing dynamics was dominated by strong winds ($G > 1$) and by convection due to heat loss into the atmosphere ($G < 0$, blank areas in Fig. 4.18). Several events of low wind and strong heating between March 16 and March 26 produced periods with G values between 10^{-2} and 10^{-3}, one of which coincided with the period of our TIR survey on March 22. Later, stronger winds and colder nighttime air temperatures (Fig. 4.17) result in G values above one and below zero, respectively. In a longer perspective, the overall tendency of lake surface heating should produce the negative buoyancy of the groundwater relative to the surface waters, so that the floating of groundwater in summer becomes impossible ($Ri < 0$ and $G < 0$).

The balance between buoyancy and mixing considered above suggests that the favorable conditions for groundwater floating, at least in temperate climates, should appear twice a year, in spring and in autumn, when (i) lake water densities are higher than the groundwater density, and (ii) mixing produced by the heat and momentum fluxes at the lake surface is weak. However, in autumn measurement windows might be extremely small or non-existent since water bodies cool down much slower than the atmosphere so that heat fluxes from the water surface to the atmosphere might hinder groundwater floating on top of the lake water. The condition (ii) usually varies at rather short time scales, depending on the synoptic situation. The dimensionless criterion G may be useful in this sense for planning airborne surveys based on short-term weather forecasts and on current lake water temperatures.

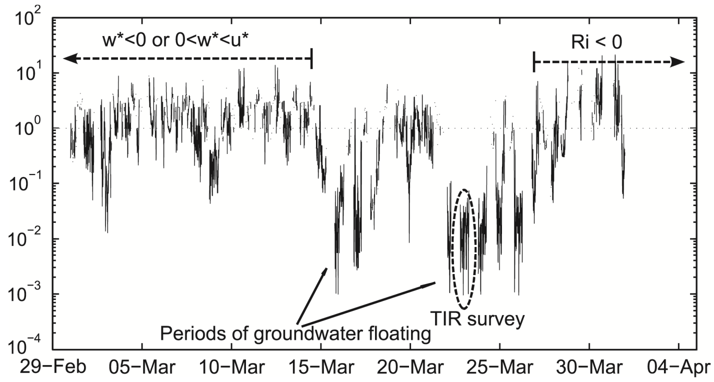

Figure 4.18 The groundwater floating criterion *G* (Eq. 4.19) in Lake Arendsee in March 2012. u_* is the friction velocity at the lake surface, w_* is the convective velocity scale, and *Ri* is the Richardson number. The gaps correspond to the periods of negative G, when no groundwater floating is possible independent of the absolute value of *G*.

4.3.5 Conclusions

Airborne measurement of TIR is a useful technique to identify groundwater discharge not only in marine systems (SGD) but also in freshwater lakes (LGD). In the present case study lake temperatures, the high amount of LGD, the LGD pattern and weather conditions before the campaign were favorable for the application of the method. We hope that the present study promotes further TIR investigations by different research groups. Simultaneous ground-based measurements of the thickness of the warmer surface layer and the temporal development of the plume are necessary for providing justification and refinement of constants used in the theoretical criterion given as Equation 4.18. In the future, the method might be applied to get a first fast snapshot of the LGD pattern and might be a useful basis for planning the application of ground-based measurement techniques. In case that a study aims at the determination of nutrient loads a combination of hydrological and biogeochemical investigations is required. For example, in the present case study, the TIR image (Fig. 4.16) revealed, that the major LGD occurs in the south-southeastern shore section where the small town of Arendsee is located. Thus, further hydrological and biogeochemical investigations should focus on this area. Based on the results of a thermal infrared image it is possible to conduct time-consuming, labor-intensive ground-based investigations more specifically in the most relevant and representative zones instead of the more or less random approach applied nowadays. Our aim is to stimulate the use of airborne thermal infrared by different scientists in different case studies since we are quite sure that a broader application of the method would be a large step forward in understanding of groundwater–lake interactions. However, attributing surface thermal anomalies to LGD depends on careful consideration of other factors that could produce similar patterns such as above-ground inflows, solar radiation, and wind as well as careful consideration of lake physics.

4.3.6 References

Anderson, J.M., Duck, R.W., McManus, J., 1995. Thermal radiometry: a rapid means of determining surface water temperature variations in lakes and reservoirs. *Journal of Hydrology*, 173(1): 131-144.

Barenblatt, G.I., 2003. *Scaling*. Cambridge University Press, 171 p.

Boehrer, B., Herzsprung, P., Schultze, M., Millero, F.J., 2010. Calculating density of water in geochemical lake stratification models. *Limnology and Oceanography: Methods*, 8(11): 567-574.

Cook, J.M., Edmunds, W.M., Robins, N.S., 1991. Groundwater contribution to an acid upland lake (Loch Fleet, Scotland) and the possibilities for amelioration. *Journal of Hydrology*, 125(1): 111-128.

Danielescu, S., MacQuarrie, K.T.B., Faux, R.N., 2009. The integration of thermal infrared imaging, discharge measurements and numerical simulation to quantify the relative contributions of freshwater inflows to small estuaries in Atlantic Canada. *Hydrological Processes*, 23(20): 2847-2859.

Deardorff, J.W., 1970. Convective Velocity and Temperature Scales for the Unstable Planetary Boundary Layer and for Rayleigh Convection. *Journal of the Atmospheric Sciences*, 27(8): 1211-1213.

Dietz, S., Lessmann, D., Boehrer, B., 2012. Contribution of Solutes to Density Stratification in a Meromictic Lake (Waldsee/Germany). *Mine Water and the Environment*, 31(2): 129-137.

Dinçer, T., 1968. The Use of Oxygen 18 and Deuterium Concentrations in the Water Balance of Lakes. *Water Resources Research*, 4(6): 1289-1306.

Duarte, T.K.e., Hemond, H.F., Frankel, D., Frankel, S., 2006. Assessment of submarine groundwater discharge by handheld aerial infrared imagery: case study of Kaloko fishpond and bay, Hawai'i. *Limnology and Oceanography: Methods*, 4(7): 227-236.

Garcia-Solsona, E., Garcia-Orellana, J., Masqué, P., Rodellas, V., Mejías, M., Ballesteros, B., Domínguez, J.A., 2010. Groundwater and nutrient discharge through karstic coastal springs (<i>Castelló</i>, Spain). *Biogeosciences*, 7(9): 2625-2638.

Harvey, F.E., Rudolph, D.L., Frape, S.K., 2000. Estimating Ground Water Flux into Large Lakes: Application in the Hamilton Harbor, Western Lake Ontario. *Ground Water*, 38(4): 550-565.

Hofmann, H., Knöller, K., Lessmann, D., 2008. Mining lakes as groundwater-dominated hydrological systems: assessment of the water balance of Mining Lake Plessa 117 (Lusatia, Germany) using stable isotopes. *Hydrological Processes*, 22(23): 4620-4627.

Hook, S.J., Prata, F.J., Alley, R.E., Abtahi, A., Richards, R.C., Schladow, S.G., Palmarsson, S.O., 2003. Retrieval of lake bulk and skin temperatures using Along-Track Scanning Radiometer (ATSR-2) data: A case study using Lake Tahoe, California. *Journal of Atmospheric and Oceanic Technology*, 20(4): 534-548.

Hupfer, M., Pöthig, R., Brüggemann, R., Geller, W., 2000. Mechanical resuspension of autochthonous calcite (Seekreide) failed to control internal phosphorus cycle in a eutrophic lake. *Water Research*, 34(3): 859-867.

Johnson, A.G., Glenn, C.R., Burnett, W.C., Peterson, R.N., Lucey, P.G., 2008. Aerial infrared imaging reveals large nutrient-rich groundwater inputs to the ocean. *Geophysical Research Letters*, 35(15): n/a-n/a.

Kishel, H.F., Gerla, P.J., 2002. Characteristics of preferential flow and groundwater discharge to Shingobee Lake, Minnesota, USA. *Hydrological Processes*, 16(10): 1921-1934.

Kluge, T., Ilmberger, J., von Rohden, C., Aeschbach-Hertig, W., 2007. Tracing and quantifying groundwater inflow into lakes using a simple method for radon-222 analysis. *Hydrology and Earth System Sciences*, 11(5): 1621-1631.

Krabbenhoft, D.P., Bowser, C.J., Kendall, C., Gat, J.R., 1994. Use of O-18 and deuterium to assess the hydrology of groundwater-lake systems. In: *Environmental Chemistry of Lakes and Reservoirs*, Baker, L.A. (Ed.). Advances in Chemistry Series, 67-90.

Lee, D.R., 1977. A device for measuring seepage flux in lakes and estuaries. *Limnology and Oceanography*, 22(1): 140-147.

Lee, K., 1969. Infrared exploration for shoreline springs: A contribution to the hydrogeology of Mono Basin, Stanford University, California, p.

Monin, A.S., Obukhov, A.M., 1954. Basic laws of turbulent mixing in the surface layer of the atmosphere. *Trudy Akademii Nauk SSSR Geophizicheski Institut*, 24: 163–187.

Oliveira Ommen, D.A., Kidmose, J., Karan, S., Flindt, M.R., Engesgaard, P., Nilsson, B., Andersen, F.O., 2012. Importance of groundwater and macrophytes for the nutrient balance at oligotrophic Lake Hampen, Denmark. *Ecohydrology*, 5(3): 286-296.

Ong, J.B., Lane, J.W., Zlotnik, V.A., Halihan, T., White, E.A., 2010. Combined use of frequency-domain electromagnetic and electrical resistivity surveys to delineate near-lake groundwater flow in the semi-arid Nebraska Sand Hills, USA. *Hydrogeology Journal*, 18(6): 1539-1545.

Ozmidov, R.V., 1990. *Diffusion of Contaminants in the Ocean. Oceanographic Sciences Library,* 4. Springer Netherlands, The Netherlands, 320 p.

Padman, L., 1991. Near-surface mixing in a freshwater lake. *Marine and Freshwater Research*, 42(6): 655-673.

Peterson, R.N., Burnett, W.C., Glenn, C.R., Johnson, A.G., 2009. Quantification of point-source groundwater discharges to the ocean from the shoreline of the Big Island, Hawaii. *Limnology and Oceanography*, 54(3): 890-904.

Pfannkuch, H.O., Winter, T.C., 1984. Effect of anisotropy and groundwater system geometry on seepage through lakebeds: 1. Analog and dimensional analysis. *Journal of Hydrology*, 75(1–4): 213-237.

Rundquist, D., Murray, G., Queen, L., 1985. Airborne thermalmapping of a “flow-through” lake in the Nebraska Sandhills. *JAWRA Journal of the American Water Resources Association*, 21(6): 989-994.

Schmidt, C., Bayer-Raich, M., Schirmer, M., 2006. Characterization of spatial heterogeneity of groundwater-stream water interactions using multiple depth streambed temperature measurements at the reach scale. *Hydrology and Earth System Sciences*, 10(6): 849-859.

Schott, J.R., 1979. Temperature-measurement of cooling water discharged from power-plants. *Photogrammetric Engineering and Remote Sensing*, 45(6): 753-761.

Schuetz, T., Weiler, M., 2011. Quantification of localized groundwater inflow into streams using ground-based infrared thermography. *Geophysical Research Letters*, 38.

Selker, J.S., Thevenaz, L., Huwald, H., Mallet, A., Luxemburg, W., de Giesen, N.V., Stejskal, M., Zeman, J., Westhoff, M., Parlange, M.B., 2006. Distributed fiber-optic temperature sensing for hydrologic systems. *Water Resources Research*, 42(12).

Shaban, A., Khawlie, M., Abdallah, C., Faour, G., 2005. Geologic controls of submarine groundwater discharge: application of remote sensing to north Lebanon. *Environmental Geology*, 47(4): 512-522.

Shaw, R.D., Prepas, E.E., 1990. Groundwater-lake interactions: II. Nearshore seepage patterns and the contribution of ground water to lakes in central Alberta. *Journal of Hydrology*, 119(1): 121-136.

Stigebrandt, A., 1985. A Model for the Seasonal Pycnocline in Rotating Systems with Application to the Baltic Proper. *Journal of Physical Oceanography*, 15(11): 1392-1404.

Torgersen, C.E., Faux, R.N., McIntosh, B.A., Poage, N.J., Norton, D.J., 2001. Airborne thermal remote sensing for water temperature assessment in rivers and streams. *Remote Sensing of Environment*, 76(3): 386-398.

Vanek, V., 1987. The interactions between lake and groundwater and their ecological significance. *Stygologia*, 3: 1-23.

Whiting, J.M., 1976. Determination of Groundwater Inflow to Prairie Lakes Using Remote Sensing. *IEEE Transactions on Geoscience Electronics*, 14(1): 60-65.

Wuest, A., Lorke, A., 2003. Small-scale hydrodynamics in lakes. *Annual Review of Fluid Mechanics*, 35: 373-412.

Zilitinkevich, S., Mironov, D.V., 1996. A multi-limit formulation for the equilibrium depth of a stably stratified boundary layer. *Boundary-Layer Meteorology*, 81(3): 325-351.

5 Discussion of the two core studies

The two studies presented in Chapter 3 proof that groundwater P concentrations can be increased far beyond natural background values. This means that P can be transported with the groundwater in relevant amounts. Here, "relevant" means that groundwater-borne P is the reason for ongoing eutrophication of Lake Arendsee. To the best of our knowledge this has never been proven by such a detailed P budget. Furthermore, the few so-far known cases of groundwater P contamination could always be referred to known P sources (e.g., sewage infiltration over decades in the catchment of Ashumet Pond in Massachusetts, USA, McCobb et al. 2003). In contrast, no obvious or known contamination source could be identified in the catchment of Lake Arendsee. Nevertheless, the severity of the contamination is confirmed by the fact that a lake of such large volume is deteriorated.

The poor trophic condition of the lake evolves from a situation in which the main LGD fluxes occur just where the groundwater is most heavily contaminated with P. However, it might be short-sighted or even ignorant to think that Lake Arendsee is a single case where several unfavorable conditions come together by accident. The reverse might actually be true, namely that many eutrophied lakes receive significant nutrient loads from groundwater exfiltration without being noticed. Reasons for the neglect of groundwater in nutrient and especially P budgets of lakes have been discussed in Chapter 2. The results presented in the Lake Arendsee-studies in Chapter 3 should stimulate lake managers and researchers to always consider groundwater as a potential source of lake eutrophication.
Putting this into action means that simple standard modelling approaches or single groundwater investigations are no sufficient means to exclude groundwater as a main nutrient source of a lake. Learning from Lake Arendsee implies that detailed *in situ*-investigations with high spatial resolutions are required. Such investigations would, at best, end up with a value for the groundwater-borne load of the target parameter. However, the studies presented here clearly show that the approach of multiplying LGD volume by parameter concentration to obtain a groundwater-borne mass load is by far not as simple as it seems. To obtain reliable results a variety of factors influencing LGD and related mass loads should be considered in such investigations. As a by-product of the Lake Arendsee-studies a conceptual scheme visualizing the most important features contributing to the magnitude of groundwater-borne mass loads has been developed (Fig. 5.1). Most of those features are characterized by either temporal or spatial heterogeneity of the target parameter or groundwater exfiltration (Chapter 2). Their contribution to a mass load is of very individual character in single systems since they might depend on a number of factors as will be discussed below. This prohibits general statements about the individual importance of these features for groundwater-borne mass loads. At the same time the large variety of factors impacting on LGD mass loads underlines the necessity for *in situ*-investigations in order to increase the reliability of lake specific mass load determinations. However, such intense investigations will be in most cases far beyond the capacities of both, research and practice, especially since investigations of all of these aspects on site are challenging and results will inevitably come along with shortcomings. Consequently, the determination of groundwater-borne mass loads is always a tradeoff between, on the one hand. addressing the features named in Figure 5.1 by detailed investigations and, on the other hand, time and costs. If, however, by means of the present studies the awareness for groundwater-borne P loads to surface waters increases, a great deal of work will have been done regarding the acceptance of an increased workload to determine the role of groundwater in a lake P budget.

The following sub-chapters discuss methods and results of the Lake Arendsee-studies (Chapter 3) in the light of the basic drivers named in the red-framed boxes in Figure 5.1.

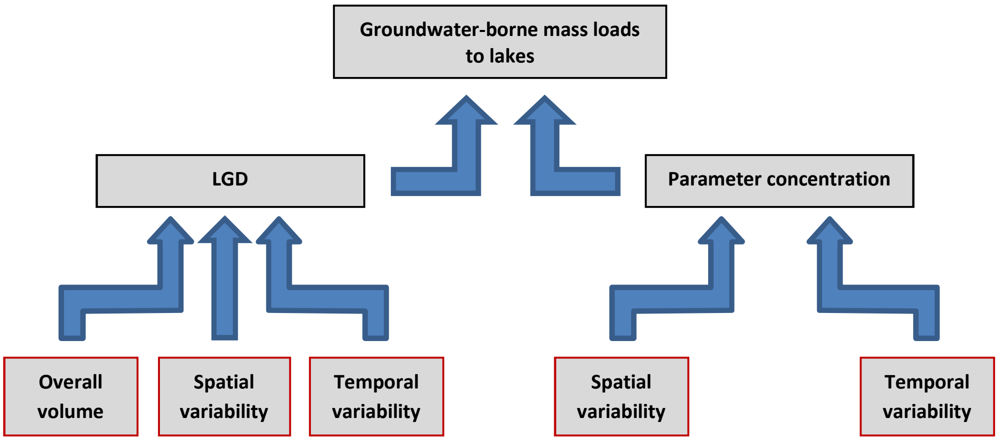

Figure 5.1 Illustration of features influencing the magnitude of groundwater-borne mass loads to lakes. Red-framed features are regarded and discussed as basic drivers for groundwater-borne mass loads that need to be addressed in studies aiming at quantifying groundwater-borne mass loads.

5.1 Lacustrine groundwater discharge

5.1.1 Overall volume of LGD

In the case of Lake Arendsee a value for the overall LGD volume was derived from groundwater recharge calculations based on geographical data with a relatively high spatial resolution (Chapter 3.1). This approach is based on the assumption that on sufficiently long time scales the same amount of groundwater exfiltrating into a lake is recharged in the catchment. A comparison of the overall LGD volume with the other terms of the water balance reveals the influence of groundwater on a lake water balance. In terms of overall LGD volumes, this holistic approach is more reliable than the upscaling of point measurements: Apart from a sufficient spatial resolution of point measurements, the accuracy of overall LGD volumes derived from them (e.g., of hydraulic gradients or lake bed temperatures) depends on assumptions and methods to determine boundary conditions (e.g., values for k_{sat}, K_{fs} or groundwater and surface water temperatures, etc.). In practice, some of those parameters are often based on "experiences" or literature values instead of being actually determined *in situ*. As a consequence, overall LGD volumes resulting from upscaling of point measurements include the sum of all errors of the individual measurements. The areal upscaling of local exfiltration rates will impose further insecurity onto the resulting overall LGD volume due to potential non-representativeness. A representative sampling setup, however, will often comprise unfeasibly large numbers of measurement points to derive a reliable value for overall LGD volumes.

Nevertheless, also groundwater recharge quantification at Lake Arendsee contained uncertainties in some aspects. In general, accuracies of LGD volumes derived from groundwater recharge can be reduced by unknown groundwater extractions from the aquifer, unsuitable or low-quality input data, and incorrect catchment delineation. Often, a lake's groundwater catchment differs at least slightly from its surface catchment (Nützmann and Mey 2007; Winter et al. 2003). However, for practical reasons this is often not considered and groundwater and surface catchments are handled to be identical. The subsurface catchment of Lake Arendsee was determined from water table measurements all around the lake (Chapter 3.1). This enabled the interpolation of groundwater contour lines and by that the delineation of the subsurface catchment which significantly differs in size and shape from the surface catchment (Fig. 5.2). A sufficient number of well distributed observation sites is a prerequisite for proper interpolations. Also at this large scale hydrogeological heterogeneity might be an issue for reliable results. At Lake Arendsee the substrates in the subsurface catchment are of varying hydraulic

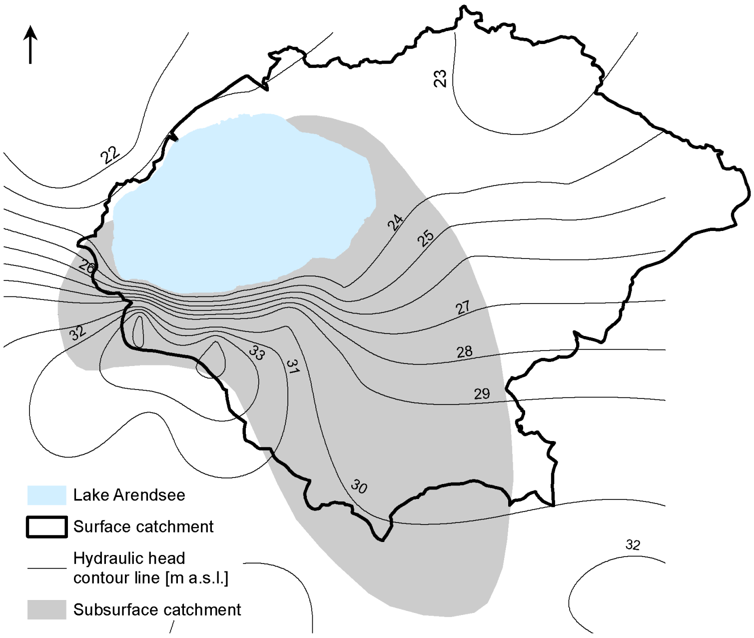

Figure 5.2 Surface and subsurface catchment of Lake Arendsee.

conductivities resulting in two separated aquifers at some locations. It is crucial to only include water table values from the aquifer of interest into the interpolations water table contour lines.

Another point to be discussed is the assumption that groundwater recharged in the catchment equals the volume of groundwater exfiltration to the lake. Abstractions of groundwater from the aquifer have to be taken into account. In the setting of Lake Arendsee agricultural drainage reduces the exfiltration volume significantly. Groundwater and vadose water are directed into ditches or tile drains by the artificially imposed gradient. While the transport of water from the saturated zone into both, surface and subsurface drains is a lateral process the transport of vadose water into subsurface tube drains is dominated by vertical, often preferential flow (Stamm et al. 2002). This preferential flow is induced by interconnected macropores which may contribute significantly to stream flow while matrix flow is of minor importance (Carluer and Marsily 2004; Stillman et al. 2006; Fig. 5.3).

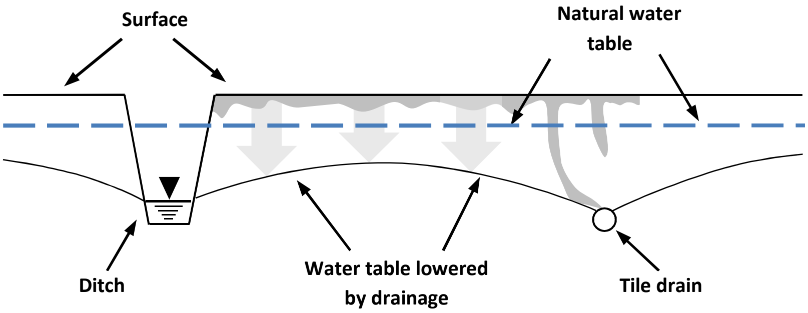

Figure 5.3 Scheme of the impact of artificial drainage on the water table. A front of vadose water (in dark grey) reaches the drains either as preferential flow directly towards the tile drain (induced by macropores) or as matrix flow towards the groundwater (light grey arrows; modified from Radcliffe et al. 2015 and Skaggs et al. 2005).

The impact of agricultural drainage on the hydrology of adjacent ecosystems is hardly quantifiable (Skaggs et al. 2005). Although large areas have been meliorated by drainage in northern Europe (Lennartz et al. 2011) studies on drainage impacts rather focus on transport and losses of nutrients and contaminants than on the consequences of the hydrological alteration of the system. The reduction of groundwater flow in regional or local water balances is hardly discussed. This is despite the fact that drain water often represents the major component in the local water balance. For example, Lennartz et al. (2011) report that tile drainage discharge accounted for 75, 87, and 68% of precipitation in three different measurement periods at the same site, respectively. These values imply a similar reduction of actual groundwater flow.

The amount of water being directed into drainage pipes and ditches is highly individual for single facilities and sites and depends on a lot of factors of which some are listed below (e.g., Dollinger et al. 2015; Radcliffe et al. 2015):

- Regional geographic settings, e.g.,
    - Soil type
    - Hydraulic connectivity of ditches to surrounding fields
    - Climate
- Local settings, e.g.,
    - Land use type
    - Season (depth to water table)
    - Intensity of macropore flow
    - Hydraulic gradient between water table and ditch
    - Hydraulic connectivity of interfaces between ditches and groundwater
- Drainage facility characteristics, e.g.,
    - Type (tile drainage or ditch system)
    - Length, slope, cross section width, orientation regarding slope of surrounding areas
    - Vegetation cover in the ditch
    - Maintenance and management
    - Ditch network design

The groundwater catchment of Lake Arendsee is mainly agricultural and a large portion of it is drained. Although it is difficult to quantify drainage losses, former GDR authorities developed extensive data on the drainage-intensity of single parcels. Drainage intensity represents the percentage of the water infiltrating into the soil that is collected by drainage facilities (i.e., drainage losses). The data are available as GIS shape files. The drainage intensity is classified in four stages: 0 – 30%, 30 – 60%, 60 – 90%, and 90 – 100%. By applying the upper boundary of a class, maximum drainage losses and minimum groundwater recharge volumes were calculated (Chapter 3.1). By that two major factors may impose uncertainty to the results of groundwater recharge calculations for the subsurface catchment of Lake Arendsee:

1. The three proposed lower classes of drainage intensity cover large ranges of 30%. Applying the maximum value of a class to calculate drainage losses for a parcel imposes a potential overestimation of drainage loss by 30% and probably a mean overestimation by 15%. Consequently, groundwater recharge (i.e., LGD) and by that groundwater-borne P loads may be potentially underestimated by up to 30% due to a lack of more precise information on drainage intensity.

2. The quality and reliability of the available data is quite questionable in itself. Due to the large number of factors impacting on drainage intensity (see above), a reliable quantification of drainage losses from the vadose zone is almost impossible. It is thus questionable to if the actual drainage losses comply with the available data at all. Furthermore, no information about the derivation of drainage intensity values was available. Thus, an evaluation of the approach was not possible at all.

It would be of great benefit to develop hands-on approaches for the on-site determination of drainage intensities. However, it seems research is still far away to be able to handle this issue.

5.1.2 Spatial heterogeneity of LGD

The spatial characteristics of LGD are related to its lake specific occurrence at various locations and scales. To visualize this, a simple scheme was developed (Fig. 5.4). LGD is often diffuse, resulting in discharge distributed over a large area. LGD rates are usually not spatially homogeneous. It is well known that LGD rates show quite heterogeneous patterns, e.g., due to (hydro-)geological conditions and other factors (Winter 1999, see also Chapter 2.1). This comprises two dimensions, the one along the shoreline where LGD is usually most intense (Type A in Fig. 5.4), as well as the one perpendicular to the shoreline (Type B in Fig. 5.4). Both refer to near-shore LGD because LGD is usually most intense close to the shoreline (McBride and Pfannkuch 1975; Pfannkuch and Winter 1984). Additional spatial heterogeneity can be introduced as "hot spots" of LGD anywhere at the lake bed (Type C in Fig. 5.4). The latter occurs independently of the diffuse areal fluxes focused on near-shore areas. It can be caused for example by preferential flow paths via locally restricted areas of larger hydraulic conductivities than surrounding areas (Krabbenhoft and Anderson 1986; Fig. 1.4). This chapter discusses the importance of the different types and scales of spatial LGD heterogeneity in the case of Lake Arendsee.

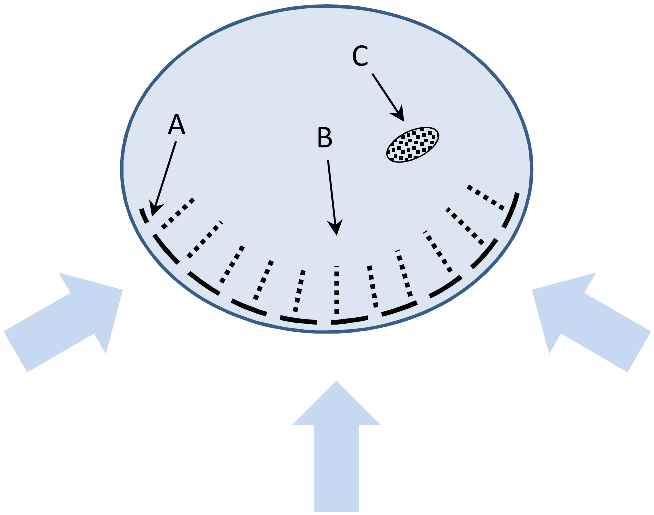

Figure 5.4 Dimensions of potential spatial heterogeneity of LGD intensity in a lake (blue circle). Large blue arrows indicate general groundwater flow direction toward the lake. Heterogeneity of LGD along the section of the shoreline where LGD occurs (Type A, dashed line), perpendicular to the shoreline (Type B, dotted lines), as well as all across the lake bed (Type C, spotted circle).

Type A - Spatial heterogeneity of LGD along the shoreline

It is well-known that most LGD occurs close to the shore (McBride and Pfannkuch 1975; Pfannkuch and Winter 1984). The general absence or presence of LGD along a lake shore is one aspect of spatial heterogeneity encompassed by Type A (Fig. 5.4). At lakes such as Lake Arendsee which are integrated in a regional flow system (flow through lakes) large scale hydrogeological settings (general groundwater flow directions and velocities) determine where groundwater predominantly discharges and by that carries mass loads to the lake.

The catchment boundaries separate groundwater in- and exfiltration zones along the shore. The spatial expansion of the catchment around the lake indicates where main LGD can be expected. Since the subsurface catchment of Lake Arendsee expands mainly south of the lake a predominant portion of groundwater is expected to enter the lake along the southern shoreline (Chapter 3.1). This was confirmed by the results of local point measurements (Fig. 3.7 in Chapter 3.1). Along the western and eastern shore groundwater exfiltration is less intensive. No LGD occurs along the northern shore. Instead, infiltration of lake water into the aquifer is assumed to take place here.

Type A-heterogeneity is not only important on the regional scale. On local scale LGD intensity along the shore can vary to a large degree and independently from large scale conditions. Besides supporting regional groundwater flow patterns, temperature depth profiles at Lake Arendsee revealed a large variation of LGD rates on medium scales (Chapter 3.1). This type of LGD heterogeneity can significantly influence groundwater-borne mass loads. If groundwater concentrations are spatially homogeneous spatial patterns of mass loads discharged by groundwater depend exclusively on spatial patterns of LGD rates. Accordingly, LGD rates determine spatial patterns of increased discharge of pollutants. If groundwater concentrations are not homogeneous, patterns of LGD rates have a severe effect on the total mass load. In a scenario of a spatially restricted contaminated plume approaching a lake there are two general options:

(a) The contaminated plume reaches the lake where LGD rates are high compared to neighboring areas. The combination of high LGD rates and high concentrations results in a large mass load to the lake.

(b) The contaminated plume reaches the lake where LGD rates are low. Resulting groundwater mass loads are small relative to scenario (a).

Lake Arendsee represents scenario (a) as shown in Chapter 3.2. The groundwater is heavily polluted where LGD has maximum rates. LGD rates were determined for 200 m-shoreline segments based on temperature depth profiles of the lake sediments. Spatial investigations of LGD rates are of large importance for mass load quantification. As will be shown below, a neglect of spatial heterogeneity of LGD rates along the shore results in an underestimation of groundwater-borne P loads. Factors controlling local LGD rates along the shore are numerous and have been discussed in Chapter 2.1. The most prominent controls of LGD are locally varying geologic conditions such as horizontal and vertical k_{sat} as well as their ratio which determines the degree of anisotropy. Sediment characteristics such as grain size distributions, porosity, and permeability influence k_{sat} at all vertical and horizontal scales, even down to the centimeter scale (Kishel and Gerla 2002). At Lake Arendsee, the complex geological situation is probably also a major factor causing LGD heterogeneity on small and medium scales. An example for such local LGD heterogeneity is measurement no. 7 in Figure 5.5. This site shows a significantly lower LGD rate than the two adjacent sites. Also the fact that the three highest LGD rates (No. 5, 13, and 18, Fig. 5.5) were found spatially independent from each other (i.e., at non-adjacent measurement sites) depicts the importance of local controls on LGD rates.

With distances of 200 m to each other, temperature based measurements at Lake Arendsee covered the medium scale and revealed substantial heterogeneity of LGD rates. Many studies, however, show that heterogeneity of groundwater discharge can also be significant at much smaller scales (e.g., Kishel and Gerla 2002). For example, transpiration of riparian vegetation is known to influence local LGD rates at the meter scales (Winter 1999). This was assumed as a reason for locally decreased exfiltration rates at a few locations of Lake Hinnensee (spatial resolution 2 m, Chapter 4.2). While the complex geological situation at Lake Arendsee probably rules LGD rates at the medium scale (about 10 to 200 m) transpiration of trees may have (amongst others) some influence at smaller scales (about 1 to 10 m). However, this influence on small scale LGD patterns is assumed to be generally superimposed by hydrogeologic conditions close to the lake.

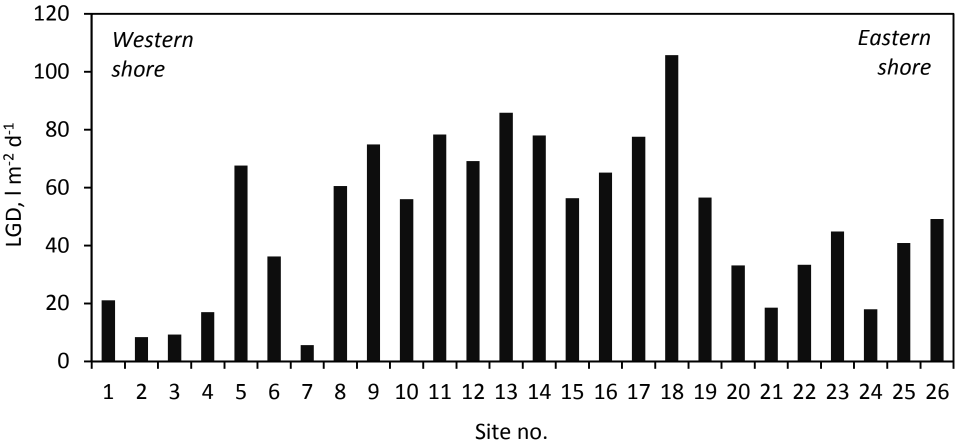

Figure 5.5 LGD rates at 26 sites along the southern shore of Lake Arendsee. Results derived from temperature depth profiles measured in 1 m distance to the shore. Distance between the measurement sites is about 200 m (see Chapter 3.1 for further information).

Type B - Spatial heterogeneity of LGD perpendicular to the shore

Due to the reasons named in Chapters 1.2 and 1.3 diffuse LGD often enters a lake primarily close to the shoreline (Fig. 1.3). Within only a few meters distance to the shore groundwater exfiltration rates usually decrease significantly (McBride and Pfannkuch 1975; Pfannkuch and Winter 1984). However, this general pattern is often superimposed or even suspended by site-specific factors impacting on LGD rates (Winter 1999). At Lake Arendsee LGD rates were derived from temperature depth profiles in 0.5, 1, 2, and 4 m distance to the shoreline (Chapter 3.1). 65% of the transects measured perpendicular to the shore (*n* = 26) showed a decrease of LGD rates with increasing distance to shore. The rest of nine transects was indifferent regarding a dependency of LGD rates to shoreline distance. Deviations from the general pattern occurred independently of the magnitude of LGD (Fig. 5.6).

Furthermore, no common pattern of LGD could be identified in this group of transects. Spatial variations of LGD rates were of individual character for each transect. The mean values of the indifferent transects show a relatively small range compared to the other group (Fig. 5.7), indicating that deviations from the general pattern do not follow specific rules but result from individual conditions at the measurement sites. Causes for are the same as mentioned for Type A-heterogeneity (e.g., geological heterogeneities). Especially great anisotropy is discussed to result in less near-shore focusing of LGD (Genereux and Bandopadhyay 2001; Pfannkuch and Winter 1984).

The results presented here show that measurements of LGD at one fixed distance to the shore might not meet the demands of the underlying research question. At Lake Arendsee temperature-derived LGD rates were applied to the total LGD volume based on groundwater recharge as a weighing factor for LGD volumes of individual shoreline segments. For this it was crucial to work with representative (comparable) values, e.g., maximum LGD rate of each transect. Measurements at a standardized distance to the shore (e.g., 1 m) might not meet this criterion.

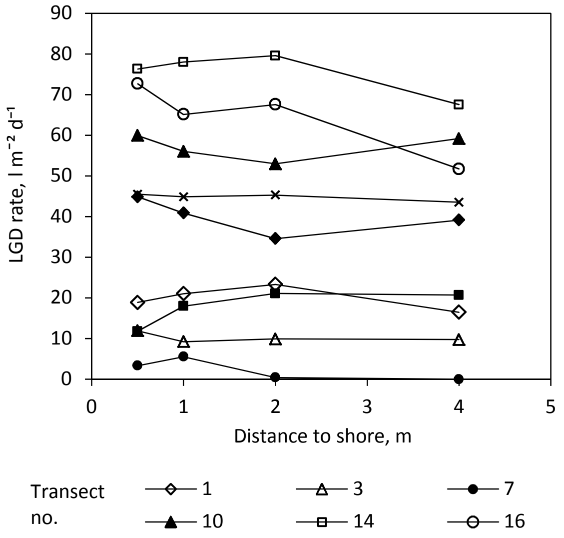

Figure 5.6 Nine transects deviating from the general pattern of decreasing LGD rates with increasing distance to shoreline.

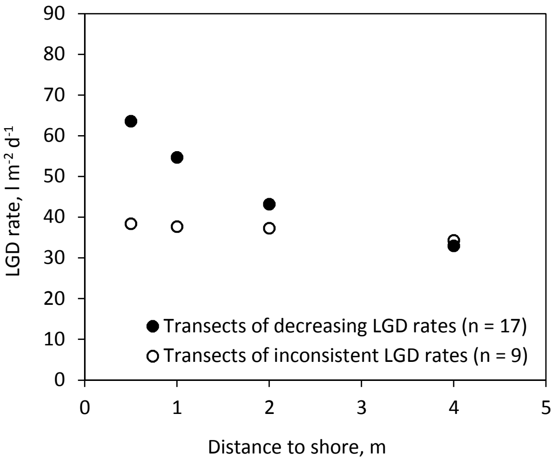

Figure 5.7 Mean LGD rates in transects of decreasing LGD rates (black dots) and transects of inconsistent LGD rates (circles) in 0.5, 1, 2, and 4 m distance to the shoreline, respectively.

Type C – Spatial heterogeneity of LGD across the lake bed due to preferential flow paths

Besides the general focusing of LGD close to the lake shore some geological settings might result in significant exfiltration in other regions of the lake bed. This can be caused, for example, by preferential flow paths in the aquifer as a result of spatially restricted areas of higher hydraulic conductivity as described in Chapter 1.2 (Krabbenhoft and Anderson 1986, see Fig. 1.4). Also, if there is more than one aquifer in contact with the lake bed LGD will occur right at the lower boundary of the separating aquitard (Rosenberry and LaBaugh 2008, Fig. 5.8).

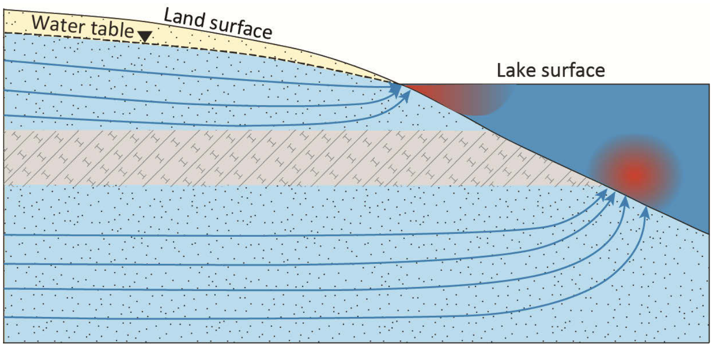

Figure 5.8 LGD (indicated in red) occurring close to and independently from the lake shore due to a low-conductivity layer separating two aquifers in contact with the lake (example for Type C-heterogeneity).

Having said this it seems that Type C of spatial LGD heterogeneity occurs rather locally restricted as LGD hotspots or in the case of Figure 5.8 as a linear section of increased LGD while Type A and B are restricted to shore areas and are mainly of a diffusive character. This imposes some difficulties to detect Type C-heterogeneity since the survey of a whole lake bed requires some effort. To exclude the occurrence of this Type C-heterogeneity LGD fiber-optic cables were deployed on the lake bed of Lake Arendsee at multiple locations as several 100 m long transects perpendicular to the lake shore (unpublished data). The results have not indicated any spatial hotspots of LGD beyond the immediate shore area. Other than the intensely investigated LGD in vicinity to the shore (heterogeneity-types A and B) LGD of Type C is assumed to not contribute significant groundwater volumes to Lake Arendsee.

5.1.3 Temporal variability of LGD

Due to generally slow groundwater flow velocities a potential temporal variability of LGD is probably limited to medium or long time scales (i.e., months to years). Consequently, temporal variability of LGD is usually less pronounced than spatial heterogeneity of LGD. Nevertheless, investigators should evaluate results of LGD measurements carefully regarding temporal changes of factors influencing LGD rates. Actually, spatial heterogeneity of LGD is often coupled to temporally fluctuating influences. In Chapters 4.2 and 4.3 transpiration of riparian vegetation is assumed to cause locally differing LGD rates. This phenomenon is largely limited to the growing season and by that may even result in transient reversals of flow conditions (Meyboom 1967; Winter 1999; Winter and Rosenberry 1995). During the colder seasons LGD rates at contiguous measurement sites might be more uniform (given that hydrogeological and other conditions are the same).

Surface water levels are probably the most variable features acting on groundwater surface water-interactions (Winter 1999). Seasonal changes of river stages for example may lead to a variability of exchanges of river water with the local groundwater flow system (Squillace et al. 1997). And the filling of reservoirs after dam building can significantly influence even regional flow systems (Van Everdingen 1967).

At Lake Arendsee the temperature-based measurements of LGD patterns might be affected by transpiration since they were conducted in summer and the shore is at least partly vegetated by larger trees. Furthermore, outside of the vegetation period, groundwater recharge may induce temporally varying LGD. Since the water table is usually close to land surface in vicinity to lakes (i.e., the unsaturated zone is thin) percolating water reaches the water table quite quickly. This may result in changes of hydraulic gradients after precipitation and by that of exchanged volumes (Winter 1983; Winter 1999). As a conclusion, the perfect timing for measurement of representative LGD patterns is probably difficult to find.

5.2 P concentrations in groundwater and LGD

Besides the LGD volume the concentration of the target parameter in LGD is the second factor of a groundwater-borne mass load. Similar to the hydrological component, i.e., the LGD volume, it will in most cases show heterogeneities in space and, although to a less extent, in time. LGD parameter concentrations are controlled by the following steps:

1) Origin in the subsurface catchment of the lake: natural conditions (e.g., geological setting) and/or anthropogenic contaminations

2) Travelling towards the lake: potential modification of original concentrations, e.g., due to biogeochemical processes in the aquifer (retention, degradation, etc.) and/or inhomogeneous spatial distribution due to hydrogeological settings
3) Passage of the reactive sediment-water interface: potential alteration of the parameter concentration during the passage of the reactive aquifer-lake interface; induced by changes in biogeochemical conditions

Within the Lake Arendsee-studies, the first two aspects were addressed by intense and frequent groundwater quality investigations with a high spatial resolution (Chapter 3.2). The intrusion of a pollutant into an aquifer will usually result in the formation of a three-dimensional contaminant plume. In this context temporal and spatial heterogeneity of parameter concentrations are not independent of each other. Sediment and contaminant characteristics but also the duration and/or the time elapsed after contamination impact on the spatial extent of such plumes (and vice versa) and their persistence (see Chapter 2.2 for N and P). However, while spatially varying concentrations of groundwater compounds may cover all scales, from small to large ones, short-term temporal variability of groundwater parameters can usually be neglected. Travel velocities of compounds in the aquifer are usually slow. In settings with very low hydraulic conductivity where advection is of minor importance, dissolved components spread only by diffusion, which results in even slower distribution in the aquifer. Furthermore, the reactivity of the contaminant itself can significantly delay the spreading of a contamination. P for example is known to travel significantly slower than the groundwater flow because of sorption and precipitation (Appelo and Postma 1999; Correll 1998; Harman et al. 1996; Lamontagne 2002; Robertson 2008; Robertson et al. 1998; Stumm and Morgan 1996). As a consequence, temporal variability of groundwater concentrations is limited to medium and long time scales.

As described in detail in Chapter 2.2 a number of biogeochemical processes have the potential to modify eventual parameter concentrations in the groundwater approaching reactive the interface (Beck et al. 2007; Carlyle and Hill 2001; Dean et al. 2003; Frape and Patterson 1981; Kroeger and Charette 2008; LaBaugh et al. 1997; Moore 2010; Moore et al. 2006; Schuster et al. 2003). Due to its redox sensibility P concentrations might be prone to alteration when passing the reactive interface. For example, increased availability of biodegradable material at the interface may enhance mineralization and cause reducing redox conditions which might result in a release of sorbed P (Chapter 2.2). However, the direction and degree of P concentration changes in LGD or SGD (submarine groundwater discharge) compared to groundwater seem to be specific for individual lakes. While some authors described increasing concentrations others found that they are decreased (Brock et al. 1982; Griffioen 1994; Hofmann and Lessmann 2006; Holman et al. 2010; Vanek 1991).

In the following sub-sections I discuss some of the results presented in Chapter 3 in detail in order to evaluate the spatial and temporal heterogeneity of P concentrations on LGD-derived P loads to Lake Arendsee.

5.2.1 Spatial heterogeneity of P concentrations

Horizontal heterogeneity of P concentrations in LGD

P concentrations in LGD of Lake Arendsee were obtained from sampling of near-shore temporary piezometers. Samples were collected from a depth of about 2 m below land surface by a peristaltic pump from manually drilled boreholes (Chapter 3.2). The results reveal a heavy contamination of the groundwater along a 2 km long stretch of the southern shore where the city Arendsee is located. The P concentrations show some variation along this stretch. This would not have been captured by the four sites along the shoreline equipped with groundwater observation wells alone. A maximum concentration of more than 4.000 µg SRP l^{-1} represents the severe contamination of LGD. Resulting groundwater-borne P loads contribute significantly to lake eutrophication which proves Hypothesis 1 (Chapter 1.5).

The approach does not capture potential alterations of the groundwater P concentrations while passing the reactive sediment-water interface. As mentioned above this interface is assumed to potentially influence the quality of LGD. In the case of P the most probable concept implies a decrease of P concentrations when LGD passes the interface. Based on the assumption that P concentrations are linked to negative redox potentials in groundwater the gradient from reducing (groundwater) to mostly oxic (lake) water will result in the precipitation of P binding compounds, e.g., induced by oxidation of Fe^{2+} to Fe(III). P is bond to the resulting Fe-complexes and deposited in the sediment instead of being discharged into the lake water. Paradoxically it seems that the intense contamination of groundwater at Lake Arendsee goes along with explicitly oxic conditions. This condition is also reflected by high nitrate concentrations parallel to high P concentrations (Chapter 3.2). The findings imply that the redox gradient at the reactive interface is not very steep, which legitimates near-shore P concentrations to be representative for actual LGD P concentrations.

Vertical heterogeneity of P concentration in LGD

P concentrations of LGD represent a depth-integrated mean of the vertical gradient of P concentrations in the plume. Groundwater flow lines in Figure 2.2 depict the focusing of LGD to near-shore areas and imply that vertical concentration gradients in the groundwater are transferred in a horizontal direction at the lake bottom by the upward bending of groundwater flow lines. This results in decreasing concentrations in LGD with increasing distance to the shoreline (Fig. 5.9). However, this concept is hardly implementable in investigations of groundwater-borne mass loads. Knowledge about P concentrations in different aquifer depths or in lake sediments would be necessary to represent the vertical gradient for every measurement location. Furthermore, it would be necessary to assign those concentrations to a representative LGD rate in order to calculate mass loads from individual depths. For a research area of the dimension at Lake Arendsee (at least 2 km of contaminated shoreline reach) a representative approach would have exceeded the capacities of the project by far. Thus, the results for Lake Arendsee underlie some uncertainty since the vertical dimension of the P concentrations was only included to a minor extent.

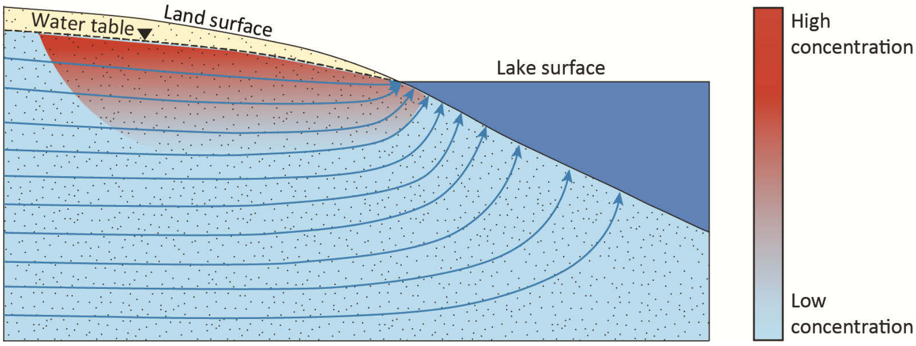

Figure 5.9 Conceptual scheme of a groundwater contamination plume (indicated in red) discharging into a lake.

Spatial heterogeneity in the groundwater of the catchment

On the one hand spatial heterogeneities of LGD concentrations depend on groundwater concentrations upgradient of the lake and on the other hand on advective and diffusive transport mechanisms. Regarding contaminant plumes the results of the Lake Arendsee-studies confirmed that groundwater concentrations can vary spatially to an extreme extent in the catchment (Chapter 3.2). This was found for P as well as for other nutrients, especially N. Unfortunately, the effort of sampling groundwater in the subsurface catchment with a high spatial resolution did not allow an explicit localization of a contamination site as it was hypothesized in Chapter 1.5 (Hypothesis 2). Currently, a final reason for this cannot be named. However, based on the statements made in Chapters 3.2 and 5.1 it might be an interaction of various factors driving the spatial picture of P concentrations in the groundwater below the city Arendsee:

- Extremely heterogeneous geology (i.e., sediment characteristics) resulting in
  - spatially differing hydraulic conductivity, i.e., different advective transport times and preferential flow paths
  - sediments with different P retention (especially sorption) capacities
- Multiple independent contaminations/origins:
  - Different locations
  - Different durations
  - Different sources (e.g., leakages of waste water facilities and inorganic fertilization of domestic gardens)

Contaminant plumes do not only disperse horizontally but also vertically. When the horizontal pattern of groundwater concentrations is in the focus of investigations, it must be assured that available sampling facilities are of similar depths to legitimate a comparison of results (Chapter 3.2). The vertical distribution of groundwater parameters depends on aquifer characteristics such as the hydraulic conductivity. Additional heterogeneity in the three-dimensional space is introduced by anisotropy. As a result of the above-mentioned aspects even highly resolved spatial groundwater quality data might not deliver information on origins and flow paths of contaminations. Figure 3.14d in Chapter 3.2 represents this for the case study of Lake Arendsee.

5.2.2 Temporal variability of P concentrations

Temporal variability of groundwater concentrations is usually low at short and medium time-scales. This was also found for P concentrations in the catchment of Lake Arendsee. The groundwater sampled from ten observation wells along the shoreline did not reveal significant changes during more than 3.5 years of regular surveys. It can be concluded that the impact of the contamination on the lake trophy will not decrease within the near future. This steady state of P concentrations is an advantage for the determination of groundwater-borne P loads. Any kind of recurring (e.g., seasonal) fluctuations would have required accordingly repeated groundwater sampling at Lake Arendsee in order to achieve representative P concentrations for LGD. Instead, sampling groundwater from temporary piezometers once was sufficient to achieve representative information on P concentrations.

5.3 Final evaluation

Besides the vertical gradient of P concentrations in LGD the Lake Arendsee-studies covered all of the features identified to influence groundwater-borne mass loads (Fig. 5.1 and Table 5.1). By this, the lake is probably one of the most intensely investigated ones regarding groundwater-borne P loads. To evaluate the effort of such intense investigations of LGD and P concentrations three scenarios are introduced and compared (Table 5.2). The first one represents the Lake Arendsee-studies as described in Chapter 3.2 in which spatial heterogeneity of both, LGD intensities and SRP concentrations, are taken into account to determine groundwater-borne P loads. Scenario 2 is introduced in Chapter 3.1.

Here, the spatial heterogeneity of SRP concentrations was reduced to concentrations found at the four upper observation wells along the southern shoreline while temporary piezometer results were not included. By upscaling those four values to the exfiltration reach a much lower spatial resolution of SRP concentrations was considered. The third scenario excludes spatial heterogeneity of LGD intensities. It is based on the overall LGD volume derived from groundwater recharge calculations while LGD rates from temperature depth profiles are not taken into account. This results in equal LGD volumes for all sub-sections of the shore. Sub-sectional SRP concentrations from near-shore piezometers are included in this scenario.

Table 5.1 List of LGD- and concentration-related features potentially influencing groundwater-borne mass loads (as a follow-up of Figure 5.1). Check marks indicate the specific consideration in the P load determinations for Lake Arendsee.

LGD	
Overall volume	✓
Spatial variability along the shore (Type A)	✓
Spatial variability perpendicular to the shore (Type B)	✓
Spatial variability across the whole lake area (Type C)	✓
Temporal variability	✓

Parameter concentration	
Horizontal variability	✓
Vertical variability	
Temporal variability	✓

Presuming that Scenario 1 accounts for the exact amount of SRP being discharged to the lake via LGD, Scenario 2 would underestimate LGD-derived SRP loads by about 50%. Excluding the spatial heterogeneity of LGD rates from SRP load calculations (Scenario 3) reduces groundwater-borne SRP load results by more than 25% (Table 5.2). The results of the three scenarios prove very well the importance of considering the spatial heterogeneity of both, LGD rates and concentrations, for LGD derived P loads. By that they confirm the third of the overarching hypotheses (Chapter 1.5) which predicted a significant influence of both factors on LGD-derived P loads.

Table 5.2 Scenarios for LGD-derived SRP load determination. Scenario 1 includes spatial heterogeneity of LGD rates by using results of temperature depth profiles as weighing factor for shoreline segments. SRP concentrations are taken from 44 near-shore temporary piezometers, allowing to assign individual SRP concentrations to the segments and by that including spatial heterogeneity of SRP concentrations. Scenario 2 reduces this heterogeneity of SRP to a minimum by upscaling only four concentrations from near-shore groundwater observation wells. Scenario 3 includes SRP heterogeneity from temporary piezometers but does not take into account heterogeneity of LGD rates based on the measurement of temperature depth profiles.

	Taking into account spatial heterogeneity of		LGD-derived SRP load	% of Scenario 1
	LGD	SRP		
Scenario 1	yes	yes	830	100
Scenario 2	yes	no	425	51
Scenario 3	no	yes	610	73

Since, besides variations of vertical P concentrations, all other factors given in Figure 5.1 have been included thoroughly into the investigations the final result of groundwater-borne P loads is of high accuracy. This is of major importance since groundwater is still regarded to be of generally low significance for lake P budgets by many researchers and lake managers. Contrasting findings will only be recognized and accepted if the investigations have been encompassing and done thoroughly.

5.4 References

Appelo, C.A.J., Postma, D., 1999. *Geochemistry, groundwater and pollution*. Balkema, Rotterdam, 536 p.

Beck, A.J., Tsukamoto, Y., Tovar-Sanchez, A., Huerta-Diaz, M., Bokuniewicz, H.J., Sanudo-Wilhelmy, S.A., 2007. Importance of geochemical transformations in determining submarine groundwater discharge-derived trace metal and nutrient fluxes. *Applied Geochemistry*, 22(2): 477-490.

Brock, T.D., Lee, D.R., Janes, D., Winek, D., 1982. Groundwater seepage as a nutrient source to a drainage lake - Lake Mendota, Wisconsin. *Water Research*, 16(7): 1255-1263.

Carluer, N., Marsily, G.D., 2004. Assessment and modelling of the influence of man-made networks on the hydrology of a small watershed: implications for fast flow components, water quality and landscape management. *Journal of Hydrology*, 285(1–4): 76-95.

Carlyle, G.C., Hill, A.R., 2001. Groundwater phosphate dynamics in a river riparian zone: effects of hydrologic flowpaths, lithology and redox chemistry. *Journal of Hydrology*, 247(3-4): 151-168.

Correll, D.L., 1998. The role of phosphorus in the eutrophication of receiving waters: A review. *Journal of Environmental Quality*, 27(2): 261-266.

Dean, W.E., Neff, B.P., Rosenberry, D.O., Winter, T.C., Parkhurst, R., 2003. The Significance of Ground Water to the Accumulation of Iron and Manganese in the Sediments of Two Hydrologically Distinct Lakes in North-Central Minnesota: A Geological Perspective. *Ground Water*, 41(7): 951-963.

Dollinger, J., Dagès, C., Bailly, J.-S., Lagacherie, P., Voltz, M., 2015. Managing ditches for agroecological engineering of landscape. A review. *Agronomy for Sustainable Development*, 35(3): 999-1020.

Frape, S.K., Patterson, R.J., 1981. Chemistry of Interstitial Water and Bottom Sediments as Indicators of Seepage Patterns in Perch Lake, Chalk-River, Ontario. *Limnology and Oceanography*, 26(3): 500-517.

Genereux, D., Bandopadhyay, I., 2001. Numerical investigation of lake bed seepage patterns: effects of porous medium and lake properties. *Journal of Hydrology*, 241(3–4): 286-303.

Griffioen, J., 1994. Uptake of Phosphate by Iron Hydroxides during Seepage in Relation to Development of Groundwater Composition in Coastal Areas. *Environmental Science & Technology*, 28(4): 675-681.

Harman, J., Robertson, W.D., Cherry, J.A., Zanini, L., 1996. Impacts on a sand aquifer from an old septic system: Nitrate and phosphate. *Ground Water*, 34(6): 1105-1114.

Hofmann, H., Lessmann, D., 2006. Hydrogeochemistry of groundwater seepage into an acidic mining lake. *Proceedings of the International Association of Theoretical and Applied Limnology*, 29: 1452–1456.

Holman, I.P., Howden, N.J.K., Bellamy, P., Willby, N., Whelan, M.J., Rivas-Casado, M., 2010. An assessment of the risk to surface water ecosystems of groundwater P in the UK and Ireland. *Science of The Total Environment*, 408(8): 1847-1857.

Kishel, H.F., Gerla, P.J., 2002. Characteristics of preferential flow and groundwater discharge to Shingobee Lake, Minnesota, USA. *Hydrological Processes*, 16(10): 1921-1934.

Krabbenhoft, D.P., Anderson, M.P., 1986. Use of a numerical groundwater-flow model for hypothesis-testing. *Ground Water*, 24(1): 49-55.

Kroeger, K.D., Charette, M.A., 2008. Nitrogen biogeochemistry of submarine groundwater discharge. *Limnology and Oceanography*, 53(3): 1025-1039.

LaBaugh, J.W., Winter, T.C., Rosenberry, D.O., Schuster, P.F., Reddy, M.M., Aiken, G.R., 1997. Hydrological and chemical estimates of the water balance of a closed-basin lake in north central Minnesota. *Water Resources Research*, 33(12): 2799-2812.

Lamontagne, S., 2002. Groundwater delivery rate of nitrate and predicted change in nitrate concentration in Blue Lake, South Australia. *Marine and Freshwater Research*, 53(7): 1129-1142.

Lennartz, B., Janssen, M., Tiemeyer, B., 2011. Effects of artificial drainage on water regime and solute transport at different spatial scales. In: *Soil hydrology, land use and agriculture: measurement and modelling*, Shukla, M.K. (Ed.). CAB International, Wallingford, UK, 434.

McBride, M.S., Pfannkuch, H.O., 1975. Distribution of seepage within lakebeds. *Journal of Research of the U.S. Geological Survey*, 3(5): 505-512.

McCobb, T.D., LeBlanc, D.R., Walter, D.A., Hess, K.M., Kent, D.B., Smith, R.L., 2003. Phosphorus in a ground-water contaminant plume discharging to Ashumet Pond, Cape Cod, Massachusetts, 1999. *U.S. Geological Survey Water Resources Investigations Report* 02-4306: 70 p.

Meyboom, P., 1967. Mass-transfer studies to determine the groundwater regime of permanent lakes in hummocky moraine of Western Canada. *Journal of Hydrology*, 5(0): 117-142.

Moore, W.S., 2010. The Effect of Submarine Groundwater Discharge on the Ocean. *Annual Review of Marine Science*, 2: 59-88.

Moore, W.S., Blanton, J.O., Joye, S.B., 2006. Estimates of flushing times, submarine groundwater discharge, and nutrient fluxes to Okatee Estuary, South Carolina. *Journal of Geophysical Research-Oceans*, 111(C9).

Nützmann, G., Mey, S., 2007. Model-based estimation of runoff changes in a small lowland watershed of north-eastern Germany. *Journal of Hydrology*, 334(3-4): 467-476.

Pfannkuch, H.O., Winter, T.C., 1984. Effect of anisotropy and groundwater system geometry on seepage through lakebeds: 1. Analog and dimensional analysis. *Journal of Hydrology*, 75(1–4): 213-237.

Radcliffe, D.E., Reid, D.K., Blomback, K., Bolster, C.H., Collick, A.S., Easton, Z.M., Francesconi, W., Fuka, D.R., Johnsson, H., King, K., Larsbo, M., Youssef, M.A., Mulkey, A.S., Nelson, N.O., Persson, K., Ramirez-Avila, J.J., Schmieder, F., Smith, D.R., 2015. Applicability of Models to Predict Phosphorus Losses in Drained Fields: A Review. *Journal of Environmental Quality*, 44(2): 614-628.

Robertson, W.D., 2008. Irreversible phosphorus sorption in septic system plumes? *Ground Water*, 46(1): 51-60.

Robertson, W.D., Schiff, S.L., Ptacek, C.J., 1998. Review of phosphate mobility and persistence in 10 septic system plumes. *Ground Water*, 36(6): 1000-1010.

Rosenberry, D.O., LaBaugh, J.W., 2008. Field Techniques for Estimating Water Fluxes Between Surface Water and Ground Water. *U.S. Geological Survey Techniques and Methods* 4-D2: 128 p.

Schuster, P.F., Reddy, M.M., LaBaugh, J.W., Parkhurst, R.S., Rosenberry, D.O., Winter, T.C., Antweiler, R.C., Dean, W.E., 2003. Characterization of lake water and ground water movement in the littoral zone of Williams Lake, a closed-basin lake in north central Minnesota. *Hydrological Processes*, 17(4): 823-838.

Skaggs, R.W., Chescheir, G.M., Phillips, B.D., 2005. Methods to determine lateral effect of a drainage ditch on wetland hydrology. *Transactions of the Asae*, 48(2): 577-584.

Squillace, P.J., Burkart, M.R., Simpkins, W.W., 1997. Infiltration of atrazine and metabolites from a stream to an alluvial aquifer. *Journal of the American Water Resources Association*, 33(1): 89-95.

Stamm, C., Sermet, R., Leuenberger, J., Wunderli, H., Wydler, H., Flühler, H., Gehre, M., 2002. Multiple tracing of fast solute transport in a drained grassland soil. *Geoderma*, 109(3–4): 245-268.

Stillman, J.S., Haws, N.W., Govindaraju, R.S., Suresh C. Rao, P., 2006. A semi-analytical model for transient flow to a subsurface tile drain. *Journal of Hydrology*, 317(1–2): 49-62.

Stumm, W., Morgan, J.J., 1996. *Aquatic Chemistry*. Wiley, New York.

Van Everdingen, R.O., 1967. Influence of the South Saskatchewan reservoir (Canada) on piezometric levels in underlying bedrock aquifers. *Journal of Hydrology*, 5: 351-IN2.

Vanek, V., 1991. Riparian zone as a source of phosphorus for a groundwater-dominated lake. *Water Research*, 25(4): 409-418.

Winter, T.C., 1983. The interaction of lakes variably saturated porous-media. *Water Resources Research*, 19(5): 1203-1218.

Winter, T.C., 1999. Relation of streams, lakes, and wetlands to groundwater flow systems. *Hydrogeology Journal*, 7(1): 28-45.

Winter, T.C., Rosenberry, D.O., 1995. The interaction of ground-water with prairie pothole wetlands in the Cottonwood Lake area, east-central North-Dakota, 1979-1990. *Wetlands*, 15(3): 193-211.

Winter, T.C., Rosenberry, D.O., LaBaugh, J.W., 2003. Where Does the Ground Water in Small Watersheds Come From? *Ground Water*, 41(7): 989-1000.

6 Learning from experiences

6.1 Discussion of studies to improve and develop methods for LGD identification and quantification

The studies presented in Chapters 2, 3, and 4 demonstrate that lacustrine groundwater discharge is difficult to determine and that a variety of specifics has to be considered. A "golden way" for such investigations does not exist. The objectives of the investigations on quality (LGD patterns) or quantity (LGD volumes/rates) will specify which approach to apply. Furthermore, the spatial (and in some cases also the temporal) scale determines the investigation strategy.

While some techniques are already well-established and widely applied, others are still under development and a successful application is not always ensured. Applying different methods to the same area and parameter might lead to significantly differing results. To account for this, this chapter wraps up the results of the three side-projects introduced in Chapter 4. All of them deal with the determination and/or quantification of LGD patterns and/or rates but they differ in intentions, applied methods, and spatial scales.

Chapter 4.1 is also focusing on Lake Arendsee and is a critical evaluation of findings from the hydrological core study in Chapter 3.1. One of the objectives was the confirmation of groundwater in- and exfiltration zones along the lake shore by measurements of stable isotopes of the water molecules in near-shore groundwater. In Chapter 3.1 in- and exfiltration zones were separated by the boundaries of the subsurface catchment which had been established from hydraulic head contour lines. The signatures of groundwater stable isotopes differed from those of the lake water signature at the south-western, southern, eastern, and north-eastern shoreline. The results basically confirmed the location of in- and exfiltration zones at Lake Arendsee.

Reproducing results with a different method is one of the best options to eventually proof measurement results. Additionally, repeated measurements with the same method can be conducted to support the accuracy of empirically achieved results. Unfortunately, measurements with the same method do not always show compatible results. An example for this is given in the same chapter (4.1) where the results of temperature depth profiles of the lake sediment presented in Chapter 3.1 are compared to those of a first field campaign conducted one year earlier by the same method. While the general focus of LGD along the southern shoreline was found in both data sets, deviations occurred at single locations. However, differing findings do not necessarily reject the original ones. In the present studies potential reasons for mismatching results of temperature-derived LGD rates are numerous, e.g., deviation of sampling specifics or small scale heterogeneities of LGD. A careful assessment of the results and their generation is necessary to facilitate a decision for the most plausible results. In the case of Lake Arendsee, comparing groundwater head contour lines as another independent approach with the results of the two temperature profile measurement campaigns indicates that the second campaign has delivered the most representative results.

In Chapter 4.2 lake bed temperatures measured by FO-DTS were tested as proxies for LGD fluxes over a large area: Single transects of LGD fluxes derived from two different methods, vertical hydraulic gradients and temperature depth profiles, respectively, were used to develop transfer functions for the temperature pattern measured with FO-DTS. A large range of LGD fluxes were determined from temperature profiles within the 20 m x 4 m-shore section (0 - 170 l m^{-2} d^{-1}). It turned out that FO-DTS measurements calibrated by such transfer functions delivered plausible results of 2D-spatial heterogeneity of LGD rates for the investigated shore section. However, the approaches have of course some degree of inaccuracy in representing actual LGD rates along the 20 m-shore section. Projecting this approach to a larger scale, e.g., the whole exfiltration reach at Lake Arendsee, might result in larger mismatches, e.g., due to a shift in the parameters controlling local LGD (such as a change of riparian vegetation type). The reference measurements along a 20 m-reach might not represent the actual conditions at another reach and upscaled fluxes might be wrong. Consequently, an upscaling approach like this needs reference measurements to be repeated with sufficiently high spatial resolution. Factors controlling the performance of upscaling approaches might depend on the spatial scale. Further efforts on routinizing upscaling techniques will have to consider the aspects controlling LGD fluxes at different scales. Nevertheless, the results of the study are promising and imply that quantitative large scale investigations of LGD are possible in the near future.

Thermal infrared radiation (TIR) was tested as a novel approach to visualize LGD at Lake Arendsee in Chapter 4.3. The picture seemed to impressively match the findings of Chapter 3.1 and revealed a large plume of warmer water at the southern shoreline. Lake-physical considerations supported the conclusion that the layer of warm water is caused by exfiltrating groundwater floating on the lake surface due to temperature-driven density differences compared to the lake water. The findings were a great success in reproducing LGD patterns with an independent method. However, further investigations revealed a very different picture and eventually lead to the conclusion that the temporal patterns depicted by the first TIR images have actually not or only to a minor extent been driven by LGD. Instead, Pöschke et al. (2015) found internal lake water movements (upwelling of seiches) to be most likely responsible for layers of warmer water floating on top of the lake water body. This lake-internal upwelling has been found in much larger lakes before (e.g., Steissberg et al. 2005; Plattner et al. 2006; Troitskaya et al. 2014), but had never been observed for a lake of the relatively small dimension of Lake Arendsee so far. This failure shows another factor in empirical research: Misinterpreting of data probably happens a lot, and results of new methods might be especially prone to errors due to missing experiences regarding method application and/or data analysis and interpretation.

Using TIR was a promising approach for a large scale overview on areas of intense LGD. Nevertheless, even if this approach had been successful it would still not have facilitated a large-scale quantitative picture of LGD. The trade-off between quantitative measurement options which mostly refer to only small or medium scales and the need to cover large areas for reliable overall LGD values is often the limiting factor in studies dealing with LGD. Upscaling of point measurements is more or less the only option so far but the determination of a sufficient spatial resolution for point measurements is laborious and difficult.

6.2 References

Plattner, S., Mason, D.M., Leshkevich, G.A., Schwab, D.J., Rutherford, E.S., 2006. Classifying and forecasting coastal upwellings in Lake Michigan using satellite derived temperature images and buoy data. *Journal of Great Lakes Research*, 32(1): 63-76.

Pöschke, F., Lewandowski, J., Engelhardt, C., Preuss, K., Oczipka, M., Ruhtz, T., Kirillin, G., 2015. Upwelling of deep water during thermal stratification onset-A major mechanism of vertical transport in small temperate lakes in spring? *Water Resources Research*, 51(12): 9612-9627.

Steissberg, T.E., Hook, S.J., Schladow, S.G., 2005. Characterizing partial upwellings and surface circulation at Lake Tahoe, California-Nevada, USA with thermal infrared images. *Remote Sensing of Environment*, 99(1-2): 2-15.

Troitskaya, E., Blinov, V., Ivanov, V., Zhdanov, A., Gnatovsky, R., Sutyrina, E., Shimaraev, M., 2015. Cyclonic circulation and upwelling in Lake Baikal. *Aquatic Sciences*, 77(2): 171-182.

7 Conclusions

7.1 Implications for Lake Arendsee

As hypothesized in Chapter 1.5 the studies presented in Chapter 3 proof that LGD is responsible for eutrophication of Lake Arendsee. The problem is caused anthropogenically induced by a severe contamination of the groundwater discharging into the lake. Unlike what was hypothesized a high spatial resolution of groundwater quality information did not reveal a coherent plume which could be tracked to a potential origin. The contamination is distributed over large areas. Thus, its elimination from the aquifer is no feasible option to mitigate the effects on the lake. Given the very high water residence time of the lake (50 – 60 years) the addition of P-binding materials seems to be the only option to induce a fast and effective decrease of pelagic P concentrations. However, without stopping the P source from entering the lake this measure will probably not be sustainable and P concentrations will again increase above those of the natural trophic state within some years or few decades (Hupfer et al. 2016).

Although it seems to be impossible to eliminate the plume(s) from the entire aquifer it might be an option to prevent the contaminated groundwater from discharging into the lake in order to increase the sustainability of P-precipitation measures (Chapter 3.2). Especially interesting might be the *in situ*-precipitation of P in LGD just as it enters the lake. For this the lake bottom can be equipped with P binding materials which remove P from the exfiltrating groundwater as this was successfully tested at Ashumet Pond (McCobb et al. 2009).

Further research at Lake Arendsee

Unfortunately, it was not possible to identify the source or local origin of the groundwater contamination. The most plausible reason is that not only one but several contamination sites cause the indifferent and heterogeneous picture of P concentrations in the urban groundwater. Potential contamination sources might be active or former leakages of waste water facilities such as sewers, house connection sewers or former sewage pits. A first approach of identifying waste water tracers in the contaminated groundwater did not reveal explicit results. A number of commonly applied pharmaceuticals were not present or only present in concentrations close to the detection limit in the groundwater (data not shown). At one observation site the artificial sweetener acesulfame was found in significant concentrations. This supports the hypothesis that ongoing waste water leakage is at least one source of groundwater contamination in the catchment of Lake Arendsee. Further research to proof this should probably focus on near-surface groundwater which might be stronger enriched by waste water indicators than groundwater from observation wells in large depths (Fig. 5.9).

A second potential source for nutrient enrichment of groundwater and LGD might be mineral fertilizers applied to private yards and gardens. Since their usage is not limited by law they are potentially applied regularly and in high doses. A trace species for this is uranium which is a geologic by-product in many mineral P-fertilizers (Cuoco et al. 2015; Engstrom et al. 2006). Also the presence of herbicides and/or pesticides could be interpreted as an "overshoot" of private gardening activities. For all of these substances, of course, it has to be confirmed that they origin from domestic instead of agricultural sources.

A focus of further investigations should be the identification of processes leading to a simultaneous presence of redox-sensitive species which usually do not occur parallel, as shown in Chapter 3.2. At one site nitrate and ammonium are both found in very high concentrations and increased P concentrations go along with explicitly positive redox-potentials. To understand the biogeochemical processes resulting in such inconsistencies investigations of sediment characteristics in both, the vadose and the saturated zones are recommended. The hypothesis proposed in Chapter 3.2 about high concentrations of dissolved P under high redox-potentials due to saturated P storage capacities (Jarvie et al. 2013) of the sediments could in principle be confirmed by the determination of sorption isotherms of soils and sediments in the catchment.

The studies presented within this thesis did not cover the potential role of the reactive interface between groundwater and lake. It was assumed that no significant modification of groundwater-borne P loads occurs during the passage of the interface (Chapters 3.2 and 5.2). Empirical data to confirm the assumption can be gathered from depth profiles of P concentrations in the lake bed, e.g., from multilevel piezometers (see Chapter 2.2 and Annex I). Another option is the installation of passive samplers which provide spatially highly resolved data from lake bed sediments (Chapter 2.1 and Annex I).

7.2 Implications for research on groundwater-lake interaction

P contamination of groundwater – a single and very special case?

The case of Lake Arendsee confirms the hypotheses that P can be dissolved and transported with groundwater and LGD in significant concentrations. By that LGD contributes significantly to eutrophication of the lake. This basic outcome of the two core studies in Chapter 3 should encourage researchers, lake managers, and policy makers to consider LGD as a main contributor to P budgets of lakes. In the light of severely P contaminated groundwater at Lake Arendsee research in the field of lake eutrophication might put a future focus on the identification of further lakes affected by excess P from groundwater discharge. This should apply especially for lakes with human settlements and activities (e.g., villages, cities, camping and other leisure facilities) in close proximity to shores where LGD takes place. When restoration measures have been conducted with unsatisfying results it might be worthwhile to investigate exfiltrating groundwater in detail.

For a first overview, investigations should cover the analysis of near-shore/near-surface groundwater in the discharge sections right at the lake shore, as done in Chapter 3.2. Potential in- and exfiltration zones along a lake shoreline can be roughly delineated from hydrogeological maps. Due to the proximity to the shoreline water tables are usually close to the surface and thus easily accessible for sampling (e.g., with temporary mini-piezometers as done at Lake Arendsee, Chapter 3.2, see also Annex I). If necessary and/or feasible, processes at the reactive interface can be investigated as a second step to evaluate LGD quality. Methods for this are presented in Chapter 2.2 and Annex I.

In terms of general surveys (e.g., within the EU Water Framework Directive) nutrient budgets for lakes are usually set up by standardized approaches to determine values for single input paths. Based on areal information on land use, vegetation, soil characteristics, drainage, and land sealing nutrient loads from groundwater, erosion, and drainage discharges are roughly estimated. Especially the diffuse inputs of nutrients are often estimated without taking empirical data into account. Any catchment-specific deviations from such standardized approaches are not captured. For the various reasons mentioned in the chapters above, the groundwater component is usually not explicitly considered in P budgets of lakes. The Lake Arendsee-studies will hopefully contribute to a general reconsideration of the potential role of groundwater for lake eutrophication. However, it will still take a lot more time to legally consolidate the necessity of including groundwater into P budgets of lakes.

Further conclusions and implications

A further conclusion from the Lake Arendsee-studies can be drawn from the active inclusion of residents into the investigations. It is common practice nowadays to accompany any planning of investigation or restorations of ecosystems which are closely related to human activities by intense information of the public. As a next step and Citizen Science-approach, private well owners were requested to supply well water for analysis in order to improve the spatial picture of the P contamination in the aquifer (Chapter 3.2). Besides the information yield about groundwater quality data in the catchment the action raised awareness for the problem within the local community. The lake is a major source of income in the region around the city Arendsee and the possibility to actively contribute to the identification of the problem obviously mobilized many inhabitants to support our project. In the context of the rising popularity of Citizen Science in many research disciplines this approach might serve as a model for other projects in the field of groundwater research. At least for the presented study the cost-benefit-ratio was a very valuable one.

The efforts regarding the quantification of groundwater recharge in the subsurface catchment revealed a substantial lack of knowledge about the influence of subsurface agricultural drainage measures on landscape hydrology (Chapters 3.1 and 5.1.1). Although some quantitative areal data on the volumes of vadose water being diverted as drainage water existed for the catchment of Lake Arendsee their accuracy and reliability should be considered with caution. In practice, data on drainage intensity hardly exist. This inhibits general statements on drainage intensity and complicates the development of applicable approaches for drainage quantification on medium or large scales. However, the effect on groundwater recharge and other components of the water balance is very relevant on both, local and regional scales. More effort should be invested in methods for the reliable quantification of subsurface drainage intensity.

Upscaling LGD point measurements is a big issue in the field of groundwater-surface water interactions nowadays. The studies and their discussions presented above demonstrate the urgent need for effective and (if possible) standardized routines of such approaches.

The different studies presented in this Ph.D. thesis touch a variety of aspects of LGD. Besides its function in the water and nutrient budgets of lakes the *in situ*-investigation of LGD is in focus. New and highly relevant outcomes go along with the recognition of issues and questions which have to be tackled by future research. By visualizing the complexity of factors contributing to LGD generation and occurrence in simplified schemes (Figures 5.1 and 5.4) lake managers might be encouraged to address the role of LGD also in practice. I hope that my work will be inspiring for scientists, managers, and policy makers working in the fields of groundwater-lake interactions and lake eutrophication.

7.3 References

Cuoco, E., Darrah, T.H., Buono, G., Verrengia, G., De Francesco, S., Eymold, W.K., Tedesco, D., 2015. Inorganic contaminants from diffuse pollution in shallow groundwater of the Campanian Plain (Southern Italy). Implications for geochemical survey. *Environmental Monitoring and Assessment*, 187(2): 17.

Engstrom, D.R., Schottler, S.P., Leavitt, P.R., Havens, K.E., 2006. A reevaluation of the cultural eutrophication of Lake Okeechobee using multiproxy sediment records. *Ecological Applications*, 16(3): 1194-1206.

Hupfer, M., Reitzel, K., Kleeberg, A., Lewandowski, J., 2016. Long-term efficiency of lake restoration by chemical phosphorus precipitation: Scenario analysis with a phosphorus balance model. *Water Research*, 97: 153-161.

Jarvie, H.P., Sharpley, A.N., Spears, B., Buda, A.R., May, L., Kleinman, P.J.A., 2013. Water Quality Remediation Faces Unprecedented Challenges from "Legacy Phosphorus". *Environmental Science & Technology*, 47(16): 8997-8998.

McCobb, T.D., LeBlanc, D.R., Massey, A.J., 2009. Monitoring the removal of phosphate from ground water discharging through a pond-bottom permeable reactive barrier. *Ground Water Monitoring and Remediation*, 29(2): 43-55.

Annex I

Methods for the determination of groundwater-surface water interactions (in German)

Karin Meinikmann,[1,2] Michael Hupfer,[3] Gunnar Nützmann,[1,2] and Jörg Lewandowski[1,2]

[1] Department of Ecohydrology, Leibniz-Institute of Freshwater Ecology and Inland Fisheries, Berlin, Germany

[2] Geography Department, Humboldt-Universität zu Berlin, Berlin, Germany

[3] Department of Chemical Analytics and Biogeochemistry, Leibniz-Institute of Freshwater Ecology and Inland Fisheries, Berlin, Germany

Citation:
Meinikmann, K., Hupfer, M., Nützmann, G., Lewandowski, J., 2016. Methoden zur Erfassung von Grundwasser-Oberflächenwasser-Interaktionen. (Methods for the determination of groundwater-surface water interactions, in German). In: Handbuch Angewandte Limnologie: Grundlagen - Gewässerbelastung - Restaurierung - Aquatische Ökotoxikologie - Bewertung - Gewässerschutz. III:1:2.2: 1–39. DOI: 10.1002/9783527678488.hbal2015005.

Abstract

Hydraulische Interaktionen zwischen Grund- und Oberflächenwasser bewirken den Austausch von Nähr- und Schadstoffen zwischen beiden Systemen. Die Erfassung dieser Wasser- und Stoffflüsse ist allerdings schwierig. Dies ist ein wesentlicher Grund für die langjährige Vernachlässigung des Grundwassers bei der Aufstellung von Wasser- und Stoffbilanzen von Gewässern. Die Auswirkungen von Grundwasser-Oberflächenwasser-Interaktionen werden dabei häufig unterschätzt, z. B. wenn das Grundwasser maßgeblich an der Wasserbilanz eines Gewässers beteiligt ist. Kontaminationen des Grundwassers können großen Einfluss auf die ökologische Qualität aquatischer Ökosysteme haben, weil auch ein geringer Grundwasserzustrom eine große Wirkung entfalten kann. Der vorliegende Beitrag beschreibt die wesentlichen Mechanismen, die die Interaktion zwischen Grundwasser und Oberflächengewässern antreiben und erläutert gängige Methoden, um diese zu untersuchen. Die hier vorgestellten Ansätze sind in den letzten Jahren und Jahrzehnten entwickelt und optimiert worden. Ihre praktische Anwendung außerhalb wissenschaftlicher Studien ist bislang noch begrenzt.

III-1.2.2

Methoden zur Erfassung von Grundwasser-Oberflächenwasser-Interaktionen

KARIN MEINIKMANN, MICHAEL HUPFER, GUNNAR NÜTZMANN und JÖRG LEWANDOWSKI

Inhalt

III-1.2.2 Methoden zur Erfassung von Grundwasser-Oberflächenwasser-Interaktionen

III-1.2.2

Methoden zur Erfassung von Grundwasser-Oberflächenwasser-Interaktionen

KARIN MEINIKMANN, MICHAEL HUPFER, GUNNAR NÜTZMANN und JÖRG LEWANDOWSKI

1 Einleitung

Grundwasser und Oberflächengewässer wurden lange Zeit als voneinander getrennte Systeme bewirtschaftet und erforscht (WINTER et al. 1998). Dabei wurde häufig übersehen, dass viele Oberflächengewässer überwiegend grundwassergespeist sind, sodass ihre Wasser- und Stoffhaushalte vom zuströmenden Grundwasser mitbestimmt oder sogar maßgeblich gesteuert werden. Umgekehrt versickert vielfach Oberflächenwasser in Grundwasserleiter, was die Beschaffenheit des Grundwassers beeinflussen kann. Menschliche Eingriffe in eines der beiden Systeme können Konsequenzen für das jeweils andere haben. Die Entnahme von Grundwasser oder Oberflächenwasser kann Position, Richtung und Raten des Wasser- und Stoffaustausches zwischen den Systemen verändern. Für das Verständnis von gewässerinternen Prozessen, um zukünftige Szenarien zu modellieren, aber auch um effektive Managementmaßnahmen durchzuführen, ist es unerlässlich, den Wasser- und Stoffaustausch zwischen Grund- und Oberflächenwasser zu berücksichtigen.

Für eine möglichst genaue Quantifizierung von Wasser- und Stoffflüssen zwischen Oberflächen- und Grundwasser sprechen verschiedene Gründe, von denen im Folgenden die drei Wichtigsten genannt werden sollen. Detailliertere Ausführungen hierzu finden sich in ROSENBERRY et al. (2015) und LEWANDOWSKI et al. (2015).

- Bilanzierung der Wasser- und Stoffhaushalte von Flüssen und Seen: Das Grundwasser wurde und wird in derartigen Berechnungen oft nur als Differenz der übrigen Ein- und Austragsterme berücksichtigt. Die Fehler in den anderen Bilanztermen summieren sich auf diese Weise im Grundwasserterm auf. Dass der Term im Vergleich zur Gesamtbilanz meist klein ist, impliziert einen geringen Einfluss des Grundwassers auf das jeweilige Gewässer. Der Eindruck der Wasserbilanz täuscht jedoch häufig, da das Grundwasser hohe Konzentrationen an Nähr- oder Schadstoffen haben kann. Die empirische Erfassung von Qualität und Quantität des zuströmenden Grundwassers wertet die Güte einer Bilanzrechnung im Einzelfall erheblich auf und verhindert Fehlinterpretationen.
- Bereitstellung von empirischen Daten zu Grundwasser-Oberflächenwasser-Interaktionen für die Einzugsgebiets- oder Grundwassermodellierung: Die Modellierung ist ein wichtiges Instrument zur Erarbeitung von Managementstrategien im Gewässer- und Grundwasserschutz. Auch im Rahmen der Trinkwasserversorgung ist die Modellierung unverzichtbar für die Sicherstellung von Qualität und Quantität der Ressource. Die Kalibrierung von Modellergebnissen erfordert die Verfügbarkeit gebietsspezifischer Daten, die häufig nicht in der benötigten Qualität vorliegen, sodass entsprechende Messungen nötig werden.
- Räumliche Eingrenzung von Grundwasserkontaminationen, die ein Oberflächengewässer erreichen: Schadstofffahnen breiten sich im Grundwasserleiter sowohl horizontal als auch vertikal aus; dies ist jedoch fallspezifisch. Erreicht eine solche Fahne einen Fluss oder See, werden auch die Qualität des Oberflächenwassers und damit das gesamte Ökosystem beeinflusst. Beim Eintritt des kontaminierten Grundwassers kommt es an der Sediment-Wasser-Grenze vielfach zu Umsatzprozessen, die die Beschaffenheit und damit die Wirkung einer Verschmutzung beeinflussen. Die Erfassung derartiger Interaktionen kann entschei-

dend zur Erarbeitung von geeigneten Sanierungs- oder Restaurierungsmaßnahmen beitragen.

Wechselwirkungen zwischen Grund- und Oberflächenwässern können maßgeblich zur Bildung und Erhaltung oder auch Schädigung von aquatischen Habitaten führen. Hier besteht einerseits weiterhin großer Forschungsbedarf, während andererseits eine Sensibilisierung für diese Zusammenhänge auch auf der Anwendungsebene notwendig ist. Ein Beispiel dafür sind Tagebaurestseen, die nach der Stilllegung durch den Wiederanstieg des Grundwassers entstehen. An einigen Standorten transportiert das einströmende Grundwasser Fe^{2+} und H^+ aus der Pyritverwitterung in die Seen, was vielfach zu einer Versauerung der Gewässer führt (Grunewald und Schoenheinz 2014; Schultze et al. 2010; Kap. V-1.3.1). Diese Prozesse schränken nicht nur die Nutzung der Gewässer (z. B. als Badeseen) extrem ein. In derart saurem Milieu können die meisten Organismen nicht überleben. Eine Abschätzung der Folgen eines Grundwasserwiederanstiegs ist nur möglich, wenn räumliche Muster der Austauschraten zwischen den beiden Systemen bekannt sind (Fleckenstein et al. 2009; Neumann et al. 2013).

In der Spree führt die Oxidation von Fe^{2+}, das mit dem Grundwasser aus dem Lausitzer Kohlerevier in den Fluss gelangt, außerdem zu einer Trübung und Braunfärbung des Wassers sowie zur Ausbildung einer teilweise vielen Dezimeter mächtigen Kolmationsschicht aus Eisenocker. Auch hier kommt es zum Ab- und Aussterben der meisten Tier- und Pflanzenarten. Die Pyritverwitterung führt außerdem zur Freisetzung von großen Mengen an Sulfat (SO_4^{2-}), das mit dem Grundwasser ebenfalls in die Flüsse und Seen transportiert wird. Dies kann in einigen Gebieten mittelfristig zu einer Einschränkung der Trinkwassergewinnung aus Uferfiltrat führen. So wird beispielsweise das Trinkwasser von Berlin aus ufernahen Brunnen an der Spree gewonnen, die nicht nur Grundwasser, sondern auch in den Grundwasserleiter infiltriertes Flusswasser fördern. Die extrem hohen SO_4^{2-}-Konzentrationen im Spreewasser könnten mittelfristig zu einer Überschreitung des Trinkwassergrenzwertes für SO_4^{2-} (TrinkwV 2001) führen und vielfältige Folgen für Oberflächengewässer haben (Kap. V-1.2.5).

Neben den beschriebenen Prozessen steht vor allem die Anreicherung von Grund- und Oberflächenwässern mit Nährstoffen im Fokus von Studien zum Austausch zwischen den Systemen (Abschnitt 2.1). Die Eutrophierung von Gewässern wurde bisher kaum mit dem Grundwasser in Verbindung gebracht. Die Reduktion der Nährstoffeinträge in Flüsse und Seen aus Punktquellen (z. B. Abwasserzuleitungen) und diffusen anderen Einträgen (z. B. aus der Landwirtschaft) führte aber nicht überall zu der gewünschten Trophieverbesserung (Gulati und van Donk 2002; Sharpley et al. 2013). Vielmehr stellt die Eutrophierung weiterhin eine der größten Gefahren für limnische Systeme weltweit dar. Es liegt daher nahe, dass an vielen Stellen ein diffuser Zustrom von bisher unberücksichtigten Stofffrachten über das Grundwasser für weiterhin hohe Belastungen im Freiwasser verantwortlich ist. Der vorliegende Beitrag erläutert zunächst die Prozesse und Mechanismen, die dem Austausch zwischen Grund- und Oberflächenwasser zugrunde liegen, und thematisiert dabei die Unterschiede zwischen Seen und Fließgewässern. Anschließend werden Methoden zur Erfassung des hydrologischen und des stofflichen Austausches zwischen den Systemen beschrieben. Die Entwicklung dieser Methoden ist noch im Gange, und einige davon werden bislang nur für Forschungszwecke angewandt. Ausgehend vom Stand der Entwicklung soll für einige Methoden ihr möglicher Nutzen und das Potenzial für praktische Fragestellungen diskutiert werden. Die Verfahren sind, soweit nicht explizit erwähnt, sowohl für Fließgewässer als auch für Seen anwendbar. Es werden zudem wichtige Anwendungsgrenzen und -hinweise sowie Fehlerquellen beschrieben.

2 Grundlagen

2.1 Grundwasser-Oberflächenwasser-Interaktion: Eine lange vernachlässigte Wechselwirkung

Die fehlende Betrachtung der Systeme Grundwasser und Oberflächengewässer als ein hydrologisches Kontinuum (Winter et al. 1998) hat viele Gründe. Zunächst ist anzuführen, dass erste Forschungen jeweils von unterschiedlichen Disziplinen betrieben wurden. Die Limnologie befasst sich traditionell mit den Wechselwirkungen von Organismen und Umweltbedingungen in den Oberflächengewässern. Die Hydrogeologie ist dagegen „die Wissenschaft von den Erscheinungsformen des Wassers, insbesondere in der Erdkruste als Grundwasser“ (Müller 1999). Der Fokus dieser Disziplin liegt auf der Bildung, der räumlichen Verteilung, Verbreitung und dem Austritt des Grundwassers sowie dessen Beschaffenheit und

Qualität (Müller 1999). Damit ist sie ein Teilgebiet sowohl der Hydrologie als auch der Geologie. Obwohl in manchen Definitionen von Hydrogeologie die „Austauschvorgänge mit dem Wasser der Atmosphäre und dem der Erdoberfläche als Teilvorgänge des natürlichen Wasserkreislaufs“ (Hötzl 2001) genannt werden, steht in der Praxis oft die Bestimmung von Quantität und Beschaffenheit des unterirdischen Wassers im Fokus. Dies ist u. a. der Tatsache geschuldet, dass das Grundwasser in vielen Teilen der Welt die bedeutendste Trinkwasserressource ist. In Deutschland werden 70 % des Trinkwassers aus Grund- und Quellwässern entnommen (Bartel et al. 2013). Die Qualitätssicherung hinsichtlich gesundheitlicher Aspekte hat daher oberste Priorität, während die ökologische Relevanz des Grundwassers in Bezug auf Oberflächengewässer bisher weniger Beachtung fand. Davon ausgenommen ist die ubiquitäre Grundwasserbelastung mit Nitrat durch die Industrialisierung der Landwirtschaft. Sowohl die gesundheitsgefährdende Wirkung von zu hohen Nitratkonzentrationen im Grundwasser als auch die damit verbundene Gefahr der Eutrophierung benachbarter Ökosysteme geben seit mehreren Jahrzehnten Anlass zu intensiver Forschung. Tatsächlich ist eine häufige Motivation für die Untersuchung von Grundwasser-Oberflächenwasser-Interaktionen eine ungeklärte Anreicherung von Nähr- oder Schadstoffen im Oberflächengewässer (Behrendt et al. 2002). Der Zustrom von kontaminiertem Grundwasser kann im Einzelfall große Auswirkungen auf die Gewässerqualität haben. Nähr- oder Schadstofffahnen erreichen ein Oberflächenwasser aufgrund der langsamen Grundwasserfließgeschwindigkeiten oft stark verzögert, unter Umständen erst Jahre oder gar Jahrzehnte nach der eigentlichen Kontamination. Bis dahin bleiben sie häufig völlig unbemerkt. Ein Beispiel dafür ist der Arendsee im Norden Sachsen-Anhalts. Hier stiegen die Phosphorkonzentrationen im Freiwasser innerhalb der letzten Jahrzehnte stetig an. Maßnahmen wie die Fernhaltung von kommunalem Abwasser, die bereits in den 1970er Jahren ergriffen wurden, scheinen keine signifikant positive Wirkung zu haben. Die Frachten aus anderen Eintragspfaden, z. B. aus Landwirtschaft oder durch rastende Zugvögel, reichen jedoch nicht aus, um die Belastung des Gewässers zu erklären. Eine intensive Untersuchung des Einzugsgebiets offenbarte eine starke Kontamination des Grundwassers mit Phosphor und anderen Nährstoffen (Meinikmann et al. 2015). Die Quantifizierung der grundwasserbürtigen Phosphorfrachten erfolgte daraufhin anhand der Kombination von hydro(geo) logischen und geochemischen Methoden. Exfiltrationsraten und Phosphorkonzentrationen wurden für einzelne Uferabschnitte individuell bestimmt und miteinander multipliziert. Die abschnittsweisen Ergebnisse wurden zu einer grundwasserbürtigen Gesamt-Phosphorfracht aufsummiert. Es zeigte sich, dass das Grundwasser mehr als 50 % der gesamten externen Phosphorfracht in den See einträgt und somit maßgeblichen Anteil an der Eutrophierung des Gewässers hat (Meinikmann et al. 2013, 2015).

Bisher ungeklärt sind Ursachen und Eintragswege von ansteigenden Konzentrationen an gelöstem organischem Kohlenstoff (TOC bzw. DOC), die in vielen Oberflächengewässern in der nördlichen Hemisphäre beobachtet wurden (Arvola et al. 2010; Brothers et al. 2014; Clark et al. 2010; Evans et al. 2005; Kokorite et al. 2012; Monteith et al. 2007). Einige Autoren vermuten einen Zusammenhang mit dem globalen Klimawandel oder mit Veränderungen in der atmosphärischen Deposition (Monteith et al. 2007; Worrall et al. 2003). Andere sind der Auffassung, dass es sich um einzugsgebietsbezogene Prozesse handelt, die den verstärkten diffusen Zutritt von organischem Kohlenstoff antreiben (z. B. Findlay 2005). Die Differenzierung der beteiligten Prozesse in der vadosen und gesättigten Zone und deren Bedeutung für das Phänomen ansteigender Kohlenstoffkonzentrationen in Gewässern ist bisher jedoch noch kaum Forschungsgegenstand gewesen.

Den genannten Beispielen entsprechend befasst sich die Forschung im Bereich der Grundwasser-Oberflächenwasser-Interaktion häufig mit der Quantifizierung von Stofffrachten, die mit dem zuströmenden Grundwasser in ein Gewässer gelangen. Der inverse Prozess des in den Grundwasserleiter versickernden Oberflächenwassers wird vor allem im Zusammenhang mit der Uferfiltration betrachtet. Bei der Uferfiltration wird die Retardation von Schadstoffen im Grundwasserleiter genutzt, um Oberflächenwasser von Seen oder Flüssen durch die Untergrundpassage zu reinigen und dann als Trinkwasser zu nutzen.

Der Austausch von Wasser zwischen den Systemen erfolgt über das Gewässersediment, das eine Grenz- und Übergangszone darstellt, in der oft steile physikalische, chemische und biologische Gradienten auftreten. Die Mächtigkeit dieser Grenzzone lässt sich nicht eindeutig definieren. Sie umfasst in der Regel die obersten Zentimeter bis Dezimeter des Gewässersediments und kann zeitlich und räumlich variieren. Viele der hier vorgestellten Untersuchungsmethoden finden an dieser Grenzzone Anwendung. Generell kann ein Austausch überall im Gewässerbett stattfinden. Physikalische Gesetzmäßigkeiten sorgen allerdings dafür, dass der Großteil der Interaktionen überwiegend im Uferbereich eines Gewässers stattfindet und damit in einem Bereich, der für Messungen leichter zugänglich ist als Bereiche in größerer Wassertiefe (Abschnitt 2.2). Dennoch sind die hydraulischen und chemischen Prozesse, die sich zwischen Grund- und Oberflächenwasser abspielen, aus folgenden Gründen nur schwer zu quantifizieren:

- Der Austausch verläuft in den meisten Fällen diffus, also (groß-)flächig. Er ist visuell meist nicht wahrnehmbar und damit umso schwerer zu erfassen. Es existieren nur wenige äußerliche Indikatoren für diese Prozesse, obwohl in einigen Studien die Wasservegetation als Zeiger für Grundwasser-Oberflächenwasser-Interaktionen genutzt wurde (Rosenberry et al. 2000; Sebestyen und Schneider 2004). Die exakte Ausdehnung der Bereiche eines Gewässers, in denen Interaktionen mit dem Grundwasser stattfinden, ist schwer zu bestimmen. Für eine repräsentative Auswahl von Untersuchungsstandorten sind daher häufig aufwendige Voruntersuchungen notwendig. Die Repräsentativität einzelner Standorte wird außerdem durch die Heterogenität des Gewässersediments eingeschränkt. Die hydraulischen Verhältnisse können sich innerhalb weniger Meter bis Zentimeter signifikant voneinander unterscheiden, weil beispielsweise die Sortierung des Substrates oft kleinräumig variiert.
- Die Untersuchung von (bio-)geochemischen Prozessen, die innerhalb der Grenzzone stattfinden, erweist sich ebenfalls als schwierig. Auch hier können in vertikaler und horizontaler Richtung kleinräumig signifikante Unterschiede auftreten.
- Die technische Umsetzbarkeit von Untersuchungen an der Grenzzone zwischen Gewässer und Grundwasser ist im Einzelfall begrenzt. Die Zugänglichkeit der zu untersuchenden Bereiche kann beispielsweise durch starken Pflanzenbewuchs eingeschränkt sein. Große Gewässertiefen lassen die Installation von Messgeräten nur vom Boot aus oder per Taucher zu. Auch Strömung oder starker Wellengang können Untersuchungen vor Ort erschweren.

Die genannten Faktoren sind einige der Gründe für die lange andauernde Vernachlässigung des Grundwassers in den Wasser- und Nährstoffhaushalten von Oberflächengewässern. Diese Vernachlässigung hat zur Folge, dass viele hydrologische und biogeochemische Prozesse im Bereich der Grenzzone noch immer nicht richtig verstanden sind. Deshalb wird hier zunächst auf die Mechanismen von Grundwasser-Oberflächenwasser-Interaktionen eingegangen.

2.2 Wechselwirkung zwischen Grund- und Oberflächenwasser: Termini und Mechanismen

Interaktionen zwischen Grund- und Oberflächenwässern werden entsprechend den hydrogeologischen Konventionen in diesem Beitrag aus der Sicht des Grundwasserkörpers betrachtet. Der Austritt von Grundwasser in einen See oder einen Fluss wird Exfiltration genannt, während der in entgegengesetzter Richtung stattfindende Prozess, der Zustrom von Oberflächenwasser in das Grundwasser, Infiltration heißt (Abb. 1). Erfolgt die Betrachtung aus Sicht des Oberflächengewässers, ist die Terminologie genau umgekehrt. Ob ex- oder infiltrierende Verhältnisse vorliegen, hängt vom hydraulischen Gradienten zwischen Grund- und Oberflächenwasser ab. Liegt die Grundwasseroberfläche oberhalb des Gewässerspiegels, exfiltriert Grundwasser in das Oberflächenwasser. Befindet sich die Grundwasserspiegel unterhalb der Oberfläche des Gewässers, so infiltriert Fluss- oder Seewasser in den Grundwasserleiter und trägt zu einer Neubildung von Grundwasser bei. Der Austausch zwischen Grund- und Oberflächenwasser er-

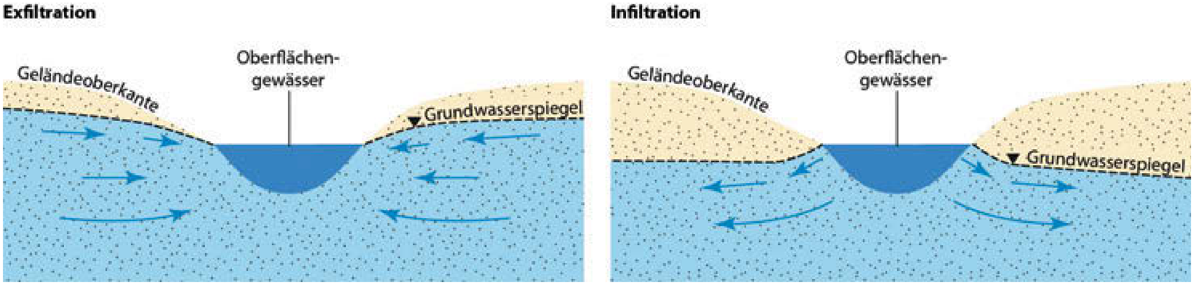

Abb. 1: Schematische Darstellung von Exfiltration (a) und Infiltration (b). Die blauen Pfeile repräsentieren Grundwasserfließpfade. (Nach Winter et al. 1998)

folgt über das Gewässersediment, das in diesem Zusammenhang auch als (Sediment-Wasser-)Grenzzone bezeichnet wird.

An der Uferlinie treffen Grundwasseroberfläche und die horizontale Oberfläche des Gewässers zusammen. Bei exfiltrierenden Verhältnissen hat der Neigungsunterschied zwischen den beiden Wasseroberflächen eine abrupte Druckentlastung im Grundwasserkörper zur Folge. Die Grundwasserfließpfade driften daraufhin in Richtung dieses Druckentlastungspunktes ab, was einen Wechsel von einer horizontalen in eine aufwärtsgerichtete Fließbewegung des Grundwassers bedingt (Abb. 2). Die Orientierung der Grundwasserfließpfade zu diesem Druckentlastungspunkt führt dazu, dass ein Großteil der Exfiltration im unmittelbaren Uferbereich stattfindet und die Exfiltrationsraten mit zunehmendem Uferabstand abnehmen.

Im Einzelfall hängt die räumliche Verteilung der Exfiltrationsraten jedoch in erster Linie von den Sedimenteigenschaften vor Ort ab. Vor allem Korngrößenzusammensetzung und Lagerungsdichte der Substrate bestimmen die hydraulische Leitfähigkeit (k_f) des Grundwasserleiters und damit Fließgeschwindigkeiten und Austauschraten. Grundwasserleiter sind in der Regel heterogen bezüglich ihrer hydraulischen Leitfähigkeit, was zu entsprechenden räumlichen Unterschieden in den Austauschraten auf kleinen und mittleren Skalen zu führt. Auch am Gewässergrund abgelagerte allochthone Sedimente, die sich in ihrer Beschaffenheit deutlich von denen des angrenzenden Grundwasserleiters unterscheiden können, haben Einfluss auf den Austausch zwischen Grundwasser und Oberflächengewässer.

An der Sediment-Wasser-Grenze selbst wirken viele Faktoren, die zu zusätzlicher Variabilität im Austausch zwischen Grund- und Oberflächenwasser führen können. Die Sedimente werden z. B. durch Ufererosion, Wellengang und Strömung oder durch wechselnde Wasserstände bearbeitet und umgelagert. Das führt neben räumlichen auch zu zeitlichen Heterogenitäten im Austausch zwischen den beiden Systemen. Der Eintrag neuer Sedimentfrachten, z. B. nach Starkniederschlägen, und die Einarbeitung von organischem Material (Totholz o. Ä.) in das Gewässersediment verstärkt ebenfalls die Heterogenität der Grenzzone. Nicht zu unterschätzen ist außerdem der Einfluss von Benthos, Fischen, Vögeln und anderen Organismen, die das Sediment in verschiedener Weise nutzen und verändern. Räumlich variierende Austauschraten können auch durch Vegetation verursacht werden. So kann zum Beispiel die Transpiration von Baumbeständen im direkten Uferbereich zu lokal verringertem Grundwasserzustrom führen (Abb. 3). Die Transpiration der Ufervegetation kann auch saisonal und sogar diurnal variierende Fließ- und Austauschraten verursachen (Doss 1993; Fraser et al. 2001; Winter und Rosenberry 1995). Ist der Verlust in die Atmosphäre so groß, dass der Grundwasserspiegel unter die Gewässeroberfläche sinkt, kommt es zum Wechsel von exfiltrierenden zu infiltrierenden Verhältnissen.

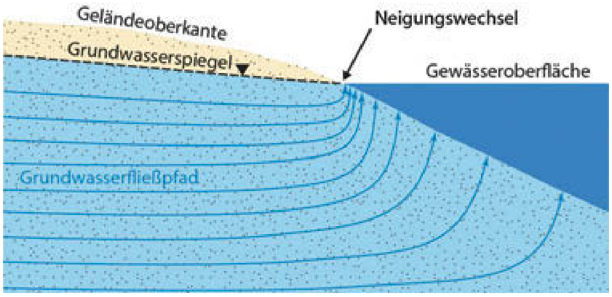

Abb. 2: Räumliche Entwicklung der Grundwasserfließpfade bei Exfiltration. (Nach Winter et al. 1998)

Die verschiedenen Einflüsse können zu unterschiedlichen Richtungen der Grundwasser-Oberflächenwasser-Interaktionen entlang eines Transektes führen, wie am Beispiel von Abbildung 3 erläutert werden soll. Während im unmittelbaren Uferbereich die Transpiration der Vegetation zu zeitweise infiltrierenden Verhältnissen führt, kann die lokale Grundwasserfließrichtung in einiger Uferentfernung zum Zustrom von Grundwasser in das Gewässer führen. In einiger Uferentfernung tritt eine geringleitende Schicht auf den Wasserkörper, der das obere Grundwasserstockwerk von einem unteren separiert. In die-

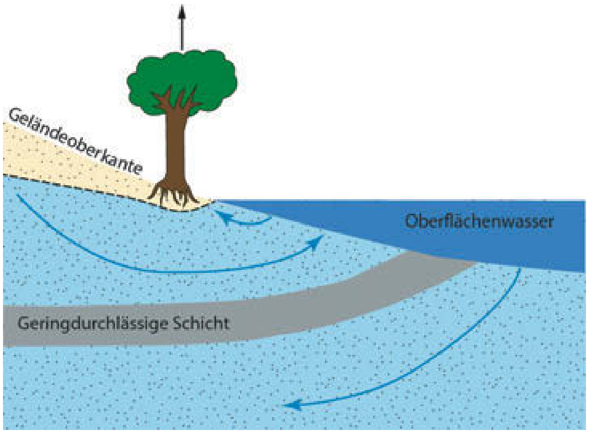

Abb. 3: Beispiel für räumliche Heterogenität der Grundwasser-Oberflächenwasser-Interaktion, verursacht beispielsweise durch Transpiration der Ufervegetation und unterschiedliche Sedimenteigenschaften. (Nach Winter et al. 1998)

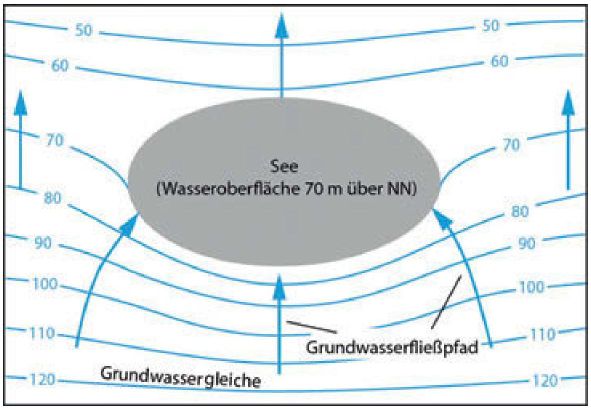

Abb. 4: Grundwassergleichen (hellblaue Linien, in m über NN) und Grundwasserfließpfade (Pfeile) in der Umgebung eines Sees (Durchflusstyp).

sem Bereich findet kein Austausch mit dem Oberflächenwasser statt. Der Austausch mit dem unteren Stockwerk wiederum ist von Infiltration geprägt, beispielsweise weil die regionale Fließrichtung des Grundwassers entgegen derjenigen des oberen Grundwasserstockwerkes verläuft (Abb. 3).

2.3 Unterschiede zwischen Fließgewässern und Seen

Neben den bereits genannten Mechanismen, die für alle Gewässertypen gelten, zeigen Fließgewässer und Seen einige jeweils spezifische Eigenschaften im Austausch mit dem Grundwasser. Fließgewässer sind schnell fluktuierende Systeme, was auch für die Dynamik der Interaktion mit dem Grundwasser zutrifft. Es ist außerdem davon auszugehen, dass im Oberlauf Exfiltrationsprozesse dominieren, während in tiefer liegenden Abschnitten zunehmend Verluste durch Infiltration auftreten. Da diese Prozesse aber ständigen räumlichen und zeitlichen Veränderungen unterliegen, sind allgemeingültige Aussagen nur bedingt gültig. Hochwässer beispielsweise können die üblicherweise vorherrschenden exfiltrierenden Bedingungen umkehren, da der Pegel im Fluss oft schneller ansteigt als der Grundwasserspiegel und diesen letztendlich übersteigt (Lewandowski et al. 2009). Seen sind dagegen weniger dynamisch und lassen sich daher in drei Typen einteilen (vgl. Kap. IV-1.1.3): den *Zuflusstyp*, bei dem im gesamten Gewässerbett Exfiltration stattfindet, den *Abflusstyp*, bei dem ausschließlich Infiltration stattfindet, sowie den *Durchflusstyp*, der als Teil des lokalen oder regionalen Grundwasserströmungssystems in einem Bereich grundwassergespeist ist und in anderen Bereichen Wasser an den Grundwasserleiter verliert (Abb. 4).

Ein weiterer Unterschied zwischen den Systemen ist die Lage der Grundwassergleichen (Linien gleichen Grundwasserstandes, Isohypsen genannt) in Bezug zum Gewässer. Im Einzugsgebiet eines Sees verlaufen die Grundwassergleichen im Allgemeinen parallel zur Uferlinie. Der Grundwasserzufluss erfolgt daher in senkrechter Richtung zum Seeufer (Abb. 4). Im Einzugsgebiet von Fließgewässern verlaufen die Isohypsen dagegen überwiegend senkrecht zum Ufer, sodass Grundwasser und Fluss die gleiche Strömungsrichtung haben. Ein Austausch zwischen beiden Systemen wird durch die Krümmung der Isohypsen im unmittelbaren Uferbereich angezeigt. Erfolgt sie in Richtung des Oberflächengefälles (d. h. in Fließrichtung des Oberflächenwassers), so liegen infiltrierende Verhältnisse vor (Abb. 5a). Im Falle von Grundwasserzustrom in das Gewässer (Exfiltration) krümmen sich die Isohypsen in Ufernähe entgegen der oberflächlichen Fließrichtung (Abb. 5b).

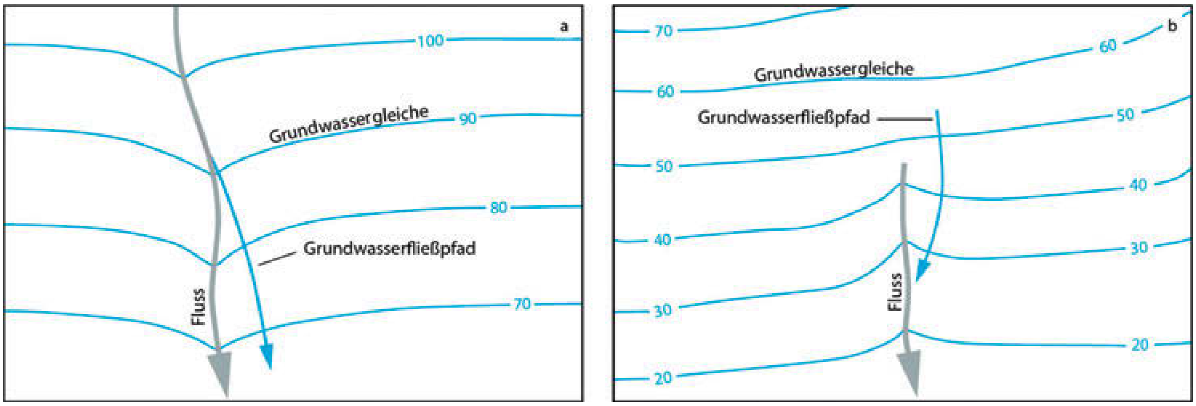

Abb. 5: Infiltration von Flusswasser in das Grundwasser (a) und Exfiltration von Grundwasser in den Fluss (b). Grundwassergleichen (hellblaue Linien, in m über NN). (Verändert nach Winter et al. 1998)

Ein zusätzlicher Aspekt, der fließende Gewässer von Seen unterscheidet, ist die Bedeutung der Grenzzone zwischen Sediment und Freiwasser. Anders als in den meisten Seen findet hier neben dem Austausch mit dem Grundwasser ein relativ schneller und reversibler Austausch zwischen dem Freiwasser und dem Porenwasser des Flussbettes statt. Dieser wird angetrieben durch die Fließbewegung im Fluss und den morphologisch bedingten Gefällewechseln zwischen Stromschnellen und Kolken, aber auch durch kleinräumigere Bodenstrukturen und Hindernisse im Gewässer (Totholz, Wasserpflanzen, etc.). Flusswasser wird immer wieder in das Gewässersediment gedrückt, wo es als Porenwasser deutlich langsamer weitertransportiert wird, bis es an anderer Stelle wieder in das Freiwasser austritt. Die Wassermenge in dieser Grenzzone, der hyporheischen Zone, kann einen großen Anteil am Abfluss des Gewässers haben. Die komplexen chemischen Prozesse, die innerhalb dieser Zone stattfinden, sind daher von großer Bedeutung für die Beschaffenheit des Flusswassers. In Abhängigkeit vom aktuellen Abflussvolumen ist auch die zeitliche Variabilität der Grenzzone von Flüssen durchaus höher als die der Grenzzone von Stillgewässern. Die Quantifizierung des Anteils exfiltrierenden Grundwassers kann deswegen in Fließgewässern komplizierter als in Seen sein, da es sich mit dem vorübergehend infiltrierenden Oberflächenwasser vermischt.

3 Methoden zur Erfassung des hydrologischen Austausches

Im Folgenden werden Methoden zur Bestimmung von Mustern und/oder Raten des Wasseraustausches zwischen Grundwasser und Oberflächengewässern beschrieben. Generell ist zwischen zwei Arten von Methoden zu unterscheiden. Die Messung von Austauschraten mithilfe von Seepagemetern (Abschnitt 3.1) ist die bisher einzige *direkte* Methode zur Quantifizierung von Wasserflüssen zwischen den beiden Systemen. Bei allen weiteren Verfahren handelt es sich um *indirekte* Methoden, denen Parameter zugrunde liegen, die (zum Teil) von Richtung und Intensität der Grundwasser-Oberflächenwasser-Interaktion abhängig sind. Ist ein Verfahren nur bedingt auf beide bzw. ausschließlich auf einen der beiden Gewässertypen anwendbar, so wird an entsprechender Stelle darauf hingewiesen. In Abschnitt 5 werden die hier vorgestellten Methoden zur Erfassung des hydrologischen Austausches zwischen Grund- und Oberflächenwasser noch einmal gegenübergestellt.

3.1 Seepagemeter

Seepagemeter sind die einzigen Instrumente, die eine direkte Erfassung von Austauschraten zwischen Grund- und Oberflächenwässern ermöglichen. Sie werden deshalb an dieser Stelle besonders ausführlich behandelt. Es handelt sich dabei um einseitig offene Zylinder (meist aus Stahl), die mit ihrer offenen Seite in das Gewässersediment gedrückt werden (Abb. 6). Das innerhalb des Zylinderdurchmessers exfiltrierende Grundwasser verdrängt das im Zylinderhohlraum eingeschlossene Wasser, das daraufhin in einen mit einem Schlauch am Zylinder angeschlossenen Sammelbeutel aus Plastik weitergeleitet wird. Über die Wägung des Plastikbeutels wird das Exfiltrationsvolumen ermittelt. Die Umrechnung auf die Fläche des Zylinders und den Messzeitraum ermöglicht die Kalkulation der Exfiltrationsrate. Umgekehrt können auch Infiltrationsraten bestimmt werden, indem der Verlust von Wasser aus dem Plastikbeutel gemessen wird.

Durchmesser und Höhe des Zylinders sind variabel und maßgeblich durch die Handhabbarkeit limitiert. Seepagemeter mit größeren Durchmessern erzielen genauere Ergebnisse, was vor allem bei kleinen Fließraten von Bedeutung ist. Außerdem integrieren sie kleinskalige Heterogenitäten des Grundwasserzustroms besser. Je größer allerdings ein Seepagemeter ist, desto schwieriger ist seine Handhabung, wobei vor allem das Entfernen aus dem Sediment nach Gebrauch große Probleme bereiten kann. Auch die Installation von größeren Seepagemetern kann schwieriger sein, weil vor allem bei groben und unebenen Sedimenten die Abdichtung im Gewässergrund oft nicht optimal gelingt. ROSENBERRY (2005) schlägt daher als Kompromiss vor, mehrere normalgroße Seepagemeter einem einzigen Plastikbeutel zuzuführen, um eine größere Fläche (und damit räumliche Variabilität im Grundwasserfluss) abzudecken (Abb. 6). Die übliche Größe für Seepagemeter ist etwa 0,25 m^2, wobei vielfach einfache Konstruktionen aus den oberen und unteren Teilen alter Stahl- oder Plastikfässer verwendet werden. Diese kostengünstigen Konstruktionen wurden zuerst von Lee (1977) eingeführt und seitdem von vielen Autoren verfeinert und optimiert. Denn so einfach und logisch diese Art der Messung von Austauschraten auch erscheinen mag, so sehr liegen Probleme bei der Anwendung oft im Detail. Das Einbringen ins Sediment ist beispielsweise häufig

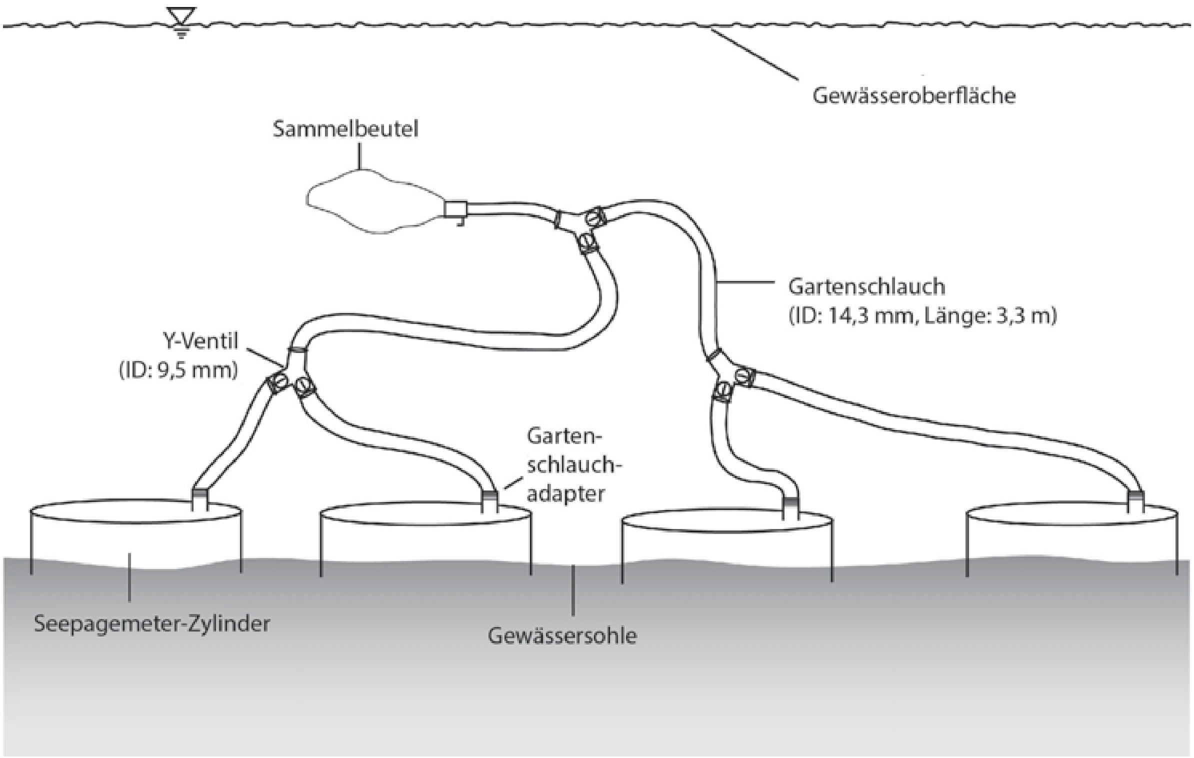

Abb. 6: Schematische Darstellung von vier Seepagemetern, die über handelsübliche Gartenschläuche und entsprechende Ventile miteinander verbunden sind, um die Auswirkungen räumlicher Heterogenitäten im Grundwasser-Oberflächenwasser-Austausch auf die Messergebnisse zu reduzieren. (Nach Rosenberry 2005)

schwierig, weil zu grobes Sediment ein gleichmäßiges Einbringen erschweren oder ganz verhindern kann. Möglichst dünne Wandungen erleichtern die Installation im Sediment. Auch das Anschärfen der Kanten führt zu einem leichteren und gleichmäßigen Einbringen in das Sediment. Rosenberry und LaBaugh (2008) empfehlen bei großem Widerstand (vor allem in sandigen und kiesigen Gewässerbetten), sich auf das Seepagemeter zu stellen und es mit vorsichtigen Bewegungen vor und zurück in das Sediment zu treiben. Allerdings sollte beachtet werden, dass ein zu schnelles Einbringen das Sediment innerhalb des Zylinders kompaktieren kann, was zu Veränderungen der ursprünglichen Fließraten führt.

Der Plastikbeutel, der das exfiltrierende Wasservolumen auffangen soll, wird erst nach dem Einbringen des Zylinders angebracht, da bei der Installation des Zylinders überschüssiges Wasser oder Gas entweichen muss. Größe und Art der Beutel wurden vielfach diskutiert. Überwiegend werden einfache Vorratsbeutel (z. B. Gefrierbeutel) mit einem Volumen von etwa vier Litern verwendet. Es wurden allerdings auch Studien mit handelsüblichen Kondomen (150 ml; Schincariol und McNeil 2002) oder Mülltüten (15 l; Erickson 1981) durchgeführt. Manche Autoren bevorzugten dickwandigere Plastikbeutel, um Fraßschäden, z. B. durch Fische, vorzubeugen (Erickson 1981). Beliebt waren in diesem Zusammenhang Urinbeutel oder Beutel für Infusionen, weil an diese bereits ein Schlauch angeschlossen ist, der mit dem Seepagemeter verbunden werden kann. Dickwandige Beutel zeigen im Vergleich zu dünnwandigen Varianten jedoch einen größeren Widerstand gegenüber eintretendem Wasser, was zu Verfälschungen der Fließraten führen kann. Daher raten erfahrene Seepagemeter-Nutzer von dickwandigen Plastikbeuteln ab.

Es hat sich außerdem bewährt, die Plastikbeutel mit einem gewissen Wasservolumen aufzufüllen, bevor sie an den Zylinderkörper angeschlossen werden. Plastiktüten unterliegen einem produktionsbedingten *memory effect*, der einen geringen Unterdruck auslöst, wenn ihre ursprüngliche Form durch mechanische Einwirkung verändert wird. Dieser *memory effect* forciert einen übermäßigen Zustrom von Wasser in den Beutel. Das ist vor allem bei geringen Fließraten zu berücksichtigen. Fehlmessungen lassen sich daher durch ein bestimmtes Initialvolumen im Beutel (ca. 1 l bei einem Gesamtvolumen von 4 l) vermeiden.

Werden am Untersuchungsstandort infiltrierende Verhältnisse erwartet, so ist es sowieso unabdingbar, dass der Plastikbeutel ausreichend mit Wasser befüllt ist, da der Beutel in diesem Fall Wasser verliert. Im Folgenden werden die wichtigsten Empfehlungen und Fehlerquellen genannt, die bei der Anwendung von Seepagemetern zu beachten sind (nach Rosenberry und LaBaugh 2008):

1. Anforderungen an das Instrument und die Installation: Seepagemeter sollten aus stabilem und unelastischem Material bestehen (z. B. Edelstahl, Hartplastik). Ein Durchmesser von 0,5 m ist ein guter Kompromiss zwischen größtmöglich abgedeckter Fläche und praktikabler Handhabung. Es muss sichergestellt sein, dass das Seepagemeter mit seinem gesamten Umfang mindestens einige Zentimeter tief im Gewässersediment installiert ist und nicht nur mit seiner Kante auf dem Sediment aufliegt.
2. Undichtigkeiten zwischen Seepagemeter und Sediment: Zwischen Sediment und Seepagemeter muss eine gute Abdichtung gewährleistet wird, um ein Entweichen des exfiltrierenden Grundwassers aus dem Zylinder ins Freiwasser zu verhindern. Die Zylinderwandung sollte daher vollständig und so weit wie möglich in das Sediment eingebracht werden. Dies ist außerdem wichtig, um die Stabilität der Konstruktion auch bei starkem Wind und/ oder Wellenschlag zu gewährleisten.
3. Zeitabstand zwischen Installation des Seepagemeter und erster Messung: Durch die Installation des Seepagemeters wird das Sediment kompaktiert, und ursprüngliche Fließraten können verändert werden. Deswegen sollte ausreichend Zeit eingeplant werden, damit sich das ursprüngliche Gleichgewicht des Systems wieder herstellen kann. Es sollte mindestens ein Tag zwischen dem Einbringen und der ersten Messung liegen. Generell benötigen feinkörnigere Sedimente (Lehme oder Tone) eine längere Regenerationsphase als gröbere Sedimente.
4. Mangelhafte Verbindung zwischen Zylinder und Plastikbeutel: Da die meisten Seepagemeter Eigenbauten sind, gibt es kein „Patentrezept“ für die Verbindung zwischen Plastikbeutel und Zylinder. Als Verbindungsstücke werden meist Polyethylen- oder auch Gartenschläuche verwendet. Die Schlauchverbindungen sollten vor allem bei höheren Austauschraten einen ausreichend großen Durchmesser haben. Ist dieser zu klein, entsteht ein Widerstand, der die Ergebnisse verfälschen kann. Der Schlauchdurchmesser sollte mindestens 9 mm betragen. Die Verbindung zum Seepagemeter erfolgt oft über einen Gummipfropfen an einer Öffnung an der Oberseite oder der Wandung des Zylinders. Hier sollte großer Wert auf Dichtheit gelegt werden, ebenso wie auf der Seite des Plastikbeutels.
5. Installation und Entfernung des Auffangbeutels: Während des Anbringens des Beutels kann es schnell zu ungewolltem Ein- oder Austritt von Wasser kommen. Generell ist bei der Installation jeglicher Druck auf den Beutel zu vermeiden, da der Austausch von Wasser zwischen Beutel und Zylinder das Ausgangsvolumen und -gewicht des Beutels verändert. Dies kann verhindert werden, indem ein Ventil als Verbindungsstück zum Zylinder genutzt wird (z. B. Gartenschlauchzubehör), das erst nach der Installation des Beutels geöffnet wird. Ein solches Ventil verhindert zusätzlich die Ansammlung von Luft im Beutel während der Installation. Nach dem Einfüllen des Wassers wird die vorhandene Luft im Beutel herausgepresst und das Ventil geschlossen, sodass die Ausgangsbedingungen bis zur Installation erhalten bleiben. Luft im Beutel kann das Ergebnis verfälschen. Harvey et al. (2000) führten beispielsweise einen übermäßigen Zufluss auf den durch eingeschlossenes Gas verursachten Auftrieb des Beutels zurück. Nicht repräsentative Flüsse können außerdem durch das Gewicht des Bearbeiters entstehen, der sich dem Seepagemeter nähert, um den Beutel anzubringen oder zu entfernen. Gerade bei weichen Sedimenten wurde beobachtet, dass das durch das Gewicht verdrängte Wasser kurzfristig zu deutlich erhöhten Seepageraten führt (Rosenberry und Morin 2004). Dies ist vor allem bei kleinen Flussraten von Bedeutung. Wenn möglich, sollte die Installation der Beutel daher vom Boot aus erfolgen. Alternativ lässt sich der Beutel auch in einigem Abstand (1–2 m) vom Seepagemeter an einem Verlängerungsschlauch anbringen.
6. Wellenschlag und Wellenbewegung: In Fließgewässern kann es durch die Strömung ebenfalls zu Fehlern in der Seepage-Messung kommen. Dies ist auf den von der Fließgeschwindigkeit induzierten dynamischen Druck (Staudruck) als Teil des Gesamtdrucks im Gewässer zurückzuführen. Anders als im Gewässer selbst ist die dynamische Druckhöhe im Beutel gleich null, weil dort keine signifikante Wasserbewegung auftritt. Daraus kann sich ein nicht unerheblicher Druckgradient an der elastischen Beuteloberfläche ergeben. Dieser Gradient führt dazu, dass bei Fließgeschwindigkeiten von mehr als 0,1 m s^{-1} signifikante Feh-

ler auftreten: Bei exfiltrierenden Verhältnissen fließt mehr Wasser in den Beutel, als Grundwasser exfiltriert, bei infiltrierenden Verhältnissen wird das aus dem Beutel herausfließende Volumen reduziert. Ähnliche Effekte können auch bei Wellenschlag, z. B. im Uferbereich von Seen, auftreten Murdoch und Kelly, (2003). Derartige Fehler können vermieden werden, indem die Beutel durch ein weiteres Gehäuse aus stabilerem Material vom fließenden Wasser abgeschottet werden. Der Druckgradient hat, anders als bei den elastischen Plastikbeuteln, bei einem stabilen Gehäuse keine Auswirkungen. Eine solche Schutzkonstruktion sollte auch gewährleisten, dass der Schlauch zwischen Zylinder und Plastikbeutel nicht eingequetscht und der Austausch zwischen den beiden Elementen verhindert wird. Verschiedene Alternativen sind beispielsweise in Schneider et al. (2005) und Sebestyen und Schneider (2001) beschrieben.

Mittlerweile werden auch automatisierte Seepagemeter eingesetzt. Sie ermöglichen die Erfassung kurzfristiger Schwankungen der Austauschraten. Neben den bereits genannten Wellenbewegungen können auch Seiches (windinduzierte interne Wellen im Wasserkörper) oder verstärkte Grundwasserneubildung nach Regenereignissen Auslöser dafür sein. Automatisierte Seepagemeter sind auf der Zylinderoberseite mit einem Fließgeschwindigkeitsmesser ausgestattet, der Fließbewegungen in das Seepagemeter oder aus dem Seepagemeter heraus quantifiziert. Beispiele entsprechender Studien finden sich in Paulsen et al. (2001), Menheer (2004) und Rosenberry und Morin (2004). Andere automatisierte Seepagemeter nutzen Heat-Pulse-Technologien oder chemische und Farbtracer. Eine Übersicht dazu findet sich bei Rosenberry und LaBaugh (2008). Der Vorteil automatisierter Seepagemeter besteht neben der hohen zeitlichen Auflösung darin, dass das in- oder exfiltrierende Wasser nicht aufgefangen werden muss und damit die vielfältigen Fehler bei der Anwendung der Beutel entfallen.

3.2 Hydraulische Gradienten

Nach dem Gesetz von Darcy ist der Volumenstrom Q (in m^3 s^{-1}), der eine Querschnittsfläche A (in m^2) in einem porösen Medium laminar passiert, proportional zum hydraulischen Gradienten i:

$$\frac{Q}{A} = v_\mathrm{f} = -k_\mathrm{f} \cdot i \tag{1}$$

Der Quotient aus Q und A ist die sogenannte Darcy-Geschwindigkeit v_f (in m s^{-1}) als Annäherung für die tatsächliche Grundwasserfließgeschwindkeit. Der hydraulische Gradient i beschreibt das Verhältnis des Druckhöhenunterschiedes Δh (in m) zwischen zwei Standrohren zur Fließlänge L (in m) zwischen eben diesen Standrohren,

$$i = \frac{\Delta h}{L} \tag{2}$$

In Bezug auf den Austausch zwischen Grund- und Oberflächenwasser gilt: Liegt der Grundwasserspiegel oberhalb der Gewässeroberfläche, exfiltriert Grundwasser in das Gewässer (b in Abb. 7). Wenn Wasser aus dem Oberflächengewässer in den Grundwasserleiter fließt, liegt der Grundwasserspiegel un-

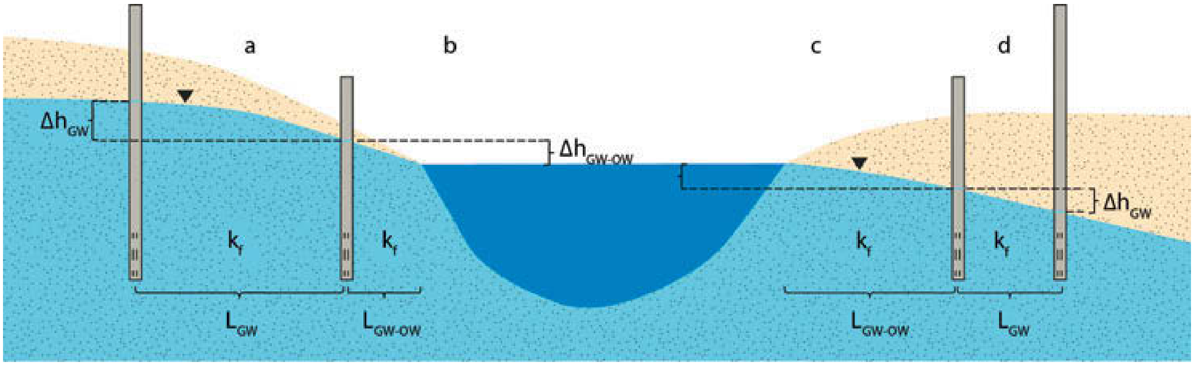

Abb. 7: Ableitung der Richtung des Grundwasser-Oberflächenwasser-Austausches anhand der hydraulischen Gradienten innerhalb des Grundwasserleiters (a und d) oder zwischen Grundwasser und Oberflächenwasser (b und c). Liegt der Grundwasserspiegel oberhalb der Wasseroberfläche (positiver Wert für Druckhöhenunterschied Δh), exfiltriert Grundwasser in das Gewässer (a und b). Im umgekehrten Fall (Grundwasserspiegel liegt unterhalb der Wasseroberfläche, negativer Wert für Δh) infiltriert Oberflächenwasser in das Grundwasser (c und d). Das Verhältnis von Δh zur Fließlänge L (Distanz zwischen den Beobachtungsstellen; GW = Grundwasser; OW = Oberflächenwasser) entspricht dem hydraulischen Gradienten. Bei bekanntem Durchlässigkeitsbeiwert des Sedimentmaterials (k_f) lässt sich daraus die Darcy-Geschwindigkeit berechnen (s. Gl. 3).

Tab. 1: Durchlässigkeitsbeiwerte der einzelnen Korngrößen nach DIN 18130-1 (Größenordnungen)

Lockergestein	**Durchlässigkeitsbeiwert k_f (in m s^{-1})**
reiner Kies	10^{-1}–10^{-2}
grobkörniger Sand	$\approx 10^{-3}$
mittelkörniger Sand	10^{-3}–10^{-4}
feinkörniger Sand	10^{-4}–10^{-5}
schluffiger Sand	10^{-5}–10^{-7}
toniger Schluff	10^{-6}–10^{-9}
Ton	$<10^{-9}$

Tab. 2: Einteilung der Durchlässigkeitsbeiwerte nach DIN 18130-1

Einteilung	**Durchlässigkeitsbeiwert k_f (in m s^{-1})**
sehr stark durchlässig	$>10^{-2}$
stark durchlässig	10^{-2}–10^{-4}
durchlässig	10^{-4}–10^{-6}
schwach durchlässig	10^{-6}–10^{-8}
sehr schwach durchlässig	$<10^{-8}$

terhalb der Gewässeroberfläche (c in Abb. 7). Der Vergleich der Druckhöhen ermöglicht also eine Aussage über die Richtung des hydrologischen Austausches zwischen den beiden Systemen. Der Gradient i ist ein Indikator für die Intensität des Austausches.

Aus den Gleichungen 1 und 2 ergibt sich:

$$v_f = -k_f \cdot \frac{\Delta h}{L} \tag{3}$$

k_f (in m s^{-1}) ist dabei der Durchlässigkeitsbeiwert, der die Wasserdurchlässigkeit des Aquifermaterials quantifiziert (auch gesättigte hydraulische Leitfähigkeit genannt). k_f-Werte sind überwiegend von der Korngrößenzusammensetzung des Grundwasserleiters abhängig und lassen sich entweder direkt anhand von ungestörten Stechzylinderproben oder indirekt beispielsweise über eine Korngrößenanalyse ermitteln (s. Hartge und Horn 2009). Beide Verfahren sind allerdings fehleranfällig, sodass mit ihnen ermittelte Werte für dieselbe Probe oft signifikant unterschiedlich sind. Je nach Korngröße variieren hydraulische Leitfähigkeiten über mehrere Größenordnungen und werden in Klassen von „sehr stark durchlässig“ ($>10^{-2}$ m s^{-1}) bis „sehr schwach durchlässig“ ($<10^{-8}$ m s^{-1}) eingeteilt (Tab. 1 und Tab. 2). Ist der Durchlässigkeitsbeiwert k_f des Sediments bekannt, so lässt sich anhand der Grundwasserspiegelhöhen die Darcy-Geschwindigkeit v_f zwischen zwei Beobachtungsstandorten anhand von Gleichung 3 berechnen. Ist zusätzlich die Ausdehnung des Grundwasserleiters in horizontaler und vertikaler Richtung bekannt (Fläche A in Gleichung 1), kann auch der Volumenstrom Q zwischen den beiden Standrohren aus den Grundwasser-Spiegelhöhen ermitteln werden. Für die Austauschraten zwischen Grundwasser und Oberflächengewässern gilt analog: Ist die Fläche bekannt, an der ein Austausch stattfindet, lassen sich Gesamtvolumina (Q in Gl. 1) für In- und Exfiltration berechnen. Meistens ist jedoch eine Abschätzung der vertikalen Ausdehnung dieser Fläche schwierig.

Die Grundwasserspiegelhöhen werden üblicherweise in Grundwassermessstellen von Hand mithilfe eines Lichtlotes oder automatisch mit Drucksensoren gemessen. Um die Werte in Relation zueinander setzen zu können, müssen sie auf eine definierte Bezugsfläche für Höhenmessungen bezogen werden. Dies ist in Deutschland meistens Meter über Normalnull (NN).

Das Prinzip der hydraulischen Gradienten gilt nicht nur für laterale Flüsse, sondern lässt sich auch auf die Vertikalflüsse anwenden, die den Austausch zwischen Grund- und Oberflächenwässern vor allem in Seen dominieren (Abb. 2, Abschnitt 2.2). Vertikale hydraulische Gradienten (VHG) lassen sich durch im Gewässersediment niedergebrachte Piezometer erfassen. Dabei handelt es sich um am unteren Ende geschlitzte oder perforierte Rohre (meist mit geringem Durchmesser), die manuell oder mit Schlaghammer in das Gewässersediment getrieben werden (s. auch Abschnitt 4.2). Δh ist dabei wiederum die Differenz zwischen der Wasserspiegelhöhe im Piezometer und der Gewässeroberfläche (Abb. 8). Liegt die Grundwasseroberfläche oberhalb des Oberflächenwasser-

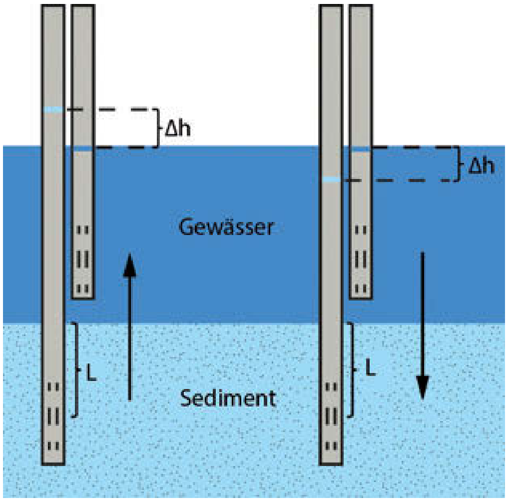

Abb. 8: Ableitung der Richtung des vertikalen Austausches zwischen Grund- und Oberflächenwasser (schwarze Pfeile) anhand von vertikalen hydraulischen Gradienten. Links: Exfiltration; rechts: Infiltration.

spiegels, exfiltriert das Grundwasser in das Oberflächengewässer. Wenn das Grundwasser im Piezometer unterhalb des Oberflächenwassers ansteht, infiltriert Oberflächenwasser in den Grundwasserleiter. Die Fließlänge L entspricht hier der Sedimenttiefe, in der das Piezometer niedergebracht ist, wobei die Filterstrecke nur zur Hälfte einzubeziehen ist (Abb. 8). Die bei bekanntem k_f-Wert resultierende Fließgeschwindigkeit kann dann für eine Fläche A des Gewässergrundes mit gleichem hydraulischem Gradienten extrapoliert werden, um Austauschraten zu quantifizieren. Vertikale hydraulische Gradienten (VHG) sind mit relativ geringem Aufwand und hoher räumlicher Auflösung erfassbar. Bei starkem Wellengang im Gewässer ist es sinnvoll, die Differenz zwischen dem Wasserstand im Piezometer und der Gewässeroberfläche innerhalb eines weiteren Rohres zu messen. Dieses ist ebenfalls mit einem Filter ausgestattet und/oder am unteren Ende offen und lässt sich einfach und schnell am Piezometer anbringen wie in Abbildung 8 angedeutet. Wind und Wellen haben in einem solchen Rohr deutlich weniger Auswirkungen, sodass sich der Wasserstand zuverlässiger bestimmen lässt. Befinden sich die oberen Enden der beiden Rohre auf gleicher Höhe, entspricht die Differenz der Wasserstände unter der Rohroberkante dem Wert für Δh, sodass eine weitere Umrechnung auf eine Bezugsfläche überflüssig wird. Die größte Unsicherheit dieser Methode liegt in der Genauigkeit der k_f-Werte, die vor allem in Bereich der Sediment-Wasser-Grenze innerhalb von wenigen Metern bis Zentimetern um mehrere Größenordnungen variieren können. Wie bereits erwähnt ist außerdem deren Bestimmung ist mit großen Unsicherheiten verbunden. Näherungsweise können k_f-Werte aus Siebkornanalysen abgeleitet werden (HARTGE und HORN 2009). Vielfach werden Pumpversuche und Slug-Tests in Grundwassermessstellen oder Piezometern durchgeführt, um standortspezifische k_f-Werte für Aquifer und Gewässersedimente zu ermitteln. Beim Pumpversuch wird die Auswirkung der Wasserentnahme an einem Standort auf die Wasserstände der Umgebung ausgewertet. Slug-Tests werden dagegen zur Bestimmung lokaler hydraulischer Kenngrößen eingesetzt. Dabei wird der Wasserstand in einer Grundwassermessstelle oder einem Piezometer durch Entnahme abgesenkt und der Zeitraum ausgewertet, innerhalb dessen sich der ursprüngliche Wasserstand wiederherstellt. Auch die Zugabe von Wasser in ein Piezometer ist eine Variante des Slug-Tests. Gewässer, Grundwassermessstellen oder auch die kleineren Piezometer lassen sich einfach mit Datenloggern ausstatten. Das ermöglicht die Erfassung von hydraulischen Gradienten und Austauschraten über lange Zeitreihen hinweg.

3.3 Wasserbilanzverfahren

3.3.1 Wasserhaushalt von Seen

Lassen sich die übrigen Komponenten des Wasserhaushaltes eines Sees (Abb. 9) mit gewisser Sicherheit quantifizieren, ergibt sich die Grundwasserkomponente aus der Summe aller Abflusskomponenten. Die Wasserhaushaltsbilanz eines Sees lautet wie folgt:

$$\begin{aligned}\frac{\Delta V}{\Delta t} \pm R = P + OW_{\mathrm{zu}} + GW_{\mathrm{ex}} \\ - ET - OW_{\mathrm{ab}} - GW_{\mathrm{in}}\end{aligned} \tag{4}$$

mit $\Delta V/\Delta t$ als Änderung des Wasservolumens im See pro Zeitintervall, P als Niederschlag auf die Gewässeroberfläche, der direkt auf die Seefläche fällt, OW_{zu} dem Zustrom aus oberirdischen Zuflüssen (Dränagen, Bäche, Flüsse, etc.), GW_{ex} als grundwasserbürtigem Zustrom (Grundwasserexfiltration), ET als Evaporation von der Seeoberfläche plus Transpiration von emergenten Wasserpflanzen, OW_{ab} als oberirdischem Abstrom aus dem Gewässer und GW_{in} als unterirdischem Abstrom (Grundwasserinfiltration). R repräsentiert den Restterm, also weitere Abflusskomponenten, die z. B. aufgrund ihrer mengenmäßigen Bedeutung nicht berücksichtigt werden. Dies betrifft häufig Oberflächen- und Zwischenabfluss (Interflow). Beide Komponenten sind schwer zu bestimmen, haben allerdings auch oft vernachlässigbar kleine Anteile an der Gesamtbilanz. Gleichung 4 kann für den Nettoterm der Grundwasserkomponente inklusive R aufgelöst werden:

$$\begin{aligned}&GW_{\mathrm{ex}} - GW_{\mathrm{in}} \pm R \\ &= \frac{\Delta V}{\Delta t} + ET + OW_{\mathrm{zu}} - P - OW_{\mathrm{ab}}\end{aligned} \tag{5}$$

Damit liegt die Grundwasserkomponente in der Bilanz lediglich als Nettoterm vor, eine Differenzierung zwischen In- und Exfiltration ist nicht möglich. Ein weiterer Nachteil ist, dass neben den nicht berücksichtigten Abflusskomponenten (R) auch die aufsummierten Fehler aller übrigen Einzelterme der Wasserbilanz in die Grundwasserkomponente einfließen. Dadurch erhöht sich die Unsicherheit in dieser Komponente um ein unbekanntes Maß. Dieser „althergebrachte“ Ansatz ist als erste Näherung zu empfehlen, wenn die übrigen Terme mit entsprechender Sicherheit zu bestimmen sind. Für spezifische Fragestellungen bezüg-

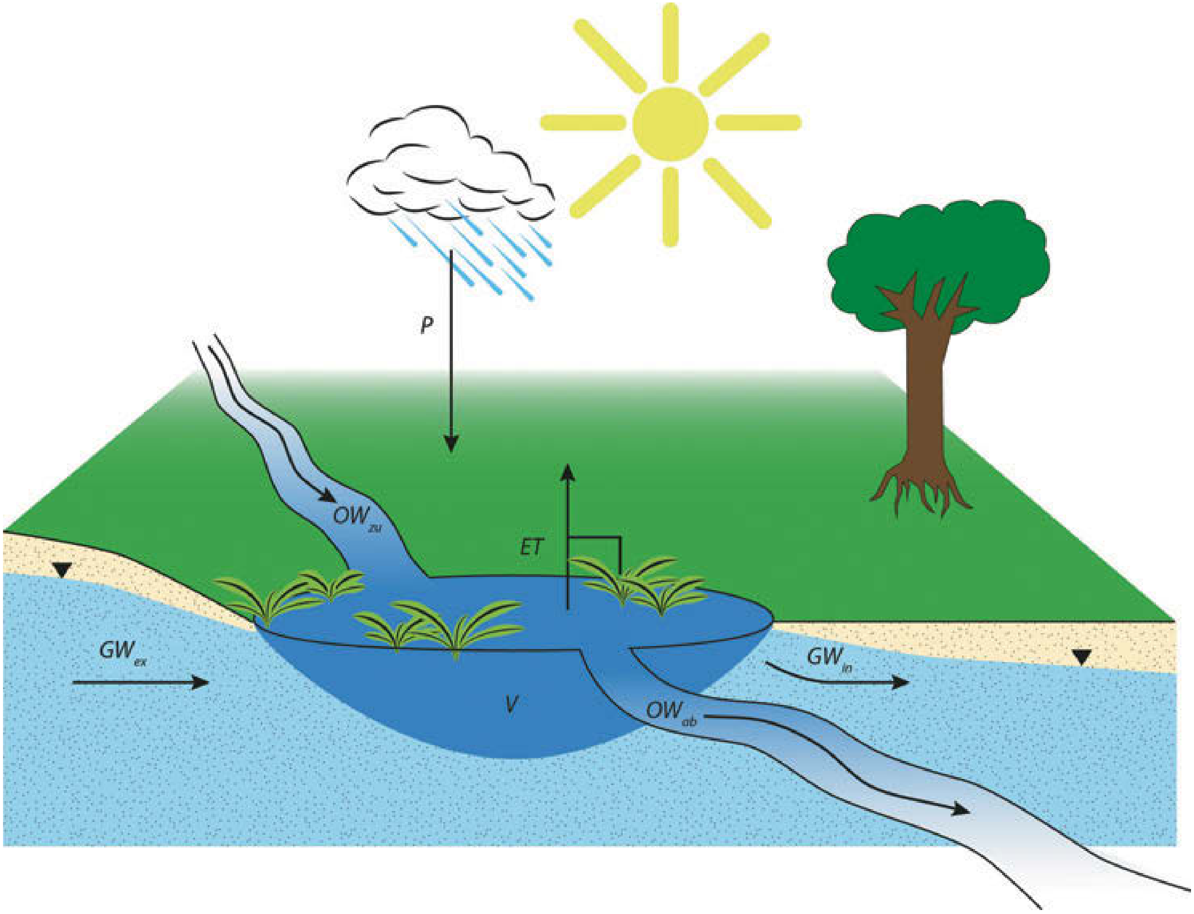

Abb. 9: Wasserhaushalt eines Sees mit den Zuflusstermen Niederschlag auf die Seeoberfläche (*P*) sowie Zustrom durch Oberflächenwasser (OW_{zu}) und Grundwasserexfiltration (GW_{ex}). Verlustterme sind die Evaporation von der freien Wasseroberfläche und die Transpiration von Vegetation (zusammen *ET*), der Abstrom über Oberflächenwasser (OW_{ab}) und die Grundwasserinfiltration (GW_{in}). *V* ist das Seevolumen.

lich des Austausches zwischen See und Grundwasser sollte jedoch auf die weiteren in diesem Beitrag beschriebenen Methoden zurückgegriffen werden.

3.3.2 Abflussdifferenzmessung im Fließgewässer

In einem Fließgewässer lässt sich der Austausch mit dem Grundwasser als Abflussdifferenz zwischen Anfang und Ende einer Messstrecke quantifizieren. Unter der Voraussetzung, dass es innerhalb dieser Messstrecke zu keinen weiteren Zuwächsen des Abflusses (z. B. durch Zusammenflüsse mit anderen Fließgewässern) oder Verlusten (z. B. durch künstliche Entnahmen) kommt, entspricht die Differenz des Abflussvolumens zwischen Anfang und Ende der Messstrecke dem Nettoterm der Grundwasserkomponente (Differenz zwischen GW_{ex} und GW_{in}, s. Gl. 5). Dieser simple Ansatz hat den Nachteil, dass, wie auch bei der Seewasserbilanz, lediglich ein Nettoterm quantifiziert wird, aber keine Differenzierung zwischen Exfiltration und Infiltration vorgenommen werden kann. Bei der Auswahl der Messstrecke ist auf eine ausreichende Länge zu achten, da die Abflussdifferenz größer sein sollte als der zu erwartende Fehler der Abflussmessung. Abflussmessungen im Fließgerinne gelten im Allgemeinen als sehr anfällig für Unsicherheiten. Als vergleichsweise zuverlässig gelten in diesem Zusammenhang Messwehre. Sie lassen sich mit Drucksensoren zur regelmäßigen Wasserstandsmessung ausstatten. Außerdem ist zu beachten: Je größer der Abfluss, desto länger sollte der entsprechende Gewässerabschnitt sein. Bei kleineren, flachen und langsam fließenden Gewässern können die Evaporation von der Wasseroberfläche und die Transpiration durch Wasserpflanzen signifikante Verlustgrößen sein, die gegebenenfalls separat zu quantifizieren sind.

3.3.3 Einzugsgebietsbezogene Grundwasserneubildungsrechnungen

Ausgehend von der Annahme, dass sich ein Gewässer bezüglich seines Wasserhaushaltes im langjährigen Gleichgewicht befindet, entspricht die Menge des pro Zeiteinheit in seinem Einzugsgebiet neugebildeten Grundwassers der Grundwasserexfiltration in das Gewässer. Als Grundwasserneubildung ist der „Zugang von in den Boden infiltriertem Wasser zum Grundwasser“ definiert (Hölting und Coldewey 2009; DIN 4049-3). Das Grundwasser wird überwiegend aus der Versickerung von Niederschlagswasser gespeist. Die Infiltration von Oberflächenwasser in den Grundwasserleitern spielt quantitativ eine untergeordnete Rolle. Im Wesentlichen wird die Grundwasserneubildung durch die Evaporation des Niederschlagswassers von Boden- und Pflanzenoberflächen und die Transpiration der Vegetation gesteuert (*ET* in Gl. 5). Diese Verlustgrößen bestimmen, welcher Anteil des Niederschlags tatsächlich in den Boden infiltriert und als Sickerwasser den Grundwasserkörper erreicht. Höhe und Intensität der Evapotranspiration und damit der Grundwasserneubildung hängen von verschiedenen, interagierenden Faktoren ab (z. B. Länge der Vegetationsperiode, Flächennutzung, Witterungsverhältnisse, Bodensättigung, etc.). Viele Verfahren zur Bestimmung von Grundwasserneubildungsraten beruhen daher auf der überwiegend rechnerischen Bestimmung der Evapotranspiration. Zu nennen sind hier beispielsweise das Bagrov-Verfahren (Bagrov 1953, 1954), das von Glugla et al. (2003) für das Gebiet von Deutschland weiterentwickelt wurde, oder das Verfahren nach Schroeder und Wyrwich (1990). Für diese Verfahren werden teilweise hoch aufgelöste Daten für Standortparameter wie Nutzung, Bodenart, Feldkapazität, Grundwasserflurabstand u. v. m. benötigt. Häufig werden auch meteorologischen Daten einbezogen. Die genannten Ansätze beruhen dabei auf langjährigen Datensätzen und Ergebnissen intensiver Verdunstungsmessungen. Die Verfügbarkeit und die räumliche und zeitliche Auflösung der entsprechenden Eingangsdaten sind häufig limitierend beim Einsatz dieser Methoden.

Die Bestimmung der Grundwasserneubildung wird für das Grundwassereinzugsgebiet eines Gewässers vorgenommen. Das unterirdische Einzugsgebiet stimmt häufig nicht mit dem topografischen Einzugsgebiet überein. Ist die Ausdehnung des Grundwassereinzugsgebietes nicht bekannt, helfen Informationen zu den Grundwasserständen im obersten Grundwasserleiter in der Umgebung des Gewässers weiter. Mithilfe dieser Daten können Grundwassergleichen interpoliert werden, die eine ungefähre Abgrenzung des Grundwassereinzugsgebietes ermöglichen. Die einzugsgebietsbezogene Grundwasserneubildung kann für Fließgewässer auch über die Analyse von Trockenwetterganglinien kalkuliert werden. Diese Methode wird im folgenden Abschnitt beschrieben.

3.4 Ganglinienanalyse und Separation des Basisabflusses bzw. der Grundwasserneubildung

In vielen Oberflächengewässern wird ein Großteil des Abflusses durch exfiltrierendes Grundwasser generiert. Zumindest für Fließgewässer ist die Ableitung von Grundwasserspeichervolumen oder Grundwasserneubildungsraten aus Abflussmessungen daher ein naheliegendes Instrument. Die Anteile der jeweiligen Abflusskomponenten sind jedoch in unterschiedlichen Systemen sehr variabel und dynamischen Prozessen wie Niederschlagsereignissen oder Vegetationsperioden unterlegen. Zur Quantifizierung des grundwasserbürtigen Anteils müssen daher der Basisabfluss, der überwiegend durch Grundwasser gespeist wird, und der Direktabfluss (Oberflächen- und Zwischenabfluss) voneinander separiert werden. Dies geschieht anhand der so genannten Trockenwetterganglinie, die die individuelle Reduktion des Durchflusses (Rezession, Abb. 10) in Perioden ohne abflusswirksame Niederschläge charakterisiert. Trockenwetterganglinien können meist mit Exponentialfunktionen beschrieben werden. Sie basieren auf Zeitreihen von täglichen Durchflüssen am Gewässerquerschnitt und lassen Rückschlüsse auf die Speicher- und Auslauf-

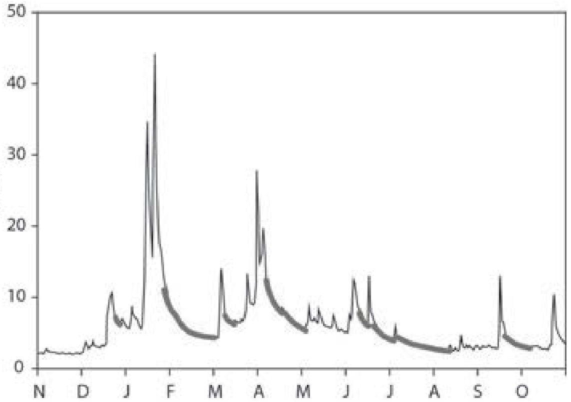

Abb. 10: Beispielhafte Ganglinie täglicher Durchflüsse der Leine (Pegel Göttingen) in einem Wasserwirtschaftsjahr mit typischen Rezessionen (in grau) (Nach DWA, 2013).

eigenschaften des Grundwasserleiters zu. Abweichungen von der Trockenganglinie kommen überwiegend durch ansteigende Durchflüsse nach Niederschlagsereignissen zustande und können dem daraufhin einsetzenden Direktabfluss zugeordnet werden. Die Analyse der typischen Rückgangskurven an einem Gewässerquerschnitt wird heutzutage mithilfe von Modellen durchgeführt. Ihnen zugrunde liegen verschiedene theoretische Ansätze, die die Eigenschaften des Grundwasserspeichers betreffen. Der Ansatz des linearen Speichers geht davon aus, dass der Basisabfluss immer proportional zum Füllungsvolumen des Grundwasserspeichers (Speicherinhalt *S*) ist. Tatsächlich ist diese Beziehung jedoch keineswegs linear, sodass auch nichtlineare Verfahren entwickelt wurden. Eine Zusammenfassung zu den verschiedenen Ansätzen findet sich in DWA (2013).

Mithilfe von Trockenwetterganglinien lässt sich also der grundwasserbürtige Anteil des Gesamtabflusses in einem Zeitintervall berechnen bzw. modellieren. Der Basisabfluss, dessen Volumen mithilfe der Trockenwetterganglinien als Anteil des Gesamtabflusses berechnet werden kann, entspricht der Menge an Grundwasser, die den Grundwasserleiter im Zeitintervall *i* in Richtung des Vorfluters verlässt. Damit ist die einzugsgebietsbezogene, grundwasserbürtige Abflusskomponente in Fließgewässern quantifizierbar. In Abhängigkeit von der Fragestellung kann es jedoch notwendig sein, nicht nur den Basisabfluss im Gewässer selbst, sondern die Grundwasserneubildung (GWN) im Einzugsgebiet zu bestimmen. Dazu muss neben dem Basisabfluss Q_B der Zufluss in den Grundwasserspeicher im Zeitintervall *i* berücksichtigt werden:

$$GWN_i = S_i - S_{i-1} + \int_{i-1}^{i} Q_B \, \Delta t \tag{6}$$

mit *S* als Speicherinhalt zu Beginn und am Ende des Zeitintervalls *i* und $\int Qe \, \Delta t$ als Volumen des Basisabflusses im selben Zeitintervall *i*. Unter Umständen sind außerdem zusätzliche Verluste (z. B. durch Verdunstung oder Grundwasserentnahmen) zu berücksichtigen. Unter der Annahme eines linearen Speichers ergibt sich eine proportionale Beziehung zwischen *S* und Q_B folgendermaßen:

$$S = k \cdot Q_B \tag{7}$$

k repräsentiert die durchschnittliche Zeit, die das Wasser nach der Versickerung im Grundwasserspeicher verbleibt. Der Wert ergibt sich aus der Trockenwetterganglinie eines linearen Speichers, die der folgenden Exponentialfunktion entspricht:

$$Q_{Bt} = Q_{Bt-\Delta t} \cdot e^{\frac{-\Delta t}{k}} \tag{8}$$

mit $Q_{Bt-\Delta t}$ als Basisabfluss zu Beginn und Q_{Bt} als aktuellem Basisabfluss in einer Zeitspanne *t* ohne abflusswirksame Niederschlagsereignisse.

Wie oben beschrieben, ist der Zusammenhang zwischen Grundwasser und Fließgewässern in Form des Abflussvolumens messbar und teilweise sogar sichtbar. Für Seen gilt dies meistens nicht. Die vergleichsweise langen Verweilzeiten des Wassers in Seen sowie das Verhältnis von Seewasservolumen zu Exfiltrationsvolumen vermindern die Reaktion auf Abflussereignisse, vor allem, wenn das Grundwasser nur einen geringen Anteil an der Wasserbilanz des Sees hat. Das oben beschriebene Verfahren der Separation der Trockenwetterganglinien lässt sich daher nicht für Seen anwenden. Allerdings kann es auf Grundwasserganglinien in Einzugsgebieten von Seen (und Fließgewässern) übertragen werden. Aus Abweichungen von Rezessionslinien des Grundwasserstandes kann die Grundwasserneubildung für einen Standort abgeleitet werden. Sie entspricht dem Direktabfluss im Fließgewässer, der in der Abflussganglinie als Abweichung zur Trockenwetterganglinie zum Ausdruck kommt. Die anhand der Grundwasserstände eines einzelnen Standortes abgeleitete Grundwasserneubildungsrate resultiert aus den örtlichen Bedingungen, wie zum Beispiel Boden- und Substrateigenschaften, Vegetationsbedeckung und Grundwasserflurabstand. Sie lassen sich daher, wie üblich bei Punktmessungen, in den wenigsten Fällen auf ein gesamtes Einzugsgebiet übertragen. Stattdessen sollten die Daten möglichst vieler Grundwasserbeobachtungsstellen im Einzugsgebiet für eine Ganglinienanalyse herangezogen werden. Bei der Auswahl der Beobachtungsstellen ist Folgendes zu beachten:

- Die Messstelle muss im obersten, ungespannten Grundwasserleiter verfiltert sein, da Stauschichten eine repräsentative Reaktion der Grundwasseroberfläche verhindern.
- Generell sollten Standorte gewählt werden, deren Grundwasserflurabstand ausreichend groß ist, um nicht durch Evaporation oder Transpiration beeinflusst zu werden. Nur so lassen sich die beobachteten Grundwasserschwankungen ausschließlich auf Änderungen im Speicherinhalt *S* (s. Gl. 6) zurückführen.
- Die Lage der Beobachtungsstelle sollte zudem weit genug von der Vorflut entfernt sein, da es im Austauschbereich kurzfristige hydraulische Interaktio-

nen zwischen den Systemen gibt, die die Grundwasserneubildungsprozesse überlagern können.

- Bei sehr tiefen Beobachtungsstellen ist zu beachten, dass die Grundwasserneubildung zeitlich verzögert ist, sodass eine eindeutige Zuordnung zum auslösenden Ereignis unter Umständen schwierig ist.

3.5 Natürliche Tracer

Da sich Grund- und Oberflächenwässer in einigen Parametern (z. B. bestimmten Wasserinhaltsstoffen) grundlegend unterscheiden, können diese als natürliche Tracer verwendet werden. Ein solcher Tracer sollte möglichst konservativ sein, damit es im Verlaufe des Transports durch den Grundwasserleiter nicht zu einer signifikanten Modifikation durch chemische, physikalische oder biologische Prozesse kommt. Im Folgenden werden einige Methoden zu diesem Thema vorgestellt. Ein besonderer Fokus liegt dabei auf der Nutzung von Temperatur bzw. Wärme als Tracer für Grundwasser-Oberflächenwasser-Interaktionen, weil dieser Parameter in der Forschung besonders intensiv genutzt wird (Abschnitt 3.5.3).

3.5.1 Stabile Isotope von Sauerstoff und Wasserstoff

Stabile Isotope von Wasser (^{1}H und ^{2}H – Deuterium –, sowie ^{16}O, ^{17}O und ^{18}O) können genutzt werden, um Grundwasser-Oberflächenwasser-Interaktionen zu untersuchen. Verschiedene physikalische Prozesse führen zur Isotopenfraktionierung, die in spezifischen Verhältnissen von schweren zu leichten Isotopen resultiert. Eine solche Isotopenfraktionierung ergibt sich beispielsweise aus dem Mehrbedarf an Energie bei der Verdunstung isotopisch schwererer Wassermoleküle im Vergleich zu leichteren. Die Verdunstung führt zu einer Abreicherung an isotopisch leichten Wassermolekülen in Oberflächengewässern im Vergleich zum Grundwasser. Dieser Umstand kann sowohl zur qualitativen als auch zur quantitativen Abschätzung von Grundwasser-Oberflächenwasser-Interaktionen genutzt werden. So kann eine Differenzierung von In- und Exfiltrationsbereichen anhand der Isotopensignatur des ufernahen Grundwassers im Vergleich zum Seewasser erfolgen. Abbildung 11 zeigt die Isotopensignaturen des Sauerstoffs im oberflächennahen Grundwasser rund um einen See (Arendsee, Sachsen-

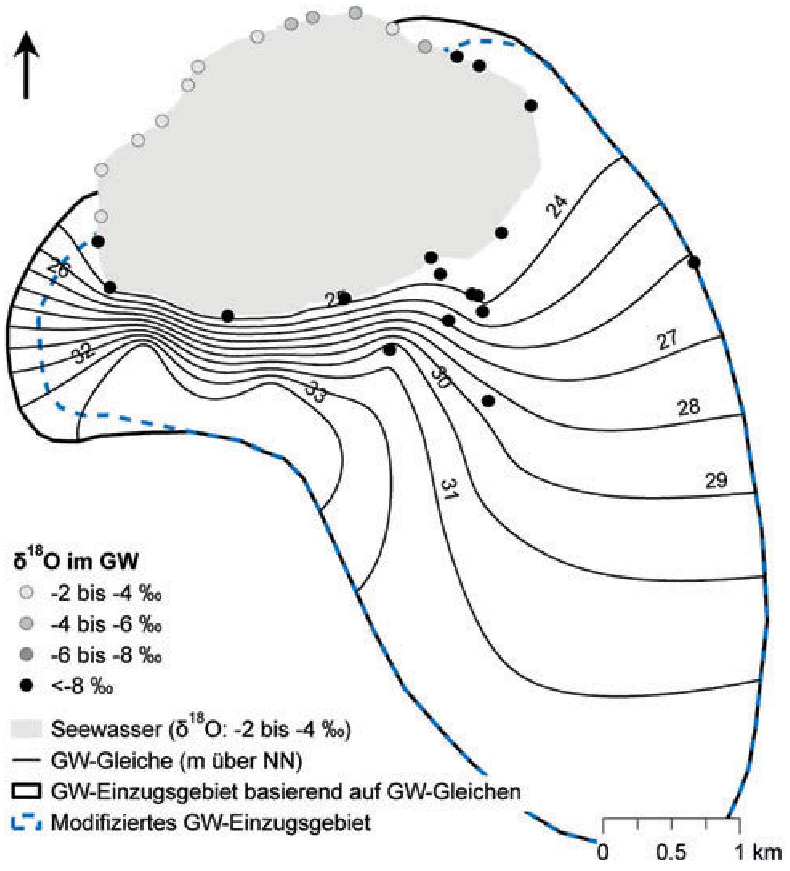

Abb. 11:
Nutzung von stabilen Isotopen des Sauerstoffs im ufernahen Grundwasser zur Validierung der In- und Exfiltrationsbereiche am Arendsee (Sachsen-Anhalt). Die Farbskala der Punkte ist als Ähnlichkeit der Isotopensignatur des Grundwassers mit derjenigen des Seewassers zu interpretieren (hellgrau: große Ähnlichkeit, schwarz: geringe Ähnlichkeit). Die Ergebnisse bestätigen im Wesentlichen die Abgrenzung der In- und Exfiltrationsbereiche, die auf der Grundlage von Grundwassergleichen (schwarze Linien) vorgenommen wurde.

Anhalt) sowie in einigen Grundwassermessstellen im Einzugsgebiet. Die spezifische Isotopensignatur einer Probe wird als Abweichung (δ) des Verhältnisses des schwereren zum leichteren Isotop vom Vienna Standard Mean Ocean Water (VSMOW) angegeben. Der Wert δ bezieht sich immer auf das schwerere Isotop und ergibt für Sauerstoff:

$$\delta^{18}\mathrm{O} = \frac{\left(\frac{^{18}O}{^{16}O}\right)_{\mathrm{Probe}} - \left(\frac{^{18}O}{^{16}O}\right)_{\mathrm{VSMOW}}}{\left(\frac{^{18}O}{^{16}O}\right)_{\mathrm{VSMOW}}} \cdot 1000\ ‰ \tag{9}$$

Für Wasserstoff gilt entsprechend:

$$\delta\mathrm{D} = \frac{\left(\frac{D}{^{1}H}\right)_{\mathrm{Probe}} - \left(\frac{D}{^{1}H}\right)_{\mathrm{VSMOW}}}{\left(\frac{D}{^{1}H}\right)_{\mathrm{VSMOW}}} \cdot 1000\ ‰ \tag{10}$$

Am Arendsee wurde das Grundwassereinzugsgebiet anhand von Grundwassergleichen bestimmt (Abb. 11). Die Isotopensignaturen des Grundwassers im Uferbereich weisen eine deutliche Differenzierung auf und bestätigen die räumliche Abgrenzung von In- und Exfiltrationsbereichen. Während die Proben im Exfiltrationsbereich ähnliche Signaturen wie das Grundwasser im Einzugsgebiet aufweisen, sind die Signaturen des Infiltrationsbereiches denjenigen des Seewassers ähnlicher. Das infiltrierende Seewasser prägt dort die Isotopenverhältnisse des ufernahen Grundwassers. Mit diesem Ergebnis konnte die Abgrenzung des Einzugsgebietes auf der Grundlage der Grundwassergleichen im Wesentlichen bestätigt und optimiert werden (Abb. 11, blaue gestrichelte Linie).

Mithilfe einer einfachen Mischungsrechnung lässt sich der Anteil des Grundwassers an der Wasserbilanz eines Sees auf der Grundlage der Isotopensignaturen aller beteiligten Komponenten quantifizieren. Für einen See, der sich bezüglich seines Wasserhaushaltes und der Isotopensignaturen in einem Steady State befindet, gilt:

$$\begin{aligned} 0 = {} & \delta_{\mathrm{P}} P + \delta_{\mathrm{GW_{ex}}} GW_{\mathrm{ex}} + \delta_{\mathrm{OW_{zu}}} OW_{\mathrm{zu}} - \delta_{\mathrm{E}} E \\ & - \delta_{\mathrm{GW_{in}}} GW_{\mathrm{in}} - \delta_{\mathrm{OW_{ab}}} OW_{\mathrm{ab}} \end{aligned} \tag{11}$$

mit den Volumina des Niederschlags P, der Grundwasserexfiltration GW_{ex} und des oberirdischen Zuflusses OW_{zu} auf der Habenseite und den Volumina der Evaporation E von der Gewässeroberfläche, der Grundwasserinfiltration GW_{in} und des oberirdischen Abflusses OW_{ab} aus dem Gewässer auf der Verlustseite. δ entspricht der Isotopensignatur der jeweiligen Komponente der Wasserbilanz (s. Gl. 9 und Gl. 10). Außerdem wird die Isotopensignatur des Seewassers (δ_{See}) benötigt. Als Resultat der Mischung aller Zuflusskomponenten und der weiteren Fraktionierung des Seewassers durch die Evaporation ist sie wesentlicher Bestandteil der folgenden Mischungsrechnung:

$$\begin{aligned} & \delta_{\mathrm{P}} P + \delta_{\mathrm{GW_{ex}}} GW_{\mathrm{ex}} + \delta_{\mathrm{OW_{zu}}} OW_{\mathrm{zu}} - \delta_{\mathrm{E}} E \\ & = (P + GW_{\mathrm{ex}} + OW_{\mathrm{zu}} - E) \cdot \delta_{\mathrm{See}} \end{aligned} \tag{12}$$

Die Isotopensignaturen der Abstromkomponenten aus dem See (GW_{in} und OW_{ab}) haben keinen Einfluss auf diejenige des Seewassers. Vielmehr entsprechen sie eben jener und sind daher in der Mischungsrechnung (Gl. 12) nicht mehr von Bedeutung. Aus Gleichung 12 ergibt sich nach Umstellung:

$$\begin{aligned} & GW_{\mathrm{ex}} \\ & = \frac{P(\delta_{\mathrm{See}} - \delta_{\mathrm{P}}) + OW_{\mathrm{zu}}(\delta_{\mathrm{See}} - \delta_{\mathrm{OW_{zu}}}) - E(\delta_{\mathrm{See}} - \delta_{\mathrm{E}})}{(\delta_{\mathrm{GW_{ex}}} - \delta_{\mathrm{See}})} \end{aligned} \tag{13}$$

Außer δ_E lassen sich die Terme in Gleichung 13 relativ leicht erfassen. Die Berechnung von δ_{E} erfolgt nach CRAIG und GORDON (1965, s. auch KENDALL und MCDONNELL 2003). Bei Gewässern ohne oberirdische Zuflüsse entfällt der entsprechende Term in Gleichung 13. Bei Fließgewässern ist eine hohe Dynamik der Isotopensignaturen zu erwarten, da auch hier verschiedene Abflusskomponenten zusammenkommen, die individuell auf saisonale und witterungsbedingte Schwankungen reagieren. Die damit verbundene Unsicherheit reduziert die Zuverlässigkeit der Methode auf überwiegend grundwassergespeiste Gewässer. Auch bezogen auf die anderen Komponenten der Wasserbilanz ist zu berücksichtigen, dass ihre Isotopensignaturen saisonal schwanken können, z. B. aufgrund verringerter Verdunstungsraten im Winter. Diese Prozesse können jedoch auch zur Erfassung saisonaler Unterschiede von Grundwasser-Oberflächenwasser-Interaktionen genutzt werden.

Traditionell werden Isotope massenspektrometisch gemessen, was sehr aufwendig und vergleichsweise teuer ist. Vor wenigen Jahren ist die Cavity-Ring-Down-Spektroskopie auf den Markt gekommen (BERDEN et al. 2000). Damit können die Messungen mit wesentlich geringerem Aufwand durchgeführt werden (MUNKSGAARD et al. 2011).

3.5.2 Radon

In den letzten Jahren sind vermehrt Radonbilanzen zur Quantifizierung des Grundwasserzustroms in Oberflächengewässer herangezogen worden. Radon ist ein radioaktives Element, das zu den reaktionsträgen Edelgasen gehört. Es existieren verschiedene Radonisotope, von denen ^{222}Rn das stabilste ist. ^{222}Rn (im folgenden Rn) hat eine Halbwertszeit von 3,8 Tagen und entsteht als Zerfallsprodukt aus Radium (^{226}Ra) in der natürlichen Zerfallsreihe von Uran (^{238}U). ^{238}U ist natürlicher Bestandteil vieler Gesteine und Sedimente und unterliegt als solches entsprechenden Verwitterungsprozessen. In deren Verlauf gelangt Rn in das Grundwasser und die Bodenluft, bevor es in die Atmosphäre ausgast oder zu Polonium (^{218}Po) zerfällt. Grundwasser ist daher mit Rn angereichert. Neu gebildetes Grundwasser reichert sich innerhalb von 15 Tagen mit Rn an (Hoehn und Vongunten 1989). In Oberflächengewässern sind die Rn-Konzentrationen üblicherweise gering, weil es über die Wasseroberfläche ausgast oder zerfällt. Die Neuproduktion von Rn aus dem Zerfall von ^{226}Ra im Freiwasser kann diese Verluste nicht aufwiegen.

Rn-Konzentrationen werden in der Einheit Becquerel (Bq) angegeben. Bq ist ein Maß für die Aktivität einer bestimmten Menge einer radioaktiven Substanz (Aktivitätskonzentration). Sie entspricht der mittlere Anzahl an Atomkernen, die innerhalb von einer Sekunde radioaktiv zerfallen (1 Bq = 1 s^{-1}). Die Aktivitätskonzentration wird meistens auf ein Volumen bezogen (z. B. Bq l^{-1} oder Bq m^{-3}). Im Grundwasser liegt die Aktivitätskonzentration von Rn in Abhängigkeit von den geologischen Bedingungen zwischen 1000 und 100 000 Bq m^{-3}, während sie im Oberflächenwasser um mehrere Größenordnungen darunter liegt (1–100 Bq m^{-3}). Dieser Unterschied macht Rn zu einem attraktiven Tracer für Grundwasser-Oberflächenwasser-Interaktionen, obwohl die Analytik vergleichsweise aufwendig ist (Kluge et al. 2007).

Bei der Messung von Rn in Flüssigkeiten ist größte Behutsamkeit schon während der Probenahme notwendig. Da die Gasphase gemessen wird, sollte jegliche Ausgasung und Blasenbildung während und nach der Probenahme vermieden werden. Aufgrund der geringen Halbwertszeit ist außerdem eine zügige Messung nach der Probenahme geboten. Die Wasserprobe wird während der Messung mit Reinluft begast, sodass das Radon ausgetrieben wird. Es wird in ein Kreissystem geleitet, in dem ein Detektor zur Erfassung der Rn-Konzentration zwischengeschaltet ist. Das Prinzip der Messung beruht auf der Zählung der radioaktiven Zerfallsprozesse. Dabei wird das Kreislaufsystem so lange mit Probenmaterial beschickt, bis sich eine gleichmäßige Anzahl an Zerfallsprozessen einstellt. Bei den relativ hohen Rn-Konzentrationen im Grundwasser werden nur entsprechend geringe Probenvolumina (ca. 250 ml) benötigt. Im Oberflächenwasser sind die Konzentrationen dagegen so gering, dass zur Etablierung eines Gleichgewichts im Kreislauf große Probenmengen notwendig sind und der konstante Nachschub unter Umständen direkt aus dem Gewässer in das System gepumpt werden muss.

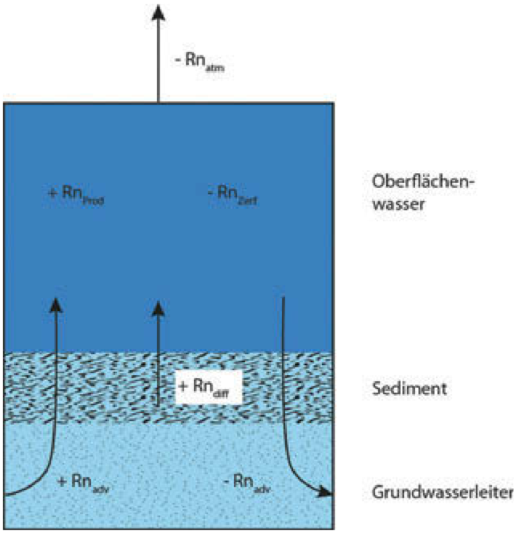

Abb. 12: Box-Modell der Radonbilanz eines Gewässers mit den Termen $\mathrm{Rn}_{\mathrm{adv}}$ (advektiver Zutritt bzw. Abstrom mit dem Grundwasser), $\mathrm{Rn}_{\mathrm{diff}}$ (diffusiver Zutritt aus dem Gewässersediment) und $\mathrm{Rn}_{\mathrm{Prod}}$ (Zuwachs aus dem Zerfall von ^{226}Ra) sowie den Verlusttermen $\mathrm{Rn}_{\mathrm{Zerf}}$ (Zerfall von Rn) und $\mathrm{Rn}_{\mathrm{atm}}$ (Ausgasung von der Gewässeroberfläche in die Atmosphäre).

Häufige Fehlerquelle während der Messung ist eine zu hohe Luftfeuchtigkeit im Kreislaufsystem. Daher sind Trocknungseinheiten in das System eingebettet, die der Luft die Feuchtigkeit entziehen, bevor die Messung erfolgt. Für die Messung von Rn wird häufig das Messgerät RAD7 der Firma Durridge verwendet.

Die Radon-Bilanz eines rein grundwassergespeisten, gut durchmischten Sees lautet (z. B. Tuccimei et al. 2005 und Kluge et al. 2007; Abb. 12):

$$\mathrm{Rn}_{\mathrm{adv}} + \mathrm{Rn}_{\mathrm{diff}} + \mathrm{Rn}_{\mathrm{Prod}} - \mathrm{Rn}_{\mathrm{Zerf}} - \mathrm{Rn}_{\mathrm{atm}} = 0 \tag{14}$$

Gleichung 14 gilt unter der Voraussetzung, dass Grundwasserexfiltration und -infiltration gleich groß sind, d. h. keine Verluste durch Evaporation auftreten (Niederschlag = Evaporation). In dem Fall repräsentiert $\mathrm{Rn}_{\mathrm{adv}}$ den advektiven Zutritt und Verlust von Rn mit dem Grundwasser und ergibt sich aus dem

Volumen der Grundwasserex- bzw. -infiltration (Q, in m^{-3}) und der Rn-Aktivitätskonzentration des Grundwassers (C_{GW}) und derjenigen des Oberflächenwassers (C_{OW}, beide in Bq m^{-3}; Abb. 12):

$$\mathrm{Rn}_{\mathrm{adv}} = Q \cdot (C_{\mathrm{GW}} - C_{\mathrm{OW}}) \tag{15}$$

Neben dem advektiven Transport kommt es zu einem diffusiven Zutritt von Rn aus dem Gewässersediment in die Wassersäule ($\mathrm{Rn}_{\mathrm{diff}}$). Dieser Term beinhaltet einerseits den diffusiven Fluss des zum Zeitpunkt der Probenahme im Sediment vorhandenen Radons und andererseits den Fluss, der sich aus dem Zerfall von $^{226}\mathrm{Ra}$ im Sediment ergibt. Rn_{diff} wird empirisch anhand von Gleichgewichtsexperimenten mit dem Gewässersediment bestimmt. Methodische Ansätze dazu sind beispielsweise bei Corbett et al. (1997), Corbett et al. (1998), Corbett et al. (2000) oder Martens et al. (1980) zu finden. Andere Studien berücksichtigen den diffusen Fluss von Rn aus dem Gewässersediment nicht und betrachten die anhand dieser Methode ermittelten Grundwasserexfiltrationsraten als Maximalwerte (Kluge et al. 2007).

Im Freiwasser zerfällt Rn zu $^{218}\mathrm{Po}$ (Rn_{Zerf}), was anhand der Rn-Aktivitätskonzentration im Oberflächenwasser (C_{OW}, Bq m^{-3}), der Rn-Zerfallskonstante (λ_{Rn}, 0,181 d^{-1}) und dem Seevolumen V (m^3) zu quantifizieren ist:

$$\mathrm{Rn}_{\mathrm{Zerf}} = C_{\mathrm{OW}} \cdot \lambda_{\mathrm{Rn}} \cdot V \tag{16}$$

Durch den Zerfall von $^{226}\mathrm{Ra}$ im Freiwasser kommt es wiederum zu einem Zuwachs von Rn ($\mathrm{Rn}_{\mathrm{prod}}$), der sich Gleichung 16 entsprechend auf der Grundlage der $^{226}\mathrm{Ra}$-Konzentration des Oberflächenwassers (C_{Ra}, Bq m^{-3}) ergibt:

$$\mathrm{Rn}_{\mathrm{prod}} = C_{\mathrm{Ra}} \cdot \lambda_{\mathrm{Rn}} \cdot V \tag{17}$$

C_{Ra} lässt sich durch eine Rn-Messung des Seewassers nach etwa vier Wochen Lagerungszeit ermitteln. Nach dieser Zeit ist der Anteil der Seewasser-Rn-Konzentration aus Rn_{adv} vernachlässigbar gering, sodass der gemessene Wert der Rn-Produktion aus dem Zerfall von $^{226}\mathrm{Ra}$ entspricht.

Weiterhin kommt es zu einem diffusiven Verlust von Rn aus dem Oberflächenwasser durch Ausgasung in die Atmosphäre (Rn_{atm}). Dieser Term ist nicht ohne Weiteres bestimmbar. Neben den Rn-Aktivitätskonzentrationen des Freiwassers (C_{OW}) und der Luft (C_{atm}) wird auch ein Wert für die Rn-Transfergeschwindigkeit an der Wasser-Luft-Grenze k (in m min^{-1}) benötigt:

$$\mathrm{Rn}_{\mathrm{atm}} = k(C_{\mathrm{OW}} - \alpha C_{\mathrm{atm}}) \tag{18}$$

α ist der dimensionslose Ostwald-Koeffizient (Löslichkeitskoeffizient). k hängt neben der Viskosität des Wassers und dem Diffusionskoeffizienten von Rn in Wasser maßgeblich von der Turbulenz an der Wasseroberfläche ab. In Stillgewässern ist diese überwiegend von der Windgeschwindigkeit abhängig. Informationen zur Ableitung der windgetriebenen Gas-Transfergeschwindigkeit k finden sich beispielsweise bei MacIntyre et al. (1995), Dulaiova und Burnett (2006) oder Burnett et al. (2007).

Sind alle weiteren Terme bestimmt, ergibt sich aus Gleichung 14 für Rn_{adv}:

$$\mathrm{Rn}_{\mathrm{adv}} = \mathrm{Rn}_{\mathrm{Zerf}} + \mathrm{Rn}_{\mathrm{atm}} - \mathrm{Rn}_{\mathrm{diff}} - \mathrm{Rn}_{\mathrm{Prod}} \tag{19}$$

Auf dieser Grundlage lässt sich unter Einbezug der Rn-Aktivitätskonzentration des Grundwassers (C_{GW}) und des Oberflächenwassers (C_{OW}) das Volumen von Grundwasserex- und -infiltration (Q) durch Umstellen von Gleichung 15 berechnen:

$$Q = \mathrm{Rn}_{\mathrm{adv}} \cdot (C_{\mathrm{GW}} - C_{\mathrm{OW}})^{-1} \tag{20}$$

Vorsicht ist geboten, wenn der Wasserverlust durch Evaporation größer ist als die Niederschlagsmenge. Dadurch kann es zu einer signifikanten Aufkonzentration von Rn im Oberflächenwasser kommen (Atkinson et al. 2015; Cartwright und Gilfedder 2015). In diesem Fall reduziert sich die Grundwasserinfiltration (GW_{in}) um die Differenz zwischen Niederschlag und Evaporation. Zusätzlich ist die Aktivitätskonzentration des Oberflächenwassers C_{OW} nicht mehr repräsentativ für den Verlust von Rn über abströmendes Grundwasser.

Neben den genannten Termen sind weitere potenzielle Rn-Zuwachs- oder Verlustterme, wie z. B. der künstliche Entzug von Oberflächenwasser oder oberirdische Zu- und Abläufe über Flüsse oder Gräben, ebenfalls in Gleichung 14 bzw. Gleichung 19 zu berücksichtigen.

Für Fließgewässer lassen sich Gleichung 14 bzw. Gleichung 19 auf einzelne Gewässerabschnitte anwenden. Zu beachten ist, dass, anders als bei Seen, die Turbulenz an der Gewässeroberfläche weniger windabhängig ist, sondern überwiegend von Fließgeschwindigkeit und Gewässertiefe kontrolliert wird (Atkinson et al. 2015). Dementsprechend unterscheiden sich die Ableitungen von k für Seen und Fließgewässer. Beispiele und Literatur zur Bestimmung von k in Fließgewässern werden u. a. bei Atkinson et al. (2015) genannt. Die Bestimmung von k wird von einigen Autoren als die größte Unsicherheit bei der

Rn-Bilanzierung in Fließgewässern gehalten (Cook et al. 2006).

Rn als Tracer für Grundwasser-Oberflächenwasser-Interaktionen ist ein vielversprechender Ansatz. Probenahme und Analytik der einzelnen Komponenten der Rn-Bilanz sind jedoch aufwendig und fehleranfällig, sodass Kosten und Nutzen bei der Planung derartiger Untersuchungen mit Umsicht abgewogen werden sollten. Gute Erfolge wurden mit der Lokalisierung von Hotspots des Grundwasserzustroms durch Rn-Messungen am Gewässergrund gemacht. Lokal erhöhte Rn-Aktivitätskonzentrationen deuten auf verstärkte Grundwasserexfiltration hin, wobei auch der diffuse Rn-Fluss aus dem Sediment (Rn_{diff}) ursächlich dafür sein kann (Kluge et al. 2007). Die Ergebnisse solcher Analysen können als Ausgangspunkt für weitere Untersuchungen dienen.

3.5.3 Wärme als Tracer

Unter bestimmten Voraussetzungen lassen die Temperaturunterschiede zwischen Grund- und Oberflächenwasser eine Quantifizierung von Austauschraten zu. Während die Temperaturen des Grundwassers im Jahresverlauf nur wenig schwanken, ist Oberflächenwasser im Winter häufig deutlich kälter bzw. im Sommer deutlich wärmer als das zuströmende Grundwasser. Die Untersuchung von Temperaturen an und in der Grenzzone zwischen Grund- und Oberflächenwasser ermöglicht nicht nur die Erfassung von räumlichen Mustern des Austausches, sondern auch die Kalkulation von Austauschraten. Voraussetzung dafür ist eine ausreichend große Differenz der Temperaturen zwischen den beiden Systemen. Untersuchungen dazu finden deshalb überwiegend in den Sommer- oder Wintermonaten statt. Entsprechende Methoden werden im Folgenden vorgestellt.

Faseroptische Temperaturmessung

Zur Lokalisation von Grundwasserexfiltration in Seen und Flüssen wird zunehmend die faseroptische Temperaturmessung (engl. *fibre-optic distributed temperature sensing*, FO-DTS) genutzt. Wird eine Glasfaser mit Laserimpulsen beschickt, werden verschiedene Signale zurückgestreut. Eines dieser Rückstreusignale (Raman-Antistokes) ist temperaturabhängig, sodass mit der Erfassung des rückgestreuten Raman-Signals und der Laufzeit des Lichtes Temperaturänderungen entlang der Glasfaser erkannt und lokalisiert werden können. Entsprechende Glasfaserkabel werden entlang des Gewässerbodens ausgelegt. Mit einer räumlichen Auflösung von mehreren Metern bis wenigen Dezimetern werden die Temperaturen entlang des Kabels erfasst. Abweichungen von der Temperatur des überstehenden Wassers deuten auf den Zutritt von kühlerem oder wärmerem Grundwasser hin. Das Ergebnis der Messung sind die Temperaturen entlang des Kabels in der zuvor gewählten räumlichen Auflösung (z. B. ein Meter). Auf diese Weise können über mehrere hundert Meter räumlich hoch aufgelöst Standorte mit verstärkter Grundwasserexfiltration lokalisiert werden (Abb. 13). Das Verfahren visualisiert also die Muster des Grundwasserzustroms und eignet sich besonders für

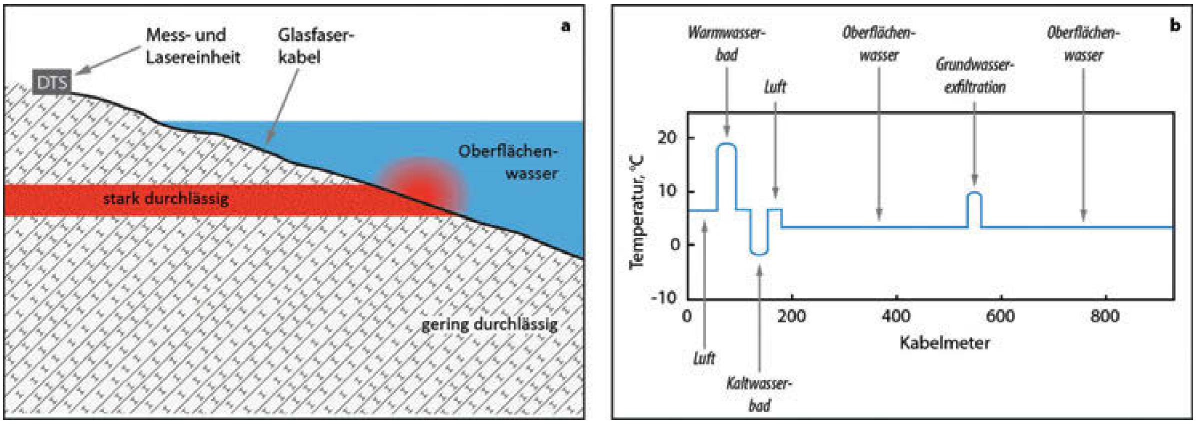

Abb. 13: Lokalisierung von Standorten mit verstärkter Grundwasserexfiltration anhand faseroptischer Temperaturmessungen (*fiber-optic distributed temperature sensing*, FO-DTS). a) Wärmeres (oder kälteres) Grundwasser, das beispielsweise aufgrund lokal höherer Durchlässigkeit des Grundwasserleiters verstärkt exfiltriert, verursacht beim Eintritt in den See eine lokale Erwärmung (oder Abkühlung) am Gewässergrund. b) Schematisches Beispiel für das Ergebnis einer DTS-Messung in einem gut durchmischten See (ca. 4 °C) mit punktueller Exfiltration von wärmerem Grundwasser.

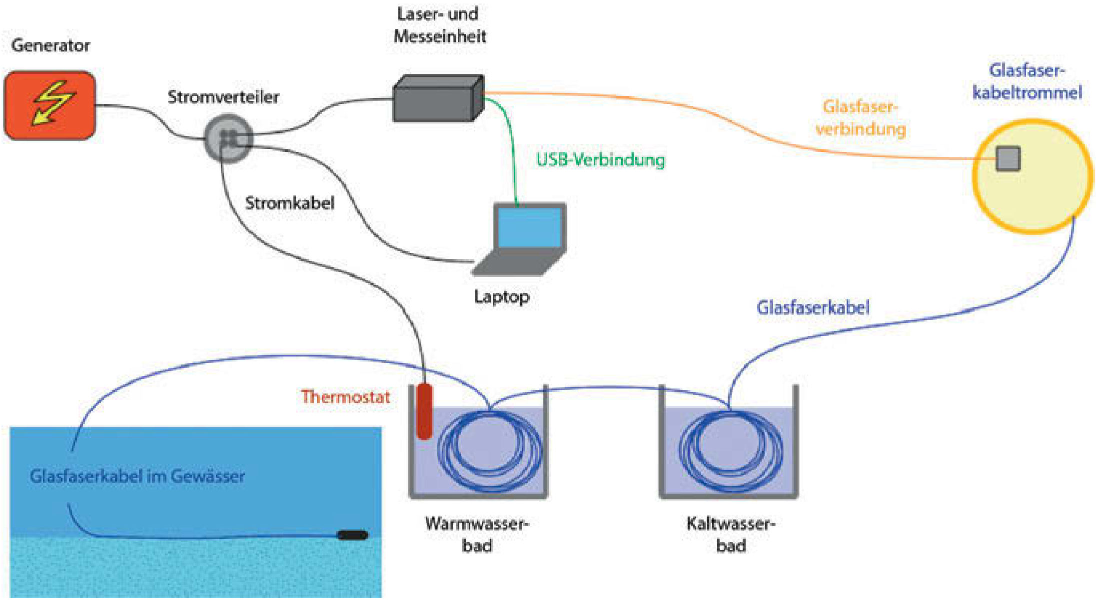

Abb. 14: Schematisches Beispiel für den Aufbau von DTS-Messungen im Gewässer.

die Detektion lokaler Grundwasserzutritte. Die Anwendung zur Erfassung von diffusen Flüssen hat sich dagegen in der Praxis bisher kaum bewährt, da ein großflächiger Zustrom kein eindeutiges Temperatursignal bewirkt. In ausgesprochen homogenen Systemen ist es möglich, das DTS-Signal mit einigen Punktmessungen zu kalibrieren und dann aus dem beobachteten Muster der Temperaturverteilung die lokalen Exfiltrationsraten zu berechnen (Blume et al. 2013).

Der Aufbau einer DTS-Messung besteht im Wesentlichen aus dem DTS-Kabel, der Mess- und Lasereinheit, unter Umständen dem damit verbundenen Computer und einer externen Stromquelle (Abb. 14). Am Kabelende ist die Glasfaser entweder terminiert oder wird umgebogen und mit einer weiteren Faser verspleißt, sodass das Signal wieder zurückgeführt wird. Neben der Glasfaser ist das DTS-Kabel meist mit weiteren Fasern und Materialien zu deren Schutz ausgestattet, da Glasfasern sehr anfällig für Beschädigungen sind. In flachen Gewässern ist es oft möglich, das DTS-Kabel mit Steinen oder Bodenankern manuell zu befestigen. DTS-Kabel, die speziell für Untersuchungen in tieferen Gewässern hergestellt werden, sind mittlerweile zusätzlich mit einem Metalldraht (z. B. aus Kupfer) ausgerüstet, um das Kabel zu beschweren und ein gleichmäßiges Absinken auf die Sedimentoberfläche zu gewährleisten. Das Ausbringen des Kabels in tieferen Gewässern erfolgt am besten vom Boot aus. Bei schwierigen Bedingungen kann es notwendig sein, das Kabel von Tauchern auslegen zu lassen.

Um die Ergebnisse später räumlich zuordnen zu können, ist es sinnvoll, die abgefahrene Route mit einem GPS zu verfolgen. Die Verortung der Ergebnisse kann in der Praxis schwierig sein. Durch Wind und Wellen können Kabel und Boot ungleichmäßig verdriftet werden, was die spätere Georeferenzierung der Ergebnisse erschwert. Günstig ist es, markante Standorte in das Kabeltransekt einzubeziehen, an denen (evtl. auch erst nach dem Verlegen des Kabels) Koordinaten und zugehörige Kabelmeter zuverlässig erfasst werden können.

Die Messungen werden üblicherweise über einen längeren Zeitraum durchgeführt. Gerätebedingt unterliegen die Ergebnisse über den Zeitraum einer Messung einer gewissen Drift, sodass es notwendig ist, die Ergebnisse im Nachhinein kalibrieren zu können. Dazu sollten mehrere Kabelmeter jeweils in einem Warm- und einem Kaltwasserbad bekannten Temperaturen ausgesetzt sein (Abb. 14). Um die Temperaturen in den Bädern räumlich und zeitlich konstant zu halten, empfiehlt es sich, sie mit Tauchpumpen auszustatten, um die Ausbildung einer Temperaturschichtung zu verhindern. Während die Temperatur im Warmbad beispielsweise mit einem Aquarienthermostat aufrechterhalten werden kann, erfolgt die Kühlung des Kaltbades am besten mit Eis. Die Überwachung der Temperaturen mit Handgeräten sollte immer durch eine kontinuierliche Erfassung der Temperaturen mithilfe von Datenloggern unterfüttert werden. Dies ermöglicht eine Nachkalibrierung für jeden einzelnen

Zeitpunkt der Messung. Die eigentlichen Messungen dauern, je nach räumlichem und zeitlichem Setup sowie der zugrunde liegenden Fragestellung, mehrere Minuten bis Stunden. Eine einzelne Messung von wenigen Sekunden produziert ein relativ großes „Rauschen“, das durch die Mittelung vieler aufeinanderfolgender Messungen geglättet wird.

Zu beachten ist zudem, dass in den Uferbereichen der Gewässer oder in flachen Seen und Flüssen die Sonneneinstrahlung bzw. die räumlichen Wechsel von Sonne und Schatten Einfluss auf die Temperaturen entlang des Kabels haben können. Wind und Tagesgänge der Sonneneinstrahlung induzieren eine zusätzliche Dynamik. Entsprechende räumlich oder zeitlich auftretende Temperatursignale sind daher mit Vorsicht auszuwerten.

In Seen werden DTS-Messungen am besten während der Durchmischungsphasen durchgeführt, um eine gleichmäßige Temperatur in der Wassersäule und damit entlang des Gewässerbodens zu gewährleisten. Problematisch ist, dass während dieser Zeiträume die Temperaturdifferenz zwischen Grund- und Freiwasser nicht groß genug sein kann. Im Sommer allerdings, wenn die Temperaturunterschiede am größten sind, ist auch die thermische Schichtung besonders ausgeprägt. In diesen Fällen müssen auftretende Temperatursignale sorgfältig auf ihre Ursache hin überprüft werden, da sie nicht nur durch zutretendes Grundwasser, sondern auch durch vertikale Temperaturgradienten in der Wassersäule verursacht werden können. Dabei ist zu beachten, dass exfiltrierendes Grundwasser im Epilimnion im Verhältnis zum Freiwasser ein kaltes Temperatursignal verursacht, während dies in größeren Tiefen ein warmes Signal ist. Zusätzlich besteht die Gefahr, dass der Grundwasserzustrom nicht erkannt wird, weil im Vertikalprofil des Freiwassers grundwassergleiche Temperaturen auftreten können. Die Aufnahme eines Temperaturprofils der Wassersäule an der tiefsten Stelle des Sees ist als Referenz für die Temperaturen entlang des Kabels in verschiedenen Tiefen in jedem Fall sinnvoll. Im Optimalfall werden Temperaturprofile des Freiwassers an mehreren Stellen aufgenommen. Zusätzlich sollten die Gewässertiefen beim Verlegen des Kabels in regelmäßigen Abständen aufgenommen werden. So kann einem Standort entlang des Kabels neben der GPS-Position auch eine Tiefe und die zugehörige potenzielle Temperatur zugewiesen werden. Echolotmessungen ermöglichen die Erfassung der Gewässertiefe während der Platzierung des Kabels.

Ein weiteres Phänomen, das bei der Messung in Seen zu Fehlinterpretationen führen kann, sind interne Wellen, sogenannte Seiches. Diese windinduzierten Wasserbewegungen führen zu im Tagesverlauf periodisch auftretenden Temperaturschwankungen, die ebenfalls die Interpretation der Ergebnisse erschweren können.

In der Entwicklung befindet sich aktuell noch das so genannte aktive DTS. Dabei werden entweder die Ummantelung eines Stahlkabels oder einzelne, im Kabel befindliche Metalladern aufgeheizt. In diesem Fall wird die Geschwindigkeit der Wiederabkühlung des Kabels als Proxy für den Zutritt von Grundwasser in das Gewässer genutzt. Strömt viel Wasser am Kabel vorbei, kühlt es sich schneller ab. Der Vorteil ist, dass diese Methode unabhängig von Temperaturdifferenzen zwischen Grund- und Oberflächenwasser eingesetzt werden kann.

Heat-Pulse-Sensor

Der Heat-Pulse-Sensor ist ein Messgerät, mit dem sich Fließrichtung und Fließgeschwindigkeit in der hyporheischen Zone von Fließgewässern in etwa 10 cm Tiefe unter der Sediment-Wasser-Grenze messen lassen. Das Prinzip der Messung beruht ebenfalls auf Wärme als Tracer. Im Gegensatz zu den anderen Methoden wird nicht die natürliche Temperaturdifferenz zwischen Grund- und Freiwasser genutzt. Statt-

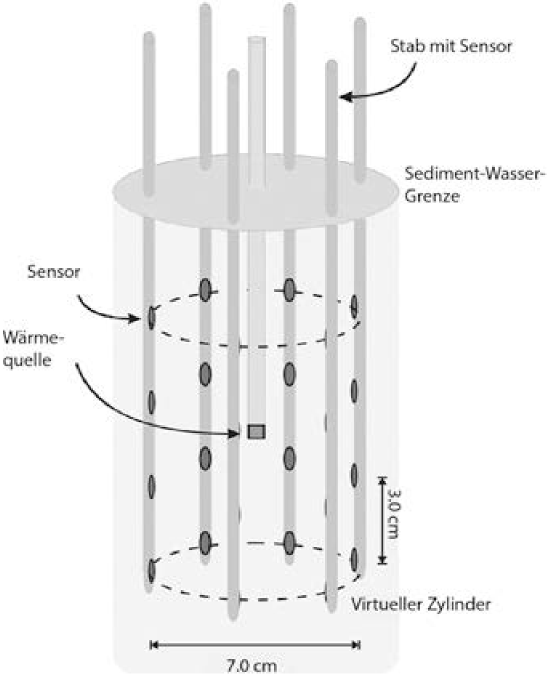

Abb. 15: Schematische Darstellung eines Heat-Pulse-Sensors. (Verändert nach ANGERMANN et al. 2012a)

dessen wird, wie beim aktiven DTS, mit einem Heizelement ein kurzer Wärmeimpuls in das Sediment eingetragen. Auf einem virtuellen Zylinder um die Heizquelle mit 7 cm Durchmesser sind 24 Temperatursensoren angeordnet, die die Durchbruchskurven des Heizimpulses erfassen (Abb. 15). Daraus lassen sich Fließrichtung und -geschwindigkeit der Wasserbewegung in der hyporheischen Zone ableiten. Bei der Ermittlung der Fließgeschwindigkeit ist die Retardation des Wärmetransportes im Sediment zu berücksichtigen. Eine einfache, aber recht ungenaue Auswertung, die nur die Peaks der Durchbruchskurven verwendet, wird in Lewandowski et al. (2011a) präsentiert. Basierend auf dieser ersten Näherung wird durch eine analytische Lösung der Wärme-Transport-Gleichung unter Einbezug aller Durchbruchskurven der Sensoren die Berechnung optimiert (Angermann et al. 2012b).

Erste Ergebnisse haben sehr heterogene Fließmuster im oberflächennahen Sediment gezeigt (Angermann et al. 2012a, 2012b; Lewandowski et al. 2011a). Weitere systematische Untersuchungen stehen noch aus. Auch wurde der Sensor bislang nicht in Seesedimenten eingesetzt. Seit Anfang 2015 gibt es auch einen kommerziell erhältlichen Heat-Pulse-Sensor.

Temperaturtiefenprofile des Gewässersediments

In Abhängigkeit von Richtung und Intensität des Wasserflusses zwischen Grund- und Oberflächenwasser ergibt sich ein standortcharakteristischer vertikaler Temperaturgradient in der Grenzzone. Dieser Gradient resultiert aus dem advektiven, also an die Strömung gebundenen, und dem konduktiven Transport von Wärme (Abb. 16).

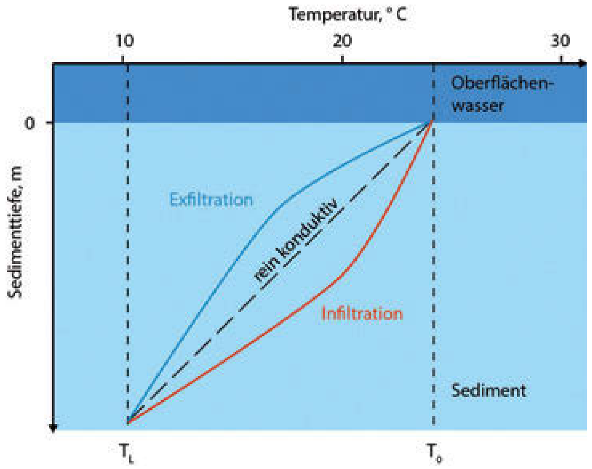

Abb. 16: Schematische Darstellung von Temperaturgradienten im Sediment eines Oberflächengewässers innerhalb der Randbedingungen T_0 und T_L (in °C). Rein konduktiver Wärmetransport ohne Massenflüsse (gestrichelte Linie), nach oben gerichteter Fluss (Exfiltration, blaue Linie) und nach unten gerichteter Fluss (Infiltration, rote Linie).

Das Temperaturtiefenprofil, das sich aufgrund dieses Austausches in vertikaler Richtung in der Grenzzone einstellt, ist stärker gekrümmt, je größer die Austauschraten sind. Die verlässlichsten Ergebnisse entsprechender Untersuchungen lassen sich in Zeiträumen erzielen, in denen die Temperaturunterschiede zwischen Grund- und Oberflächenwasser maximale Werte erreichen. Anibas et al. (2009) empfehlen daher, die Messung von Temperaturtiefenprofilen im Hoch- oder Spätsommer bzw. im Winter durchzuführen.

Ausgehend von der Annahme, dass der Austausch ausschließlich bzw. überwiegend in vertikaler Richtung stattfindet (s. Abschnitt 2.2 und Abb. 2), lässt sich dieser Prozess mit der folgenden eindimensionalen Wärme-Transport-Gleichung beschreiben:

$$K_{\mathrm{fs}}\left(\frac{\partial^2 T}{\partial z^2}\right) - q_z c_{\mathrm{f}} \rho_{\mathrm{f}} \frac{\partial T}{\partial z} = \rho c \frac{\partial T}{\partial t} \qquad (21)$$

wobei T (in °C) die Temperatur, K_{fs} (in J s^{-1} m^{-1} K^{-1}) die thermische Leitfähigkeit des Sediment-Wasser-Gemisches in der Grenzzone, ρc (in J m^{-3} K^{-1}) die volumetrische Wärmekapazität des Sediment-Wasser-Gemisches, $\rho_f c_f$ (in J m^{-3} K^{-1}) die volumetrische Wärmekapazität des Wassers, q_z (in m s^{-1}) die vertikale Fließgeschwindigkeit (Darcy-Geschwindigkeit) des Wassers in der Sedimenttiefe z (in m) und t die Zeit (in s) ist. In Gleichung 21 beschreiben die beiden Terme auf der linken Seite die Konvektion und die Advektion. Der Term auf der rechten Seite steht für die zeitliche Änderung der Temperatur. Unter der Annahme, dass der Austausch nur in vertikaler Richtung und mit konstanter Fließgeschwindigkeit q_z stattfindet, kann die Gleichung analytisch gelöst werden. Aus der folgenden Formel ergibt sich für jeden Punkt auf der z-Achse die Temperatur $T(z)$ (Bredehoeft und Papadopulos 1965):

$$T(z) = \left(\frac{\exp\left(\frac{q_z \rho_{\mathrm{f}} c_{\mathrm{f}}}{K_{\mathrm{fs}}} z\right) - 1}{\exp\left(\frac{q_z \rho_{\mathrm{f}} c_{\mathrm{f}}}{K_{\mathrm{fs}}} L\right) - 1} \cdot (T_{\mathrm{L}} - T_0) \right) + T_0 \qquad (22)$$

Mithilfe dieser Gleichung lässt sich nun die Fließgeschwindigkeit q_z auf der Grundlage der Temperaturverteilung in der Grenzzone zwischen Grund- und

Oberflächenwasser quantifizieren. Neben den in Gleichung 22 enthaltenen Parametern (volumetrische Wärmekapazität des Wassers $\rho_f c_f$, thermische Leitfähigkeit des Sediment-Wasser-Gemisches in der Grenzzone K_{fs}; beide sind der Fachliteratur zu entnehmen, z. B. Häfner et al. 1992) müssen folgende Größen bekannt sein:

- die Mächtigkeit L (in m) der Grenzschicht, in der sich die Temperaturen aufgrund des Wasseraustausches in vertikaler Richtung verändern,
- die Temperatur T_L (in °C) am unteren Ende dieser Grenzschicht (Grundwassertemperatur), und
- die Temperatur T_0 (in °C) am oberen Ende der Grenzschicht (unmittelbar an der Sediment-Wasser-Grenze).

L, T_L und T_0 sind aus Freilandmessungen zu ermitteln, sodass sich die gesuchte Fließgeschwindigkeit q_z aus der Minimierung der folgenden Fehlerfunktion berechnen lässt:

$$O(q_z) = \sum_{j=1}^{N} \left[T_j - \left(\frac{\exp\left(\frac{q_z \rho_f c_f}{K_{fs}} z_j\right) - 1}{\exp\left(\frac{q_z \rho_f c_f}{K_{fs}} L\right)} \cdot (T_L - T_0) + T_0 \right) \right]^2 \tag{23}$$

Dabei sind T_j die gemessenen Temperaturen entlang des Tiefenprofils und N die Anzahl der Messpunkte im Gewässersediment. Der Fehler $O(q_z)$ entspricht der Summe der quadrierten Differenzen zwischen gemessener Temperatur T_j und berechneter Temperatur in der Tiefe z_j bei den gegebenen Parametern und Randbedingungen. Die Strömungsgeschwindigkeit q_z innerhalb der Temperaturgrenzzone L ist die zu variierende Größe (Schmidt et al. 2006). Die Lösung derartiger Optimierungsprobleme ist mit gängigen Softwareprodukten durchzuführen. In Microsoft Excel© steht dafür beispielsweise die „Solver-Funktion" zur Verfügung.

Messungen der Temperaturen im Gewässersediment sind im Allgemeinen einfach und kostengünstig durchzuführen. Die meist ufernahe Exfiltration von Grundwasser erleichtert die Untersuchungen, da die Gewässertiefe in diesen Bereichen oft recht gering ist. Zur Erfassung von Temperaturprofilen des Gewässersediments werden beispielsweise lanzenartige Messgeräte genutzt, in die in vertikaler Richtung Temperatursensoren integriert sind. Nach dem Einbringen in das Sediment (0,5 bis 1 m) und einer gewissen Periode zur Wiederherstellung der dadurch gestörten natürlichen Bedingungen sind die Temperaturen in Abhängigkeit von der verwendeten Technik nach relativ kurzer Zeit ablesbar.

Der Wert für die Wärmeleitfähigkeit des gesättigten Sediments (K_{fs}) ist über Messungen vor Ort bestimmbar. Stehen dazu keine direkten Methoden zur Verfügung (z. B. entsprechende Sonden), kann K_{fs} auch über die Porosität n des Substrats abgeschätzt werden:

$$K_{fs} = K_S^{(1-n)} + K_f^n \tag{24}$$

wobei K_f die Wärmeleitfähigkeit der Flüssigkeit ist (für Wasser: 0,56 J s^{-1} m^{-1} $°C^{-1}$) und K_S die Wärmeleitfähigkeit des Feststoffes (Gewässersediment, in J s^{-1} m^{-1} $°C^{-1}$) ist. Stonestrom und Constantz (2003) geben auf der Grundlage verschiedener Studien Werte zwischen 0,2 und 2,5 J s^{-1} m^{-1} $°C^{-1}$ für K_{fs} an. Weitere Informationen zur Bestimmung von K_{fs} finden sich beispielsweise bei Menberg et al. (2013).

Temperaturen im Gewässersediment unterliegen nicht nur saisonalen, sondern auch diurnalen Schwankungen. Die Schwankungen in Zeitreihen der vertikalen Temperaturen im Gewässersediment lassen sich ebenfalls nutzen, um Austauschraten zu berechnen (Hatch et al. 2006). Zwei Alternativen stehen dabei zur Berechnung der vertikalen Fließgeschwindigkeit v_f (entspricht q_z in Gl. 21–23) zur Verfügung:

Entweder

$$v_f = v_{Ar} \cdot \gamma \tag{25}$$

mit v_{Ar} als Geschwindigkeit der thermalen Front, die auf der Grundlage des Verhältnisses der Amplitude des tiefsten Temperaturwertes (A_{ti} in Abb. 17) zu derjenigen des flachsten Temperaturwertes (A_{fl} in Abb. 17) abgeleitet wird. Die Amplitude spiegelt die

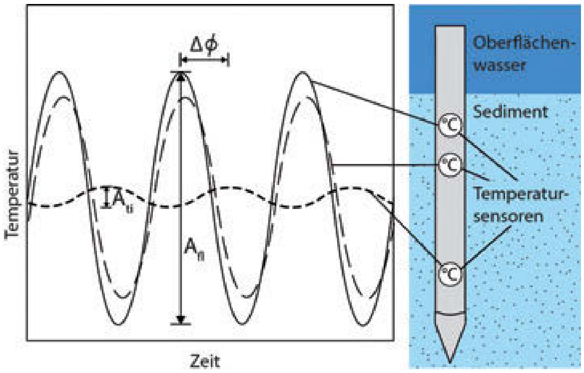

Abb. 17: Schematische Darstellung von Temperaturamplituden im Gewässersediment (a), ermittelt anhand von Temperaturen in unterschiedlichen Tiefen des Gewässersediments (b). (Verändert nach Hatch et al. 2006)

Dämpfung des Temperatursignals in der entsprechenden Sedimenttiefe wider.

Oder

$$v_\mathrm{f} = v_{\Delta\varphi} \cdot \gamma \qquad (26)$$

mit $v_{\Delta\varphi}$ als Geschwindigkeit der thermalen Front, die auf der Grundlage der Phasenverschiebung ($\Delta\varphi$) zwischen den Amplituden des tiefsten Temperarturwertes (A_ti in Abb. 17) und des flachsten Temperaturwertes (A_fl in Abb. 17) abgeleitet wird. Die Phasenverschiebung ergibt sich aus der zeitlichen Verzögerung der vertikalen Ausbreitung des Temperatursignals in das Sediment. Beide, Dämpfung und Phasenverschiebung, sind abhängig vom advektiven Wärmetransport zwischen den Systemen.

γ ist dabei das Verhältnis von volumetrischer Wärmekapazität des Sediment-Wasser-Gemisches (ρc, in $\mathrm{J\,m^{-3}\,K^{-1}}$) zu volumetrischer Wärmekapazität des Wassers ($\rho_\mathrm{f} c_\mathrm{f}$, in $\mathrm{J\,m^{-3}\,K^{-1}}$).

Anders als bei den oben beschriebenen Temperaturtiefenprofilen werden für diese Methode nur zwei Temperatursensoren im Sediment benötigt. Zur genauen Beschreibung der Herleitung von v_Ar und $v_{\Delta\varphi}$ wird an dieser Stelle auf Hatch et al. (2006) verwiesen. Eine Weiterentwicklung dieses Ansatzes findet sich außerdem bei Vandersteen et al. (2015).

4 Methoden zur Erfassung von Stoffflüssen zwischen Grund- und Oberflächenwasser

Neben den hydraulischen Interaktionen ist oft auch der Stoffaustausch zwischen Grund- und Oberflächenwasser Gegenstand von empirischen Untersuchungen. Fragestellungen dazu beinhalten beispielsweise die Lokalisierung des Zutritts von Nähr- oder Schadstofffahnen in einem Gewässer. Von Interesse sind außerdem die biologischen und geochemischen Prozesse, die sich an der Grenzzone zwischen Grund- und Oberflächenwasser abspielen. Hier kann es zum Beispiel durch veränderte Redox-Bedingungen zu signifikanten Veränderungen der Beschaffenheit des in- oder exfiltrierenden Wassers kommen. Die Quantifizierung der grundwasserbürtigen Fracht eines Stoffes erfolgt in der Regel als getrennte Bestimmung von Volumen und Konzentration der Grundwasserkomponente und anschließende Multiplikation der beiden Größen. Oft erfordert die räumliche Variabilität beider Terme die separate Untersuchung von Teilabschnitten oder -bereichen, sodass eine große räumliche Auflösung und damit eine genaue Bestimmung der grundwasserbürtigen Fracht erzielt werden. Im Folgenden werden einige Methoden vorgestellt, die die Erfassung von Stoffkonzentrationen auf verschiedenen räumlichen Skalen und Ausdehnungen ermöglichen.

4.1 Beprobung von Grundwassermessstellen

Grundwassermessstellen erlauben neben der bereits erwähnten Feststellung des Grundwasserstandes die Entnahme von Grundwasserproben, die entweder *on-site* oder im Labor auf die Untersuchungsgrößen (z. B. Nähr- oder Schadstoffe) analysiert werden. Die Untersuchung der Grundwasserqualität im Einzugsgebiet von Gewässern kann erste Hinweise darauf geben, ob die Belastung eines Gewässers durch die Exfiltration von Grundwasser verursacht wird. Obwohl deutschlandweit eine Vielzahl von Messstellen existiert (13 000 Messstellen sind bei der EU zur Umsetzung der Wasserrahmenrichtlinie gemeldet; Bannick et al. 2008), werden Schad- oder Nährstofffahnen (vor allem aus Punktquellen) im Einzelfall oft nur durch Zufall erfasst. Zusätzlich bilden Kontaminationen oft vertikale Gradienten von hohen Konzentrationen im oberen Bereich der gesättigten Zone zu geringeren Konzentrationen in tieferen Regionen aus. In Abhängigkeit von Filterlängen und Filtertiefen der Grundwassermessstellen werden Belastungen daher unter Umständen nicht erkannt oder als geringfügig eingestuft. Außerdem werden bei der routinemäßigen Beprobung des Grundwassers häufig nur bestimmte Inhaltsstoffe gemessen. Beispielsweise wird der ökologisch wichtige Pflanzennährstoff Phosphor im Grundwasser in der Regel nicht oder nicht mit ausreichenden Bestimmungsgrenzen gemessen, weil Phosphor im Grundwasserleiter selbst weder ökologisch noch humantoxikologisch bedeutsam ist. Die schädliche (d. h. eutrophierende) Wirkung entfaltet dieser Nährstoff erst, wenn er aus dem Grundwasserleiter in ein Oberflächengewässer gelangt.

Ufernahe Grundwassermessstellen repräsentieren die Beschaffenheit von exfiltrierendem Grundwasser besser als solche, die sich in größerer Entfernung zum Gewässer befinden. Bei der Passage der reaktiven Grenzzone kann es zu Prozessen kommen, die die Beschaffenheit des letztendlich exfiltrierenden Grundwassers deutlich verändern. Daher repräsentieren Grundwassermessstellen auch in unmittelbarer Ufernähe nicht unbedingt die Beschaffenheit des exfiltrierenden Grundwassers. Untersuchungen der Beschaffenheit des Wassers direkt in der Grenzzone liefern diesbezüglich verlässlichere Ergebnisse. Im Folgenden werden einige Möglichkeiten dafür erläutert.

4.2 Mini-Piezometer

Zur Untersuchung von biogeochemischen Prozessen in der reaktiven Grenzzone zwischen Grund- und Oberflächenwasser werden häufig Mini-Piezometer eingesetzt. Dabei handelt es sich im Prinzip um Miniaturen von Grundwassermessstellen. Sie bestehen aus Rohren aus Polyethylen oder Stahl, die am unteren Ende geschlitzt oder perforiert sind und mit relativ geringem Aufwand bis in Tiefen von wenigen Metern installiert werden können (Abb. 18). Mini-Piezometer erfüllen mehrere Funktionen. Außer in Gewässersedimenten lassen sie sich auch an grundwassernahen Standorten (also auch im Uferbereich von Gewässern) installieren und als provisorische Grundwassermessstellen nutzen. Dabei ermöglichen sie das Monitoring von Grundwasserdruckhöhen, Grundwasserqualität sowie die Erfassung der hydraulischen Leitfähigkeit. Sie sind kostengünstig, lassen sich, wenn nötig, auch in Eigenarbeit herstellen und sind vergleichsweise leicht zu installieren. Sie haben meist einen geringen Durchmesser (empfohlen werden etwa 1–2″), um die manuelle Installation im Sediment zu erleichtern. Daher lassen sich oft keine Pumpen in die Piezometer einführen. Stattdessen erfolgt die Probenahme beispielsweise mit einer Peristaltikpumpe, deren Schlauch in das Rohr geführt wird, um das in das Piezometerrohr infiltrierende Porenwasser an die Oberfläche zu pumpen. In der Praxis ergeben sich zum Teil Probleme durch zu große Schlitz-/Lochweiten im Filterbereich, sodass das geförderte Wasser hohe Feinsedimentfrachten enthält, was das Filtern der Proben und/oder die Analytik erschwert oder behindert. Zu geringe Schlitz-/Lochweiten können dagegen zu Verstopfungen führen. Rivett et al. (2008) verwenden Lochweiten von 4 mm. Häufig sind jedoch deutlich geringere Loch- oder Schlitzweiten besser geeignet. Im Handel sind Schlitzweiten von 0,3 mm problemlos erhältlich. Zusätzlich kann der Filterbereich von außen mit einem feinmaschigen Material ausgestattet werden, um eine weitere Filterwirkung zu erzielen (Abb. 19). Hier eignen sich reißfeste und abbauresistente Nylonmaterialien, aber auch empfindlichere Nylon-Damenstrumpfhosen werden verwendet (Savoie und Leblanc 1998). Die Befestigung dieses Außenfilters kann beispielsweise mit rostfreiem Bindedraht oder Kabelzugbändern erfolgen.

Ein Gewinde am unteren Ende des Rohres ermöglicht das Anbringen einer Spitze und erleichtert so das Einbringen des Piezometers in den Untergrund. Per Hand oder motorbetriebener Schlagkraft wird das Piezometer in das Sediment getrieben. Da das Material jedoch bei der Installation leicht Schaden nehmen kann, werden die Piezometer teilweise nicht direkt in das Sediment eingebracht. Stattdessen kann an der Stelle, an der das Piezometer gesetzt werden soll, mit einem Handbohrer vorgebohrt werden. Auch wenn das Loch nach Entnahme des Handbohrers wieder

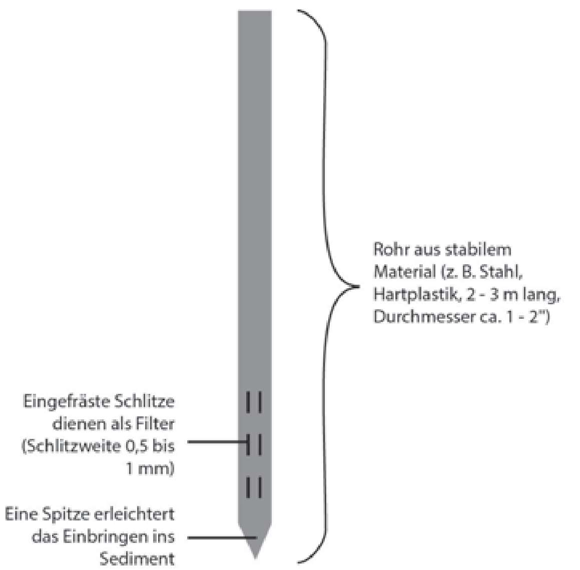

Abb. 18: Skizze eines Mini-Piezometers (Beispiel).

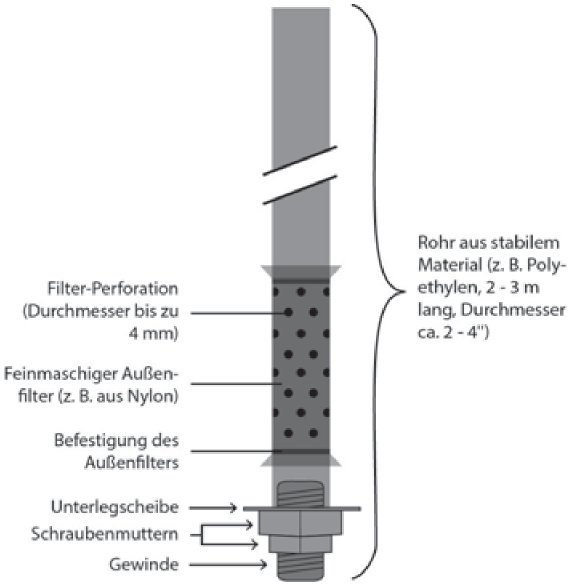

Abb. 19: Mini-Piezometer in Anlehnung an Rivett et al. (2008).

zusammenfällt, lässt sich das Piezometer anschließend leichter in den aufgelockerten Untergrund einbringen.

Rivett et al. (2008) empfehlen, am unteren Ende des Piezometers eine Kombination von Unterlegscheiben und mehreren Schraubenmuttern in absteigender Größe als provisorische Spitze aufzuschrauben (Abb. 19). Wichtig ist dabei, dass die Unterlegscheibe einen größeren Durchmesser als das Piezometerrohr hat. Bei der Installation dient sie als Stütze für ein Vortriebsrohr (vorzugsweise aus Stahl), das über die Piezometerkonstruktion gestülpt wird. Diese Einheit aus Vortriebsrohr mit innenliegendem Piezometer wird dann in das Gewässersediment getrieben, wobei die gesamte Schlagkraft auf dem Vortriebsrohr und der Unterlegscheibe liegt und nicht auf dem Piezometer. Ist die gewünschte Tiefe erreicht, lässt sich das Vortriebsrohr herausziehen, während das Mini-Piezometer im Sediment verbleibt.

Das Einbringen von Mini-Piezometern kann z. B. bei groben Sedimenten sehr schwierig sein. Hier kann auch das Prinzip der „verlorenen Spitze“ helfen. Dabei wird zunächst ein Rohr, das mit einer Spitze versehen ist (Material aus Stahl), mit einem motorbetriebenen Schlaghammer in das Sediment eingebracht. Das Mini-Piezometer wird erst danach in dieses oben offene Rohr eingeführt. Beim Herausziehen des äußeren Rohres löst sich die Spitze und verbleibt zusammen mit dem Piezometer im Sediment. Entsprechende Technik wird von verschiedenen Firmen angeboten (z. B. Eijkelkamp Agrisearch Equipment).

Transekte bestehend aus mehreren Mini-Piezometern orthogonal zum Ufer erlauben die Erfassung der Grundwasserbeschaffenheit vom nahen Uferbereich bis in die In- oder Exfiltrationszone im Gewässer. Parallel zueinander bzw. zum Ufer angeordnet können Mini-Piezometer helfen, die räumliche Ausdehnung von Schad- oder Nährstofffahnen zu bestimmen. Zwischen der Installation und der ersten Probenahme liegen im Optimalfall mehrere Tage oder auch Wochen, damit sich die ursprünglichen hydraulischen und geochemischen Verhältnisse, die durch die Installation gestört wurden, wieder einstellen können. Mini-Piezometer können theoretisch nach den einzelnen Probenahmen noch tiefer ins Sediment getrieben werden, um tiefengestufte Ergebnisse zu erhalten, wobei allerdings der zeitliche Abstand zwischen den Probenahmen beim Vergleich der Ergebnisse zu berücksichtigen ist. Alternativ dazu können mehrere Piezometer in geringem Abstand zueinander in verschiedenen Tiefen niedergebracht werden. Andererseits sollte eine gewisse Mindestdistanz zwischen den Messpunkten eingehalten werden, um die hydraulische Integrität des Substrats aufrecht zu erhalten. Dabei ist wiederum die kleinskalige, laterale Heterogenität der biogeochemischen Beschaffenheit des Porenwassers zu beachten. Bei der Probenahme im Gewässersediment ist darauf zu achten, dass die Pumpleistung nicht zu hoch gewählt wird, um ein Ansaugen von Oberflächenwasser in das Sediment entlang des Piezometerrohres zu vermeiden.

4.3 Multilevel-Piezometer

Multilevel-Piezometer erlauben die punktuelle vertikale Beprobung des Porenwassers im Gewässersediment in hoher räumlicher Auflösung. Sie stellen eine Modifikation des oben beschriebenen Mini-Piezometers dar: Anstatt eines einzelnen Filterrohres bestehen Multilevel-Piezometer aus einem Bündel von Schläuchen, die als Probenahmeports in unterschiedlichen Tiefen im Gewässersediment enden (Abb. 20).

Abb. 20: Beispiel eines Multilevel-Piezometers (a). Die vom Rohrinneren nach außen geführten Schläuche sind mit einer Gaze als Filtermaterial ausgestattet und mit Kabelbindern an der Haltestange fixiert (b). Auf einer mobilen Vorrichtung befinden sich die Mehrkanalpumpe inklusive farblich kodierter Anschlussschläuche (c) sowie eine Haltevorrichtung für Probengefäße (d). (Fotos: Jörg Lewandowski, Franziska Pöschke, Katharina Amelung).

Häufig werden Schläuche aus Polyethylen oder Polytetrafluorethen (Teflon®) verwendet. Letzteres hat den Vorteil, dass es inert ist und keine Sorption an den Oberflächen stattfindet. Nachteilig ist jedoch, dass es sauerstoffdurchlässig ist und es zur Oxidation von anoxischen Probenwässern, und damit zu verfälschten Ergebnissen, kommen kann. Zur Beprobung wird an jeden der einzelnen Schläuche ein Unterdruck angelegt, was eine simultane tiefengestufte Beprobung des Porenwassers im Gewässersediment oder von oberflächennahem Grundwasser ermöglicht. Auf diese Weise können Prozesse, die innerhalb der Passage der reaktiven Grenzzone auf der Dezimeterskala stattfinden, mit geringem Kosten- und Arbeitsaufwand erfasst und evaluiert werden. Multilevel-Piezometer können im Eigenbau hergestellt werden. Die Schläuche mit einem Durchmesser von wenigen Millimetern werden entlang einer zentralen Stützstange (z. B. aus nichtrostendem Stahl, Durchmesser 5–10 mm) angebracht. Zur Befestigung der Schläuche können rostfreier Draht oder Kabelbinder verwendet werden. Ähnlich wie für die Mini-Piezometer beschrieben, sollten die im Sediment endenden Schläuche mit einem Filter aus reißfestem Material (z. B. aus Nylon) ausgestattet werden.

Bei Multilevel-Piezometern mit dem oben beschriebenen Design (nach Rivett et al. 2008) ist auf ein Vortriebsrohr zum Schutz des Materials und zur Vermeidung von Verschiebungen der einzelnen Schläuche kaum zu verzichten. Dazu kann die Stützstange mit einem Gewinde, einer angeschraubten Spitze und einer zwischengeschalteten Unterlegscheibe ausgestattet werden, wie bereits für die Mini-Piezometer beschrieben. Alternativ kann aber auch hier die Methode der „verlorenen Spitze“ zum Einsatz kommen (s. Abschnitt 4.2). Vor der ersten Beprobung sollten wiederum mehrere Tage vergehen, damit sich das gestörte Sediment und die geochemische Beschaffenheit des Porenwassers wieder einstellen können.

Problematisch bei Multilevel-Piezometern können präferenzielle Fließwege sein, die sich entlang der äußeren Oberflächen der Schläuche und des Rohres ausbilden können. Während der Probenahme kann dadurch beispielsweise Oberflächenwasser in das Sediment gesogen werden und zu nicht repräsentativen Ergebnissen führen. Zum Teil werden die Schläuche auch innerhalb eines Rohres nach unten geführt. Dadurch verringert sich die äußere Oberfläche, an der sich präferenzielle Fließwege bilden können. Dieses erfordert jedoch einigen Mehraufwand bei der Konstruktion, da an den Schlauchenden entsprechende Öffnungen im Rohr eingebaut werden müssen und das untere Ende der Schläuche jeweils so in dieser Öffnung fixiert werden muss, dass es hydraulischen Kontakt zum Sediment hat und dabei keine Undichtigkeit auftritt. Die Beprobung der einzelnen Schläuche erfolgt im Optimalfall simultan mit Mehrkanalschlauchquetschpumpen. Die gleichzeitige Beprobung verhindert, dass Wasser aus benachbarten Sedimentschichten angesogen und das Vertikalprofil verfälscht wird. Fehler können durch falsche Zuordnungen von Schläuchen und Sedimenttiefen auftreten. Farblich unterschiedliche Schläuche erlauben die Differenzierung der beprobten Sedimenttiefe von der Oberfläche aus. Auch andere Markierungsmethoden können helfen, Verwechslungen zu vermeiden, müssen aber dauerhaft stabil und gegen Witterungsbedingungen resistent sein.

4.4 Porenwassersammler (Peeper)

Porenwassersammler (auch Dialyse- oder Diffusionssammler) ermöglichen die vertikal hoch aufgelöste Beprobung von Porenwasser in wassergesättigten Sedimenten (Hesslein 1976). Sie werden auch „Peeper“ genannt (von engl. *to peep*, spähen, linsen). Peeper

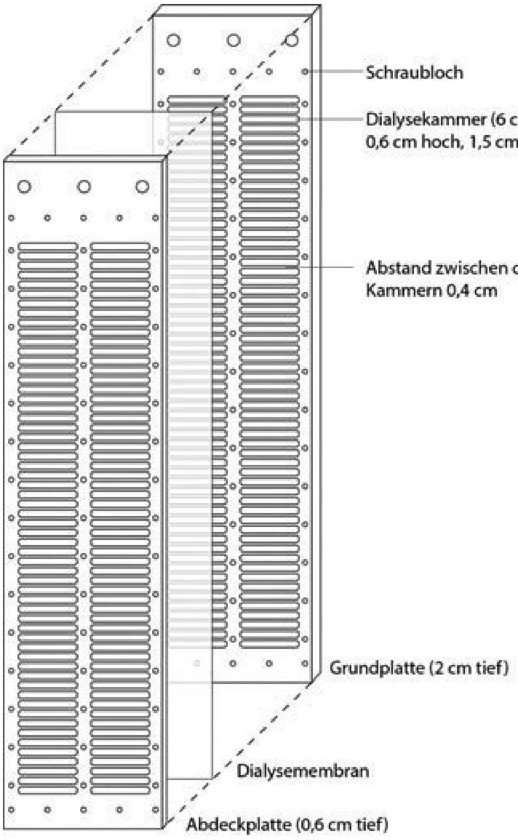

Abb. 21: Schematisches Beispiel eines Porenwassersammlers. (Nach Lewandowski 2002)

bestehen aus einer Platte, in die im Abstand von einigen Millimetern Vertiefungen (Kammern) eingelassen sind (Abb. 21). Als Material wird häufig durchsichtiger Acrylkunstoff (Plexiglas) verwendet. Die Kammern werden mit deionisiertem Wasser gefüllt, bevor sie mit einer semipermeablen Dialysemembran (z. B. aus Polysulfon) und einer Deckplatte abgedeckt werden. Der Peeper wird in das Gewässersediment eingebracht. Ionen diffundieren durch die Membran, sodass sich die Beschaffenheit des Wassers in den Kammern an die des Porenwassers angleicht. Die Porengröße der Membran bestimmt die Größe der Partikel und Ionen, die in die Kammern hineindiffundieren können und sollte entsprechend der Fragestellung gewählt werden. Auch die Wahl des Folienmaterials sollte mit Blick auf die zu bestimmenden Parameter vorgenommen werden. Biologische Abbaubarkeit oder die säureinduzierte Lösung von Stoffen (z. B. Bor, Calcium, Kalium, u. v. m.) aus der Membran heraus können die ursprüngliche Porenwasserzusammensetzung verändern. Der fertig zusammengestellte Peeper sollte vor der Exposition 24 Stunden lang mit Stickstoff begast werden. Das Wasser in den Kammern ist dann weitgehend sauerstofffrei, sodass Ausfällungen von Eisen und andere redoxabhängige Prozesse während der Exposition im Gewässer unterbleiben.

Die Expositionsdauer des Peepers ist so zu wählen, dass Störungen des Sedimentes nach dem Einbringen des Peepers weitgehend abgeklungen sind. Weiterhin ist so lange abzuwarten, bis sich zwischen dem Porenwasser und dem Wasser in den Kammern ein (dynamisches) Gleichgewicht eingestellt hat. Häufig wird eine Expositionsdauer von 14 Tagen gewählt, wobei etwa eine Woche auf die Gleichgewichtseinstellung entfällt. Die tatsächliche Gleichgewichtseinstellung hängt von Parametern wie der Temperatur, der Porosität der Membran, der chemischen Zusammensetzung des Porenwassers, der Kammertiefe und dem Ort der Nachlieferung (Freisetzung im Sediment unmittelbar vor der Membran oder Transport von Stoffen aus der Umgebung) ab.

Nach der Entnahme können die einzelnen Kammern auf die gewünschten Inhaltsstoffe hin analysiert werden. Das Probenvolumen in den Kammern beträgt nur wenige Milliliter. Die Entnahme erfolgt mit Spritzen oder Pipetten, die durch die Membran gestochen werden. Der Zeitraum zwischen Entnahme und Beprobung sollte so kurz wie möglich sein, da vor allem der Kontakt zur sauerstoffhaltigen Atmosphäre Redox-Prozesse in den Proben induzieren kann. Teilweise werden 5-Minuten-Zeiträume für die Beprobung der Kammern empfohlen (z. B. Adams 1991), was aber in der Praxis aufgrund der Vielzahl der Kammern kaum umsetzbar ist.

Der Vorteil eines Peepers ist, dass die passive Art der Beprobung verhindert, dass sich Wasser aus unterschiedlichen Tiefen in der Probe mischt oder Sauerstoff in die Probe gelangt, da kein Unterdruck angelegt wird. Werden die oben beschriebenen Details wie geeignete Membranen, ausreichende Gleichgewichtseinstellungszeiten, zügige Analytik etc. ausreichend berücksichtigt, stellen Peeper eine optimale Methode zur räumlichen Erfassung der Porenwasser-Konzentrationen in Bezug auf mikrobiologische und geochemische Fragestellungen dar (Brandl und Hanselmann 1991).

Das klassische Anwendungsfeld von Peepern ist die diffusive Rücklösung von Stoffen aus marinen und limnischen Sedimenten. Sie können aber auch benutzt werden, wenn advektive Transportprozesse wie Grundwasserzu- und -abstrom eine Rolle spielen. Anhand von Peepern können die Stoff-Konzentration des zuströmenden Grundwassers und damit die Frachten ermittelt werden. Darüber hinaus bieten Peeper aber auch die Möglichkeit, Veränderungen der Biogeochemie entlang von Transportpfaden über die Sediment-Wasser-Grenzzone hinweg zu erfassen (Abb. 22) und so den Stoffumsatz in der reaktiven Grenzzone zu quantifizieren.

Wie bei den Temperaturtiefenprofilen (Abschnitt 3.5.3) können sich auch Tiefenprofile konservativer (also nichtreaktiver) Ionen wie beispielsweise Chlorid an der Sediment-Wasser-Grenze einstellen – vorausgesetzt, dass Oberflächenwasser und Grundwasser sich deutlich in den Konzentrationen des entsprechenden Ions unterscheiden. Diese mit einem Peeper erfassbaren Gradienten können analog zu Temperaturtiefenprofilen ausgewertet werden, um die Flüsse über die Sediment-Wasser-Grenze zu quantifizieren (s. Abschnitt 3.5.3).

Die Dialysetechnik wurde an verschiedene Fragestellungen und Bedingungen angepasst. Zu diesen Entwicklungen gehören der Einsatz von 2D-Peepern (Hupfer und Lewandowski 2005; Laskov et al. 2007), die Erfassung der Porenwasserdynamik an einem festen Standort durch den Austausch des Kammervolumens mittels Schläuchen (Jacobs 2002) sowie die Kombination von Mini-Peepern mit Laborexperimenten (Zak et al. 2006). Höhere vertikale Auflösungen werden durch die Anwendung von Gelsammlern erreicht (Krom et al. 1994).

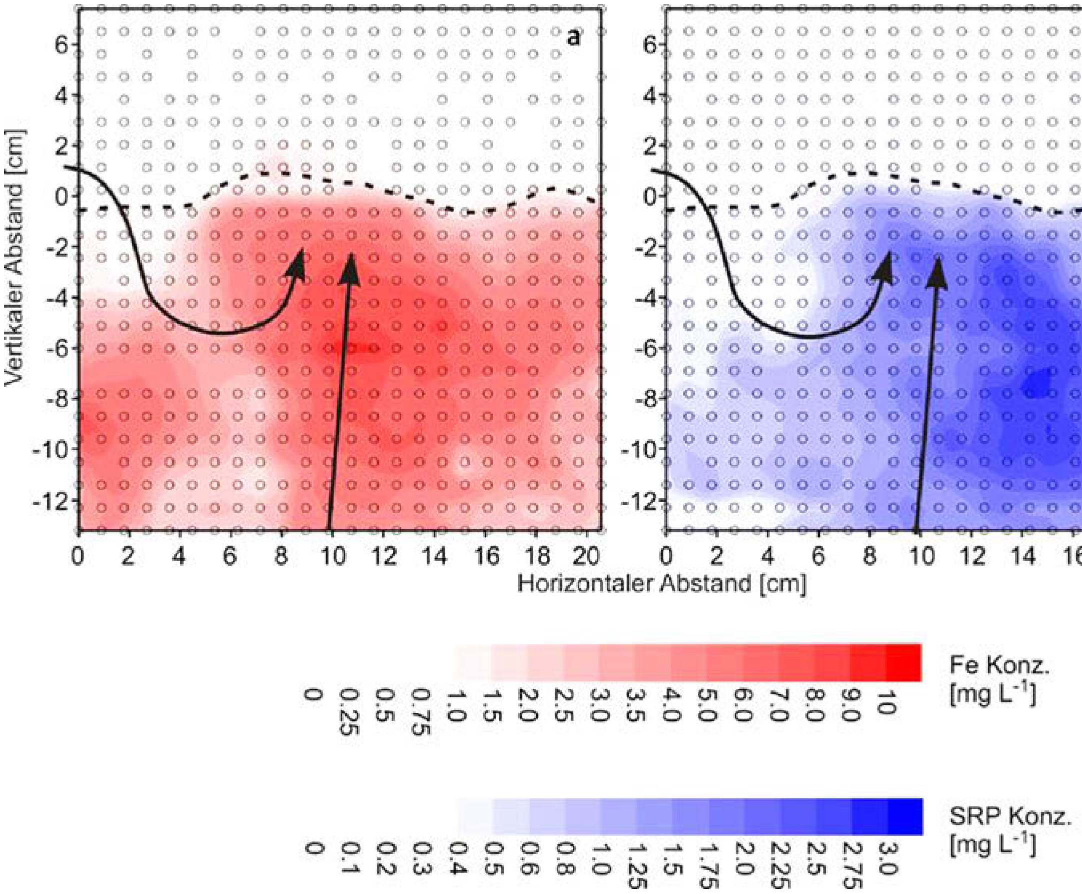

Abb. 22: Konzentrationen von gelöstem Eisen (Fe, links) und von gelöstem reaktivem Phosphor (SRP, rechts) in der hyporheischen Zone der Spree. Die gestrichelte Linie markiert die Sediment-Wasser-Grenze. Kreise repräsentieren Porenwasserkammern, Pfeile beschreiben potenzielle Fließpfade des Porenwassers in der hyporheischen Zone, abgeleitet aus den Ergebnissen der Porenwasseranalytik. (Lewandowski und Nützmann 2010)

4.5 Seepagemeter

Seepagemeter können neben der Quantifizierung (Abschnitt 3.1) auch zur Erfassung der Beschaffenheit von exfiltrierendem Grundwasser genutzt werden. Das sich im Plastikbeutel sammelnde Wasser kann zur Analyse der gewünschten Parameter herangezogen werden. Das im System eingeschlossene Oberflächenwasser (Zylinder und angeschlossener Plastikbeutel) muss jedoch zunächst ausgetauscht werden, um das tatsächlich exfiltrierende Grundwasser zu erfassen. Ein mehrmaliger Austausch des Seepagemeter-Volumens ist vorteilhaft. Wie in Abschnitt 3.1 dargestellt, sollten die Plastikbeutel außerdem beim Anschluss an den Zylinder mit einer gewissen Wassermenge vorgefüllt sein, um den Widerstand zu verringern, der durch einen leeren Beutel verursacht wird. Menge und Beschaffenheit (Konzentration) des anfänglich im Beutel befindlichen Wassers müssen bekannt sein, um die Konzentration des exfiltrierenden Grundwassers berechnen zu können.

Probleme können durch die Entwicklung anoxischer Bedingungen innerhalb des Seepagemeter-Systems verursacht werden. Bei redoxsensitiven Parametern wie Phosphor oder Ammonium kann dies zu einem nicht repräsentativen Konzentrationsanstieg führen (Downing und Peterka 1978; Belanger und Mikutel 1985; Belanger et al. 1985; Zimmermann et al. 1985). Im Einzelfall ist es schwierig zu differenzieren, ob diese Prozesse ein Artefakt des Seepagemeter-Systems sind, oder ob die Veränderungen natürlicherweise während der Passage der reaktiven Grenzzone hervorgerufen werden.

Auch die Störung des Gewässersediments während des Einbringens eines Seepagemeters kann zu verfälschten Ergebnissen führen. Die Aufwirbelung von organischem Material während der Installation kann zu erhöhten Umsatzprozessen führen. Andererseits könnte das Ausbleiben von frischem organischem Material aus der Wassersäule entsprechende Umsatzraten innerhalb der vom Seepagemeter abgedeckten Fläche reduzieren.

5 Zusammenfassung und Ausblick

Die Erfassung von Wasser- und Stoffflüssen zwischen Grund- und Oberflächenwasser ist schwierig. Neben der generellen Unterschätzung der Auswirkung dieser Prozesse ist das ein wesentlicher Grund für die langjährige Vernachlässigung dieser Wechselwirkungen bei der Aufstellung von Wasser- und Stoffbilanzen von Gewässern (Abschnitt 2.1). Die hier vorgestellten Methoden sind in den letzten Jahren und Jahrzehnten entwickelt und optimiert worden. Ihre praktische Anwendung außerhalb wissenschaftlicher Studien ist bislang noch begrenzt. Es ist aber davon auszugehen, dass das Bewusstsein für die Bedeutung der Grundwasser-Oberflächenwasser-Wechselwirkungen weiter zunimmt, denn die Gefährdung der Süßwasserökosysteme durch diffuse Belastungen nimmt voraussichtlich weiter zu. Dies betrifft neben den klassischen Nähr- und Schadstoffen zunehmend auch die Belastung durch organische Spurenstoffe (Medikamentenrückstände, Hormone, Kosmetika, Pflanzenschutzmittel, Biozide, Industriechemikalien, etc.). Bis vor einigen Jahren traten derartige Substanzen in natürlichen Systemen kaum in Erscheinung. Die entsprechenden Transport-, Um- und Abbauprozesse, sowie die Wirkung auf Organismen und Ökosysteme sind daher häufig noch weitgehend unbekannt. Zum Teil sind die Analysetechniken auch noch nicht so weit ausgereift, dass sie in den meist geringen Konzentrationsbereichen, in denen diese Stoffe im Feld auftreten, aussagekräftige Ergebnisse erzielen.

Aktuell beziehen sich Studien zu organischen Schadstoffen in Grundwasser und Oberflächengewässern häufig auf lokal begrenzte Belastungen durch Kanalisationsleckagen oder Abwasserreinigungsanlagen (z. B. Lewandowski et al. 2011b; Mueller et al. 2012). Vor allem im urbanen Bereich sind allerdings bereits großflächigere Grundwasserbelastungen durch Abwässer belegt (Bremer und Harter 2012; Schaider et al. 2014; Wolf et al. 2012). Sie müssen als Indiz dafür angesehen werden, dass großflächige und intensive Belastungen von urbanen Grund- und Oberflächenwässern mit diesen Substanzen häufiger vorkommen als bislang angenommen.

Auch die Gefahr durch Nährstoffüberschüsse scheint noch lange nicht gebannt. Dabei deutet der Fall des Arendsees (Abschnitt 2.1) darauf hin, dass beispielsweise die grundwasserbürtigen Phosphorfrachten in die Oberflächengewässer bislang unterschätzt wurden. Das Monitoring zum Erfolg von Maßnahmen gegen zu hohe Nitratkonzentrationen im Grundwasser zeigt ernüchternde Ergebnisse (Balzer und Schulz 2014; BMU 2012). Besonders oberflächennahes Grundwasser ist weiterhin stark stickstoffbelastet, und eine Trendumkehr scheint nicht in Sicht zu sein. Es besteht also auch weiterhin ein großes Eutrophierungspotenzial durch Grundwasserexfiltration für die Oberflächengewässer.

Die vielfältigen Belastungen der Gewässer, die sich aus der intensiven Nutzung von Ressourcen und Landschaft ergeben, werden vermutlich eine verstärkte Auseinandersetzung mit den Interaktionen zwischen den aquatischen Ökosystemen forcieren. Auch die immer schneller voranschreitende Entwicklung von Methoden und Techniken in den Disziplinen Hydro(geo)logie, Limnologie und chemische Analytik wird hoffentlich dazu beitragen, dass die Austauschprozesse zunehmend einfacher und kostengünstiger zu untersuchen sind, sodass sie in Zukunft auch immer häufiger berücksichtigt werden. Damit wäre ein wichtiger Beitrag zum Schutz von Quantität und Qualität der Süßwasserressourcen geleistet.

Tabelle 3 liefert einen zusammenfassenden Überblick über die in Abschnitt 3 vorgestellten Methoden, die eine Erfassung des hydrologischen Austausches zwischen Grundwasser und Oberflächenwasser ermöglichen. Eine detaillierte Darstellung erfolgt jeweils in den entsprechenden Abschnitten.

Die Quantifizierung von Stoffflüssen zwischen Grundwasser und Oberflächengewässern erfordert die Messung der Konzentration des Zielparameters. Anders als bei der Erfassung des hydrologischen Austausches geschieht dies meist direkt, sodass die Konzentration als Messgröße auch die Ergebnisgröße ist (vgl. Tab. 3). Methoden zur Erfassung von Stoffkonzentrationen werden in Tabelle 4 zusammengefasst. Es liegt nahe, dass entsprechende Untersuchungen überwiegend punktuell durchgeführt werden können, sodass die Repräsentativität eingeschränkt ist. Daher sind oft viele Untersuchungen an unterschiedlichen Standorten notwendig, um die Qualität des exfiltrierenden Grundwassers beurteilen zu können. Zur Quantifizierung von Stofffrachten sind die gemessenen Konzen-

Tab. 3: Übersicht über hydrologische Methoden zur Erfassung von Grundwasserin- und -exfiltration

Methode	**Geeignet für**		**Messgröße**	**Einheit der Messgröße***	**Ergebnis-/ Kalkulationsgröße**	**Einheit der Ergebnisgröße***	**Räumliche Skala****	**Quantitativ (als Fließgeschwindigkeit/ Menge)**	**Qualitativ (räumliche Muster)**	**Abschnitt**
	Fließgewässer	**See**								
Seepagemeter	ja	ja	In-/Exfiltrationsvolumen	$l\ m^{-2}\ d^{-1}$	–	–	klein	ja	ja	3.1
vertikale hydraulische Gradienten	ja	ja	Wasserstandsdifferenz bezogen auf Entfernung	$cm\ m^{-1}$	Darcy-Geschwindigkeit	$cm\ d^{-1}$	klein	ja	ja	3.2
Wasserhaushalt	bedingt	ja	–	–	Nettovolumen des Grundwasserterms	$m^3\ a^{-1}$	mittel bis groß	ja	nein	3.3.1
Abflussdifferenzmessung im Fließgewässer	ja	nein	Durchfluss	$m^3\ sec^{-1}$	Nettovolumen des Grundwasserterms	$m^3\ m^{-1}$	mittel bis groß	ja	bedingt	3.3.2
Grundwasserneubildung im EZG	ja	ja	–	–	Volumen der Grundwasserexfiltration	$m^3\ a^{-1}$	mittel bis groß	ja	nein	3.3.3
Ganglinienanalyse im Gewässer	ja	nein	Durchfluss	$m^3\ sec^{-1}$	Basisabfluss	$m^3\ sec^{-1}$	mittel bis groß	ja	nein	3.4
Ganglinienanalyse im Grundwasser	ja	ja	Grundwasserstand bezogen auf Bezugsfläche (z. B. GOK)	m	Grundwasserneubildungsrate	$m\ a^{-1}$	mittel	ja	nein	3.4
stabile Isotope (Wasser)	bedingt	ja	Konzentration bezogen auf VSMOW	‰	Anteil des Grundwassers an der Wasserbilanz	m^3	mittel bis groß	ja	nein	3.5.1
	ja	ja	Konzentration bezogen auf VSMOW	‰	Unterscheidung von In- und Exfiltrationsbereichen	Δ‰ (See- und Grundwasser)	klein bis mittel	nein	ja	3.5.1
Radon	bedingt	ja	Aktivitätskonzentration	$Bq\ l^{-1}$	Bilanzierung des Grundwasserterms im Wasserhaushalt eines Gewässers	m^3	mittel bis groß	ja	nein	3.5.2
	ja	ja	Aktivitätskonzentration	$Bq\ l^{-1}$	Unterscheidung von In- und Exfiltrationsbereichen	$Bq\ l^{-1}$	klein	nein	ja	3.5.2
FO-DTS	ja	ja	Temperatur als Indikator für Standorte mit verstärkter Grundwasserexfiltration	°C	–	–	mittel bis groß	nein	ja	3.5.3

Tab. 3: (Fortsetzung)

Methode	**Geeignet für**		**Messgröße**	**Einheit der Messgröße***	**Ergebnis-/ Kalkulationsgröße**	**Einheit der Ergebnisgröße***	**Räumliche Skala****	**Quantitativ (als Fließgeschwindigkeit/ Menge)**	**Qualitativ (räumliche Muster)**	**Abschnitt**
	Fließgewässer	**See**								
Heat-Pulse-Sensor	ja	nicht getestet	Temperatur	°C	Richtung und Geschwindigkeit der hyporheischen Fließbewegung	cm d^{-1}	klein	ja	ja	3.5.3
Temperaturprofile des Gewässersediments	ja	ja	Temperatur als Indikator für Darcy-Geschwindigkeit	°C	Darcy-Geschwindigkeit	cm d^{-1}	klein	ja	ja	3.5.3

* Entspricht die Messgröße nicht der Ergebnisgröße, so ist letztere ebenfalls angegeben. Die Einheiten der Mess- und Ergebnisgrößen variieren in Abhängigkeit von Fragestellung, Messgerät, räumlicher und zeitlicher Auflösung der Messungen, Bezugseinheiten etc.** klein: Zentimeter bis wenige Meter; mittel: wenige Meter bis einige Hundert Meter; groß: einige Hundert Meter bis Kilometer

Tab. 4: Übersicht über Methoden zur Erfassung der Konzentrationen des exfiltrierenden Grundwassers

Methode	**Einsatz in**		**Prinzip/ Technik**	**Erfasstes Medium**	**Räumliche Skala***		**Räumliche Auflösung**		**Abschnitt**
	(ufernahem) Grundwasser	**Porenwasser im Gewässersediment**			**vertikal**	**horizontal**	**vertikal**	**horizontal**	
Grundwassermessstellen	ja	nein	Pumpen	Grundwasser	mittel	–	integrierend in Abhängigkeit von Filterlänge	punktuell	4.1
Seepagemeter	nein	ja	passives Auffangen	exfiltrierendes Grundwasser	mittel	klein bis mittel	–	kleinräumig integrierend	4.5
Mini-Piezometer	ja	ja	Pumpen	Grundwasser knapp unterhalb der Sediment-Wasser-Grenze	klein	klein	integrierend in Abhängigkeit von Filterlänge	punktuell	4.2
Multilevel-Piezometer	ja	ja	Pumpen	Grundwasser knapp unterhalb der Sediment-Wasser-Grenze und/ oder Sedimentporenwasser	klein bis mittel	klein	einige Zentimeter oder Dezimeter, abhängig vom Abstand der einzelnen Probenahmeports	punktuell	4.3
Porenwassersammler	nein	ja	diffus, Ausgleich von Konzentrationsgradienten	Grundwasser im Bereich der Sediment-Wasser-Grenze und/ oder Sedimentporenwasser	klein	klein	einige Zentimeter, abhängig vom Abstand der Kammern	punktuell	4.4

* klein: Zentimeter bis wenige Dezimeter; mittel: wenige Dezimeter bis einige Meter; groß: einige Meter bis Hunderte Meter

trationen mit repräsentativen hydrologischen Austauschraten zu multiplizieren. Da Wasserflüsse und Stoffkonzentrationen unabhängig voneinander stark heterogen sind, ist die Untersuchung kleiner Ufersegmente zu empfehlen. Die abschnittsweise ermittelten Stofffrachten werden dann aufsummiert.

Literatur

Adams, D.D. (1991): Sediment pore water sampling. In: Mudroch, A., Mac Knight, S.D. (eds): CRC Handbook of Techniques for Aquatic Sediments Sampling: 171–202. CRC Press, Boca Raton.

Angermann, L., Krause, S., Lewandowski, J. (2012a): Application of heat pulse injections for investigating shallow hyporheic flow in a lowland river. Water Resources Research 48.

Angermann, L., Lewandowski, J., Fleckenstein, J.H., Nutzmann, G. (2012b): A 3D analysis algorithm to improve interpretation of heat pulse sensor results for the determination of small-scale flow directions and velocities in the hyporheic zone. Journal of Hydrology 475: 1–11.

Anibas, C., Fleckenstein, J.H., Volze, N., Buis, K., Verhoeven, R., Meire, P., Batelaan, O. (2009): Transient or steady-state? Using vertical temperature profiles to quantify groundwater-surface water exchange. Hydrological Processes 23: 2165–2177.

Arvola, L., Rask, M., Ruuhijarvi, J., Tulonen, T., Vuorenmaa, J., Ruoho-Airola, T., Tulonen, J. (2010): Long-term patterns in pH and colour in small acidic boreal lakes of varying hydrological and landscape settings. Biogeochemistry 101: 269–279.

Atkinson, A.P., Cartwright, I., Gilfedder, B.S., Hofmann, H., Unland, N.P., Cendon, D.I., Chisari, R. (2015): A multi-tracer approach to quantifying groundwater inflows to an upland river; assessing the influence of variable groundwater chemistry. Hydrological Processes 29: 1–12.

Bagrov, N.A. (1953): O srednem mnogoletnem ísparenii s poverchnosti suši (Über den vieljährigen Verdungstungsdurchschnitt von der Oberfläche des Festlandes). Meteorologia i Gidrologia, Nr. 10, S. 20–25, Leningrad, (russ.).

Bagrov, N.A. (1954): O rasčete ísparenija s poverchnosti suši (Über die Berechnung der Verdunstung von der Oberfläche des Festlandes). Meteorologia i Gidrologia, Nr. 2, S. 12–18, Leningrad, (russ.).

Balzer, F., Schulz, D. (2014): Umweltbelastende Stoffeinträge aus der Landwirtschaft Möglichkeiten und Maßnahmen zu ihrer Minderung in der konventionellen Landwirtschaft und im ökologischen Landbau. UBA Umweltbundesamt (Hrsg.), Hintergrund, Dessau-Roßlau, 31 S.

Bannick, C., Engelmann, B., Fendler, R., Frauenstein, J., Ginzky, H., Hornemann, C., Ilvonen, O., Kirschbaum, B., Penn-Bressel, G., Rechenberg, J., Richter, S., Roy, L., Wolter, R. (2008): Grundwasser in Deutschland. BMU – Bundesministerium für Umwelt, Naturschutz und Reaktorsicherheit (Hrsg.), Reihe Umweltpolitik, Berlin, 71 S.

Bartel, H.H., Dieter, H.H., Feuerpfeil, I., Grummt, H.-J., Grummt, T., Hummel, A., Konietzka, R., Litz, N., Rapp, T., Rechenberg, J., Schaefer, B., Schlosser, F.-U., Vigelahn, L. (2013): Rund um das Trinkwasser. – UBA Umweltbundesamt (Hrsg.), 3. Auflage, Dessau-Roßlau, 86 S.

Behrendt, H., Kornmilch, M., Opitz, D., Schmoll, O., Scholz, G. (2002): Estimation of the nutrient inputs into river systems – experiences from German rivers. Regional Environmental Change 3: 107–117.

Belanger, T.V., Mikutel, D.F. (1985): On the use of seepage meters to estimate groundwater nutrient loading to lakes. Water Resources Bulletin 21(2): 265–273.

Belanger, T.V., Mikutel, M., Opitz, D.F., Churchill, P.A., (1985): Groundwater seepage nutrient loading in a Florida lake. Water Research 19(6): 773–781.

Berden, G., Peeters, R., Meijer, G. (2000): Cavity ring-down spectroscopy: Experimental schemes and applications. International Reviews in Physical Chemistry 19: 565–607.

Blume, T., Krause, S., Meinikmann, K., Lewandowski, J. (2013): Upscaling lacustrine groundwater discharge rates by fiber-optic distributed temperature sensing. Water Resources Research 49: 7929–7944.

BMU – Bundesministerium für Umwelt, Naturschutz und Reaktorsicherheit (Hrsg.) (2012): Nitratbericht. Bonn, 94 S.

Brandl, H., Hanselmann, K.W. (1991): Evaluation and application of dialysis porewater samplers for microbial studies at sediment-water interfaces. Aquatic Sciences 53: 54–73.

Bredehoeft, J.D., Papaopulos, I.S. (1965): Rates of vertical groundwater movement estimated from the Earth's thermal profile. Water Resources Research 1: 325–328.

Bremer, J.E., Harter, T. (2012): Domestic wells have high probability of pumping septic tank leachate. Hydrology and Earth System Sciences 16: 2453–2467.

Brothers, S., Köhler, J., Attermeyer, K., Grossart, H.P., Mehner, T., Meyer, N., Scharnweber, K., Hilt, S., (2014): A feedback loop links brownification and anoxia in a temperate, shallow lake. Limnology and Oceanography 59: 1388–1398.

Burnett, W.C., Santos, I.R., Weinstein, Y., Swarzenski, P.W., Herut, B., (2007): Remaining uncertainties in the use of Rn-222 as a quantitative tracer of submarine groundwater discharge. In: Sanford, W., Langevin, C., Polemio, M., Povinec, P. (eds): A new focus on groundwater-seawater interactions: 109–118. IAHS Publication No. 312, Perugia, Italy.

Cartwright, I., Gilfedder, B. (2015): Mapping and quantifying groundwater inflows to Deep Creek (Maribyrnong catchment, SE Australia) using Rn-222, implications for protecting groundwater-dependant ecosystems. Applied Geochemistry 52: 118–129.

Clark, J.M., Bottrell, S.H., Evans, C.D., Monteith, D.T., Bartlett, R., Rose, R., Newton, R. J., Chapman, P. J. (2010): The importance of the relationship between scale and process in understanding long-term DOC dynamics. Science of the Total Environment 408: 2768–2775.

Cook, P.G., Lamontagne, S., Berhane, D., Clark, J.F. (2006): Quantifying groundwater discharge to Cockburn River, southeastern Australia, using dissolved gas tracers 222Rn and SF6. Water Resources Research 42: W10411.

Corbett, D.R., Burnett, W.C., Cable, P.H., Clark, S.B. (1997): Radon tracing of groundwater input into Par Pond, Savannah River Site. Journal of Hydrology 203: 209–227.

Corbett, D.R., Burnett, W.C., Cable, P.H., Clark, S.B. (1998): A multiple approach to the determination of radon fluxes from sediments. Journal of Radioanalytical and Nuclear Chemistry 236: 247–252.

Corbett, D.R., Dillon, K., Burnett, W., Chanton, J. (2000): Estimating the groundwater contribution into Florida Bay via natural tracers, Rn-222 and CH4. Limnology and Oceanography 45: 1546–1557.

Craig, H., Gordon, L.I. (1965): Deuterium and oxygen-18 variations in the ocean and the marine atmosphere. In: Tongiorgi, E. (ed.): Stable Isotopes in Oceanographic Studies and Paleotemperatures, Spoleto: 9–130. Consiglio Nazionale delle Ricerche, Pisa, Italien.

Doss, P.K. (1993): The nature of a dynamic water-table in a system of non-tidal, fresh-water coastal wetlands. Journal of Hydrology 141: 107–126.

Downing, J.A., Peterka, J.J. (1978): Relationship of rainfall and lake groundwater seepage. Limnology and Oceanography. 23 (4): 821–825.

Dulaiova, H., Burnett, W.C. (2006): Radon loss across the water-air interface (Gulf of Thailand) estimated experimentally from Rn-222-Ra-224. Geophysical Research Letters 33: issue 5, article no. L05606.

DWA – Deutsche Vereinigung für Wasserwirtschaft, Abwasser und Abfall e. V. (Hrsg.) (2013): Wechselwirkungen zwischen Grund- und Oberflächenwasser. DWA-Themen T2/2013, Hennef, 157 S.

Erickson, D.R., (1981): A study of littoral groundwater seepage at Williams Lake, Minnesota, using seepage meters and wells: Minneapolis, University of Minnesota., M.S. thesis, 135 S.

Evans, C.D., Monteith, D.T., Cooper, D.M. (2005): Long-term increases in surface water dissolved organic carbon: Observations, possible causes and environmental impacts. Environmental Pollution 137: 55–71.

Findlay, S.E.G. (2005): Increased carbon transport in the Hudson River: unexpected consequence of nitrogen deposition? Frontiers in Ecology and the Environment 3: 133–137.

Fleckenstein, J.H., Neumann, C., Volze, N., Beer, J. (2009): Spatio-temporal patterns of lake-groundwater exchange in an acid mine lake. Grundwasser 14: 207–217.

Fraser, C.J.D., Roulet, N.T., Lafleur, M. (2001): Groundwater flow patterns in a large peatland. Journal of Hydrology 246: 142–154.

Glugla, G., Jankiewicz, P., Rachimow, C., Lojek, K., Richter, K., Fürtig, G., Krahe, P., (2003): BAGLUVA – Wasserhaushaltsverfahren zur Berechnung vieljähriger Mittelwerte der tatsächlichen Verdunstung und des Gesamtabflusses. Bundesanstalt für Gewässerkunde, BfG-Bericht 1342, Koblenz, 103 S.

Grunewald, U., Schoenheinz, D. (2014): Acidification of water bodies due to mining activities in the Lower Lusatia region – causes, severity and remedial conceptions. Hydrologie und Wasserbewirtschaftung 58: 274–285.

Gulati, R.D., van Donk, E. (2002): Lakes in the Netherlands, their origin, eutrophication and restoration: state-of-the-art review. Hydrobiologia 478: 73–106.

Häfner, F., Sames D., Voigt, H.-D. (1992): Wärme- und Stofftransport – Mathematische Methoden. Springer Verlag, Berlin, Heidelberg, New York, 626 S.

Hatch, C.E., Fisher, A.T., Revenaugh, J.S., Constantz, J., Ruehl, C. (2006): Quantifying surface water-groundwater interactions using time series analysis of streambed thermal records: Method development. Water Resources Research 42: issue 10, article no. W10410.

Hartge, K.H., Horn, R. (2009): Die physikalische Untersuchung von Böden. 4. Auflage, Schweizerbart, 178 S.

Harvey, J.W., Krupa, S.L., Gefvert, C.J., Choi, J., Mooney, R.H., Giddings, J.B. (2000): Interaction between ground water and surface water in the northern Everglades and relation to water budgets and mercury cycling–study methods and appendixes. U. S. Geological Survey Open-File Report 2000–168, 395 S.

Hesslein, R.H. (1976): An in situ sampler for close interval pore water studies. Limnology and Oceanography 21: 912–914.

Hoehn, E., Vongunten, H.R. (1989): Radon in groundwater – a tool to assess infiltration from surface waters to aquifers. Water Resources Research 25: 1795–1803.

Hölting, B., Coldewey, G.W. (2009): Hydrogeologie – Einführung in die Allgemeine und Angewandte Hydrogeologie. 7. Auflage, Spektrum Akademischer Verlag, Heidelberg, 383 S.

Hötzl, H. (2001): Hydrogeologie. In: Lexikon der Geowissenschaften, Bd. 2: S. 458f. Spektrum Akademischer Verlag, Heidelberg, Berlin.

Hupfer, M., Lewandowski, J. (2005): Retention and early diagenetic transformation of phosphorus in Lake Arendsee (Germany) – consequences for management strategies. Archiv fuer Hydrobiologie 164: 143–167.

Jacobs, P.H. (2002): A new rechargeable dialysis pore water sampler for monitoring sub-aqueous in-situ sediment caps. Water Research 36: 3121–3129.

Kendall, C., McDonnell, J.J. (Hrsg.) (2003): Isotope tracers in catchment hydrology. 3. Auflage, Elsevier, Amsterdam, 839 S.

Klaus, J., McDonnell, J.J. (2013): Hydrograph separation using stable isotopes: Review and evaluation. Journal of Hydrology 505: 47–64.

Kluge, T., Ilmberger, J., von Rohden, C., Aeschbach-Hertig, W. (2007): Tracing and quantifying groundwater inflow into lakes using a simple method for radon-222 analysis. Hydrology and Earth System Sciences 11: 1621–1631.

Kokorite, I., Klavins, M., Rodinov, V., Springe, G. (2012): Trends of natural organic matter concentrations in river waters of Latvia. Environmental Monitoring and Assessment 184: 4999–5008.

Krom, M.D., Davison, P., Zhang, H., Davison, W. (1994): High-resolution pore-water sampling with a gel sampler. Limnology and Oceanography 39: 1967–1972.

Laskov, C., Herzog, C., Lewandowski, J., Hupfer, M. (2007): Miniaturized photometrical methods for the rapid analysis of phosphate, ammonium, ferrous iron, and sulfate in pore water of freshwater sediments. Limnology and Oceanography-Methods 5: 63–71.

Lee, D.R. (1977): Device for measuring seepage flux in lakes and estuaries. Limnology and Oceanography 22: 140–147.

Lewandowski, J. (2002): Untersuchungen zum Einfluss seeinterner Verfahren auf die Phosphor-Diagenese in Sedimenten. Humboldt-Universität zu Berlin, Dissertation, 84 S.

Lewandowski, J., Nützmann, G. (2010): Nutrient retention and release in a floodplain's aquifer and in the hyporheic zone of a lowland river. Ecological Engineering 36: 1156–1166.

Lewandowski, J., Lischeid, G., Nutzmann, G. (2009): Drivers of water level fluctuations and hydrological exchange between groundwater and surface water at the lowland river Spree (Germany): field study and statistical analyses. Hydrological Processes 23: 2117–2128.

Lewandowski, J., Angermann, L., Nutzmann, G., Fleckenstein, J.H. (2011a): A heat pulse technique for the determination of small-scale flow directions and flow velocities in the streambed of sand-bed streams. Hydrological Processes 25: 3244–3255.

Lewandowski, J., Putschew, A., Schwesig, D., Neumann, C., Radke, M. (2011b): Fate of organic micropollutants in the hyporheic zone of a eutrophic lowland stream: Results of a preliminary field study. Science of the Total Environment 409: 1824–1835.

Lewandowski, J., Meinikmann, K., Nützmann, G., Rosenberry, D. O. (2015): Groundwater – the disregarded component in lake water and nutrient budgets. 2. Effects of groundwater on nutrients. Hydrological Processes: 29(13): 2922–2955.

MacIntyre, S., Wanninkhof, R., Chanton, J.P. (1995): Trace gas exchange across the air-water interface in freshwater and coastal marine environments. In: Matson, P.A., Harriss, R.C. (eds): Methods in ecology – biogenic trace gases: measuring emissions from soil and water: 52–97. Blackwell, Cambridge.

Martens, C.S., Kipphut, G.W., Valklump, J. (1980): Sediment-water chemical exchange in the coastal zone traced by in situ Radon-222 flux measurements. Science 208: 285–288.

Meinikmann, K., Lewandowski, J., Nützmann, G. (2013): Lacustrine groundwater discharge: Combined determination of volumes and spatial patterns. Journal of Hydrology 502: 202–211.

Meinikmann, K., Hupfer, M., Lewandowski, J. (2015): Phosphorus in groundwater discharge – a potential source for lake eutrophication. Journal of Hydrology 524: 214–226.

Menberg, K., Steger, H., Zorn, R., Reuss, M., Proll, M., Bayer, P., Blum, P. (2013): Bestimmung der Wärmeleitfähigkeit im Untergrund durch Labor und Feldversuche und anhand theoretischer Modelle. Grundwasser 18: 103–116.

Menheer, M.A. (2004): Development of a benthic-flux chamber for measurement of ground-water seepage and water sampling for mercury analysis at the sediment-water interface. U.S. Geological Survey Scientific Investigations Report 2004–5298, 14 S.

Monteith, D.T., Stoddard, J.L., Evans, C.D., de Wit, H.A., Forsius, M., Hogasen, T., Wilander, A., Skjelkvale, B.L., Jeffries, D. S., Vuorenmaa, T., Keller, B., Kopacek, J., Vesley, J. (2007): Dissolved organic carbon trends resulting from changes in atmospheric deposition chemistry. Nature 450: 537–440.

Müller, T. (1999): Wörterbuch und Lexikon der Hydrogeologie. Springer, Berlin, Heidelberg, 367 S.

Mueller, B., Scheytt, T., Asbrand, M., de Casas, A.M. (2012): Pharmaceuticals as indictors of sewage-influenced groundwater. Hydrogeology Journal 20: 1117–1129.

Munksgaard, N.C., Wurster, C.M., Bird, M.I. (2011): Continuous analysis of delta O-18 and delta D values of water by diffusion sampling cavity ring-down spectrometry: a novel sampling device for unattended field monitoring of precipitation, ground and surface waters. Rapid Communications in Mass Spectrometry 25: 3706–3712.

Murdoch, L.C., Kelly, S.E. (2003): Factors affecting the performance of conventional seepage meters: Water Resources Research, v. 39, no. 6, p. SWC 2–1.

Neumann, C., Beer, J., Blodau, C., Peiffer, S., Fleckenstein, J.H. (2013): Spatial patterns of groundwater-lake exchange – implications for acid neutralization processes in an acid mine lake. Hydrological Processes 27: 3240–3253.

Paulsen, R.J., Smith, C.F., O'Rourke, D., Wong, T.F. (2001): Development and evaluation of an ultrasonic ground water seepage meter. Ground Water 39: 904–911.

Rivett, M.O., Ellis, R., Greswell, R.B., Ward, R.S., Roche, R.S., Cleverly, M.G., Walker, C., Conran, D., Fitzgerald, P.J., Willox, T., Dowle, J. (2008): Cost-effective mini drive-point piezometers and multilevel samplers for monitoring the hyporheic zone. Quarterly Journal of Engineering Geology and Hydrogeology 41: 49–60.

Rosenberry, D.O. (2005): Integrating seepage heterogeneity with the use of ganged seepage meters. Limnology and Oceanography-Methods 3: 131–142.

Rosenberry, D.O., LaBaugh, J.W. (2008): Field Techniques for Estimating Water Fluxes Between Surface Water and Ground Water. U.S. Geological Survey, Techniques and Methods 4-D2, 128 S.

Rosenberry, D.O., Morin, R.H. (2004): Use of an electromagnetic seepage meter to investigate temporal variability in lake seepage. Ground Water 42: 68–77.

Rosenberry, D.O., Striegl, R.G., Hudson, D.C. (2000): Plants as indicators of focused ground water discharge to a northern Minnesota lake. Ground Water 38: 296–303.

Rosenberry, D.O., Lewandowski, J., Meinikmann, K., Nützmann, G. (2015): Groundwater – the disregarded component in lake water and nutrient budgets. Part 1: effects of groundwater on hydrology. Hydrological Processes: 29(13): 2895–2921.

Savoie, J., Leblanc, D.R. (1998): Water-Quality Data and Methods of Analysis for Samples Collected Near a Plume of Sewage-Contaminated Ground Water, Ashumet Valley, Cape Cod, Massachusetts, 1993-94. U.S. Geological Survey, Water-Resources Investigations Report 97-4269, 113 S.

Schaider, L.A., Rudel, R.A., Ackerman, J.M., Dunagan, S.C., Brody, J.G. (2014): Pharmaceuticals, perfluorosurfactants, and other organic wastewater compounds in public drinking water wells in a shallow sand and gravel aquifer. Science of the Total Environment 468: 384–393.

Schincariol, R.A., McNeil, J.D. (2002): Errors with small volume elastic seepage meter bags. Ground Water 40: 649–651.

Schmidt, C., Bayer-Raich, M., Schirmer, M. (2006): Characterization of spatial heterogeneity of groundwater-stream water interactions using multiple depth streambed temperature measurements at the reach scale. Hydrology and Earth System Sciences 10: 849–859.

Schneider, R.L., Negley, T.L., Wafer, C. (2005): Factors influencing groundwater seepage in a large, mesotrophic lake in New York. Journal of Hydrology 310: 1–16.

Schroeder, M., Wyrwich, D. (1990): Eine in Nordrhein-Westfalen angewendete Methode zur flächendifferenzierten Ermittlung der Grundwasserneubildung. Deutsche Gewässerkundliche Mitteilungen 34: 12–16.

Schultze, M., Pokrandt, K.-H., Hille, W. (2010): Pit lakes of the Central German lignite mining district: Creation, morphometry and water quality aspects. Limnologica – Ecology and Management of Inland Waters 40: 148–155.

Sebestyen, S.D., Schneider, R.L. (2001): Dynamic temporal patterns of nearshore seepage flux in a headwater Adirondack lake. Journal of Hydrology 247: 137–150.

Sebestyen, S.D., Schneider, R.L. (2004): Seepage patterns, pore water, and aquatic plants: hydrological and biogeochemical relationships in lakes. Biogeochemistry 68: 383–409.

Sharpley, A., Jarvie, H. P., Buda, A., May, L., Spears, B., Kleinman, P. (2013): Phosphorus legacy: overcoming the effects of past management practices to mitigate future water quality impairment. Journal of Environmental Quality 42: 1308–1326.

Stonestrom, D.A., Constantz, J. (eds) (2003): Heat as a tool for studying the movement of ground water near streams. U.S. Geological Survey, Circular 1260, 96 S.

TrinkwV (2001): Verordnung über die Qualität von Wasser für den menschlichen Gebrauch. Trinkwasserverordnung in der Fassung der Bekanntmachung vom 2. August 2013 (BGBl. I S. 2977).

Tuccimei, P., Salvati, R., Capelli, G., Delitala, M.C., Primavera, P. (2005): Groundwater fluxes into a submerged sinkhole area, Central Italy, using radon and water chemistry. Applied Geochemistry 20: 1831–1847.

Vandersteen, G., Schneidewind, U., Anibas, C., Schmidt, C., Seuntjens, P., Batelaan, O. (2015): Determining groundwater-surface water exchange from temperature-time series: Combining a local polynomial method with a maximum likelihood estimator. Water Resources Research 51: 922–939.

Winter, T.C., Rosenberry, D.O. (1995): The interaction of ground-water with prairie pothole wetlands in the Cottonwood Lake area, east-central North-Dakota, 1979–1990. Wetlands 15: 193–211.

Winter, T.C., Harvey, J.W., Franke, O.L., Alley, W.M. (1998): Ground water and surface water a single resource. U.S. Geological Survey, Circular 1139, 79 S.

Wolf, L., Zwiener, C., Zemann, M. (2012): Tracking artificial sweeteners and pharmaceuticals introduced into urban groundwater by leaking sewer networks. Science of the Total Environment 430: 8–19.

Worrall, F., Burt, T., Shedden, R. (2003): Long term records of riverine dissolved organic matter. Biogeochemistry 64: 165–178.

Zak, D., Kleeberg, A., Hupfer, M. (2006): Sulphate-mediated phosphorus mobilization in riverine sediments at increasing sulphate concentration, River Spree, NE Germany. Biogeochemistry 80: 109–119.

Zimmermann, C.F., Montgomera, J.R., Carlson, P.R. (1985): Variability of dissolved reactive phosphate flux rates in nearshore estuarine sediments – effects of groundwater-flow. Estuaries 8(2B): 228–236.

DIN 4049-3 (1994): Hydrologie; Begriffe zur quantitativen Hydrologie – Abschnitt 3: Unterirdisches Wasser. Beuth, Berlin.

DIN 18130-1 (1998): Baugrund; Untersuchung von Bodenproben; Bestimmung des Wasserdurchlässigkeitsbeiwerts – Teil 1: Laborversuche. Beuth, Berlin.

DIN 18130-1 (2003): Baugrund; Untersuchung von Bodenproben; Bestimmung des Wasserdurchlässigkeitsbeiwerts – Teil 2: Feldversuche. Beuth, Berlin. Entwurf.

Empfohlene, weiterführende Literatur

Adams, D.D. (1991): Sediment pore water sampling. In: Mudroch, A., Mac Knight, S.D. (eds): Handbook of Techniques for Aquatic Sediments Sampling: 171–202. 2. ed., CRC Press.

Anderson, M.P. (2005): Heat as a Ground Water Tracer. Ground Water 43: 951–968.

Brandl, H., Hanselmann, K.W. (1991): Evaluation and application of dialysis porewater samplers for microbial studies at sediment-water interfaces. Aquatic Sciences 53: 54–73.

Constantz, J. (2008): Heat as a tracer to determine streambed water exchanges. Water Resources Research 44: 1–20.

DWA – Deutsche Vereinigung für Wasserwirtschaft, Abwasser und Abfall e. V. (Hrsg.) (2013): Wechselwirkungen zwischen Grund- und Oberflächenwasser. DWA-Themen T2/2013, Hennef, 157 S.

Hartge K.H., Horn, R. (2009): Die physikalische Untersuchung von Böden. 4. Auflage, Schweizerbart, 178 S.

Healy, R.W., Ronan, A.D. (1996): Documentation of computer program VS2Dh for simulation of energy transport in variably saturated porous media; modification of the US Geological Survey's computer program VS2DT. USGS Water-Resources Investigations Report 96-4230, 40 S.

Hesslein, R.H. (1976): An in situ sampler for close interval pore water studies. Limnology and Oceanography 21: 912–914.

Hölting, B., Coldewey, G.W. (2009): Hydrogeologie – Einführung in die Allgemeine und Angewandte Hydrogeologie. 7. Auflage, Spektrum Akademischer Verlag, Heidelberg, 383 S.

Kendall, C., McDonnell, J.J. (Hrsg.) (2003): Isotope tracers in catchment hydrology. 3. Auflage, Elsevier, Amsterdam, 839 S.

Krabbenhoft, D.P., Bowser, C.J., Kendall, C., Gat, J.R. (1994). Use of O-18 and deuterium to assess the hydrology of groundwater-lake systems. In: Baker, L.A. (ed.), Environmental Chemistry of Lakes and Reservoirs: 67–90. Advances in Chemistry Series.

Lewandowski, J., Meinikmann, K., Nützmann, G., Rosenberry, D. O. (2015): Groundwater – the disregarded component in lake water and nutrient budgets. 2. Effects of groundwater on nutrients. Hydrological Processes : .

Müller, T. (1999): Wörterbuch und Lexikon der Hydrogeologie. Springer, Berlin-Heidelberg, 367 S.

Rosenberry, D.O., Lewandowski, J., Meinikmann, K., Nützmann, G. (2015): Groundwater – the disregarded component in lake water and nutrient budgets. Part 1: effects of groundwater on hydrology. Hydrological Processes: 29(13): 2895–2921.

Rosenberry, D.O., LaBaugh, J.W. (2008): Field Techniques for Estimating Water Fluxes Between Surface Water and Ground Water. U.S. Geological Survey, Techniques and Methods 4-D2, 128 S.

Stonestrom, D.A., Constantz, J., (Hrsg.) (2003): Heat as a Tool for Studying the Movement of Ground Water near Streams. U.S. Geological Survey, Circular 1260, 96 S.

Winter, T.C., Harvey, J.W., Franke, O.L., Alley, W.M. (1998): Ground Water and Surface Water – a Single Resource. U.S. Geological Survey, Circular 1139, 79 S.

Karin Meinikmann[1, 2], Michael Hupfer[1], Gunnar Nützmann[1, 2], Jörg Lewandowski[1, 2]

[1] Leibniz-Institut für Gewässerökologie und Binnenfischerei
Müggelseedamm 310
12587 Berlin

[2] Humboldt-Universität zu Berlin
Geographisches Institut
Rudower Chaussee 16
12489 Berlin

Annex II

Declaration of independent work

I hereby declare that this thesis and the work presented in it is entirely my own except where otherwise indicated. I have only used the documented utilities and references.

Hiermit erkläre ich, dass ich die vorliegende Dissertation selbständig verfasst habe und keine anderen als die angegebenen Quellen und Hilfsmittel verwendet habe.

Berlin, 20 December 2016 ……………………………………………….
Karin Meinikmann